

Climate Change and Atlantic salmon (*Salmo salar*): Changes in Flow and Freshwater Habitat in the Burrishoole Catchment

A thesis submitted for the Degree of
Doctor of Philosophy

Presented by
Ciaran J. Broderick M.Sc.

Department of Geography
Faculty of Social Science
National University of Ireland, Maynooth
Kildare

May 2012

Head of Department:

Prof. Mark Boyle

Research Supervisors:

Dr. Rowan Fealy and Dr. Conor Murphy



NUI MAYNOOTH

Ollscoil na hÉireann Má Nuad

Acknowledgements

I thank my supervisors Dr. Rowan Fealy and Dr. Conor Murphy for their support and advice throughout the process. Their guidance was always appreciated and contributed greatly to my development as a researcher. I also extend my thanks to Prof. John Sweeney for making the facilities in ICARUS available to me. Acknowledgements must also be extended to Prof. Mark Boyle and Dr. Jan Rigby for their role in nurturing postgraduate research in the department. I also thank Dr. Frank Mulligan and Prof. Chris Kilsby for acting as my internal and external examiners respectively. Their words of encouragement will provide solace during any difficult times ahead. Special mention must go to Dr. Priscilla Mooney who helped me along each step in the process, and gave very generously of her time whenever it was needed. I'd also like to extend my deepest appreciation to everyone in ICARUS for their friendship and encouragement throughout my PhD - especially during those (quite regular) periods when patience was running thin and stress levels were reaching a critical point. The atmosphere created by the individuals who work there meant that spending a long day in the office was a pleasurable experience. The support offered by this group of people is undoubtedly one of ICARUS's greatest strengths, and without it the last few years would have been much more difficult. I wish to extend my appreciation to the Marine Institute who supported my research financially. I also thank all those who work in the Burrishoole catchment; they were very generous with their data and always giving of their time when assistance was needed.

I'm also very grateful for the support and guidance provided by my family and friends. My brother Killian and sister Deirdre, along with my Mum, Dad and Grandmother, were always willing to listen to regular updates on my progress with enthusiasm. A mention must be given to my uncle Harry; he showed me that science and the pursuit of knowledge is something to be cherished and seized upon at all available opportunities. Last but not least a special mention must go to Selina for all her support, never ending patience and encouragement. With her words of wisdom she always kept my feet on the ground, particularly with her mantra, "oh don't worry, you'll get it done". Just a word of warning, now that I'm finished I get to decide what we watch on TV.

Abstract

Climate change is anticipated to impact the flow regime of riverine systems with resultant consequences for the freshwater habitat of Atlantic salmon (*Salmo salar*) and the long-term sustainability of their population numbers. The Burrishoole catchment, a relatively small but productive salmon catchment (~90 km²) located on Ireland's west coast, is used as a case study to investigate this. A series of high resolution climate scenarios were employed to examine potential changes in the climate and hydrology of this catchment. The climate scenarios used represent different combinations of greenhouse gas emission scenarios, driving GCMs and statistical/dynamical downscaling models; in addition, three different rainfall-runoff models (HBV, HYSIM and TOPMODEL) were employed – integrating across both structural and parameter uncertainty. By considering multiple model pathways this study attempts to sample across the uncertainties encountered at each stage in the process of translating prescribed anthropogenic forcings into local scale responses in the catchment system. The hydrological projections were examined in the context of the habitat and flow requirements of Atlantic salmon at key stages in their life-cycle (e.g. spawning, migration).

Model projections suggest that the catchment is likely to become warmer, with wetter winters and drier summers occurring. The results of the hydrological modelling suggest that this will be accompanied by an increase in the seasonality of its flow regime - manifest in an increase in low (Q95) summer and high (Q05) winter flows. If realised, these changes are likely to impact salmon through a reduction in the availability of preferred habitat, a loss in connectivity across the catchment system and a disruption to the evolved synchrony between the occurrence of optimal in-stream conditions and the time at which certain life history events occur. Each of these factors is likely to impact the processes of migration, reproduction and recruitment - each of which is critical for the long-term viability of healthy, self-sustaining wild stocks in the catchment. Based on the projected flow data it is likely that the carrying capacity and productivity of the catchment may be reduced. In addition, by affecting those life stages which are already subject to significant mortality losses (e.g. fry emergence, smolt migration), changes in climate may result in population collapse - particularly if successive year-classes are affected. The results of the hydrological modelling highlight the sensitivity of smaller spatey catchments to changes in climate. Given that the Burrishoole system is typical of

many catchment systems found along Ireland's western seaboard, the results highlight a vulnerability to climate change which is present more generally across the region.

CONTENTS

List of Figures	ix
-----------------------	----

List of Tables.....	xviii
---------------------	-------

1. Introduction

1.1 Research Background.....	1
1.2 The intensification of the natural greenhouse effect.....	3
1.3 Observed changes in the global climate.....	6
1.4 The ecological response to recent warming.....	9
1.5 Projected future climate change.....	11
1.6 Climate change and salmonids.....	13
1.7 Research aims and objectives.....	14
1.7.1 Aims.....	15
1.7.2 Research Outline.....	15
1.8 RESCALE (Review and Simulate Climate and Catchment Responses at Burrishoole).....	16
1.9 Chapter Summaries.....	17

2. Climate Change, freshwater ecosystems and Atlantic salmon

2.1 Observed changes in the climate system.....	19
2.1.1 Temperature.....	20
2.1.2 Precipitation.....	22
2.1.3 The Intensification of the Hydrological Cycle.....	26
2.1.4 Changes in European Extremes.....	28
2.2 Climate change indicators for Ireland.....	29
2.3 Projected changes in the global climate system.....	30
2.4 Projected changes in the hydrological cycle.....	33
2.5 Climate change impacts on freshwater ecosystems.....	34
2.6 A summary of the anticipated impacts of climate change on freshwater ecosystems	43
2.7 Climate change and salmonids.....	45
2.7.1 Species distribution and life cycle.....	45
2.7.2 Climate change impacts on salmonids in freshwaters.....	47
2.8 A summary of the Anticipated Impacts of Climate Change on Salmonids.....	51
2.9 Conclusion.....	54

3. The Burrishoole catchment

3.1 Background.....	55
3.2 Characterizing the catchment system.....	56
3.3 Observed climatology	63
3.4 Sub-catchments of the Burrishoole system	64
3.5 Instruments and data	66
3.5.1 Furnace weather station	66
3.5.2 Belmullet weather station.....	67
3.5.4 Water Level Recorders.....	67
3.5.4 Water level records.....	68
3.4.5 Data Quality Issues	69
3.6 Indicators of climate change in the Burrishoole catchment	72
3.7 The status of Atlantic salmon (<i>Salmo salar</i>) in the Burrishoole catchment.....	73
3.8 Conclusion.....	73

4. Uncertainty and predictability in climate modelling

4.1 Introduction	75
4.2 Emission scenarios and atmospheric greenhouse gas concentrations.....	78
4.3 Climate sensitivity and radiative forcing.....	80
4.4 Climate predictability.....	83
4.5 Uncertainty in the development of high resolution climate scenarios	86
4.6 Uncertainty in climate impacts	88
4.7 Managing uncertainty in climate projections	90
4.8 Probabilistic projections and weighting criteria	92
4.9 ENSEMBLES: weighting scheme	95
4.10 Conclusion.....	97

5. Approaches to statistical and dynamical downscaling

5.1 Climate modelling and downscaling.....	99
5.2 A review of different downscaling techniques	101
5.2.1 Dynamical Downscaling	101
5.2.2 Statistical Downscaling	104
5.2.2.1 Classification schemes	109
5.2.2.2 Stochastic Weather Generators	111
5.2.2.3 Regression Models	113
5.3 An inter-comparison of statistical downscaling methods.....	115
5.4 Relative skill of statistical and dynamical downscaling	120

5.5 Conclusion.....	126
6. High resolution climate scenarios for the Burrishoole catchment	
6.1 Introduction	128
6.2 Statistical downscaling of GCM output: data and methods	129
6.2.1 <i>Datasets: Statistical Downscaling</i>	130
6.2.1.1 <i>NCEP Reanalysis Data</i>	130
6.2.1.2 <i>Global Climate Model data for the Irish grid box</i>	131
6.2.2 <i>Model Description: Linear Regression (SDSM)</i>	132
6.2.3 <i>Model Description: Generalized Linear Model (GLM)</i>	134
6.2.4 <i>Predictor selection</i>	135
6.2.5 <i>Temperature: calibration and validation</i>	137
6.2.6 <i>Precipitation: calibration and validation</i>	143
6.2.6.1 <i>Linear Regression (SDSM)</i>	144
6.2.6.2 <i>Generalised Linear Model (GLM)</i>	145
6.2.6.3 <i>Model comparison</i>	145
6.2.7 <i>Other meteorological parameters</i>	152
6.2.7.1 <i>Wind speed</i>	152
6.2.7.2 <i>Relative humidity</i>	153
6.2.7.3 <i>Solar radiation and potential evaporation</i>	153
6.3 Dynamically downscaled datasets	154
6.3.1 <i>ENSEMBLES</i>	155
6.3.2 <i>ERA-40 RCM evaluation</i>	159
6.3.2.1 <i>Minimum temperature</i>	164
6.3.2.2 <i>Maximum temperature</i>	169
6.3.2.3 <i>Precipitation</i>	175
6.4 Development and application of a model weighting scheme	185
6.4.1 <i>Formulation of a weighting scheme</i>	186
6.4.1.1 <i>RCM weights</i>	190
6.4.1.2 <i>GCM weights</i>	193
6.4.1.3 <i>Model pathway weighting scheme</i>	194
6.4.1.4 <i>Final aggregated weights</i>	200
6.5 Conclusion.....	203
7. Projected changes in climate for the Burrishoole catchment	
7.1 Introduction	206
7.2 Projected changes in temperature	206
7.3 Projected changes in precipitation	214
7.4 Probability distribution for reference period and climate scenarios	221
7.5 Model response to climate forcing.....	228
7.6 Other climate variables.....	233

7.6.1	<i>Wind speed</i>	233
7.6.2	<i>Relative humidity</i>	235
7.6.3	<i>Solar radiation & potential evaporation</i>	235
7.7	Conclusion	235
8. Hydrological modelling and climate impact studies		
8.1	Introduction	238
8.2	Global and regional scale impact studies	238
8.3	Approaches to hydrological modelling in impact studies	243
8.4	Addressing stationarity	249
8.5	Uncertainty in hydrological modelling studies	251
8.5.1	<i>Data Uncertainty</i>	254
8.5.2	<i>Model Structure Uncertainty</i>	256
8.5.3	<i>Uncertainty in the Model Parameters</i>	261
8.6	Uncertainty in climate change impact studies	268
8.7	Conclusion	272
9. The hydrological response of the Burrishoole system to future climate change		
9.1	Introduction	274
9.2	Data	275
9.2.1	<i>Bias correction of RCM data</i>	275
9.2.1.1	<i>Background</i>	276
9.2.2.2	<i>Quantile mapping</i>	279
9.2.2	<i>Mapping of climate scenarios within the catchment</i>	282
9.2.3	<i>Evaporation Data</i>	284
9.3	Hydrological model selection	285
9.3.1	<i>HBV-light</i>	288
9.3.2	<i>TOPMODEL</i>	290
9.2.3	<i>HYSIM</i>	292
9.4	Sensitivity analysis	294
9.5	Methodology	300
9.3.1	<i>Generalized Likelihood Uncertainty Estimation (GLUE)</i>	300
9.3.2	<i>Monte Carlo simulation of probabilistic flow projections</i>	306
9.6	Model performance under observed conditions	310
9.6.1	<i>Glenamong</i>	310
9.6.2	<i>Srahrevagh</i>	319
9.7	The contribution of rainfall-runoff models to uncertainty	325

9.8 Components of uncertainty.....	328
9.9 Projected changes in flow	328
9.9.1 Glenamong	331
9.9.1.1 Median Flow (Q50): Individual Climate Pathways.....	331
9.9.1.2 Median Flow (Q50): Probabilistic Flow Projections.....	332
9.9.1.3 High Flows (Q05): Individual Climate Pathways	336
9.9.1.4 High Flows (Q05): Probabilistic Flow Projections	336
9.9.1.5 Low Flows (Q95): Individual Climate Pathways	340
9.9.1.6 Low Flows (Q95): Probabilistic Flow Projections.....	340
9.9.2 Srahrevagh.....	344
9.9.2.1 Median Flows (Q50): Probabilistic Flow Projections	344
9.9.2.2 High Flows (Q05): Probabilistic Flow Projections	344
9.9.2.3.Low Flows (Q95): Probabilistic Flow Projections.....	34
9.10 Conclusion	353

10. Climate change impacts on Atlantic salmon (*Salmo salar*): linking projected changes in flow to habitat requirements

10.1 Introduction.....	354
10.2 The potential impacts of changing flow regimes on salmonids.....	356
10.2.1 Salmonid eggs and fry.....	359
10.2.2 Salmonid parr and Smolt production.....	363
10.2.3 Smolt migration	366
10.2.4 Migration into and through river systems.....	368
10.2.5 Impacts on habitat maintenance.....	372
10.2.6 Adaptation.....	373
10.3 Methodology.....	374
10.4 Ideal Flow Parameters	381
10.5 Results	383
10.5.1 Reliability Resilience and Vulnerability (RRV Analysis).....	383
10.5.2 Changes in flow and habitat availability.....	386
10.5.2.1 Survival and upstream migration: adult salmon	386
10.5.2.2 Changes in the availability of ideal spawning habitat.....	388
10.5.2.2 Habitat availability for spawning and juvenile salmon	388
10.6 Discussion of Results	390
10.7 Conclusion	392

11. Conclusion

11.1 Introduction.....	398
11.2 Summary of key findings	401

11.3 The potential impacts on Atlantic salmon (<i>Salmo salar</i>)	405
11.4 Points of discussion and scope for further work.....	409
11.4.1 Addressing uncertainty	409
11.4.2 The ENSEMBLES dataset	412
11.4.3 Natural variability and extreme events.....	413
11.4.4 The development and application of a weighting scheme.....	414
11.4.5 Hydrological modelling	417
11.4.6 Habitat modelling.....	418
11.5 Addressing the potential impacts of climate change	419
11.6 Final conclusion	420
Bibliography	423
Appendix I: Projected changes in mean temperature (minimum and maximum) for the Burrishoole catchment estimated on a seasonal and monthly basis	I
Appendix II: Projected changes (%) in mean precipitation receipts for the Burrishoole catchment estimated on a seasonal and monthly basis.....	VIII
Appendix III: Dotty plots from the Monte Carlo simulation conducted for each of the three rainfall-runoff models used in this study (TOPMODEL, HYSIM and HBV)	XII
Appendix IV: Projected changes in median (Q50), high (Q05) and low (Q95) flows for the Glenamong and Srahrevagh catchments respectively; estimated on a seasonal and monthly basis.....	XVI
Appendix V: Results of the Reliability, Resilience and Vulnerability analysis conducted for the Glenamong and Srahrevagh catchments.....	XXXV

List of Figures

Figure 1.1	Principal anthropogenic and natural components of radiative forcing as outlined in the IPCC AR4 (2007). The values represent the contribution of different radiative forcings for the year 2005 relative to the beginning of the industrial revolution (circa. 1750) (Source: IPCC, 2007).....	4
Figure 1.2	Atmospheric concentrations of carbon dioxide sampled directly from the atmosphere at the Mauna Lao observatory Hawaii. The records indicate in parts per million the increase in atmospheric CO ₂ since 1958. Smaller fluctuations in the general trend are indicative of seasonal variations in atmospheric CO ₂ . (Source: http://www.esrl.noaa.gov/gmd/ccgg/trends/ , accessed 27/11/2011)	5
Figure 1.3	Records of atmospheric carbon dioxide and surface temperature extracted from the Vostok ice core - drilled in east central Antarctica - which stretch back over 400,000 years (Petit <i>et al.</i> , 1999). Current observations of CO ₂ sampled directly from the atmosphere are higher than at any period in the ice core record. (Source: http://en.wikipedia.org/Image:Vostok-ice-core-petit.pngfile , accessed 27/11/2011).....	6
Figure 1.4	Atmospheric CO ₂ concentrations measured at the Mauna Loa observatory (ppmv; in red). Surface ocean pCO ₂ (µatm; in blue) and surface ocean pH (in green) measured at the ALOHA Ocean station (Source: Doney <i>et al.</i> , 2009).....	7
Figure 1.5	Global temperature anomalies for the period 1850–2011 relative to the 1961–1990 average. This time series is compiled jointly by the Climatic Research Unit (CRU) and the UK Met Office	8
Figure 1.6	Projected patterns of future regional surface temperature change for the early and late 21st century relative to the period 1980–1999. The central and right panels show the AOGCM multimodel average projections for the B1 (top), A1B (middle) and A2 (bottom) SRES scenarios averaged over the decades 2020– 2029 (centre) and 2090–2099 (right). Shown in the left panel are probability distribution functions of the estimated global average temperature increase from an ensemble of different AOGCM and Earth System Model of Intermediate Complexity studies for the same periods.(Source: IPCC, 2007)	12
Figure 1.7	Schematic illustrating the main components of the study and how they are related.....	16
Figure 2.1	Observed global annual average temperature (°C) deviations for the period 1850–2010. Deviations are relative to the 1961-90 reference period means. Show in blue are estimated changes in the global mean surface temperature from the combined UK Met Office Hadley Centre and Climate Research Unit dataset HadCRUT3. Shown in red are estimated temperature changes from NASA's GISS dataset - anomalies are calculated relative to the period 1951-1980. (Source: http://www.eea.europa.eu/data-and-maps/figures . accessed 27/12/2011).	21
Figure 2.2	Connections between human activity, hydrological and geomorphological processes and ecosystem/fish responses. (Adapted from Milner <i>et al.</i> , 2010).....	35
Figure 2.3	A schematic of the four principles outlined by Bunn & Arthington (2002) which describe the link between aquatic biodiversity and the natural flow regime of a river system. Flow regimes can be defined as patterns of variability in flow that describe the full range of behaviour exhibited by river systems (e.g. long term average flows, seasonality, low and high flow statistics, interannual variability). Bunn and Arthington (2002) state that flow regimes influence the diversity of aquatic flora and fauna via several interrelated mechanisms that operate on different spatial and temporal scales. The first principle outlined above highlights the importance of flow as a key determinant of physical habitat at different temporal and spatial scales (i.e. from the scale of the catchment to the scale of microhabitats along the channel reach). This is driven by both high and low flow components; high flows are important for determining the channel form and shape which low flows may limit habitat availability. The second principle outlined above refers to the synchronicity between the life history strategy of aquatic organisms and patterns of flow. The life cycle of aquatic species have evolved in response to natural flow regimes, as such the seasonality of the flow regime and the timing of key flow events (e.g. spates) are intrinsically linked to the completion of different stages in an organism's life cycle. The third principle highlights the importance of flow for maintaining lateral and longitudinal connectivity across river systems. Flow act as a medium facilitating migration and movement between different parts of river systems and between in-stream and floodplain habitats. High flows may be particularly important for facilitating access to different parts of the network. The fourth of Bunn & Arthington's (2002) principles states that altered flow regimes may be more conducive to the ingress and proliferation of exotic species at the expense of native biota, provided the former are more adapted to the modified flow regime. Figure 2.3 is adapted from Bunn & Arthington (2002). (Source: www.awsaplanning.com/Presentations_files/RJG-ReportPresentation.ppt)	41
Figure 2.4	Potential impacts of climate change on the various life-stages of Atlantic salmon (<i>Salmo salar</i>) (Source: Walsh & Kilsby, 2007)	53

Figure 3.1	Location of the Burrishoole catchment and Belmullet synoptic station; also shown are the RCM grid boxes overlying the catchment.....	57
Figure 3.2	Map of the Burrishoole catchment showing each of the five constituent sub-catchments. Also shown is the Glendahurk catchment.....	58
Figure 3.3	Aquifer productivity across the Burrishoole catchment (Source: GSI, 2003).....	60
Figure 3.4	Soil cover across the Burrishoole catchment.....	61
Figure 3.5	Land cover type across the Burrishoole catchment (Source: CORINE, 2003)	62
Figure 3.6	Climograph depicting average monthly precipitation receipts (mm) and mean monthly temperature °C for the Burrishoole catchment. The plot is estimated using records from the Furnace weather station (Figure 3.2) averaged over the period 1961-2000.....	63
Figure 3.7	Double mass rating curves showing the cumulative monthly streamflow (mm) for each catchment plotted against data from the Glenamong recorder	71
Figure 3.8	Smoothed time series for the Goulan catchment showing change in both the mean and variance of the flow series subsequent to an extreme event (circa. 14/12/2006).....	71
Figure 3.9	The number of wild adult salmon which returned to the Burrishoole catchment on an annual basis, recorded over the period 1970–2009 (Source: Fealy <i>et al.</i> , 2010)	73
Figure 4.1	Uncertainty arises at each step in the process of modelling the potential climate response to altered forcing conditions (Source: IPCC, 2007).....	76
Figure 4.2	Key uncertainties in climate impact assessments represented using the “uncertainty explosion”. Uncertainty is amplified as it is propagated through each stage of the modelling process; (modified after Jones, 2000 and “cascading pyramid of uncertainties” in Schneider, 1983 (Source: IPCC, 2001).....	76
Figure 4.3	The relative contribution of each source of uncertainty to decadal mean surface temperature projections shown by the fractional uncertainty (the 90% confidence level divided by the mean prediction) for (a) the global mean, relative to the warming from the 1971–2000 mean, and (b) the British Isles mean, relative to the warming from the 1971–2000 mean (Source: Hawkins & Sutton, 2007). The plots are constructed using the Coupled Model Intercomparison Project phase 3 (CMIP3) multimodel air temperature projections also used in the IPCC AR4 (2007).....	85
Figure 6.1	Seasonal scatter plots of downscaled versus observed (Furnace weather station) daily minimum temperature for the Furnace weather station. Temperature is downscaled using NCEP reanalysis data for the calibration (1961-1978; 1994-2000) (left panel) and validation (1979-1993) (right panel) periods respectively. Values for the explained variance, standard error and slope of the least squares fitted line are provided	139
Figure 6.2	Seasonal scatter plots of downscaled versus observed (Furnace weather station) daily maximum temperature for the Furnace weather station. Temperature is downscaled using NCEP reanalysis data for the calibration (1961-1978; 1994-2000) (left panel) and validation (1979-1993) (right panel) periods respectively. Values for the explained variance, standard error and slope of the least squares fitted line are provided	140
Figure 6.3	Correspondence between observed (Furnace weather station) and downscaled temperature over the calibration (1961-1978; 1994-2000) and validation (1961-1978; 1994-2000) periods. Maximum (left panel) and minimum (right panel) temperature are downscaled for the Furnace weather station using NCEP reanalysis data. Datasets are averaged based on the day of year (1-366).....	141
Figure 6.4	Correspondence between the interannual variability of the observed (Furnace weather station) and downscaled maximum (left panel) and minimum (right panel) temperature series. Temperature is downscaled using NCEP reanalysis data for the calibration (1961-1978; 1994-2000) and validation (1979-1993) periods.....	142
Figure 6.5	Monthly percent wet-days (≥ 0.2 mm) for the downscaled and observed (Furnace weather station) precipitation series estimated over the calibration (1961-1978; 1994-2000) and validation (1979-1993) periods respectively. Precipitation is downscaled from NCEP reanalysis data using both the SDSM and GLM models	147

Figure 6.6(a)	Mean monthly wet-spell length (≥ 0.2 mm) for the downscaled and observed (Furnace weather station) precipitation series estimated over the calibration (1961-1978; 1994-2000) and validation (1979-1993) periods respectively. Precipitation is downscaled from NCEP reanalysis data using both the SDSM and GLM models	147
Figure 6.6(b)	Mean monthly dry-spell length (< 0.2 mm) for the downscaled and observed (Furnace weather station) precipitation series estimated over the calibration (1961-1978; 1994-2000) and validation (1979-1993) periods respectively. Precipitation is downscaled from NCEP reanalysis data using both the SDSM and GLM models	148
Figure 6.7	Monthly mean precipitation receipts for the downscaled and observed (Furnace weather station) series estimated over the calibration (1961-1978; 1994-2000) and validation (1979-1993) periods respectively. Precipitation is downscaled from NCEP reanalysis data using both the SDSM and GLM models.....	149
Figure 6.8	Interannual variability (total annual receipts) estimated for the downscaled and observed (Furnace) precipitation series over the calibration (1961-1978; 1994-2000) and validation (1979-1993) periods respectively. Precipitation is downscaled from NCEP reanalysis data using both the SDSM and GLM models.....	149
Figure 6.9	Monthly variance of the downscaled and observed (Furnace weather station) precipitation series over the calibration (1961-1978; 1994-2000) and validation (1979-1993) periods respectively. Precipitation is downscaled from NCEP reanalysis data using both the SDSM and GLM models. Both the inflated and non-inflated downscaled SDSM data is plotted	150
Figure 6.10	Seasonal Q-Q plots for the observed and downscaled (Furnace weather station) precipitation series over the calibration (1961-1978; 1994-2000) (left panel) and validation (1979-1993) (left panel) periods respectively. Precipitation is downscaled from NCEP reanalysis data using both the SDSM and GLM models. The plots are constructed using rainfall amounts only. The enlarged green dots are used to highlight those values relating to the following percentiles: 25 th , 50 th , 75 th , 90 th , 95 th and 99 th	151
Figure 6.11	GCM-RCM/GCM-SDSM model combinations - or ‘model pathways’ - (colour coded according to driving GCM) used to produce the downscaled data employed in this study. (***) mark those simulations which run until the year 2100. (**) mark those scenarios for which the dynamical weighting scheme is formulated (Figure 6.24). Note that the HadCM3 GCM is run in three sensitivity configurations (Q0, Q16 and Q3). The abbreviations in brackets denote the main centre responsible for the corresponding model pathway.....	156
Figure 6.12	Total error is shown as the sum of the systematic and random components. Different metrics can be used to assess each type of model error. (Source: http://www.met.ed.ucar.edu/nwp/model_derivedproducts/navmenu.php?tab=1&page=4.4.0 , accessed 24/11/2011)	164
Figure 6.13(a)	Skill of the RCMs used in the ENSEMBLES project at simulating observed winter (top panel) and spring (bottom panel) minimum temperature for the period 1961-2000. Model skill is assessed using the observed temperature series from the Furnace weather station. The MSE, bias and variance of the error are calculated for 15 RCMs, each driven using ERA-40 reanalysis data. These metrics are plotted together as they provide a measure of the total, systematic and random model error respectively. Error bars for each metric are calculated based on 10,000 bootstrapped samples and represent the 95% confidence interval.....	165
Figure 6.13(b)	Skill of the RCMs used in the ENSEMBLES project at simulating observed summer (top panel) and autumn (bottom panel) maximum temperature for the period 1961-2000. Model skill is assessed using the observed temperature series from the Furnace weather station. The MSE, bias and variance of the error are calculated for 15 RCMs, each driven using ERA-40 reanalysis data. These metrics are plotted together as they provide a measure of the total, systematic and random model error respectively. Error bars for each metric are calculated based on 10,000 bootstrapped samples and represent the 95% confidence interval.....	166
Figure 6.14	Taylor diagrams showing model skill at simulating observed winter (top left panel), spring (top right panel), summer (bottom left panel) and autumn (bottom right panel) minimum temperature for the period 1961-2000. On each plot the output from 15 RCMs, each run using ERA-40 reanalysis data, is compared to the observed temperature series from the Furnace weather station (denoted as ‘reference’). The plots provide a graphical summary of the similarity between the patterns of variability in the observed and modelled series - quantified in terms of their correlation, their centered root-mean-square difference and the amplitude of their variations (represented by the standard deviation) (Taylor, 2001).....	167

Figure 6.15	Interannual variability of observed and model simulated minimum temperature for the period 1961-2000. The output from 15 RCMs, each run using ERA-40 reanalysis data, is compared to the observed temperature series from the Furnace weather station	168
Figure 6.16(a)	Skill of the RCMs used in the ENSEMBLES project at simulating observed winter (top panel) and spring (bottom panel) maximum temperature for the period 1961-2000. Model skill is assessed using the observed temperature series from the Furnace weather station. The MSE, bias and variance of the error are calculated for 15 RCMs, each driven using ERA-40 reanalysis data. These metrics are plotted together as they provide a measure of the total, systematic and random model error respectively. Error bars for each metric are calculated based on 10,000 bootstrapped samples and represent the 95% confidence interval.....	170
Figure 6.16(b)	Skill of the RCMs used in the ENSEMBLES project at simulating observed summer (top panel) and autumn (bottom panel) maximum temperature for the period 1961-2000. Model skill is assessed using the observed temperature series from the Furnace weather station. The MSE, bias and variance of the error are calculated for 15 RCMs, each driven using ERA-40 reanalysis data. These metrics are plotted together as they provide a measure of the total, systematic and random model error respectively. Error bars for each metric are calculated based on 10,000 bootstrapped samples and represent the 95% confidence interval.....	171
Figure 6.17	Taylor diagrams showing model skill at simulating observed winter (top left panel), spring (top right panel), summer (bottom left panel) and autumn (bottom right panel) maximum temperature for the period 1961-2000. On each plot the output from 15 RCMs, each run using ERA-40 reanalysis data, is compared to the observed temperature series from the Furnace weather station (denoted as 'reference'). The plots provide a graphical summary of the similarity between the patterns of variability in the observed and modelled series - quantified in terms of their correlation, their centered root-mean-square difference and the amplitude of their variations (represented by the standard deviation) (Taylor, 2001).....	173
Figure 6.18	Interannual variability of observed and model simulated maximum temperature for the period 1961-2000. The output from 15 RCMs, each run using ERA-40 reanalysis data, is compared to the observed temperature series from the Furnace weather station	174
Figure 6.19(a)	Observed and model simulated monthly mean precipitation receipts averaged over the period 1961-2000. The output from 15 RCMs, each run using ERA-40 reanalysis data, is compared to the observed precipitation series from the Furnace weather station	176
Figure 6.19(b)	Percent bias in the model simulated monthly rainfall receipts estimated for the period 1961-2000. The output from 15 RCMs, each run using ERA-40 reanalysis data, is compared to the observed precipitation series from the Furnace weather station.....	176
Figure 6.20	Interannual variability of observed and model simulated annual precipitation receipts for the period 1961-2000. The output from 15 RCMs, each run using ERA-40 reanalysis data, is compared to the observed precipitation series from the Furnace weather station	177
Figure 6.21	Frequency bias of the model simulated data estimated on a seasonal basis for the period 1961-2000. The output from 15 RCMs, each run using ERA-40 reanalysis data, is compared to the observed precipitation series from the Furnace weather station. Nine different threshold levels are used to discretize the datasets (≥ 0.2 mm, 1 mm, 2 mm, 5 mm, 10 mm, 20 mm, 25 mm, and 30 mm). Perfect score = 1; overestimating >1 ; underestimating <1	179
Figure 6.22(a)	Seasonal ROC curves for 15 RCMs each run using ERA-40 reanalysis data. The output from 15 RCMs, each run using ERA-40 reanalysis data, is compared to the observed precipitation series from the Furnace weather station. Nine different threshold levels are used to discretize the datasets (≥ 0.2 mm, 1 mm, 2 mm, 5 mm, 10 mm, 20 mm, 25 mm, and 30 mm).....	180
Figure 6.22(b)	Area under the ROC curves shown in Figure 6.22(a). All values have been standardized on a seasonal basis	181
Figure 6.23(a)	Q-Q plots of the observed and model simulated precipitation series for winter. The output from 15 RCMs, each run using ERA-40 reanalysis data for the period 1961-2000 is compared to the observed precipitation series from the Furnace weather station. The enlarged green dots are used to highlight those values relating to the following percentiles: 25 th , 50 th , 75 th , 90 th , 95 th and 99 th	182
Figure 6.23(b)	Q-Q plots of the observed and model simulated precipitation series for summer. The output from 15 RCMs, each run using ERA-40 reanalysis data, is compared to the observed precipitation series from the Furnace weather station over the period 1961-2000. The enlarged green dots are used to highlight those values relating to the following percentiles: 25 th , 50 th , 75 th , 90 th , 95 th and 99 th	183

Figure 6.24	Schematic of the model weighting scheme. To ensure equitability when comparing all climate projections the data was collapsed based on the respective emission scenarios; thus a separate set of weights were developed for the dynamical (A1B) and statistical (A2 and B2) pathways independent of one another.....	190
Figure 6.25	Aggregated seasonal weights formulated for each of the 13 RCMs used to downscale GCM data for the period 1961-2050. The seasonal weights for each variable are shown in the top (minimum temperature), middle (maximum temperature) and bottom (precipitation) panels. Prior to plotting the weights were normalized on a seasonal basis.....	193
Figure 6.26	Observed and model simulated mean monthly precipitation receipts averaged over the 30 year control period (1961-1990). Climate scenarios from 25 model pathways (19 GCM-RCM; 6 GCM-SD) are compared to observed precipitation from the Furnace weather station	196
Figure 6.27	Smoothed empirical probability distribution functions of observed and model simulated monthly mean precipitation receipts for the control period (1961-1990). Climate scenarios from 25 model pathways (19 GCM-RCM; 6 GCM-SD) are compared to observed precipitation from the Furnace weather station.....	197
Figure 6.28	Aggregated seasonal weights formulated for each of the 17 GCM-RCMs pathways which run up until 2050. The weights are normalized on a seasonal basis for each variable	199
Figure 6.29	Aggregated seasonal weights for the dynamically downscaled temperature and precipitation scenarios. Darker/lighter shading denotes those scenarios assigned a higher/lower weighting.....	202
Figure 6.30	Aggregated seasonal weights for the statistically downscaled temperature and precipitation ensemble members. Darker/lighter shading denotes those scenarios assigned a higher/lower weighting.....	202
Figure 7.1	The projected 10-year moving average (mean) temperature for the Burrishoole catchment (1961-2100) plotted for each of the 19 ensemble members whose projections cover the period 1961-2099. Also shown is the 10 year moving average for mean temperature observed in the catchment. This is calculated using data from the Furnace weather station.....	208
Figure 7.2	The projected 10-year moving average (mean) temperature for the Burrishoole catchment estimated based on the unweighted (A1B, A2, B2 and all scenarios) and weighted ensemble average (A1B) for each SRES scenario. The plot includes the equally weighted mean ensemble calculated using all 19 ensemble members. The shaded area is used to illustrate the range in the model response to perturbed forcing. Also shown is the 10 year moving average for mean temperature observed in the catchment. This is calculated using data from the Furnace weather station.....	209
Figure 7.3	Projected changes in average monthly maximum temperature for the Burrishoole catchment. Changes are estimated relative to the 30 year control period (1961-1990) for the 2020s (top), 2050s (middle) and 2080s (bottom) respectively. The range in projected changes from the A1B model pathways are plotted using the grey bar; model projections relating to the A2 and B2 emission scenarios are plotted separately. Also shown is the equally weighted and weighted mean ensemble for the A1B ensemble members	210
Figure 7.4	Projected changes in average monthly minimum temperature for the Burrishoole catchment. Changes are estimated relative to the 30 year control period (1961-1990) for the 2020s (top), 2050s (middle) and 2080s (bottom) respectively. The range in projected changes from the A1B model pathways are plotted using the grey bar; model projections relating to the A2 and B2 emission scenarios are plotted separately. Also shown is the equally weighted and weighted mean ensemble for the A1B ensemble members	212
Figure 7.5	Projected changes in the 90th and 95th percentile of summer and winter temperature (minimum and maximum)	213
Figure 7.6	Projected changes in average monthly precipitation receipts for the Burrishoole catchment. Changes are estimated relative to the 30 year control period (1961-1990) for the 2020s (top), 2050s (middle) and 2080s (bottom) respectively. The range in projected changes from the A1B model pathways are plotted using the grey bar; model projections relating to the A2 and B2 emission scenarios are plotted separately. Also shown is the equally weighted and weighted mean ensemble for the A1B ensemble members	216
Figure 7.7(a)	Projected changes in the 20 th , 40 th , 50 th , 60 th , 80 th , 90 th and 95 th percentiles of winter rainfall amounts. A wet day threshold of ≥ 2 mm is used.....	218
Figure 7.7(b)	Projected changes in the 20 th , 40 th , 50 th , 60 th , 80 th , 90 th and 95 th percentiles of summer rainfall amounts. A wet day threshold of ≥ 2 mm is used.....	219

Figure 7.8	Projected changes in the seasonal variance of rainfall amounts (≥ 2 mm) for the Burrishoole catchment.....	220
Figure 7.9	Smoothed probability distribution functions (PDFs) constructed using downscaled temperature (maximum) projections for the Burrishoole catchment. The PDFs for each ensemble member and shown (grey) along with the weighted mean ensemble PDF for each emission scenario (A1B, A2 and B2). The weighting scheme used is discussed in Chapter six. Also shown is the smoothed PDF of observed maximum temperature for the period 1961-1990. The PDFs for summer and winter only are shown.....	222
Figure 7.10	Smoothed probability distribution functions (PDFs) constructed using downscaled temperature (minimum) projections for the Burrishoole catchment. The PDFs for each ensemble member and shown (grey) along with the weighted ensemble mean PDF for each emission scenario (A1B, A2 and B2). The weighting scheme used is discussed in Chapter six. Also shown is the smoothed PDF of observed maximum temperature for the period 1961-1990. The PDFs for summer and winter only are shown.....	223
Figure 7.11	Empirical cumulative distribution functions (ECDFs) constructed using downscaled temperature (maximum) projections for the Burrishoole catchment. The ECDFs for each ensemble member and shown (grey) along with the weighted ensemble mean ECDF for each emission scenario (A1B, A2 and B2). The weighting scheme used is discussed in Chapter six. Also shown is the ECDF of observed maximum temperature for the period 1961-1990. The ECDFs for summer and winter only are shown	224
Figure 7.12	Empirical cumulative distribution functions (ECDFs) constructed using downscaled temperature (minimum) projections for the Burrishoole catchment. The ECDFs for each ensemble member and shown (grey) along with the weighted ensemble mean ECDF for each emission scenario (A1B, A2 and B2). The weighting scheme used is discussed in Chapter six. Also shown is the ECDF of observed maximum temperature for the period 1961-1990. The ECDFs for summer and winter only are shown	225
Figure 7.13	Smoothed probability distribution functions (PDFs) constructed using downscaled temperature (maximum) projections for the Burrishoole catchment. The PDFs for each ensemble member and shown (grey) along with the weighted ensemble mean PDF for each emission scenario (A1B, A2 and B2). The weighting scheme used is discussed in Chapter six. The equally weighted PDF for each emission scenario (A1B, A2 and B2) is also shown	226
Figure 7.14	Projected changes in temperature and precipitation for each respective model pathway. The plot illustrates the individual response of each model pathway to prescribed anthropogenic forcings.....	229
Figure 7.15	Bivariate probability density functions representing the multi-model response to future climate forcing. The contour plots overlay the response of individual model pathways (+). In this case each of the twenty five ensemble members is considered, and each is given an equal weighting when calculating the overall ensemble response	230
Figure 7.16	Bivariate probability density functions representing the response of the multi-model ensemble to future climate forcing. The contour plots overlay the response of individual model pathways (+). In this case the A1B ensemble members are considered. The weighting scheme discussed in Chapter 6 is used to weight the ensemble response	231
Figure 7.17	Bivariate probability density functions representing the response of the multi-model ensemble to future climate forcing. The contour plots overlay the response of individual model pathways (+). In this case the ensemble members relating to the A1B emission scenarios are considered - each is given an equal weighting when calculating the overall response	232
Figure 9.1	Quantile mapping applied to a synthetic dataset. Panels (a) and (b) show the respective differences in the probability distribution functions for each dataset. Shown in panel (c) are the equivalent cumulative distribution functions (cdfs) of the data shown in panels (a) and (b). Panel (d) illustrates how well the cdf of the corrected Y dataset conforms to the cdf of the X dataset. Panels (e) and (d) show the adjustment brought about by applying the correction.....	280
Figure 9.2	Percent bias in the mean of the corrected and non-corrected downscaled precipitation data. Quantile mapping is applied on a monthly basis	281
Figure 9.3	Percent bias in the variance of the corrected and non-corrected downscaled precipitation data. Quantile mapping is applied on a monthly basis	282
Figure 9.4	HBV-light model structure (Source: Siebert, 2000).....	289
Figure 9.5	TOPMODEL: model structure (Source: Lin <i>et al.</i> , 2010).....	291

Figure 9.6	HYSIM: model structure (Source: Manley, 2006).....	294
Figure 9.7	Results of the regional sensitivity analysis (RSA) conducted for the nine process parameters used in HBV-light. Parameter sensitivity is expressed by the accumulated distribution functions formulated using the Nash Sutcliffe (NS) efficiency scores returned for individual parameter sets (y-axis). Parameters are classified as behavioural if they attain a NS score of ≥ 0.7	296
Figure 9.8	Results of the regional sensitivity analysis (RSA) conducted for TOPMODEL. Both Sr0 and qs0 are initialization parameters. Parameter sensitivity is expressed by the accumulated distribution functions formulated using the Nash Sutcliffe (NS) efficiency scores returned for individual parameter sets (y-axis). Parameters are classified as behavioural if attaining a score ≥ 0.7	297
Figure 9.9	Results of the regional sensitivity analysis (RSA) conducted for HYSIM. Parameter sensitivity is expressed by the accumulated distribution functions formulated using the Nash Sutcliffe (NS) efficiency scores returned for individual parameter sets (y-axis). Parameters are classified as behavioural if attaining a NS score ≥ 0.7	298
Figure 9.10	Steps involved in the application of the Generalized Likelihood Uncertainty Estimation (GLUE) method of Beven and Binley (1992).....	300
Figure 9.11	Schematic of the Monte Carlo sampling procedure used to formulate the posterior distribution for the selected flow statistic (Q50, Q05 or Q95).....	307
Figure 9.12(a)	Shown in the top panel is the median and 90% confidence interval derived from the multimodel simulation for the Glenamong catchment (Aug 2006 to April 2007; 200 days); also shown are the observed data points for the same time period. The observed precipitation is shown in the lower panel.....	313
Figure 9.12(b)	Shown in the top and lower panels is the median and 90% confidence interval (Aug 2006 to April 2007; 200 days) for the Glenamong catchment simulated using HBV and HYSIM respectively. Also shown are the observed data points for the same time period.....	314
Figure 9.12(c)	Shown in the top panel is the median and 90% confidence interval (Aug 2006 to April 2007; 200 days) for the Glenamong catchment simulated using TOPMODEL. Shown in the lower panel is the median series estimated for each CRR model (HBV, HYSIM and TOPMODEL). Also plotted are the median series and 90% confidence interval for the multimodel simulation	315
Figure 9.13	Observed and model simulated monthly mean (upper panel) and variance (lower panel) flow values for the Glenamong catchment plotted along with the median and 90% confidence interval for each CRR model (HBV, HYSIM and TOPMODEL). Also plotted are the median and 90% confidence interval for the multimodel simulation	317
Figure 9.14	Q-Q plots of observed versus simulated flow values for the Glenamong catchment. The median series for each CRR model (HBV, HYSIM and TOPMODEL), as well as the multimodel simulation, is plotted. The green dots are used to highlight those flow values relating to the following percentiles: 20 th , 40 th , 50 th , 60 th , 80 th , 90 th and 95 th	317
Figure 9.15(a)	Shown in the top panel is the median and 90% confidence interval derived from the multimodel simulation for the Srahrevagh catchment (June 2006 to January 2007; 300 days); also shown are the observed data points for the same time period. The observed precipitation is shown in the lower panel.....	321
Figure 9.15(b)	The median series derived for each CRR model (HBV, HYSIM and TOPMODEL) plotted over the median and 90% confidence interval from the multimodel simulation (June 2006 to January 2007; 300 day). Also shown are the observed data points for the same period	322
Figure 9.16	Observed and model simulated monthly mean (upper panel) and variance (lower panel) flow values for the Srahrevagh catchment plotted along with the median and 90% confidence interval for each CRR model (HBV, HYSIM and TOPMODEL). Also plotted are the median and 90% confidence interval for the multimodel simulation	323
Figure 9.17	Q-Q plots of observed versus simulated flow for the Srahrevagh catchment. The median series for each CRR model (HBV, HYSIM and TOPMODEL), as well as the multimodel simulation, is plotted. The green dots are used to highlight those flow values relating to the following percentiles: 25 th , 50 th , 75 th , 90 th , 95 th and 99 th	324
Figure 9.18	Average width of the 90% prediction interval (PI) simulated using the retained behavioral parameter sets for each of the three CRR (HBV, HYSIM and TOPMODEL); also shown in the average width of the 90% PI for the multimodel simulation. The PI is shown as a percentage of the mean monthly flow value calculated using the median simulation for that period.....	326

Figure 9.19	Percentage change in the Q50 flow statistic for the Glenamong catchment calculated relative to the 30 year control (1961-1990) period for the 2020s (top), 2050s (middle) and 2080s (bottom) respectively. The range in projected changes from the A1B model pathways are plotted using the grey bar; model projections relating to the A2 and B2 emission scenarios are plotted separately. Also shown is the weighted mean ensemble for the A1B ensemble members 333
Figure 9.20	Monthly boxplots of the percent change in the Q50 median flow statistic for the Glenamong catchment. Changes are estimated relative to the 30 year control (1961-1990) period for the 2020s (top), 2050s (middle) and 2080s (bottom) respectively. The plots are formulated based on the posterior distribution of the Monte Carlo simulation conducted for the A1B based climate scenarios. On each box the central mark represents the median, the edges represent the 25 th and 75 th percentiles and the whiskers represent the 90% confidence interval..... 334
Figure 9.21	Monthly boxplots of the percent change in the Q50 median flow statistic for the Glenamong catchment. Changes are estimated relative to the 30 year control (1961-1990) period for the 2020s (left), 2050s (middle) and 2080s (right) respectively. The plots are formulated based on the posterior distribution of the Monte Carlo simulation conducted for the A2 (top), B2 (middle) and A2/B2 based climate scenarios (bottom). On each box the central mark represents the median; the edges represent the 25 th and 75 th percentiles and the whiskers represent the 90% confidence interval..... 335
Figure 9.22	Percentage change in the Q05 flow statistic for the Glenamong catchment calculated relative to the 30 year control (1961-1990) period for the 2020s (top), 2050s (middle) and 2080s (bottom) respectively. The range in projected changes from the A1B model pathways are plotted using the grey bar; model projections relating to the A2 and B2 emission scenarios are plotted separately. Also shown is the weighted mean ensemble for the A1B ensemble members 337
Figure 9.23	Monthly boxplots of the percent change in the Q05 median flow statistic for the Glenamong catchment. Changes are estimated relative to the 30 year control (1961-1990) period for the 2020s (top), 2050s (middle) and 2080s (bottom) respectively. The plots are formulated based on the posterior distribution of the Monte Carlo simulation conducted for the A1B based climate scenarios. On each box the central mark represents the median, the edges represent the 25 th and 75 th percentiles and the whiskers represent the 90% confidence interval..... 338
Figure 9.24	Monthly boxplots of the percent change in the Q05 median flow statistic for the Glenamong catchment. Changes are estimated relative to the 30 year control (1961-1990) period for the 2020s (left), 2050s (middle) and 2080s (right) respectively. The plots are formulated based on the posterior distribution of the Monte Carlo simulation conducted for the A2 (top), B2 (middle) and A2/B2 based climate scenarios (bottom). On each box the central mark represents the median; the edges represent the 25 th and 75 th percentiles and the whiskers represent the 90% confidence interval 339
Figure 9.25	Percentage change in the Q95 flow statistic for the Glenamong catchment calculated relative to the 30 year control (1961-1990) period for the 2020s (top), 2050s (middle) and 2080s (bottom) respectively. The range in projected changes from the A1B model pathways are plotted using the grey bar; model projections relating to the A2 and B2 emission scenarios are plotted separately. Also shown is the weighted mean ensemble for the A1B ensemble members 341
Figure 9.26	Monthly boxplots of the percent change in the Q95 median flow statistic for the Glenamong catchment. Changes are estimated relative to the 30 year control (1961-1990) period for the 2020s (top), 2050s (middle) and 2080s (bottom) respectively. The plots are formulated based on the posterior distribution of the Monte Carlo simulation conducted for the A1B based climate scenarios. On each box the central mark represents the median, the edges represent the 25 th and 75 th percentiles and the whiskers represent the 90% confidence interval..... 342
Figure 9.27	Monthly boxplots of the percent change in the Q95 median flow statistic for the Glenamong catchment. Changes are estimated relative to the 30 year control (1961-1990) period for the 2020s (left), 2050s (middle) and 2080s (right) respectively. The plots are formulated based on the posterior distribution of the Monte Carlo simulation conducted for the A2 (top), B2 (middle) and A2/B2 based climate scenarios (bottom). On each box the central mark represents the median; the edges represent the 25 th and 75 th percentiles and the whiskers represent the 90% confidence interval..... 343
Figure 9.28	Monthly boxplots of the percent change in the Q50 median flow statistic for the Srahrevagh catchment. Changes are estimated relative to the 30 year control (1961-1990) period for the 2020s (top), 2050s (middle) and 2080s (bottom) respectively. The plots are formulated based on the posterior distribution of the Monte Carlo simulation conducted for the A1B based climate scenarios. On each box the central mark represents the median, the edges represent the 25 th and 75 th percentiles and the whiskers represent the 90% confidence interval..... 345

Figure 9.29	Monthly boxplots of the percent change in the Q50 median flow statistic for the Srahrevagh catchment. Changes are estimated relative to the 30 year control (1961-1990) period for the 2020s (left), 2050s (middle) and 2080s (right) respectively. The plots are formulated based on the posterior distribution of the Monte Carlo simulation conducted for the A2 (top), B2 (middle) and A2/B2 based climate scenarios (bottom). On each box the central mark represents the median; the edges represent the 25 th and 75 th percentiles and the whiskers represent the 90% confidence interval	346
Figure 9.30	Monthly boxplots of the percent change in the Q05 median flow statistic for the Srahrevagh catchment. Changes are estimated relative to the 30 year control (1961-1990) period for the 2020s (top), 2050s (middle) and 2080s (bottom) respectively. The plots are formulated based on the posterior distribution of the Monte Carlo simulation conducted for the A1B based climate scenarios. On each box the central mark represents the median, the edges represent the 25 th and 75 th percentiles and the whiskers represent the 90% confidence interval.....	347
Figure 9.31	Monthly boxplots of the percent change in the Q05 median flow statistic for the Srahrevagh catchment. Changes are estimated relative to the 30 year control (1961-1990) period for the 2020s (left), 2050s (middle) and 2080s (right) respectively. The plots are formulated based on the posterior distribution of the Monte Carlo simulation conducted for the A2 (top), B2 (middle) and A2/B2 based climate scenarios (bottom). On each box the central mark represents the median; the edges represent the 25 th and 75 th percentiles and the whiskers represent the 90% confidence interval.	348
Figure 9.32	Monthly boxplots of the percent change in the Q95 median flow statistic for the Srahrevagh catchment. Changes are estimated relative to the 30 year control (1961-1990) period for the 2020s (top), 2050s (middle) and 2080s (bottom) respectively. The plots are formulated based on the posterior distribution of the Monte Carlo simulation conducted for the A1B based climate scenarios. On each box the central mark represents the median, the edges represent the 25 th and 75 th percentiles and the whiskers represent the 90% confidence interval.....	350
Figure 9.33	Monthly boxplots of the percent change in the Q95 median flow statistic for the Srahrevagh catchment. Changes are estimated relative to the 30 year control (1961-1990) period for the 2020s (left), 2050s (middle) and 2080s (right) respectively. The plots are formulated based on the posterior distribution of the Monte Carlo simulation conducted for the A2 (top), B2 (middle) and A2/B2 based climate scenarios (bottom). On each box the central mark represents the median; the edges represent the 25 th and 75 th percentiles and the whiskers represent the 90% confidence interval.	351
Figure 10.1	Schematic illustrating the interaction between those abiotic factors known to affect salmon and trout parr (Source: Armstrong <i>et al.</i> , 2003).....	355
Figure 10.2	The significance which different components of the hydrograph have for freshwater ecosystems and salmonid species (Source: Poff <i>et al.</i> , 1997).....	357
Figure 10.3	Idealized trapezoidal shape used to model the hydraulics of study reaches.....	378
Figure 10.4	Aerial photograph of the Glenamong study reach	380
Figure 10.5	Aerial photograph of the Srahrevagh study reach.....	380
Figure III-1	Dotty plots for the HBV-light model constructed using 10,000 sampled parameters sets. The Nash Sutcliffe (NS) efficiency criterion is used (y-axis). The red square denotes the parameter value with the highest NS score.....	XIII
Figure III-2	Dotty plots for the TOPMODEL model constructed using 10,000 sampled parameters sets. The Nash Sutcliffe (NS) efficiency criterion is used (y-axis). The red square denotes the parameter value with the highest NS score.....	XIV
Figure III-3	Dotty plots for the HYSIM model constructed using 10,000 sampled parameters sets. The Nash Sutcliffe (NS) efficiency criterion is used (y-axis). The red square denotes the parameter value with the highest NS score.....	XV

List of Tables

Table 3.1	Physical attributes of the five constituent sub-catchments of the greater Burrishoole system (Figure 3.2). Also listed are the physical properties of the Glendahurk catchment.....	65
Table 3.2	Datasets from the Furnace weather station.....	66
Table 3.3	Datasets from the Burrishoole catchment’s upland rain gauge network. The record length and the proportion of missing values for each gauge is shown.....	68
Table 3.4	Streamflow records from the Burrishoole catchment. The length of the record provided by each recorder and the proportion of missing values is shown	69
Table 5.1	Summary of the relative strengths and weaknesses of statistical and dynamical approaches to downscaling (adapted from Wilby & Wigley, 1997).....	121
Table 6.1	Candidate (NCEP and GCM) predictor variables available from the UKSDSM data archive. Note: Italics indicate secondary airflow indices calculated from pressure fields (surface, 500 and 850 hPa).....	131
Table 6.2	Predictors used to downscale daily minimum and maximum temperature. Also shown is the explained variance (%) for the calibration (1961–1978; 1994–2000) and independent validation (1979-1993) periods.....	137
Table 6.3	Percent bias for selected statistics calculated over the independent validation period (1979-1993) on a monthly basis for maximum and minimum temperature respectively; also shown is the coefficient of determination. The temperature series are downscaled from NCEP reanalysis data and compared to observations from the Furnace weather station (Figure 3.2)	138
Table 6.4	Predictors used to downscale precipitation for each season	144
Table 6.5	Explained variance (%) for the calibration (1961-1978; 1994-2000) and validation (1979-1993) periods estimated on a seasonal basis. The explained variance is calculated for the linear component of SDSM (i.e. with the variance inflation disabled) and the GLM amounts model respectively. Prior to estimating the explained variance a fourth root transformation is applied to the modelled and observed precipitation data. Also shown is the HSS for the GLM occurrence model. Due to the stochastic modelling of wet days the HSS was not calculated for SDSM	146
Table 6.6	Explained variance (%) calculated on a seasonal basis for the calibration (1961-1978; 1994-2000) and validation (1979-1993) period respectively. Wind speed is downscaled to the Belmullet synoptic station using NCEP reanalysis data. The explained variance is calculated for the linear component of SDSM (i.e. with the variance inflation disabled) and the GLM respectively.....	153
Table 6.7	Explained variance (%) calculated on a seasonal basis for the calibration (1961-1978; 1994-2000) and validation (1979-1993) periods. Relative humidity is downscaled to the Belmullet synoptic station using NCEP reanalysis data. The explained variance is calculated for the linear component of SDSM (i.e. with the variance inflation disabled).....	153
Table 6.8	Explained variance (%) calculated on a seasonal basis for the calibration (1981-1988; 1995-2000) and validation (1989-1993) periods respectively. The explained variance is calculated for the linear component of SDSM. Solar radiation is downscaled to the Belmullet synoptic station using NCEP reanalysis data and point-scale temperature records	154
Table 6.9	Explained variance (%) calculated on a seasonal basis for the calibration (1971-1981) and validation (1982-1987) periods respectively. The explained variance is calculated for the linear component of SDSM. Potential evaporation is downscaled to the Belmullet synoptic station using NCEP reanalysis data and point-scale temperature records	154
Table 6.10	Institutions, model names and abbreviations of the ENSEMBLES RCM simulations used in this study. The Hadley Centre contributed a perturbed physics ensemble consisting of three different RCM simulations, each of which was tuned to have a different climate sensitivity: standard (HC-Q0), low (HC-Q3) and high (HC-Q16). The RPN (GEMLAM) and CHMI (ALADIN) institutes did not use their RCMs to downscale GCM data.....	155
Table 6.11	Institutions, model names and abbreviations of the GCMs used as boundary conditions for the ENSEMBLES RCM simulations. The Hadley Centre contributed a perturbed physics ensemble consisting of three different versions of the HadCM3, each of which was tuned to have a different climate sensitivity: standard (HC-Q0), low (HC-Q3) and high (HC-Q16).....	156
Table 6.12	Metrics used to evaluate model performance	162

Table 6.13	Results for continuous evaluation metrics (mean absolute error (MAE), the standard deviation of the error (STD Error), bias and Pearson's r) estimated seasonally. The output from 15 RCMs, each run using ERA-40 reanalysis data for the period 1961-2000, is compared to the observed precipitation series from the Furnace weather station. A fourth root transformation is used prior to estimating the skill scores.....	184
Table 6.14	GCM weights (Déqué & Somot, 2010)	194
Table 6.15	The 17 GCM-RCMs pathways which run up until 2050 ranked (highest to lowest) according to their assigned weighting - the weights are averaged across seasons. The pathways are colour coded according to the driving GCM used.....	200
Table 7.1	The daily probability of precipitation estimated for different event thresholds (5 mm, 10 mm, 20 mm, 30 mm); probabilities are calculated using wet days only (≥ 2 mm). The weighted and equally weighted mean ensemble for winter and summer is shown. Daily probabilities for the observed series are also shown (1961-1990).....	227
Table 7.2	Model projected changes in wind speed, relative humidity and potential evaporation. Scenarios for each variable are statistically downscaled from three GCMs (HadCM3, CSIROmk2 and CGCM2) each run using both the A2 and B2 emission scenario. Both SDSM and a generalized linear model (GLM) were employed to downscale wind speed. The table is colour coded to highlight increases/decreases.....	234
Table 8.1	Methods for addressing uncertainty in hydrological modelling studies (Source: Montanari, 2011). AMALGAM, a multialgorithm genetically adaptive method for multiobjective optimization; BATEA, Bayesian total error analysis; BFS, Bayesian forecasting system; BMA, Bayesian multimodel analysis; DYNIA, dynamic identifiability analysis; GLUE, generalized likelihood uncertainty estimation; IBUNE, integrated Bayesian uncertainty estimator; MOSCEM-UA, multiobjective shuffled complex evolution University of Arizona; SCE-UA, shuffled complex evolution university of Arizona.....	253
Table 9.1	HBV-light: model parameters and sampling ranges	289
Table 9.2	TOPMODEL: model parameters and sampling ranges	291
Table 9.3	HYSIM: model parameters and sampling ranges	294
Table 9.4	Results of the Kolmogorov–Smirnov test (significance level 0.05) used to quantify differences between the accumulated distribution functions of the behavioural and non-behavioural parameter sets for the HBV-light model. Differences are highlighted as being significant if underlined.....	297
Table 9.5	Results of the Kolmogorov–Smirnov test (significance level 0.05) used to quantify differences between the accumulated distribution functions of the behavioural and non-behavioural parameter sets for TOPMODEL. Differences are highlighted as being significant if underlined	298
Table 9.6	Results of the Kolmogorov–Smirnov test (significance level 0.05) used to quantify differences between the accumulated distribution functions of the behavioural and non-behavioural parameter sets for HYSIM. Differences are highlighted as being significant if underlined.....	298
Table 9.7	The number of Monte Carlo simulations conducted for each emission scenario. The MC simulation is used to estimate the posterior distribution of the selected flow indices over each successive horizon (2020s, 2050s and 2080s). The numbers of simulations is altered according to the number of climate pathways considered	309
Table 9.8	Efficiency scores for the Glenamong catchment returned by the 100 behavioural parameter sets retained for each CRR model estimated over the calibration and validation periods respectively	310
Table 9.9	Efficiency scores for the Glenamong catchment returned by the median series for each CRR model as well as the median of the multimodel simulation. The efficiency scores are estimated for the calibration and validation period respectively.....	311
Table 9.10	Efficiency scores for the Srahrevagh catchment returned by the 100 behavioural parameter sets retained for each CRR model estimated over the calibration and validation periods respectively	319
Table 9.11	Efficiency scores for the Shrevagh catchment returned by the median series for each CRR model as well as the median of the multimodel simulation. The efficiency scores are estimated for the calibration and validation period respectively.....	320

Table 9.12	Projected changes (%) in mean flow for the 2080s horizon (2070-2099) relative to the 30 year control period (1961-1990). Changes in flow are estimated for the Glenamong catchment. The range in projected mean monthly and seasonal flow for each uncertainty component is shown. The range is taken as the difference in the projected flow suggested when each component in the uncertainty chain is altered whilst the others are held constant. The cells are colour coded to highlight higher/lower values.....	329
Table 10.1	Dimensions of the 50 m Glenamong and Srahrevagh study reaches.....	378
Table 10.2	Ideal minimum values of discharge per metre width (q) for adult Atlantic salmon (Source: Stewart, 1969).....	382
Table 10.3	Ideal minimum flow depth and velocity values for juvenile Atlantic salmon (Hendry & Cragg-Hine, 1997)	383
Table 10.4	Results of the Reliability, Resilience and Vulnerability (RRV) analysis for the Glenamong and Srahrevagh catchments. The analysis is conducted for three flow statistics representing median (Q50), low (Q95) and high flows (Q05); four different time periods including the control (1961-1990), 2020s (2010-2039), 2050s (2040-2069) and 2080s (2070-2099) are considered in the analysis. The results represent the median of the posterior distribution estimated using the MC simulation approach discussed in section 9.3.2. The ensemble weighting scheme outlined in chapter six was used when estimating changes in the RRV criteria.....	385
Table 10.5	Results of the habitat modelling conducted using the hydraulic parameters outlined for each life stage. 10.5(i) Percentage of time that flow corresponding to the minimum ideal discharge per metre width (q) is exceeded. 10.5(ii) Percentage of time that flow corresponding to the minimum ideal water depth and Froude number is exceeded. 10.5(iii) Percentage of time that flow corresponding to the minimum ideal water depth and velocity is exceeded. Four different time periods including the control, 2020s, 2050s and 2080s are considered. The results represent the median of the posterior distribution estimated using the MC sampling approach discussed in section 9.3.2. The ensemble weighting scheme outlined in chapter six was used when estimating changes in each parameter	387
Table I-1	Projected changes in mean monthly and seasonal maximum temperature for the Burrishoole catchment calculated over the 2020s horizon (2010-2039) relative to the 30 year control period. (1961-1990). The table is colour coded to highlight increases/decreases.....	II
Table I-2	Projected changes in mean monthly and seasonal maximum temperature for the Burrishoole catchment calculated over the 2050s horizon (2040-2069) relative to the 30 year control period. (1961-1990). The table is colour coded to highlight increases/decreases.....	III
Table I-3	Projected changes in mean monthly and seasonal maximum temperature for the Burrishoole catchment calculated over the 2080s horizon (2070-2099) relative to the 30 year control period. (1961-1990). The table is colour coded to highlight increases/decreases.....	IV
Table I-4	Projected changes in mean monthly and seasonal minimum temperature for the Burrishoole catchment calculated over the 2020s horizon (2010-2039) relative to the 30 year control period. (1961-1990). The table is colour coded to highlight increases/decreases.....	V
Table I-5	Projected changes in mean monthly and seasonal minimum temperature for the Burrishoole catchment calculated over the 2050s horizon (2040-2069) relative to the 30 year control period. (1961-1990). The table is colour coded to highlight increases/decreases.....	VI
Table I-6	Projected changes in mean monthly and seasonal minimum temperature for the Burrishoole catchment calculated over the 2080s horizon (2070-2099) relative to the 30 year control period. (1961-1990). The table is colour coded to highlight increases/decreases.....	VII
Table II-2	Projected changes (%) in mean monthly and seasonal precipitation receipts for the Burrishoole catchment calculated over the 2020s horizon (2010-2039) relative to the 30 year control period. (1961-1990). The table is colour coded to highlight increases/decreases.....	IX
Table II-1	Projected changes (%) in mean monthly and seasonal precipitation receipts for the Burrishoole catchment calculated over the 2050s horizon (2040-2069) relative to the 30 year control period. (1961-1990). The table is colour coded to highlight increases/decreases.....	X
Table II-3	Projected changes (%) in mean monthly and seasonal precipitation receipts for the Burrishoole catchment calculated over the 2080s horizon (2070-2099) relative to the 30 year control period. (1961-1990). The table is colour coded to highlight increases/decreases.....	XI

Table IV-15	Projected changes (%) in the Q05 low flow statistics calculated on a monthly and seasonal basis for the Shrevagh catchment. Changes are estimated for the 2080s horizon (2070-2099) relative to the 30 year control period. (1961-1990). Projected changes in Q05 are estimated using the median series from the multimodel simulation. The table is colour coded to highlight increases/decreases.....XXXI	
Table IV-16	Projected changes (%) in the Q95 low flow statistics calculated on a monthly and seasonal basis for the Shrevagh catchment. Changes are estimated for the 2020s horizon (2010-2039) relative to the 30 year control period. (1961-1990). Projected changes in Q95 are estimated using the median series from the multimodel simulation. The table is colour coded to highlight increases/decreases..... XXXII	
Table IV-17	Projected changes (%) in the Q95 low flow statistics calculated on a monthly and seasonal basis for the Shrevagh catchment. Changes are estimated for the 2050s horizon (2040-2069) relative to the 30 year control period. (1961-1990). Projected changes in Q95 are estimated using the median series from the multimodel simulation. The table is colour coded to highlight increases/decreases.....XXXIII	
Table IV-18	Projected changes (%) in the Q95 low flow statistics calculated on a monthly and seasonal basis for the Shrevagh catchment. Changes are estimated for the 2080s horizon (2070-2099) relative to the 30 year control period. (1961-1990). Projected changes in Q95 are estimated using the median series from the multimodel simulation. The table is colour coded to highlight increases/decreases.....XXXIV	
Table V-1	The projected reliability of median (Q50), low (Q95) and high (Q05) flows estimated on an annual basis for the Glenamong and Srahrevagh catchments respectively. Each statistic is calculated for three future time horizons (2020s, 2050s and 2080s) relative to the 30 year control period (1961-1990). Projected changes in each statistic are estimated using the median series from the multimodel simulation. The table is colour coded to highlight differences in the results from individual climate scenarios..... XXXVI	
Table V-2	The projected resilience of median (Q50), low (Q95) and high (Q05) flows estimated on an annual basis for the Glenamong and Srahrevagh catchments respectively. Each statistic is calculated for three future time horizons (2020s, 2050s and 2080s) relative to the 30 year control period (1961-1990). Projected changes in each statistic are estimated using the median series from the multimodel simulation. The table is colour coded to highlight differences in the results from individual climate scenarios.....XXXVII	
Table V-3	The projected vulnerability of median (Q50), low (Q95) and high (Q05) flows estimated on an annual basis for the Glenamong and Srahrevagh catchments respectively. Each statistic is calculated for three future time horizons (2020s, 2050s and 2080s) relative to the 30 year control period (1961-1990). Projected changes in each statistic are estimated using the median series from the multimodel simulation. The table is colour coded to highlight differences in the results from individual climate scenarios..... XXXVIII	

Chapter 1

Introduction

1.1 Research Background

Climate change is considered one of the most complex and important environmental issues currently facing the global community. It poses a major challenge to human society and threatens to undermine the functioning of terrestrial and aquatic ecosystems, with resultant consequences for biodiversity, species distribution and community structures (Walther *et al.*, 2002; Thomas *et al.*, 2004; Hare, 2006; Warren *et al.*, 2010). Indeed there is a growing body of evidence which suggests that recent climate change has affected a wide range of species with diverse life-strategies and geographic profiles (Hughes, 2000; Wuethrich, 2000; McCarthy, 2001; Walther *et al.*, 2002; Parmesan & Yohe, 2003). According to Parmesan (2006:2) “the direct impacts of anthropogenic climate change have been documented on every continent, in every ocean, and in most major taxonomic groups”.

The latest report released by the Intergovernmental Panel on Climate Change (IPCC, 2007a) states with “very high confidence” (90% probability) that since the beginning of the industrial era (circa. 1750) the globally averaged effect of human activity on the Earth’s energy balance has been one of warming. The report states that, relative to pre-industrial levels (1750), a net increase of +1.6 (with a +0.6 to +2.4 90% confidence range) Wm^{-2} in the planet’s radiative forcing has occurred (IPCC, 2007a). Such changes in the planetary energy balance translate into an increase in the globally averaged surface air temperature which, according to the Goddard Institute for Space Studies (GISS), have increased over the period 1880 to 2010 by an average of 0.8°C (Hansen *et al.*, 2010). In addition, it is estimated that the rate at which warming has occurred since the beginning of the industrial era has been unprecedented in more than 10,000 years (IPCC, 2007a). The observed changes in the Earth’s radiative balance are attributed to rising concentrations of atmospheric greenhouse gases (GHGs) which, along with positive feedbacks initiated in the system (e.g. increases in atmospheric water vapour (Solomon *et al.*, 2010)), have had the effect of enhancing the Earth’s natural greenhouse effect. This has occurred despite human (e.g. the release of aerosols such as sulphate,

organic carbon, black carbon) and natural forcings (e.g. volcanic activity) exerting a cooling influence on the planet (IPCC, 2007a).

Importantly for this study freshwater ecosystems are highlighted as being particularly vulnerable to changes in climate, not least because they are already heavily degraded by human activity, but also because of their geographically fragmented nature and the associated lack of thermal refugia for more sensitive species. Given their sensitivity to changes in climate, it is suggested that freshwaters act as 'sentinel systems', providing an insight into the possible biological, chemical and physical responses of other ecological systems to changes in climate (Adrian *et al.*, 2009; Woodward *et al.*, 2010). With respect to freshwaters, recent climate change is manifest primarily through alterations in the thermal regime of river and lake systems - changes in which reflect warming trends evident in global and regional surface air temperatures. Changes in climate have also been detected through the response of various biological indicators; this includes alterations in the phenology of some aquatic biota and changes in the distributional range of more mobile species. Whilst the majority of impact studies have focused on temperature as the key driver of change in lotic ecosystems, owing to its influence on water quality, food abundance and the availability of physical habitat, as well as its role in providing refuge, migratory cues and connectivity across freshwater systems, hydrology is as important as water temperature for determining the ecological status of river systems and their long-term capacity to sustain populations of some freshwater and anadromous fish species - including Atlantic salmon (*Salmo salar*).

This study seeks to contribute to the existing scientific discourse concerning the potential impacts of climate change on the freshwater habitat of Atlantic salmon. The study focuses on the Burrishoole catchment - a relatively small but productive catchment system (~90 km²) located on Ireland's west coast. In recent decades there has been an observed progressive decline in the population numbers of this ecologically important and environmentally sensitive species in many of Ireland's waterways (Stefansson *et al.*, 2003; Peyronnet *et al.*, 2007). Given that populations are subject a wide range of anthropogenic stressors, and that their natural environment has already been significantly degraded, it is important that the potential future impacts of climate change on this species are investigated.

Although climate change is anticipated to affect all aspects of riverine ecosystems, this study focuses on how changes in key climate variables are likely to impact the hydrological regime of the study catchment. Projected changes in patterns of flow

behaviour and the nature of extreme events are examined with respect to the habitat requirements of Atlantic salmon at critical stages in their life cycle. The study findings should offer some insight into how climate change may affect those catchment systems located on Ireland's west coast - many of which are similar in nature to the Burrishoole. In addition, the study should provide an empirical contribution to how catchment management and fish stocking strategies are formulated, whereby in order to guard against further population declines, a strong emphasis will need to be placed on mitigating the most deleterious effects of climate change on the freshwater environment.

1.2 The intensification of the natural greenhouse effect

The link between rising concentrations of atmospheric GHGs, alterations in the global radiative balance and changes in the climate system are framed by the Earth's natural greenhouse effect. Without a certain naturally occurring concentration of GHGs in the atmosphere, the Earth would be too cold to sustain life. GHGs such as carbon dioxide (CO₂), methane (CH₄), nitrous oxide (N₂O) and water vapor (H₂O) absorb and subsequently radiate long-wave energy emitted by the Earth's surface - thereby heating the planet's surface and atmosphere.

If the Earth's radiative balance is perturbed, the global surface temperature will respond in order to adjust to a new equilibrium state. An externally imposed energy imbalance in the system, either natural or anthropogenic in origin, is termed radiative forcing; the relationship between alterations in this forcing and changes in the equilibrium surface temperature (ΔT_s) is given by:

$$\Delta T_s = \lambda \Delta F$$

where ΔF is the radiative forcing and λ is the climate sensitivity K/(W/m⁻²). This parameter is a measure of how responsive the climate system is to a change in forcing.

In addition to changes in land-use and the intensification of agricultural practices, the release of carbon dioxide through the mass combustion of fossil fuels has led to the observed increases in atmospheric GHGs - whose levels currently far exceed those of the pre-industrial era (IPCC, 2007a). The IPCC (2007a) states that enhanced atmospheric concentrations of CO₂ are the single largest contributing factor to the overall increase experienced in the Earth's radiative forcing (Figure 1.1). Fossil fuels

such as natural gas, petroleum and coal - representing vast geological deposits of decomposed organic material rich in hydrocarbons - when burned produce carbon dioxide. The historical and continued reliance of industrialized nations on fossil fuels as a cheap energy resource has meant that carbon dioxide and other GHGs have been emitted in quantities which far exceed the natural rate of uptake by terrestrial and aquatic systems (le Quéré *et al.*, 2009). If the current rate of GHG emissions continue, it could potentially lead to a doubling or even tripling of pre-industrial atmospheric concentrations of CO₂ (~280 ppmv; parts per million volume) before the end of the present century (Tans, 2009).

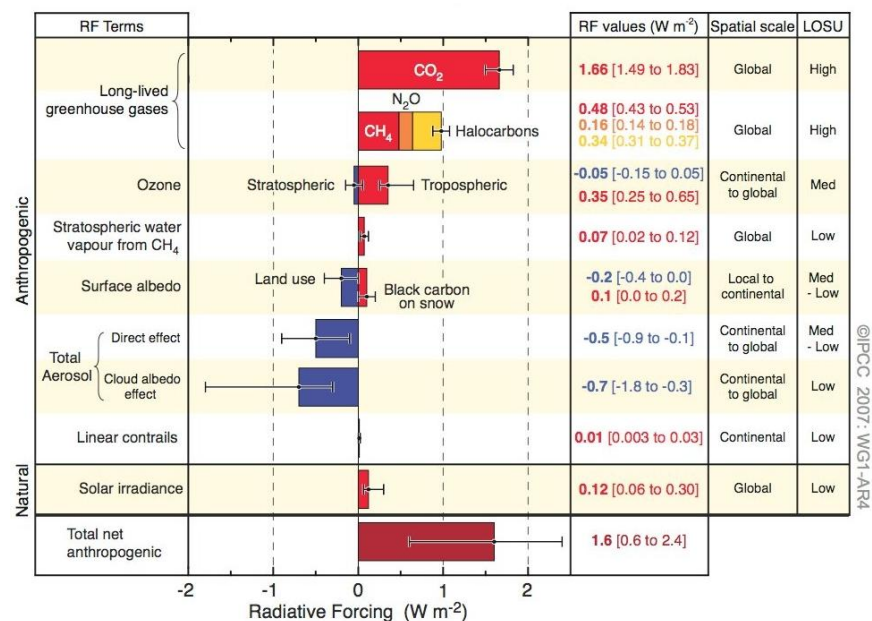


Figure 1.1 Principal anthropogenic and natural components of radiative forcing as outlined in the IPCC AR4 (2007). The values represent the contribution of different radiative forcings for the year 2005 relative to the beginning of the industrial revolution (circa. 1750) (Source: IPCC, 2007).

In recent years an increase in the demand for energy in emerging economies, and a return to coal as a key resource for energy production, has helped contribute to further increases in atmospheric GHGs (Le Quéré *et al.*, 2009). In the year 2008, total anthropogenic emissions of CO₂ approximated to 10 billion tons of carbon annually (equivalent to one million tons per hour or, on a per capita basis, ~ 0.2 kg person⁻¹ h⁻¹). Of this amount 8.7 ± 0.5 billion tons originated from the combustion of fossil fuels and cement production; it is estimated that deforestation was responsible for a further 1.2 ± 0.7 billion tons (Le Quéré *et al.*, 2009).

Data from the Mauna Loa observatory, located on the island of Hawaii in the South Pacific Ocean, illustrates the observed upward trend in atmospheric carbon dioxide. Since 1956, CO₂ levels have been monitored at the observatory using air samples taken directly from the atmosphere (Keeling, 1960). The observatory's location at an altitude

where the air is undisturbed by the localized effects of vegetation or human activity means its records provide a reliable indicator of changes in the elemental composition of the Earth's atmosphere. In addition, the dataset from Mauna Loa constitutes the longest continuous record of atmospheric CO₂ in existence.

Records from the observatory indicate that between 1959 and 2011 atmospheric concentrations CO₂ increased from ~316 ppmv to ~391 ppmv (Figure 1.2). In line with observed trends in carbon dioxide, atmospheric concentrations of methane and nitrous oxide have also increased. Over the period 1750-2005 methane levels rose from 715ppbv (parts per billion volume) to 1772 ppbv, while concentrations of nitrous oxide increased from 270 ppbv to 319 ppbv (IPCC, 2007). Along with the consumption of fossil fuels, increases in atmospheric concentrations of these gases are attributed to the intensification of agriculture and greater industrial activity.

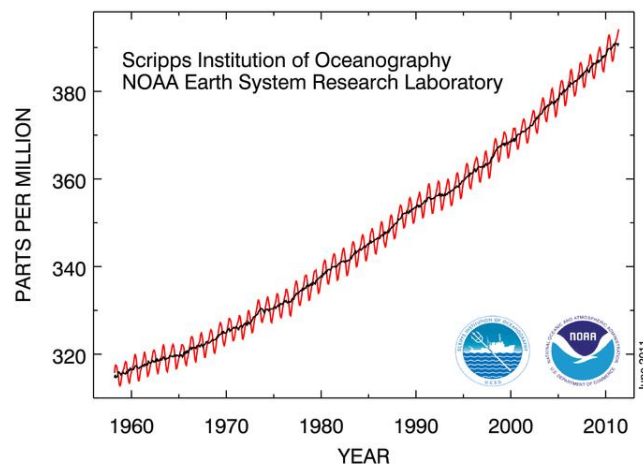


Figure 1.2 Atmospheric concentrations of carbon dioxide sampled directly from the atmosphere at the Mauna Lao observatory Hawaii. The records indicate in parts per million the increase in atmospheric CO₂ since 1958. Smaller fluctuations in the general trend are indicative of seasonal variations in atmospheric CO₂. (Source: <http://www.esrl.noaa.gov/gmd/ccgg/trends/>, accessed 27/11/2011)

Ice core samples constitute an important historical record of changes in the chemical composition of the Earth's atmosphere. The Vostok ice core drilled in central east Antarctica provides a record of past variations in atmospheric carbon dioxide and other gases stretching back 800,000 years and spanning four interglacial cycles (Lüthi *et al.*, 2008). Data from the Vostok site indicates that current atmospheric concentrations of CO₂ far exceed the natural range of variability which, records suggest varies between 180ppmv and 280ppmv (Petit *et al.*, 1999). Carbon dioxide measured at Mauna Loa and other monitoring sites currently exceed the upper bound of this range by ~40%. The records suggest that the current rate of increase in atmospheric CO₂ is as much as 30 times greater than natural rates in the geological past, and at present, levels are currently higher than at any time throughout the last 800,000 years (IPCC, 2007a; Lüthi *et al.*,

2008); furthermore it is likely that the rate of increase in atmospheric CO₂ during the 20th century is unprecedented in at least the past 16,000 years (IPCC, 2007a). Ice cores also provide a record of variations in global temperature and hold information on the occurrence of natural events (e.g. volcanic eruptions). Information on historic conditions is extracted by analysing small bubbles of air - which contain a sample from the atmosphere - enclosed in the ice. Data from the Vostok site has been used to explore the relationship between surface temperature and atmospheric CO₂. The records illustrate the degree to which fluctuations in air temperature and atmospheric carbon dioxide co-vary (Figure 1.3); ice-core data thus provides an insight into the possible response of the climate system to changes in the elemental composition of the Earth's atmosphere.

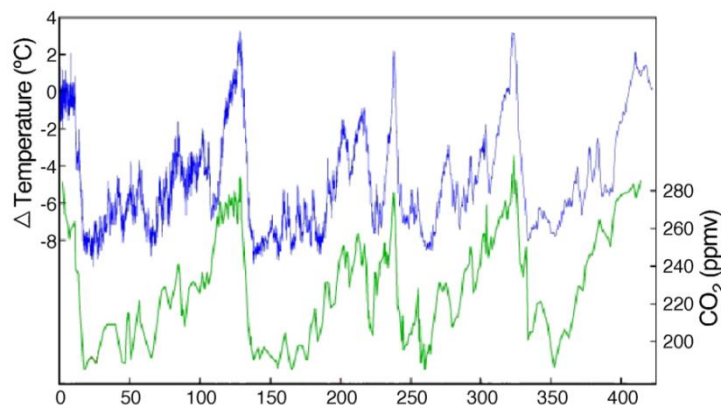


Figure 1.3 Records of atmospheric carbon dioxide and surface temperature extracted from the Vostok ice core - drilled in east central Antarctica - which stretch back over 400,000 years (Petit *et al.*, 1999). Current observations of CO₂ sampled directly from the atmosphere are higher than at any period in the ice core record. (Source: <http://en.wikipedia.org/wiki/Image:Vostok-ice-core-petit.png#file>, accessed 27/11/2011)

Records from the Vostok site suggests a lag between CO₂ and temperature in the initial warming phase of each cycle, then CO₂ appears to lead. It is likely that this is associated with a weakening in the orbital forcing (Milankovitch cycle), combined with the positive feedbacks of reduced albedo - resulting from the decay of the Northern Hemisphere ice sheets - and increased concentrations of atmospheric CO₂ and CH₄ (Lorius *et al.*, 1990). Essentially changes in the quantity of radiation the Earth receives triggers a series of positive feedbacks in the system, leading to increases in atmospheric GHGs which appear to lag behind increases in temperature. This illustrates the importance of feedback mechanisms and their role in amplifying the climate response.

1.3 Observed changes in the global climate

The IPCC (2007a:30) states that, “at continental, regional and ocean basin scales numerous long-term changes in climate have been observed. These include changes in

arctic temperatures and ice, widespread changes in precipitation amounts, ocean salinity, wind patterns and aspects of extreme weather including droughts, heavy precipitation, heat waves and the intensity of tropical cyclones”. Warming of the climate system is evident in the melting of ice sheets in Greenland (Hanna *et al.*, 2008) and Antarctica, a process which, along with the thermal expansion of oceanic water, has contributed to a rise in global sea levels (Church & White, 2006; Shepard & Wingham, 2007). It is estimated that sea levels rose by ~170 mm during the 20th century. Additionally it is estimated that over the period 1961 to 2003 sea levels have risen at an average rate of 1.8 mm per annum (1.3 to 2.3 mm) (IPCC, 2007a). The rate of increase in the last decade is estimated to be approximately double that occurring over the last century (Church & White, 2006).

Warming is evident in the widespread melting of glaciers and reductions in the extent of arctic sea-ice and snow cover (Polyak *et al.*, 2010). Instrumental records of global surface air and ocean temperatures also provide evidence for recent changes in the climate system (Levitus, 2000; 2005). It is estimated that since 1978 the annual average arctic sea-ice extent has shrunk by $2.7 \pm 0.6\%$ per decade (IPCC, 2007a). Increases in atmospheric CO₂ have led to the oceans becoming more acidic. Records indicate that surface water pH levels have decreased by an average of ~0.1 since 1750 - equivalent to a ~ 30% increase in hydrogen ion (H⁺) concentration (Orr *et al.*, 2005; IPCC, 2007a). Figure 1.4 illustrates the relationship between increases in atmospheric CO₂ measured at Mauna Loa, and surface ocean pH levels measured at the ALOHA ocean station (Doney *et al.*, 2009; Dore *et al.*, 2009).

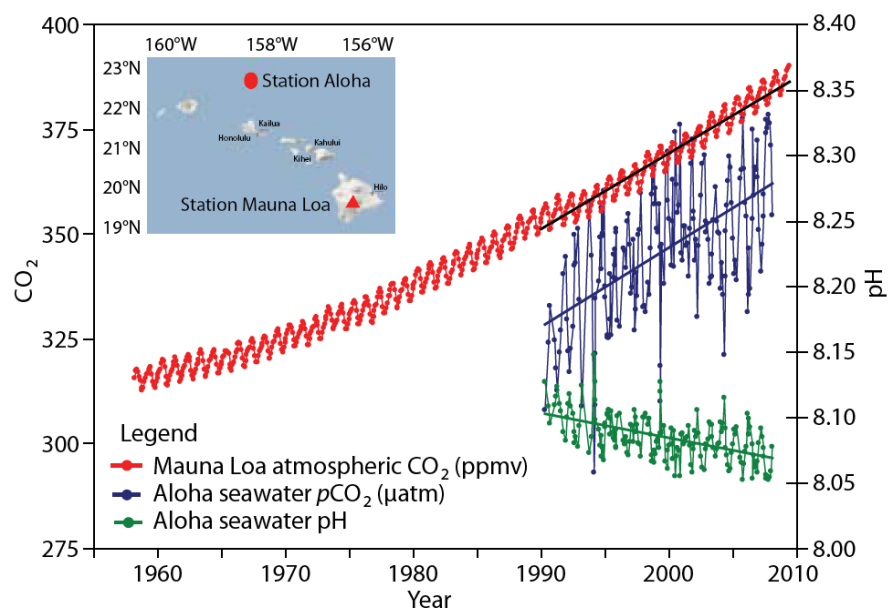


Figure 1.4 Atmospheric CO₂ concentrations measured at the Mauna Loa observatory (ppmv; in red). Surface ocean pCO₂ (µatm; in blue) and surface ocean pH (in green) measured at the ALOHA Ocean station (Source: Doney *et al.*, 2009).

Over the instrumental period of record (with widespread measurements from 1880) average global air temperatures have increased by approximately 0.8°C (GISS, 2010). Figure 1.5 shows the recorded increase in globally averaged air temperatures for the past ~160 years. According to the World Meteorological Organisation (WMO), over the period 2001-2010, global temperatures averaged 0.46°C above the 1961-1990 average - this is noted as the warmest decade on record since instrumental records began (WMO, 2011).

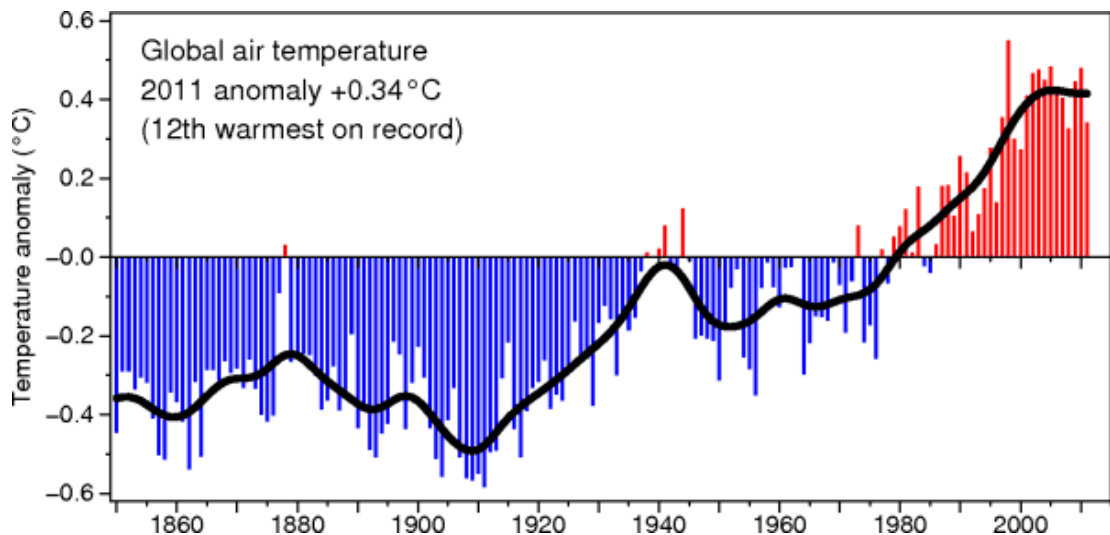


Figure 1.5 Global temperature anomalies for the period 1850–2011 relative to the 1961–1990 average. This time series is compiled jointly by the Climatic Research Unit (CRU) and the UK Met Office.

Globally the warmest year on record was 2010 - followed by 2005 and 1998 respectively (WMO, 2011). Significantly, the rate of warming experienced during the latter half of the 20th and beginning of the 21st century has been greater than at any other time during the past 1,000 years (IPCC, 2007a). Global observations indicate an increase in the number of warm extremes and a reduction in the number of cold day extremes - such changes in extreme conditions are consistent with the general upward trend in global temperature (Alexander *et al.*, 2006; IPCC, 2007a). Rising air temperatures lead to a corresponding increase in the moisture-holding capacity of the atmosphere (Douville *et al.*, 2002; Trenberth *et al.*, 2003; Trenberth, 2011), the result of which is altered precipitation patterns and changes in the nature (i.e. intensity, frequency and type) of heavy precipitation events. It is estimated that on a globally averaged basis precipitation over land has increased by approximately 2% since the beginning of the 20th century (Dai *et al.*, 1997; Hulme *et al.*, 1998; Huntington, 2006); this increase is however not spatially or temporally uniform - with regional variations in more general trends being apparent. It is noted that changes in total precipitation

receipts have been accompanied by an increase in the intensity of heavy or extreme precipitation events (Groisman *et al.*, 2005; Alexander *et al.*, 2006).

1.4 The ecological response to recent warming

Across both terrestrial and aquatic systems recent changes in climate have been found to correlate with changes in the distributional range of some species and alterations in the time at which seasonal events occur (Hughes 2000; Parmesan & Yohe 2003; Root *et al.* 2003, Hickling *et al.*, 2005; 2006). Observed changes in the phenology (Roy & Sparks, 2000; Menzel *et al.*, 2001; Hays *et al.* 2005, Adrain *et al.* 2006; Visser & Both 2005; Parmesan, 2006), distribution (Beaugrand *et al.* 2002; Root *et al.*, 2003; Parmesan & Yohe, 2003), abundance (Hickling *et al.*, 2005) and physiological response (Janzen, 1994; Hughes, 2000) of various plant, animal and fish species have been attributed to recent climate change (IPCC, 2007a).

A number of authors indicate that the most prominent response of temperate aquatic ecosystems to climate warming has been a change in phenology (Gerten & Adrian, 2002; Adrian *et al.*, 2006). Studies examining the response of biological indicators to recent climate change have highlighted the earlier onset of spring events and a lengthening of the growing season. Menzel and Fabian (1999) found that since the 1960s the average annual growing season in Europe has lengthened by 10.8 days which, the authors attribute to an increase in regional air temperatures. A subsequent study by Menzel *et al.* (2006) - which considered 125,000 observational series of some 542 plant and 19 animal species in 21 European countries over the period 1971–2000 - found that on average the onset of spring/summer in Europe has advanced by 2.5 days per decade. Menzel *et al.* (2006) state that the observed changes in the timing of seasonal events match warming trends evident in European temperature records.

In addition to changes in phenology, there has been a noted migration poleward of more mobile species (Walther *et al.*, 2002; Root *et al.*, 2003). When investigating the relationship between biological trends and recent climate change, a study by Parmesan and Yohe (2003) - which considered more than 1,700 species, the data for which varied in length and time period covered - detected a significant range shift towards the poles of 6.1 km per decade. Additionally, with respect to the phenological response of the species considered, Parmesan and Yohe (2003) found an advance in the mean onset of

spring events by 2.3 days per decade. Observed changes in the composition of ecological communities as well as the greater abundance of non-native species have also been linked to observed changes in climate (Walther *et al.*, 2002).

There is substantial evidence linking observed trends in marine and freshwater biological systems to increases in water temperature. Changes in these systems have also been linked to warming-related trends in ice cover, salinity, ocean circulation and dissolved oxygen (Weyhenmeyer *et al.*, 1999; Beaugrand, 2002; Gerten & Adrian, 2002; Edwards & Richardson, 2004; Winder & Schindler, 2004; Hays *et al.* 2005; Adrian *et al.*, 2006). Climate-mediated changes in marine and freshwater ecosystems include:

- shifts in the distributional range and abundance of algal, plankton and fish species in high-latitude oceans
- increases in algal and zooplankton abundance in high-latitude and high-altitude lakes
- the earlier migration of riverine fish species and shifts in their distributional range

(Source: IPCC, 2007b)

The earlier onset of spring events have been found in a range of taxonomically diverse organisms in the aquatic environment - including species of marine (Edwards & Richardson, 2004) and freshwater plankton (Gerten & Adrian, 2002; Winder & Schindler, 2004). The rapid response of marine species to short-term and episodic changes in sea-surface temperatures - such as those accompanying El Niño events - highlights the sensitivity of aquatic species to ocean warming and their potential response to future climate change (Hughes, 2000).

Changes in climate are anticipated to push the distributional range of some fish species towards areas at higher latitudes. Already there is evidence of shifts in the distribution of some marine fish species relative to their thermal tolerances. Over a 20 year period (1974-1993) Holbrook *et al.* (1997) found that the composition of Californian reef fish populations had changed such that the proportion of southern warm affinity species increased from approximately 25% to 35%; this was found to occur in parallel with a ~17% decline in the proportion of northern, cold affinity species. Similarly, a study of fish populations in the North Sea by Perry *et al.* (2005) found that over a 25 year period

both exploited and non-exploited species had responded to recent warming by shifting their latitudinal range further northward, and/or by altering their swimming depth.

Beaugrand *et al.* (2002) detected a macro-scale change in the biogeography of calanoid copepod crustaceans in the northeastern region of the North Atlantic Ocean. Over the period 1960-1999 strong biogeographical shifts in all copepod assemblages were found to have occurred. In the north-east Atlantic it was found that the distribution of warm affinity species had shifted northward by 10° (latitude), this was accompanied by a retreat in the distributional range of cold water species towards more northerly latitudes. Observed changes in the calanoid copepod species composition were attributed to an increase in regional sea surface temperatures. Beaugrand *et al.* (2002) indicate that the range shift in copepod assemblages is commensurate with trends detected in the phenology and distribution of many taxonomic groups in terrestrial ecosystems located at similar latitudes. Following from this, Beaugrand and Reid (2003) investigated the long-term response of zooplankton, phytoplankton and Atlantic salmon to changes in hydro-meteorological forcing in the northeast Atlantic. It was found that recent increases in regional sea-surface temperatures had an impact on all three trophic levels. The authors point to a marked increase in Northern Hemisphere temperature anomalies at the end of the 1970s (consistent with trends in the North Atlantic Oscillation) as a critical period when all biological variables show a pronounced change. Rijnsdorp *et al.* (2009) assessed the impact of recent climate change on the life cycle of various aquatic species, focusing primarily on fish species in the Northeast Atlantic region. The authors found that during the early stages of their life-history, fish species are particularly sensitive to climatic drivers. The study findings suggest that further changes in the climate system are likely to influence growth, mortality and recruitment, with resultant consequences for the overall productivity and abundance of fish stocks in this region.

1.5 Projected future climate change

The results of model experiments conducted to examine past variations in the climate system suggest it is very unlikely that the warming experienced over the latter half of the 20th century can be attributed to natural forcing alone (IPCC, 2007a). It is anticipated that if GHGs continue to be emitted at or above current rates, it is very likely that the warming trend evident in observed records will continue, and that changes

experienced in the global climate during the 21st century will be greater than those experienced over the course of the 20th century. Global climate models (GCMs) are the primary tool used for understanding past variations in the Earth's climate, and when employed in a climate change context, provide a means for exploring the potential response of the climate system to a change in forcing. Depending on the particular pathway human development may take, model experiments suggest an increase in global temperatures of between 1.8°C (B1 low emissions scenario) and 4°C (A1FI high emissions scenario) by the end of the present century (2090-2099 relative to 1980-1989) (IPCC, 2007a; Knutti *et al.*, 2008) (Figure 1.6). This however represents a best estimate or the point around which the majority of model simulations converge. Based on the results of model experiments the projected range in temperature increase is between 1.1°C (B1 scenario) and 6.4°C (A1FI scenario). Model simulations also suggest an increase in precipitation at higher latitudes; it is anticipated that this will be accompanied by a corresponding decrease in receipts across the subtropics (IPCC, 2007a).

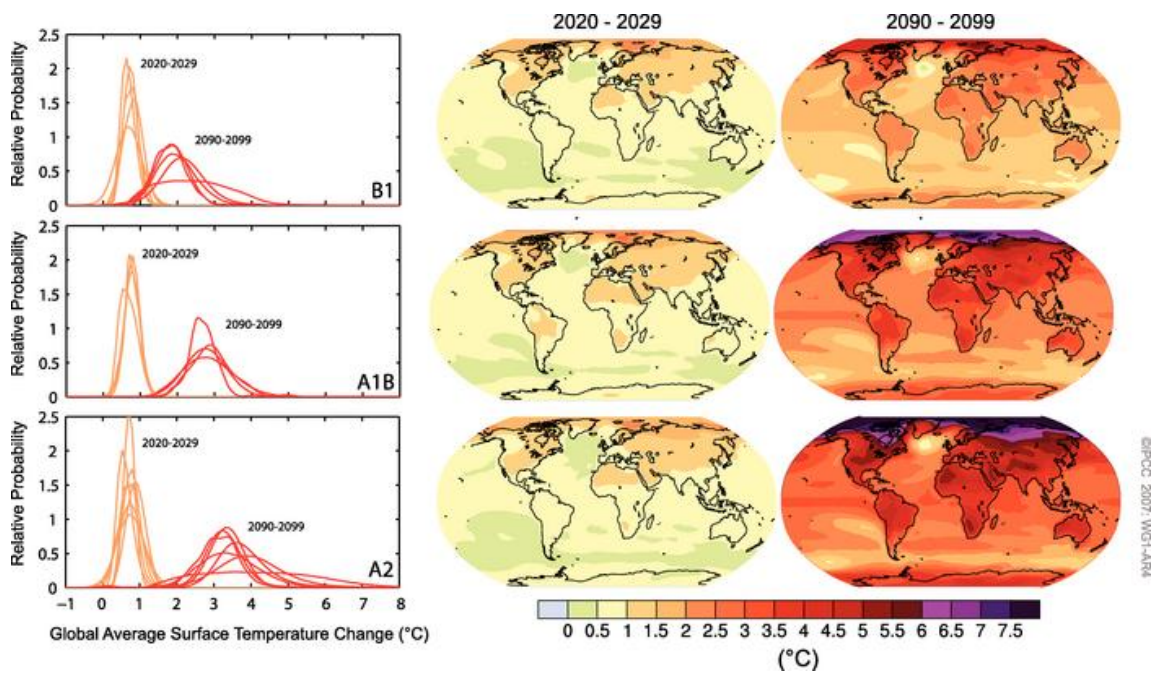


Figure 1.6 Projected patterns of future regional surface temperature change for the early and late 21st century relative to the period 1980–1999. The central and right panels show the AOGCM multimodel average projections for the B1 (top), A1B (middle) and A2 (bottom) SRES scenarios averaged over the decades 2020–2029 (centre) and 2090–2099 (right). Shown in the left panel are probability distribution functions of the estimated global average temperature increase from an ensemble of different AOGCM and Earth System Model of Intermediate Complexity studies for the same periods. (Source: IPCC, 2007).

An increase in the occurrence of extreme precipitation and drought events is also suggested to occur. Regions that are likely to experience increased precipitation receipts include the Arctic, Northern Europe and the northeast USA (Hayhoe *et al.*, 2006; IPCC, 2007a). If realised such changes in climate are likely to impact food production,

heighten flood risk and reduce the availability of water resources - thus climate change has potentially far reaching implications for the functioning of human and societal systems. Similarly, projected changes in climate have the potential to negatively affect natural systems with associated consequences for species abundance, biodiversity and habitat conservation; it is thus critical that the most potentially deleterious aspects of future climate change are explored.

1.6 Climate change and salmonids

Any shift or fundamental alteration in dominant climate conditions has the potential to affect the integrity of freshwater ecosystems and adversely impact the availability of suitable in-stream habitats, thus undermining the future viability of some populations of freshwater and anadromous fish species, including the Atlantic salmon (*Salmo salar*). This species is listed in Annex II and V of the EU Habitats Directive (1992) and thus has been identified as a threatened species deserving of conservation action. Given that they are highly sensitive to changing environmental conditions (i.e. being cold-adapted and requiring high dissolved oxygen levels), the success of native stocks and their productivity is considered a key indicator for the overall ecological well-being of freshwater systems.

Salmonids have complex life cycles consisting of several stages (egg, larvae, juveniles and adult) each of which have different dietary, growth and habitat requirements (Rijnsdorp *et al.*, 2010). This picture is complicated by the requirement of some salmonid species to migrate between the marine and freshwater environments, undergoing significant physiological change and travelling great distances in order to complete their lifecycle; consequently, salmon are regarded as a species which are particularly vulnerable to climate change. This is due to their innate sensitivity to environmental conditions and the fact that their life-cycle necessarily exposes them to climate-mediated changes in both the marine and freshwater environments.

In terms of the Atlantic salmon, Ireland remains one of a small number of European countries which retain a viable native brood stock and attractive freshwater environment for breeding; however, the continued survival of this once abundant species in many of Ireland's waterways has increasingly come under threat from human activity (Parrish *et al.*, 1998; Stefansson *et al.*, 2003). An analysis of long-term survival and productivity

trends for Irish stock suggest that many populations have gone into decline (Stefansson *et al.*, 2003). This mirrors a decline which has occurred more generally across their distributional range, but particularly along their southernmost limits where many populations have become extinct (Parrish *et al.*, 1998). It is anticipated that with further increases in water temperature, the distributional range of this species will be redrawn further northward where habitat conditions are likely to remain favourable for success during the freshwater phase of their life cycle (McCarthy & Houlihan, 1997; Friedland *et al.*, 2003; Jonsson & Jonsson, 2009).

Climate-mediated changes in water temperature, precipitation and streamflow all have long-term implications for the life-history strategy of salmonids and the local-carrying capacity of river systems. Changes in climate have the potential to alter the time at which key stages in their life cycle occur (e.g. smoltification, sexual maturity) (Berglund, 1991; Beaugrand & Reid, 2003; Jonsson & Jonsson, 2009; Graham & Harrod, 2009), as a result impacting the processes of recruitment, reproduction and migration, each of which is critical for the long-term productivity of salmonid stocks. Whilst changes in climate may directly affect salmon by altering aspects of their phenology (e.g. time of swim-up), physiology and behaviour (e.g. feeding); it may also affect them indirectly by reducing the availability of preferred habitat, altering food web-dynamics and changing the nature of interspecific relationships. The decline in many populations which has been observed in recent decades is an indication of the impact human activity has had on their environment (e.g. pollution, dams, over-abstraction and aquaculture) (Parrish, 1998; Stefansson *et al.*, 2003). Climate change brings the added complication that it is likely to amplify the effects of any current anthropogenic stressors; in this respect it presents additional challenges for the management and sustainable restoration of freshwater habitats.

1.7 Research aims and objectives

The objective of this study is to examine how changes in climate may impact the flow regime of the Burrishoole catchment - a relatively small but productive upland system typical of many catchments found along Ireland's western seaboard. Projected changes in the catchment hydrology are examined in the context of the freshwater habitat and flow requirements of Atlantic salmon (*Salmo salar*) at different stages in their life cycle. While the results of this study are specific to the Burrishoole catchment, the general

findings are likely to be of relevance to the future management of catchment systems which possess similar physical and ecological characteristics.

1.7.1 Aims

- Examine changes in key climate variables for the catchment using a series of high-resolution climate projections.
- Analyse changes in different aspects of the catchment's flow regime using the output from a plausible set of hydrological models.
- Assess the potential implications that projected changes in the flow regime may have with respect to the physiological and habitat requirements of Atlantic salmon (*Salmo salar*) at different stages in their life cycle.
- Implement a robust methodological approach for dealing with those uncertainties which affect a climate impact study of this nature.

1.7.2 Research Outline

Climate change is anticipated to alter the flow regime of riverine systems with consequences for the freshwater habitat of salmonids and the long-term sustainability of their population numbers. The Burrishoole catchment, an internationally important sentinel site for salmonid monitoring located on Ireland's west coast is used as a case study to investigate this. Changes in the catchment's flow regime under a range of future climate forcings are explored using a set of high resolution climate scenarios as input to multiple rainfall-runoff models (integrating across different parameter sets and model structures).

To examine how alterations in the hydrological regime correspond to changes in those variables (depth, velocity, etc.) which are more closely linked to the availability of physical habitat, the projected hydrological flow series are subsequently used to model changes in the channel hydraulics of two selected stream reaches. Explicit consideration is given to the habitat requirements of Atlantic salmon (*Salmo salar*) at different stages in their life cycle (e.g. spawning, migration). To manage the uncertainties which pervade the translation of different GHG emission scenarios and coarse scale GCM projections into changes in flow and habitat availability at the reach scale, methods for

quantifying uncertainty in the final results are adopted. Figure 1.7 provides a schematic of the key components of this study.

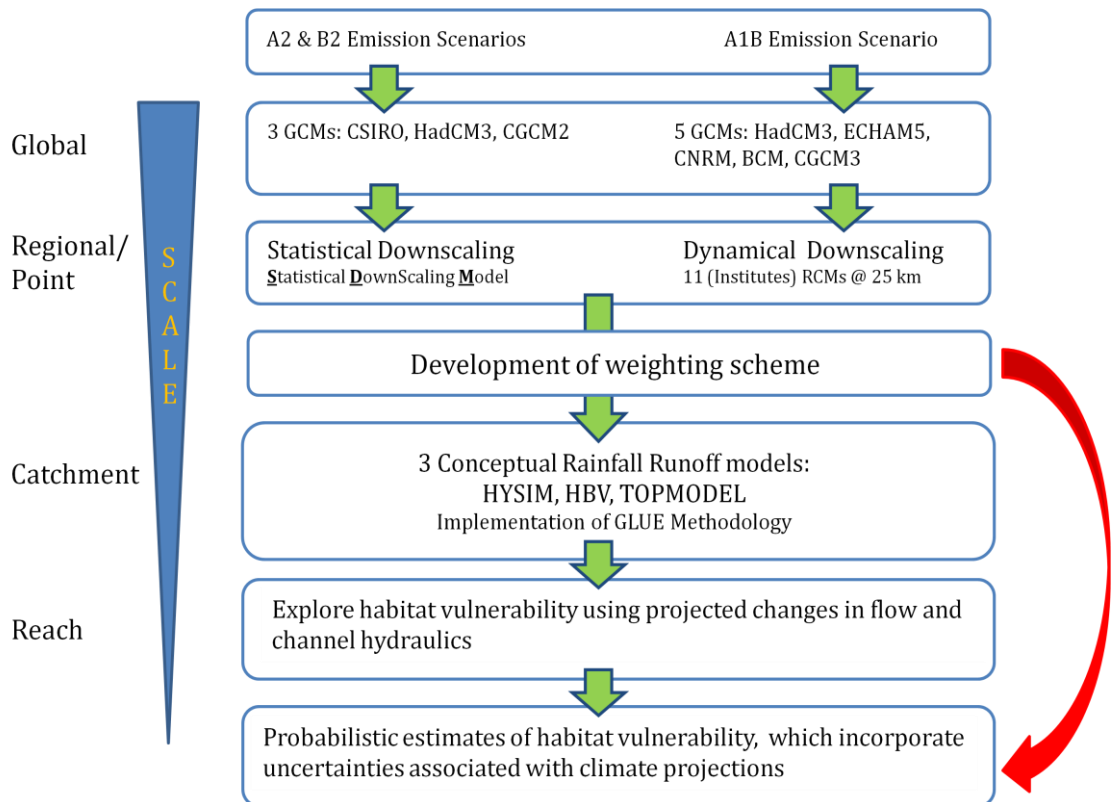


Figure 1.7 Schematic illustrating the main components of the study and how they are related.

1.8 RESCALE (Review and Simulate Climate and Catchment Responses at Burrishoole)

Some of the work conducted for this study contributed to RESCALE (*Review and Simulate Climate and Catchment Responses at Burrishoole*) - a multi-disciplinary project carried out to examine the potential impacts of climate change on the Burrishoole catchment (Fealy *et al.*, 2010). The project remit was to investigate how changes in streamflow, temperature and water quality (DO, DOC and pH) may affect the productivity of salmon stocks in the catchment. Some of the work documented in the subsequent chapters - relating primarily to the statistical downscaling - was conducted for the purposes of RESCALE and is not of direct relevance to the findings of this study; however, as it allows for a greater exploration of the methodological approach adopted, where appropriate the results from RESCALE are discussed.

1.9 Chapter Summaries

Chapter 2 sets the context for the study being undertaken - providing background information on observed changes in climate and ecosystem functions at a global, regional and national level. Anticipated changes in the climate system and hydrological cycle are discussed. The significance of natural flow regimes with respect to the functioning of freshwater ecosystems and the availability of suitable in-stream habitats is highlighted; in addition the potential impacts of climate change on aquatic ecosystems and salmonid species are explored.

Chapter 3 provides background information on the Burrishoole catchment and the observed datasets used in this study. The importance of the catchment as an international centre for research into migratory fish species is highlighted; the physical properties of the catchment are subsequently outlined. There is evidence that the catchment has experienced warming consistent with trends found both nationally and at a global scale. Given the significance of this for the study being undertaken, a discussion on observed changes in precipitation and temperature for the catchment is provided.

Chapter 4 examines each link in the “cascade of uncertainty”, describing how each one contributes to the overall uncertainty in the results from impact studies. The importance of accounting for uncertainty at each step in the process of translating storylines of future socio-economic development into local scale climate impacts is highlighted. In addition, the various methods for quantifying uncertainty are discussed.

Chapter 5 critically examines the methods employed for downscaling coarse resolution GCM data to the finer spatial scales relevant for conducting local to regional scale impact studies.

Chapter 6 describes the application of a statistical model used to downscale climate data for the Burrishoole catchment. As dynamically downscaled data from the ENSEMBLES (van der Linden & Mitchell, 2009) data archive is also employed in this study, a description of the GCM-RCM ‘model pathways’ used to generate this data is given. An assessment of model skill at simulating present day climate conditions for the catchment is subsequently provided. A performance based weighting system is devised for use in this study - the various criteria used to develop this are outlined.

Chapter 7 examines projected changes in climate for the catchment. Despite a general agreement between the respective ensemble members, a considerable amount of uncertainty regarding future change in climate is evident. The added benefit of employing a multi-model ensemble in-conjunction with the formulated weighting scheme is considered.

Chapter 8 discusses the issues associated with conducting hydrological impact studies. The limitations of different hydrological models and the assumptions implicit in their application in a climate change context are examined. A discussion on the sources of uncertainty in hydrological modelling is provided; the various methods employed to address them are also outlined.

Chapter 9 describes the hydrological models used in this study. It highlights the difficulties of selecting models specific to the physical characteristics of the Burrishoole system and the responsive nature of its flow regime; in addition, the merits of employing a multi-model approach are explored. Model projected changes in the hydrological regime of the study catchments are subsequently examined.

Chapter 10 provides contextual information on the link between hydrological processes and the success of salmonids at different stages in their life cycle. This chapter also discusses the methods used to model changes in habitat availability under future climate. The results of the hydrological and hydraulic modelling are discussed in the context of the known habitat and flow requirements of Atlantic salmon at different stages in their life-cycle.

Chapter 11 provides an overview of the study and its findings; in addition key points of discussion and potential areas for future research are highlighted. The relevance of the findings from this study for the future management of catchment systems similar in nature to the Burrishoole is explored.

Chapter 2

Climate change, freshwater ecosystems and Atlantic salmon

2.1 Observed changes in the climate system

Rising atmospheric concentrations of carbon dioxide and other GHGs have contributed to an increase in the planet's radiative forcing and altered the energy balance of the climate system, leading to a warming of the Earth's oceans and atmosphere. The current scientific consensus attributes most of the observed increase in atmospheric GHGs to human activity, principally the mass consumption of fossil fuels; a practice which has underpinned the development of industrialised society.

Evidence suggests that concentrations of atmospheric carbon dioxide have increased from a pre-industrial level of ~280 ppmv to a current level of ~391 ppmv - a rise of ~40% (IPCC, 2007a). If current rates of fossil fuel consumption continue, it is likely to result in a doubling or even tripling of atmospheric CO₂ (relative to pre-industrial levels) by the end of the 21st century (Trans, 2009). An analysis of ice core data indicates that atmospheric concentrations of carbon dioxide are presently greater than at any time in at least the past 800,000 years (Luthi *et al.*, 2008); whilst records of past variations in atmospheric CO₂ - estimated from various marine and terrestrial proxies - suggest that current levels are greater than at any time in the past several million years (Royer *et al.*, 2006).

The results of model experiments indicate that the warming experienced since the mid-20th century cannot be attributed to natural forcing alone, and it is only when models are run using both natural and anthropogenic forcing that the temperature increases observed over the past century are replicated - highlighting the impact which human activity has had on the climate system (IPCC, 2007a). There are a number of indicators which provide evidence that changes in the global climate have occurred, this includes:

- the melting of ice sheets in Greenland and Antarctica (Hanna *et al.*, 2008; Velicogna, 2009; Rignot, 2011)
- a rise in global average sea levels (Church & White, 2006; Sheperd & Wingham, 2007)

- a reduction in glacier mass balance, contractions in snow cover and declines in the extent of arctic sea-ice (IPCC, 2007a; Polyak *et al.*, 2010)
- increases in global air (Jones *et al.*, 1999) and ocean temperatures (Levitus, 2000; Levitus *et al.*, 2009)
- changing precipitation patterns (Hulme *et al.*, 1998)
- the acidification of the world's oceans (Doney *et al.*, 2009)

Evidence that the climate system is undergoing fundamental changes can also be found in the biological responses of natural systems - of which climate is a key determining variable. Observed changes in marine and terrestrial ecosystems which have been linked with changes in the global climate include an advance in the timing of seasonal events and a reduction in the abundance of some species of flora and fauna; alterations in the distributional range of more mobile species have also been linked to recent climate change (e.g. Hughes, 2000; Wuethrich, 2000; McCarthy, 2001; Walther *et al.*, 2002; Hickling *et al.*, 2005, 2006).

2.1.1 Temperature

The three principal reconstructions of global surface temperature (National Oceanic and Atmospheric Administration (NOAA); Climate Research Unit (CRU); Goddard Institute for Space Studies (GISS)) all indicate that the Earth has experienced significant warming since the 1880s (Jones *et al.*, 1999; Hansen *et al.*, 2011) - with most of this warming occurring since the 1970s (Figure 2.1).

Between 1906 and 2005 globally averaged surface air temperatures increased by $0.74^{\circ}\text{C} \pm 0.18^{\circ}\text{C}$ (IPCC, 2007a). Over the past 50 years the rate of warming has almost doubled to 0.13°C per decade, and it is likely that the current rate of warming is greater than at any time in the last one thousand years (IPCC, 2007a). More recently, GISS have indicated that since 1880 globally averaged air temperatures have increased by $\sim 0.8^{\circ}\text{C}$ (Hansen *et al.*, 2010). According to the World Meteorological Organisation (WMO) - over the period 2001-2010 - global temperatures averaged 0.46°C above the 1961-1990 average which, is the highest ever recorded for a 10-year period (WMO, 2011). When estimating changes in temperature the WMO considers each of the datasets maintained by the three organisations referred to above. Recent data assessed by GISS suggests that 2010 tied with 2005 as the warmest year in the 131 year instrumental record (Hansen *et al.*, 2010). The three warmest years on record include 2010, 2005 and 1998; in addition

records indicate that sixteen of the warmest years have occurred since 1990 (WMO, 2011). Kennedy and Parker (2010) indicate that warming experienced in 2010 was in part related to the El Niño that developed in 2009, this is also the case with the high temperatures recorded in 1998; however, no such natural factor can be attributed to the warming experienced in 2005.

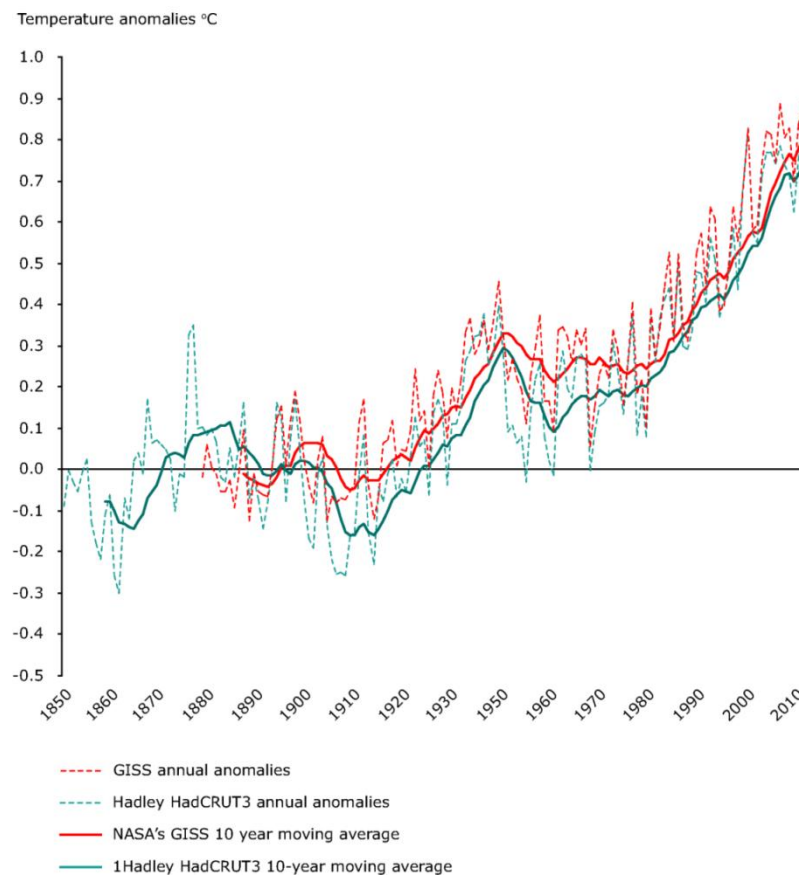


Figure 2.1 Observed global annual average temperature ($^{\circ}\text{C}$) deviations for the period 1850–2010. Deviations are estimated relative to the mean values for the 1961-90 reference period. Show in blue are estimated changes in the global mean surface temperature from the combined UK Met Office Hadley Centre and Climate Research Unit dataset HadCRUT3. Shown in red are estimated temperature changes from NASA's GISS dataset - anomalies are calculated relative to the period 1951-1980. (Source: <http://www.eea.europa.eu/data-and-maps/figures>. accessed 27/12/2011).

According to the dataset maintained by the UK Met Office (Climate Research Unit), the period 2001-2010 (0.44°C above 1961-90 mean) was 0.20°C warmer than the period 1991-2000 (0.24°C above 1961-90 mean). Their analysis indicates that 1998, with a temperature of 0.55°C above the 1961-90 mean, is the warmest year on record. The next nine warmest years all occur in the decade 2001-2010. During this period 2008 is the only year which does not appear in the ten warmest years. Despite 2008 being the coldest year of the 21st century, it is still the 12th warmest on record.

Despite an increase in global temperature, spatial disparities in the rate and magnitude of warming exist. For example, warming has been greater over land (0.27°C per decade since 1979) as opposed to the oceans (0.13°C per decade since 1979) (IPCC, 2007a); in

addition temperature increases have been greatest at high northern latitudes. This is exemplified by average spring and winter temperatures in the arctic which, over the past 100 years have increased by approximately double the global average (IPCC, 2007a). In contrast, parts of the Antarctic continent and Pacific Ocean have exhibited little or no evidence of warming (IPCC, 2007a). The WMO (2011) indicate that recent warming has been especially strong in Africa, as well as in parts of Asia and the Arctic (WMO, 2011). The Saharan/Arabian, East African, Central Asian and Greenland/Arctic/Canadian sub-regions have all experienced temperature increases in the range of 1.2°C to 1.4°C over the last decade (2001-10) - relative to the long-term average - and are 0.7°C to 0.9°C warmer than in any previous decade (WMO, 2011). According to the European Environment Agency (EEA) average annual surface temperatures over the European ocean area and land mass have increased by 1.1°C (1850-2009 relative to the 1850-1899 average) (EEA, 2010); when ocean areas are excluded surface temperatures for the same period were found to have increased by 1.3°C.

Observational records indicate an increase/decrease in the occurrence of warm/cold day extremes; also of note is an increase in the duration and frequency of heat waves (IPCC, 2007a). Alexander *et al.* (2006) found that, for the period 1951-2003, over 70% of the global land area considered by their study exhibited a significant decrease in the annual occurrence of cold nights; this was accompanied by a significant increase in the frequency of warm nights - with some regions experiencing a doubling of these indices. Similarly, Firch *et al.* (2002) found a decrease in the number of frost days, an increase in the occurrence of warm summer nights and a reduction in the intra-annual extreme temperature range. Instrumental records also show an increase in the incidence of precipitation occurring as rain rather than snow, this finding is consistent with studies focusing on temperature change in high latitudes (Mote, 2003; Knowles *et al.*, 2006).

2.1.2 Precipitation

Linked with warmer air temperatures is an increase in the moisture carrying capacity of the atmosphere - the theoretical basis for which is the Clausius-Clapyeron relation. There is however a considerable degree of uncertainty regarding whether humidity will increase in accordance with the Clausius-Clapyeron relation or at a lower rate (Allen & Ingram, 2002; Held & Soden, 2000; Trenberth, 2011). Allen and Ingram (2002) found

that the precipitation response in a number of GCMs was approximately $3.4\% \text{ K}^{-1}$. This was related to evaporation being constrained at a rate lower than that required to satisfy the $7\% \text{ K}^{-1}$ increase in specific humidity estimated by the Clausius–Clapyeron relation. Observational data does however support increases at rates which are consistent with the Clausius–Clapyeron relation (Huntington, 2006; Allan & Soden, 2007; Wentz *et al.*, 2007; Zhang *et al.*, 2007; Willet *et al.*, 2008). Changes in the energy balance of the climate system mean alterations in the spatial distribution and variability of precipitation is likely to occur. A change in forcing is also likely to alter the frequency of occurrence and intensity of extreme events, and lead to changes in the type and amount of precipitation which occurs.

Precipitation records indicate an overall, although not significant increase in precipitation and an intensification of the water cycle over the 20th century (Trenberth *et al.*, 2007). On a globally averaged basis precipitation over land is estimated to have increased by approximately 2% since the beginning of the 20th century (Jones and Hulme, 1996; Dai *et al.*, 1997; Hulme *et al.*, 1998; Huntington, 2006). This is however not spatially or temporally uniform, with regional variations being apparent (Karl & Knight, 1998). The increase is most pronounced polewards of 30° in both hemispheres, with many regions experiencing a 6-8% increase over the period 1900-2005 (IPCC, 2007a).

Zhang *et al.* (2007) found that the observed increase in the Earth's radiative forcing has not been detected in precipitation at a global scale; the authors indicate that this is partly due to changes in different regions cancelling each other out. Zhang *et al.* (2007) compared trends found in land precipitation records over the 20th century with trends found in model simulated data (based on a suite of 14 climate models). By considering observed trends in the context of model simulations the authors state that anthropogenic forcing has had a discernible influence on changes in precipitation across different latitudinal bands. Zhang *et al.* (2007) indicate that regional and global precipitation trends cannot be explained either by internal climate variability or natural forcing alone; thus the authors point to anthropogenic forcing as the primary driver of observed changes in large scale precipitation regimes. Zhang *et al.* (2007) note increases in precipitation over the Northern Hemisphere mid-latitudes, and state that this has been accompanied by a decrease in yields over the subtropics/tropics; the authors also highlight the sensitivity of regions like the Sahel - constituting the region between the

Sahara desert to the north and African savannah to the south - to altered precipitation patterns.

According to a number of studies the high latitudes of the northern hemisphere have experienced an increase in the amount and variability of precipitation - particularly during the wetter winter months (Alexander *et al.*, 2006; Meehl *et al.*, 2006; Trenberth *et al.*, 2007). Increased receipts in the mid and high latitudes are in contrast with decreases experienced in the northern sub-tropics (Houghton *et al.*, 2001). Record low precipitation yields have been observed in equatorial regions since 1995, and there has been a persistent decline in precipitation in the Sahel since the late 1960s (Dore, 2005). According to Dore (2005) precipitation across the African continent has declined by 5-10% between the periods 1931–1960 and 1968–1997; this trend has been most pronounced over the Sahel region where - over the same period - precipitation receipts are estimated to have declined by between 20% and 49%.

Marked increases in precipitation have been detected in northern Europe; however, increases have been accompanied by a general decline in precipitation yields towards southern Europe and across the Mediterranean region (Schonwiese & Rapp, 1997). Over the 20th century it is estimated that precipitation amounts in northern Europe increased by 10–40%; in contrast some parts of southern Europe have dried by as much as 20% (Dore, 2005). Such trends reflect a wider hemispherical pattern of divergent zonal mean precipitation trends between high and low latitudes (Dai *et al.*, 1997; Hulme *et al.*, 1998).

Several studies have detected increases in precipitation receipts in a number of regions (Dai *et al.*, 1997; Alexander *et al.*, 2005), including areas of the United States (Karl & Knight, 1998; Groisman *et al.*, 1999) and Canada (Mekis & Hogg, 1999), South America (Haylock *et al.*, 2006a), the Arctic (Min *et al.*, 2008), northern Taiwan (Yu *et al.* 2006), Australia (Hennessy *et al.*, 1999; Manton *et al.*, 2001) and the UK (Osborn & Hulme, 2002).

In some regions an overall increase/decrease in total annual receipts has been accompanied by changes in the seasonality of the precipitation regime. This is the case in the UK where records indicate an increase in winter rainfall amounts, which has been accompanied a notable decline in summer receipts - the latter of which is manifest through an increasing frequency in the occurrence of drought events (Osborn & Hulme, 2002). An increase in the seasonality of the precipitation regime has been detected in

different regions across Germany. In this case researchers have found that an increase/decrease in winter/summer rainfall amounts had occurred over the periods 1958-2001 (Hundecha & Bardossy, 2005) and 1851-2006 (Hansel *et al.*, 2009) respectively.

Linked with increases in precipitation amounts are changes in the occurrence and intensity of heavy rainfall events (Groisman *et al.*, 2005; Alexander *et al.*, 2006). According to Dore (2005) it is likely that over the latter half of the 20th century there has been a 2-4% increase in the frequency of heavy or 'extreme' precipitation in the Northern Hemisphere - particularly across the mid to high latitudes. Regional studies focusing on the United States (Karl & Knight, 1998; Kunkel *et al.*, 1999), China (Liu *et al.*, 2005; Zhai *et al.*, 2005), Canada (Stone *et al.*, 1999), Switzerland (Frei & Schar, 2001; Schmidli & Frei, 2005), Japan (Iwashima & Yamamoto, 1993; Yamamoto & Sakurai, 1999) and the Mediterranean (Kostopoulou & Jones, 2005) have all indicated an increase in either the intensity of precipitation events or the contribution of extreme events to total annual receipts. Similar conclusions were drawn from studies focusing on northern Italy (Brunetti *et al.*, 2000), the UK (wintertime precipitation) (Osborne *et al.* 2000; Osborne & Hulme, 2002), Scotland (Fowler & Kilsby, 2003), South Africa, northeast Brazil and the former USSR (Groisman *et al.*, 1999; Gruza *et al.*, 1999; Easterling *et al.*, 2000). Based on a comparison between observed and model simulated data for the latter half of the 20th century, Min *et al.* (2011) suggests that the increase in heavy precipitation events observed over the Northern Hemisphere land area is linked to anthropogenic forcing.

Dore (2005) indicates that increases in mean annual receipts are reflected disproportionately in increased incidences of heavy precipitation, suggesting an amplified response in the intensity of precipitation events to climate forcing (Groisman *et al.*, 1999; Gruza *et al.*, 1999; Easterling *et al.*, 2000). Essentially in cases where an increase in total receipts has been observed, the relative increase in the frequency of extreme precipitation events has been disproportionately greater (Dore, 2005). It follows that where a reduction in rainfall amounts has been experienced, so too has a decrease in the frequency of extreme events (Katz, 1999; Groisman *et al.*, 1999); however, as stated by Dore (2005) this generalization does not always hold as increases in higher order events have also been observed in areas where an overall decline in yields has occurred - pointing to more fundamental changes in the probability distribution of precipitation (Buffoni *et al.*, 1999; Groisman *et al.*, 1999; Brunetti *et al.*, 2000; Dore, 2005).

2.1.2 The Intensification of the Hydrological Cycle

It is argued that increasing atmospheric concentrations of carbon dioxide and other GHGs have led to an intensification of the hydrological cycle - manifest in an increase in the flux of water between the terrestrial, atmospheric and aquatic spheres (Trenberth, 1999, 2011; Huntington, 2006; Held & Soden, 2000, 2006; Chang & Jung, 2010). By fundamentally altering the Earth's energy balance, climate change is likely to affect all aspects of the hydrological cycle (Bates *et al.*, 2008; Trenberth *et al.*, 2007) including, evaporation rates, the spatial and temporal variability of precipitation patterns and the quantity as well as timing of flow through freshwater systems; furthermore, climate change has the potential to alter the characteristics (frequency, duration and intensity) of extreme events such as floods, drought and severe storms. The relationship between changes in the Earth's energy budget and the intensification of the hydrological cycle - otherwise interpreted as the sensitivity of the hydrologic response to climate warming - is encapsulated by the Clausius–Clapyeron relation (Held & Soden, 2000). Measurable changes in the processes and components of the hydrological cycle are important indicators of warming in the climate system (DelGenio *et al.*, 1991; Loaciga *et al.*, 1996; Trenberth, 1999; Held & Soden, 2000; Arnell *et al.*, 2001).

Trends found in a range of hydroclimatic variables including: precipitation (Houghton, *et al.*, 2001), runoff (Groisman *et al.*, 2001), atmospheric water vapour (New *et al.*, 2000) and glacier mass balance (Oerlemans, 2005) indicate that during all or part of the 20th century there was an acceleration of the hydrological cycle - observed at both regional and continental scales (Huntington, 2006). Similar trends observed in the length of growing seasons (Cooter & LeDuc, 1995), evapotranspiration rates (Golubev *et al.*, 2001) and soil moisture deficits (Robock *et al.*, 2000) also support an intensification of the hydrological cycle. However, due to the various inconsistencies between individual studies - *vis-à-vis* the variables/regions considered, as well as the limitations of available datasets - a significant degree of uncertainty is associated with the assertion that an acceleration of the hydrological cycle has occurred (Huntington, 2006).

Trends detected in patterns of global runoff by Labat *et al.* (2004) and Labat *et al.* (2005) suggest an increase in continental runoff (estimated over the period 1920-1995), supporting the contention that an intensification of the water cycle has occurred. Their study suggested a 4% increase in global runoff per 1°C increase in air temperatures

during the 20th century - with regional variations evident around this trend. Legates *et al.* (2005) however highlight a number of shortcomings in both studies - which include the small sample considered and the potential confounding influence of non-climatic drivers on changing runoff patterns. It is argued this undermines the findings of both Labat *et al.* (2004) and Labat *et al.* (2005).

The IPCC (2007b) states that there is a broadly consistent pattern of change in annual runoff, with some areas, particularly those at higher latitudes, experiencing an increase; conversely, in regions including west Africa, southern Europe and southern Latin America, reductions in annual runoff have been experienced (Milly *et al.*, 2005; IPCC, 2007b). At a regional scale studies have detected an increase in runoff in parts of China (Tao *et al.*, 2003; He *et al.*, 2010), Finland (Hyvarinen, 2003) and the coterminous USA (Walter *et al.*, 2004). In addition, increases in precipitation over a number of river catchments in the United States have been detected using hydrometric data (Lins & Slack, 1999; Groisman *et al.*, 2001; McCabe & Wolock, 2002).

Giorgi *et al.* (2011) proposed the hydroclimatic intensity index (HY-INT) as a measure for detecting warming related trends in the water cycle. In order to explore the response of the hydrological cycle to climate warming the authors applied the index to observed station and gridded datasets of daily precipitation. The results suggested an increasing trend in the index over the last decades of the 20th century which the authors attribute to anthropogenic forcing.

Theoretically, the observed increases in higher order precipitation events (Groisman *et al.*, 2004) should lead to a corresponding increase in the frequency of flooding and extreme flow events; however, evidence from regional studies conducted in the USA (Lins & Slack, 1999; Douglas *et al.*, 2000; McCabe & Wolock, 2002; Vogel *et al.*, 2002), Scandinavia (Hyvarinen, 2003; Lindstrom & Bergstrom, 2004), Canada (Zhang *et al.*, 2001) and central Europe (Mudelsee *et al.*, 2003) do not consistently support this. The findings of these studies are generally at odds with those of Milly *et al.* (2002) who reported an increase in the frequency of flood events over the 20th century (with discharges exceeding 100-year return periods). This study examined runoff patterns in 29 river basins - each with an area greater than 200,000km² - spanning different continents and climatic zones. The authors indicate that the link between increases in the occurrence of flood events and radiatively induced climate change is a tentative one, but consistent with model simulations. In a study of 195 catchments, Kundzewicz *et al.* (2005) found that 137 of the selected catchments exhibited no trend in the annual

maximum series; however 31 returned a positive trend and 27 exhibited a negative trend. Petrow and Merz (2009) analysed 145 discharge gauges distributed across Germany for trends in flooding events. According to the authors the spatial and seasonal coherence of the results from individual records and river catchment suggests that detected changes in flood behaviour are climate driven. Both Robson (2002) and Robson *et al.* (1998) examined flow series from catchments in the UK for changing flood patterns; both studies indicated that no clear evidence for warming related trends in flood behaviour could be found.

2.1.3 Changes in European Extremes

The EU funded project ‘STARDEX’ (**ST**Atistical **R**egional **D**ownscaling of **EX**tremes for European regions) was undertaken to examine changes in the frequency and intensity of extreme precipitation and temperature across Europe. Observational records from 491 European-wide stations, covering the period 1958-2000 were used in the study. The results indicated an increase in mean temperatures across Europe consistent with trends found in global datasets. This was found to be accompanied by an increase in the occurrence of extreme temperature and precipitation events.

The indices used in STARDEX have been employed in several region specific studies (e.g. Hundscha & Bardossy, 2005; McElwain & Sweeney, 2007). When examining trends in daily precipitation and temperature across western Germany using the STARDEX indices, Hundscha and Bardossy (2005) found an increase in daily maximum and minimum extreme temperatures. With the exception of the summer season the authors also found an increase in both the magnitude and frequency of extreme precipitation events. The results of the STARDEX project can be summarized on a seasonal basis as follows (STARDEX Final Report, 2005):

Winter

- With the exception of south-western Europe, there has been a general increase in extreme maximum temperature.
- Extreme minimum temperature has increased to a greater degree than extreme maximum temperature.
- With the exception of small decreases noted in parts of Greece, Scandinavia and the Iberian Peninsula, extreme minimum temperature has increased over the entire region.

- The longest winter dry period increased in Southern Europe; this is contrasted with observed decreased in Northern Europe.
- The indices used indicated an increase in heavy rainfall across the UK, central Europe and Scandinavia.
- In Eastern Europe, Greece and western part of the Iberian Peninsula the indices suggested a general decrease in extreme precipitation.

Summer

- With the exception of Eastern Europe, northern Scandinavia and Russia, extreme maximum temperature was found to have increased in most regions.
- With the exception of a small number of stations, extreme minimum temperature increased in most areas for this season.
- In contrast to winter, trends for the longest dry period during summer were less spatially coherent; however, stations in central Europe, the UK and southern Scandinavia exhibited a general increase in this index.
- In Scandinavia, northwest Russia and across southwest Europe a positive trend in the incidence of extreme precipitation events was found.
- Across the northern Iberian Peninsula, the UK and northeast Europe a decrease in heavy rainfall during this season was found to have occurred.

2.2 Climate change indicators for Ireland

Trends detected in observed temperature and precipitation records from synoptic stations located across Ireland indicate that its climate has undergone changes commensurate with trends found in European and global datasets. A study by McElwain and Sweeney (2007) found that, over the period 1890-2004, Ireland's mean annual surface air temperature increased by 0.7°C. The general positive trend in air temperature follows a similar pattern to that found globally; however, Ireland's trend was found to exhibit greater interannual variability and displayed a tendency to lag the global trend - a finding which may be due in part to the temperate maritime nature of the climate and the moderating influence of the Gulf Stream (McElwain & Sweeney, 2007).

Analysis of the instrumental records indicates that two distinct periods of warming occurred (1910-1940 and 1980-2004). During the latter period of warming temperatures

increased by 0.42°C per decade - almost double the rate of the first period (0.23°C per decade). The records used also indicated that six of the ten warmest years on record occurred between 1995 and 2004. McElwain and Sweeney (2007) found that 1945 was the warmest year on record – this is followed by 1998 which was the second warmest. This is similar to global datasets where 1998 (at the time of this study) is noted as being the warmest year (Jones *et al.*, 1999). The synoptic records indicated that for the majority of stations an increase in mean temperatures (maximum and minimum) had occurred; there was also a noted increase in the number of hot days (defined as maximum temperature >18°C) and a decrease in the occurrence of frost days (minimum temperature < 0°C) - a trend accompanied by a shortening in the length of the frost season (McElwain & Sweeney, 2007).

McElwain and Sweeney (2004) suggest that trends found in precipitation records are consistent with patterns found at a European scale. Total annual precipitation yields were found to have increased in the north and west of the country, in contrast on the southern and south-eastern seaboard a slight negative trend in receipts was found. Stations located on the west coast suggested an increase in the maximum number of consecutive wet days; additionally, increases in the precipitation intensity ($\geq 10 \text{ mm d}^{-1}$), as well as the frequency of events greater the 90th percentile were found for these stations. Positive trends in the persistence and intensity of rainfall are consistent with increases in annual receipts for stations located on the west coast.

2.3 Projected changes in the global climate system

The IPCC (2007a) state that if atmospheric concentrations of aerosols and GHGs were held constant at year 2000 levels it is likely that a further warming of ~ 0.1°C per decade would still occur over the next two decades. This is due to the timescales associated with climatic feedbacks and the slow response of the oceans to warming. Depending on which emissions pathway is considered more likely, climate models suggest an increase in global temperatures of between 1.8°C (B1 low emissions scenario) and 4°C (A1FI high emissions scenario) by the end of the present century (2090-2099 relative to 1980-1989) (IPCC, 2007a; Knutti *et al.*, 2008)

Model simulations indicate that temperature increases are likely to be greatest over land and at higher latitudes; in contrast relatively less warming is projected to occur over the North Atlantic and Southern Oceans (IPCC, 2007a). Model experiments also indicate

that the negative trend observed in snow cover and glacier mass balance will continue. It is likely this will negatively impact the availability of water resources in those regions supplied by melt waters (Barnett, 2005). The results of a study conducted by Schneeberger *et al.* (2003) on 11 glaciers sampled from different climatic regions suggest a volume loss of 60% by the 2050s.

Increases in air temperature are also likely to result in a continuation and further enhancement of the negative trend observed in the sea-ice extent. In some model projections, by the latter part of the 21st century Arctic late-summer sea-ice disappears almost entirely (IPCC, 2007a). Model simulations also indicate that the warming suggested to occur over the present century is likely to result in a 20-35% decrease (by the 2050s) in the permafrost area of the Northern Hemisphere. Melting of the Antarctic and Greenland ice sheets is likely to continue, further contributing to increases in sea level rise - estimates for which indicate that by the last decade of the 21st century, relative to the last two decades of the 20th century, sea-levels may have risen by between 0.18m (B1 scenario) and 0.59m (A1FI scenario) (IPCC, 2007a). These findings are similar to Horton *et al.* (2008) who suggest an increase of between 0.42m and 0.57m in sea levels by the end of the present century. The intensity of tropical cyclones is also likely to increase; in addition, model projections indicate a poleward shift in extra-tropical storm tracks (IPCC, 2007a).

Bates *et al.* (2008) document results from a multi-model experiment consisting of fifteen climate models, each run using the A1B emission scenario. Model simulations projected an increase in atmospheric water vapour, evaporation and precipitation - consistent with an intensification of the global hydrological cycle. Despite a general concordance between individual models, strong seasonal and regional differences were found to occur. For the period 2080–2099 (relative to 1980-1999) an increase of up to 20% in annual mean precipitation receipts across high latitudes was suggested. In contrast the models indicated a decrease of 20% in annual yields across the subtropics. A decline in receipts of up to 20% over the Mediterranean and Caribbean regions, as well as the sub-tropical western coasts of each continent were also projected to occur (Bates *et al.*, 2008). Regions likely to experience an increase in precipitation included the Arctic, Northern Europe, Canada and the northeast United States (Hayhoe *et al.*, 2006; Bates *et al.*, 2008).

GCM experiments consistently suggest an increase in the variability, frequency and intensity of heavy precipitation events - albeit with significant regional variations. The

frequency of extreme precipitation is likely to increase over most areas during the 21st century (e.g. tropical and high-latitude zones) (Bates *et al.*, 2008). Projected increases in the precipitation intensity will likely result in an increase in the magnitude and duration of high flow and flooding events. Mid-continental drying, most notably in the subtropics, low and mid-latitudes, is likely to increase during summer - leading to a greater risk of drought conditions (Sheffield & Wood, 2007; Bates *et al.*, 2008).

In their study of model simulated precipitation data for a European domain, Kundzewicz *et al.* (2006) found a marked contrast between projected changes in winter and summer precipitation patterns. Although not spatially uniform, wetter winters were suggested to occur throughout the continent; with respect to changes in summer rainfall patterns, a distinction between northern and southern Europe was made. It is likely that southern Europe will experience drier summers whilst over northern Europe winter precipitation yields are projected to increase. Due to changing precipitation patterns problems of water quality and supply are likely to be exacerbated, particularly over southern Europe during the drier summer months. A study by Palmer and Räisänen (2002) suggested an increase in the frequency of 'very' wet winters across northern Europe which, the authors link to an increase in the intensity of mid-latitude storms. According to Palmer and Räisänen (2002), for a doubling of CO₂ (61–80 years from present), a five-fold increase in the likelihood of very wet winters is projected for Scotland, Ireland and much of the Baltic Sea basin, whilst a seven fold increase is projected for parts of Russia.

With regards to changes in the intensity of precipitation over Europe, the highest quartiles of daily rainfall amounts are anticipated to increase in many areas (Christensen & Christensen 2003; Kundzewicz *et al.* 2006). In keeping with trends found over the past century (Dore, 2005) the frequency and intensity of heavy precipitation events is projected to increase in regions which also experience a general reduction in total receipts (Christensen & Christensen 2003; Kundzewicz *et al.* 2006; Frei *et al.*, 2006). This is one of the key findings of a study by Christensen and Christensen (2003) who examined the impacts of climate change on severe summertime flooding across Europe. For southern and central Europe rising air temperatures are likely to increase soil moisture deficits, leading to the more frequent occurrence of drought events and intense summer drying (Douville *et al.*, 2002; Christensen *et al.*, 2007a).

A study by Fowler and Ekström (2009), which considered projections from a multi-model ensemble (obtained from PRUDENCE project), found that extreme precipitation

across the UK during winter, spring and autumn is likely to increase. The absolute magnitude of increases ranged from 5% to 30% (2070–2100 relative to the 1961-1990 control) depending on region and season considered.

2.4 Projected changes in the hydrological cycle

Model projections suggest that by the mid 21st century across the high latitudes, water availability and mean annual runoff will have increased (Bates *et al.*, 2008); in contrast, over drier regions - particularly those in the mid-latitudes and the dry tropics - a decrease in the availability or water resources is likely to occur (e.g. western USA, Mediterranean, southern Africa and northeastern Brazil) (Bates *et al.*, 2008). Milly *et al.* (2005) used 12 climate models to explore global trends in runoff and water availability under perturbed forcing conditions. For the year 2050 the models projected a 10% to 40% increase in runoff in eastern equatorial Africa and the La Plata basin (South America). This was also the case across the high latitudes of North America, Eurasia and some major islands of the equatorial eastern Pacific Ocean. A decrease in runoff (typically 10-30% by 2050) was suggested for southern Africa, the Middle East, southern Europe and the mid-latitude region of western North America.

Using four different GCM-based climate scenarios, Arnell (1999) explored the potential hydrological response of a defined European domain to projected changes in climate. Although inter-model differences were evident, the projections broadly suggested a decrease in annual runoff at latitudes south of 50°N (-25% to -50%); in contrast increases were suggested for areas north of 50°N latitude. Projected changes in patterns of flood behaviour for Europe indicate that over large parts of the continent a reduction in return periods is likely (Lehner *et al.*, 2006; Hirabayashi *et al.*, 2008; Dankers & Feyen, 2008); however, the results from individual studies are inconsistent, highlighting the uncertainties inherent in modelling climate and hydrological extremes - even at large spatial scales.

There have been several studies focusing on the potential impacts of climate change on river flows in the United Kingdom (e.g. Arnell & Reynard, 1996; Sefton & Boorman, 1997; Pilling & Jones, 1999, 2002; Arnell, 2004). In general the results suggest that annual, winter and summer runoff is likely to decrease in southern regions; in contrast, over northern areas flows are likely to increase throughout the year, particularly during

winter. The principle findings from similar studies conducted in an Irish context (e.g. Charlton & Moore, 2003; Murphy & Charlton, 2008; Steele-Dunne *et al.*, 2008) are summarised below.

- The seasonality of runoff is likely to increase, with higher flows in winter and spring; extended dry periods are suggested to occur during the summer and autumn months.
- The projected increase in winter runoff is more pronounced in westerly river basins.
- All areas are anticipated to experience a reduction in summer runoff; however, the greatest decreases are likely to occur during the autumn months. In addition catchments situated along the eastern seaboard are likely to experience the greatest decrease in runoff.
- It is likely that the magnitude and frequency of flooding events will increase nationally, but particularly in those catchments located on the western seaboard.
- A number of catchments exhibited an increase in the incidence and duration of low flow events.
- Those catchments which lack the storage potential with which to moderate the effects of an increasingly seasonal rainfall regime are most vulnerable to changes in climate.

2.5 Climate change impacts on freshwater ecosystems

Given that variations in localised climate conditions have had a central role in shaping the abiotic and biotic composition, as well as structure of freshwater ecosystems, it is likely that any change in such an elemental variable will have a significant impact on all facets of freshwater systems. This includes, for example, individual organisms, interspecific relationships, community structures, nutrient cycling and the nature of food web-dynamics. Climate change is also likely to affect a range of abiotic factors including the substrate cover, flow regime and water chemistry. In doing so it may impact the quantity and quality of available habitat and create conditions conducive to the ingress of invasive species (Walther, 2001; Mckee *et al.*, 2003; Moss *et al.*, 2003; Burgmer, 2007; Senerpont Domis *et al.*, 2007; Walsh & Kilsby, 2007; King *et al.*, 2008; Rahel & Olden, 2008; Heino *et al.*, 2009; Döll & Zhang, 2010; Perkins *et al.*, 2010; Woodward *et al.*, 2010; Wrona *et al.*, 2010).

Given the level of interconnection which exists between hydrological processes, the functioning of riverine ecosystems and the productivity of salmonid populations, it is important that the impacts of climate change on Atlantic salmon are framed within the wider context of potential impacts on freshwater ecosystems. Figure 2.2 highlights how changes in streamflow may affect salmonid species both directly, by altering their habitat conditions, and indirectly, by affecting wider ecosystem functions.

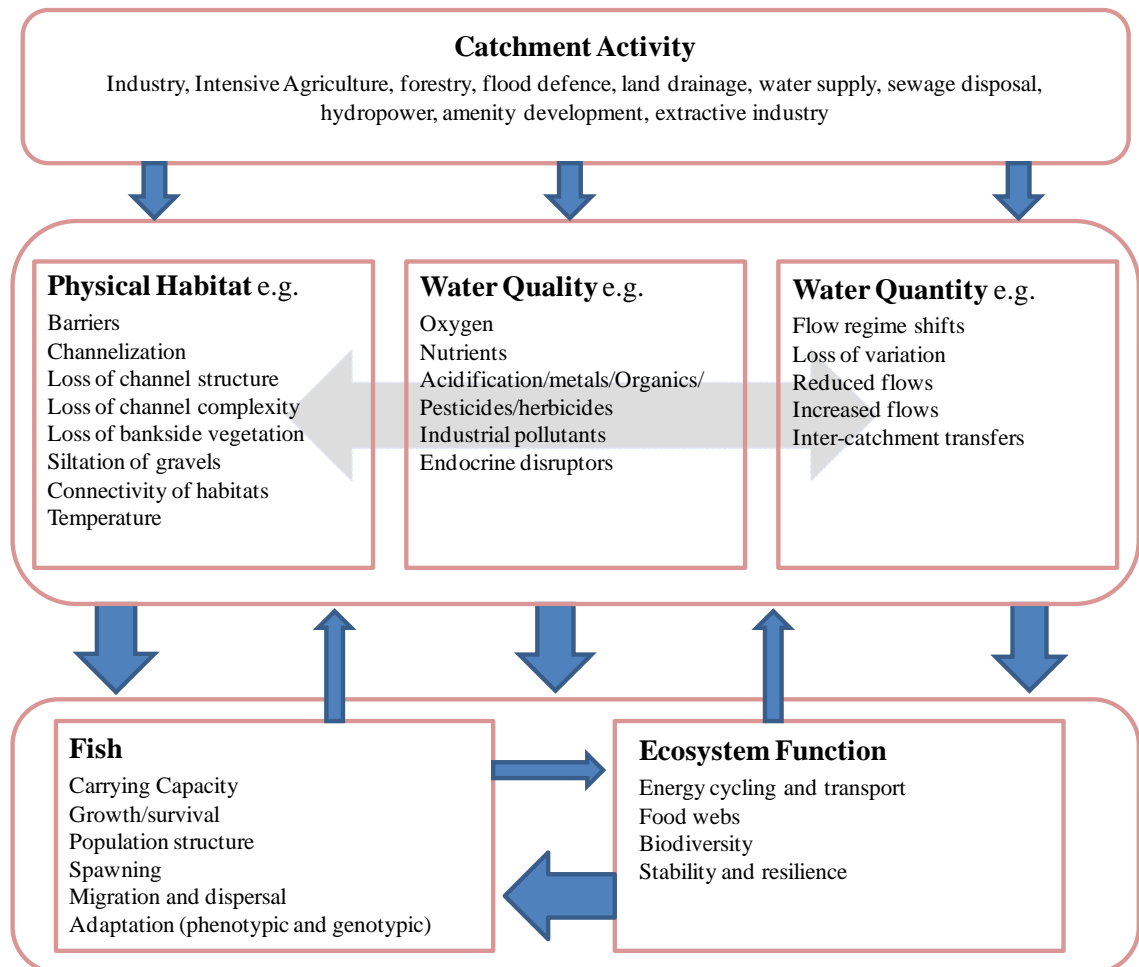


Figure 2.2 Connections between human activity, hydrological and geomorphological processes and ecosystem/fish responses. (Adapted from Milner *et al.*, 2010)

As they are physically fragmented and subject to numerous anthropogenic stressors, freshwaters are considered particularly vulnerable to changes in climate (Woodward *et al.*, 2010). Based on an assessment of changes in biodiversity, Sala *et al.* (2000) considered lentic (i.e. ponds and lakes) and lotic (i.e. rivers and streams) ecosystems to be the most sensitive to climate change when considered alongside marine and terrestrial systems. Woodward *et al.* (2010) indicate that freshwaters at higher latitudes and altitudes - where globally some of the fastest rates of warming have occurred (Hansen, 2010) - may act as 'sentinel systems', providing an indication of larger scale

changes which may occur in less vulnerable and more complex systems (i.e. species rich).

Given the level of interdependence within ecosystems, together with regional disparities in their response to climate forcing and the confounding influence of human impacts, it is difficult to demonstrate a direct causal link between recent climate change and observed changes in freshwater ecosystems. Despite this there is evidence that changes in climate have had an impact on the biological, physical and chemical characteristics of freshwaters - both directly through changes in precipitation and air temperature, and indirectly through interactions with other stressors (Nickus *et al.*, 2010).

Climate change is manifest primarily in those aspects of freshwater systems which are temperature-dependent. Due to its influence on the rate at which biological and chemical processes occur (e.g. photosynthesis, behaviour, dissolved oxygen saturation, metabolic rate) temperature is a primary driver of ecological change in aquatic environments (Harley *et al.*, 2006). According to the IPCC (2007b) recent warming has brought about an increase in river and lake water temperatures and contributed to changes in the composition of community structures and the timing of seasonal events. In addition climate change has influenced changes in the productivity of freshwater systems and affected the abundance of individual organisms (IPCC, 2007b). The Millennium Ecosystem Assessment (2005) indicated that recent climate warming has been a major driver of biodiversity loss in freshwater ecosystems. In global scale studies investigating observed declines in biodiversity, warming related trends in water temperature and alterations in patterns of flow behaviour are highlighted as having the most significant impacts on biodiversity loss (Lake *et al.*, 2000; Xenopoulos *et al.*, 2005; Heino *et al.*, 2005). For example, studies by Hickling *et al.* (2005, 2006) attributed shifts in the distributional range of some freshwater and terrestrial taxa in Britain to changes in climate observed over the period 1960-2000.

The most immediate effects of recent climate change have been experienced as increased river and lake water temperatures. Increases in water temperature have generally mirrored the upward trend evident in regional air temperatures observed over the past ~100 years (Winder & Schindler, 2004; Hari *et al.*, 2006; Hammond & Pryce, 2007; Arvola *et al.*, 2010). The IPCC (2007b) indicate that since the 1960s, water temperatures have increased by between 0.2°C and 2.0°C in rivers and lakes across Europe, Asia and North America. The EEA (European Environment Agency) state that

during last century water temperatures in European rivers and lakes have increased by between 1°C and 3°C (2007). Langan *et al.* (2007) reports that in an upland Scottish river (Girnock burn), winter and spring maximum stream water temperatures increased by 2°C over the last 30 years. Hari *et al.* (2006) examined water temperatures in rivers and streams across Switzerland - their study covered an altitudinal range of almost 4000m. The results indicated that warming was evident at all altitudes, with trends being reflective of increases in regional air temperature observed over the past 40 years.

An analysis of temperature records from Lake Baikal (Russia) indicated that over the past 60 years surface water temperatures have increased at a rate of 0.2°C per decade (Hampton, 2008). Similarly records from Lake Constance (Germany) indicated that mean annual lake water temperature increased by 0.17°C per decade (since the 1960s) (Straile *et al.*, 2003). An analysis of deep lake water temperatures - indicative of more long-term temperature trends - suggest increases which are consistent with trends found in surface waters (IPCC, 2007b). Records indicate that since the early 1900s several large East African lakes including, Edward, Albert, Kivu, Victoria, Tanganyika and Malawi, have warmed by between 0.2 and 0.7°C (IPCC, 2007b).

Enhanced air and water temperatures are reflected in the more prolonged stratification of lake waters and increases in the length of ice-free seasons. Changes in water temperature, wind speed and precipitation patterns affect the time at which overturning occurs and the extent of lake mixing, thus altering the persistence of thermal stratification. By affecting the thermal regime of lacustrine systems, changes in climate may alter the distribution of nutrients and oxygen; in addition it may change the overall heat content and quality of surface waters. Changes in the persistence of thermal stability may disrupt biological cycles, alter phytoplankton dynamics and impact primary production (IPCC, 2007b; Adrian *et al.*, 2009). According to Bates *et al.* (2008), the freeze-up date of rivers and lakes has on average been delayed by a rate of 5.8 ± 1.6 days per century (when averaged over all available datasets, spanning 150 years), whilst the date for break-up has occurred earlier, at a rate of 6.5 ± 1.2 days per century. Also reported is a lengthening in the stratified period (by 2-3 weeks) of several lakes in Europe and North America (IPCC, 2007b).

An analysis of 20 year records (1969-1988) from lakes in northwestern Ontario (Canada) indicated that both air and lake water temperatures had increased by 2°C; in addition the observed data indicated that the ice-free season had extended by three

weeks (Schindler, 1996). Several other studies also linked increasing temperatures to the earlier break-up and later freezing of seasonal ice-cover on rivers and lakes (Livingstone 1999; Magnuson *et al.*, 2000). A study by Coats *et al.* (2006) of Lake Tahoe (USA) found that - over the period 1970-2002 - lake water temperatures had increased by approximately 0.15°C per decade, associated with which was an increase in the persistence of thermal stratification. An analysis of records from Lake Zurich (covering the period 1947-1998) by Livingstone (2006) suggested an increase in the period of summer stratification of roughly 2-3 weeks, in addition thermal stability was found to have increased by 20%.

Studies examining the potential response of lake systems to projected changes in climate generally indicate that water temperatures - particularly in the epilimnion - are likely to increase. In addition, temperature profiles, thermal stability and mixing patterns are likely to be altered, leading to further increases in the persistence and extent of summer stratification (Hondzo & Stefan, 1993; Stefan *et al.*, 1998).

By altering biological and chemical processes, climate-mediated changes in water temperature, flow patterns and precipitation are likely to impact the various parameters relating to water quality (e.g. biological oxygen demand, dissolved oxygen (DO), dissolved organic carbon (DOC)), (e.g. Jennings *et al.*, 2009; Naden *et al.*, 2010; Whitehead *et al.*, 2009; Nickus *et al.*, 2010). With respect to this, Grimalt *et al.* (2010) explored the impacts of climate change on the mobility of persistent organic pollutants in freshwater bodies. The study highlighted how changes in climate may exacerbate the impacts of any current anthropogenic stressors on water quality. As DOC influences acidity, light penetration, nutrient availability and potential toxicity, it is an important parameter in terms of the overall ecological health of freshwater ecosystems. Due to the influence which temperature and precipitation patterns have on the production and outwash of DOC, trends observed in the concentration levels of DOC in freshwater lakes provide an indicator of changes in climate. During the past two decades increases in DOC in areas of the UK, central Europe and North America have been detected (Freeman *et al.*, 2001; Evans *et al.*, 2005; Monteith *et al.*, 2007). These increases have, at least in part, been attributed to recent changes in climate (Freeman *et al.* 2001; Hudson *et al.*, 2003; Evans *et al.*, 2006; Worrall *et al.*, 2006; Erlandsson *et al.*, 2008). Over the coming decades changing precipitation patterns are anticipated to increase the frequency of acid-pulses and releases of DOC - a key mechanism for which is the more regular occurrence of post-drought floods (Arnell, 1998; Whitehead, 2009; Fealy *et al.*,

2010). Temperature is a key physical determinant of oxygen solubility, consequently further increases in air temperatures are likely to result in a reduction in the DO content of surface waters. DO levels are anticipated to be impacted also by temperature-induced increases in the rate of microbial activity. Changes in temperature and DO have implications for the ecological well-being of freshwater bodies and the diversity of plant and animal species which they can sustain (Hauer *et al.*, 1997).

There is evidence that the recent warming of freshwaters and the associated change in water quality has affected a diverse range of taxonomic groups including riverine plants, invertebrate and fish species (e.g. Fry, 1971; Stefansson *et al.*, 2003; Davidson & Hazelwood, 2005; Zydlewski *et al.*, 2005; King *et al.*, 2007; McGinnity *et al.*, 2009). Fish and invertebrate species whose thermal limits may have already been reached or exceeded are most vulnerable to further increases in temperature. In addition, those species sensitive to changes in environmental conditions will come under increased pressure - this is particularly relevant for cold-adapted species which require high DO levels such as salmonids. Under future climate conditions, cold-affinity species may be replaced by species such as cyprinids which are more tolerant of low oxygen conditions and are better adapted to warmer environments (e.g. Daufresne *et al.*, 2004). With respect to this, recent climate change has been detected in long-term fish and invertebrate data collected from the upper Rhone (at Bugey). These records, which cover the period 1979 to 1999, were examined to determine whether recent climate change has had a discernible influence on the structure of either community. It was found that the more frequent occurrence of low flows, along with observed increases in water temperature had favoured southern, thermophilic fish species (e.g. chub, barbel) at the expense of northern, cold-adapted species (e.g. dace). In addition, thermophilic invertebrate taxa (e.g. Athricops, Potamopyrgus) were found to have replaced cold-water invertebrate taxa (Daufresne *et al.*, 2004). The results indicate that the observed change in community structure was in part attributable to changes in the thermal regime of the river system - changes in which reflect long term trends evident in regional air temperatures.

Increasing temperatures are likely to affect freshwater and anadromous fish species at all stages in their life cycle (e.g. hatching, migration, spawning and growth) - although the response may vary depending on the species and life stage considered (Elliott, 1991; Jonsson *et al.*, 2001; Jonsson & Jonsson, 2009). In many cases global climate change represents an additional stressor for fish populations which may already be subject a

range of human-induced pressures (Allan & Flecker, 1993). A study by Mc Ginnity *et al.* (2009) suggested that, while Atlantic salmon may have the capability to adapt to increasing temperatures (with certain caveats attached), the presence of additional stressors, including the supplementation of wild populations with hatchery fish, may result in catastrophic population collapses within a relative short period of time.

Studies have shown that the flow regime is a key component of lotic ecosystems, central for determining the availability of suitable habitat and important for regulating ecological processes like migration and reproduction (Bunn & Arthington, 2002; Verdonshot *et al.*, 2010). Poff *et al.* (1998) highlight that natural flow regimes are essential for aquatic and riparian species and list five components of the flow regime which are regarded as critical for maintaining the ecological integrity of riverine systems. These include the magnitude, frequency, duration, timing and rate of change in hydrologic conditions. It has been shown that anthropogenically imposed alterations (e.g. impoundments, water abstraction, channelization, diversions, etc.) on natural flow regimes can have considerable consequences for the overall ecological well-being of river systems and their capacity to nurture viable populations of more sensitive species (Poff & Ward, 1989; Bunn & Arthington, 2002; Gilvear *et al.*, 2002; Johnsen *et al.*, 2010; Poff & Zimmerman, 2010). As outlined by Bunn and Arthington (2002) changing flow regimes have the potential to affect each link in the relationship between flow, habitat and biotic diversity (Figure 2.3).

Under altered flow conditions increases in the variability of available habitat may limit access to resources, resulting in a decrease in the local carrying capacity of river systems (Wright *et al.*, 2004). In addition, changes in hydrology may lead to a decoupling of the evolved relationship between established patterns of flow behaviour and the occurrence of various stages in the life history of aquatic biota. The various components of the flow regime - particularly the seasonality and timing of more extreme events - are critical for the successful completion of different life stages (e.g. spawning, recruitment, migration) (Dudgeon *et al.*, 2006). In a climate change context alterations in flow are complicated by changes in the thermal regime of river systems which may alter the phenology of some aquatic biota, possibly resulting in a further narrowing in the window of opportunity whereby flow conditions are aligned with the habitat and physiological requirements of individual organisms at a specific stages in their life cycle.

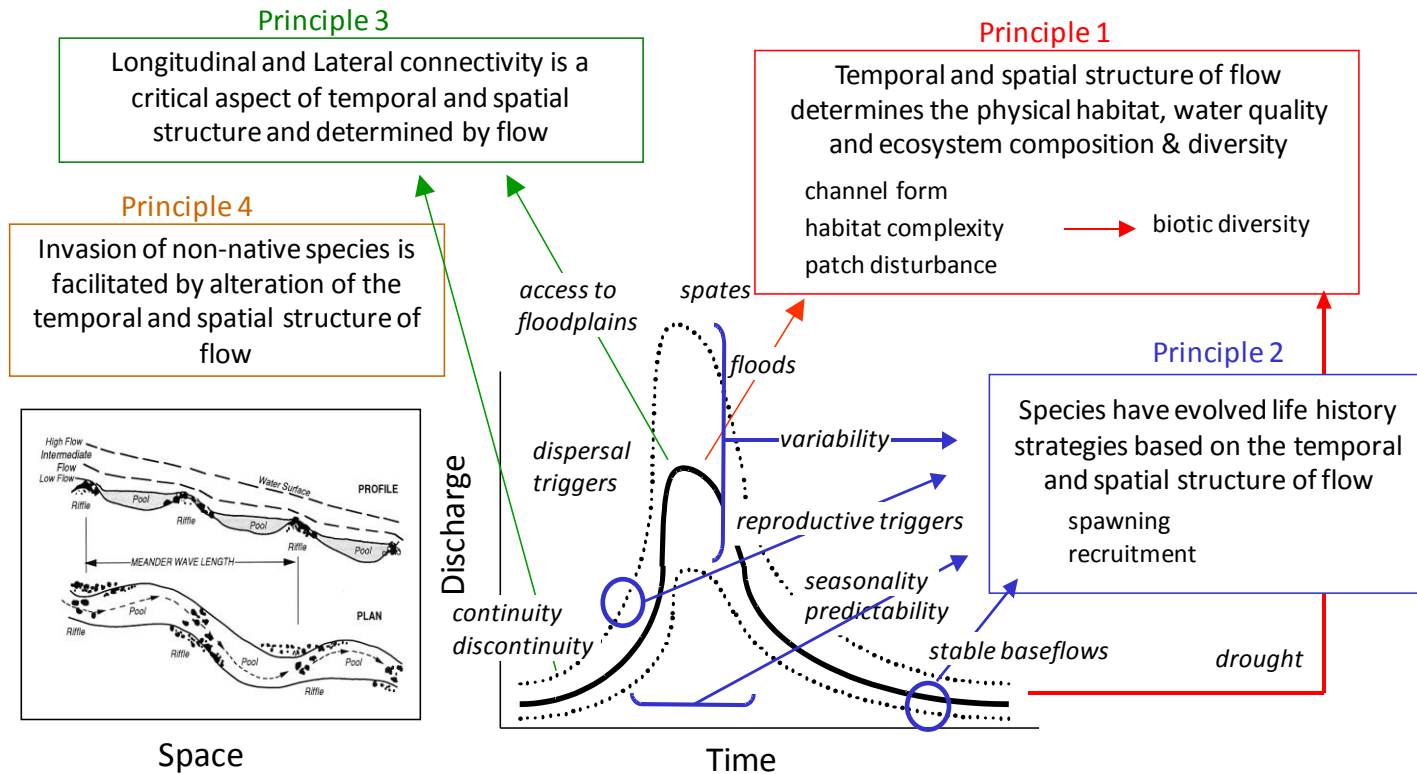


Figure 2.3 A schematic of the four principles outlined by Bunn & Arthington (2002) which describe the link between aquatic biodiversity and the natural flow regime of a river system. Flow regimes can be defined as patterns of variability in flow that describe the full range of behaviour exhibited by river systems (e.g. long term average flows, seasonality, low and high flow statistics, interannual variability). Bunn and Arthington (2002) state that flow regimes influence the diversity of aquatic flora and fauna via several interrelated mechanisms that operate on different spatial and temporal scales. The first principle outlined above highlights the importance of flow as a key determinant of physical habitat at different temporal and spatial scales (i.e. from the scale of the catchment to the scale of microhabitats along the channel reach). This is driven by both high and low flow components; high flows are important for determining the channel form and shape which low flows may limit habitat availability. The second principle outlined above refers to the synchronicity between the life history strategy of aquatic organisms and patterns of flow. The life cycle of aquatic species have evolved in response to natural flow regimes, as such the seasonality of the flow regime and the timing of key flow events (e.g. spates) are intrinsically linked to the completion of different stages in an organism's life cycle. The third principle highlights the importance of flow for maintaining lateral and longitudinal connectivity across river systems. Flow act as a medium facilitating migration and movement between different parts of river systems and between in-stream and floodplain habitats. High flows may be particularly important for facilitating access to different parts of the network. The fourth of Bunn & Arthington's (2002) principles states that altered flow regimes may be more conducive to the ingress and proliferation of exotic species at the expense of native biota, provided the former are more adapted to the modified flow regime. Figure 2.3 is adapted from Bunn & Arthington (2002). (Source: www.awsaplanning.com/Presentations_files/RJG-ReportPresentation.ppt).

Changing flow regimes may also alter connectivity across river systems – thereby impeding up-stream migration and reducing access to exploitable habitats, refugia and food resources along different parts of the stream network (Bunn & Arthington, 2002; Pringle, 2003).

Any changes in flow may also impact riverine ecosystems by reducing water quality and altering those fluvial processes (e.g. rates of erosion and deposition) which are critical for the maintenance of in-stream habitats (e.g. riffle-pool sequence, refugia). For example, spates are necessary for the removal of accumulated sediment and debris, maintaining the channel form and distributing organic material (e.g. detritus, algae) (Verdonschot *et al.*, 2010). Although high flows constitute an important component in the overall flow regime, such episodic disturbances have great potential to disrupt the long-term functioning of lotic ecosystems. Under altered climate conditions an increase in the magnitude or a change in the timing of flood events may lead to a scouring of nests and benthic communities; it may also result in organisms being involuntarily displaced downstream into unfavourable habitats.

By restricting movement and access to resources, an increase in the frequency of drought events may reduce the carrying capacity of river systems and limit the dispersal of individuals along the stream network - an issue of particular concern during periods of enhanced water temperatures. With respect to potential changes in hydrology, climate change places additional pressures on river systems whose natural flow regimes have already been modified by human activity (Armitage & Pardo, 1995; Olden & Naiman, 2010; Tockner *et al.*, 2010). Using two climate scenarios and a global hydrological model Xenopoulos *et al.* (2005) found that under future climate forcing up to 75% (quartile range 4–22%) of local fish biodiversity may become extinct (by 2070) in rivers projected to experience a reduction in discharge.

In a comprehensive review study, Poff and Zimmerman (2010) found that the ecology of river systems - considering both aquatic (macroinvertebrate and fish species) and riparian organisms - overwhelmingly responds negatively to alterations in flow. Negative impacts on aquatic species included: a loss of sensitive biota, increases in non-native species, life-cycle disruption (e.g. spawning cues), reduced habitat availability, a decline in species abundance, a reduction in spawning and recruitment, the expiration of native fishes and a change in the population structure. Riparian vegetation is important for in-stream habitat as it provides shade and is an important food source. With respect

to riparian zones Poff and Zimmerman (2010) found that changes in flow resulted in: the terrestrialisation of flora, increased plant mortality, vegetation encroachment into channels; and a reduction in plant coverage, species diversity and recruitment.

2.6 A summary of the anticipated impacts of climate change on freshwater ecosystems

A summary of climate change impacts on freshwater ecosystems is provided below (after Hauer, 1997; Mooij *et al.*, 2004; IPCC, 2007a, 2007b; ; Battarbee, 2008; Bates, *et al.*, 2008; Hering *et al.*, 2010; Kernan *et al.*, 2010; Verdonschot *et al.*, 2010).

Changes relating to increased air and water temperatures

- By reducing DO levels and creating conditions conducive to the release of benthic phosphorus, increasing temperatures are likely to lower water quality in lentic systems.
- Higher temperatures are likely to enhance the thermal stability of lake systems - potentially altering primary production, nutrient cycling and phytoplankton activity.
- The ice-free season for river and lake systems is likely to be extended; as a result of which the length of time deep lakes experience hypoxic conditions may increase.
- An increase in water temperature is likely to reduce phytoplankton diversity; with a shift towards the dominance of cyanophytes expected to occur.
- For cold-adapted species enhanced water temperatures are likely to reduce recruitment success and increase exposure to parasitic transmission.
- Higher temperatures are anticipated to alter the distribution of many fish species and negatively impact benthic invertebrates - particularly in regions where thermal tolerances have already been reached or exceeded.
- It is likely that environmental conditions will favour warm-adapted species (e.g. cyprinid fish species) over cold-adapted species which are less tolerant of low DO environments (e.g. salmonids) (e.g. Daufresne *et al.*, 2004).
- An increase in the duration of summer stratification is anticipated to enhance eutrophication and lead to oxygen depletion in deep zones.

- Species extinctions are expected to occur where warm summer temperatures and anoxia eliminate deep cold-water refugia.
- Due to temperature increases significant changes are likely to occur in the species composition, phenology and production of planktonic communities (e.g. increases in toxic blue-green algal blooms).
- If a 2-3°C increase in temperature is realized there is potential for numerous arctic lakes to dry out.

Changes relating to altered precipitation and flow patterns

- Water levels are anticipated to increase in lakes at high latitudes, where climate models suggest an increase in precipitation receipts; a decline in water levels is suggested in lakes at mid and low latitudes.
- The upstream movement of river zones is likely to occur; as a result those species bound to small streams and springs in the lower reaches of river systems - which are unable to seek refuge at higher altitudes - are particularly vulnerable to changes in climate. For migratory species artificial or natural obstructions to upstream migration may reduce access to thermal refugia in higher zones.
- The distributional range of diadromous species is likely to shift poleward. Similarly, species of waterfowl, invertebrate and tropical invasive species are likely to shift poleward with some localized extinctions occurring.
- Enhanced water temperature and alterations in established flow patterns are likely to favour invasive species.
- Changes in flow are likely to impact the availability of preferred habitats (quantity and quality) and limit access to exploitable resources.
- In riverine systems changing flow regimes may lead to a divergence in the synchronicity between the timing of flow events and the occurrence of different stages in the life history of aquatic biota. This is likely to be further complicated by changes in temperature which may alter the phenology and behaviour of some species.
- Due to an increase in the incidence of drought, it is likely that some rivers will become intermittent with dry phases during the summer months.
- Changing precipitation patterns and increased soil moisture deficits are likely to increase DOC concentrations, thus altering biogeochemical cycles and changing the chemical composition of freshwaters.

- The seasonal migration patterns of many wetland species are likely to be affected, with some species becoming locally extinct.
- Due to their sensitivity to changes in the water balance, closed lake systems are most vulnerable to changes in climate. Under some climatic conditions it is possible they will disappear entirely.
- Changes in climate and land-use will place additional pressures on already-stressed ecosystems.

2.7 Climate change and salmonids

According to Graham and Harrod (2009:1143), “changes in climate, and in particular temperature, have and will continue to affect fish at all levels of biological organization: cellular, individual, population, species, community and ecosystem, influencing physiological and ecological processes in a number of direct, indirect and complex ways”. There is a growing body of evidence indicating that the recent warming of freshwaters and the associated reduction in water quality has affected the physiology (Fry, 1971; Stefansson *et al.* 2003), phenology (Zydlewski *et al.*, 2005; Mc Ginnity *et al.*, 2009), distribution (Friedland, 2003; Juanes *et al.*, 2005) and survival of some fish species (Daufresne *et al.*, 2004; King *et al.*, 2007; McGinnity *et al.*, 2009; Clews *et al.*, 2010). However, given the range of confounding factors which must be considered, isolating the direct effects of recent climate change on salmonids is a difficult task (Daufresne *et al.*, 2004); as is quantifying the possible impacts of future climate change, particularly as indirect and interacting factors may play as significant a role as those more direct effects (e.g. changes in water temperature with respect to known thermal tolerances) (Fealy *et al.*, 2010). This is illustrated by Figure 2.2 which highlights how any change in flow under altered climate conditions may impact salmonid species in a number of both direct and interacting ways (Milner *et al.*, 2010).

2.7.1 Species distribution and life cycle

Historically Atlantic salmon (*Salmo salar*) were widely distributed in all countries whose river systems discharged into the temperate and sub-arctic regions of the North Atlantic Ocean (MacCrimmon & Gots, 1979; Webb *et al.*, 2007); however, in recent decades their distribution has decreased and the number of returning adults has declined

significantly. Along with the overexploitation of stocks this decline is attributed to human interference with their ecology and habitat (Crisp, 2000). In Europe the distribution of Atlantic salmon currently ranges from northern Portugal to the Barents Sea; in addition this species can be found in the UK, Ireland, Iceland and Greenland. In North America its range extends along the eastern seaboard, from approximately 40°N to northern Quebec (Thorstad *et al.*, 2010).

Similar to many other salmonids, the Atlantic salmon is a diadromous species moving between the freshwater and marine environments in order to complete its life cycle. Typically juveniles will rear for a number of years in freshwater before undergoing a process of physiological change termed ‘smoltification’ which prepares them for life in the marine environment. Once they leave freshwater they migrate to their feeding grounds in the expanses of the North Atlantic; here they mature and become adults before returning to their natal streams and rivers with a high degree of fidelity in order to spawn and complete their life cycle (Thorstad *et al.*, 2010). Moving between the marine and freshwater environments allows them to fully exploit the resources available in both. In contrast, brown trout (*Salmo trutta*) - which is the other dominant salmonid species in Irish rivers - do not occur naturally in North America and are primarily regarded as being a European species. As it can remain resident in the freshwater environment to complete the various stages of its life cycle, this species has a much more flexible life history strategy.

Each stage in the life cycle of salmonids is intrinsically linked with variations in climate and weather events. Water temperatures influence key biological processes such as stock recruitment, growth rates and reproduction; whilst migratory behaviour, including the timing of entry to river systems and the rate of upstream progression is influenced by the flow regime (Graham & Harrod 2009, Mc Ginnity *et al.*, 2009). As salmonids use environmental variables as cues for migration, changes in flow and the timing of seasonal events have a greater potential to impact these species (Friedland, 2003).

Both salmon and trout are found in almost every river system in Ireland; however, they are more prevalent in those catchments situated along the Atlantic seaboard - particularly those catchments which have been to a lesser degree adversely impacted by human activity (Stefansson *et al.*, 2003; Harrod & Graham, 2009). Analysis of long-term survival and productivity trends suggest that populations of both species in Ireland

have suffered severe declines in recent decades (Stefansson *et al.*, 2003; Peyronnet *et al.*, 2007).

In parallel with increased sea-surface temperatures the number of adult salmon returning to Britain and Ireland has decreased significantly since the 1970s (Hendry & Cragg-Hine, 2003; Anon., 2005; Stefansson *et al.*, 2003; Beaugrand & Reid, 2003; Jonsson & Jonsson, 2004; Todd *et al.*, 2008). In England and Wales there is evidence that the number of returning adult Salmon has decreased by ~50% since the mid-1970s (Hendry & Cragg-Hine, 2003; Anon., 2005). For example, populations of Atlantic salmon and brown trout have declined in the Wye catchment by an estimated 50% and 67% respectively (over the period 1985-2004) (Clews *et al.*, 2010).

The steady decline in Irish stocks of Atlantic salmon mirrors a decline evident more generally across their distributional range. Along its southernmost limits salmon populations are mostly extirpated (Parrish *et al.*, 1998) and there is evidence that populations at more northerly latitudes, which in the past have been regarded as being relatively healthy, are also coming under threat (Graham & Harrod, 2009). Some of the causes implicated in the decline of both salmon and trout stocks include, amongst others, the over extraction of water resources, poor water quality, the intensification of aquaculture, the introduction of artificial barriers, the removal of riparian zones, the proliferation of disease, and increases in parasitic transmission (Graham & Harrod, 2009). Harrod and Graham (2009) indicate that regardless of how well stocks have been managed to date, or how well the aquatic environment has been protected in the past, climate change is likely to amplify the effects of any current anthropogenic stressors; climate change thus presents a complex set of challenges for catchment and fishery managers.

2.7.2 Climate change impacts on salmonids in freshwaters

A number of studies indicate that their sensitivity to environmental conditions (cold-adapted; requiring high DO levels), and the significant distances they must travel in order to complete their life cycle - exposing them to the rigors of the marine and freshwater environments and climate related changes in both - mean anadromous fish species are particularly vulnerable to changes in climate (Ottersen *et al.*, 2004; Harrod & Graham, 2004; Lassalle *et al.*, 2008). Although the Earth's climate has undergone

natural shifts in the past, aquatic species have been able to adapt to such changes through their evolutionary or behavioural response. However, the rate at which climate change is anticipated to occur may exceed the rate at which some species are capable of genetically or ecologically adapting. The innate ability of fish species to adapt to changes in their environment will vary according to the habitat and species considered; it will also depend on their individual tolerances, with some species benefitting and others losing out. A number of authors have indicated that Atlantic salmon may not be adapting at a quick enough rate to recent climate change; as a result localized extinctions are likely to occur (Friedland, 2003; Ottersen *et al.*, 2004; Graham & Harrod, 2009).

The thermal tolerances of salmonids at different stages in their life cycle is well-understood (Crisp, 1981; Elliott, 1991), and it is acknowledged that changes in temperature have the potential to affect each life stage differently (Crisp, 1981; Elliott, 1991; Friedland *et al.*, 2000; Friedland *et al.*, 2003; Salinger & Anderson, 2006; Peyronnet, 2008; Jonsson & Jonsson, 2009; Graham & Harrod, 2009; Mc Ginnity *et al.* 2009). For example increased water temperatures may negatively impact growth rates and productivity, reduce post-smolt survival and increase the susceptibility to disease and parasitic transmission (Hari *et al.*, 2006; Graham & Harrod, 2009; Mc Ginnity *et al.* 2009). Changes in the thermal regime of river and lake systems are also likely to alter the time at which different stages in the life history of salmonids occur. Jonsson and Jonsson (2009) state that traits such as, age at first maturity, longevity and fecundity decline with increasing temperatures. Enhanced water temperatures also have knock-on effects for water quality (e.g. eutrophication) and the wider functioning of freshwater ecosystems (e.g. food-web dynamics), thus changes in climate may impact salmonid populations in a myriad of both direct and indirect ways (Graham & Harrod, 2009).

Elliott and Elliott (2010) indicate that salmon are more sensitive to enhanced water temperatures when compared to trout, additionally the temperature tolerance for alevins is slightly lower than that for parr or smolts. Salmon eggs are noted as having the lowest thermal tolerance; consequently this life stage is highlighted as being the most vulnerable to any increase in water temperature. Elliott and Elliott (2010) state that if winter temperatures in southern Britain and Ireland continue to increase along their current trajectory it is possible they will soon exceed the upper thermal range for embryonic development in both salmon and trout. This highlights the possible

consequences climate change may have for recruitment success and the potential for population collapse to occur if particular thermal thresholds are breached.

In a study of the River Fiddich in north-east Scotland, Morrison (1989) found that Atlantic salmon parr grew faster and smolted earlier as a result of an increase in river water temperatures (between 1°C and 3°C). In the case of this river, discharges from local distilleries resulted in ambient water temperatures being increased through artificial means. Morrison (1989) discovered that the rate of parr growth was faster downstream of the effluent discharge points located along the river system. In a study of the Miramichi River - one of Canada's most productive salmon rivers - Swansburg *et al.* (2002) found that, under altered climate conditions, temperature thresholds are likely to occur earlier and for an extended period, adversely affecting the growth of juvenile salmon parr and reducing the overall productivity of the Miramichi system. Similarly, the results of a study by Lund *et al.* (2002) on the heat shock response of Atlantic salmon in the Miramichi, suggested that increases in temperature - similar to those projected to occur over the coming decades - could have significant consequences for productivity in this system. Graham and Harrod (2009) highlight the sensitivity of salmonids to DO levels, suggesting that under warmer conditions a reduction in DO would have the effect of increasing fish mortality, particularly during those more sensitive life stages (e.g. juvenile). Todd *et al.* (2010) state that enhanced water temperatures are likely to increase parr and smolt production in rivers at more northerly latitudes where productivity is currently constrained by lower water temperatures.

Davidson and Hazelwood (2005) formulated growth projections for Atlantic salmon in four UK rivers (Thames, Wye, Dee and Lune) using the UKCIP02 temperature scenarios. Their results suggested that under a low emissions scenario growth rates are projected to improve in those catchment systems located in the north and north-west. However, under a high emissions scenario, whereby thermal tolerances are exceeded over the latter half of the current century, model projections suggest a considerable decline in growth rates across all catchments (Davidson & Hazelwood, 2005). Davidson and Hazelwood (2005) state that in rivers along the southern edge of their distributional range (i.e. River Thames) - where on a regional basis warming in the UK is generally projected to be greatest - growth rates are anticipated to decline, with resultant consequences for the abundance, survival and productivity of salmon stocks in these areas.

It is widely acknowledged that temperature has a significant influence on the timing and rate of smoltification (Zydlewski *et al.*, 2005; Todd *et al.*, 2010). By altering growth rates, increasing temperatures may influence the size and age at which smoltification occurs (Jonsson & Jonsson, 2009). A study by Zydlewski *et al.* (2005) found that an earlier and more rapid increase in spring temperatures resulted in smolts migrating downstream earlier. Alterations in the timing of smoltification and the migration of smolts to sea have implications for post-smolt survival rates and success in the marine environment (Friedland *et al.*, 2003). The influence of increased temperature on growth rates and maturation in marine waters, as well as on the time of return migration have been variously explored by Martin and Mitchell (1985), Friedland (2000), Friedland *et al.* (2003) and Jonsson and Jonsson (2004).

Changes in precipitation and patterns of flow behaviour are as important for determining the impacts of climate change on salmonids as changes in other abiotic variables (Heggenes *et al.*, 1999; Mather *et al.*, 2008). Wenger *et al.* (2011) highlight that climate impact assessments conducted on freshwater biota have typically focused on temperature, ignoring critical drivers such as interspecific relationships and hydrological flow regimes. Variations in river flow determine the availability of suitable habitat and influence access to exploitable resources; as such hydrological regimes are critical for determining the local carrying capacity of river systems. Jowett (1992) found that the amount of available habitat was an important variable in determining the abundance of adult brown trout in 82 New Zealand Rivers. Similarly Gibson and Myers (1988) found a positive relationship between runoff and the survival of eggs and underyearling salmon parr in five Canadian river systems.

The life history strategy of salmonids has evolved largely in response to the hydrological conditions specific to the flow regime of their natal rivers (Dudgeon *et al.*, 2006). Consequently climate mediated changes in established patterns of flow behavior, and in particular alterations in the timing of seasonal events, may lead to a loss in the synchrony between the occurrence of various life history stages and optimal in-stream conditions. Changes in climate also have the potential to alter the nature (e.g. frequency, timing) of extreme flow events. Given their impact on mortality and the success of year-classes, any change in the occurrence of extreme flows have far reaching implications for the long-term sustainability of some salmonid populations. For example, extreme high flows can lead to the wash out of eggs and fry, whilst a reduction in flow may leave nests stranded and fish isolated in unfavourable habitats (Crisp, 1989). By

influencing fish movement and the connectivity of habitats, streamflow affects energy expenditure, feeding behaviour and the timing of migration (Armstrong *et al.*, 1998; Armstrong *et al.*, 2003; Berland *et al.*, 2004; Jonsson, 2009). For example, spates may be required for fish to ascend artificial or natural barriers and thus are essential for migratory progression. During prolonged low flow periods, upstream migration may be delayed, preventing access to more suitable spawning areas. In addition it has been shown that the occurrence of low flows can inhibit the movement of adults from coastal waters into river systems, potentially resulting in mortality and reducing recruitment levels (Soloman *et al.*, 1999; Soloman & Sambrook, 2004).

It is argued that changes in hydrology, coupled with the continued warming of both the freshwater and marine environments, will result in a northward shift in the biogeographical range of Atlantic salmon. This will result in the loss of populations in areas along the southernmost limits of their range (e.g. Iberian Peninsula and France), whilst territories further northward which are presently unsuitable (e.g. arctic rivers) are likely to be exploited (Stefansson *et al.*, 2003; Todd *et al.*, 2010). Todd *et al.* (2010) indicate that given the increases in drought and water temperature projected to occur across Europe, it is possible that populations as far north as southern England may become extinct. Similarly, it is likely that the southernmost populations of Atlantic salmon in North America will be under the greatest threat of extinction (Reist *et al.*, 2006). In reference to the British Isles, Graham and Harrod (2009) indicate that increased water temperatures may enhance productivity and growth in northern and upland populations; however, in southern and lowland areas increased temperature and a reduction in DO may result in population losses.

2.8 A summary of the anticipated impacts of climate change on salmonids

Climate change is likely to pose a significant threat to the continued existence of viable salmon stocks in many waterways across Ireland. Figure 2.4 highlights the potential impacts of climate change on the various life stages of Atlantic salmon (Walsh & Kilsby, 2007). The following is a summary of the likely impacts of climate change on Atlantic salmon and trout sourced variously from Jonsson and Jonsson (2009), Stefansson *et al.* (2003), Graham and Harrod (2009) and Milner *et al.* (2010).

- The biogeographical distribution of Atlantic salmon is likely to move further northwards, with extinctions likely along its southernmost limits.
- Increases in temperature are likely to enhance the vulnerability of populations to disease and parasitic transmission.
- In northern and southern parts of the distribution range an increase in parr mortality rates during winter is likely. This is an anticipated outcome of increasing spring and winter droughts (southern regions) and less stable flow conditions (northern regions).
- Enhanced water temperature should favour warm-adapted cyprinid fish species over salmonids. In contrast eels (*Anguilla anguilla*) may be better placed to exploit higher water temperatures.
- An increase in growth rates is likely - with the caveat that temperatures remain within the optimal thermal range for growth and food sources aren't diminished.
- It is likely that the spawning time will be delayed, occurring in the autumn or early winter
- Warmer temperatures will advance the time of egg hatching and alevin emergence.
- Smoltification is likely to occur at an earlier age, especially in northern and intermediate parts of the distribution range.
- A disproportionate increase in the rate of warming in freshwaters, as opposed to the marine environment, may result in the earlier migration of smolts to sea with consequences for post-smolt survival.
- It is likely that upstream migration will occur earlier in the year. This would have the effect of altering patterns of energy use prior to spawning, with the possibility of increased adult mortalities and reduced recruitment levels.
- An increase in flow variability and the occurrence of extreme hydrological events may delay upstream migration, increasing the possibility of fish straying to other river systems.
- Drought during upstream migration may reduce spawning stocks and improve the reproductive success of small relative to large adults.
- It is likely that there will be an immediate phenotypic response to altered climate conditions; however, over the longer-term genetic changes in traits such as smolt age, the age of maturity and disease resistance may occur.

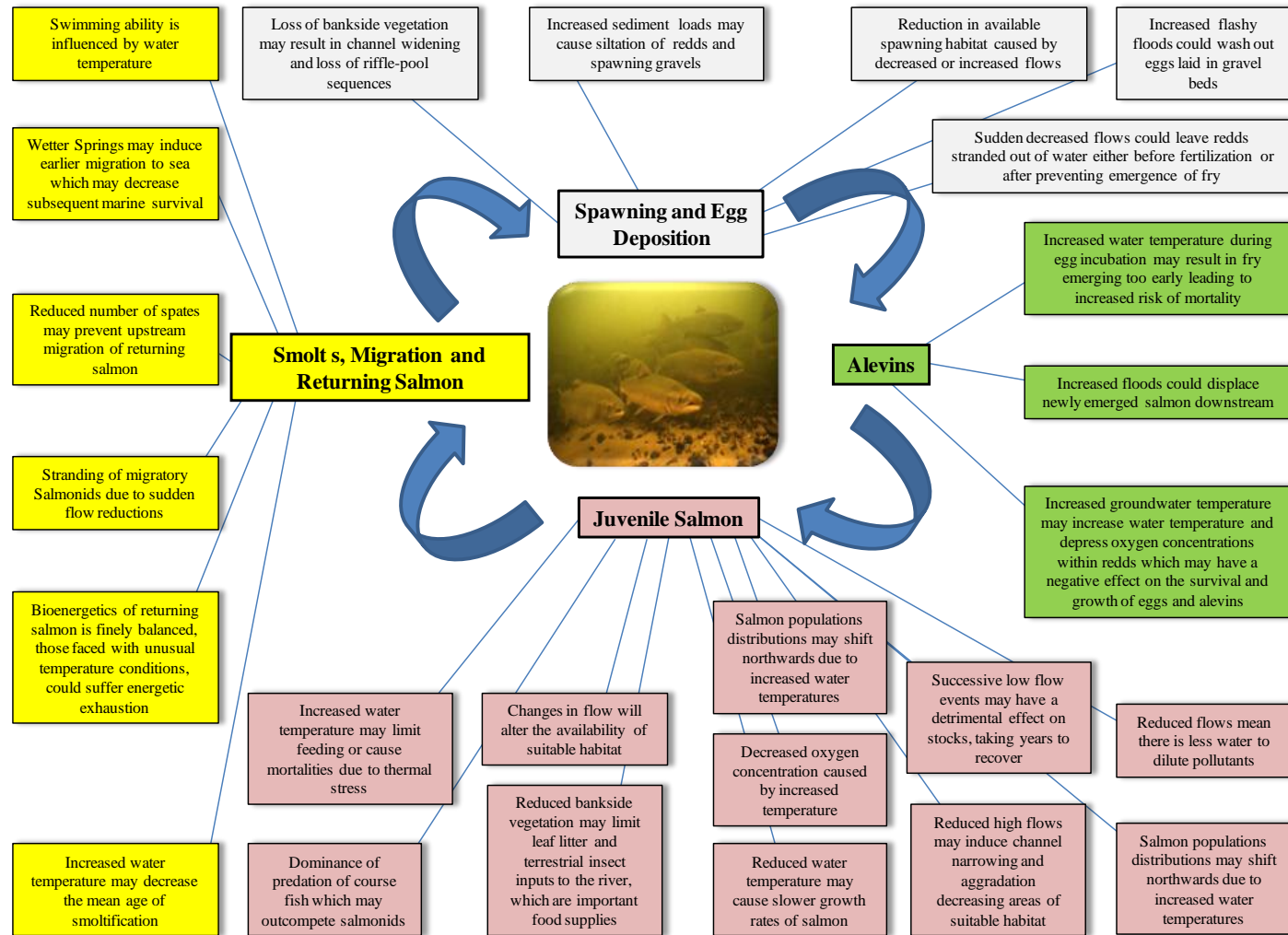


Figure 2.4 Potential impacts of climate change on the various life-stages of Atlantic salmon (*Salmo salar*) (Source: Walsh & Kilsby, 2007)

2.9 Conclusion

Scientific consensus attributes most of the recent warming experienced in the global climate to anthropogenic emissions of carbon dioxide and other greenhouse gases. If emissions remain on their current upward trajectory it is likely that the global climate will undergo further warming, with many unforeseen and possibly irreversible consequences for both human and environmental systems. Climate-mediated changes in precipitation and water temperature are likely to disrupt the functioning of freshwater ecosystems and reduce the availability of suitable in-stream habitats - with knock-on effects for the sustainability of some populations of freshwater and anadromous fish species.

The preceding sections provided evidence of anthropogenically induced changes in the global climate system, and importantly highlighted that climate change signals have already been detected in freshwater ecosystems. Although the impacts of recent climate change are more tangible with respect to changes in those physical, biological and chemical parameters which are temperature-dependent, it is suggested that over the coming decades a direct causal link between changes in lotic ecosystems and the intensification of the hydrological cycle will become increasingly apparent.

By altering the availability of suitable habitat, climate-mediated changes in patterns of flow behaviour are likely to undermine the local carrying capacity of river systems, leading to reductions in the abundance and productivity of native salmon stock. The observed progressive decline in their population numbers, along with their inherent sensitivity to environmental conditions and vulnerability to anthropogenic stressors, means it is important that the most deleterious effects of climate change on this species - which is of great ecological and cultural significance - are investigated and planned for. The study documented in the preceding chapters aims to explore how changes in climate may impact flow behaviour and habitat availability in a relatively productive upland system. The following chapter provides background information on the catchment and the datasets used.

Chapter 3

The Burrishoole catchment

3.1 Background

The Burrishoole catchment is a mainstay for much of the research conducted at both a national and international level on freshwater ecosystems and anadromous fish species - including the Atlantic salmon (*Salmo salar*), sea trout (*Salmo trutta*) and eel (*Anguilla anguilla*). The catchment holds international importance as a ‘sentinel system’ for monitoring the status of migratory fish stocks. Since the mid 1970s fish trapping facilities operated in the catchment have recorded the movement of all fish between the marine and freshwater environment of the catchment. The International Council for the Exploration of the Seas (ICES) use the fish census records from Burrishoole to gauge the overall status of fish stocks in Ireland and the North Atlantic region. In addition, much of the research conducted on anadromous species utilizes data collected from the Burrishoole catchment. The catchment is under the stewardship of the Marine Institute who have a dedicated research facility located within its confines. Along with operating the trapping facilities, they have implemented an extensive programme for monitoring environmental conditions across the catchment.

Datasets available from the catchment include long-term records of temperature and precipitation which date back nearly sixty years. Monitoring instruments installed more recently provide high-resolution data on thermal profiles and several water quality parameters (e.g. pH, DOC and DO). It is the availability of both long and short-term environmental datasets, along with the fish census records, and extensive empirical/local knowledge of the system which means it provides an ideal basis for studying the potential impacts of climate change on salmonid species. The similarity of the Burrishoole catchment to many catchment systems found along Ireland’s west coast - in terms of its ecology, hydrology and geomorphological characteristics - mean its response to altered forcing conditions provides an indication of the impacts climate change may have more generally across the region. This is significant given that Ireland’s most productive salmon rivers are located along the western seaboard.

3.2 Characterizing the catchment system

The Burrishoole catchment is located Ireland's on west coast near Newport Co. Mayo (9° 34' 20" W 53° 55' 22" N) (Figure 3.1) and comprises part of the Western Region Basin District (WRBD). The catchment (Figure 3.2) is nestled at the heart of the Nephin Beg mountain range and drains in a north-south direction from its upland headwaters through a freshwater lake and stream network, before reaching a brackish tidal lake system (*L. Furnace*) located in its lower confines. The Burrishoole catchment discharges into the Atlantic Ocean at the northeast corner of Clew bay. It takes on an almost idealized amphitheatre like shape with steep slopes to the north, west and east delineating its drainage boundary. The surrounding terrain is complex being characterised by localised valleys, steeply sloping mountain ranges and a flat alluvial valley floor at the confluence of the catchment's stream and lake systems. Its altitudinal range spans approximately 700 metres - from 10 m at the outlet point to over 700 m at the highest peaks on upland contributing areas. The western and upper parts of the catchment hold status as a Special Area of Conservation (Site name Owenduff/Nephin Complex; Site Code 000534).

Fish trapping facilities operated in the catchment are located on two channels known as the "Salmon Leap" and "Mill Race" which connect Lough Feeagh with the tidal Lough Furnace (Figure 3.2). These trapping installations are used to record the movement of all migratory fish between the freshwater environs of the catchment and coastal waters. Since 1970 a complete census of fish movement (both upstream and downstream) has been compiled; however, the catchment was first used as a site for fish trapping in 1958, and the records for some species date back this far.

The total area of the freshwater component of the Burrishoole system is 89.5 km². The catchment has a dense drainage network comprised of approximately 45 km of interconnecting shallow streams and rivers. In addition it encompasses seven lakes of various sizes; the three largest of which include Lough Bunaveela (0.54 km²), Lough Feeagh (4.1 km²) - both of which are freshwater lakes - and the brackish Lough Furnace (1.41 km²) (Whelan *et al.*, 1998). Both Lough Furnace and Lough Feeagh are situated in the lower parts of the Burrishoole valley, whilst the Bunaveela is located in the upper reaches of the Goulan sub-catchment.

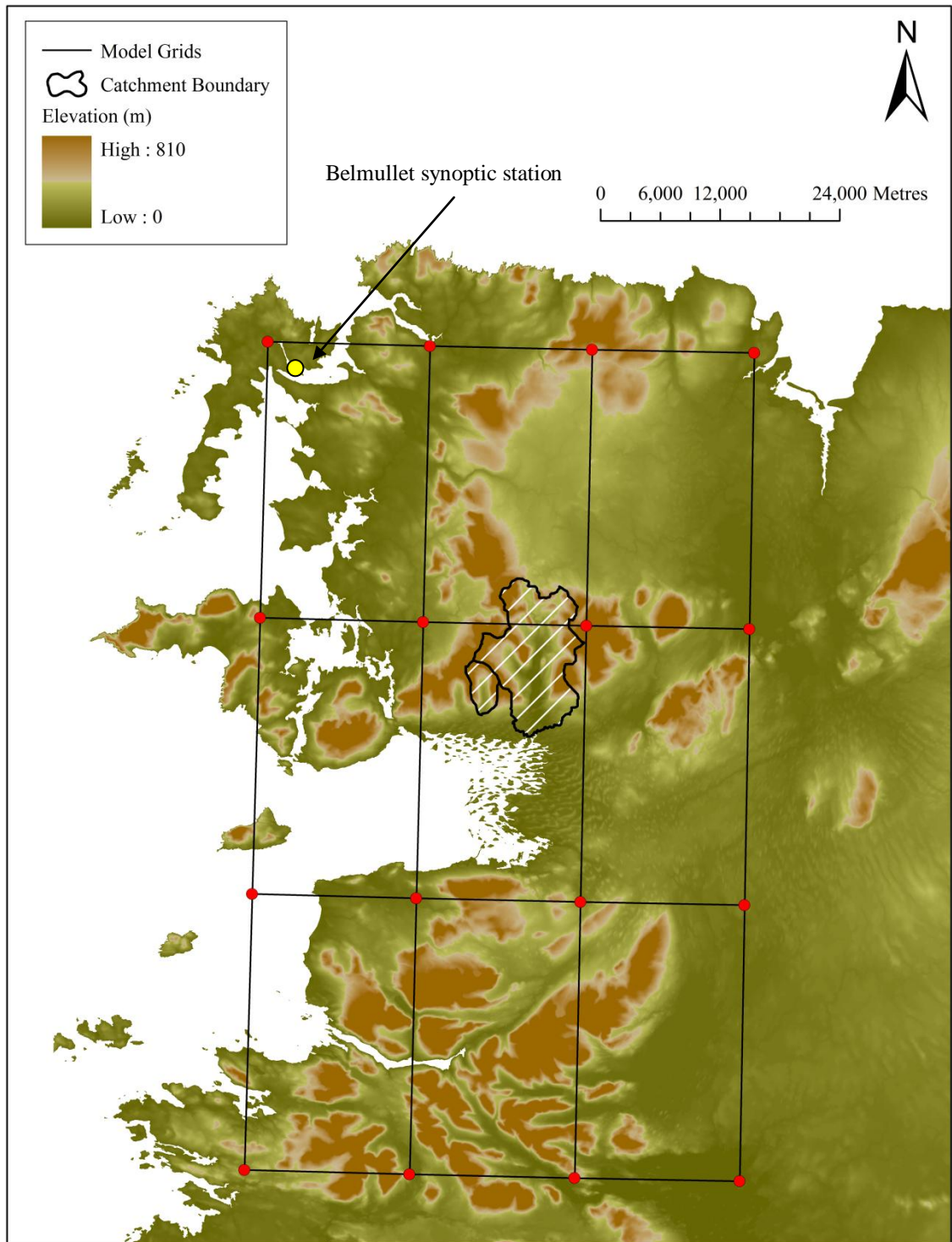


Figure 3.1 Location of the Burrishoole catchment and Belmullet synoptic station; also shown are the RCM grid boxes overlying the catchment.

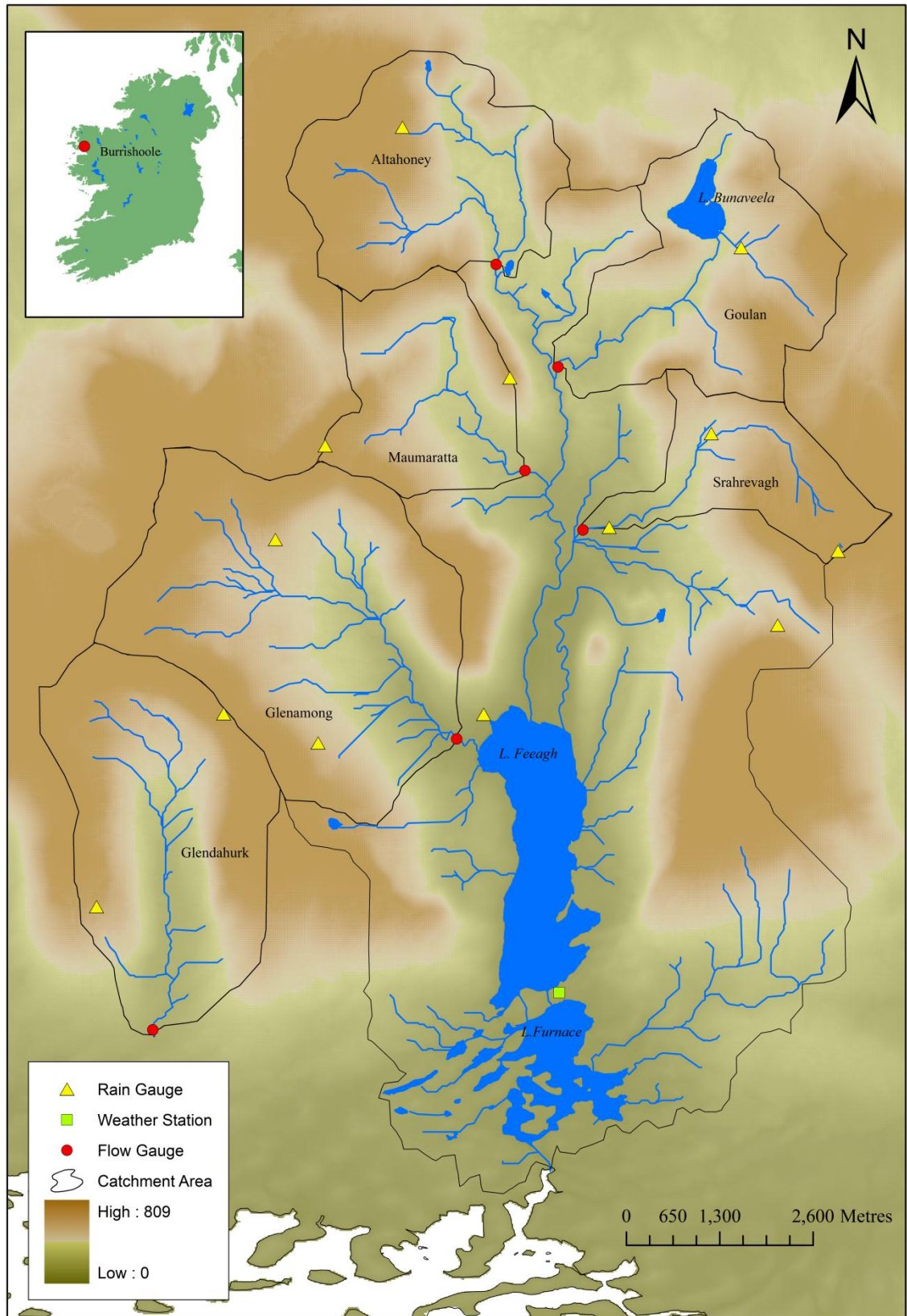


Figure 3.2 Map of the Burrishoole catchment showing each of the five constituent sub-catchments. Also shown is the Glendahurk catchment.

Metamorphic rock from the late Precambrian era comprises the bedrock geology of the catchment and can be apportioned accordingly; 44% quartzites, 44% schists/gneiss, 11% and 1% sandstone and limestone (Parker, 1977; Long *et al.*, 1992; Irvine *et al.*, 2000). In the lower parts of the catchment, towards its outlet point, metamorphic rocks dip below Devonian Old Red Sandstone and Carboniferous limestone. A terminal moraine delineating the boundary between the metamorphic and sedimentary rocks which underlie the catchment is located between Lough Furnace and Lough Feeagh.

Spatial differences in the underlying geology are reflected in the water chemistry and biological productivity of the catchment. Rivers on the western side of the catchment are generally more acidic and have a low buffering capacity (alkalinity in the order of -2.7 to $2.7 \text{ mg L}^{-1} \text{ CaCO}_3$); this is in contrast to those rivers draining the eastern side of the catchment, which generally have a pH level closer to circumneutral (in the order of 15 - $20 \text{ mg L}^{-1} \text{ CaCO}_3$) and as a result have a higher aquatic productivity (Fealy *et al.*, 2010).

Due to its underlying geology the catchment is characterised as having a relatively poor groundwater storage and transmissivity capacity. Figure 3.3 illustrates that the catchment is underlain by aquifers classified as being only locally productive (PI) (GSI, 2003). The overlying soils are mainly poorly drained peaty podzols and gleys, with blanket peatlands covering the mountain slopes to the north (Figure 3.4). Land cover (Figure 3.5) in the catchment comprises 64% peat bog and 23% forestry, with the remainder (13%) generally consisting of localised pockets of natural grassland, scrub, transitional woodland and agricultural land (CORINE, 2003).

Vegetation cover on the blanket peats is dominated by *Molinia caerulea*, *Schoenus nigricans* and *Scirpus caespitosus* (O'Sullivan, 1993). The predominant agricultural activity in the catchment is sheep grazing, with much of the peat bog area being treated as commonage (Weir, 1996). The Burrishoole catchment has a history as a site for commercial forestry activity. Afforestation schemes commenced in the catchment in 1951 and expanded between 1960 and 1969. Of the 23% of the catchment under forest, a large proportion of it is the result of commercial afforestation. The main species covering the catchment include Sitka spruce (*Picea sitchensis*) (26%) and Lodgepole pine (*Pinus contorta*) (70%); albeit that small areas of native oak woodland exist.

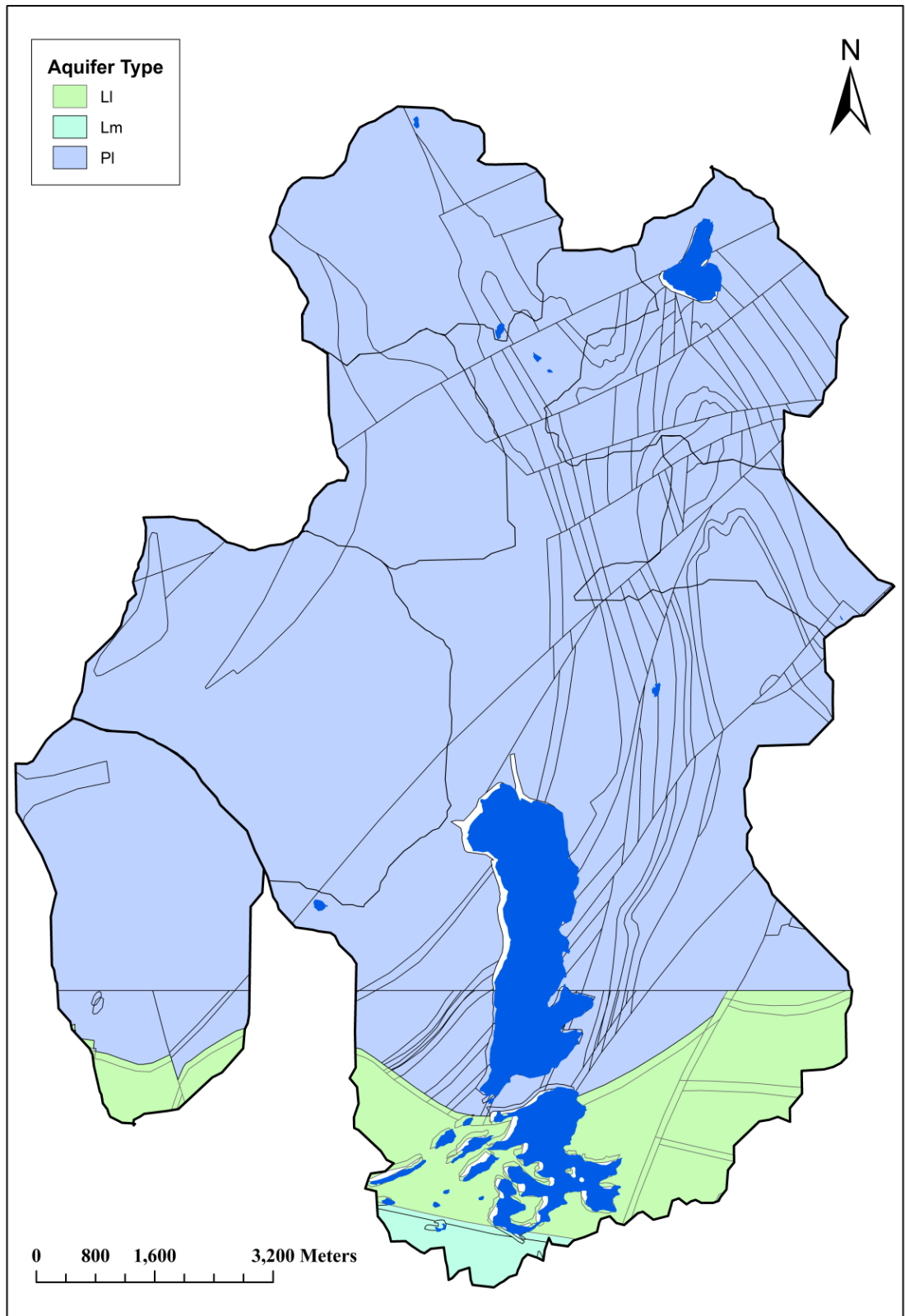


Figure 3.3 Aquifer productivity across the Burrishoole catchment (Source: GSI, 2003)

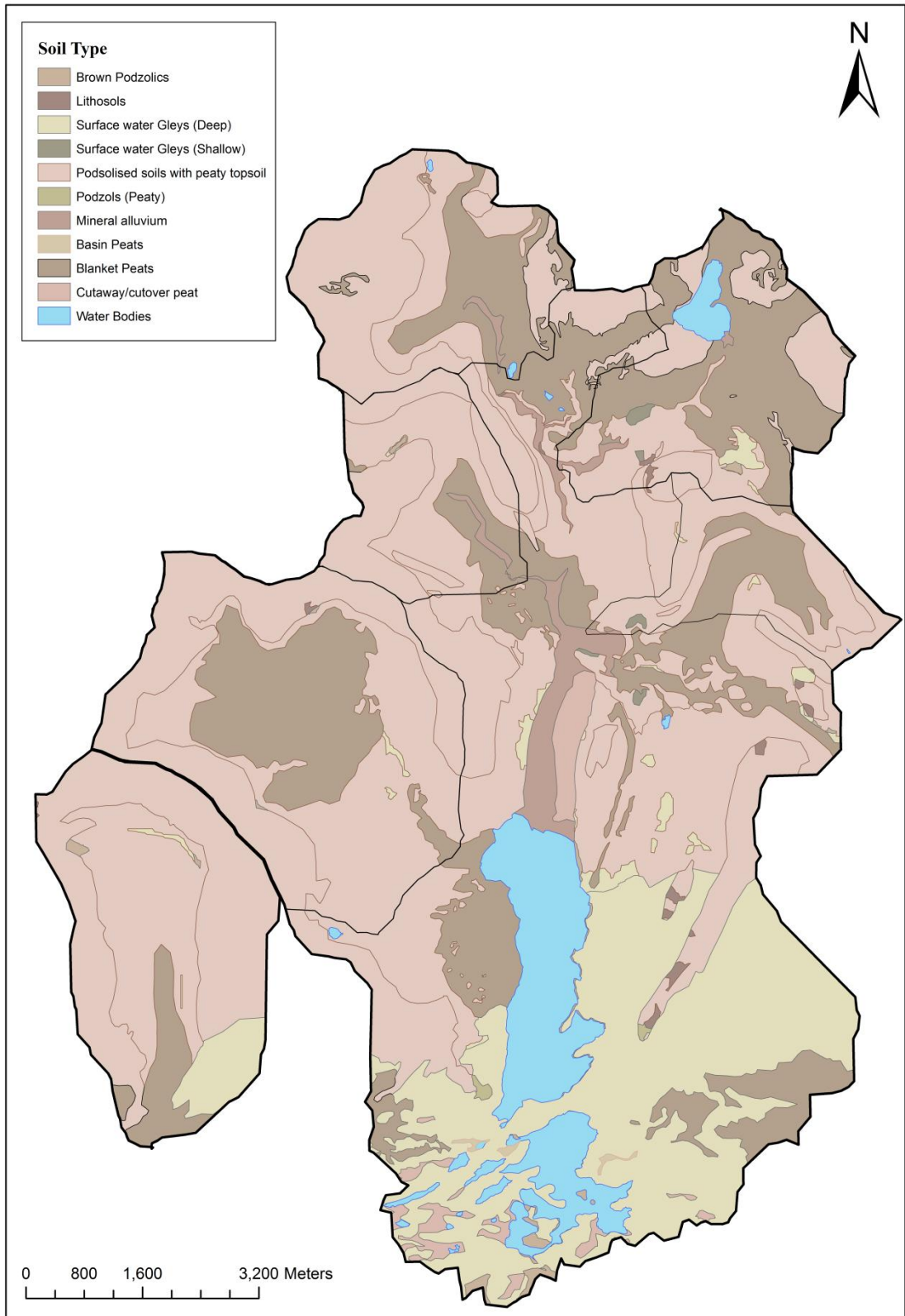


Figure 3.4 Soil cover across the Burrishoole catchment. (Source: Daly & Fealy, 2006)

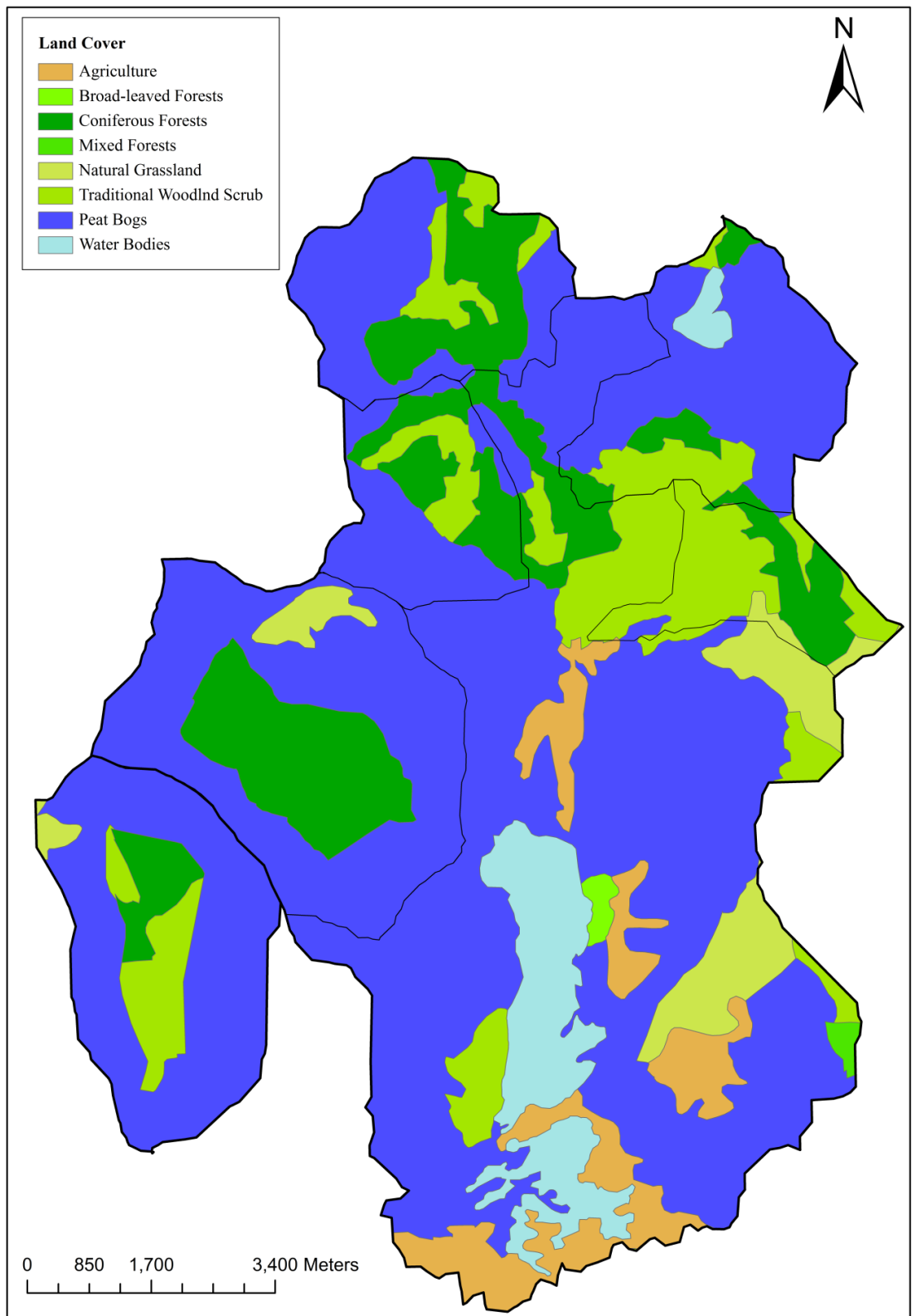


Figure 3.5 Land cover type across the Burrishoole catchment (Source: CORINE, 2003)

In the 1990s, clearfelling of forest plantations began; to date approximately 672 hectares or ~30% of the total plantation area has been removed. A number of studies have indicated that overgrazing and afforestation have impacted the catchment; however, any link between such impacts and a reduction in fish stocks has not been conclusively established.

3.3 Observed climatology

Owing to its close proximity to the Atlantic Ocean the catchment has a temperate maritime climate. The climograph in Figure 3.6 shows values for mean monthly temperature (°C) and precipitation receipts (mm) calculated over the period 1961-2000. Records indicate that annual average mean temperatures range from 9°C (1986) to 11.4°C (2007), in addition the records show that (averaged over the 40 year period 1961-2000) August (15.2°C), July (15.1°C) and June (13.8°C) are generally the warmest months whilst January (5.7°C), February (5.8°C) and December (6.5°C) are the coolest.

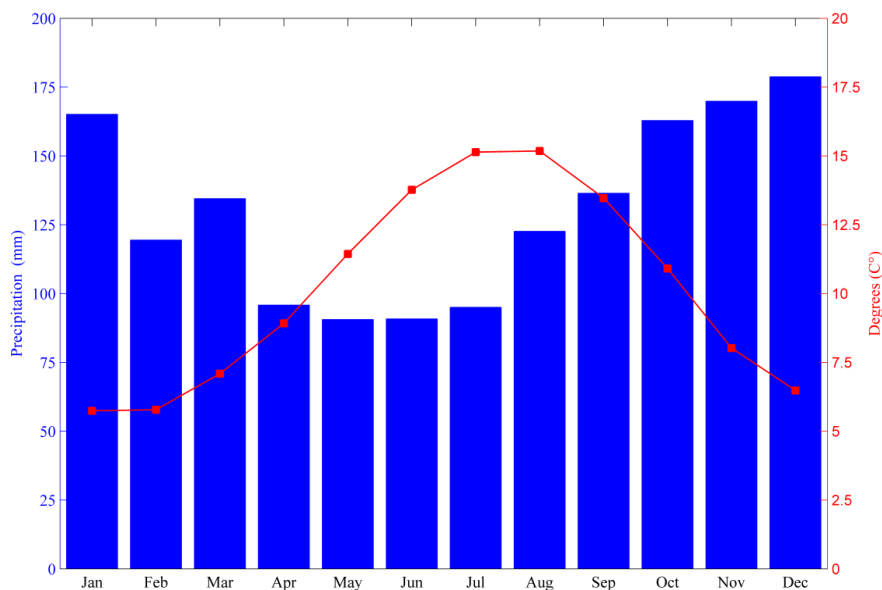


Figure 3.6 Climograph depicting average monthly precipitation receipts (mm) and mean monthly temperature °C for the Burrishoole catchment. The plot is estimated using records from the Furnace weather station (Figure 3.2) averaged over the period 1961-2000.

Precipitation receipts in the catchment are relatively high; this is due to the surrounding, upland terrain - which is conducive to orographic uplift - and the catchment's coastal location directly in the path of the prevailing rain bearing westerlies/south-westerlies. Multi-year annual precipitation yields range from 1118 mm (2009) to 1930 mm (2001), and records indicate that (averaged over the 40 year period 1961-2000) December (179 mm), November (170 mm) and January (165 mm) are generally the wettest months, whilst June (90 mm), May (95 mm) and July (95 mm) are typically the driest.

The complexity of the local topography leads to highly heterogeneous precipitation patterns across the catchment. Records from the catchment's own rain gauge network indicate that localized events - particularly with respect to extreme and heavy rainfall events - are an important feature of its precipitation regime. The spatially heterogeneous nature of precipitation is demonstrated by an extreme event (> 250 year return period) which occurred on the 2nd of July 2009 between 7 p.m. and 9 p.m. During this two hour period approximately 50 mm of rain fell on the eastern side of the catchment; however, over the same period, gauges on the western side recorded as little as 16 mm of rainfall. The precipitation which occurred is reflected in measurements from water level recorders located in the Goulán (6.48 m) and Srahrevagh (4.86 m) sub-catchments; however, given that the flow levels lie outside the ranges for which the recorders are rated, it is likely that these measurements represent an underestimation of the true values (Fealy *et al.*, 2010). Flooding events in both rivers are typically in the region of 1.2 to 2 m in height. It is noted that during this event water levels rose almost concurrently with the amount of precipitation recorded (Fealy *et al.*, 2010).

3.4 Sub-catchments of the Burrishoole system

As delineated by the location of gauging points across its stream network, the Burrishoole catchment can be divided into a series of five sub-catchments consisting of the Glenamong, Maurmatta, Altahoney (located in the west and north-west parts of the catchment) Goulán and Srahrevagh (situated in the north-east and east parts of the catchment). Each of these sub-catchments, either directly or through the larger stream network, drains into the two lakes situated on the valley floor. Also included is the Glendahurk catchment which lies adjacent to the Burrishoole catchment along its western drainage boundary. Although this is not part of the Burrishoole system, monitoring of this catchment system is conducted as part of monitoring operations carried out across the Burrishoole.

Of each catchment considered the Glenamong (17.2 km²) and Glendahurk (12.4 km²) (Table 3.1) are the largest, with the Srahrevagh (4.9 km²) being the smallest. Peat is overwhelmingly dominant in all sub-catchments, particularly the Altahoney (78% coverage), Goulán (100%) and Srahrevagh (89%). The Glenamong (70%) and Glendahurk (75%) are also notable for a high proportion of blanket peat coverage.

Lough Bunaveela, located in the Goulan catchment, is the only surface water body of notable size located in the any of the sub-catchments.

	Catchment					
	<i>Glendahurk</i>	<i>Glenamong</i>	<i>Maurmatta</i>	<i>Altahonev</i>	<i>Goulan</i>	<i>Sraheevagh</i>
CORINE Land Cover (%)						
<i>Agriculture</i>	-	-	-	-	-	1
<i>Coniferous forests</i>	9	28	32	32	11	30
<i>Natural grassland</i>	2	4	-	0	-	7
<i>Transitional woodland scrub</i>	15	-	16	13	14	59
<i>Peat bogs</i>	74	68	52	55	70	2
<i>Water bodies</i>	-	-	-	-	5	-
Aquifer Classification (%)						
<i>Poor aquifer, generally unproductive except in local zones (PI)</i>	88	100	100	100	100	100
<i>Locally important, generally moderately productive in local zones (LI)</i>	12	-	-	-	-	-
Soil Type (%)						
<i>Blanket Peat</i>	74	68	91	78	100	89
<i>Peaty Podzols</i>	26	32	9	22	-	11
Morphometric Attributes						
<i>Area (km²)</i>	12.4	17.1	6.4	9.2	9.6	4.9
<i>Min Elevation (m)</i>	47	12	54	94	59	23
<i>Max Elevation (m)</i>	710	708	383	626	389	550
<i>Slope (°)</i>	14.0	12.0	10.0	13.0	8.8	9.0

Table 3.1 Physical attributes of the five constituent sub-catchments of the greater Burrishoole system (Figure 3.2). Also listed are the physical properties of the Glendahurk catchment.

The flow regime of each sub-catchment is highly responsive to rainfall events, and exhibits behaviour typically associated with runoff dominated systems. This is related to the geometric properties of each drainage basin (e.g. steep slope, small area) and the poor productivity of the underlying aquifers. Both these factors contribute to the inability of each catchment to attenuate the rapid movement of water through their system or to dampen the streamflow response to heavy precipitation events. The low contribution of baseflow to catchment discharge - which is particularly evident during the drier summer months - underlines each catchment's lack of storage potential. Streamflow records for two of the sub-catchments indicate that they had completely dried up on at least one occasion after a sustained period without rainfall. The presence of blanket peatland plays a significant role in the catchment hydrology. It has been shown that well developed macropores and pipes which exist in the peat matrix provide an effective conduit for rapid subsurface flow (Holden & Burt, 2003; Holden, 2005). In addition, during storm events peat covered hillslopes are conducive to both infiltration and saturation excess overland flow. Thus in peat dominated systems rapid lateral (throughflow) and overland flow contribute to the 'flashy' nature of the storm response

(Holden & Burt, 2003; Holden, 2005). Given the history of commercial forestry in the Burrishoole catchment, it is possible that disruptions of the soil matrix may have altered its long-term hydrologic response. The extent to which this may have occurred is not known and records do not span a period long enough to investigate it.

3.5 Instruments and data

To provide a record of environmental conditions across the Burrishoole system, intensive instrumental monitoring of key climatological, chemical and ecological variables is conducted. The catchment has its own weather station whose records for temperature and precipitation date back over 60 years; it also has an extensive rain gauge network (Figure 3.2). Continuous recordings for several water quality parameters, including pH levels, DOC and DO are taken; in addition the thermal profile of the catchment's lake system is monitored, as are flow levels across its stream network. Also recorded are lake and stream water temperatures at various points across the catchment. The following sections provide information on the instrumental datasets employed in this study.

3.5.1 Furnace weather station

Instrumental records for daily temperature (maximum and minimum) and precipitation, covering the period 1961-2009, were obtained from the manually operated Furnace weather station (9°34'18"W 53°55'24"N); the station is located at an altitude of ~14m near the catchment's outlet point (Figure 3.2). Datasets from the weather station are of a high quality and a low proportion of the observed series is classified as missing or invalid (3.5% minimum temperature, 4.5% maximum temperature and 0.4% precipitation series) (Table 3.2). The weather station is operated by the Marine Institute in-conjunction with the Irish meteorological service, Met Éireann.

Variable	Record Date Start	Missing n (%)	Mean	Median	Std. Dev	95 % ile
Minimum Temperature (°C)	Jan-1960	3.5	13	13	4.4	20.3
Maximum Temperature (°C)	Jan-1960	4.5	7.3	7.4	4.1	13.7
Precipitation (mm)	Nov-1959	0.4	4.3	1.8	6.2	16.6

Table 3.2 Datasets from the Furnace weather station.

3.5.2 Belmullet weather station

Data for other meteorological variables including wind speed, relative humidity, radiation and potential evaporation were obtained from the Belmullet synoptic station (9°59'53"W 54°14'57"N) - located ~43 km to the north-west of the catchment (Figure 3.1). This is the closest synoptic station to the catchment and is operated by Met Éireann. Although monitoring for a number of these variables is also conducted in the catchment, records were either of an insufficient length or were of a poor quality; consequently synoptic records from the Belmullet station were used instead. With the exception of radiation (1981-2000) and potential evaporation (1971-2000), observed records for each variable were available for the period 1961-2000.

3.5.3 Upland rain gauge network

An extensive rain gauge network traverses the upper reaches of the catchment, with multiple gauging points being located within the boundary of each constituent sub-catchment (Figure 3.2). The observed rainfall series from the Furnace station is considerably longer (1959- 2009) than those provided by the more recently established upland gauges, many of which commenced operation in 2002. In total the datasets from twelve gauges located across the catchment are used in this study (Table 3.3).

Owing to the complexity of the local topography (e.g. elevation, slope, aspect), precipitation varies considerably across the catchment. For example, extreme events found to occur in the records from individual gauges are not found in the data series from others; this highlights the spatial heterogeneity of precipitation, even at a sub-catchment scale. The position of the weather station near sea level means it fails to capture the influence of orographic enhancement and the spatial variability of precipitation at higher elevations in the catchment. Given that the catchment system is highly responsive to rainfall events, this is an important consideration when attempting to understand and model the hydrology of each respective sub-catchment.

Gauge	Start Date	Data (days)	Missing n (%)	Altitude (m)	Mean (mm/day)	Median (mm/day)	95 % ile (mm/day)
<i>Glenamong 1</i>	May-02	1510	43.4	342	4.8	2.2	18.2
<i>Glenamong 2</i>	May-02	2397	10.2	197	5.4	3.1	20.4
<i>Glenamong 3</i>	May-02	2535	5.0	30	5.1	2.0	20.4
<i>Glenamong 4</i>	Jul-03	1925	14.4	204	6.5	2.6	24.7
<i>Maumaratta</i>	May-02	2083	21.9	263	5.2	2.2	20.8
<i>Altahoney</i>	May-02	1903	28.7	239	6.3	2.2	25.2
<i>Srahrevagh 1</i>	May-02	2505	6.1	372	4.4	1.6	18.8
<i>Srahrevagh 2</i>	May-02	2224	16.6	130	4.0	1.8	15.4
<i>Srahrevagh 3</i>	May-02	2233	16.3	23	4.8	1.8	19.3
<i>Goulan</i>	May-02	2492	6.6	131	5.1	2.0	20.1
<i>Namaroon</i>	Jan-04	1848	10.5	290	6.6	3.2	24.3
<i>Glendahurk</i>	Jun-03	1676	26.5	247	4.9	2.2	17.4

Table 3.3 Datasets from the Burrishoole catchment's upland rain gauge network. The record length and the proportion of missing values for each gauge are shown.

As shown in Table 3.3 a number of the rainfall datasets are of a poor quality; for example, ~43% of the daily entries in the Glenamong 1 series are missing. In order to obtain a complete precipitation series for the purposes of calibrating the rainfall-runoff models, the records from individual gauges were averaged. For each sub-catchment a weighted average of the available precipitation data was used to compensate for the missing entries in individual series. The weighting used was based on the correlation between the records from each gauge and the observed streamflow series. For each catchment only those gauges situated within, or in close proximity to the catchment boundary were considered; in addition, only those precipitation series which exhibited a strong correlation with streamflow were selected. This approach allowed for the spatial distribution of rainfall across each catchment to be considered, it also addressed the problematic issue of missing values in the data series. Despite the deficiencies in the datasets highlighted in Table 3.3, it must be acknowledged that the upland network provides high resolution information at a sub-catchment scale; in addition it offers good coverage of the catchment's altitudinal range.

3.5.4 Water level records

Water levels are recorded at the outlet point for each catchment on a 15 minute interval time step. Average daily volumetric flow values were obtained from recorded water levels using a rating curve formulated for each gauging point. The observed datasets were of varying lengths and quality with some displaying a high proportion of missing

values (e.g. Glendahurk ~20%). Table 3.4 provides details of the streamflow records for each catchment. The quality of available data was an important criterion for selecting which sub-catchments would be best suited for conducting in-depth hydrological modelling. Due to various deficiencies in either the precipitation or flow data, the number of catchments which could be considered for further analysis was limited to two, namely, the Glenamong and Srahrevagh.

Catchment	Start Date	End Date	Data (days)	Missing n (%)	Mean Daily (m ³ /sec)	Std. Dev (m ³ /sec)	95 % ile (m ³ /sec)
<i>Glenamong</i>	Jun-02	Aug-09	2398	10.1	0.93	1.172	3.26
<i>Maumaratta</i>	Jun-02	Aug-09	2392	10.3	0.46	0.66	1.49
<i>Altahoney</i>	May-02	Aug-09	2546	3.70	0.60	0.89	2.34
<i>Srahrevagh</i>	Jun-02	Aug-09	2419	9.30	0.32	1.85	1.03
<i>Goulan</i>	Apr-03	May-06	1096	5.30	0.34	0.38	1.11
<i>Glendahurk</i>	Jun-02	Aug-09	2125	20.4	0.18	0.30	0.71

Table 3.4 Streamflow records from the Burrishoole catchment. The length of the record provided by each recorder and the proportion of missing values is shown.

3.4.5 Data Quality Issues

As highlighted above a number of shortcomings are associated with the rain gauge and streamflow datasets available for use in this study. In terms of precipitation, the records from a number of gauging points had a high proportion of missing values - an issue compounded by the relatively short length of the datasets and the fact that deficiencies were generally common to the records obtained from all gauges. Given the highly heterogeneous nature of precipitation across the catchment, incomplete records created difficulties when attempting to calibrate the hydrological models, whereby large peaks in flow were noted to occur without the corresponding rainfall event being recorded. Despite the high density of the gauging network, the localized nature of rainfall across the catchment means that in cases where a particular gauge had failed, no record for important events (although being present in the corresponding flow data) existed. As outlined above, to overcome this shortcoming, a weighted average of the available precipitation series was used during model development.

The quality of the streamflow datasets was a key factor in determining which sub-catchments could be considered for use in this study. Similar to precipitation, a number of flow records had a high proportion of missing values, with some displaying evidence of disruption subsequent to the occurrence of an extreme event. There also appeared to be a degree of drift or/and a step change in a number of records, indicating that some

alteration of the channel shape or movement in the stage recorder had occurred. To explore the quality of the streamflow data available a double mass curve was constructed using the records from each of the six catchments (Figure 3.7). As its flow series was shown to be the most reliable when cross-referenced with other available flow and precipitation records, the streamflow series from the Glenamong catchment was used as a reference to evaluate the reliability of flow data from the other sub-catchments.

A degree of drift is evident in records from the Goulan, Maumaratta and Glendahurk; in addition a step change is noticeable in data from the Altahoney. In contrast there appears to be no such problems with the data from the Srahrevagh recorder. Given the flashy nature of the flow response and the influence this has on the channel form, it is possible that the stage-discharge relationship has changed over time, possibly leading to the drift evident in Figure 3.7. Closer inspection of the dataset from the Goulan indicates that an extreme event which occurred during December 2006 resulted in monitoring operations being disrupted - subsequent to this the instrument appears to under record flow levels (Figure 3.8). Attempts were made to correct both the streamflow and precipitation records; however, given the difficulties in pinpointing the exact time when drift appears to begin, together with the large proportion of missing values and the short record length, a robust correction could not be applied. Difficulties were compounded by the fact that both the mean and variance of some series appeared to change over time – thus a simple bias correction could not be applied. Anecdotally it is indicated that some recorders may have been moved or relocated in the event of instrument wash out occurring. Due to the data quality issues discussed above, only a sub-set of the catchments were selected for further study. This was a conscious attempt to reduce uncertainty introduced to the hydrological models by way of the observed data used (input and output); as such it is part of a wider strategy to address the issue of stationarity in the model response.

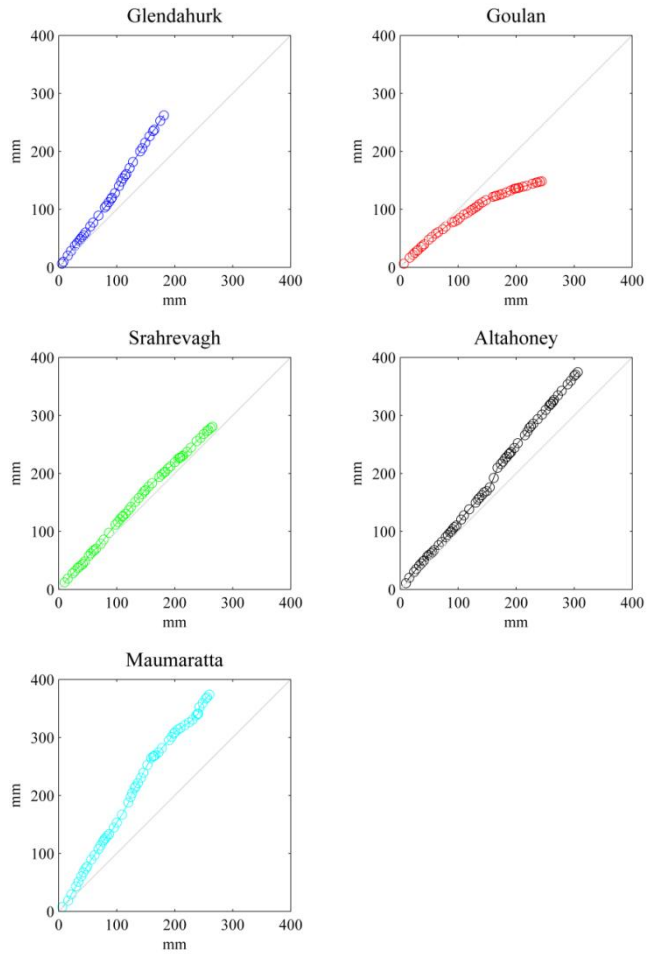


Figure 3.7 Double mass rating curves showing the cumulative monthly streamflow (mm) for each catchment plotted against data from the Glenamong recorder.

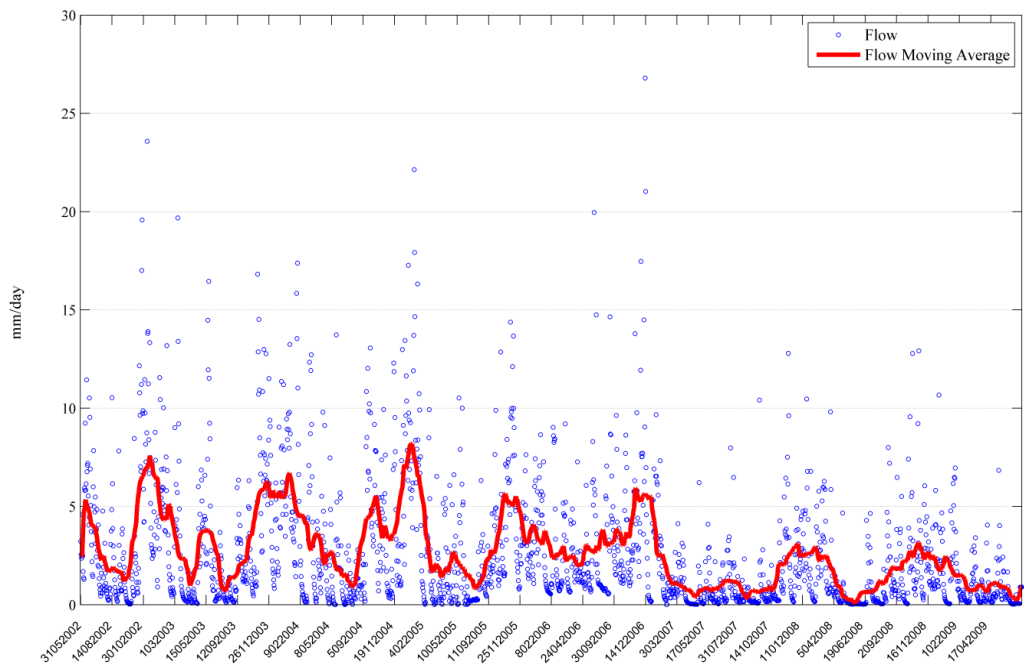


Figure 3.8 Smoothed time series for the Goulan catchment showing change in both the mean and variance of the flow series subsequent to an extreme event (circa. 14/12/2006).

3.6 Indicators of climate change in the Burrishoole catchment

Fealy *et al.* (2010) examined whether a climate change signal was present in the precipitation and temperature records from the Furnace weather station (Figure 3.2). In addition the study examined whether warming related trends were evident in records of lake water temperature. It was found that, over the period 1960-2009 (50 years), mean air temperatures in the catchment had increased significantly ($1.48\text{ }^{\circ}\text{C}$; $p < 0.001$). The rate of increase in daily maximum temperature was shown to be greater than minimum temperature (Fealy *et al.*, 2010). Seasonally, increases in mean temperature were greatest in spring ($1.8\text{ }^{\circ}\text{C}$) and winter ($1.7\text{ }^{\circ}\text{C}$); in contrast records indicated that summer ($1.5\text{ }^{\circ}\text{C}$) and autumn ($1.4\text{ }^{\circ}\text{C}$) had warmed to a lesser degree – albeit marginally so. When contrasted with Irish temperature anomalies over a similar time period (1960-2005), the mean annual increase in temperature recorded at Furnace ($1.1\text{ }^{\circ}\text{C}$) was found to have exceeded the national average ($0.9\text{ }^{\circ}\text{C}$) (Fealy *et al.*, 2010). Over the period 1960-2009 midnight lake water temperatures were found to have increased in all seasons and on an annual basis (Fealy *et al.*, 2010). Following trends in air temperature, the greatest increases in lake water temperatures were associated with winter ($1.8\text{ }^{\circ}\text{C}$) and spring ($1.79\text{ }^{\circ}\text{C}$) respectively.

An analysis of several temperature indices using metrics from the STARDEX project (STARDEX Final Report, 2005) supports evidence that the catchment has experienced warming over the past several decades. Records from Furnace indicated an increase in hot-temperature related indices and a decrease in cold-temperature related indices. For winter a significant increase was found in both the hot-day ($1.3\text{ }^{\circ}\text{C}$) and cold-day ($1.6\text{ }^{\circ}\text{C}$) thresholds. The records also indicated an increase in the duration of heat waves; this has been accompanied by an increase in the number of consecutive hot days (tmax 90th percentile).

The frequency and intensity of heavy precipitation - estimated using the 90th percentile of rain-day amounts - was found to have increased both for winter and on an annual basis (estimated over the 1960-2009). This finding is consistent with McElwain and Sweeney (2007) who found that extreme rainfall intensity has increased in the west of Ireland. The records indicated a small significant increase of 0.01 mm/year in mean annual precipitation receipts; however, on a seasonal basis, no significant increase/decrease in mean rainfall amounts was found to have occurred.

3.7 The status of Atlantic salmon (*Salmo salar*) in the Burrishoole catchment

The number of adult salmon returning to the catchment has been in decline since the 1970s (when full trapping began), with low numbers continuing each year since the 1980s (Figure 3.9). Numbers have fluctuated from a high of 1,777 in 1973 to a low of 252 in 1990 (Fealy *et al.*, 2010). Although a ban in drift netting for salmon was introduced in 2007 - which led to a notable increase in the number of returns for that year - numbers in 2008 and 2009 fell to levels similar to those recorded prior to the ban being introduced. It is noted in Fealy *et al.* (2010) that this sudden decline may be related to a decrease in marine survival consistent with a negative trend in pre-fishery abundance in Irish stocks (after Peyronnet *et al.*, 2007). The records for smolt migration show that the number of salmon recorded in downstream traps varies between a maximum of 16,136 (1976) and a minimum of 3,794 (1991) (Fealy *et al.*, 2010). Fealy *et al.* (2010) state that there is no discernible trend evident in the annual number of smolts migrating from the catchment.

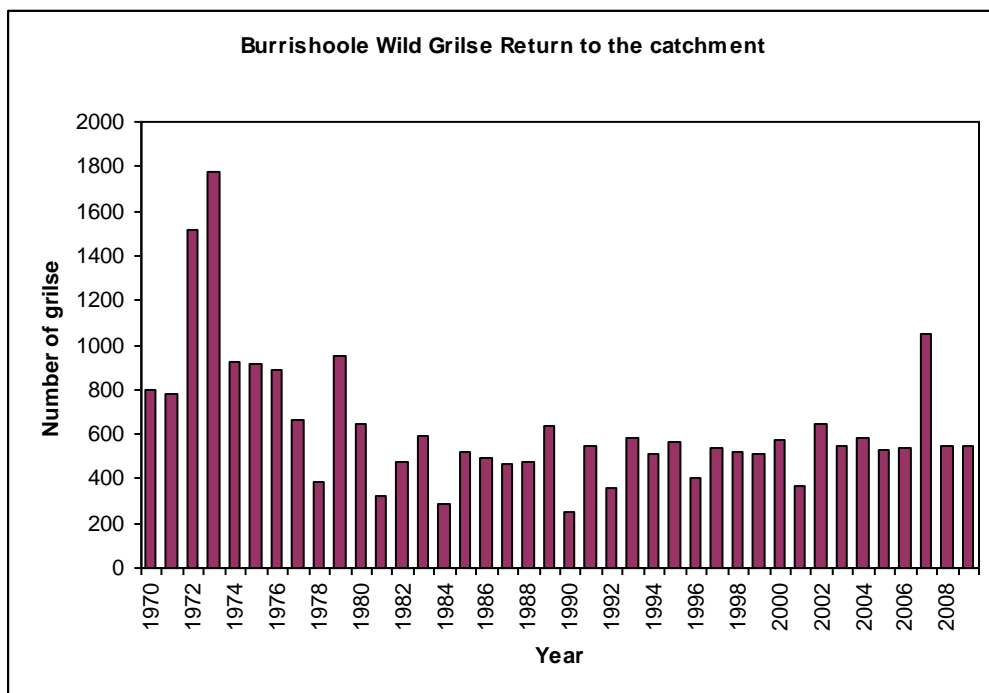


Figure 3.9 The number of wild adult salmon which returned to the Burrishoole catchment on an annual basis, recorded over the period 1970–2009 (Source: Fealy *et al.*, 2010)

3.8 Conclusion

The Burrishoole catchment provides an ideal case study for exploring the impacts of climate change on the freshwater habitat of Atlantic salmon. Although high quality

datasets for a range of environmental variables monitored in the catchment are available, deficiencies were evident in the quality of some precipitation and runoff records. Shortcomings in the observed data limited the number of catchments which could be considered for hydrological modelling. Critically trends found in long-term records from the catchment indicate that its climate has undergone warming consistent with trends found in national and global datasets. The biological and physical characteristics of the catchment - encapsulated by the fact it is a productive upland system, which is highly responsive to rainfall events and has a high peat content - suggests that the study findings should provide an insight into the potential impacts of climate change on other river systems located along the west coast, many of which are similar in nature to the Burrishoole. The following chapter outlines the uncertainties inherent in developing high-resolution climate projections for use in local to regional scale impact studies; in addition it discusses the merits of employing a performance based weighting system when using climate ensembles.

Chapter 4

Uncertainty and predictability in climate modelling

4.1 Introduction

Although we can state with a high degree of certainty that the Earth's climate system is likely to change in response to further increases in atmospheric GHGs, due to our limited understanding of feedback mechanisms and the inherent limitations to the predictability of regional or local scale climate, a large amount of uncertainty (of which a large part is irreducible) is implicitly associated with model projections of future climate change. While the scientific community is confident that anthropogenic emissions of GHGs and aerosols will alter the elemental composition of the Earth's atmosphere; there is much less confidence associated with exactly how the climate system may change in response to this (Dessai *et al.*, 2007). A considerable amount of uncertainty is associated with model estimates of future climate change – a fact illustrated by the lack of convergence in the projections from individual climate models, even in cases where the same forcing scenarios are used. This divergence applies not only to the magnitude but also to timing, spatial distribution and direction of change. These uncertainties pose major challenges for policy makers who ideally require probabilistic projections of future change which adhere to the risk assessment framework used to formulate robust adaptation strategies (Schneider, 2001).

As illustrated in Figure 4.1, uncertainty arises at each stage in the process of translating storylines of anthropogenic GHG emissions into scenarios of future climate change (Jones, 2000; Moss & Schneider, 2000; Wilby, 2005). The accumulation or propagation of uncertainty at each stage has variously been described as the “cascade of uncertainty” (Schneider, 1983) or the “uncertainty explosion” (Henderson-Sellers, 1993) (Figure 4.2). Model projected changes in the climate system are subject to a high degree of uncertainty stemming from both aleatory (‘unknowable’ knowledge) and epistemic (‘incomplete’ knowledge’) sources (Hulme & Carter, 1999; Jones, 2000; New & Hulme, 2000; Oberkampf *et al.*, 2002). The latter arises due to our limited understanding of climate system processes and their imperfect representation in climate models - both of which introduce uncertainty when modelling the climate system

response to a change in forcing. With greater knowledge and improvements in computing power this source of uncertainty has the potential to be somewhat redressed.

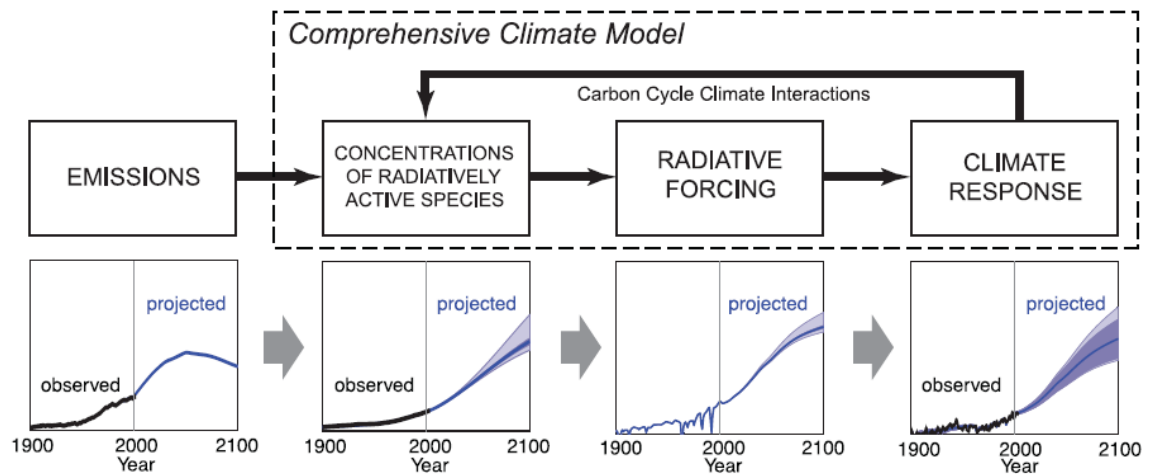


Figure 4.1 Uncertainty arises at each step in the process of modelling the potential climate response to altered forcing conditions (Source: IPCC, 2007).

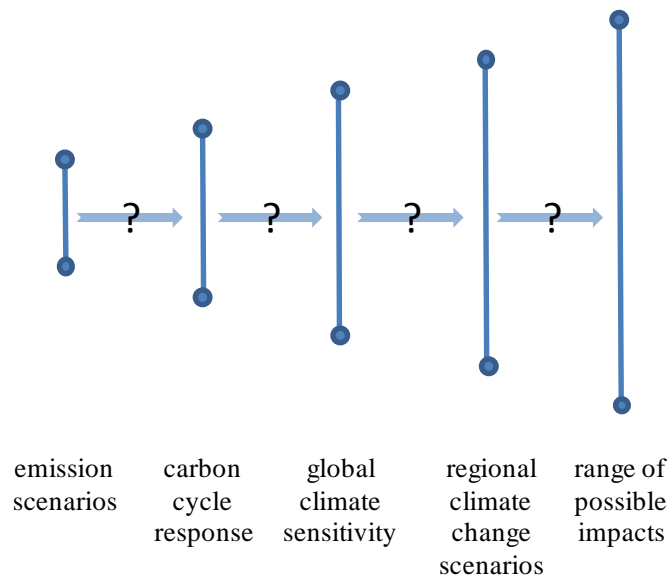


Figure 4.2 Key uncertainties in climate impact assessments represented using the “uncertainty explosion”. Uncertainty is amplified as it is propagated through each stage of the modelling process; (modified after Jones, 2000 and “cascading pyramid of uncertainties” in Schneider, 1983 (Source: IPCC, 2001).

Aleatory uncertainty refers to the unpredictable and ‘chaotic’ nature of the climate system, both in the real world and in model simulations. This source of uncertainty is most conspicuously associated with the impossibility of knowing the exact socio-economic pathway human development will take, and stemming from this, how atmospheric concentrations of carbon dioxide and other GHGs are likely to change as a result. To address uncertainties which arise due to unpredictability, different ‘scenarios’ or storylines are used to represent a range of possible outcomes or sequence of events. In terms of anthropogenic GHGs, various storylines of human-societal development are

used to formulate different emission scenarios. With respect to the ‘chaotic’ nature of the climate system, epistemic uncertainty is accounted for by performing multiple model simulations whereby the initial state of the system is adjusted between successive model runs. This approach allows a range of equally plausible yet (often) dissimilar projections of future climate, which are representative of natural climate variability, to be generated. For each simulation the temporal evolution of the system is different; however, the underlying climate signal - which is one of a warming climate - remains the same.

With respect to the predictability of local-scale climate, the principal sources of uncertainty include, the model formulation (e.g. the numerical scheme, parameterization and grid resolution), forcing scenario and natural climate variability - the latter of which includes internal unforced variability (i.e. initial conditions) and natural forced variability (e.g. solar forcing) (Maraun *et al.*, 2010). Van der Linden and Mitchell (2009) list the major sources of uncertainty identified by the EU funded ENSEMBLES project (van der Linden & Mitchell, 2009), this includes:

- The socio-economic assumptions upon which emissions scenarios are based (e.g. technological development, land-use and carbon taxation).
- Feedbacks from changes in the climate system on socio-economic systems - leading to reactionary changes in anthropogenic emissions which, in-turn, affect the projected rate of future change in the climate system.
- Translating GHG emissions into atmospheric concentrations of radiatively active gases.
- Translating atmospheric GHG concentrations to radiative forcing.
- Uncertainties associated with climate observations (e.g. distribution patterns of atmospheric constituents).
- Uncertainties associated with different classes of model error, including structural model uncertainty (stemming from basic model construction), uncertainty in the parameterisation of sub-grid scale processes (e.g. cloud physics) and stochastic uncertainties arising from the coupling between unresolved sub-grid scale variability and the resolved grid-scale flow.
- The initial model state (e.g. ocean temperatures).
- Dynamical downscaling between global (GCMs) and regional climate models (RCMs) (e.g. driving boundary conditions, the choice of GCM/RCM combination).

- Statistical downscaling of GCM output (e.g. choice of predictors, assumption of stationarity in empirical relationships).

4.2 Emission scenarios and atmospheric greenhouse gas concentrations

To model changes in the climate system arising from anthropogenic forcings, GCMs must take account of future atmospheric concentrations of GHGs (CO₂, CH₄, N₂O, etc.) and aerosol emissions. The IPCC Special Report on Emission Scenarios (SRES) outlines several different storylines which plot possible directions of human development through the 21st century (Nakicenovic *et al.*, 2000). Each storyline is based on various assumptions about future agricultural and land-use practices, demographic change and economic development; also considered is the possible role of carbon-free and renewable energy resources. These narratives are the basis for formulating different emission scenarios. Each of the SRES storylines of future development - of which there are 40 - can be related to four preliminary marker scenarios; A1, A2, B1 and B2 (Box 4.1).

A1. The A1 storyline and scenario family describes a future world of very rapid economic growth, global population that peaks in mid-century and declines thereafter, and the rapid introduction of new and more efficient technologies. Major underlying themes are convergence among regions, capacity building and increased cultural and social interactions, with a substantial reduction in regional differences in per capita income. The A1 scenario family develops into three groups that describe alternative directions of technological change in the energy system. The three A1 groups are distinguished by their technological emphasis: fossil intensive (A1FI), non-fossil energy sources (A1T), or a balance across all sources (A1B) (where balanced is defined as not relying too heavily on one particular energy source, on the assumption that similar improvement rates apply to all energy supply and end-use technologies).

A2. The A2 storyline and scenario family describes a very heterogeneous world. The underlying theme is self-reliance and preservation of local identities. Fertility patterns across regions converge very slowly, which results in continuously increasing population. Economic development is primarily regionally oriented and per capita economic growth and technological change more fragmented and slower than other storylines.

B1. The B1 storyline and scenario family describes a convergent world with the same global population, that peaks in mid-century and declines thereafter, as in the A1 storyline, but with rapid change in economic structures toward a service and information economy, with reductions in material intensity and the introduction of clean and resource-efficient technologies. The emphasis is on global solutions to economic, social and environmental sustainability, including improved equity, but without additional climate initiatives.

B2. The B2 storyline and scenario family describes a world in which the emphasis is on local solutions to economic, social and environmental sustainability. It is a world with continuously increasing global population, at a rate lower than A2, intermediate levels of economic development, and less rapid and more diverse technological change than in the A1 and B1 storylines. While the scenario is also oriented towards environmental protection and social equity, it focuses on local and regional levels.

Box 4.1 The four SRES scenario 'families' (IPCC, 2001 after Nakicenovic *et al.*, 2000).

As highlighted by New & Hulme (2000) the four marker scenarios account for approximately 80-90% of the range in future emissions. The uncertainties associated with future emission pathways stem from assumptions made about the underlying socio-economic drivers and the means by which future emissions are quantified using each narrative. Depending on the scenario considered, atmospheric concentrations of CO₂ vary significantly, ranging from 540 ppmv to 970 ppmv by 2100 (IPCC, 2007a) - much greater than present day (~391 ppmv) or pre-industrial levels (~280 ppmv).

Emission scenarios describe changes in atmospheric GHGs for a range of plausible futures; however, it is essentially impossible to provide scenarios which cover all eventualities. In this respect it is possible that a scenario never considered may come to pass. Consequently, even at this initial stage, if all scenarios were to be explored in the construction of local scale climate projections, a significant level of uncertainty would remain (Foley, 2010a). The results from model simulations presented in the IPCC Fourth Assessment Report (AR4) (2007a) suggest that the dominant factor explaining the spread in climate projections is the emission scenario used. The projections indicate that it is generally during the latter half of the current century that the emission scenario has a discernible influence on the model response; thus, uncertainty introduced by way of the emission scenario is to a certain extent dependent on the time scales considered.

Uncertainty associated with future GHG emissions is further compounded when translating the SRES scenarios into atmospheric concentrations of radiatively active gases. This is due to deficiencies in our understanding of the natural sources and sinks of each GHG and the impact climatic feedbacks may have on them. For example, global models of the coupled climate-carbon system indicate that atmospheric warming is likely to reduce the capacity of terrestrial and marine systems to absorb carbon dioxide (Cox *et al.*, 2000; Dufresne *et al.*, 2002; Friedlingstein *et al.*, 2006). An incomplete knowledge of the behaviour, spatial distribution and lifespan of GHGs in the atmosphere also contributes to uncertainties in biogeochemical cycles and estimates of future radiative forcing.

It is intended that four new scenarios of anthropogenic radiative forcing, known as representative concentration pathways (RCPs), will replace the current SRES emission scenarios (Moss *et al.*, 2009; van Vuuren *et al.*, 2009; Inman, 2011). Each pathway outlines changes in the Earth's radiative forcing (8.5 W m⁻², 6 W m⁻², 4.5 W m⁻² and 2.6 W m⁻²) arising from different socio-economic and technological development scenarios. The range covered by the RCPs is wider than previously considered in IPCC

reports (Inman, 2011); for example, they include a scenario (IMAGE 2.6) which projects that the world's emissions will drop below zero (circa. 2070), and become negative thereafter. In addition, the most warming intensive scenario (MESSAGE 8.5) suggests that atmospheric carbon dioxide would rise above 1,300 ppm by 2100. The RCPs are the basis for the most recent climate model experiments, the results of which will inform the next IPCC assessment report (AR5).

4.3 Climate sensitivity and radiative forcing

There are various uncertainties associated with our understanding of how the Earth's radiative balance may change in response to an increase in atmospheric GHGs and other radiative forcings - the most prominent of which include anthropogenic aerosols (e.g. sulphate, black carbon) and stratospheric ozone. Whilst the effects of increasing CO₂ are generally well understood, the influence which other GHGs and aerosols may have is not. It is uncertain what the dominant effect of aerosols is likely to be; this refers both to their role in cloud formation and the direct influence they have on the absorption and scattering of solar radiation. Loeb and Su (2010) indicate that radiative forcing by aerosols is the largest uncertainty in anthropogenic radiative forcing of the global climate. Uncertainty also stems from how warming related feedbacks initiated in the climate system may act to amplify or dampen changes in the radiative balance (e.g. a reduction in the Earth's albedo resulting from melting ice-caps).

Even if future concentrations of atmospheric GHGs were known, and could be translated into an exact corresponding change in the radiative balance, a considerable amount of uncertainty in the climate response would remain. Climate sensitivity is a measure of how responsive the climate system is to a change in forcing. It is defined by Roe and Baker (2007: 629) as “the equilibrium change in global and annual mean surface air temperature, T , due to an increment in downward radiative flux, R_f , that would result from sustained doubling of atmospheric CO₂ over its pre-industrial value of ~280 ppm ($2 \times \text{CO}_2 \sim 560 \text{ ppm}$)”. Assuming the climate system undergoes a doubling of forcing ΔF_{2x} (~3.7 Wm²) (IPCC, 2007a) - consistent with a doubling of atmospheric CO₂ - ΔT_{2x} is the resultant change in the globally averaged surface air temperature when the system reaches its new equilibrium state. The sensitivity of the climate system to this forcing is therefore:

$$\lambda = \Delta T_{2x} / \Delta F_{2x}$$

Based on the equation above, the anthropogenic contribution to radiative forcing can be quantified as a change in the globally averaged surface air temperature response. Understanding and quantifying the climate sensitivity, including the role of various feedbacks (e.g. cloud, ice-albedo and water vapour) and interactions which may dampen or amplify the effects of climate forcing is critical when modelling future changes in the climate system. According to Cox and Stephenson (2007) climate sensitivity is the largest source of uncertainty in projections of future climate on time scales beyond a few decades. Given that the magnitude of model projected changes in climate are strongly related to the responsiveness of the climate system, there is an onus on the scientific community to quantify, and where possible reduce uncertainty in the climate response.

On the basis of available evidence the IPCC AR4 (2007a) suggests a climate sensitivity of $\sim 3^{\circ}\text{C}$ for a normal distribution, with a likely range of approximately $2\text{--}4.5^{\circ}\text{C}$ (5 to 95% probability). For a log-normal distribution the climate sensitivity is estimated to be between 2.1°C and 4.6°C (5 to 95% probability) with a median value of 3.2°C . Although it is impossible to rule out higher values ($>4.5^{\circ}\text{C}$), it is stated that the lower sensitivity limit is very likely to be greater than 1.5°C (IPCC, 2007a; Knutti & Hegerl, 2008; Knutti *et al.*, 2008). Knutti and Hegerl (2008) reviewed the current scientific understanding of climate sensitivity; based on the various studies they considered - which spanned different timescales and methodological approaches - the authors concluded that sensitivity is within the generally accepted range of 2°C - 4.5°C .

Estimates of the climate sensitivity have been obtained through an examination of trends found in instrumental records of global temperature (~ 150 years) (Räisänen, 2007; Knutti & Hegerl, 2008). The observed climate response to solar cycles and volcanic activity has also been used to investigate the climate sensitivity. Climate model experiments and the investigation of paleoclimatological records provide two additional lines of inquiry into the response of the climate system to a change in forcing (Räisänen, 2007; Foley, 2010b). Whilst all climate models are based on the same immutable physical laws, as they variously differ with respect to their design, structure, and parameterization, as well as how important climatic processes, feedback mechanisms and system interactions are represented, the sensitivity of individual models to perturbed forcing conditions differs also. As a result the climate response can be explored by analysing the output from a multi-model ensemble (MME) of climate simulations (e.g. Yokohata *et al.*, 2008). For example, estimates of sensitivity based on

an 18 model ensemble are reported in the IPCC AR4 (2007a). Similarly, the climate sensitivity may be investigated using a perturbed-physics approach, whereby the parameters of the same model are altered between successive model runs (Piani *et al.*, 2005; Stainforth *et al.*, 2005). This approach is based on sampling those parameters (within their estimated uncertainty ranges) which influence the simulation of key system processes (Rougier *et al.*, 2009). Although the members of a perturbed-physics ensemble (PPE) share the same parent model (with the same basic structure), the responsiveness of the model's parameters is such that altering their values creates numerous permutations of the same model with widely varying degrees of sensitivity (Räisänen, 2007). Stainforth *et al.* (2005) report results from the *climateprediction.net* experiment - a perturbed model experiment consisting of over 2000 simulations. According to Stainforth *et al.* (2005) climate sensitivities were found to range from less than 2°C to more than 11°C; only 4.2% of the simulations exceeded 8°C, and most were found to cluster around 3.4°C. Piani *et al.* (2005) evaluated the *climateprediction.net* ensemble using observations of present day climate and found that the climate sensitivity was at a best estimate 3.3°C, but ranged between 2.2°C (5th percentile) and 6.8°C (95th percentile).

Paleoclimate data from sources including ice-cores and speleotherms - used as proxy records for changes in the global climate - have been employed to explore the response of the climate system to changes in forcing through geological time. A study by Zeebe *et al.* (2009), which considered changes in climate over the Palaeocene–Eocene Thermal Maximum (circa. 55 million years ago) - during which the planet warmed by between 5°C and 9°C - found that atmospheric carbon dioxide increased during the main event by less than ~70% (relative to pre-event levels). Based on the currently accepted values for climate sensitivity, this rise in CO₂ can only explain between 1°C and 3.5°C of the warming inferred from proxy data. The study concludes that, in addition to direct CO₂ forcing, other processes and/or feedbacks that are as of yet unknown must have caused a significant portion of the warming experienced during the Palaeocene–Eocene Thermal Maximum - suggesting that the climate sensitivity may be greater than currently estimated. A study by Schmittner *et al.* (2011) combined temperature reconstructions of the Last Glacial Maximum (circa 20,000 years ago) with the output from climate model simulations to explore the climate sensitivity. In contrast to the generally accepted range, their study findings suggested that sensitivity may be much lower than stated in the 2007 IPCC report (2.3°C as the median; 1.7°C to 2.6°C as the 66% probability range). As highlighted by Foley (2010a) much research is now being

undertaken to try and validate the sensitivity of climate models using paleoclimate data (e.g. Edwards *et al.*, 2007).

4.4 Climate predictability

The degree to which we can predict the climate response to a change in forcing is limited by our incomplete knowledge of the global climate system and the simplifying assumptions necessary to model a system of its complexity. Climate models provide a three-dimensional, physically-based mathematical representation of the structure and behaviour of the climate system. Despite their highly complex nature, these models remain a simplified representation of reality, based on differing assumptions about the physical processes, interactions and feedback mechanisms which underpin the workings of the true system.

With respect to the climate predictability, uncertainty is introduced by way of the model formulation (e.g. physics, parameterization schemes, parameter values, numerical algorithms, horizontal and vertical resolution), unforced climate variability and the requirement to approximate important sub-grid-scale processes. The model resolution and parameterizations used - along with the necessity of omitting some processes entirely - is required in order to balance the dynamic nature of the climate system and the model complexity against the required runtime, the current limitations of computing resources and our incomplete knowledge of the true system. According to Giorgi (2005) model configuration provides a dominant contribution to the uncertainty cascade, with almost half of the overall range in the IPCC projections of global temperature change attributed to this factor alone.

Although adequate to capture large scale variations in climate, the coarse resolution at which GCMs are run mean they fail to explicitly resolve important sub-grid scale processes (e.g. processes associated with convective cloud formation and precipitation) which must be represented parametrically. As demonstrated by Senior (1999), omitting certain processes in order to reduce the model complexity - as an alternative to representing them parametrically - can have a significant impact on the model performance. Senior (1998) found marked differences in the response of large-scale circulation and surface temperature when a scheme with interactive cloud radiative properties was included (rather than omitted) in runs of the UK Meteorological Office's GCM.

Parameterization schemes represent the effect of sub-grid processes empirically, based on their association with resolvable grid-scale fields. The parameterization of important physical processes (e.g. cloud micro-physics) which are not explicitly resolved at the grid-scale, leads to error in the model simulation and is one of the key sources of uncertainty in model projections (Tebaldi & Knutti, 2007). As the empirically derived relationships which underpin parameterization schemes are based on present day climate, applying them under altered forcing conditions incurs an assumption in the stationarity of the derived relationships. However, as the dynamical core of climate models is based on immutable physical laws, the models provide credible estimates of future climate change, despite the requirement to parameterize key physical processes (Foley, 2010b).

The climate system is an inherently dynamic, complex and non-linear system which, as it evolves over time, is subject to a range of natural fluctuations. Natural variability has the capacity to either amplify or dampen the influence of both human and natural forcings. Equally anthropogenic forcing has the capacity to disrupt natural modes of variability and cyclical climatic processes - dampening or amplifying their effects and creating feedbacks in the system (Foley, 2010b). In this respect the ability of climate models to simulate different naturally occurring modes of variability, and their response to altered forcing conditions, will affect model projections of future climate.

The degree to which climate models can capture natural variability is limited. Even in the absence of anthropogenic forcing, where the climate system remains stable, large scale modes of variability - operating across timescales from the decadal (e.g. North Atlantic Oscillation) to the millennial (e.g. thermohaline circulation) - may only be quasi-predictable (Griffies & Bryan, 1997; Foley, 2010a). Min *et al.* (2005) used a 1000-yr control simulation from the ECHO-G AOGCM (Atmosphere-Ocean General Circulation Model) to evaluate model skill at capturing two dominant signals of natural variability; the El Niño-Southern Oscillation (ENSO) and North Atlantic Oscillation (NAO). It was found that the model captured the ENSO reasonably well; however, the simulated amplitude of the ENSO signal was found to be too large, and its occurrence too regular and frequent. With regards to the NAO, the model overestimated the warming associated with the North Pacific during the high index phase. A study by Bell *et al.* (2000) considered the ability of 16 AOGCMs to simulate the variability of global surface air temperatures. The results indicated that the majority of models considered underestimated unforced inter-annual temperature variations over the oceans; in

contrast, they were found to have overestimated variability over land masses - a finding which the authors attribute to deficiencies in the land surface schemes used.

The climate response to altered forcing is related to the interaction which occurs between the various components of the climate system (e.g. atmosphere, ocean, land surface, cryosphere and biogeochemical cycles). A lack of knowledge regarding the exact role of important feedbacks (e.g. water vapour/atmospheric warming, cloud formation/radiation, ice and snow albedo), their rate of change and whether they are linear in their response (to further climate warming) or subject to abrupt shifts leads to uncertainty in the model projections.

Hawkins and Sutton (2007) investigated the relative contribution which uncertainty in the choice of GHG emission scenario, the individual model responses and the internal unforced variability made to the total uncertainty in model projections of surface temperature. Figure 4.3 indicates that over the first two decades of the 21st century the dominant sources of uncertainty are natural variability and the predictability of the climate response. Over longer time scales, particularly past the mid-century, the greatest contribution to uncertainty stems from the climate model and emission scenario. Hawkins and Sutton (2007) indicate that the reduction in the contribution by natural variability is due to a strengthening of the climate change signal. In contrast to global projections (Figure 4.3(a)), natural variability is shown to have a greater influence at a regional scale (Figure 4.3(b)).

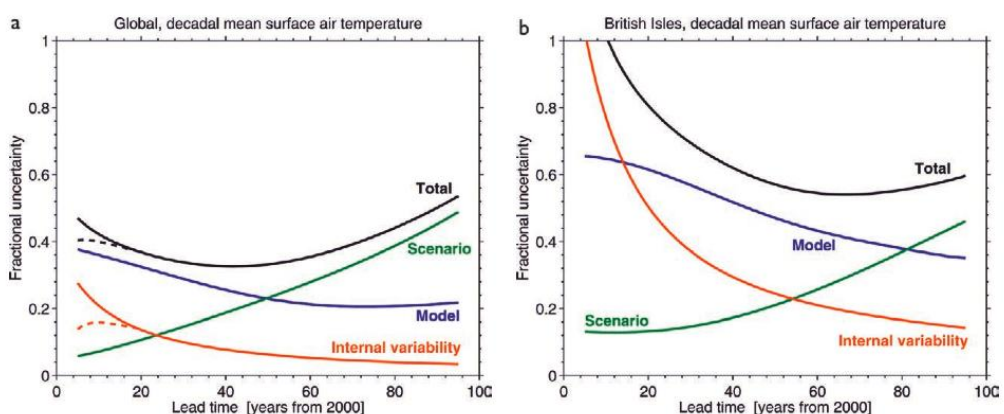


Figure 4.3 The relative contribution of each source of uncertainty to decadal mean surface temperature projections shown by the fractional uncertainty (the 90% confidence level divided by the mean prediction) for (a) the global mean, relative to the warming from the 1971–2000 mean, and (b) the British Isles mean, relative to the warming from the 1971–2000 mean (Source: Hawkins & Sutton, 2007). The plots are constructed using the Coupled Model Intercomparison Project phase 3 (CMIP3) multimodel air temperature projections also used in the IPCC AR4 (2007).

Owing to a lack of convergence in the projections from individual climate models, it is argued that considering the output from a single model in isolation may lead to the

suppression of critical uncertainties in estimates of future climate change (Hulme & Carter, 1999; Wilby & Harris, 2006). With respect to this, there are a number of approaches which can be taken to both explore the uncertainty space and quantify uncertainty in the projected climate response. Sampling model uncertainty typically involves employing a multi-model ensemble (MME) and/or, as described above, running the same model numerous times with a different internal structure, configuration or parameterization scheme (perturbed physics ensemble (PPE)).

To compare the performance of different GCMs a number of studies - including the Atmospheric Model Intercomparison Project (AMIP), the Arctic Ocean Model Intercomparison Project (AOMIP) and the Coupled Model Intercomparison Project (CMIP) - have been undertaken. The findings from these studies suggest that (a) different models reproduce different components of the climate system with varying degrees of success - with no single model being the most skilful at reproducing all aspects of observed system behaviour; and (b) the averaging of ensembles provides a better fit to observations than any one individual model in isolation (Lambert & Boer, 2001).

4.5 Uncertainty in the development of high resolution climate scenarios

GCMs can only provide a ‘broad-brush’ interpretation of how variables such as continental-scale temperature and rainfall patterns may change in response to anthropogenic forcing. As a result of the coarse spatial resolution at which GCM are run, their data cannot be applied directly in local/regional scale impact studies. Consequently, in order to generate climate data which is commensurate with the scales required for conducting impact assessments, the output from GCM experiments must be firstly subjected to some form of downscaling (Diaz-Nieto & Wilby, 2005).

The limitations and underlying assumptions implicit in downscaling climate scenarios introduces an additional level of uncertainty to local or regional scale estimates of climate change (Rowell, 2006). Dynamically downscaled scenarios are subject to many of the same uncertainties associated with GCMs (e.g. model configuration, parameterization, grid resolution and natural variability); however, regional models have the added complicating factor that any bias or error present in the driving GCM is propagated through the models (Räisänen *et al.*, 2004). When uncertainties in both the

nested regional and driving GCM interact, it may lead to the amplification of uncertainty in the downscaled data; conversely, it may also result in error cancellation, whereby the errors in the downscaling and parent model cancel each other out, producing a response which is consistent with the observations without the underlying mechanisms necessarily being correct. The uncertainty introduced to statistically downscaled scenarios arises from a number of sources including the model choice, predictor selection and training period used.

A number of European wide studies including PRUDENCE (Christensen *et al.*, 2007b), ENSEMBLES (van der Linden and Mitchell, 2009); DEMETER (Development of a European Multi-model Ensemble system for seasonal to inTERannual prediction) (Palmer *et al.*, 2004) and STARDEX (STARDEX Final Report, 2005) have been used to compare downscaling techniques and study different sources of uncertainty. Rowell (2006) explored the uncertainty introduced by the RCMs used to downscale temperature and precipitation scenarios for the UK (over the late 21st century). In the case of this study data from PRUDENCE and the IPCC Data Distribution Centre (DCC) was used. Rowell (2006) highlights that, although it is a necessary step, regional downscaling inevitably contributes a further source of uncertainty to the overall uncertainty in climate projections. The author found that the formulation of the regional models influenced the projected range in mean climate for the UK. The results indicated that the largest source of uncertainty - when all seasons and both variables were considered - was the formulation of the global-coupled model.

In a similar study, data produced through the EU funded ENSEMBLES project was used to explore different sources of uncertainty, including the choice of driving GCM and downscaling model; the study also considered the effect which interannual variability had. In accordance with the results from its predecessor PRUDENCE (Christensen *et al.* 2007b; Déqué *et al.*, 2007), the results from ENSEMBLES (van der Linden & Mitchell, 2009) indicated that over the first half of the 21st century large-scale seasonal mean changes were largely determined by the GCM, whilst differences between the respective RCMs were more closely linked to natural variability (Déqué, 2007, 2009; van der Linden & Mitchell, 2009). The choice of RCM was shown to be important, particularly as it was found that some models amplified the climate change signal whilst others tended to weaken it (van der Linden and Mitchell, 2009).

The results from ENSEMBLES (van der Linden & Mitchell, 2009) highlight that uncertainties in both global and regional scale climate processes contribute to the full range of plausible climate responses; consequently, a comprehensive sampling of both is needed in order to properly characterise the uncertainty space and inform the development of robust adaptation strategies. Due to temporal variations in their relative contribution to uncertainty in the regional scale response, it is argued that a greater number of GCMs should be sampled over the latter half of the century (e.g. 2050 onwards); in contrast, the RCMs should be more heavily sampled when modelling climate during the earlier half of the century, when conditions are closer to the present day climate (Déqué, 2007; 2009; van der Linden & Mitchell, 2009).

Chen *et al.* (2011) investigated uncertainty in a hydrological impacts study which employed climate scenarios derived using six different statistical downscaled methods, including a change factor approach and weather generator. It was found that the uncertainty range originating from the choice of 28 climate projections (seven GCMs and three emissions scenarios) was slightly larger than the uncertainty envelope associated with the choice of downscaling method. Of the methods considered regression-based statistical downscaling was found to have contributed most to the overall downscaling uncertainty.

4.6 Uncertainty in climate impacts

When attempting to model the impacts of climate change on human and environmental systems an additional source of uncertainty originates from the impact models used - represented by the final component in the chain of uncertainties (Figure 4.2). Not unlike climate models, the limitations and assumptions associated with impact models introduces uncertainty to their output. One of the greatest uncertainties is the assumption that the model remains valid under future climate conditions, of which it has no prior experience.

Several studies have examined the relative contribution of the various stages in the “cascade of uncertainty” to the overall uncertainty in impact assessments. Kay *et al.* (2000) explored the influence of uncertainty on the results of an impacts study which examined changes in flood frequency in England. Six different sources of uncertainty were considered including: the emission scenario, GCM structure, regionalization

model (including RCM structure), hydrological model (considering both the structure and parameter values) and the internal variability of the climate system (sampled by applying different GCM initial conditions). The results indicated that the greatest contribution to uncertainty came from the GCM used. The authors highlight the importance of natural variability, particularly when trying to identify clearly defined climate change signals. Graham *et al.* (2007a) examined the hydrological response of the Lule River in Northern Sweden to changes in climate using the PRUDENCE dataset (Christensen *et al.* 2007b). The study indicated that the choice of GCM had a greater influence on the projected hydrological response than the choice of emission scenario. Similarly, when examining projected changes in three river basins located in Northern and Central Europe, Graham *et al.* (2007b) found that the choice of GCM had a significant influence on the projected hydrological response.

Wilby *et al.* (2006) used two emission scenarios and three GCMs to investigate uncertainty in an impact study which focused on the future availability of water resources. The magnitude of projected changes was found to differ depending on the GCM selected. A study by Jasper *et al.* (2004), which examined the response of two alpine river basins (Switzerland) to projected climate change, concluded that large uncertainties are introduced by way of the GCMs used. The emission scenario was also found to have a noticeable influence on the results. The study employed 17 climate projections derived from seven GCMs and four emission scenarios. Prudhomme and Davies (2009a; 2009b) examined different sources of uncertainty in model projected changes in the hydrological regime of four river catchments in the UK. The results indicated that the GCMs were the largest source of uncertainty in the results; however, uncertainty stemming from the downscaling method and emission scenario used was of a similar magnitude, but generally less than the GCM.

In their study of climate change impacts on the hydrology of a Nordic catchment (Chute-du-Diable, Quebec), Minville *et al.* (2008) found that the choice of GCM contributed most to the overall uncertainty in the projected hydrological response. Wilby and Harris (2006) conducted a comprehensive assessment of uncertainty in hydrological impact studies; their study focused on low flows in the River Thames. It was found that the hydrological model projections were most affected by uncertainty stemming from the choice of GCM. Uncertainties due to the emission scenario and hydrological model parameters were shown to be of lesser significance. In this study

Wilby and Harris (2006) highlighted the benefits of adopting a probabilistic framework as a means for characterising uncertainty in the results from climate impact studies.

4.7 Managing uncertainty in climate projections

Due to the significant implications it has for policy decisions and the potential for maladaptation to occur, addressing uncertainty in local scale projections of future climate has become an issue of critical importance for impact assessors. Although it is common practice, the over-reliance on a single realisation of future climate - typically derived using a single emissions pathway and climate model - may lead to the suppression of key uncertainties in estimates of future climate change. Hulme and Carter (1999) go so far as to state that this practice is ‘dangerous’, as any subsequent policy decisions will be founded only on a partial assessment of the true risk posed by climate change. In this respect it is important that the uncertainty space is adequately sampled if the results from impact studies are to be used for the development of robust adaptation responses. Thus, employing a single projection of future climate is an inappropriate strategy for conducting impact studies (Wilby & Harris, 2006). It is now widely recognized that comprehensive impact assessments must address the issue of uncertainty by employing multiple realizations of future climate. As a result there is an onus on the climate modelling community not to produce a single deterministic account of future climate, but rather a range of plausible climate pathways which allow for some consideration of the uncertainties encountered at each stage in the process of developing regional or local scale climate projections. Indeed current research has moved somewhat beyond this towards producing probabilistic projections of future climate based on the output from multi-model ensembles. Advancing this approach, it is possible to attach some weighting to the projections from individual models or ensemble members based on their ability to capture different aspects of present day climate.

As highlighted above, an important finding of inter-comparison studies like AMIP, AOMIP and CMIP3, as well as projects like PRUDENCE (Christensen *et al.*, 2007b) and ENSEMBLES (van der Linden & Mitchell, 2009), is that irrespective of whether operating at a global or regional scale, models display disparate skill levels, with some being more proficient at capturing certain aspects of observed system behaviour when compared with others. In addition, in any ensemble generally no single model outperforms its competitors in all aspects of performance. For example, models which

accurately replicate large-scale modes of circulation or different climatic regimes may be poor at capturing extreme events or regional-scale forcings. It is generally acknowledged that by allowing the respective strengths of different models to be combined, climate ensembles are likely to provide a more reliable estimate of future climate change (Tebaldi & Knutti, 2007). Thus, when examining the potential local scale response to perturbed forcing it is advised that an ensemble based approach is adopted - both as a means of incorporating uncertainties relating to the climate predictability (i.e. to capture the spread of climate responses) and as an acknowledgement that the performance of the ensemble is likely to be better than any of its constituent ensemble members when considered in isolation (Buser *et al.*, 2009). As stated by Weigel *et al.* (2010), combining the output from different models is a more pragmatic approach for addressing uncertainty and producing reliable estimates of future change. Using an ensemble not only allows the strengths of different models to be exploited, it also facilitates attaching a conditional likelihood value to different model outcomes. In addition it dispels the over-confidence implicitly associated with using a single realization of future climate (Weigel *et al.*, 2008).

Maraun *et al.* (2010) state that uncertainty in the model response (i.e. formulation, parameterization, unforced variability) can be addressed by using multi-model and/or perturbed physics ensembles (Benestad, 2004; Murphy *et al.*, 2004; Stainforth *et al.*, 2005; Tebaldi & Knutti, 2007). The former allows sampling of the uncertainty associated with inter-model variability, whilst the latter allows for an exploration of uncertainty associated with the internal model configuration (e.g. parameterization). As the model parameters can be methodically reconfigured between successive runs, perturbed physics ensembles (PPEs) allow for a more systematic sampling of uncertainty when compared with multi-model ensembles (MMEs). In the case of the latter, differences which exist between individual models are to a certain extent arbitrary. As a result the assumption that the models used in a MME are independent from one another may not be valid (i.e. different models share similar structural assumptions); this may lead to an oversampling of a particular region of the model space, creating a bias in the final ensemble and any probabilistic projections derived from it. However, whilst the PPE may appear to offer a more systematic and less subjective approach to addressing model uncertainty, as it is essentially the same model which is altered between successive runs, it cannot capture inter-model differences. Given their highlighted shortcomings, an optimum approach - whereby both the internal

and inter-model variability could be sampled - would be to employ a multi-model perturbed-physics ensemble (Collins *et al.*, 2010; Foley, 2010a).

4.8 Probabilistic projections and weighting criteria

In order for climate ensembles to be considered reliable it is important that the performance of individual members is scrutinized and that the methodological approaches used to generate them are valid. A key issue when employing climate ensembles is whether to use information about the skill of individual members under present day climate to inform their relative contribution to the overall ensemble under future forcing (Foley, 2010b). Model weighting has been shown to improve prediction skill and thus, when employed in a climate change context, may provide a means of reducing uncertainty in future projections (Weigel *et al.*, 2008; 2010). As outlined by Weigel *et al.* (2010), the criteria employed for model weighting in the past has included an assessment of systematic bias over the control period (e.g. Giorgi & Mearns 2003; Tebaldi *et al.*, 2005) and model skill in capturing observed trends (e.g. Greene *et al.*, 2006; Hawkins & Sutton 2009; Boé *et al.*, 2009); weighting schemes have also been formulated using composites of several other performance criteria (Murphy *et al.*, 2004).

The issue of whether to apply a weighting scheme is a particularly contentious one, not least because it requires an assumption that model performance is both time and state invariant. It also requires that a robust methodological approach for evaluating the performance of competing models is employed. This is an issue which Weigel *et al.* (2010) highlights as a critical weakness in weighting schemes, and is one underlined by the fact that no consensus regarding what constitutes best practice in this area currently exists. The principle argument in favour of model weighting is that it is difficult to expect a model which has little or no skill under current conditions to be a reliable estimator of future climate; the converse of this is that a model's performance with respect to current day climate is in no way a guarantee of its validity under altered forcing, and thus each ensemble member should be considered equally plausible. Weigel *et al.* (2010) state that it may be more pragmatic to simply omit poorly performing models from the ensemble which, in some cases may be justifiable; however, given the unpredictability of the climate system and our dearth of knowledge regarding its true workings - particularly under altered forcing conditions - it may be

better to err on the side of caution and include a larger number of models which exhibit disparate skill levels, but which may contain the true outcome, rather than be overconfident in a smaller number of models which may not (Foley, 2010a). In addition, as it effectively constrains the uncertainty space, omitting ensemble members on the basis of performance may lead to an underestimation of uncertainty. Based on the points outlined above, model weighting may be considered a means of reducing uncertainty, or conversely may simply add an additional layer of uncertainty which must be explored.

The generation of multi-model ensembles and the development of methods like the reliability ensemble averaging (REA) framework (Giorgi & Mearns, 2002; 2003), are part of a wider undertaking by the modelling community to produce probabilistic projections of future climate; however, one of the impediments to the widespread application of this approach is the uncertainty surrounding which techniques are most suitable for combining model simulations (Knutti *et al.*, 2010). As they are more appropriate for expressing uncertainty, and are applicable to combining the information from individual ensemble members, Bayesian methods have typically been employed to produce probabilistic projections based on ensemble data (Dessai & Hulme, 2004). Among the first to employ a Bayesian framework was Tebaldi *et al.* (2005); in this case the authors produced weighted probability distributions of changes in mean temperature over 22 different (Giorgi) regions of the global landmass. Tebaldi *et al.* (2005) employed the criteria of model bias and convergence from the REA method proposed by Giorgi and Mearns (2002). This method assigns a weighting to each ensemble member based on its ability to simulate present day climate; an additional measure which considers model convergence under perturbed forcing is also used. Despite its widespread application, the REA method has been the subject of some criticism, the main focus of which has been the incorporation of the convergence criterion. For example, Xu *et al.* (2010) state this term artificially narrows the probability distribution of projected change. In addition, it is argued that using the criterion may not be valid given that there is no observed data with which to benchmark model performance; furthermore it assumes independence in the ensemble members. Xu *et al.* (2010) updated the REA method by omitting the convergence criterion and including supplementary measures for quantifying model performance; in addition, the approach proposed by Xu *et al.* (2010) considers model performance with respect to multiple climate variables.

As outlined by Buser *et al.*, (2009), the methodological framework set out by Tebaldi *et al.* (2005) has been generalized and advanced by others (e.g. Furrer *et al.* 2007; Min & Hense, 2007; Jun *et al.*, 2008; Buser *et al.*, 2009; Smith *et al.*, 2009). The framework has also been applied in a statistical downscaling context by Hashmi *et al.* (2009). In this case a Bayesian weighted multi-model ensemble approach was used to combine the precipitation scenarios produced from three different statistical models.

Lopez *et al.* (2006) compared the Bayesian framework of Tebaldi *et al.* (2005) to the approach devised by Allen *et al.* (2003) - which is based on the detection of climate change signals (Allen *et al.*, 2000, 2003; Stott & Kettleborough, 2002). It was found that the underlying assumptions of both methods resulted in the predicted distributions being significantly different from one another. Min *et al.* (2007) applied Bayesian model averaging (BMA) to produce weighted distributions of temperature change for different continental regions. Bayes factors and the expectation-maximization algorithm were compared as methods for estimating the weighting factors. This study also examined differences in the projections from the weighted (derived using BMA) and unweighted (arithmetic) mean ensemble. Min *et al.* (2007) found that that the BMA approach was sensitive to the training period used; in addition it suggested greater increases in mean temperature and produced broader distributions when compared to the unweighted mean ensemble. Greene *et al.* (2005) employed a Bayesian linear model to estimate probability distribution functions of regional temperature change using a multi-model ensemble of AOGCMs.

As discussed above, the use of weighted probabilistic methods requires that some criteria are used to assign a measure of reliability to the output from competing models. The REA approach, along with Bayes factor and expectation-maximization algorithm referred to above, are indicative of the methods used to formulate model weights. Approaches to model evaluation have predominantly focused on how well models reproduce different aspects of observed climate (e.g. mean and higher order statistics, inter-annual/decadal variability and geographical patterns) and system behaviour (e.g. different mode of large-scale circulation, North Atlantic Oscillation index). Murphy *et al.* (2004) devised the climate prediction index (CPI) which weighted GCMs depending on how well they reproduced various statistical descriptors of present-day climate. The index was formulated based on model performance at simulating multiple climate variables. Wilby and Harris (2006) employed the CPI criteria (Murphy *et al.*, 2004) to weight GCMs used in a catchment scale impacts assessment. The weighting scheme is

referred to as an impact relevant climate prediction index (IRCPI). In this case the index was estimated based on the skill of each GCM at reproducing variables considered important for capturing low flows in the study catchment (Thames, UK).

Brekke *et al.* (2008) employed six metrics to quantify (GCM) model skill at capturing the observed climatology of Northern California. In this study a multi-model ensemble consisting of 75 ensemble members - generated by 17 AOGCMs - was assessed. To formulate the model weights three different evaluation criteria were employed. The first was based on the model's ability to reproduce the local climatology of the study region; the second examined model performance at capturing global-scale climatic processes. The third criterion was based on how well each model described the link between the local scale climate response and global scale forcings (i.e. teleconnections). Thus, in order for the scenarios to be considered reliable, the models used to generate them had to capture the connection between global and local scale climate processes; they also had to simulate these processes with a high degree of skill.

4.9 ENSEMBLES: weighting scheme

As part of the ENSEMBLES project (van der Linden & Mitchell, 2009) a performance based weighting system was developed and subsequently employed to produce probabilistic projections of future climate change for Europe using the ENSEMBLES dataset. The work carried out for this is reported in a special edition of Climate Research entitled "Regional Climate Model evaluation and weighting" (volume 44, 2010). A holistic approach was taken when formulating the ENSEMBLES weighting scheme, whereby each group involved considered contrasting aspect of model performance and explored the use of different evaluation metrics.

Coppola *et al.* (2010) proposed a weighting system for RCMs based on model performance at simulating the sub-GCM-grid scale mesoscale climate signal (i.e. the signal not explicitly resolved by low resolution climate models). The signal is representative of the value added by the running GCM data through a higher resolution dynamical model, and is indicative of how well the RCM captures the influence of sub-grid scale features (e.g. coastlines, topography). For this the performance of each ERA-40 driven RCM was assessed on a seasonal basis and both temperature and precipitation were considered. Five metrics were used to quantify each model's ability to reproduce

observed spatial patterns of variability in mesoscale signals for each variable independently. It was found that, when evaluated using the same performance criteria, the weighted mean ensemble performed better than the unweighted mean ensemble - particularly over topographically complex regions (e.g. Alpine region).

Kjellström *et al.* (2010) assessed the ability of 16 RCMs - when run using ERA-40 boundary conditions - to reproduce daily and monthly statistics of temperature and precipitation for the period 1961-2000. The degree to which the empirical probability distribution function of the observations matched that of the simulated series was employed as a quantitative measure of model skill. Kjellström *et al.* (2010) found that the weighted ensemble was a slightly better approximation to the observations than the corresponding unweighted ensemble for most regions, variables and seasons. Lenderink (2010) devised a weighting system based on how well the RCMs simulated precipitation extremes. For this the 99th, 99.9th and 99.99th percentiles of daily modelled precipitation were compared on a seasonal basis with the E-OBS dataset. In their contribution to the ENSEMBLE weighting scheme Lorenz and Jacob (2010) considered RCM (ERA-40 driven) skill at simulating observed linear trends in annual mean temperature over 8 different European regions for the period 1961-2000. Skill scores were assigned to individual RCMs based on differences between observed and model simulated trends.

Also included in the overall ENSEMBLES weighting system are the results from Sanchez-Gomez *et al.* (2009) who assessed RCM performance at simulating large-scale circulation patterns. The models were evaluated based on how well they reproduced the frequency of occurrence, composite pattern, persistence, interannual variability and long-term trends in the occurrence of different circulation types. In addition Halenka *et al.* (unpublished) provided ensemble weights formulated based on how well each model reproduced the annual cycle in both temperature and precipitation (Kjellström & Giorgi, 2010).

Christensen *et al.* (2010) investigated how the model weights derived from each of the six studies outlined above could be combined into a single comprehensive weighting system. The authors investigated the effects of differently aggregating the individual skill scores to produce the overall model weights; it was found that the final weights were sensitive to the aggregation method used. Crucially, this study indicated that using the formulated weights did not bring about any improvement above using the

unweighted mean ensemble. One of the reasons proposed for this is that mean biases were not explicitly considered by any of the performance criteria employed. The findings of Christensen *et al.* (2010) are generally in keeping with the results from other studies (e.g. Wilby & Harris, 2006; Fowler & Ekström, 2009; Knutti *et al.*, 2010). Although the weighting scheme appears to add little value in terms of simulating current day climate, it is argued that, as the weights have been objectively formulated, the weighted mean ensemble may still provide a more reliable estimate of future climate when compared to the unweighted mean ensemble (i.e. where an equal weighting is applied). In this respect employing model weights may be considered a more defensible approach, despite appearing to have little influence on the overall outcome.

Déqué and Somot (2010) employed the weighting scheme derived for the regional models used in ENSEMBLES to produce probabilistic climate projections for three European cities (Budapest, Lisbon and Dublin). Here the same RCMs were employed to dynamically downscale GCM simulations; the resulting datasets were combined using the ENSEMBLES weighting scheme outlined above. Over the control period (1961-1990) there was no evidence that the use of the weights produced a weighted probability distribution function (PDF) which was closer to the observed PDF than if equal or randomly drawn weights were used. Additionally, it was found that irrespective of the model weighting employed (equal, random or quantitatively derived), a similar response to future climate forcing was elicited. Déqué and Somot (2010) state that as the ENSEMBLES weights are based on a physical and multi-purpose approach, they are more robust than equal weights - even if the unweighted and weighted mean ensemble return similar results.

4.10 Conclusion

Our ability to translate theorized storylines of future socio-economic development into alterations in the elemental composition of the atmosphere and changes in local or regional climate is limited by both what is ‘unknown’ and what is ‘unknowable’ about the workings, temporal evolution and sensitivity of the climate system. When simulating the climate response to a change in forcing, uncertainty is introduced by way of the simplifications imposed on the climate system in order to make it solvable with respect to current computing power and our incomplete knowledge of system processes.

Uncertainty in climate models stems principally from their coarse resolution, internal model configuration, and critically the requirement to approximate important sub-grid scale processes. The necessity to parameterize key physical processes, not resolvable at the grid-scale, incurs an assumption in the validity of empirically derived relationships under perturbed forcing. In addition, the predictability of the climate system is limited by the chaotic nature of the system itself, both in the real world and in model simulations. It is also limited by our incomplete understanding of the role feedback mechanisms may have and how such feedbacks are represented in climate models; this is of particular importance with respect to their interaction with natural modes of variability and cyclical climate processes.

The principal means of addressing uncertainty in climate models is through the use of multi-model or perturbed physics ensembles, both of which allow key uncertainties to be sampled when estimating the climate response. Different methods for combining the information contained in such ensembles to produce probabilistic projections of future change exist. One of the foremost critical issues associated with this is whether to apply some weighting criteria to the ensemble members in order to constrain their relative contribution to the aggregated ensemble response. Typically the weighting criteria used is based on the ability of each respective ensemble member to capture some aspect of observed climate behaviour. Whilst a model's ability to simulate observed climate may not be indicative of its skill when applied under altered forcing conditions, it can equally be said that a model which is unable to simulate past behaviour is also likely to be less reliable when used to model future climate. Given these conflicting viewpoints, the application of a weighting scheme comes with the caveat that a robust approach for quantifying model skill is adopted.

As highlighted above the uncertainty which pervades climate change impact studies is introduced not only by the predictability of the large-scale climate response, but also through the emission scenario, regionalization technique and impact model used. Figure 4.2 illustrates how uncertainty is accumulated or amplified as it passes through each link in the chain, underlining the importance of independently sampling the uncertainties present at each stage. The following chapter critically examines the various methodological approaches employed for downscaling coarse scale GCM data; the chapter also provides an outline of the various uncertainties associated with downscaling climate data and how they can be addressed.

Chapter 5

Approaches to statistical and dynamical downscaling

5.1 Climate modelling and downscaling

Understanding how the Earth's climate may change in response to further increases in atmospheric GHGs, and the possible impacts any such changes may have on human and environmental systems, is critical for developing robust adaptation strategies and formulating appropriate policy decisions. Global climate models (GCMs) are the primary tool used for studying past variations in the Earth's climate, and are employed in a climate change context to explore the potential response of the climate system to a change in forcing. These models are three-dimensional numerical representations of the structure and behaviour of the global climate system; they describe the dynamics of the Earth's oceans and atmosphere in a physically explicit manner, and account for the complex workings and interactions of the various sub-systems which comprise the global climate system. Climate models are a key instrument for exploring the possible evolutionary pathways of the Earth's climate under prescribed anthropogenic forcings; as such their projections provide the primary source of information used for conducting impact studies and developing climate change adaptation responses.

GCMs describe climate behaviour by integrating a range of chemical, biological and fluid-dynamical equations which are either derived directly from physical laws (e.g. Newton's first law of motion) or are formulated by more empirical means. There are both atmospheric GCMs (AGCMs) and ocean GCMs (OGCMs); both of which can be coupled to form an atmosphere-ocean GCM (AOGCM) which, along with the addition of various sub-models (e.g. sea-ice, land model and carbon cycle model), forms the basis of a model which provides a more complete representation of the climate system. Modelling future climate based on a global domain is necessary in order to ensure that the interactions between different climate regimes are handled correctly. Previous studies have shown that GCMs have the capability to simulate the large-scale features and dynamics of the climate system (e.g. general circulation of the oceans and atmosphere, sub-continental patterns of temperature and precipitation); for example, some have been shown to be skillful at capturing important climatic tele-connections such as those associated with ENSO (El Niño-Southern Oscillation) (Leung *et al.*,

1999). Despite their recognized skill at a global scale, the coarse resolution at which they operate restricts their capacity to provide a realistic description of both the workings and condition of the system at finer spatial scales (Grotch & MacCracken, 1991; Zorita & Von Storch, 1999). This aspect of GCMs severely limits the direct use of their output in regional/local scale impact applications, for which higher resolution data is required (Giorgi & Mearns, 1991; Wilby & Wigley 1997, McGuiffie *et al.*, 1999; Wilby *et al.*, 1999; Giorgi *et al.* 2001; Prudhomme *et al.*, 2002).

GCMs are currently run at a relatively coarse spatial resolution - typically of the order of 300-500 km. Operating at this scale is necessary given the constraints of currently available computing power and the highly dynamic nature of the climate system. However, at this resolution the influence of important sub-grid scale features, which have a strong bearing on the local climate, cannot be explicitly accounted for. Considering local scale forcings in any plausible future scenario is particularly important where land-surface conditions significantly influence the character of regional and local scale climate. This is particularly true for regions which present highly heterogeneous environments such as coastal zones, regions with complex topographies and areas with diverse land-use types (Wilby *et al.*, 2004). Furthermore, their coarse resolution and limited physics prohibits them from explicitly resolving important climatic processes which occur at a sub-grid scale level (e.g. cloud formation, evaporation, convective rainfall) - many of which are either omitted from the model simulations or are represented using parameterization schemes. Physical processes which occur at the sub-grid level strongly affect local climate at the scales most relevant to the ecological and human environment; consequently they are often those of greatest importance to impact assessors (Cubasch *et al.*, 1996; Zorita & von Storch, 1999).

Given that the global climate is primarily the response of the climate system to large-scale factors (e.g. differences in solar forcing, the Earth's rotation, the global land-sea distribution, orographic features) (Zorita & von Storch, 1999), it is rational to expect that GCMs which are proficient at capturing global scale processes may not perform well at simulating regional climate - which is primarily the response of the climate system to regional scale forcings and climate processes which cannot be resolved based on the grid resolutions currently employed. Ideally the climate scenarios used to drive impact assessments should reflect sub-grid scale processes and capture locally specific climate details lacking in the output from GCMs. Reflecting the heterogeneity of the sub-GCM grid scale climate necessitates 'downscaling' coarse resolution model output

to the finer spatial scales relevant for conducting impact studies. This may be to higher resolution grids or point specific locations on the Earth's surface commensurate with instrumental stations. Downscaling is based on the principle that local or regional climate is primarily determined by climate conditions on a much larger scale (Wilby *et al.*, 2004). Developing models with which to capture this relationship allows changes in local-scale variables to be explored using coarse resolution GCM projections.

5.2 A review of different downscaling techniques

Downscaling methods can be broadly divided into two categories: empirical/statistical downscaling and dynamical techniques. Empirical downscaling is based on developing statistical models which describe the relationship between the large scale climate or atmospheric state (e.g. circulation patterns) and the regional or local scale response (e.g. point/grid scale precipitation); dynamical downscaling is conducted using limited area models which employ the same or similar numerical schemes and parameterizations as larger scale GCMs. Downscaling methods, as reviewed by Wilby and Wigley (1997), Wilby *et al.* (2004), Mearns *et al.* (2003) and Fowler *et al.* (2007) can be divided into four general categories: dynamical downscaling (Mearns *et al.*, 1995; Teutschbein & Seibert, 2010; Rummukainen, 2010), regression based methods (Hewitson & Crane, 1996; Wilby *et al.*, 1999), weather classification (Yarnal, 2001) and stochastic weather generators (Richardson, 1981; Racsko *et al.*, 1991; Semenov & Barrow, 1997; Corte-Real & Hu, 1999; Kilsby *et al.*, 2007).

5.2.1 Dynamical Downscaling

Dynamical downscaling typically involves embedding a higher resolution regional climate model (RCM) within a coarse resolution global model, wherein the nested model is driven by lateral boundary conditions from the parent GCM. This is done so with the aim of explicitly accounting for regional scale forcings (e.g. complex topographical features and heterogeneous land cover) and mesoscale climate processes not adequately captured by large-scale models (Giorgi & Mearns, 1991; Giorgi & Mearns, 1999; Rummukainen, 2010).

RCMs are similar to GCMs in that they both rely on the same physical-dynamical description of fundamental climate processes; however, RCMs are run over a limited

area at a much higher resolution. Over the domain on which the model is focused the physical dynamics of the atmosphere are simulated using horizontal grids with a resolution typically of the order of 20-50 km. Information on large scale climate variables (e.g. pressure, vorticity, temperature, humidity etc.) are provided to the regional climate model from the driving GCM. This data is supplied as lateral boundary conditions and processed in a physically consistent manner to produce more spatially detailed climate simulations. Along with regional climate models there are two further approaches to dynamical downscaling (Rummukainen, 2010). The first employs a high resolution atmospheric global model; the second uses a global model with a variable-resolution grid. Here the resolution of the computational grid is increased over a particular area of the global domain. The computational cost of this approach is currently much greater than that of a GCM, prohibiting its widespread application in climate studies (Rummukainen, 2010).

A key benefit of employing RCMs is that they are capable of resolving important sub-GCM-grid scale processes dynamically; thus, as highlighted by Fowler *et al.* (2007), RCMs are able to explicitly model important regional climate features such as orographic enhancement, local winds and extreme weather events (Murphy, 1999; Frei *et al.*, 2003; Fowler *et al.*, 2005; Frei *et al.*, 2006). Frei *et al.* (2003) assessed the performance of five RCMs used to simulate precipitation over the European Alps. Despite inter-model differences being apparent, the models were shown to be capable of skillfully simulating the mesoscale features of heavy precipitation over an area with a complex topography. Schmidli *et al.* (2006) state that the ability of RCMs to incorporate information about regional land-use and topography makes dynamical downscaling more skilful than statistical methods over areas of complex terrain.

The influence which sub-grid scale topographic features (e.g. orographic forcing, rain shadow effects) can have on local climate means that regional climate signals may be significantly different from those simulated by GCMs - highlighting the added benefit of employing dynamical downscaling (Leung *et al.*, 2004; Fowler *et al.*, 2007). In addition, the ability of RCMs to simulate mesoscale precipitation processes in a physically explicit manner means they potentially provide more plausible scenarios of future change in extreme rainfall and regional scale variability (Fowler *et al.*, 2007).

Despite their high resolution some climate processes (e.g. cloud formation) will still occur on too fine a spatial scale to be explicitly resolved and must be represented parametrically (i.e. statistically approximated). As highlighted by Frei *et al.* (2003), the

requirement to represent some climate processes in this manner can lead to inter-model differences in projections of future climate, and introduces uncertainty to the model simulations. In addition, the resolution at which RCMs are currently run means their output may still lack the detail required for conducting local scale impact studies - thus necessitating the application of statistical methods. One of the key assumptions of dynamical downscaling, and climate modelling more generally, is that of stationarity - where the empirical relationships derived under observed climate are assumed to remain valid under the forcing conditions of possible future climates. This essentially non-verifiable assumption underlies the parameterizations used in RCMs (and GCMs); however, as the core basis of climate models is immutable physics and not unverifiable assumptions, it is proposed that this makes a stronger argument for their validity (when compared to statistical methods) under perturbed forcing (Foley, 2010a).

The requirement to parameterize important sub-grid scale processes, along with biases inherited from the driving GCM, necessarily introduces uncertainty to the downscaled RCM projections. Uncertainty stemming from the model configuration (e.g. grid resolution, model structure, parameterization, etc.) and the internal variability of the climate system also contribute to the overall uncertainty in the projected regional scale response (Hagemann *et al.*, 2004). It is argued that in order to address this, it is preferable to adopt a multi-model approach, whereby an ensemble of plausible climate projections is used to explore possible changes in regional climate (Fowler *et al.*, 2007). However, dynamical models are computationally demanding, limiting their application in multiple scenario assessments. In order to overcome this, a number of pan European projects, including PRUDENCE (European FP5 Prediction of Regional scenarios and Uncertainties for Defining European Climate change risks and Effects) (Christensen *et al.*, 2007b) and ENSEMBLES (van der Linden & Mitchell, 2009) (van der Linden & Mitchell, 2009) have been undertaken. Projects like those referred to above facilitate the co-ordination of model experiments and the sharing of information - as part of which the various institutes involved make the output from their model simulations (conducted for a common domain and time period) freely available. In doing so such projects provide the data required for addressing some of the uncertainties inherent in future estimates of regional climate change.

5.2.2 *Statistical Downscaling*

According to Mehrotra and Sharma (2011) statistical downscaling is the most favoured method for transferring large-scale synoptic information from GCM simulations of future climate to the point or catchment grid scales required for conducting impact assessments. Statistical methods are based on the principle that local and regional climate is conditioned by two factors: the large-scale climatic or atmospheric state and regional physiographic features such as topography, land-sea distribution and land-cover (von Storch; 1995, 1999). Based on this a quantitative relationship can be established between large-scale predictors (e.g. circulation patterns, grid-scale humidity) and sub-grid scale climate (e.g. temperature, precipitation) or other surface environmental variables (predictands). Once established under observed conditions, the statistical model is used to derive local point or grid scale scenarios for the surface predictand using coarse resolution GCM data. A study by Trigo and Palutikof (2001) demonstrated that statistical downscaling was more skilful in reproducing the mean, variance and distribution of precipitation across the Iberian Peninsula when compared to the GCM data without downscaling being applied; as such the study demonstrated the ‘added value’ in employing statistical downscaling.

Depending on the particular approach taken and the research question posed, the statistical relationship developed between the large-scale atmospheric predictors and local-scale predictand(s) can be expressed in a deterministic and/or stochastic manner. Statistical downscaling does not demand significant computing resources, meaning it is suited to producing large ensembles of local-scale climate scenarios; consequently this approach to downscaling is widely used for conducting uncertainty assessments. One of the key drawbacks of statistical downscaling is that it requires good quality long-term instrumental records - this is to ensure that a robust statistical relationship can be established. As a result statistical methods are well-suited to areas where the observational network is particularly dense, and high quality coverage of localised climate conditions is provided (Zorita & von Storch, 1999; Wilby *et al.*, 2004).

A number of key assumptions underlie statistical downscaling, the most fundamental of which is that the predictor-predictand relationships established under present day climate remain valid under the forcing conditions of possible future climates. The assumption of stationarity can be tested through ‘model transferability’ - whereby the model is validated using a period from the instrumental record which is representative of a climate regime ‘different’ to that used for model fitting (Charles *et al.*, 2004).

However, given that future climate may lie outside the bounds of what may have been experienced previously - a fact which is underlined by the non-linear nature of the climate system and the potential for it to undergo abrupt changes - this assumption remains somewhat unverifiable.

As stated by Fowler *et al.* (2007) this assumption has been shown to be questionable in the observed record (e.g. Huth, 1997; Slonsky *et al.*, 2001; Fowler & Kilsby, 2002). In a study of the relationship between continental scale circulation and surface climate Huth (1997) found that the derived statistical relationship did not remain stable over time and exhibited considerable intra- and inter-decadal variations. The author states that this casts doubts on the applicability of circulation type approaches - which was the method employed by Huth (1997) - in statistical downscaling. It is argued that non-stationarity can be attributed to temporal changes in the structure of the climate system. It can also be attributed to employing a calibration period which does not adequately sample the natural range of variability and/or by employing a predictor set which fails to reflect low-frequency variations in climate (Wilby, 1998; Fowler *et al.*, 2007).

Statistical downscaling also assumes that the large-scale predictors employed to derive local-scale climate projections are physically meaningful, capture climatic variability across a range of timescales and are well simulated by the driving GCMs (Giorgi *et al.*, 2001); in addition, it is assumed that the large-scale predictors used adequately capture the climate change 'signal' (Hewiston & Crane, 1996, 2006). With respect to this it is widely acknowledged that downscaling models which employ circulation based predictors only may fail to reflect changes in humidity under altered climate conditions (Wilby & Wigley, 1997, 2000; Charles *et al.*, 1999; Murphy, 2000; Fowler *et al.*, 2007). Trenberth *et al.* (2003) point out that future changes in precipitation are likely to occur through increases in the moisture content of the atmosphere resulting from enhanced air temperatures. This underlines the requirement to include variables which are physically sensible, even if they appear to be non-informative under observed conditions. With respect to the points made above, some measure of humidity is typically used as a predictor when downscaling precipitation (Wilby & Wigley, 1997; Easterling, 1999; Murphy, 2000; Beckmann & Buishand, 2002); indeed it is highlighted that an increase in model skill can be brought about by including some measure of atmospheric humidity (Murphy, 1999).

Fowler *et al.* (2007) indicates that the inclusion of a humidity variable in the predictor set can lead to a convergence in the projections from dynamical and statistical models.

A study by Charles *et al.* (1999) found that when relative humidity was included in the set of atmospheric predictors used, the model (a nonhomogeneous hidden Markov model) produced rainfall projections which were consistent with those from an RCM - subsequent studies by Timball *et al.* (2008) and Vrac *et al.* (2007) produced similar results. However, it is argued that when compared with other variables (e.g. temperature, humidity), circulation based predictors are more skilfully simulated by climate models (Cavazos & Hewiston, 2005); thus, in order to satisfy other assumptions, such variables should be used exclusively in statistical models. This apparent contradiction is indicative of the difficulties which underlie the process of predictor selection - which is an important aspect of statistical methods and a critical source of uncertainty in the downscaled projections. Cavazos & Hewiston (2005) evaluated the skill of 29 individual NCEP (National Centers for Environmental Prediction) predictors in capturing daily precipitation at 15 sites sampled across diverse climatic regimes. In this study an artificial neural network (ANN) was used. The results indicated that predictors representing mid-tropospheric circulation and specific humidity were the most relevant controls of daily precipitation for all locations and seasons. Tropospheric thickness, along with 2m and 850 hPa meridional wind components were also important; however, their explanatory power was found to be more regionally and seasonally dependent.

In addition to predictor selection, the size and location of the predictor domain used is an important consideration. Brinkmann (2002) assessed the association between winter precipitation using correlation fields and large-scale circulation patterns of daily 700 hPa pressure data for three different North American precipitation regimes. Brinkmann (2002) found that the optimum grid-point location for downscaling may be a function of the time scale under consideration, and as such may not be a function solely of the target area. At the daily time scale, the optimum grid point was not that located within the region for which precipitation was being downscaled, but was rather a point offset to the west or northwest of it. Wilby and Wigley (2000) found that the location and spatial extent of the predictor domain was an important factor affecting the stability and realism of the downscaled precipitation scenarios. This study examined the applicability of 15 predictors used to downscale precipitation for six regions in the conterminous USA. The pattern analysis conducted by Wilby and Wigley (2000) suggested that the maximum correlations between precipitation and MSLP (mean sea level pressure) were greatest away from the grid-box (i.e. where the predictors were spatially remote from

the predictands); in contrast, maximum correlations for specific humidity occurred when the data was propinquitous (i.e. in close proximity). Spak *et al.* (2007) compared the data downscaled using a multiple linear regression model with that from a dynamical model (MM5). In this case both models were used to downscale monthly (June, July and August) mean surface temperature over the eastern region of North America. It was shown that the domain size had little effect on the skill of the regression model under current climate conditions; however, it was found that the domain had a greater influence on the projected changes in surface temperature than any other factor considered - including the training period and predictor set used.

One of the key weaknesses statistical approaches have (particularly regression and weather typing approaches) is that they tend to underestimate the variability of local climate, and as a result may fail to fully capture the changing nature of extreme events. The under prediction of variance is particularly evident when downscaling those surface variables which are to a lesser degree controlled by the large-scale atmospheric state, and are instead more strongly influenced by local scale forcings (e.g. precipitation, local winds). Essentially the inability of statistical approaches (particularly regression based models and circulation typing) to explicitly account for local or regional scale forcings (e.g. orographic enhancement) results in the downscaled series lacking the ‘noise’ component originating from small-scale atmospheric processes. This component of the time series is essential for characterising local scale weather and patterns of climate variability.

A number of techniques aimed at enhancing the variability of the downscaled data have been proposed. Variance inflation - as implemented by Karl *et al.* (1990) - uses a scaling factor to linearly rescale the downscaled series so that its variance better accords with that of the observations. Von Storch (1999) criticizes this approach for its assumption that all local-scale variability can be traced back to variability in the large-scale predictors. It is argued that this assumption is not valid given that the predictors are based on synoptic scale fields, and thus hold no information on sub-grid scale variability. Von Storch (1999) advocates the use of an alternative method termed ‘randomization’, whereby the variability not captured by the model is represented through the addition of ‘white noise’ (Buma & Dehn, 1998, 1999; Wilby *et al.* 1999; Kysely, 2002). This approach can be represented as:

$$\sigma_{tot}^2 = \sigma_{explained}^2 + \sigma_{noise}^2$$

Randomization has also been employed as a method for bias correcting RCM data (Jakob *et al.*, 2011). Buma and Dehn (1998) state that autoregressive character of the observed (predictand) series should determine whether white (entirely independent) or red noise (dependent on the past) is added. Bürger (1996; 2002) developed a more complex technique based on canonical correlation analysis termed ‘expanded downscaling’ (e.g. Huth, 1999; Dehn *et al.*, 2000, Müller-Wohlfeil *et al.*, 2000). As explained by Cannon (2009) the method adds a constraint to the regression cost function which forces the observed and predicted variances to be similar. Bürger and Chen (2005) conducted a review of each method and found that no one optimal approach exists. Randomization was found to perform well with respect to present climate conditions, but was unable to represent local scale changes in atmospheric variability when used to model future climate. In contrast expanded downscaling was shown to be skillful at capturing atmospheric variability in a climate change context. When downscaling climate data to multiple sites variance inflation was found to misrepresent spatial correlations - resulting in a loss of the temporal coherence between climate series downscaled to individual sites. Expanded downscaling was also noted as being sensitive in instances where the predictors/predictands deviated from normality. Cannon (2009) proposes an additional method based on a multivariate ridge regression model (Hoerl & Kennard, 1970; Brown & Zidek, 1980) with negative parameters (Hua & Gunst, 1983). The technique is conceptually similar to expanded downscaling but is able to maintain the covariance structure between variables.

As discussed above one of the most critical aspects of statistical downscaling is predictor selection. Ideally the atmospheric variables used as large-scale predictors should:

- have a strong and physically sensible relationship with the target variable
- explain low-frequency (i.e. multi-decadal) climate variability and observed trends in climate data
- have a stable and time invariant relationship with the predictand
- be at an appropriate scale (i.e. in relation to important physical processes and GCM performance)
- account for a significant proportion of the variability exhibited by the observed series
- be realistically simulated by the driving global (or regional) model
- adequately capture the climate change signal (e.g. humidity used to downscale precipitation)

- maintain the covariance structure between climate variables
- maintain the spatial coherence between different target sites/areas

(after Wilby & Wigley, 1997; Giorgi *et al.*, 2001; STARDEX Final Report 2005)

The various techniques developed for statistical downscaling can be grouped into three main categories: regression models, weather generators and weather typing schemes.

5.2.2.1 Classification schemes

This synoptic type approach to downscaling seeks to establish a relationship between variations in local or regional climate and the occurrence of particular ‘weather types’ (Giorgi *et al.*, 2001). Weather or circulation typing involves grouping days into discrete classes based on their synoptic similarity (Wilby *et al.*, 2004). In a downscaling context weather classes have been defined using indices of air flow applied to sea level pressure (Conway *et al.*, 1996) or by applying some type of cluster analysis to atmospheric pressure data (Enke & Spekat, 1997; Fowler *et al.*, 2000; 2005). Similarly pressure data may be discretized using correlation analyses (Beck *et al.*, 2000), eigenvector techniques (Goodess & Palutikof, 1998), optimization algorithms (Phillip *et al.*, 2007; Küttel *et al.*, 2009), fuzzy rules (Bárdossy *et al.*, 2002; 2005; Wetterhall *et al.*, 2009) or self-organising maps (Michaelides *et al.*, 2007; Tumbo *et al.*, 2010). Such methods come under the broad heading of objective classification schemes. Large-scale circulation data may also be classified subjectively using approaches such as the Lamb weather type (Lamb, 1972) and Hess–Brezowsky Groszwetterlagen (Hess & Brezowsky, 1952, 1977). Such schemes employ a predefined set of rules and expert knowledge to classify circulation data; typically it is the objectivised versions of these schemes which are used (e.g. Jenkinson-Collison types) (Jenkinson & Collison, 1977; James, 2006).

The application of weather typing in a downscaling context involves developing conditional probability distributions for observed statistics (e.g. mean wet-day amount) which describe the relationship between a particular weather class and the surface predictand. Once this relationship is established the same classification criteria is applied to the output from GCMs; local scale changes are then estimated by examining projected changes in the frequency of weather types (Hay *et al.*, 1991; Corte-Real *et al.*, 1998; Goodess & Palutikof, 1998).

Huth *et al.* (2008) highlights different approaches for using circulation classifications in a downscaling context. This includes the use of an independent downscaling model for each respective circulation class (e.g. Enke *et al.*, 1997) and employing monthly or seasonal frequencies of daily circulation types as predictors of monthly/seasonal mean values for the predictand (e.g. Goodess & Jones, 2002). The first approach is based on the fact that the predictand/predictor relationship may vary depending on the occurrence of a particular circulation pattern. Huth (1999) employed this approach to downscale temperature for Europe; in this study atmospheric data was classified into circulation patterns using PCA (Principal Component Analysis) and k-means clustering. A series of linear regression models were subsequently produced, each of which was specific to a particular circulation type. When using this downscaling approach the absence of other atmospheric variables from the driving data assumes that pressure patterns alone capture the main processes governing local scale weather and climate. In some cases this may weaken the connection between the surface predictand and changes in the large-scale atmospheric state - which is particularly important when estimating the predictand response to altered forcing conditions (e.g. humidity when modelling precipitation) (Karl *et al.*, 1990; Murphy, 2000; Beckham & Buishand, 2002). Weather typing differs from circulation classifications in that the former may incorporate additional atmospheric variables (e.g. precipitable water).

Weather typing has the benefit of being based on the sensible linkages between the large-scale atmospheric state and variations in climate at a local and regional scale. The approach also has the advantage of being able to downscale a range of environmental variables and can be employed in multi-site applications. There is however a number of weaknesses associated with this approach. One of the main shortcomings shared by all weather typing and circulation classification schemes is their insensitivity to within-type variability (e.g. wet circulation types which include the occurrence of dry days) (Brinkmann, 1999; 2000). In addition, a number of assumptions are implicit when using synoptic typing as a downscaling tool, the most fundamental of which is that the characteristics of each type remain the same under altered forcing conditions. A study by Widmann and Schar (1997) found that changes in the nature of daily precipitation across Switzerland were not due to changes in the frequency of particular circulation patterns (based on sea level pressure), but were in fact the result of within-type changes in rain producing circulation types, whereby the amount of rainfall associated with wet-types was found to have increased. The study was conducted using records for the

periods 1901-1990 (with 113 continuously operating rain-gauge sites) and 1961-1990 (with 304 sites) respectively. This highlights the possible non-stationarity of empirically derived relationships between circulation types and surface weather; it also suggests that additional atmospheric descriptors may be required (e.g. humidity). A study by Wilby (1994) found that classification approaches had limited success in reproducing the persistence of wet and dry-spells at two sites in southern England. In this study Wilby (1994) identified the subjectivity introduced by the classification scheme and the non-stationarity of the precipitation characteristics associated with individual types as important weaknesses in this approach.

5.2.2.2 *Stochastic Weather Generators*

Stochastic downscaling methods employ weather generators (WGs) - such as WGEN (Wilks, 1992), LARS-WG (Racsko *et al.*, 1991; Semenov & Barrow, 1997) and EARWIG (Kilsby *et al.*, 2007) - to produce multiple synthetic series of daily or sub-daily weather data conditioned using large-scale GCM projections. The generated data series replicate the statistical attributes of local climate variables, but not the observed sequence of events (Wilks & Wilby, 1999; Hashmi *et al.*, 2009). WGs are a versatile tool and have been employed for a range of tasks including generating data for use in hydrological and agricultural risk assessments (e.g. Mavromatis & Hansen, 2001), extending the simulation of daily weather to unobserved sites (e.g. Semenov & Brooks, 1999) and producing site-specific climate scenarios for impact assessments (e.g. Dubrovsky *et al.* 2004, Evans *et al.*, 2008; Semenov, 2009; Semenov & Halford, 2009; Semenov & Stratonovitch, 2010).

Generally WGs firstly determine the occurrence of wet and dry days; this is done typically by employing variants of Markov chain models (e.g. two state first-order markov chain) with specified transition probabilities (Richardson, 1981) or by using empirical distributions of the wet/dry spell length (Semenov & Brooks, 1999). Secondary variables - including rainfall amounts, temperature, solar radiation and evaporation - are subsequently modelled conditional on precipitation occurrence. In the case of precipitation, a gamma distribution is typically used to model wet-day amounts. Although first order models are often employed when modelling rainfall occurrence, second and third order models have been used to improve performance at simulating both the occurrence and persistence of wet/dry spell lengths. Improvements in the

ability of WGs to reproduce both higher order events and the variability of a climatic time-series have been brought about by the development of the Neyman-Scott Rectangular Pulses (NSRP) stochastic precipitation model (Fowler *et al.*, 2007; Kilsby *et al.*, 2007; Burton *et al.*, 2010). In the case of this model, rainfall (both occurrence and amounts) is simulated as a single continuous variable. Precipitation is modelled as a sequence of storm events (storm times are represented as a Poisson process) consisting of temporal clusters of raincells, each of which has an associated intensity. The amount of rainfall occurring for a given time step is calculated by accumulating the individual raincell intensities (Burton, *et al.*, 2008).

WGs are adapted for statistical downscaling by conditioning their parameters on variations in large-scale atmospheric predictors (Katz, 1996; Semenov & Barrow, 1997, Wilks, 1999; Wilby *et al.*, 2004). WGs have also been used in-conjunction with circulation patterns (e.g. Corte-Real *et al.*, 1999), whereby the model parameters are set conditional on the occurrence of different circulation types. Projected changes in the large-scale atmospheric state are then reflected in the stochastically generated local-scale climate series. Corte-Real *et al.* (1999) found that when conditioned using four circulation patterns (identified using PCA and k-means clustering), a weather generator was able to simulate the important features of local precipitation (e.g. the distribution of wet and dry spell lengths, extreme precipitation) over southern Portugal with a high degree of skill - highlighting the applicability of this approach for downscaling future precipitation.

Several studies comparing the performance of different weather generators have been conducted. Semenov *et al.* (1998) assessed the performance of the LARS-WG and WGEN; for the purposes of comparing model performance 18 sites in the USA, Europe and Asia - representative of different climatic regions - were selected. Whilst it was shown that both models were unable to capture some aspects of observed climate - including the annual variability in monthly means - the WGEN model performed better than the LARS-WG at simulating mean monthly temperature and precipitation. The authors attribute this to the WGEN having a greater number of parameters and allowing more complex distributions to be fitted.

Stochastic downscaling techniques have the advantage of capturing the variability of local climate and thus allowing for a better representation of higher order events in the driving data for impact studies. In this respect WGs have an advantage over regression or weather type approaches which, as discussed above, tend to underestimate the true

variability of local-scale climate. WGs also have the advantage of allowing multiple variables to be modelled concurrently, thus ensuring that the temporal coherence between them is maintained. One of the key benefits of employing stochastic methods is the ability to generate large ensembles of climate data for use in risk assessments (e.g. crop modelling, water resources management). Similarly stochastically generated data can be used to represent natural climate variability - an issue of increasing importance given the need to address this source of uncertainty in climate impact studies. Weather generators also have the benefit of being able to produce climate series with a high temporal resolution (e.g. sub-daily rainfall data).

The key weaknesses associated with employing stochastic models in a climate change context are related to the difficulties in modifying the model parameters. It has been found that altering the precipitation parameters can result in inconsistent changes in the secondary variables (Wilks, 1992). In addition, an assumption in the stationarity of inter-variable relationships under future climate forcing is implicitly associated with the downscaled datasets.

5.2.2.3 Regression Models

Regression models or transfer functions establish a direct statistical relationship between the observed local-scale predictand (e.g. point scale precipitation) and a suite of large-scale atmospheric predictors (e.g. mean sea level pressure, vorticity, meridional velocity). The coarse scale output from GCMs is then used to drive this relationship, allowing changes in the corresponding local scale variable to be estimated. Although the basic methodology remains the same, specific approaches differ according to the transfer function and predictor set employed; they also differ with respect to the statistical fitting procedure used. The often complex and non-linear predictor-predictand relationships which exist have necessitated the use of a wide range of regression models including, linear and non-linear regression (Huth, 1999; Hellström *et al.*, 2001; Fealy & Sweeney, 2008), generalized linear models (Fealy & Sweeney, 2007) artificial neural networks (ANNs) (Crane & Hewitson, 1998; Wilby *et al.*, 1998), singular value decomposition (SVD) (Huth, 1999; Chu & Yu, 2010), multi-variate splines (Corte-Real *et al.*, 1995) and canonical correlation analysis (CCA) (von Storch *et al.*, 1993; Huth, 1999).

Huth (1999) compared the performance of several linear models when used to downscale daily mean winter temperature for 39 stations across central Europe. The study considered CCA, SVD and three multiple regression models (stepwise regression of principal components (PCs) and regression of PCs with and without the stepwise screening of gridded values). The predictors used in the study included 500 hPa heights, MSLP, 850 hPa temperature and 1000–500 hPa thickness. The model incorporating PCs with stepwise screening was found to perform best according to the evaluation criteria employed. Each of the other methods performed comparably but only when a large number of the predictor's PCs were used; in addition Huth (1999) indicates that the SVD method performed worst. When evaluating the explanatory power of the predictors used Huth (1999) found that those models which employed temperature variables returned more accurate results than those using circulation variables alone. The best performing models were those using a combination of 850 hPa, temperature and 500 hPa. Huth (1999) indicates that the results may be different for other seasons, particularly summer when the link between surface weather and low-frequency circulation features is much weaker. It is noted however that by using GCM output rather than reanalysis data (as was used in this study) the models may produce different results. The author indicates that this is due to GCMs simulating atmospheric predictors and large scale climate features (e.g. teleconnections, modes of variability) - when compared with reanalysis data - with varying degrees of accuracy.

Fealy and Sweeney (2007) employed a generalized linear modelling approach to downscale precipitation scenarios for 14 synoptic stations across Ireland. In this case a two step approach was taken, whereby precipitation occurrence was downscaled using logistic regression; rainfall amounts were subsequently modelled for wet-days only using a generalized linear model with a gamma distribution and log-link function. In a subsequent study Fealy and Sweeney (2008) employed a step-wise linear regression model to downscale temperature, radiation and potential evapotranspiration for multiple sites across Ireland.

Regression methods have the benefit of allowing a direct and physically sensible relationship to be established between local-scale weather events and the large-scale atmospheric state (Wilby, 1997). As regression models incur minimal computational costs, the approach is suited for conducting uncertainty assessments. The key weaknesses associated with regression type downscaling are related to the

underestimation of variance. The results from regression models are also affected by uncertainty introduced by way of the predictors and model domain used.

5.3 An inter-comparison of statistical downscaling methods

A number of studies comparing the relative merits of different approaches in statistical downscaling have been conducted. Weichert and Bürger (1998) compared linear and nonlinear (Radial Basis Function) downscaling models using the same atmospheric circulation data. In this case the models were used to downscale temperature, precipitation and vapor pressure for a station located in central Europe. The results indicated that when downscaling precipitation both modelling approaches performed poorly, capturing only a small proportion of the observed variability (correlation ~40%). The authors state that despite this, clear differences in the applicability of both models were evident. The artificial neural network was better at capturing rainfall occurrence; in addition it was found that heavy precipitation events occurring during convective storms were often detected by the non-linear model only. However, while the model was able to detect these events, the amount of precipitation it simulated for them was so low as to be inconsequential in the overall model output. Weichert and Bürger (1998) highlight the underestimation of variance as a key weakness of (non-)linear models. The authors also highlight the limitations of analogue methods, pointing to their inability to model new and possibly unforeseen climatic changes which lie outside the bounds of what has occurred over the observed period of record.

Huth (2008) also explored differences between linear and non-linear downscaling approaches; for this study temperature was downscaled to 8 stations across Europe. Huth (2008) compared seven models, including linear regression of grid point values and PC regression of predictor's principal components; the other models used included variants of ANNs and regression models based on individual circulation types. Conditional on the evaluation criteria employed, pointwise linear regression appeared to be the best performing method. Both the pointwise neural network (NN) and linear regression models were better than the PC- based NN and linear models. It is noted by the author that using the principal components may result in a loss of critical information in the predictor fields. Huth (2008) indicates that the skill of the linear model used may be due to the predictand-predictor relationship being intrinsically linear, as a result of which little value is added by employing a non-linear approach. The

number of parameters which must be adjusted in neural networks, and the uncertainty associated with calibrating them (i.e. difficulties in determining a global optimum), is also cited as a possible reason for their relatively poor performance.

Zorita and von Storch (1999) compared an analogue approach to more complex models (CCA, ANNs and classification and regression tree approach) based on their ability to downscale monthly and daily winter rainfall for 92 stations located across the Iberian Peninsula. The results indicated that the relatively simple analogue method performed as well as the more complex methods considered. It was found the analogue approach could be applied to non-normally distributed variables and was capable of reproducing the observed variability of the predictand; it also had the additional benefit of preserving inter-site correlations. In contrast the results indicated that the linear model and neural networks used underestimated the variability of observed precipitation; however, the authors state that the linear model offers a more physically sensible approach for capturing the relationship between local and large scale variability. This is in contrast to the more complex classification and neural network methods which, Zorita and von Storch (1999) indicate do not directly offer a physical interpretation of this relationship. The authors argue that this supports more strongly the validity of linear models under perturbed forcing conditions - provided that the variability of their output can be augmented to reflect the true variance of the target predictand.

As highlighted by Fowler *et al.* (2007), ANNs have been reported to perform poorly in the simulation of daily precipitation - particularly with respect to the simulation of the wet day occurrence (e.g. Wilby & Wigley, 1997; Wilby *et al.*, 1998; Zorita & von Storch, 1999; Khan *et al.*, 2006). Schoof and Pryor (2001) compared the performance of multiple-linear regression to a series of ANNs when used to downscale daily (maximum and minimum) air temperature, precipitation and total monthly precipitation receipts for a site in Indianapolis (USA). The findings indicated that both approaches performed well when used to downscale temperature, but were found to underestimate the variability of precipitation, particularly over shorter time scales. The ANNs performed better when used to model total monthly precipitation as opposed to daily precipitation; in addition, when the models were used to downscale temperature, model performance was found to improve when an autoregressive term was included.

Diaz-Nieto and Wilby (2005) compared the use of change factors to a statistical downscaling model using a case study of low flows in the River Thames - both baseline and future climate conditions were considered. The authors highlight that the

assumption implicit when using change factors - that the temporal structure of the future climate is the same as the baseline climatology - is a key weakness of this approach. The catchment response was found to be more complex and conservative when modelled using the statistically downscaled data as opposed to data derived using the change factor approach. Diaz-Nieto and Wilby (2005) attribute this to the differential treatment of multi-decadal natural variability and the temporal structuring of daily climate variables.

Harpham and Wilby (2005) compared the performance of three different models (Radial Basis Function, Multi Layer Perceptron and SDSM) when used to downscale heavy precipitation for multiple sites in northwest and southeast England respectively. It was found that SDSM (Statistical DownScaling Model; Wilby *et al.*, 2002) produced more spatially coherent inter-site correlations. This model was also shown to provide a better representation of daily precipitation quantiles; however, for individual sites, the ANNs were shown to be more skillful. All models considered had the greatest skill for those indices relating to the persistence of large-scale winter precipitation.

A number of other studies have compared SDSM to alternative downscaling methods/models (e.g. Dibike & Coulibaly, 2005; Khan *et al.*, 2006; Diaz-Nieto & Wilby, 2005). Chen *et al.* (2010) compared SDSM to a support vector machine (SVM) and multivariate analysis when used to downscale climate data for the Shih-Men Reservoir basin in Taiwan. It was found that SDSM performed better than the other models at capturing daily precipitation events less than 10 mm; however, the results indicated that the SVM method produced a more accurate simulation of daily precipitation when compared with either SDSM or the multivariate model. A study by Liu *et al.* (2008) compared SDSM with a time lagged feedforward neural network (TLFN) and an evolutionary polynomial regression (EPR) technique for downscaling numerical weather ensemble forecasts generated by a medium range forecast model. The selected methods were employed for downscaling daily precipitation and temperature data for the Chute-du-Diable basin located in northeastern Canada. The TLFN and EPR models were found to be more efficient techniques when applied to downscale daily precipitation and temperature respectively.

Liu *et al.* (2011) compared the performance of SDSM and a nonhomogeneous hidden Markov model (NHMM) when used to downscale daily precipitation to the Tarim River basin located in northwest China. The NHMM showed greater skill at simulating

monthly precipitation and wet-day amounts, in addition SDSM performed relatively poorly at reproducing the higher quantiles of rainfall amounts - particularly for dry stations (those with an annual precipitation yield of <200 mm). Hashmi *et al.* (2010) compared the performance of SDSM and the LARS-WG when used to simulate the frequency of extreme precipitation events for the Clutha river catchment (located in South Island, New Zealand). Both models exhibited a comparable level of skill in reproducing the monthly mean and standard deviation of the observed series, additionally each model was found to reproduce present-day extreme events with a reasonable level of skill; however, when used to downscale data from the same GCM both produced diverging accounts of future extremes.

Dibike and Coulibaly (2005) employed the LARS-WG and SDSM to downscale temperature and precipitation scenarios for a catchment system (Chute-du-Diable) in northern Quebec. Under observed conditions SDSM was found to underestimate the wet-spell length for most months of the year, in contrast the LARS-WG was more skillful at reproducing wet and dry spell lengths. Both models reproduced daily precipitation reasonably well, with little difference being evident in their respective performance. For the majority of months SDSM tended to overestimate temperature, while the LARS-WG both over and under estimated temperature during different periods of the year. Although the models reproduced observed climate conditions with a similar level of skill, each produced diverging projections of future change when forced using the same GCM data. While the regression model suggested an increase in both the mean and variability of daily precipitation, data downscaled using the LARS-WG did not suggest such a trend - this highlights the uncertainty introduced by way of the downscaling method used. Khan *et al.* (2006) conducted a similar study to that of Dibike and Coulibaly (2005) using the same catchment system - here the authors compared SDSM, an ANN and the LARS-WG. The study indicated that SDSM was the best performing model at capturing the statistical attributes (e.g. skewness, dry-spell lengths) of observed daily precipitation and temperature; the results indicated that the ANN was the worst performing model.

Benestad (2001) compared empirical orthogonal functions (EOFs) to the more conventional approach of CCA for downscaling mean monthly temperature in Norway. The results suggested that the smallest errors were associated with scenarios derived using EOFs. Benestad (2001) state that EOFs have several advantages over using non-transformed predictors; this includes the ability to filter out noise and provide predictor

fields with a high spatial resolution. In addition the EOFs have the benefit of limiting the potential for overfitting the statistical model.

A study by Teutschbein *et al.* (2011) compared the performance of three different approaches (analog method, multi-objective fuzzy-rule-based classification and SDSM) used for downscaling precipitation to a meso-scale catchment in southwest Sweden. It was found that SDSM performed well at reproducing precipitation values for winter and spring, but slightly underestimated precipitation during summer and autumn. In contrast the analogue method was found to reproduce the annual cycle well. Based on the findings of the study Teutschbein *et al.* (2011) considered SDSM to be the most suitable approach for downscaling precipitation.

Wetterhall *et al.* (2007) compared four different statistical downscaling methods (two analog methods, multi-objective fuzzy-rule-based classification and SDSM) based on their ability to reproduce the statistical characteristics of daily precipitation at seven stations in south-central Sweden. The results indicated that both SDSM and the classification method performed equally well or better than both analogue approaches; however, no one method was found to perform best for all seasons. It was also found that SDSM skilfully captured the interannual variability of the precipitation series, whilst the classification approach performed best at reproducing the persistence and distribution of dry spells - although it tended to overestimate precipitation amounts. Similar to Teutschbein *et al.* (2011), Wetterhall *et al.* (2007) state that SDSM may be best suited for downscaling precipitation under altered forcing conditions. The authors give reasons for this including that the analogue approach is based only on sampling historical data and therefore cannot factor in unobserved changes. In addition, Wetterhall *et al.* (2007) highlight that, when employing methods based on classification approaches, an assumption must be made that the identified circulation patterns have the same variability under future forcing as under present day climate. The authors state that although the assumption of stationarity is implicitly associated with each method, SDSM and the fuzzy rule based classification approaches have the potential to produce reliable results when applied under altered forcing conditions.

Chiew *et al.* (2010) compared the performance of three models used to downscale precipitation for an area covering the head waters of the Murray River in south-east Australia. The models used included a daily scaling model, an analogue model and two stochastic models: GLIMCLIM (Generalised Linear Model for daily Climate time series software package) (Chandler, 2002), and NHMM (nonhomogeneous hidden Markov

model) (Hughes *et al.*, 1999). Chiew *et al.* (2010) highlight the usefulness of the simpler scaling and analogue methods for impact studies focused over very large regions (i.e. where smoothed data has less potential to affect the results); however, the authors state that the parametric models offer potential improvements as they capture a fuller range of the daily precipitation characteristics.

Frost *et al.* (2011) examined the performance of five statistical models when used to downscale multi-site daily precipitation to a set of thirty point locations across south-eastern Australia. The methods used included a scaling and analogue model GLIMCLIM (Chandler, 2002) as well as two stochastic models: NHMM and MMM-KDE (modified Markov model – kernel probability density estimation). The models were assessed based on their ability to reproduce a range of statistics including the inter-annual variability, spatial coherence and extremes. The study found that the relatively simple scaling approach provided robust results for a range of statistics; however, the stochastic models were better able to capture higher order statistics. The authors advocate the use of stochastic models in cases where capturing the full range of (day-to-day) variability in the downscaled series is important. It is argued that in the case of macro-scale impact studies, where less detailed climate data is required, scenarios obtained using a scaling approach should suffice (Frost *et al.*, 2011). In this respect the most appropriate statistical method to use can be, at least in-part, determined based on the intended application of the downscaled data.

5.4 Relative skill of statistical and dynamical downscaling

As outlined in Table 5.1 there are various strengths and weakness associated with both dynamical and statistical approaches. Given its low computational demands statistical downscaling is ideal in cases where multiple local-scale scenarios are required; as a result this approach may be more applicable when conducting uncertainty assessments. However, unlike dynamical methods, statistical downscaling cannot explicitly resolve the physical processes which condition regional-scale climate. Instead empirical methods seek only to quantitatively describe the relationship between large and local scale variability, without any requirement to necessarily understand this relationship – albeit that there is an implicit assumption that the relationship would be physically sensible.

There is a broad consensus within the downscaling community that both dynamical and statistical approaches exhibit a comparable level of skill when applied under observed climate conditions (Kidson & Thompson 1998, Mearns *et al.* 1999, Murphy 1999, Hellström *et al.*, 2001). Indeed it is suggested that there may be no single optimum approach to downscaling, and that the most appropriate method may depend more on the research question posed, the complexity of the target region and the variable(s) for which data is required.

	Statistical Downscaling	Dynamical Downscaling
<i>Strengths</i>	<ul style="list-style-type: none"> ▪ Can derive point-scale climate information from GCM-scale output ▪ Computationally inexpensive ▪ Allows the easy production of climate ensembles for risk/uncertainty analyses ▪ Easily transferable to other regions ▪ Can be used to downscale variables not available from RCMs 	<ul style="list-style-type: none"> ▪ 10-50 km resolution climate information from GCM-scale output ▪ Responds to different forcing conditions in a physically consistent way ▪ Capable of resolving important physical processes dynamically (e.g. orographic rainfall) ▪ Consistency with GCM
<i>Weaknesses</i>	<ul style="list-style-type: none"> ▪ Dependent on the realism of GCM boundary forcing; effected by biases in driving GCM ▪ Choice of domain size and location affects results ▪ Necessitates good quality data of a sufficient length to development and test statistical models ▪ Dependent upon choice of predictors ▪ Domain size, climatic region and season affects downscaling skill ▪ Fundamental assumption of model stationarity is not verifiable 	<ul style="list-style-type: none"> ▪ Dependent on the realism of GCM boundary forcing ▪ Choice of domain size and location influences results ▪ Requires significant computing power ▪ Limited to producing few ensembles of climate scenarios

Table 5.1 Summary of the relative strengths and weaknesses of statistical and dynamical approaches to downscaling (adapted from Wilby & Wigley, 1997).

Despite having a similar level of skill under current climate, both statistical and dynamical models may produce significantly different results when employed under perturbed forcing conditions (Cubasch *et al.*, 1996; Wilby & Wigley, 1997; Wilby *et al.*, 1998; Mearns *et al.*, 1999; Murphy, 2000). Hence the choice of downscaling method is one of the key sources of uncertainty in regionalized climate scenarios. One of the reasons suggested for this is that the statistical relationships established under present day climate may not hold true when used to extrapolate beyond conditions for which they were initially established (Collins, 2007). This must be prefaced with the caveat that dynamical models are themselves not exempt from making such assumptions.

Regional models incorporate statistical approximations of important climate processes which occur on too small a spatial scale to be resolved dynamically. The parameterization schemes used to represent these processes are based on empirical

relationships derived under present day climate, and as such may be invalid when applied under altered forcing conditions. However, as the core basis of dynamical models is immutable physical laws and not unverifiable assumptions, it is argued this provides a stronger foundation for their validity under perturbed forcing (Foley, 2010). A number of studies have compared the performance of statistical and dynamical methods under contrasting conditions (e.g. across different timescales, in diverse regions and under multiple future forcing conditions) using a range of evaluation criteria.

Kidson and Thompson (1998) compared the performance of the Regional Atmospheric Modelling System (RAMS) to a regression based statistical downscaling model. In this study the models were assessed based on their ability to simulate observed daily precipitation and temperature recorded at 78 sites across New Zealand (covering the period 1980-1994). The statistical predictors used included five EOFs of pressure data (1000 & 500 hPa) and a series of local-scale secondary variables. The results indicated that both methods performed well at simulating the daily and monthly station anomalies of each variable; however, the regional model was found to be more skilful at reproducing convective precipitation. Although Kidson and Thompson (1998) highlight the low computational requirements of statistical downscaling as one of its strong points, the authors state that dynamical models may be more appropriate when modelling climate conditions which are beyond the range of what has been previously experienced.

Murphy (1999) compared the skill of an RCM to that of a regression based statistical model when employed to downscale precipitation and temperature for 976 sites across Europe (covering the period 1983-1994). The performance of both the statistical and dynamical approaches was considered alongside the unaltered grid-scale output from the driving GCM – as such this study highlighted the ‘added value’ of employing a downscaling model. The skill of each approach was compared based on the correlation between the estimated and observed time series of monthly anomalies. Both the RCM and statistical model exhibited a similar level of skill; additionally both were superior to the grid scale GCM (without downscaling applied). The regression model was more skilful at capturing summer temperature while the dynamical approach was slightly better at downscaling winter precipitation. With respect to precipitation, Murphy (1999) highlights the greater skill levels of the RCM over areas with more complex topographical features (e.g. coastlines, mountainous areas). Applying the same

methods/models as Murphy (1999), Murphy (2000) produced climate scenarios for a European domain using GCM data (2080-2100). The results indicate that while the RCM and statistical models both simulated observed climate with a comparable level of skill, when forced using GCM data they produced diverging projections of future climate change. Changes in temperature suggested by the regression and dynamical models respectively were found to differ by 40-50%; differences were also apparent in the precipitation scenarios obtained using each model (RCM, GCM and statistical). To address uncertainty in the projections the author suggests attaching a measure of reliability to each method/model; however, it is highlighted that this would introduce a degree of subjectivity to the results. With regards to the statistical model used, Murphy (2000) found that the observed (based on reanalysis data) predictor-predictand relationship was not the same as the corresponding relationship estimated using GCM data. This highlights the influence which inconsistencies inherited from the driving GCM can have on the predictor-predictand relationship initially established using observed or reanalysis data.

Differences in the climate projections downscaled using both a dynamical (RegCM2) and statistical (WG) approach is also a feature of a study by Mearns *et al.* (1999). Similar to the findings of Murphy (2000), both the statistical and regional models used performed comparably when employed to downscale observed climate series (temperature and precipitation); however, when the models were applied under perturbed forcing they were found to respond differently. The RCM simulated both increases and decreases in the probability of precipitation; in contrast the statistical model suggested increases only. In addition, for 40% of the locations and months considered, the models disagreed as to the direction of mean change. The requirement of the statistical model to extrapolate beyond observed conditions is cited as a possible reason for the apparent lack of convergence between the model projections.

Hellström *et al.* (2001) compared precipitation downscaled for Sweden using the Rossby Centre RCM (RCA1) with data downscaled using a multiple-linear regression model. In this study circulation indices and atmospheric humidity were used as large-scale predictors. Two different GCMs were considered (HadCM2 and ECHAM4) and each model (including the GCMs) was assessed based on its ability to reproduce the observed seasonal cycle. Each of the downscaling models brought about an improvement in the skill of the GCMs, highlighting the value added by employing an intermediate downscaling step. Hellström *et al.* (2001) indicate that both the statistical

and dynamical models exhibited equal skill in reproducing the annual precipitation regime. An assessment of the downscaled projections indicated that differences between those series derived using the regression models (i.e. forced by different GCMs) were greater than differences between those derived using the dynamical models. The seasonally averaged difference between the dynamical and statistical scenarios obtained using the ECHAM4 GCM was 12%; in contrast there was a 21% difference in the scenarios downscaled from the HadCM2.

Wilby *et al.* (2000) found that a multiple-linear regression model performed better than an RCM (RegCM2) when used to downscale precipitation and temperature for a mountainous catchment in Colorado (Animas basin); in this study NCEP reanalysis data was used. A study by Hay and Clark (2003), which focused on three mountains catchments in the USA (located in Washington, Nevada and Colorado), produced similar results to Wilby *et al.* (2000). In this study NCEP reanalysis data was downscaled using the RegCM2 regional model; statistical downscaling was conducted using multiple-linear regression. It was found that both the statistical and dynamical models were able to capture gross aspects in the seasonal cycles of observed temperature and precipitation respectively; however, the authors highlight the requirement to bias correct the dynamically downscaled data as a key drawback of this approach, particularly as it is unknown whether the correction - empirically derived observed climate data - remains valid under perturbed forcing conditions (i.e. whether the correction is both time and state invariant).

Spak *et al.* (2007) employed multiple-linear regression alongside a dynamical model (MM5) to downscale monthly mean surface temperature over the eastern region of North America. The predictors used in the regression models included mean sea level pressure (MSLP) and 2 m temperature (decomposed into EOFs). The models employed exhibited comparable skill levels when used to simulate observed conditions, in addition their projections suggested similar changes in mean temperature (2000-2087); however, the models produced significantly different spatial patterns in the climate response, highlighting that the projections may not only diverge on a temporal basis, but also spatially.

Hanssen-Bauer *et al.* (2003) downscaled temperature and precipitation for a Norwegian domain using multiple-linear regression and a dynamical (HIRHAM) model. Temperature and MSLP were used as predictors in the statistical model for both variables. Differences in the projections from each model were found not to be

statistically significant; however, disparities in the spatial pattern of warming were found to occur. Hanssen-Bauer *et al.* (2003) indicate that the RCM projections for summer precipitation were more likely to be reliable when considered against the projections from the empirical model. In contrast to the dynamically downscaled data, it was found that the statistically downscaled projections did not suggest any change in summer precipitation. This was attributed to surface temperature not being included as a predictor when modelling summer precipitation. It is argued this resulted in a loss of the climate change signal, with the result that variations in MSLP only determined the extent of future change. This highlights the importance of predictor selection and the uncertainty which it can introduce.

Schmidli *et al.* (2007) conducted a study to assess the performance of six statistical models and three RCMs when used to downscale precipitation for the European Alps. The statistical models used included: linear regression, CCA, weather typing, a weather generator, an analog approach and a model based on local intensity scaling. For each of the models considered the complexity of the terrain and time of year was found to influence performance. The results generally indicated that the RCMs performed best during winter over mountainous areas; in contrast, during the summer months, over flatter terrain disparities in the performance of the statistical and dynamical models were reduced. The scenarios downscaled from the dynamical and statistical models respectively were found to exhibit similar biases; however, the statistical methods strongly underestimated the interannual variability, particularly during summer. Schmidli *et al.* (2007) attributes this to the greater importance of stochastic processes during this season and the inability of the statistical models to consider the affects of local scale forcings. The study concludes that for this region, the methods used significantly contribute to uncertainty in the downscaled scenarios. This was particularly evident for summer where large differences between the individual statistical models, as well as between the projections from the statistical and regional models, were found to occur.

Haylock *et al.* (2006b) compared the performance of six statistical (CCA, ANNs, SDSM) and two dynamical models (HadRM3, CHRM) when used to downscale precipitation for two station networks in southeast and northwest England respectively. The ability of each model to capture seven indices of heavy precipitation (e.g. mean, 90th percentile) was used to gauge model performance. It was found that the models performed best for winter as opposed to summer, and were better able to reproduce the

mean rather than extreme statistics. The ANNs were best at reproducing interannual variability but tended to underestimate the extremes. When used to downscale precipitation from the HadAM3P GCM, run using both the A2 and B2 SRES emission scenario, the results indicated that inter-model differences - with respect to projected changes in each of the indices considered - were at least as large as the differences evident between the emission scenarios. Thus, the results of the study highlight the uncertainty which can be introduced by way of the downscaling model/method used.

In their study of the hydrological impact of climate change on the Seine river basin (France) Boé *et al.* (2007) compared data downscaled from the Météo-France ARPEGE GCM using both a statistical and dynamical approach. The statistical downscaling method employed was based on weather typing and conditional resampling. It was found that the statistical approach was more skilful at reproducing the temporal and spatial autocorrelation properties of observed temperature and precipitation; however, the hydrological simulations produced using both sets of data were found to be relatively similar. In addition both were found to reproduce the seasonal cycle as well as the distribution of daily runoff with a high degree of accuracy.

5.5 Conclusion

Whilst it is clear that downscaling adds considerable value to GCM generated data, as highlighted by the various review studies undertaken (e.g. Wilby & Wigley, 1997; Murphy, 1999; STARDEX Final Report, 2005; Fowler *et al.*, 2007; Maraun *et al.*, 2010), no one optimum approach to downscaling exists. There are strengths, weaknesses and assumptions implicit in all; furthermore, with respect to present day climates at least, dynamical methods appear to hold little advantage over the various statistical techniques available (Fowler *et al.*, 2007). It would appear that the answer to the question of which is the best method is study specific - the most appropriate approach may depend on the study area (e.g. topographic complexity, availability of observational data) and datasets required (e.g. target variable, stochastic/deterministic, single/multiple sites); crucially it also depends on the nature of the study being undertaken (e.g. water balance studies, flood assessments).

RCMs have the advantage of being able to resolve local scale forcings dynamically, and add considerable detail to coarse scale GCM data; this is exemplified by their notable

skill over topographically complex regions. Although their physical basis means they are potentially more reliable under perturbed forcing, the requirement to represent key physical processes parametrically means regional models are dependent on the stationarity of the empirically derived relationships under perturbed forcing. Maraun *et al.* (2010) highlight the sensitivity of dynamical downscaling to the model configuration (e.g. grid resolution, numerical scheme); they also highlight the requirement to represent sub-grid scale processes parametrically and the influence which biases inherited from the driving GCM can have as sources of uncertainty in the downscaled scenarios.

Similarly statistical methods are subject to a range of uncertainties and are heavily dependent on the assumption of stationarity. Predictor selection is a critical step in the application of statistical models, and one which necessarily introduces uncertainty to the downscaled data. In a climate change context it is important that predictors which capture the warming signal are considered, even if under observed conditions they appear to add little explanatory power to the model. As highlighted above, there are various shortcomings associated with all statistical methods; for example, although linear-regression provides a direct link between local and large-scale variability, the propensity for regression models to underestimate the true variance of the local-scale predictand is an important weakness, particularly in terms of how extreme events are represented. In order to address the uncertainty introduced by way of the downscaling method used, Fowler *et al.* (2007) advocate employing a range of methods within a probabilistic framework, whereby the convergence/divergence in the projections from each can be accounted for. The following chapter discusses the various methods used to downscale climate scenarios for the Burrishoole catchment.

Chapter 6

High resolution climate scenarios for the Burrishoole catchment

6.1 Introduction

The climate scenarios used in this study represent multiple combinations of driving GCMs, GHG-emission scenarios and statistical/dynamical downscaling models - each representing a different 'model pathway'. By considering multiple model pathways this study attempts to sample across the uncertainties encountered at each stage in the 'cascade of uncertainty' (Figure 4.2) (Schneider, 1983). Although it is common practice the over-reliance on a single realisation of future climate may lead to the suppression of key uncertainties in estimates of future climate change. The uncertainties which permeate the development of high resolution climate projections are manifest in the degree to which different climate models - when forced using the same driving data - produce conflicting projections of future change (Jenkins & Lowe, 2003). The inconsistencies between model projections apply not only to the magnitude but also the timing, spatial distribution and direction of change. Thus, where policy decisions are based on a single realisation of future climate, there is potential for an over- or under-estimation of the true risk posed by climate change, increasing the likelihood of maladaptation and the implementation of ineffective response decisions.

Employing multiple climate models, along with different downscaling methods/models, is a more pragmatic approach which recognizes that all models or regionalization techniques are lacking in skill (with respect to how well they capture different aspects of observed system behaviour), and consequently it is not advisable to rely on any single method or model pathway in isolation. Adopting a multi-model approach allows the strengths of different models to be combined. In addition it recognizes that all model pathways represent a plausible future, and by utilizing the output from many different pathways a greater number of these plausible futures can be sampled - thus providing a more robust basis for climate change adaptation and policy decisions.

Although the uncertainty inherent in local-scale climate projections is to a certain extent unavoidable, it is possible to quantify the uncertainty range using prior knowledge about the relative skill of the particular model pathways or methods used to develop them. Attaching a weighting to each ensemble member - based on model skill under current climate - has the advantage of constraining the influence which poorly performing

models have on the overall ensemble response. Weighting ensemble members is however a somewhat subjective process, and it is argued that the development and implementation of weighting systems - in terms of the particular aspects of model performance which are assessed, the metrics used to evaluate them and the weighting different metrics are themselves given in the final scheme - simply adds an additional layer of uncertainty which must be explored (Christensen *et al.*, 2010). Furthermore, the implementation of a weighting scheme also comes with the assumption that model performance is both time and state invariant. Tebaldi and Knutti (2007) argue however that weighting schemes can be made more robust by using multiple diagnostics and by attempting to account for as much uncertainty as is possible. The converse of employing a weighting scheme is to treat the output from all models as being equally plausible, irrespective of performance under present day conditions. Although this negates the requirement to employ a weighting scheme, not attempting to attach some probability to model simulations implicitly assumes that all models produce equally reliable projections of future climate, despite the fact that some may be poor at capturing the (large and local scale) mechanisms which are important for determining climate variability across different temporal and spatial scales.

With respect to the points raised above, concerning both the need to address uncertainty and the benefits of employing multiple climate scenarios, a climate ensemble consisting of both statistically and dynamically downscaled data from multiple GCMs was used in this study. In this case the dynamically downscaled projections were obtained from RCM experiments conducted as part of the EU funded ENSEMBLES project (van der Linden & Mitchell, 2009). The following sections discuss the statistical models used to downscale climate scenarios for the catchment, in addition details of the dynamically downscaled climate projections are provided; following from this the weighting scheme developed for use in the study is outlined.

6.2 Statistical downscaling of GCM output: data and methods

In order to address those uncertainties stemming variously from the emission scenario, GCM structure, model parameterization and climate sensitivity, the output from three different GCMs (HadCM3, CGCM2 and CSIROmk2), each run using two different emission scenarios (A2 and B2) were used as input data for the statistically downscaled scenarios. In this study linear regression was used when downscaling climate data to the catchment. The application of regression type methods involves five steps (Wilby *et al.*,

2000; Wilby *et al.*, 2002; Wilby *et al.*, 2006): (1) predictor selection; (2) model calibration; (3) simulation of observed series using reanalysis data; (4) model validation; and (5) the generation of future time-series using GCM output. Daily data for the target variables was obtained from the catchment's weather station (Figure 3.2; Table 3.2). In cases where data for a particular variable was unavailable, records from the Belmullet synoptic station were used (Table 3.2).

6.2.1 Datasets: Statistical Downscaling

The datasets used for model training and validation were selected on the basis that they contained information on a range of contrasting conditions and were in some way representative of (likely) future climate. The years 1990-2000 are some of the warmest on record for the catchment and thus were considered to be representative of atmospheric conditions under future climate forcing; for this reason, where observed records were available for the years 1961-2000, the periods 1961–1978 and 1994–2000 respectively were used for model calibration. These periods were also selected as they are consistent with the time periods used in the EU funded STARDEX project - one of the aims of which was to conduct an inter-comparison of statistical downscaling methods (STARDEX Final Report, 2005; Wetterhall *et al.*, 2007). In order for the calibrated model to be applicable under perturbed forcing conditions, it is important that the statistical relationship was shown to remain valid for an independent validation period. To this end observed records for the years 1979-1993 were withheld for model testing.

6.2.1.1 NCEP Reanalysis Data

The gridded atmospheric data used to establish the predictor-predictand relationship was obtained from the UKSDSM data archive (Wilby & Dawson, 2004). The source of this data is the National Centers for Environmental Prediction (NCEP) reanalysis project (Kalnay *et al.*, 1996). For downscaling purposes the NCEP data was previously regridded (i.e. interpolated onto a common grid) to conform to the 2.5° latitude 3.75° longitude grid of the Hadley Centre's coupled atmosphere-ocean global climate model: HadCM3 (Harris, 2004). The UKSDSM archive contains daily predictors for the period 1961-2000 which variously describe atmospheric circulation, airflow and vapour content at three different levels in the atmosphere (surface, 850 hPa and 500 hPa) (Table

6.1). Reanalysis data from the UKSDSM archive is available for nine regions or grid-boxes covering the British Isles.

The 1-day lead and lag of each predictor was also included in the dataset; this allowed for any temporal offset between the NCEP predictors (averaged over the period 00:00–24:00) and point-scale observations (e.g. precipitation is recorded daily over the period 09:00–09:00 h) (Wilby *et al.*, 2002; Haylock *et al.*, 2006b; Fealy & Sweeney, 2007). To ensure the downscaled scenarios were not compromised by systematic biases in the driving data, candidate predictors (both NCEP and GCM) were standardized with respect to their 1961-1990 climatology (after Karl *et al.*, 1990) – this was done by subtracting the long term mean value and dividing the difference by its standard deviation. It is common practice when developing local-scale scenarios to take climate information from the grid box directly overlying the study area, thus large-scale datasets for the Irish grid box only were considered in this study.

Variable	Abbreviation
Mean temperature	temp
Mean sea level pressure	mslp
500 hPa geopotential height	p500
850 hPa geopotential height	p850
Near surface relative humidity	rhum
Relative humidity at 500 hPa	r500
Relative humidity at 850 hPa	r850
Near surface specific humidity	shum
<i>Geostrophic airflow velocity</i>	<i>f</i>
<i>Vorticity</i>	<i>z</i>
<i>Zonal velocity component</i>	<i>u</i>
<i>Meridional velocity component</i>	<i>v</i>
<i>Wind direction</i>	<i>th</i>
<i>Wind Divergence</i>	<i>zh</i>

Table 6.1 Candidate (NCEP and GCM) predictor variables available from the UKSDSM data archive. Note: Italics indicate secondary airflow indices calculated from pressure fields (surface, 500 and 850 hPa).

6.2.1.2 Global Climate Model data for the Irish grid box

Future climate scenarios were generated using predictor variables from three different GCMs, each run using both the medium-high A2 and medium-low B2 SRES (Special Report on Emission Scenarios) emissions scenarios (Nakicenovic *et al.*, 2000). GCM data for the Irish grid box was obtained from the UKSDSM data archive (Wilby & Dawson, 2004) and covers the period 1961–2100. The GCMs considered included: HadCM3, from the Hadley Centre for Climate Prediction and Research (Met Office, UK); CCGCM2, from the Canadian Centre for Climate Modelling and Analysis

(CCCMA; Canada); and CSIRO-Mk2 from the Commonwealth Science and Industrial Research Organisation (CSIRO, Australia). The same predictors available from the NCEP reanalysis dataset (listed in Table 6.1) were available for each of the three GCMs.

6.2.2 Model Description: Linear Regression (SDSM)

Linear regression was implemented through the statistical downscaling model SDSM (Statistical DownScaling Model) (Wilby *et al.*, 2002; Wilby & Dawson, 2004) - a software package used for downscaling multiple-scenarios of surface weather variables at individual sites on a daily time-step using grid resolution re-analysis and GCM data. SDSM is best described as a ‘hybrid’ of the stochastic weather generator and regression based downscaling methods (Wilby *et al.*, 2002). The model has previously been applied in a host of meteorological, hydrological and environmental assessments across diverse climatic regions (e.g. Hassan *et al.*, 1998; Wilby *et al.*, 1999, 2000; Hay *et al.*, 2000; Harpham & Wilby, 2005; Dibike *et al.*, 2008; Chen *et al.*, 2010; Souvignat & Heinrich, 2011; Liu *et al.*, 2011).

SDSM has both a deterministic and stochastic component which allows it to incorporate the strengths of both the regression and weather generator type approaches to downscaling. Linear regression comprises the core deterministic component of the model and is used to establish a direct relationship between a set of large-scale atmospheric predictors and the target variable. This relationship can be written as:

$$Y_t = \partial_0 + \sum_{j=1}^n \partial_j u_t^{(j)} + \varepsilon_i$$

where Y_t is the local predictand on day t , ∂_j is the regression parameter optimized using ordinary least squares, $u_t^{(j)}$ represents n large-scale atmospheric predictors, and ε_i is a random error term represented by the Gaussian distribution $N(0, \sigma_\varepsilon^2)$.

The underestimation of variance is one of the key shortcomings of regression type approaches to downscaling (see section 5.2.2). To address this SDSM incorporates an additional stochastic component which is used to artificially inflate the variance of the downscaled series. Variance inflation is conducted using a pseudo-random number generator which samples values from a normal distribution with a mean of zero and a standard deviation equal to the standard error ($N(0, \sigma_\varepsilon^2)$). These values are added to the

deterministically derived output for each day. Variance inflation is necessary given the importance of representing extreme and higher quantile events in the downscaled series - particularly with respect to the data used in impact studies. Variance inflation is implemented by tuning the amount of white noise (e_i) which is added to the deterministic model output using the following:

$$e_i = \sqrt{\frac{VIF}{12}} z_i S_e + b$$

where z_i are normally distributed random numbers, S_e is the standard error of the estimate (produced from the initial regression equation), b is the model bias and VIF is the variance inflation factor. Both the VIF and b parameters are adjusted so that the model output better accords with the observed series. In the equation above VIF is divided by a scaling factor which remains constant in the model.

The weather generator element of SDSM enables multiple synthetic series or ensembles of daily weather data to be produced using a common set of grid-scale predictors. Ensemble members differ with respect to their individual time-series evolution but possess the same statistical attributes. The degree to which the respective series differ is dependent on the relative significance of the stochastic component in the model structure. For those variables which are to a greater degree determined by large-scale atmospheric forcing, a high proportion of the variance will be accounted for by regression alone; however, where the grid-scale predictors account only for a fraction of the observed variance, the stochastic element has a comparatively greater weighting. This applies to variables like precipitation which display more ‘noise’ arising from localised factors not captured by the grid-scale predictor fields. Stochastically generating multiple climate realizations has the advantage of allowing the range of internal variability displayed by the local climate to be somewhat represented in the downscaled data. When using the SDSM model, where a variable did not conform to the conventions of linear regression, a transformation was applied. This ensured the datasets approximated to the required normal distribution. In this study SDSM was employed to downscale climate scenarios for the following variables:

- Temperature (minimum and maximum) (°C)
- Precipitation (mm) (occurrence and amounts)

- Wind Speed (km h^{-1})
- Relative Humidity (%)
- Solar Radiation (Mj m^{-2})
- Potential Evapotranspiration (PET) (mm)

6.2.3 Model Description: Generalized Linear Model (GLM)

Whilst conventional linear regression requires the response variable to be normally distributed, generalized linear models (GLMs) have the advantage of being able to model data series which follow probability distributions from the exponential family (e.g. Gamma, Binomial, Poisson) (Mc Cullagh & Nelder, 1989). Thus, the use of GLMs avoids the need for data transformation, which is desirable given the loss of information which can occur when rescaling is employed. In addition the relationship between the response and explanatory variables may be more complex than the simple linear form required for standard regression; with respect to this, GLMs have the added benefit of allowing non-linear relationships to be modelled. As GLMs fit probability distributions to the target variable they should allow for a better representation of the higher quantiles; consequently they have a clear advantage over linear regression, particularly in cases where data transformation is required.

GLMs have previously been employed to study different climatological series (e.g. precipitation occurrence and amounts, wind speed) (Coe & Stern, 1982; Stern & Coe, 1984; Chandler & Wheeler, 2002a, 2002b; Yan *et al.*, 2002; Chandler, 2005; Yang *et al.*, 2006); they have also been used for the purposes of downscaling precipitation. Abaurrea and Asín (2005) employed logistic regression and a GLM with a Gamma error distribution to downscale rainfall occurrence and amounts respectively. It was found that the models were skilful in reproducing certain aspects of seasonal and daily precipitation behaviour (e.g. wet and dry spell length), but were less successful at reproducing extreme events. Fealy and Sweeney (2007) also employed two different GLMs when downscaling precipitation (occurrence and amounts) for a number of synoptic stations across Ireland. Buishand *et al.* (2004) applied a separate logistic model for downscaling daily and monthly rainfall occurrence for three stations in the Rhine basin. Buishand *et al.* (2004) also used a GLM with a Gamma distribution to downscale individual wet-day and monthly rainfall amounts for the same stations. In this study GLMs were employed to downscale daily data for precipitation and wind speed - both

of which present highly skewed distributions. A logistic regression was used to model rainfall occurrence, whilst for both precipitation amounts and wind speed a Gamma distribution with a log link function was employed. Wet-day rainfall amounts have typically been described using the Gamma distribution (e.g. Katz, 1977; Buishand, 1978). In this study the method of maximum likelihood was used to estimate the coefficient values for each regression model.

6.2.4 Predictor selection

Predictor selection is critical for determining the character of the downscaled series (Winkler *et al.*, 1997; Charles *et al.*, 1999) and represents a key source of uncertainty in estimates of local climate change (Huth, 2004); however, despite the importance of this process, there is little consensus within the downscaling community as to an optimum predictor set or selection process. Past studies have employed a diverse array of selection criteria, downscaling techniques and predictor combinations (including climate data extracted from various predictor fields), covering a range of geographical and climate contexts. As a result interpretations of what constitutes the most appropriate set of predictors for a given predictand or region differs greatly. As noted in previous studies, selecting the most appropriate set of predictors, which are sensitive to the region and timescales considered, is more pragmatic than using a single predictor or standard predictor set (Wilby *et al.*, 1998; Huth, 2004). Despite the differing and often subjective approaches taken to predictor selection, there are a number of points common to previous work which provides a guide to the selection process (listed in Section 5.2.2). These criteria are however frequently at odds with one another, indicating that a balance must be struck when choosing the most suitable predictor set. For example, in comparison to surface climate variables, climate models generally provide a more realistic description of large-scale circulation (Murphy, 1999); however, a number of studies (e.g. Kidson & Watterson, 1995; Wilby & Wigley, 1997) have shown that climate scenarios downscaled using circulation predictors only are largely insensitive to alterations in climate forcing, thus warranting the inclusion of additional variables which may be less well simulated.

In this study predictor selection was largely driven by the association shown between the candidate predictors and the target variable. Predictors were also chosen with the aim of capturing the key atmospheric mechanisms known to influence local-scale

events, even where the inclusion of such predictors appeared to add little explanatory power to the model; for example, when modelling precipitation some measure of atmospheric humidity was included for all seasons, despite humidity appearing to be generally non-informative. Care was taken to avoid multicollinearity and thus ensure stability in the model output. A separate model was developed for each season, for which the most appropriate set of predictors were selected. Modelling each predictand on a seasonal basis removed any influence which the annual cycle may have had on the coefficient values, it also allowed for temporal variations in the strength of the predictor-predictand relationship; however, where the downscaled series was shown to be sensitive to the selection of a particular variable, the same predictor was chosen for each season (e.g. the inclusion of mean sea level pressure when downscaling precipitation). This was to ensure there was some continuity in the driving data used to generate the seasonal scenarios.

In addition to employing large-scale surface and atmospheric variables as predictors, potential radiation and delta temperature (i.e. diurnal temperature range; ΔT) were used to downscale daily solar radiation and potential evaporation respectively. This approach takes its cue from conventional weather generators, whereby the data series for both variables is typically estimated based on their relationship with other meteorological parameters (Donatelli *et al.*, 2006; Fealy & Sweeney, 2008).

The quantity of solar radiation received at a given point on the Earth's surface is a function of potential radiation and some measure of atmospheric transmissivity. In this case transmissivity is related to cloud cover - for which ΔT is taken as a proxy. Bristow and Campbell (1984) demonstrated that a relationship exists between the radiation transmitted through the atmosphere and the diurnal range in near surface air temperature. Following Bristow and Campbell (1984) a modified version of ΔT was used in this study:

$$\Delta T = T_{max_t} - \frac{(T_{min_t} + T_{min_{t+1}})}{2}$$

where T_{min} and T_{max} represents point scale minimum and maximum temperature at time t . For the purposes of model calibration ΔT was calculated using observed records from the Furnace weather station (Figure 3.2). For each GCM and emissions pathway ΔT was calculated using the downscaled temperature scenarios for the catchment. Potential radiation was calculated using the following (Bristow & Campbell, 1984):

Distance from the sun:

$$dd2 = 1 + 0.0334 * \text{Cos}(0.01721 * \text{doy} - 0.0552)$$

Declination:

$$\text{dec} = \sin^{-1}(.39785 * \text{Sin}(4.869 + .0172 * \text{doy} + .03345 * \text{Sin}(6.224 + .0172 * \text{doy}))$$

Half day length:

$$hs = \cos^{-1}(-\text{Tan}(\text{dec}) * \text{Tan}(\text{lat}))$$

Potential Radiation:

$$\text{PotRad}(\text{day}) = 117.5 * dd2 * \frac{hs * \text{Sin}(\text{lat}) * \text{Sin}(\text{dec}) + \text{Cos}(\text{lat}) * \text{Cos}(\text{dec}) * \text{Sin}(hs)}{\pi}$$

where *doy* is the day of year, and *lat* is the latitude in radians. Given the influence which solar radiation has on surface evaporation, ΔT and extraterrestrial radiation were included in the predictor set when downscaling this variable. Incoming solar radiation was found to have a significant influence on potential evaporation, particularly for the winter season where its inclusion as a predictor increased the percentage of explained variance from less than ~15% to over 55% - this was a finding common to both the calibration and validation periods.

6.2.5 Temperature: calibration and validation

Temperature is a relatively homogenous variable over large areas; consequently a significant proportion of the variance exhibited at a local-scale is determined by the large-scale atmospheric state. In this study the predictors used to model point-scale temperature included 2 m surface temperature and several variables which variously describe atmospheric circulation (Table 6.2).

Season	Predictors	Maximum Temperature		Minimum Temperature		
		Calibration – (E %)	Validation – (E %)	Predictors	Calibration – (E %)	Validation – (E %)
DJF	<i>temp, u, p500, zh5</i>	72	73	<i>temp, p500, f, zh5</i>	67	65
MAM	<i>temp, u5, z, v5</i>	74	79	<i>temp, f8, z5, v5</i>	69	66
JJA	<i>temp, 8u, v</i>	65	66	<i>temp, f8, v</i>	50	52
SON	<i>temp, p500, v5, u5</i>	82	81	<i>temp, f8, zh, z5</i>	74	74

Table 6.2 Predictors used to downscale daily minimum and maximum temperature. Also shown is the explained variance (E %) for the calibration (1961–1978; 1994–2000) and independent validation (1979–1993) period.

This selection avoided the use of circulation variables alone which previous studies have indicated can lead to unrealistically low estimates of temperature change (Huth,

2004). The downscaled series captures a high proportion of the variance present in the observed data, thus within the SDSM model structure the deterministic component was dominant. Based on the explained variance and the slope of the best fit line, the seasonally downscaled series better accords with the observed data for the autumn and spring seasons (Figures 6.1 & 6.2). In contrast the lowest explained variance is associated with summer minimum temperature. Figure 6.3 and 6.4 indicate that the downscaled data captures the observed annual and inter-annual variability with a high degree of skill. Generally there appears to be no discernible difference in model skill over the validation and calibration periods. Table 6.3 compares the monthly statistics of the observed and model simulated (maximum and minimum) temperature series for the validation period. Based on this the downscaled NCEP data appears to underestimate the 5th percentile, but captures well the 95th percentile and monthly mean values. The coefficient of determination (R^2) is lowest for June and July minimum temperature.

Maximum Temperature	Jan	Feb	Mar	Apr	May	Jun	Jul	Aug	Sep	Oct	Nov	Dec
<i>Percentile 5th</i>	33.3	-13.5	-11.3	-14.6	-8.8	-6.2	-7.3	-8.2	-10.5	-10.4	-3.0	19.0
<i>Mean</i>	5.1	-2.5	2.1	-3.3	-2.7	-0.6	-1.1	0.0	-1.9	-1.6	2.9	3.4
<i>Percentile 95th</i>	5.2	2.6	11.1	-3.5	-8.4	-5.8	-4.1	0.9	1.5	4.3	5.8	3.2
<i>Std Deviation</i>	-7.4	8.3	36.8	3.7	-3.0	0.0	0.0	17.4	20.0	31.6	19.0	-7.7
<i>Range</i>	-2.5	11.7	29.3	1.2	-10.1	-3.1	3.1	14.1	0.7	20.4	21.6	-12.1
R^2	0.77	0.70	0.64	0.67	0.68	0.62	0.64	0.65	0.66	0.62	0.65	0.75
Minimum Temperature												
<i>Percentile 5th</i>	-18.2	8.3	0.0	-9.1	6.1	11.3	-5.4	1.2	10.5	10.3	16.7	0.0
<i>Mean</i>	10.3	-3.4	2.4	-3.7	0.0	1.0	-1.6	0.0	2.9	0.0	3.8	4.9
<i>Percentile 95th</i>	0.0	-6.4	0.0	4.4	2.5	0.7	3.3	-0.6	5.7	-0.8	3.1	-4.3
<i>Std Deviation</i>	-6.5	3.6	0.0	8.3	3.8	-4.5	10.5	-4.5	8.3	-3.6	0.0	-3.3
<i>Range</i>	2.9	8.7	-1.3	31.0	3.0	-18.5	14.4	-1.6	11.3	4.8	11.1	-1.2
R^2	0.67	0.57	0.56	0.59	0.53	0.38	0.43	0.51	0.53	0.65	0.57	0.67

Table 6.3 Percent bias for selected statistics calculated over the independent validation period (1979-1993) on a monthly basis for maximum and minimum temperature respectively; also shown is the coefficient of determination. The temperature series are downscaled from NCEP reanalysis data and compared to observations from the Furnace weather station (Figure 3.2).

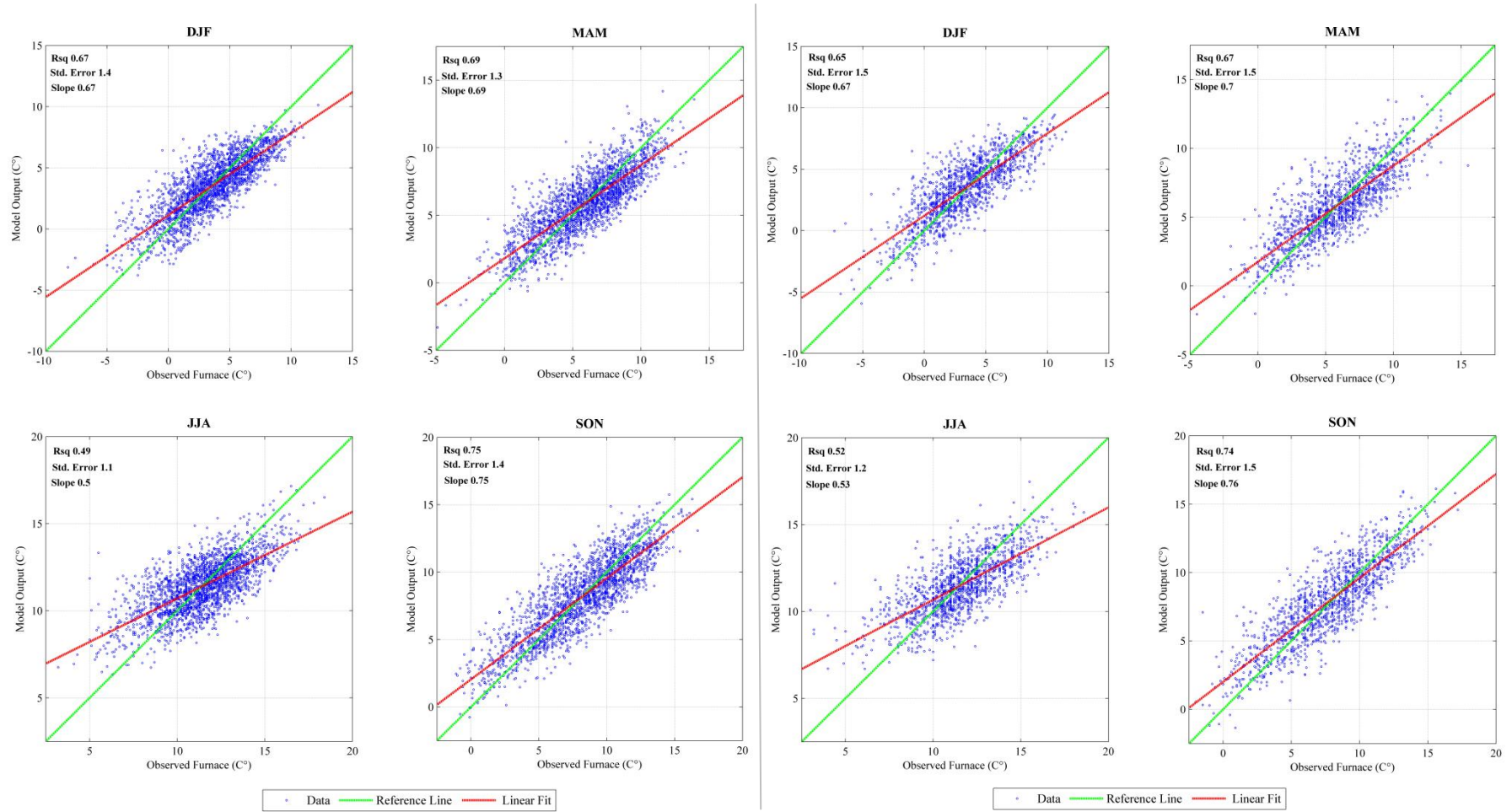


Figure 6.1 Seasonal scatter plots of downscaled *versus* observed (Furnace weather station) daily minimum temperature for the Furnace weather station. Temperature is downscaled using NCEP reanalysis data for the calibration (1961-1978; 1994-2000) (left panel) and validation (1979-1993) (right panel) periods respectively. Values for the explained variance, standard error and slope of the least squares fitted line are provided.

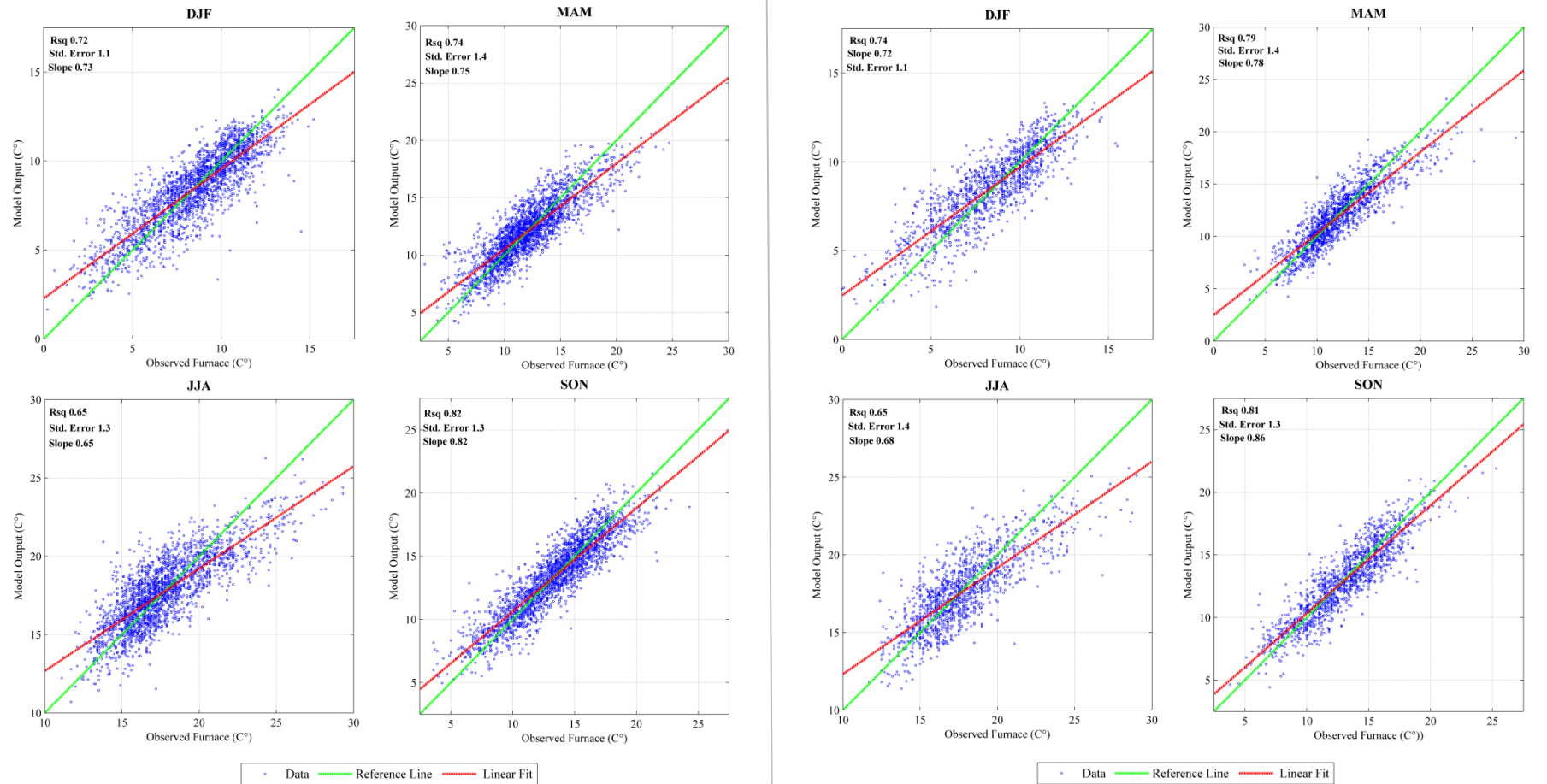


Figure 6.2 Seasonal scatter plots of downscaled *versus* observed (Furnace weather station) daily maximum temperature for the Furnace weather station. Temperature is downscaled using NCEP reanalysis data for the calibration (1961-1978; 1994-2000) (left panel) and validation (1979-1993) (right panel) periods respectively. Values for the explained variance, standard error and slope of the least squares fitted line are provided.

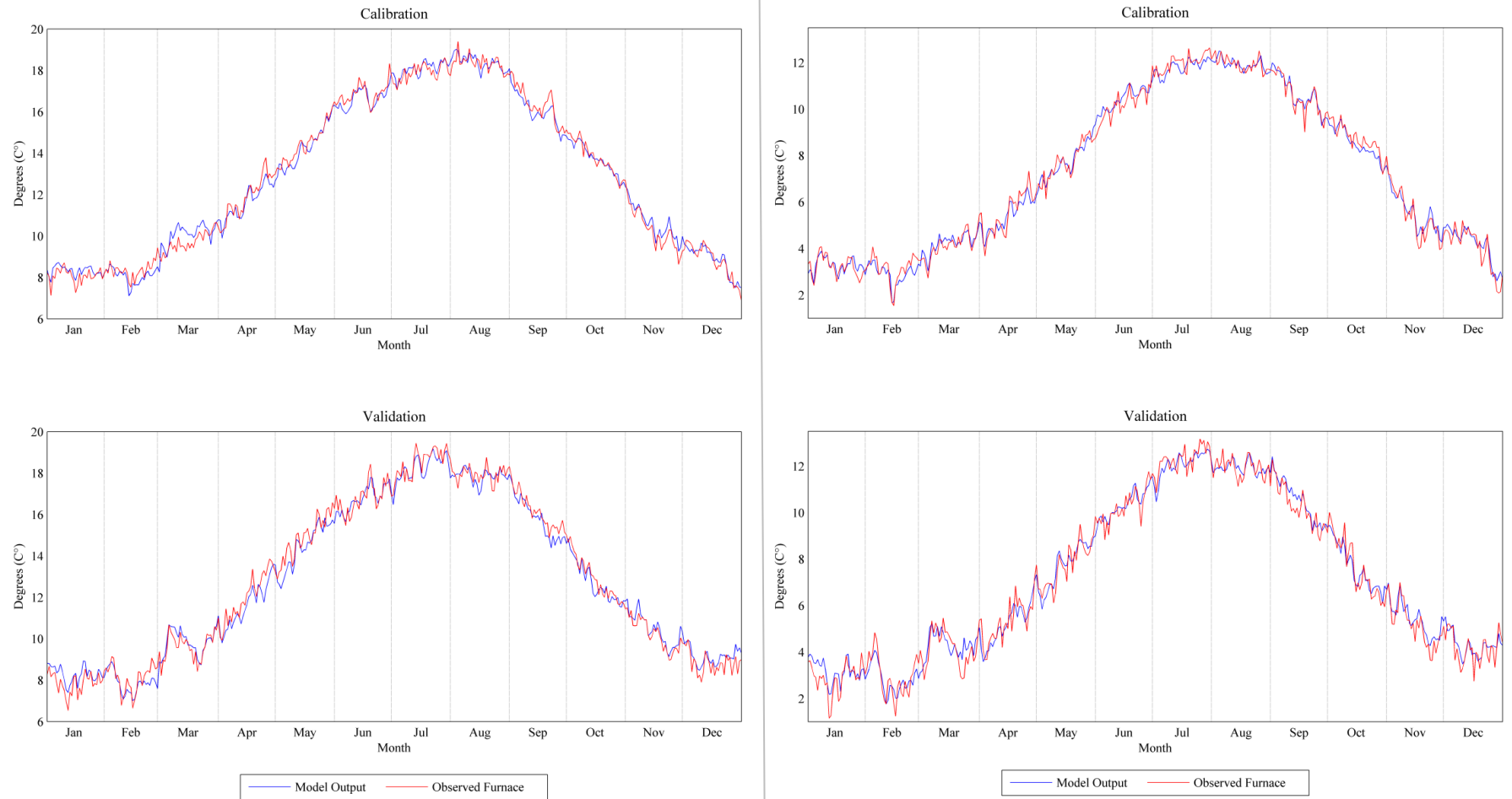


Figure 6.3 Correspondence between observed (Furnace weather station) and downscaled temperature over the calibration (1961-1978; 1994-2000) and validation (1961-1978; 1994-2000) periods. Maximum (left panel) and minimum (right panel) temperature are downscaled for the Furnace weather station using NCEP reanalysis data. Datasets are averaged based on the day of year (1-366).

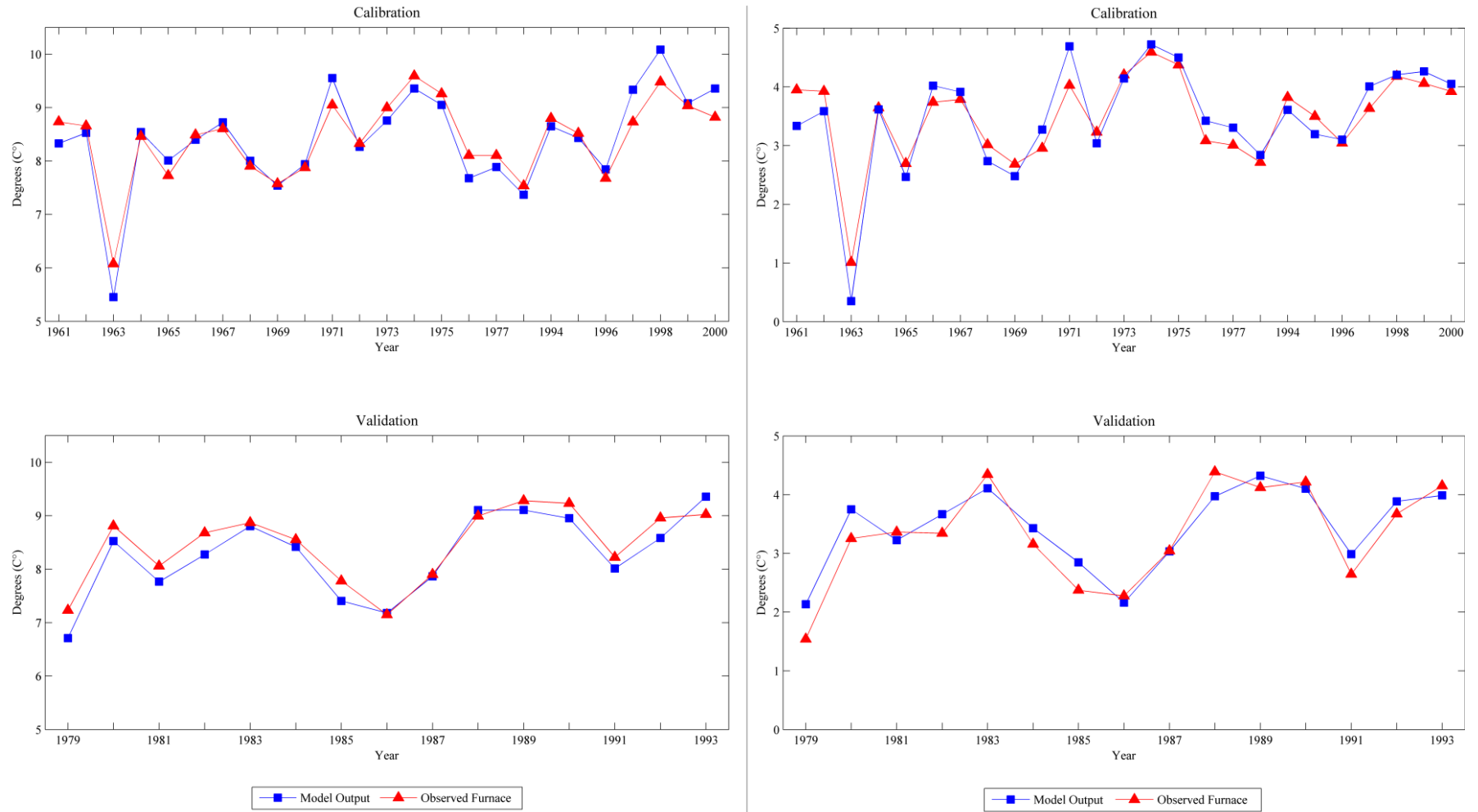


Figure 6.4 Correspondence between the interannual variability of the observed (Furnace weather station) and downscaled maximum (left panel) and minimum (right panel) temperature series. Temperature is downscaled using NCEP reanalysis data for the calibration (1961-1978; 1994-2000) and validation (1979-1993) periods.

6.2.6 Precipitation: calibration and validation

Precipitation is an extremely heterogeneous variable - both temporally and spatially - and is to a large degree influenced by localised forcings which, due to their sub-grid scale nature, are not fully captured in coarse resolution atmospheric datasets. Precipitation also presents a highly skewed discontinuous distribution where the series is punctuated by the occurrence of non-rain days. This precludes the direct application of well established and robust statistical methods which necessitate a normally distributed continuous response variable. The statistical distribution of precipitation also makes it difficult to properly characterise higher order statistics in the downscaled series.

Using both SDSM and the GLM approach, precipitation was downscaled as a two-step process (performed automatically by the SDSM software). Firstly the sequence of days on which rainfall occurs was determined; subsequent to this the quantity of rainfall estimated to occur on a given 'wet day' was simulated using a second regression model. To fit the occurrence model the observed dataset was recoded into a binary sequence signifying the occurrence of wet/dry days (≥ 0.2 mm). The predictors used to downscale precipitation are largely consistent with previous studies, being comprised of various circulation variables and some measure of atmospheric humidity. It is acknowledged that GCMs simulate those variables relating to atmospheric circulation with a high degree of skill, consequently circulation variables are frequently used when downscaling precipitation (Cavazos & Hewitson, 2005); however the use of circulation variables alone may be inappropriate as they fail to fully capture those atmospheric mechanisms - relating to thermodynamics and vapour content - which are conducive to local scale precipitation (Cavazos & Hewitson, 2005; Fowler *et al.*, 2007). The moisture content of the atmosphere is likely to be sensitive to warming climate conditions and as such humidity is an important predictor in capturing the climate change signal; furthermore, it has been shown that the inclusion of some measure of atmospheric moisture can bring about a convergence in the projections from statistical and dynamical models (Charles *et al.*, 1999). When using SDSM the same predictor set was employed when modelling wet-day occurrence as the wet-day rainfall amounts. In contrast, by allowing each parameter to be modelled independently using a different predictor set, the GLM models allowed a more flexible approach to downscaling precipitation (Table 6.4). When downscaling precipitation using SDSM those predictors which were shown to be most skilful at capturing rainfall amounts were used. In this

respect greater emphasis was placed on the model's ability to simulate receipts as opposed to the sequencing of rain/non-rain days.

Season	SDSM	GLM - Occurrence	GLM - Amounts
DJF	<i>mssl, u8, v8, shum</i>	<i>mssl, u8, v8, shum</i>	<i>mssl, u8, v8, shum</i>
MAM	<i>mssl, u, v, rhum</i>	<i>p500, u8, zh8, shum</i>	<i>mssl, u, v, rhum</i>
JJA	<i>mssl, u, v, rhum</i>	<i>p500, u, zh, rhum</i>	<i>mssl, u, v, rhum</i>
SON	<i>mssl, u, v, rhum</i>	<i>p850, u8, zh, rhum</i>	<i>mssl, u, v, rhum</i>

Table 6.4 Predictors used to downscale precipitation for each season.

6.2.6.1 Linear Regression (SDSM)

The occurrence model in SDSM is described as (Wetterhall *et al.* 2005; Wilby *et al.* 1999; 2003):

$$\omega_t = \alpha_0 + \sum_{j=1}^n \alpha_j u_t^{(j)}$$

where t is the time in days, ω_t is the conditional probability of a wet day occurring on day t , $u_t^{(j)}$ is the standardized predictor, and α_j is the regression parameter optimized by ordinary least squares. A uniformly distributed random number $r_t (0 \leq r_t \leq 1)$ is used to determine whether precipitation occurs on a given day; for each time step, a wet-day is projected to occur if $\omega_t \leq r_t$. Incorporating this stochastic element means the model is capable of producing multiple series of wet day occurrences where each series differs with respect to their sequencing of wet/dry days. On a wet day rainfall amounts is estimated using:

$$R_t^{0.25} = \beta_0 + \sum_{j=1}^n \beta_j u_t^{(j)} + \varepsilon_i$$

where which R_t is the standardized precipitation on day t , β_j is the calculated regression parameter estimated using ordinary least squares, and ε_i is a random error term represented by the normal distribution $N(0, \sigma_\varepsilon^2)$. To ensure the data conformed to the (normal) distribution required for linear regression, a fourth root transformation was applied prior to model fitting. The suitability of this transformation was tested using the Kolmogorov-Smirnov test for normality. The regression model in SDSM accounted only for a small proportion of the variance present in the observed series; as a result variance inflation had a greater bearing on the character of the model output. The current structure of the SDSM model does not allow an independent set of predictors to be used when modelling precipitation occurrence and amounts respectively; however, it

is acknowledged that it may be possible to do so using SDSM in-conjunction with external software.

6.2.6.2 Generalised Linear Model (GLM)

Logistic regression was used to model the probability of rainfall occurring on a given day conditional on the large-scale atmospheric state. The model assumes that the logistic transformation of P is a linear function of the predictors, and can be written as:

$$g(P) = \log\left(\frac{P}{1-P}\right) = a_0 + a_1x_1 + \dots + a_ix_i$$

where $g(u)$ is the link function, P is the probability of occurrence, a_0, a_1, \dots, a_i are the regression coefficients, and x_0, x_1, \dots, x_i are the predictors. In this study the regression coefficients were estimated using the method of maximum likelihood. When compared with multiple-linear regression this model is more appropriate for estimating the wet-day occurrence. This is because the model output is constrained between zero and one, allowing it to be interpreted as a true probability. Using the observed dataset a threshold probability is determined above which a rain day is assumed to occur. This threshold is taken as the conditional probability and used to classify the occurrence of a wet/dry-day in the simulated data. Precipitation amounts were modelled by relating a linear combination of the atmospheric predictors to the expected value of the response variable (specified as having a gamma distribution) through a logarithmic link function. This model structure was chosen as wet-day precipitation approximates well to a gamma distribution; it also avoids unrealistic negative values for the estimated rainfall amounts. The model can be written as:

$$\log(E(Y_i)) = \log(\mu) = \beta_0 + \beta_1x_1 + \dots + \beta_ix_i$$

The GLM approach outlined above has the advantage of allowing two different predictor sets to be used. This acknowledges that the initiation of a rainfall event, and the ensuing intensity of that event, may be controlled by different atmospheric processes.

6.2.6.3 Model comparison

Table 6.5 shows the percentage explained variance for the GLM and SDSM amounts models described above. The explained variance - listed for the respective calibration and the validation periods - is calculated based on the modelled and observed datasets

rescaled using a fourth root transformation. Table 6.5 also shows the Heidke Skill Score (HSS) for the GLM occurrence model. This metric describes the model's ability to correctly simulate the occurrence of wet and dry days. As the wet-day occurrence series was stochastically generated in SDSM, the HSS metric could not be used to assess this aspect of model performance.

The relatively low explained variance for wet day amounts - a finding common to all seasons - is consistent with previous studies and illustrates the difficulties associated with downscaling point-scale precipitation using coarse resolution atmospheric data. The percentage explained variance is greatest for winter, reflecting the stronger coupling which exists during this season between large-scale atmospheric circulation and the local-scale precipitation regime. This coupling is manifest in the greater dominance of zonal airflow and the more frequent occurrence of intense low pressure systems. In contrast, the explained variance was found to be lowest for summer, a finding which is commensurate with a general reduction in the frequency of frontal systems, a slackening in circulation and a weakening in the linkage between large-scale circulation and the local-scale response. Convective activity also makes a more significant contribution to receipts during this season, underlining the greater role local forcings play, and the inherent limitations of coarse resolution models in terms of capturing the influence which small scale perturbations in atmospheric conditions can have on the character of local precipitation.

Season	SDSM – Precipitation Amounts (E %)		GLM – Precipitation Amounts (E %)		GLM - Wet Day Occurrence HSS	
	Calibration	Validation	Calibration	Validation	Calibration	Validation
<i>DJF</i>	32	30	30	29	60	60
<i>MAM</i>	26	27	24	25	67	63
<i>JJA</i>	19	23	19	22	61	60
<i>SON</i>	20	23	28	27	61	59

Table 6.5 Explained variance (%) for the calibration (1961-1978; 1994-2000) and validation (1979-1993) periods estimated on a seasonal basis. The explained variance is calculated for the linear component of SDSM (i.e. with the variance inflation disabled) and the GLM amounts model respectively. Prior to estimating the explained variance a fourth root transformation is applied to the modelled and observed precipitation data. Also shown is the HSS for the GLM occurrence model. Due to the stochastic modelling of wet days the HSS was not calculated for SDSM.

Based on Figure 6.5 SDSM tends to underestimate the monthly wet day occurrence (%) while the GLM generally overestimates the proportion of wet days - this is particularly evident for the summer months over the calibration period. Both models do however capture the annual cycle well, particularly SDSM. The GLM consistently over-estimates the mean monthly wet (Figure 6.6(a)) and dry (Figure 6.6(b)) spell length, whilst SDSM consistently under-estimates both parameters.

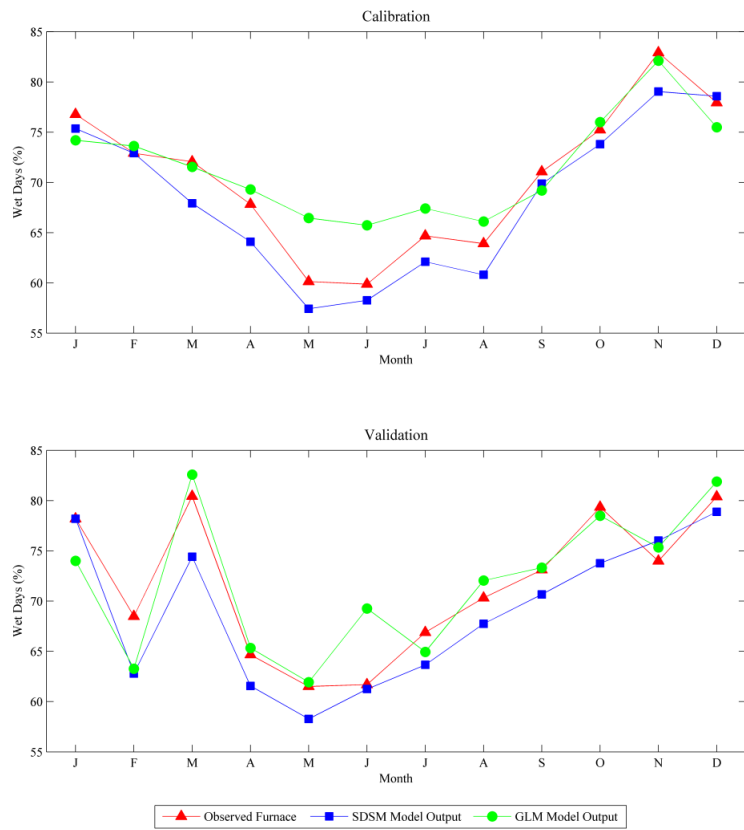


Figure 6.5 Monthly percent wet-days (≥ 0.2 mm) for the downscaled and observed (Furnace weather station) precipitation series estimated over the calibration (1961-1978; 1994-2000) and validation (1979-1993) periods respectively. Precipitation is downscaled from NCEP reanalysis data using both the SDSM and GLM models.

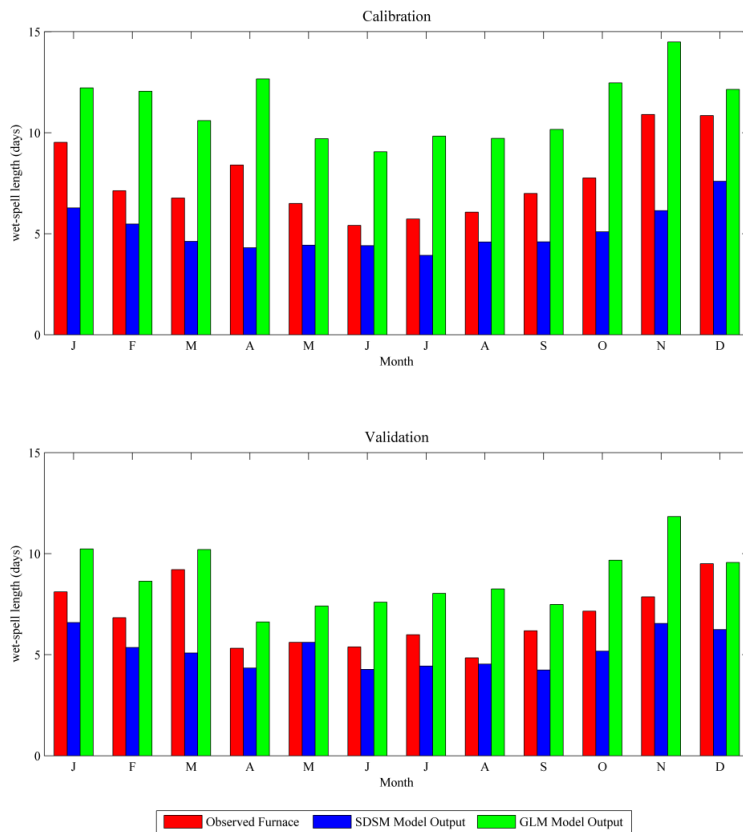


Figure 6.6(a) Mean monthly wet-spell length (≥ 0.2 mm) for the downscaled and observed (Furnace weather station) precipitation series estimated over the calibration (1961-1978; 1994-2000) and validation (1979-1993) periods respectively. Precipitation is downscaled from NCEP reanalysis data using both the SDSM and GLM models.

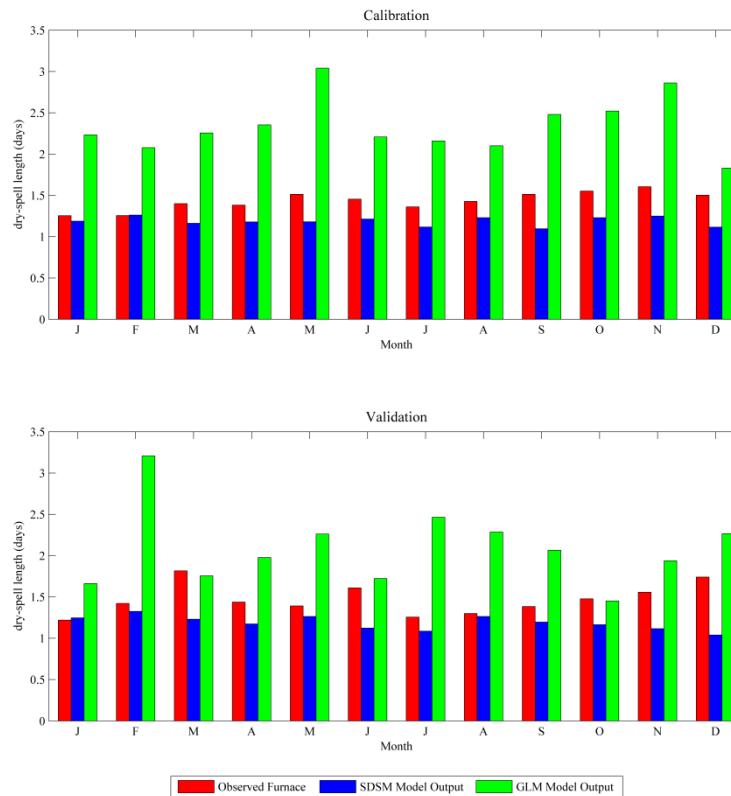


Figure 6.6(b) Mean monthly dry-spell length (<0.2 mm) for the downscaled and observed (Furnace weather station) precipitation series estimated over the calibration (1961-1978; 1994-2000) and validation (1979-1993) periods respectively. Precipitation is downscaled from NCEP reanalysis data using both the SDSM and GLM models.

Figure 6.7 and 6.8 illustrates the skill of both the SDSM and GLM models at reproducing the mean monthly, as well as inter-annual precipitation receipts for the calibration and validation periods respectively. Generally the GLM model tends to over-estimate monthly amounts; this is particularly evident for the summer months where June precipitation receipts are ~20% greater than the observed. SDSM also over-estimates June receipts for but not to the same degree (calibration 5%; validation 17%). In contrast SDSM tends to under-estimate the mean monthly values, this is most noticeable over the validation period for the months of May (14%), August (12%) and September (11%). The coefficient of determination - calculated using the observed and modelled mean monthly precipitation receipts - indicates that the GLM (calibration: 0.95; validation: 0.94) is marginally better than SDSM (calibration: 0.93; validation: 0.86) at reproducing the annual cycle. Similarly, the coefficient of determination - calculated using the observed annual precipitation amounts - indicates that the GLM (calibration: 0.65; validation: 0.61) is slightly better than SDSM (calibration: 0.64; validation: 0.60) at reproducing the observed pattern of inter-annual variability. The fact that both models exhibit similar skill at reproducing these aspects of the catchment's precipitation regime may be due to the same predictor sets (wet-day amounts) being used and the fact that both are essentially regression type models.

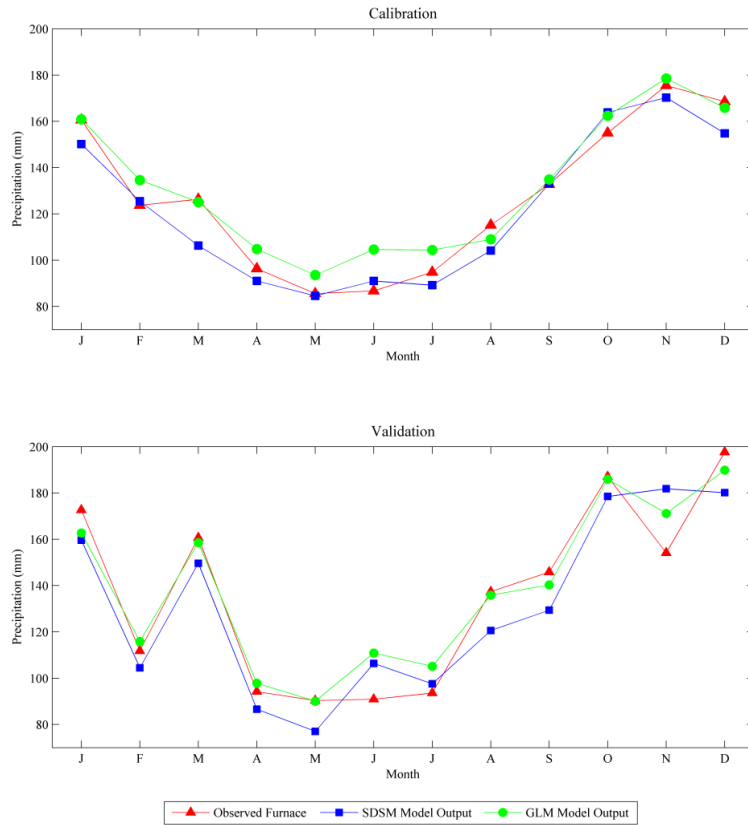


Figure 6.7 Monthly mean precipitation receipts for the downscaled and observed (Furnace weather station) series estimated over the calibration (1961-1978; 1994-2000) and validation (1979-1993) periods respectively. Precipitation is downscaled from NCEP reanalysis data using both the SDSM and GLM models.

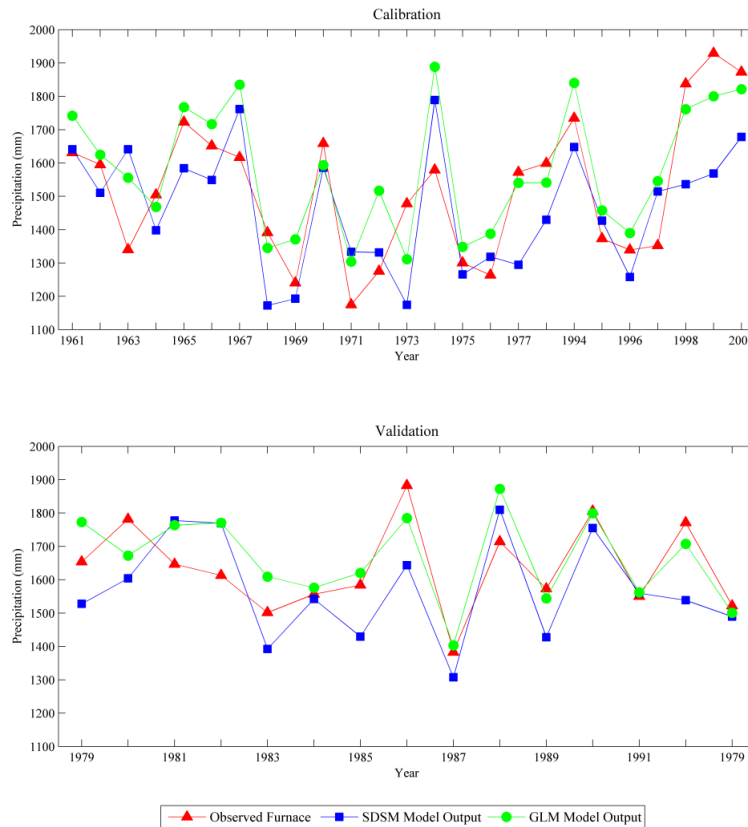


Figure 6.8 Interannual variability (total annual receipts) estimated for the downscaled and observed (Furnace) precipitation series over the calibration (1961-1978; 1994-2000) and validation (1979-1993) periods respectively. Precipitation is downscaled from NCEP reanalysis data using both the SDSM and GLM models.

Figure 6.9 shows the degree to which the GLM model, non-inflated SDSM and inflated SDSM series capture the monthly variance of the observed precipitation series over the calibration and validation periods respectively. There is a clear improvement in this aspect of model performance when variance inflation is applied. The inability of the GLM to capture the true variability of precipitation is reflected in the seasonal Q-Q plots shown in the Figure 6.10. These plots highlight that, irrespective of the season and period considered, the distribution of the rainfall data obtained using SDSM is closer to the observations than the downscaled GLM data. It is shown that the GLM underestimates the higher quantiles - particularly the 90th, 95th and 99th. With respect to the GLM derived data, Figure 6.10 illustrates the degree to which the underestimation of variance leads to a corresponding under-estimation of higher quantiles – thus highlighting the importance of applying some technique to enhance the variability of the downscaled series.

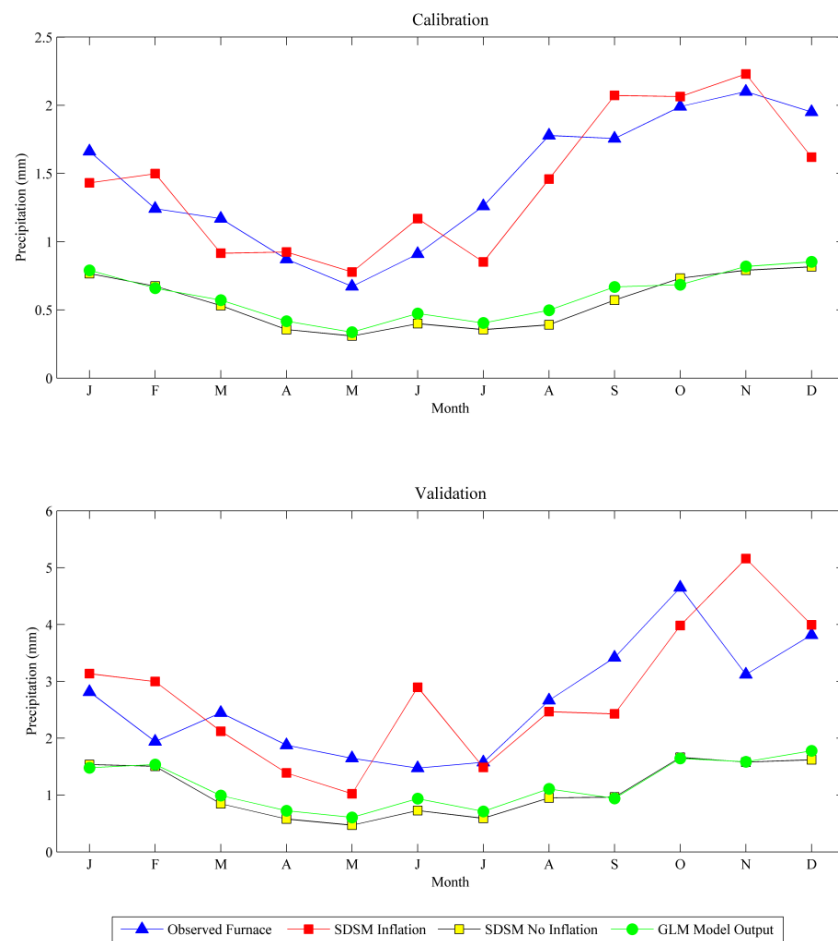


Figure 6.9 Monthly variance of the downscaled and observed (Furnace weather station) precipitation series over the calibration (1961-1978; 1994-2000) and validation (1979-1993) periods respectively. Precipitation is downscaled from NCEP reanalysis data using both the SDSM and GLM models. Both the inflated and non-inflated downscaled SDSM data is plotted.

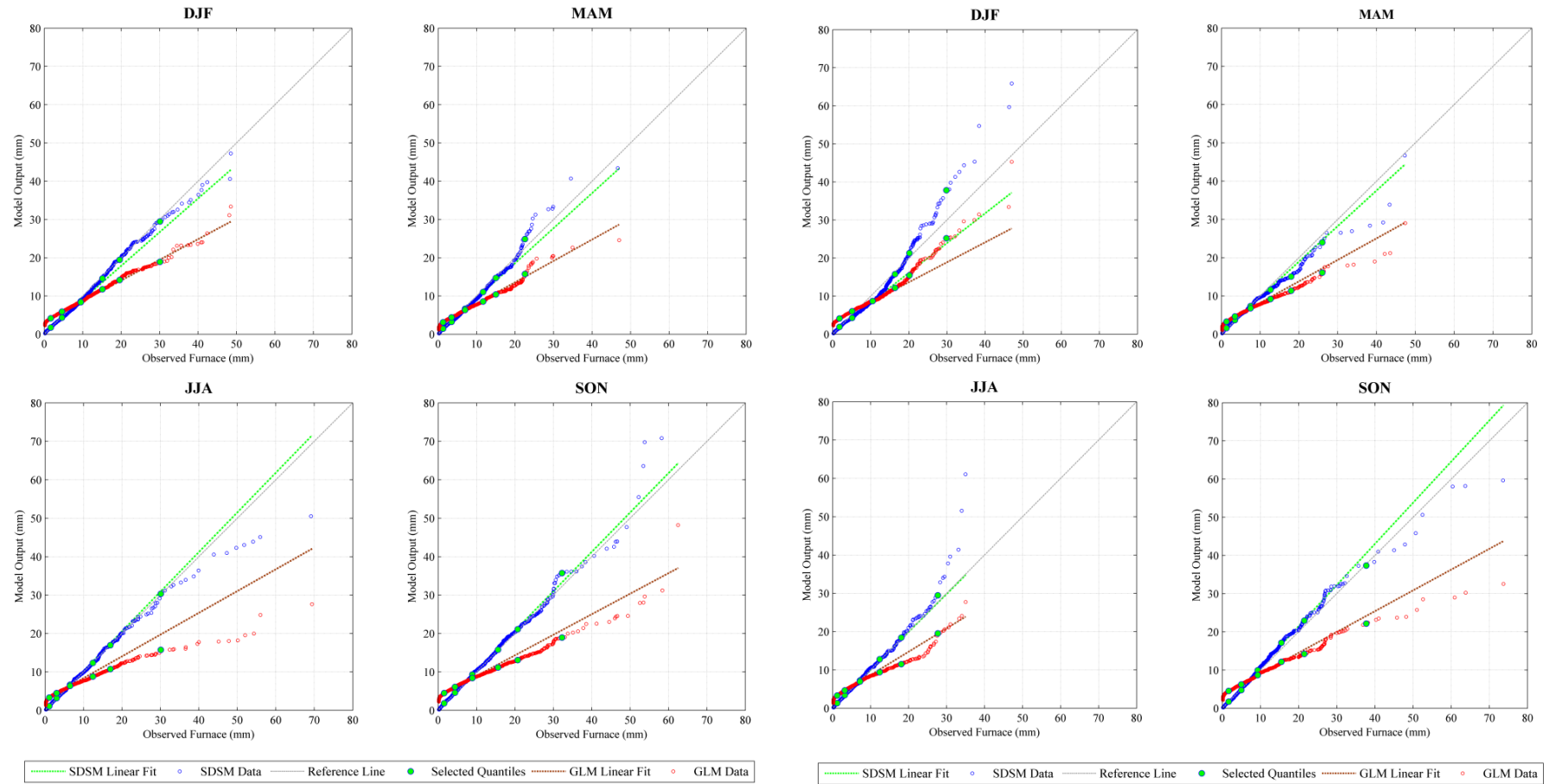


Figure 6.10 Seasonal Q-Q plots for the observed and downscaled (Furnace weather station) precipitation series over the calibration (1961-1978; 1994-2000) (left panel) and validation (1979-1993) (left panel) periods respectively. Precipitation is downscaled from NCEP reanalysis data using both the SDSM and GLM models. The plots are constructed using rainfall amounts only. The enlarged green dots are used to highlight those values relating to the following percentiles: 25th, 50th, 75th, 90th, 95th and 99th.

It cannot however be argued that variance inflation is a panacea for the problem of inadequately capturing the true variability of precipitation or the influence of local-scale forcings, nor can it be assumed that variance inflation is capable of fully characterising changes in the variability of the catchment's precipitation regime under perturbed forcing. The use of inflation techniques in statistical downscaling have been questioned; von Storch (1999) argues that variance inflation - as applied by Karl *et al.* (1990) - erroneously assumes that all local-scale variability is driven by large-scale variability in the predictor fields. In its place von Storch (1999) proposes the use of 'randomization', whereby the processes unresolved by the large-scale predictor(s) are accounted for by adding noise with some pre-defined properties to the downscaled series (see section 5.2.2). Given the degree to which the GLM approach underestimates the true variance, coupled with the fact that both approaches reproduce other statistics with a similar level of skill, the climate scenarios downscaled using SDSM only were used when modelling changes in the catchment hydrology. The results of the GLM are discussed above in order to provide a comparison of two different regression type approaches to downscaling.

6.2.7 Other meteorological parameters

A number of additional meteorological variables were downscaled for the catchment which, although not employed directly in this study, were used as part of the RESCALE project discussed in Chapter one (Fealy *et al.*, 2010). As instrumental records of sufficient length for these variables were not available from the Furnace weather station, the required observational datasets were obtained from the Belmullet synoptic station, which is located to the north-west of the catchment. Given that these variables were not used when modelling the catchment hydrology, they are not discussed in any great detail. However, they are included here as they provide additional information on the application of the downscaling method used in this study.

6.2.7.1 Wind speed

Wind speed distributions are typically positively skewed and generally approximate to either a Gamma or Weibull distribution; to accommodate this within the GLM framework a gamma distribution with a log link function was employed. SDSM was also used to downscale wind speed, in this case to conform to the distribution required for linear regression a square root transformation was applied. To reflect the processes

which govern local scale wind, predictors which describe atmospheric circulation only were employed (Table 6.6). For each season, as well as over both the calibration and validation periods, a relatively high proportion of the observed variance was accounted for in the downscaled series. The same predictor set was used in each model, this is reflected in the negligible differences in the explained variance for each; however, as with precipitation, the GLM tended to underestimate the variance of the observed series.

Season	Predictors	SDSM		GLM	
		Calibration (E %)	Validation (E %)	Calibration (E %)	Validation (E %)
DJF	<i>zh8, mslp, f8</i>	49	51	51	47
MAM	<i>f8, p500, v</i>	48	45	47	45
JJA	<i>z, f8, v</i>	46	41	47	42
SON	<i>f8, zh5, z</i>	47	47	45	45

Table 6.6 Explained variance (%) calculated on a seasonal basis for the calibration (1961-1978; 1994-2000) and validation (1979-1993) period respectively. Wind speed is downscaled to the Belmullet synoptic station using NCEP reanalysis data. The explained variance is calculated for the linear component of SDSM (i.e. with the variance inflation disabled) and the GLM respectively.

6.2.7.2 Relative humidity

Relative humidity was downscaled to the Belmullet synoptic station using the SDSM model only. Grid-scale relative humidity was included in the predictor set for each season. Incorporating this variable was considered important in order to represent the linkage between local and macro-scale atmospheric conditions. Given that they exhibited a strong correlation with point-scale humidity, a number of circulation variables were also included in the predictor set. A relatively low proportion of the variance exhibited by the observed series was captured by the downscaled data.

Season	Predictors	Calibration - (E %)	Validation - (E %)
DJF	<i>f, v, z5, rhum</i>	31	36
MAM	<i>v, f, z5, rhum</i>	30	34
JJA	<i>u, v, z5, rhum</i>	25	23
SON	<i>f5, z5, v, rhum</i>	39	39

Table 6.7 Explained variance (%) calculated on a seasonal basis for the calibration (1961-1978; 1994-2000) and validation (1979-1993) periods respectively. Relative humidity is downscaled to the Belmullet synoptic station using NCEP reanalysis data. The explained variance is calculated for the linear component of SDSM (i.e. with the variance inflation disabled).

6.2.7.3 Solar radiation and potential evaporation

When downscaling data series for both solar radiation and potential evaporation a number of large-scale predictors, along with potential radiation and ΔT were used (Table 6.8; Table 6.9). Both variables were modelled using SDSM only. Due to the influence which solar radiation has on the rate of evaporation, both variables were

downscaled using similar predictor sets. The instrumental records available for solar radiation and evaporation cover the periods 1982-2000 and 1971-2000 respectively. To overcome the short length of the data available for model training, the coefficient values were averaged across 10,000 bootstrapped samples.

Season	Predictors	Calibration - (E %)	Validation - (E %)
DJF	<i>Pot Rad, ΔT, v, $z5$, $u8$, zh</i>	65	60
MAM	<i>Pot Rad, ΔT, zh, $z5$, $u5$, $rhum$</i>	65	66
JJA	<i>Pot Rad, ΔT, $rhum$, $u5$, zh, $z5$</i>	50	48
SON	<i>Pot Rad, ΔT, zh, $u8$, $z5$</i>	73	72

Table 6.8 Explained variance (%) calculated on a seasonal basis for the calibration (1981-1988; 1995-2000) and validation (1989-1993) periods respectively. The explained variance is calculated for the linear component of SDSM. Solar radiation is downscaled to the Belmullet synoptic station using NCEP reanalysis data and point-scale temperature records.

Season	Predictors	Calibration - (E %)	Validation - (E %)
DJF	<i>Pot Rad, ΔT, v, $z5$, f, $rhum$</i>	64	55
MAM	<i>Pot Rad, ΔT, zh, $z5$, $u5$, $rhum$</i>	67	65
JJA	<i>Pot Rad, ΔT, $rhum$, $u5$, zh, $z5$, $rhum$</i>	44	45
SON	<i>Pot Rad, ΔT, v, $u8$, $z5$, $rhum$</i>	73	70

Table 6.9 Explained variance (%) calculated on a seasonal basis for the calibration (1971-1981) and validation (1982-1987) periods respectively. The explained variance is calculated for the linear component of SDSM. Potential evaporation is downscaled to the Belmullet synoptic station using NCEP reanalysis data and point-scale temperature records.

6.3 Dynamically downscaled datasets

Dynamical downscaling adds high resolution detail to the sub-GCM-grid scale climate whilst preserving the large-scale climate features simulated by the driving global model (Giorgi & Mearns, 1991; 1999; Giorgi *et al.*, 2003; Kjellström & Giorgi, 2010; Rummukainen, 2010). The strength of dynamical downscaling lies in the fact that the models are based on immutable physics and can resolve sub-grid scale processes dynamically. However, there are difficulties associated with integrating boundary conditions from the parent GCM, and there remains a need to parameterize key climate processes which occur at scales too small to be resolved explicitly. Biases in the driving data also introduce uncertainty to the model simulations, and it is argued that the resolution at which they are currently run remains too coarse for their output to be commensurate with point-scale observational data - thus necessitating the subsequent application of statistical downscaling.

The dynamically downscaled data used in this study was obtained from RCM experiments conducted as part of the EU funded ENSEMBLES project (www.ensembles-eu.org) (van der Linden & Mitchell, 2009). It constitutes one of the

largest regional climate change research projects undertaken; the work carried out for it builds on earlier EU projects such as PRUDENCE (Christensen *et al.*, 2007b), STARDEX (STARDEX Final Report, 2005), MICE (Hanson *et al.*, 2007) and DEMETER (Palmer *et al.*, 2004). The main objective of ENSEMBLES was to produce high resolution probabilistic information on future changes in climate for Europe using a multi-model ensemble. In addition the project aimed to identify methods for quantifying, and where possible reducing, the uncertainties inherent in producing regional scale projections of future climate change. Throughout the project there was an onus on participants to evaluate model performance using quality controlled gridded datasets.

6.3.1 ENSEMBLES

To produce the dynamically downscaled climate scenarios used in this study, eleven different institutes (Table 6.10) ran a series RCMs for a common European domain at a horizontal spatial resolution of 25 km (0.22°), taking lateral boundary conditions from one or more of five different AOGCMs (Table 6.11). The various model combinations employed - constituting different driving GCMs, GHG-emission scenarios and downscaling RCMs - were used to produce a multi-model ensemble of 19 dynamically downscaled climate scenarios (Figure 6.11).

Acronym	Institute	RCM	Reference
<i>C4IRCA3</i>	The Community Climate Change Consortium for Ireland, Met Éireann	RCA3	Jones <i>et al.</i> (2004)
<i>CHMIALADIN</i>	Czech Hydrometeorological Institute	ALADIN	Farda <i>et al.</i> (2010)
<i>CNRM-RM4.5</i>	Centre National de Recherches Meteorologique, Météo-France	RM4.5 (ALADIN)	Radu <i>et al.</i> (2008)
<i>DMI-HIRHAM5</i>	Danish Meteorological Institute	HIRHAM5	Christensen <i>et al.</i> (2006)
<i>ETHZ-CLM</i>	Swiss Federal Institute of Technology	CLM	Böhm <i>et al.</i> (2006)
<i>ICTP-REGCM3</i>	The Abdus Salam Intl. Centre for Theoretical Physics	REGCM3	Giorgi & Mearns (1999)
<i>KNMI-RACMO2</i>	The Royal Netherlands Meteorological	RACMO2	Lenderink <i>et al.</i> (2003)
<i>METNOHIRHAM</i>	The Norwegian Meteorological Institute	HIRHAM	Haugen & Haakenstad (2006)
<i>METO-HadRM3Q0</i>	UK Met Office, Hadley Centre for Climate Prediction and Research	HadRM3, (Q0)	Collins <i>et al.</i> (2006, 2010)
<i>METO-HadRM3Q3</i>	UK Met Office, Hadley Centre for Climate Prediction and Research	HadRM3, (Q3)	Collins <i>et al.</i> (2006, 2010)
<i>METO-HadRM3Q16</i>	UK Met Office, Hadley Centre for Climate Prediction and Research	HadRM3, (Q16)	Collins <i>et al.</i> (2006, 2010)
<i>MPI-M-REMO</i>	Max-Planck-Institute for Meteorology	REMO	Jacob (2001)
<i>OURANOSMRCC4.2.3</i>	Consortium on Regional Climatology and Adaptation to Climate Change	CRCM	Plummer <i>et al.</i> (2006)
<i>SMHI</i>	Swedish Meteorological and Hydrological Institute	RCA	Kjellström <i>et al.</i> (2006)
<i>RPN</i>	Recherche en Prévision Numérique	GEMLAM	Côté <i>et al.</i> (1998)

Table 6.10 Institutions, model names and abbreviations of the ENSEMBLES RCM simulations used in this study. The Hadley Centre contributed a perturbed physics ensemble consisting of three different RCM simulations, each of which was tuned to have a different climate sensitivity: standard (HC-Q0), low (HC-Q3) and high (HC-Q16). The RPN (GEMLAM) and CHMI (ALADIN) institutes did not use their RCMs to downscale GCM data.

Institute	Model Abb.	Reference
University of Bergen, Norway (NERSC)	BCM	Furevik <i>et al.</i> (2003)
Canadian Meteorological Service (CCCma)	CGCM3	Scinocca <i>et al.</i> (2008)
Centre National de Recherches Meteorologique, Météo-France (CNRM)	ARPEGE	Gibelin & Déqué (2003)
Max-Planck-Institute for Meteorology (MPI-M)	ECHAM5	Roeckner <i>et al.</i> (2003)
UK Met Office, Hadley Centre for Climate Prediction and Research (METO-HC)	HadCM3 (Q0)	Gordon <i>et al.</i> (2000); Collins (2010)
UK Met Office, Hadley Centre for Climate Prediction and Research (METO-HC)	HadCM3(Q3)	Gordon <i>et al.</i> (2000); Collins (2010)
UK Met Office, Hadley Centre for Climate Prediction and Research (METO-HC)	HadCM3 (Q16)	Gordon <i>et al.</i> (2000); Collins (2010)

Table 6.11 Institutions, model names and abbreviations of the GCMs used as boundary conditions for the ENSEMBLES RCM simulations. The Hadley Centre contributed a perturbed physics ensemble consisting of three different versions of the HadCM3, each of which was tuned to have a different climate sensitivity: standard (HC-Q0), low (HC-Q3) and high (HC-Q16).

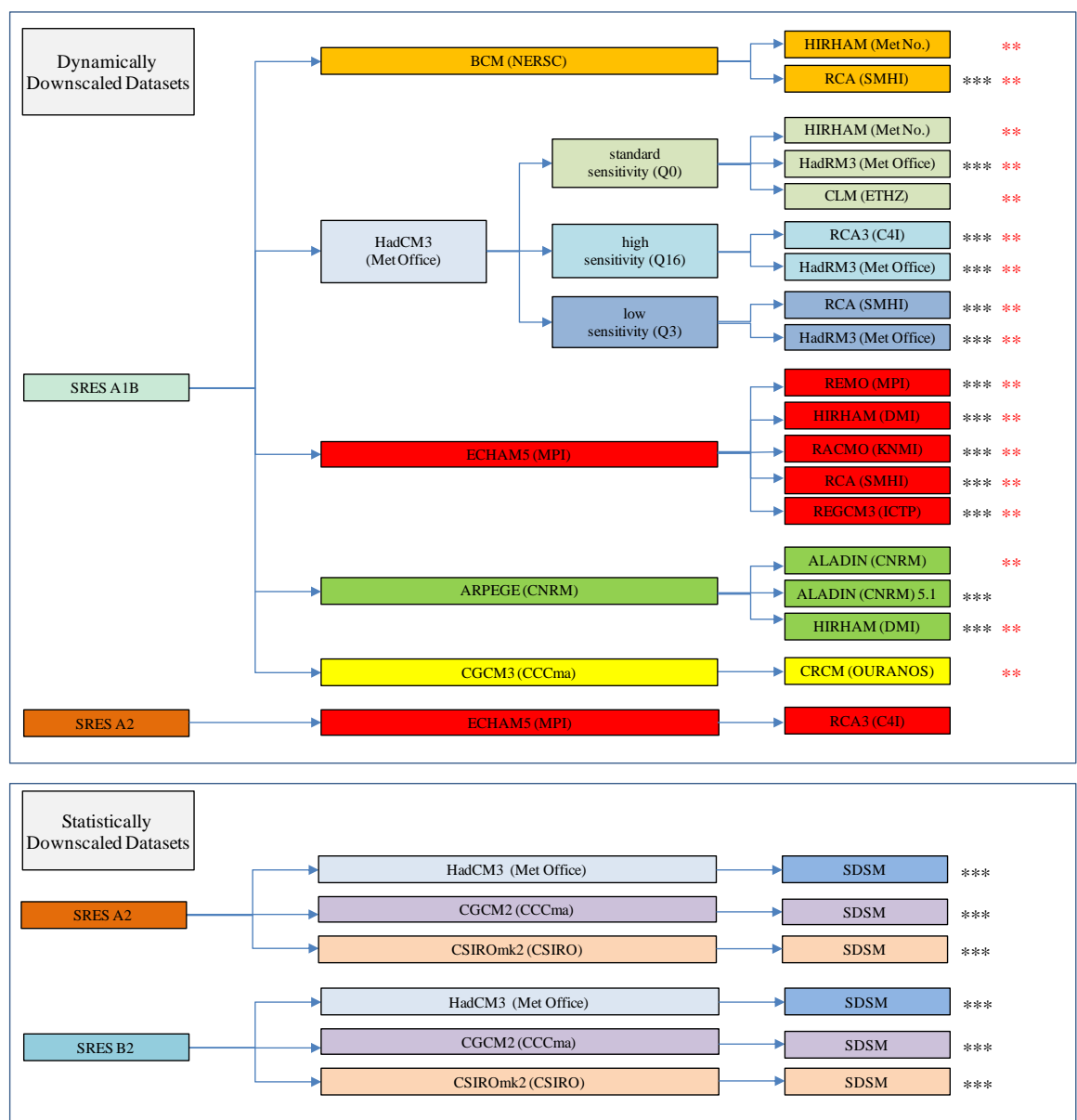


Figure 6.11 GCM-RCM/GCM-SDSM model combinations - or 'model pathways' - (colour coded according to driving GCM) used to produce the downscaled data employed in this study. (***) mark those simulations which run until the year 2100. (**) mark those scenarios for which the dynamical weighting scheme is formulated (Figure 6.24). Note that the HadCM3 GCM is run in three sensitivity configurations (Q0, Q16 and Q3). The abbreviations in brackets denote the main centre responsible for the corresponding model simulation.

All institutes - with the exception of Met Éireann (C4I) - produced data for the A1B emission scenario only; this institute downscaled GCM data for both the A1B and A2 SRES scenarios. As shown in Figure 6.11 not all of these model combinations or 'model pathways' run up until the end of the current century - five model combinations run only to the year 2050. The RCMs used to dynamically downscale GCM data have also been forced using lateral boundary conditions from the ECMWF (European Centre for Medium Range Weather Forecasts) ERA-40 reanalysis dataset (1.125° or 120 km) for the period 1961-2000 (Uppala *et al.*, 2005).

Where reanalysis data is employed the models are said to be forced using unbiased 'perfect boundary conditions' and generate data which is temporally consistent with observed climate series, allowing the sequencing of simulated and observed weather events to be compared (Maraun *et al.*, 2010). Although a number of institutes ran their regional models at a resolution of both 25 and 50 km, the higher resolution simulations only were included in this study. In addition, only those climate scenarios downscaled using models which have also been run using ERA-40 reanalysis data were used. This was to ensure that model performance - with respect to the ability of each RCM to simulate the observed climate conditions of the study area - could be assessed. As a result the datasets used represent only a sub-set of the full suite of model simulations which are available from the ENSEMBLES data archive. With the exception of the RCM used by the Canadian based Consortium on Regional Climatology and Adaptation to Climate Change (OURANOS) (Laprise *et al.*, 2003), a description of the models used in ENSEMBLES is provided by Jacob *et al.* (2007).

The data produced by each model pathway shown in Figure 6.11 can be considered a plausible scenario of detailed regional change; by sampling across a range of different GCM-RCM combinations a comprehensive exploration of the model and uncertainty space can be conducted. The various model pathways employed allow different aspects of climate model uncertainty to be considered (e.g. model formulation, parameterization, climate sensitivity and GCM/RCM model combination); this is one of the key strengths of the ENSEMBLES dataset. Of note in Figure 6.11 is that the Hadley Centre ran three members from a perturbed physics ensemble (PPE) whereby the physical parameterizations in both their RCM (HadRM3) and GCM (HadCM3) were altered to reflect a different climate sensitivity (reference sensitivity: Q0; high sensitivity: Q16 and low sensitivity Q3). Also of note in Figure 6.11 is that in some instances different institutes have employed the same RCM. With respect to an

exploration of model uncertainty, this makes an allowance for the possibility that the same model may have had a different specification (e.g. number of levels, physics routines, and parameterization scheme) or have been optimized for use in a particular region. Differences in the model configuration may result in the same models producing contrasting projections of future change.

There is however a number of limitations associated with the ENSEMBLES dataset. Firstly, the fact that the model projections are based on the A1B emission scenario means the usefulness of the dataset is limited when exploring this aspect of uncertainty. This is due to ENSEMBLES being focused primarily on addressing uncertainty in regional models rather than the full range of uncertainties which affect estimates of future climate change. Secondly, as shown in Figure 6.11, the individual model pathways are not entirely independent. In some instances the same RCM has been driven using boundary conditions from different GCMs (e.g. Met Éireann ran the RCA3 model using the HadCM3 and ECHAM5 GCMs), conversely different RCMs have been forced using data from the same parent GCM (e.g. the Hadley centre's HadCM3 GCM is used as boundary conditions for both the CLM and HIRHAM regional models). This lack of independence means an over-sampling of a particular region of the model space is likely to occur – thereby introducing bias to the ensemble and any probabilistic projections of future change derived from it.

Such bias may be addressed if every possible combination of a driving GCM and downscaling regional model were included in the ensemble; however, large gaps in the GCM-RCM matrix exist, a shortcoming related primarily to the computational costs associated with satisfying all model combinations. The dataset used in this study could be referred to as an “ensemble of opportunity” (Stone *et al.*, 2007), whereby the model output is included simply by virtue of its availability rather than because it meets some predefined criteria. Ideally, models should be more systematically sampled with the aim of preserving independence; however, given the practical difficulties associated with producing large climate ensembles, this would be a difficult objective to achieve, particularly when trying to integrate the information from different institutes - as is the case with the ENSEMBLES dataset. Given that model projections represent such a valuable source of information, it is difficult to justify excluding certain ensemble members on the basis that they lack independence. The ability to factor in independence is one of the advantages perturbed physics ensembles have – albeit that they are constrained to sampling a much narrower region of the uncertainty space. It must be

recognized that despite its shortcomings, the ENSEMBLES dataset does allow inter-model variability to be considered and facilitates an exploration of different aspects of model and climate uncertainty; as such the dataset offers clear advantages over relying on a single realization of future climate. It also represents an advance over using climate ensembles which are limited in terms of what aspects of uncertainty they can address.

For this study, downscaled (ERA-40 and GCM) daily precipitation ($\text{kg m}^{-2} \text{s}^{-1}$) and 2 m temperature (K) (maximum and minimum) were obtained from the ENSEMBLES data distribution centre - accessed via www.ensembles-eu.org. Once downloaded the data for nine grid boxes, representing the model domain of interest, were re-projected onto a common grid projection and subsequently extracted. The catchment was found to be overlain by two separate grid-boxes (Figure 3.1). Following Leander and Buishand (2007) precipitation and temperature for the catchment were calculated as a weighted average of the values from each grid box, the weights were formulated based on the proportion of the catchment falling within a specific grid box.

6.3.2 ERA-40 RCM evaluation

Christensen *et al.* (2008) state that the inability of RCMs to simulate current-day climate accurately is one of the key sources of uncertainty in climate change impact studies. It is therefore important that some analysis of RCM skill is conducted using historical observations prior to employing their output in any impact assessment. Temperature and precipitation are both of critical importance for determining the potential hydrological response of the Burrishoole catchment to changes in climate, thus it is important that the regional models used are capable of simulating these variables under current-day climate with a certain degree of skill. To this end the RCMs listed in Table 6.10 were assessed based on their ability to simulate observed climate conditions in the catchment. Although some of the RCMs examined were not used to downscale GCM data, they are included in the analysis in order to provide a comparison of model skill.

Examining the performance of regional models when driven using the same reanalysis data allows any bias in the RCMs to be isolated and ensures parity when assessing the performance of competing models. It also removes the potential for any biases inherited from the driving GCM to act as a confounding source of error when attempting to evaluate the performance of individual RCMs. Additionally, in a reanalysis driven

model the sequence of synoptic weather will be temporally consistent with observed weather patterns, as a result a direct comparison can be made between simulated and observed weather events. However, as highlighted by Maraun *et al.* (2010), discrepancies in how small scale variability is generated in RCMs - with respect to the true system processes - may lead to inconsistencies in the simulations.

Given the wide range of criteria and model diagnostics which can be applied, providing an accurate and well rounded assessment of model performance is a challenging task. For example, regional models may be evaluated based on their ability to reproduce large-scale circulation patterns or different modes of variability (e.g. North Atlantic Oscillation). They may also be appraised based on their skill at reproducing spatial patterns of surface climate and/or their ability to capture the variability in observed climatological series over a range of time-scales (from the seasonal to the decadal) or frequencies. Models may also be evaluated based on whether they capture particular weather events or extremes of conditions.

In this study the metrics used to assess model skill focused on the performance of each regional model at simulating observed precipitation and temperature in the catchment only; thus, how well they reproduced the spatial variability of either variable – or indeed other variables – was not examined. In this respect a model was considered skilful if it captured temporal patterns of variability in the observed catchment climatology; however, it may have performed poorly at simulating the temporal and spatial characteristics of climate for other regions. How well the models performed over larger spatial domains or their ability to simulate different modes of circulation and large-scale variability were aspects of model skill which were also not explored.

For a model to be considered skilful it should ideally reproduce temporal and spatial patterns of variability in surface climate across disparate scales. It should also capture important aspects of atmospheric and climate system behaviour. In light of this the potential shortcomings of the evaluation criteria employed in this study are acknowledged; however, given that the catchment is taken as the sole bounded unit of most importance in this study, it takes precedence with respect to model performance over alternative regions or larger spatial domains. In addition, given that temperature and precipitation are the most significant variables in terms of climate change impacts, it was important that model skill in reproducing these variables was considered above all others.

Given that a model which is shown to be skilful in one aspect of performance cannot be assumed to be proficient in others, it is more pragmatic to assess each model performance using a range of different criteria; to address this several different evaluation metrics were employed in this study. It has been pointed out that when evaluating the performance of RCMs the observed dataset used should be of the same spatial resolution as the model output (Maraun *et al.*, 2010). Comparing the gridded model data with point scale observations may lead to the misrepresentation of errors arising from the fact that the model output represents an areally averaged value of surface conditions and as such will have a lower variance. As a means of evaluating model performance the E-OBS gridded observational dataset was considered for use in this study (Haylock *et al.*, 2008); however, when the gridded climate series overlying the catchment was examined it did not correspond well with point-scale observations from the Furnace weather station – even allowing for the fact that the E-OBS data is spatially averaged. This may be because a small number of synoptic stations from Ireland were used when formulating the dataset. Hofstra *et al.* (2010) indicate that there are substantial biases in the E-OBS dataset over regions where the underlying station density is low. In addition, given the heterogeneous nature of precipitation in the catchment, and that point scale data is used to drive the hydrological models, it was important that a true, non-smoothed estimate of model performance was used as a benchmark. A number of studies have flagged the possibility of biases in the E-OBS data as a reason for some metrics returning low skill scores when the dataset is used for model evaluation. This is an issue which has been found to be of particular relevance when attempting to quantify how well models capture extreme events (Hofstra *et al.*, 2010; Kjellström 2010).

In the field of short-term weather-forecasting a wealth of well tested and robust methodological approaches exist for validating model forecasts (e.g. Barnston, 1992; Murphy & Wilks, 1998; Jolliffe & Stephenson, 2003; Casati *et al.*, 2008). Given that the downscaled reanalysis data is temporally consistent with the observations, many of these methods are directly transferrable to the assessment of regional model skill. It must be recognized that there is a degree of subjectivity surrounding which aspects of model performance to assess. In addition, given the wide range of evaluation metrics which are available, there is also a degree of ambiguity associated with which are the most appropriate metrics to employ. Whilst some tests are more widely used and held in higher esteem than others, in the field of numerical weather prediction (NWP) there are no universally recognized optimum set of metrics. Essentially the suitability of a

particular test must be determined based on the characteristics of the data available and the aspects of model performance which are considered most important.

The metrics used to assess model performance in this study are outlined in Table 6.12. The criteria employed variously quantify model error, bias and association; Murphy (1993) highlights these as the most important indicators of forecast quality. As both have different connotations regarding model skill, care was taken to use metrics which drew a distinction between random and systematic model error. The statistical distribution of precipitation (i.e. dichotomous, skewed and discontinuous), along with the relatively high level of noise inherent in the data, pose a number of difficulties when attempting to accurately quantify a model's ability to simulate this variable. For example, many of the skill scores (typically involving squared errors) used to describe continuous variables are sensitive to data which is not normally distributed. To overcome this diagnostics used in NWP to verify quantitative precipitation forecasts (QPF) were employed. A number of these metrics are based on categorizing precipitation events based on predefined thresholds. Contingency tables are subsequently used to estimate model skill using the various categorical type metrics available (Table 6.12).

Mean Error or Bias (Bias)	$ME = \frac{1}{N} \sum_{i=1}^N (S_i - O_i)$	Average difference between the simulated and observed values - a measure of systematic model error.
Mean Absolute Error (MAE)	$MAE = \frac{1}{N} \sum_{i=1}^N S_i - O_i $	Average magnitude of the error
Mean Squared Error (MSE)	$MSE = \frac{1}{N} \sum_{i=1}^N (S_i - O_i)^2$	Average squared magnitude of the error - a measure of total model error.
Root Mean Squared Error (RMSE)	$RMSE = \sqrt{\frac{1}{N} \sum_{i=1}^N (S_i - O_i)^2}$	Average squared magnitude of the error - gives greater weight to larger errors
Pearson's correlation coefficient (r)	$r = \frac{\sum_{i=1}^N (S_i - \bar{S})(O_i - \bar{O})}{\sqrt{\sum_{i=1}^N (S_i - \bar{S})^2} \sqrt{\sum_{i=1}^N (O_i - \bar{O})^2}}$	Measures the degree of linear association between the simulated and observed values, independent of the absolute bias.
Standard Deviation of the Error (STD Error)	$STD \text{ Error} = \sqrt{\frac{1}{N-1} \sum_{i=1}^N (e_i - \bar{e})^2}$	Square root of the average squared difference between the model error ($e_n = S_n - O_n$) and the mean model error (\bar{e}). A measure of random model error
Variance of the Error (Var Error)	$VAR \text{ Error} = \frac{1}{N-1} \sum_{i=1}^N (e_i - \bar{e})^2$	The average squared difference between the model error ($e_n = S_n - O_n$) and the mean model error (\bar{e}). A measure of random model error
Frequency Bias (FBias)	$FBias = \frac{hits + false \ alarms}{hits + misses}$	Gives the ratio of the simulated rain frequency to the observed rain frequency. Perfect = 1; overestimating >1; underestimating <1.
Probability of Detection (POD)	$POD = \frac{hits}{hits + misses}$	Measures the fraction of all observed events which were correctly predicted. Range 0 to 1 with 1 being a perfect score.
Probability of False Detection (POFD)	$POFD = \frac{false \ alarms}{correct \ rejections + false \ alarms}$	Measures the fraction of observed non-which were simulated to be events. Range 0 to 1 with 0 being a perfect score.

Table 6.12 Metrics used to evaluate model performance.

Given that temperature is a continuous normally distributed variable, well established measures for assessing model performance with respect to this variable exist. It is

widely acknowledged that model skill varies both on a temporal and regional basis, in addition some evaluation criteria (e.g. correlation coefficient) can be artificially inflated if they are applied to the annual series (i.e. capture annual trends), to address both of these issues model performance was assessed on a seasonal basis.

A number of the metrics outlined in Table 6.12 quantitatively assess differences in the respective means of the observed and modelled data; a number of others examine how well the models reproduce observed patterns of variability. The former describes the systematic bias in the model output whilst the latter is indicative of the random or non-systematic model error. Both systematic bias and random error contribute to the total error evident in model simulations. Using algebraic manipulation it can be demonstrated that the mean squared error - or the total model error - can be decomposed into:

$$MSE = (\bar{y} - \bar{o})^2 + s_y^2 + s_o^2 - 2s_y s_o r_{yo}$$

where r_{yo} is product-moment correlation between the observed and model simulated series; s_o and s_y are the standard deviations of the marginal distribution estimated from the model output and observations respectively. Finally the first term in the equation refers to the square of the mean error (Murphy, 1988). This can be re-written in a way relative to the metrics outlined in Table 6.12, whereby the mean squared error (MSE) is simply the product of the square of the model bias (Bias) and the variance of the error (VAR Error) - calculated based on the differences between the simulated and observed series.

$$\frac{1}{N} \sum_{i=1}^N (S_i - O_i)^2 = \left(\frac{1}{N} \sum_{i=1}^N |S_i - O_i| \right) + \left(\frac{1}{N-1} \sum_{i=1}^N (e_i - \bar{e})^2 \right)$$

Here N represents the number of elements in the series, S_i and O_i are the simulated and observed series respectively, e_i is the error or difference between the modelled and observed datasets, and \bar{e} is the mean model error. Figure 6.12 illustrates how total, random and systematic errors are manifest in the simulated data. Systematic model error is characterised as being a constant offset or bias from a specified reference point - typically represented using an observed data series. Random error appears as an inconsistent variation in the model over time and/or space; it is manifest in the model being unable to reproduce observed patterns of variability. In NWP systematic errors - which are assumed to remain time-invariant - can be corrected using relatively simple post-processing techniques. This is in contrast to random errors which are considered to be unpredictable and difficult to correct. In this respect random error may be regarded

as less desirable and as such the metrics used to assess it may provide a more informative picture of model performance. In the context of modelling changes in the climate system, where forcing conditions are likely to change considerably over time, and model projections are made on timescales ranging from the decadal to the centennial, systematic error may be more difficult to remediate, particularly as an assumption in the stationarity of the model bias must be made if any correction is applied.

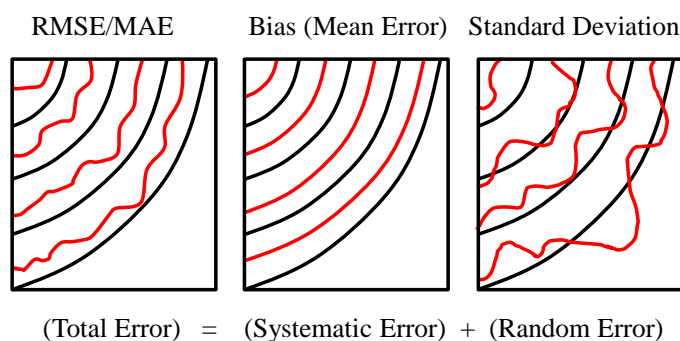


Figure 6.12 Total error is shown as the sum of the systematic and random components. Different metrics can be used to assess each type of model error. (Source: http://www.meted.ucar.edu/nwp/model_derivedproducts/navmenu.php?tab=1&page=4.4.0, accessed 24/11/2011)

The following sections document the ability of the RCMs listed in Table 6.10 to simulate observed temperature and precipitation in the catchment. Model performance is assessed based on a comparison between the output from ERA-40 driven model simulations and point-scale observational data from the Furnace weather station. For consistency model performance is generally assessed over a 30 year period; however in order to make full use of the information available a longer period (1961-2000) was chosen for this study.

6.3.2.1 Minimum temperature

Figure 6.13(a) and 6.13(b) show the MSE, squared Bias and variance of the error for each ERA-40 model simulation calculated on a seasonal basis. Of all models considered the ALADIN regional model run by Météo-France (abbreviated as CNRM-RM4.5) was generally the worst performing model. For each season it returned the highest values for the MAE and VAR Error. Figure 6.13(a) and 6.13(b) indicate that if the bias were to be used as the sole measure of model skill it would suggest that the Météo-France RM4.5 model is among the best performing models, this illustrates the need to consider multiple aspects of performance when evaluating the overall model skill. In addition it highlights the bias which may be introduced if random model error is not considered as a measure of model skill.

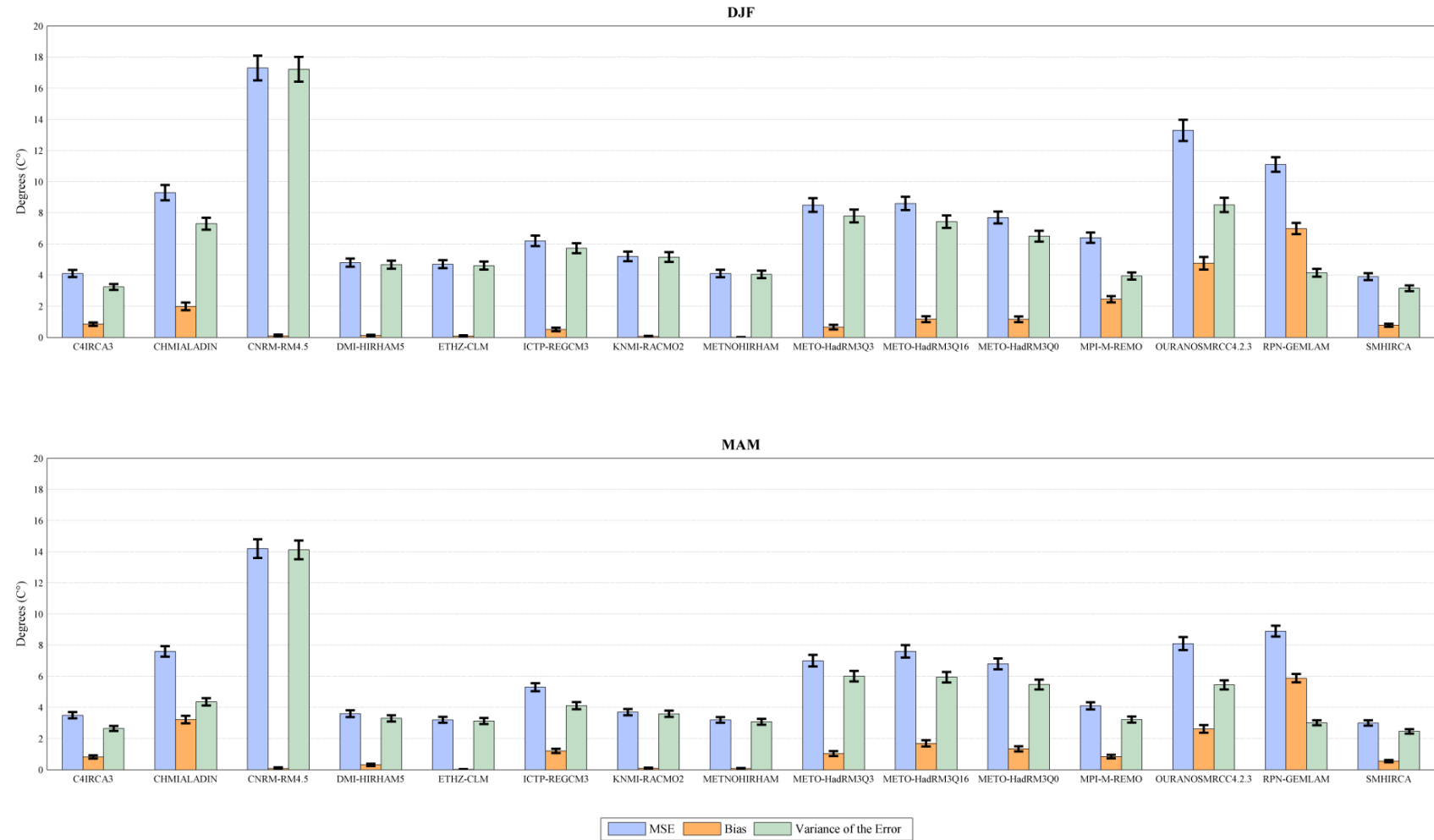


Figure 6.13(a) Skill of the RCMs used in the ENSEMBLES project at simulating observed winter (top panel) and spring (bottom panel) minimum temperature for the period 1961-2000. Model skill is assessed using the observed temperature series from the Furnace weather station. The MSE, bias and variance of the error are calculated for 15 RCMs, each driven using ERA-40 reanalysis data. These metrics are plotted together as they provide a measure of the total, systematic and random model error respectively. Error bars for each metric are calculated based on 10,000 bootstrapped samples and represent the 95% confidence interval.

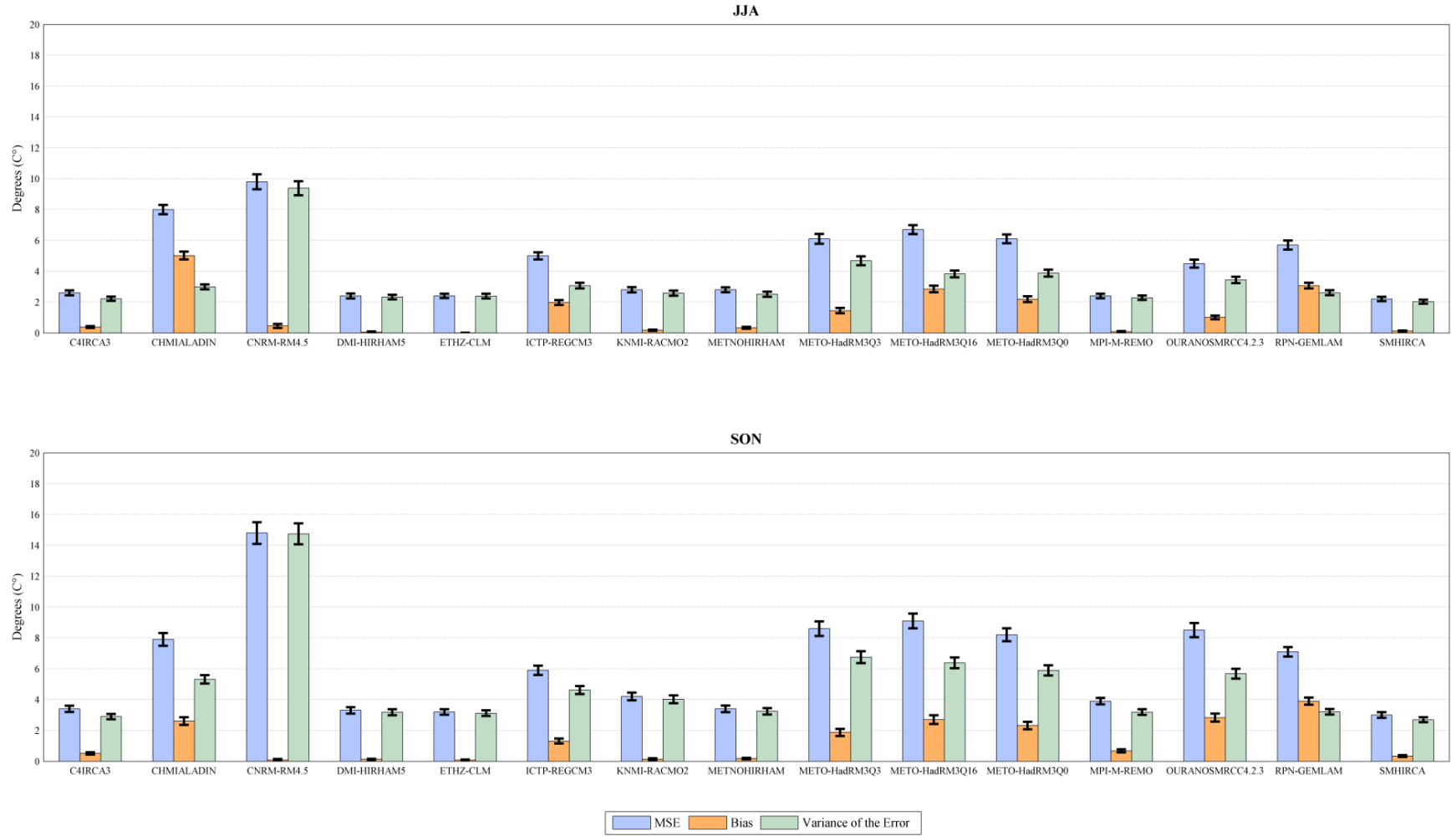


Figure 6.13(b) Skill of the RCMs used in the ENSEMBLES project at simulating observed summer (top panel) and autumn (bottom panel) maximum temperature for the period 1961-2000. Model skill is assessed using the observed temperature series from the Furnace weather station. The MSE, bias and variance of the error are calculated for 15 RCMs, each driven using ERA-40 reanalysis data. These metrics are plotted together as they provide a measure of the total, systematic and random model error respectively. Error bars for each metric are calculated based on 10,000 bootstrapped samples and represent the 95% confidence interval.

The seasonal Taylor plots (Taylor, 2001) shown in Figure 6.14 indicate that the Météo-France RM4.5 model lies furthest from the observations and appears almost as an outlier relative to other models. In this case the Taylor diagrams are used to graphically represent the scores for three metrics (RMSE, Pearson's correlation coefficient and the standard deviation). It should be noted that the mean of each series is subtracted prior to calculating the second-order statistics, thus the diagram does not provide information about overall biases but is rather used to characterize the centered pattern error. The Taylor plots highlight the weak association between the observed and CNRM model simulated data. The performance of each model is also shown by Figure 6.15 - which illustrates how well each model captured the interannual variability.

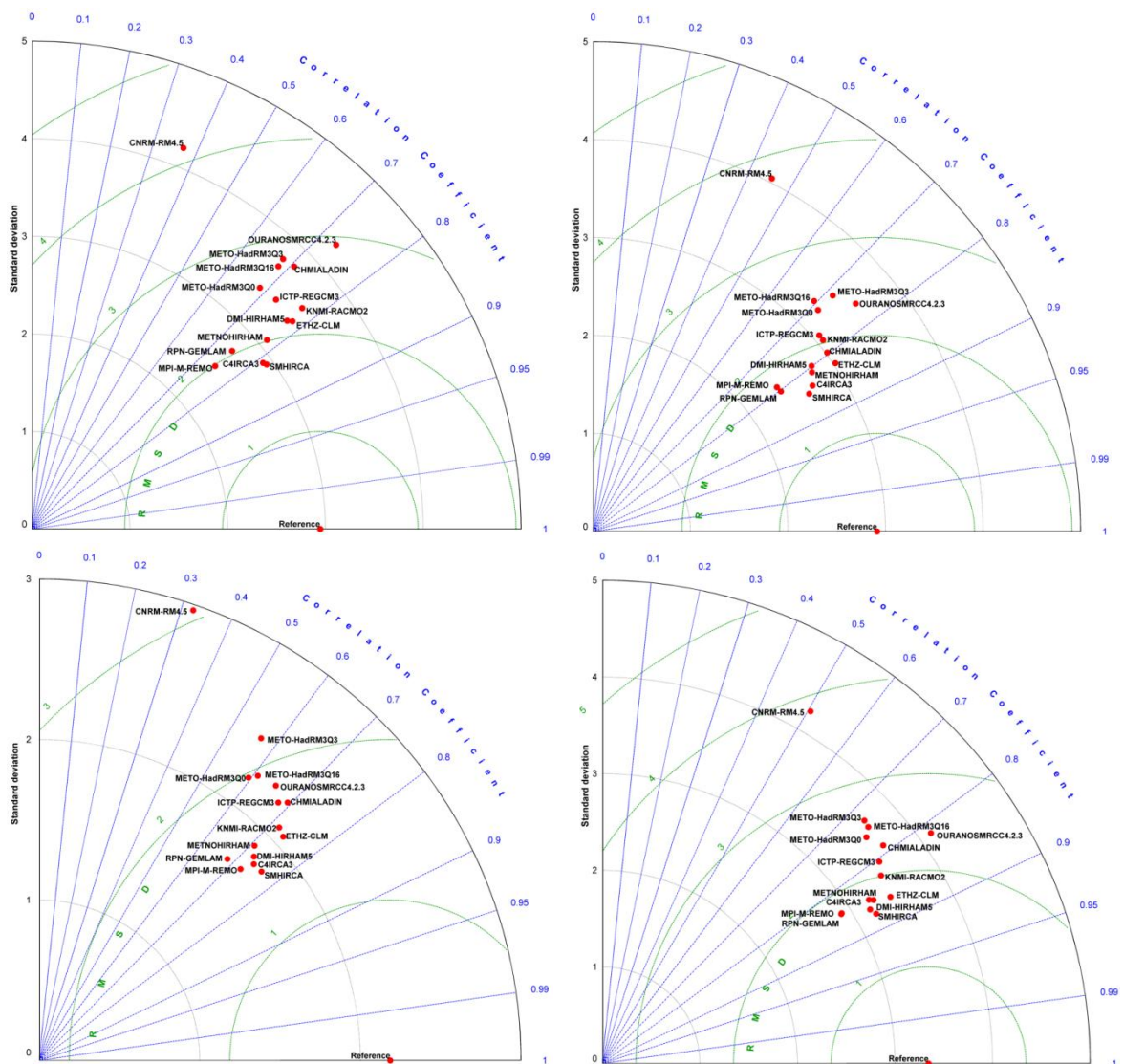


Figure 6.14 Taylor diagrams showing model skill at simulating observed winter (top left panel), spring (top right panel), summer (bottom left panel) and autumn (bottom right panel) minimum temperature for the period 1961-2000. On each plot the output from 15 RCMs, each run using ERA-40 reanalysis data, is compared to the observed temperature series from the Furnace weather station (denoted as 'reference'). The plots provide a graphical summary of the similarity between the patterns of variability in the observed and modelled series - quantified in terms of their correlation, their centered root-mean-square difference and the amplitude of their variations (represented by the standard deviation) (Taylor, 2001).

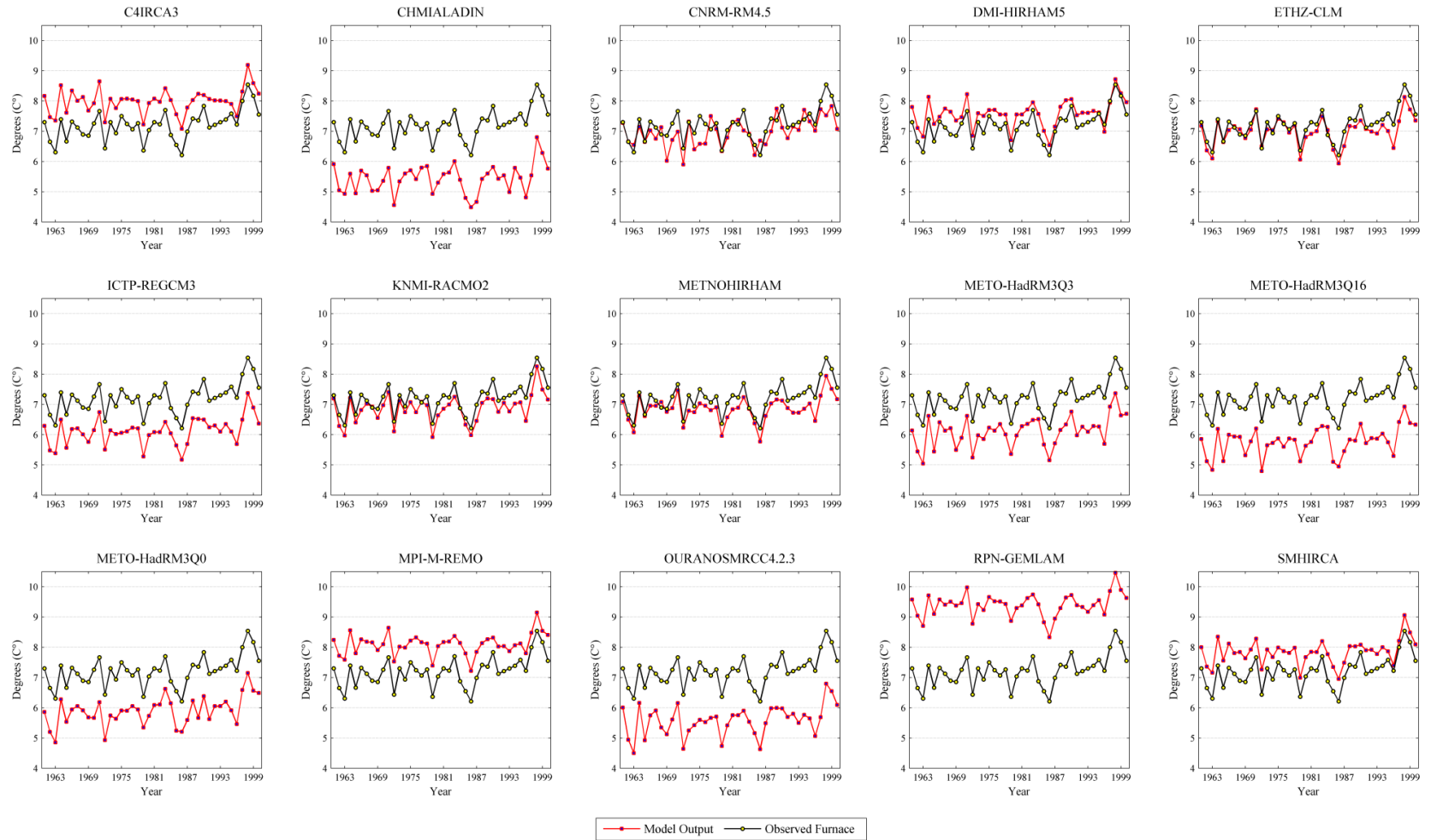


Figure 6.15 Interannual variability of observed and model simulated minimum temperature for the period 1961-2000. The output from 15 RCMs, each run using ERA-40 reanalysis data, is compared to the observed temperature series from the Furnace weather station.

Figure 6.13(a) and 6.13(b) indicate that the best performing models, at least in terms of capturing patterns of variability in the observed series, are those run by the Swedish Meteorological and Hydrological Institute (SMHI) and Met Éireann - abbreviated as SMHIRCA and C4IRCA3 respectively - both of which use the Rossby Centre Atmospheric (RCA) regional model. In all seasons the output from both models exhibits a strong association with the observed series, illustrated by the low values returned for the standard deviation of the model error (STD Error) and the proximity of both models to the reference point in each seasonal Taylor plot (Figure 6.14). There is however a degree of bias evident in the output from both models which detracts from their overall performance.

The degree to which each of these models over-estimates the mean of the observed series is illustrated by Figure 6.15. Plots of the interannual variability demonstrate the skill of both models in reproducing observed patterns of variability but also highlight the warm bias present in each. A number of models returned evaluation scores which indicated that they reproduced both the mean conditions and observed patterns of variability with a high degree of skill. This includes those models run by the Norwegian and Danish meteorological institutes - both of which used the HIRHAM regional model - similarly the models run by the Swiss (ETHZ; CLM) and German (MPI-MET; REMO) institutes performed well. The metrics indicated that a number of models had both a large systematic and random error component. Included in this are the CRCM and ALADIN regional models run by the by the Canadian (OURANOS) and Czech institutes (CHMI) respectively. The metrics employed also indicate that none of the individual model simulations conducted by the UK Met Office (HadRM3 model) performed well at reproducing observed minimum temperature in the catchment.

6.3.2.2 Maximum temperature

Figures 6.16(a) and 6.16(b) plot the seasonal skill scores returned for those metrics relating of total (MSE), random (VAR Error) and systematic (Bias) model error. In contrast to the results for minimum temperature, model performance is to a larger extent seasonally dependent; in addition the simulated data is to a greater degree affected by systematic biases in the downscaling model. With respect to this all models exhibit a cold bias, the magnitude of which varies on a seasonal basis. In some cases biases are greater in winter when compared with summer (e.g. OURANOSMRCC4.2.3), in other instances the reverse is true (e.g. C4IRCA3, SMHIRCA and RPN-GEMPLAM).

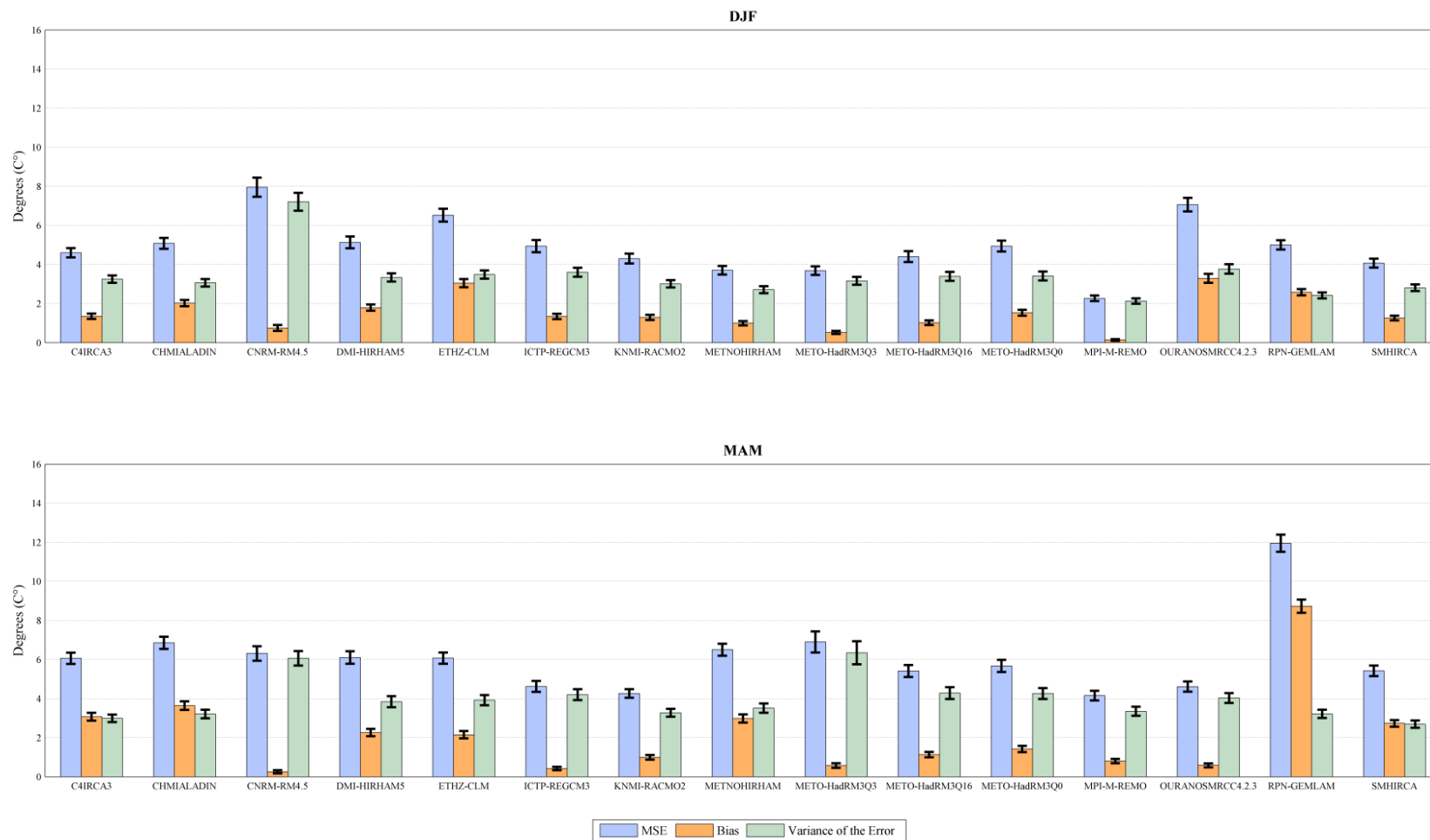


Figure 6.16(a) Skill of the RCMs used in the ENSEMBLES project at simulating observed winter (top panel) and spring (bottom panel) maximum temperature for the period 1961–2000. Model skill is assessed using the observed temperature series from the Furnace weather station. The MSE, bias and variance of the error are calculated for 15 RCMs, each driven using ERA-40 reanalysis data. These metrics are plotted together as they provide a measure of the total, systematic and random model error respectively. Error bars for each metric are calculated based on 10,000 bootstrapped samples and represent the 95% confidence interval.

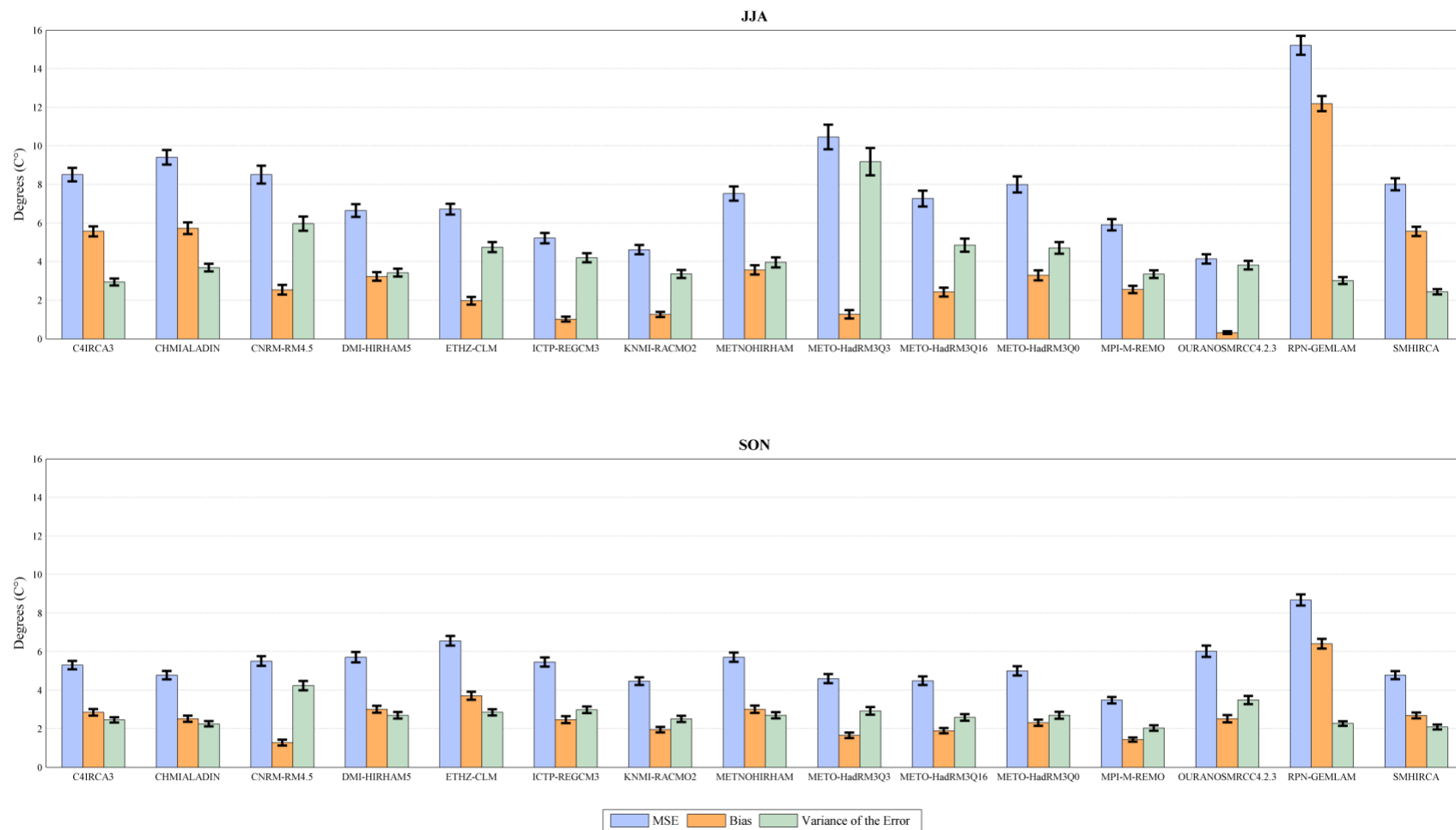


Figure 6.16(b) Skill of the RCMs used in the ENSEMBLES project at simulating observed summer (top panel) and autumn (bottom panel) maximum temperature for the period 1961-2000. Model skill is assessed using the observed temperature series from the Furnace weather station. The MSE, bias and variance of the error are calculated for 15 RCMs, each driven using ERA-40 reanalysis data. These metrics are plotted together as they provide a measure of the total, systematic and random model error respectively. Error bars for each metric are calculated based on 10,000 bootstrapped samples and represent the 95% confidence interval

The model which exhibits the largest bias is the GEM limited area model (LAM) run by the Canadian based Recherche Prévision Numérique (RPN) institute. The simulations which also exhibit a large bias include those contributed by the Irish (C4I; RCA3), Swedish (SMHI; RCA) and Czech (CHMI; ALADIN) institutes. The model simulations from Météo-France (CNRM; ALADIN) and the Max Plank Institute (MPI-MET; REMO) return the lowest values for systematic error; similarly, the UK Met Office HadRM3-Q3 model simulation - reflective of low climate sensitivity - also returns one of the lowest values for model bias. In terms of reproducing observed patterns of variability, those model simulations made available by the SMHI, MPI-MET, C4I and KNMI institutes perform well - as is evidenced by the Taylor plots shown in Figure 6.17. However, on a seasonal basis no one model is consistently the most skilful with respect to this aspect of performance.

The Canadian GEM model is the worst performing with respect to systematic error; in contrast it is among the best in terms of minimizing the random error component. Figure 6.18 illustrates the degree to which the GEM model underestimates the mean but reproduces the variability of observed conditions in the catchment. The Météo-France run ALADIN RCM is the worst performing model at simulating observed variability; the HadRM3 (Q3) model also performs poorly in this respect - as is evidenced by its relatively weak association with the observations and its distance from the reference point in each Taylor plot (Figure 6.17).

In terms of total model error the worst performing models are those run by the Canadian (RPN), French (CNRM) and Czech (CHMI) institutes; in contrast the most skilful are those run by the Max-Plank (REMO) and Royal Netherlands Meteorological (RACMO2) institutes. Both of these models exhibit consistently low mean absolute error (MAE) values for all seasons. In general the models perform best for autumn and worst for summer, this is reflected in the stronger/weaker association between the observed and model simulated series for both seasons. The models appear to be clustered in the same region of the plot for autumn, indicating little variation in performance; this is in contrast to the summer plot where a greater spread in the model values is evident.

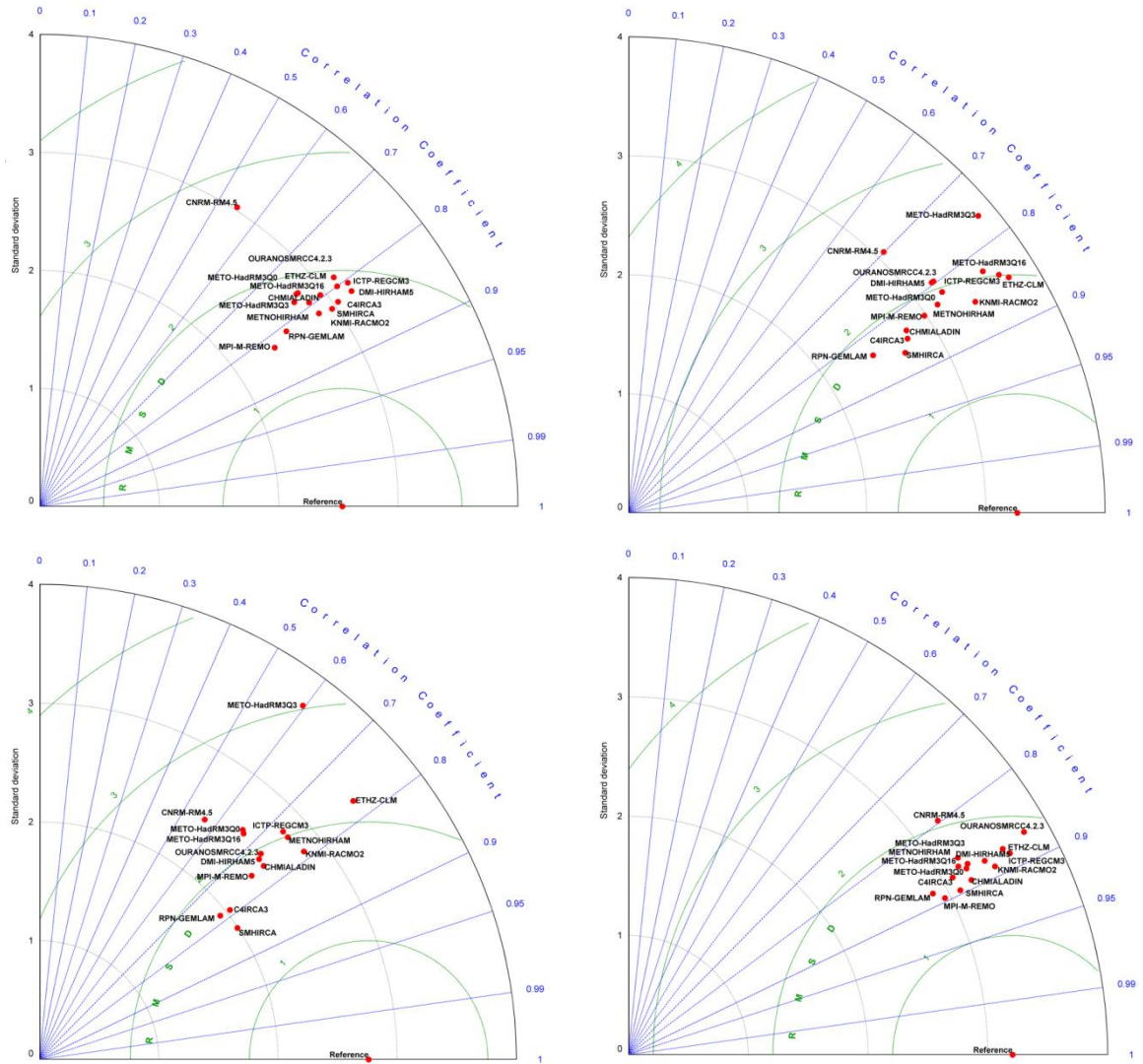


Figure 6.17 Taylor diagrams showing model skill at simulating observed winter (top left panel), spring (top right panel), summer (bottom left panel) and autumn (bottom right panel) maximum temperature for the period 1961-2000. On each plot the output from 15 RCMs, each run using ERA-40 reanalysis data, is compared to the observed temperature series from the Furnace weather station (denoted as 'reference'). The plots provide a graphical summary of the similarity between the patterns of variability in the observed and modelled series - quantified in terms of their correlation, their centered root-mean-square difference and the amplitude of their variations (represented by the standard deviation) (Taylor, 2001).

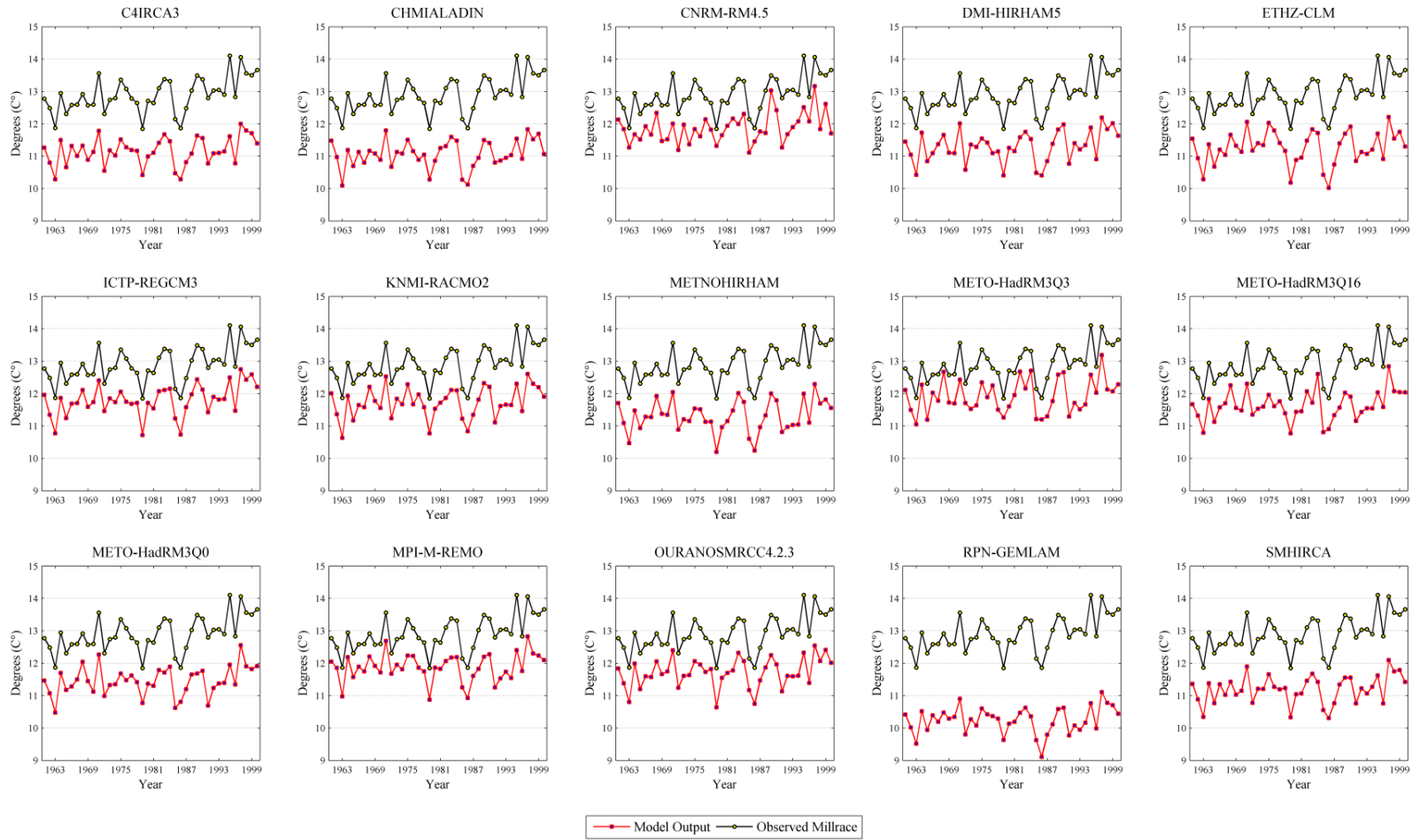


Figure 6.18 Interannual variability of observed and model simulated maximum temperature for the period 1961-2000. The output from 15 RCMs, each run using ERA-40 reanalysis data, is compared to the observed temperature series from the Furnace weather station.

6.3.2.3 Precipitation

Those more conventional metrics which are easily applied to examine model performance with respect to temperature are not as readily applicable when used to assess precipitation. A number of metrics - particularly those involving squared errors (e.g. MSE) - typically used to assess continuous variables are sensitive to large errors or inconsistencies in the modelled series. One approach to overcoming this is to normalize the data; however, this leads to a loss of information and as a result certain caveats must be associated with the estimated skill scores. The difficulties associated with evaluating precipitation as a continuous variable means that deconstructing the model error into its constituent random and systematic components is a much more complex task. The complications associated with treating precipitation as a continuous variable means QPFs are typically verified using both continuous and categorical based scores - similarly in this study both approaches are taken to assess model performance. To apply the categorical metrics outlined in Table 6.12 a number of thresholds were used to discretize the simulated and observed series. To apply the continuous based metrics a fourth root transformation was used to normalize the observed and model simulated data.

Figure 6.19(a) and 6.19(b) indicate that a number of models - including those run by the Dutch (KNMI), Italian (ICTP), Swedish (SMHI) and Czech (CHMI) institutes - simulate the catchment's annual precipitation regime with a relatively high degree of skill. Some models appear to reproduce the annual cycle but tend to over or under estimate receipts. This includes the model simulations conducted by the Danish (DMI) and Norwegian (METNO) meteorological institutes, both of which employed the HIRHAM RCM. A number of other model simulations, including those conducted by Météo-France (CNRM) and the Canadian based OURANOS institute, appear to produce a 'flat' annual cycle with large biases for both the winter and autumn months. Model skill in simulating patterns of variability and mean conditions are illustrated by how well each model reproduces the inter-annual variability of total annual precipitation receipts (Figure 6.20). It can be seen that those models which perform well at reproducing the annual cycle generally capture the inter-annual variability also. This is most evident for the model simulations provided by the ICTP, KNMI, CHMI and SMHI institutes.

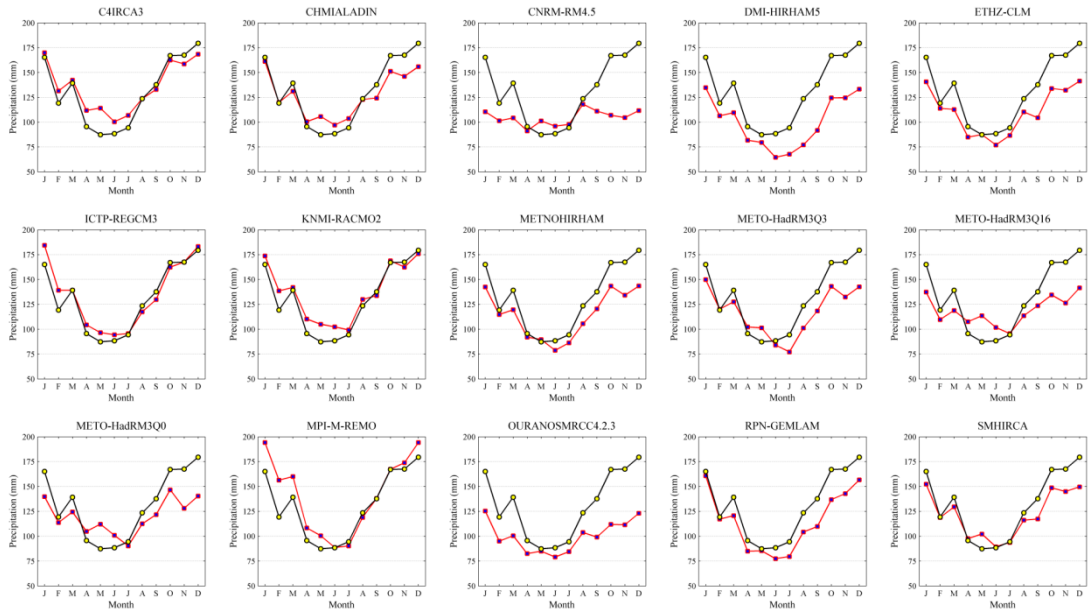


Figure 6.19(a) Observed and model simulated monthly mean precipitation receipts averaged over the period 1961-2000. The output from 15 RCMs, each run using ERA-40 reanalysis data, is compared to the observed precipitation series from the Furnace weather station.

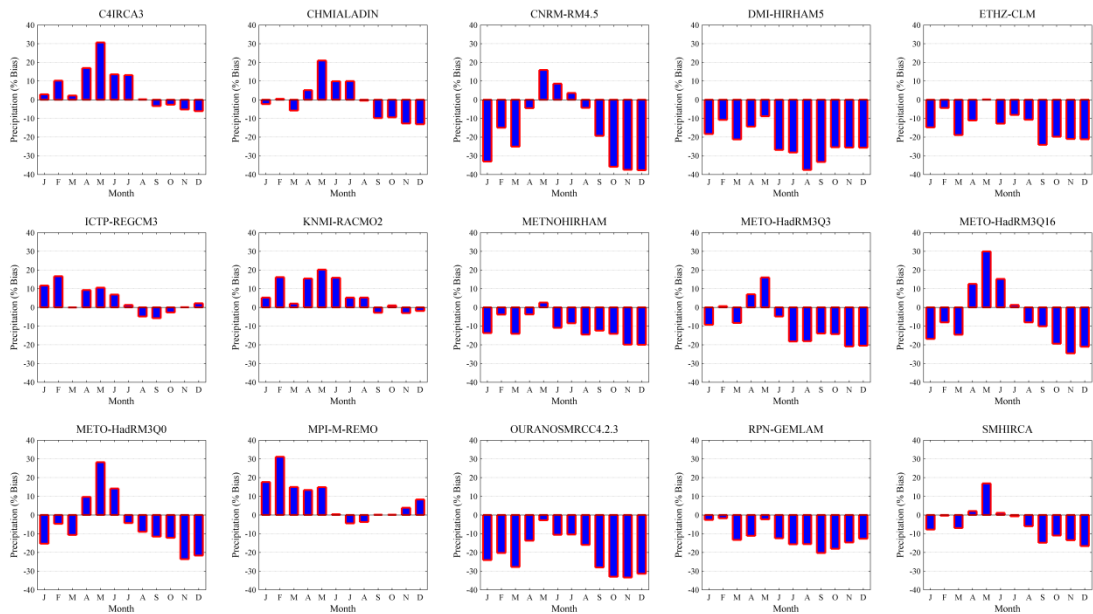


Figure 6.19(b) Percent bias in the model simulated monthly rainfall receipts estimated for the period 1961-2000. The output from 15 RCMs, each run using ERA-40 reanalysis data, is compared to the observed precipitation series from the Furnace weather station.

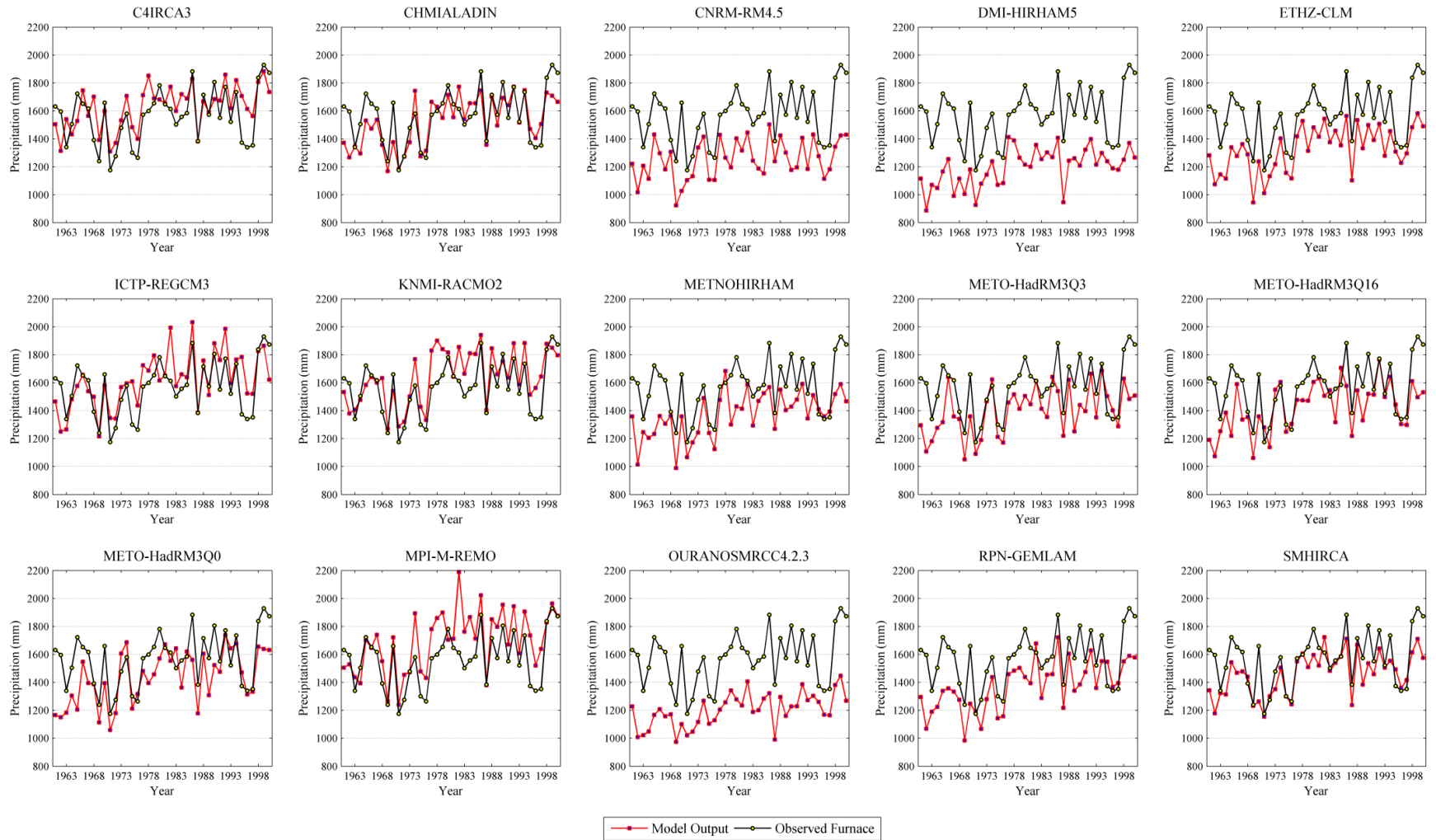


Figure 6.20 Interannual variability of observed and model simulated annual precipitation receipts for the period 1961-2000. The output from 15 RCMs, each run using ERA-40 reanalysis data, is compared to the observed precipitation series from the Furnace weather station.

The results of the categorical metrics suggest that model skill at simulating events of a given magnitude decreases as the event threshold is increased. The results from the frequency bias skill score (Figure 6.21) indicate that most models tend to underestimate the number of more intense rainfall events (e.g. ≥ 20 mm). This is particularly evident in the model simulations provided by the Czech (CNRM), Swedish (SMHI) and Canadian (OURANOS) institutes. A number of models tend to overestimate the frequency of lower threshold classes whilst at the same time underestimating the number of heavy precipitation events; this is most evident during the summer season. When individual scores are averaged across each season and threshold class those models run by the Dutch (KNMI), British (METO), Italian (ICTP) and Irish (C4I) institutes return the lowest frequency bias, whilst those run by Météo-France and both Canadian institutes (OURANOS and RPN) returned the highest values for this metric. The HIRHAM5 regional model, run by the Danish Meteorological Institute (DMI) underestimates the frequency of all event classes, a finding which is common to each season. This is consistent with the dry bias which the model exhibits in Figure 6.19 and Figure 6.20.

Figure 6.22(a) shows the relative operating characteristic (ROC) curves plotted on a seasonal basis for each model; the ROC plots are complemented by Figure 6.22(b) which quantifies the area under each curve, for visual purposes the area values have been standardized on a seasonal basis prior to graphing. The ROC curve plots the probability of detection (POD) (true positive rate) against the probability of false detection (POFD) (false positive rate). According to the curves the more accurate the model simulation the further into the upper left corner the plot extends - denoting fewer false positives and a greater proportion of correctly simulated events. The area under the curves is taken as a measure of how well each model simulated the (non-)occurrence of each event class. The seasonal curves suggest that the models perform best during winter and are worst at capturing summer precipitation; for the transition seasons of spring and autumn the models exhibit similar skill levels. Generally the best performing models - calculated based on an average of the seasonal scores - include those run by the Swedish (SMHI; RCA), Czech (CHMI; ALADIN), German (MPI-M; REMO) and Dutch (KNMI; RACMO2) institutes. In contrast the worst performing models include: ALADIN run by Météo-France, HIRHAM5 run by the Danish Meteorological Institute and the three model simulations conducted by the UK met office.

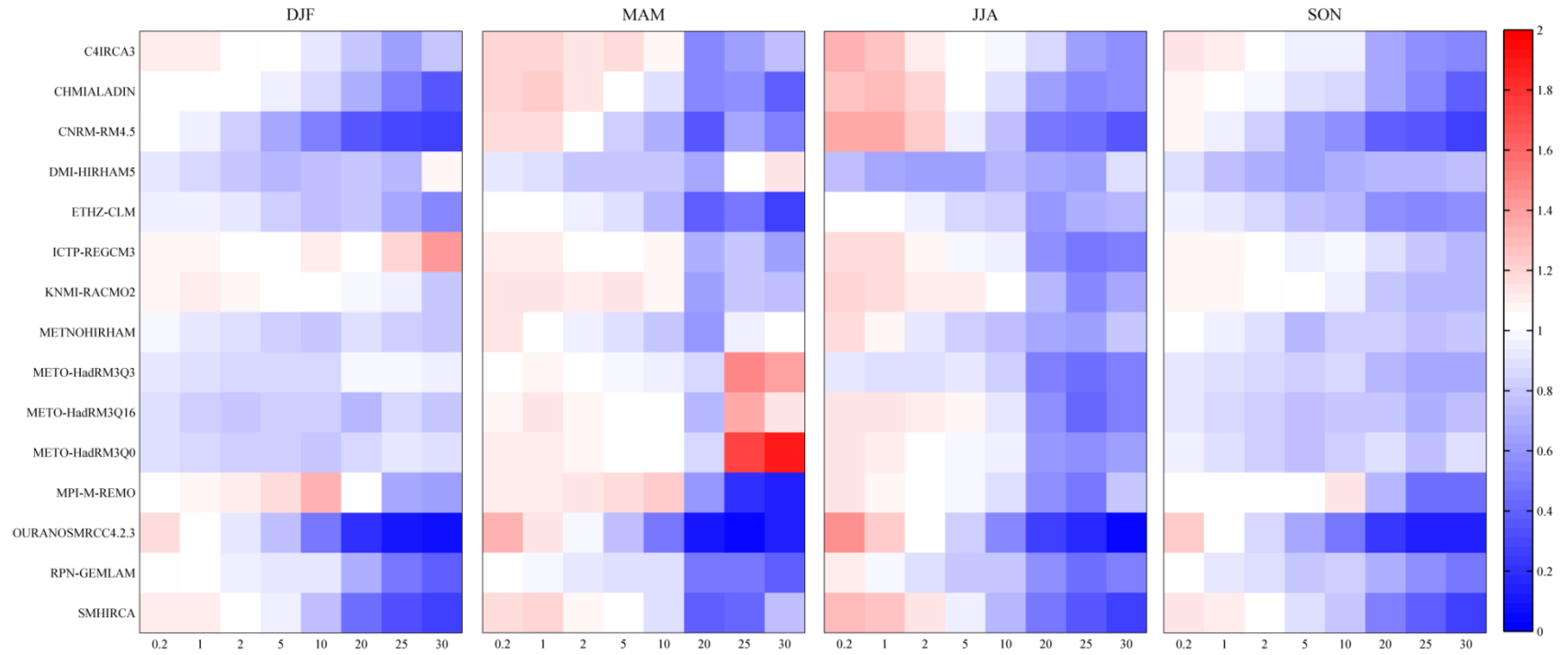


Figure 6.21 Frequency bias of the model simulated data estimated on a seasonal basis for the period 1961-2000. The output from 15 RCMs, each run using ERA-40 reanalysis data, is compared to the observed precipitation series from the Furnace weather station. Nine different threshold levels are used to discretize the datasets (≥ 0.2 mm, 1 mm, 2 mm, 5 mm, 10 mm, 20 mm, 25 mm and 30 mm). Perfect score = 1; overestimating >1 ; underestimating <1 .

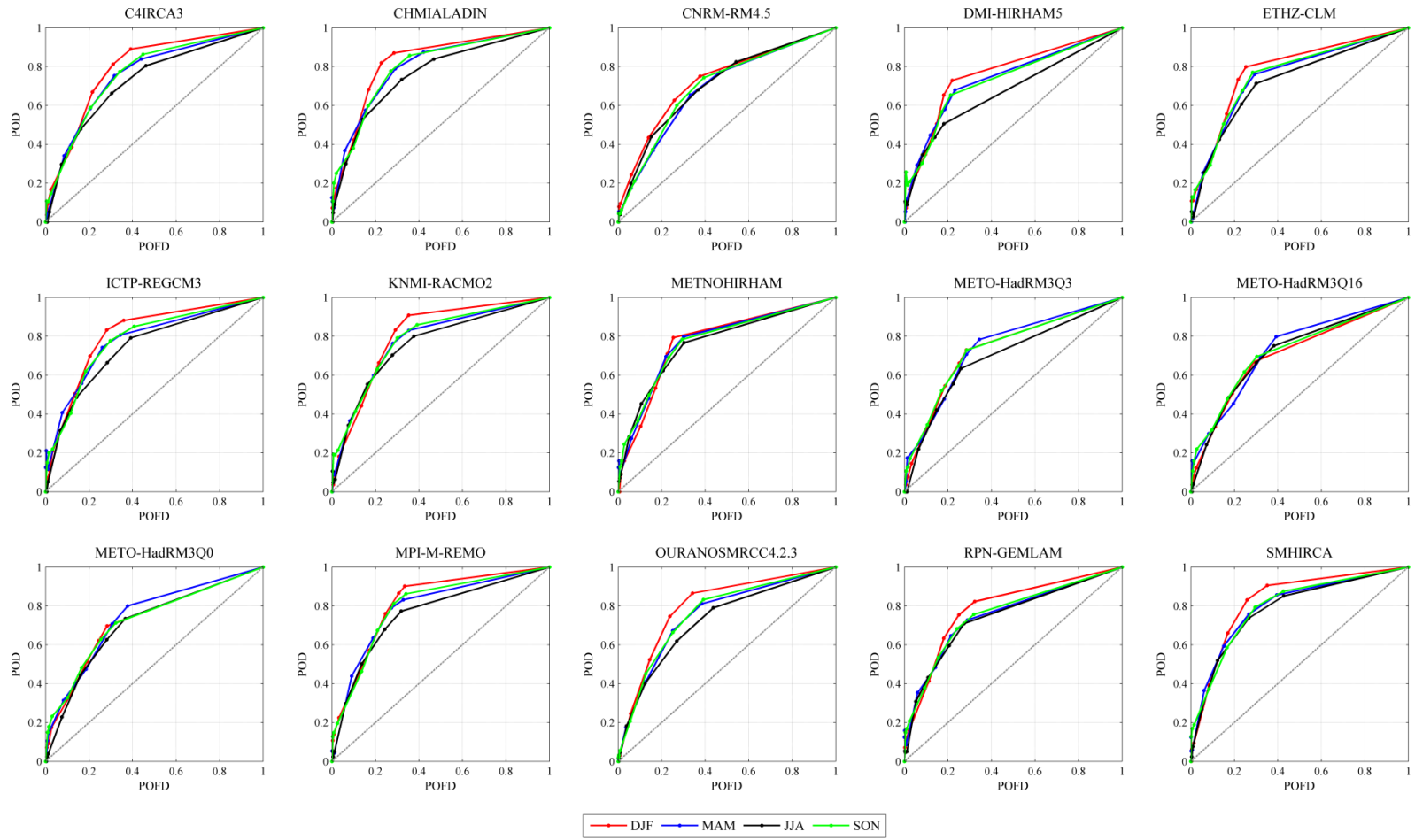


Figure 6.22(a) Seasonal ROC curves for 15 RCMs each run using ERA-40 reanalysis data. The output from 15 RCMs, each run using ERA-40 reanalysis data, is compared to the observed precipitation series from the Furnace weather station. Nine different threshold levels are used to discretize the datasets (≥ 0.2 mm, 1 mm, 2 mm, 5 mm, 10 mm, 20 mm, 25 mm, and 30 mm).

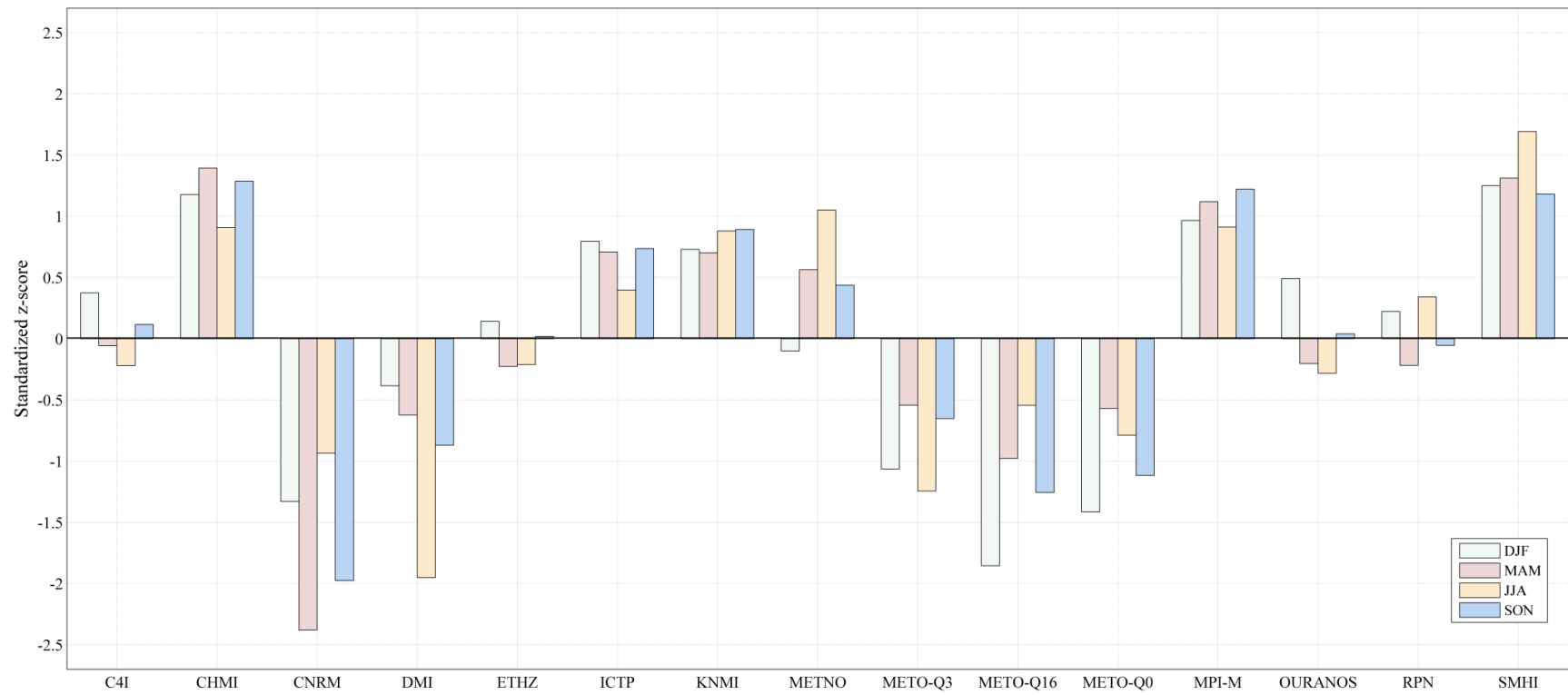


Figure 6.22(b) Area under the ROC curves shown in Figure 6.22(a). All values have been standardized on a seasonal basis.

The Canadian (CRCM) model simulation does not appear to perform as poorly according to this metric when compared with the others discussed above; this may be due to the model having a low probability of false detection (POFD).

Figure 6.23(a) and 6.23(b) show Q-Q plots for the winter and summer seasons respectively, the plots have been constructed using wet-day precipitation amounts only (≥ 0.2 mm). The plots indicate that the models perform better at capturing winter as opposed to summer precipitation - for which a decline in performance is noted. The majority of models tend to underestimate more intense events; this is particularly evident for the summer season. Those models which simulate precipitation with a high degree of skill include those run by the Irish (C4I), Danish (DMI), Italian (ICTP) and Dutch (KNMI) institutes; the model simulations conducted by the UK Met office also perform well according to the Q-Q plots. Based on the plots the least skilful simulations are those conducted by the Canadian institute (OURANOS) and Météo-France (CNRM).

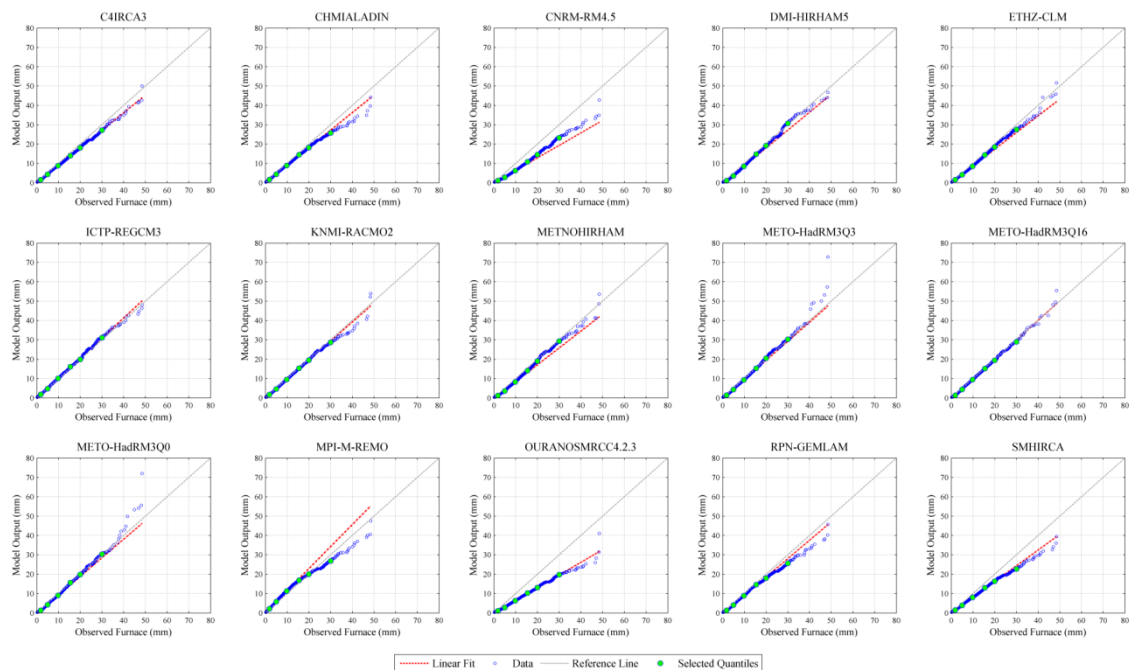


Figure 6.23(a) Q-Q plots of the observed and model simulated precipitation series for winter. The output from 15 RCMs, each run using ERA-40 reanalysis data for the period 1961-2000 is compared to the observed precipitation series from the Furnace weather station. The enlarged green dots are used to highlight those values relating to the following percentiles: 25th, 50th, 75th, 90th, 95th and 99th.

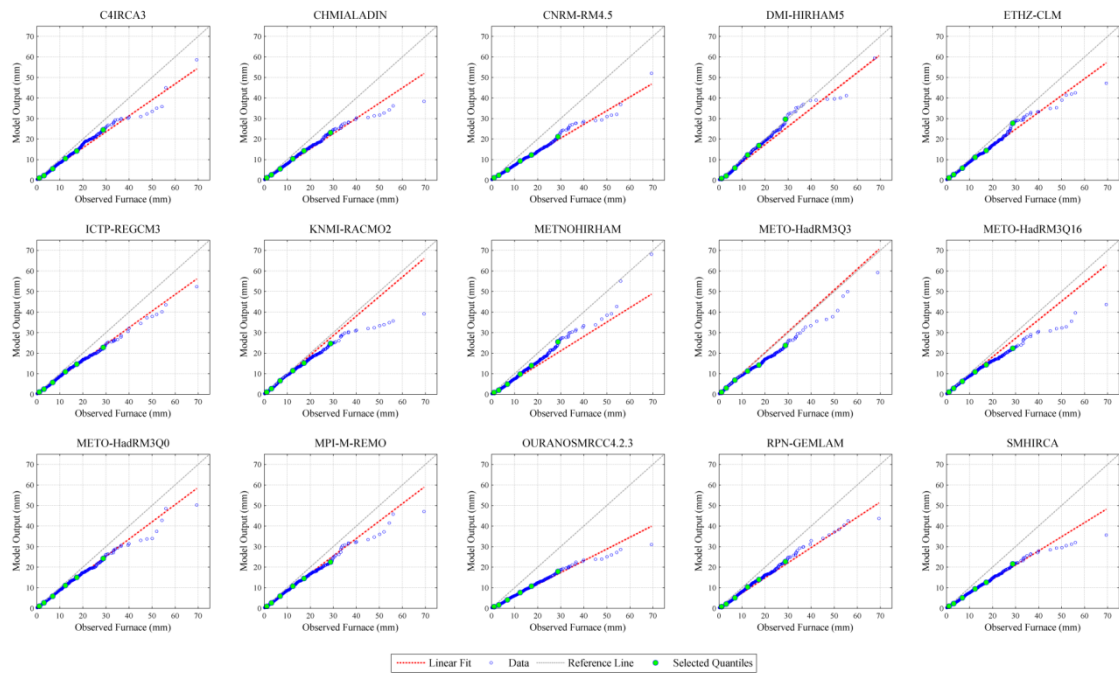


Figure 6.23(b) Q-Q plots of the observed and model simulated precipitation series for summer. The output from 15 RCMs, each run using ERA-40 reanalysis data, is compared to the observed precipitation series from the Furnace weather station over the period 1961-2000. The enlarged green dots are used to highlight those values relating to the following percentiles: 25th, 50th, 75th, 90th, 95th and 99th.

Table 6.13 show the results from continuous verification metrics applied on a seasonal basis to assess model performance. Prior to estimating each metric the observed and model simulated series was transformed using a fourth root transformation. The correlation coefficient (Pearson's r) - calculated using daily values - suggests that the model simulations made available by the Swedish (SMHI), German (MPI-M) and Czech (CHMI) institutes exhibit the strongest association with the observed data. The simulations conducted by Météo-France and the UK Met Office returned the lowest scores for this metric. Generally the models appear to have a higher correlation with the observed dataset during winter; this is in contrast to summer for which the lowest values for this metric are returned. For each season there appears to be high level of agreement between the correlation coefficients and the corresponding area under the ROC curves. The DMI and CNRM run models exhibit the highest MAE (indicative of total model error), whilst those run by the Canadian (RPN) and SMHI institutes return the lowest values for this criterion. Similarly the model simulation provided by the Swedish Meteorological and hydrological Institute has the lowest value for the standard deviation of the error (indicative of random error); whilst the UK Met Office, DMI and CNRM model simulations return the highest values for the STD Error. The model simulated data provided by the DMI generally returns the largest absolute bias (indicative of systematic error), whilst the data provided by the SMHI generally exhibits the lowest value for this metric.

Model	DJF				MAM				JJA				SON			
	MAE	Bias	STD Error	r	MAE	Bias	STD Error	r	MAE	Bias	STD Error	r	MAE	Bias	STD Error	r
<i>C4IRCA3</i>	0.12	0.12	1.23	0.62	0.24	0.24	1.19	0.55	0.24	0.24	1.3	0.47	0.08	0.08	1.31	0.56
<i>CHMIALADIN</i>	0.02	-0.02	1.11	0.71	0.19	0.19	1.07	0.61	0.23	0.23	1.2	0.53	0.04	-0.04	1.21	0.65
<i>CNRM-RM4.5</i>	0.27	-0.27	1.36	0.45	0.07	0.07	1.32	0.39	0.25	0.25	1.34	0.36	0.28	-0.28	1.47	0.41
<i>DMI-HIRHAM5</i>	0.28	-0.28	1.33	0.56	0.18	-0.18	1.2	0.56	0.37	-0.37	1.32	0.48	0.41	-0.41	1.39	0.55
<i>ETHZ-CLM</i>	0.18	-0.18	1.27	0.63	0.06	-0.06	1.15	0.6	0.05	-0.05	1.3	0.53	0.24	-0.24	1.32	0.61
<i>ICTP-REGCM3</i>	0.14	0.14	1.21	0.65	0.11	0.11	1.14	0.6	0.13	0.13	1.25	0.53	0.04	0.04	1.31	0.58
<i>KNMI-RACMO2</i>	0.12	0.12	1.21	0.67	0.17	0.17	1.14	0.61	0.19	0.19	1.23	0.55	0.07	0.07	1.27	0.62
<i>METNOHIRHAM</i>	0.16	-0.16	1.3	0.62	0.03	0.03	1.12	0.6	0.01	0.01	1.2	0.56	0.16	-0.16	1.32	0.6
<i>METO-HadRM3Q3</i>	0.19	-0.19	1.42	0.54	0.04	0.04	1.25	0.55	0.13	-0.13	1.37	0.47	0.23	-0.23	1.43	0.54
<i>METO-HadRM3Q16</i>	0.27	-0.27	1.52	0.45	0.11	0.11	1.28	0.51	0.12	0.12	1.36	0.44	0.26	-0.26	1.49	0.48
<i>METO-HadRM3Q0</i>	0.25	-0.25	1.48	0.49	0.11	0.11	1.26	0.53	0.08	0.08	1.37	0.44	0.22	-0.22	1.47	0.49
<i>MPI-M-REMO</i>	0.23	0.23	1.16	0.7	0.18	0.18	1.09	0.65	0.07	0.07	1.2	0.58	0.08	0.08	1.23	0.66
<i>OURANOSMRCC4.2.3</i>	0.13	-0.13	1.17	0.63	0.07	0.07	1.13	0.51	0.17	0.17	1.23	0.44	0.16	-0.16	1.27	0.53
<i>RPN-GEMLAM</i>	0.03	-0.03	1.24	0.59	0.05	-0.05	1.15	0.56	0.05	-0.05	1.22	0.54	0.17	-0.17	1.32	0.55
<i>SMHIRCA</i>	0.02	0.02	1.09	0.69	0.15	0.15	1.06	0.63	0.18	0.18	1.13	0.58	0	0.00	1.19	0.63

Table 6.13 Results from continuous evaluation metrics (mean absolute error (MAE), the standard deviation of the error (STD Error), bias and Pearson's r) estimated seasonally. The output from 15 RCMs, each run using ERA-40 reanalysis data for the period 1961-2000, is compared to the observed precipitation series from the Furnace weather station. A fourth root transformation is used prior to estimating the skill scores.

6.4 Development and application of a model weighting scheme

It is widely recognized that considering a single realization of future climate precludes an ample sampling of the uncertainty space - leading to overconfidence in a particular climate pathway and potential mal-adaptation to future change. As highlighted by Sánchez *et al.* (2009), employing a multi-model ensemble allows for a more accurate description of the uncertainties and limitations associated with competing models, it also allows the strengths of individual models to be combined and recognizes that no single ensemble member generally outperforms its competitors in all aspects of performance. Although this represents a more pragmatic approach for exploring the climate response to perturbed forcing, inconsistencies in the ability of individual models to capture the various features of present-day climate suggests that performance based weighting systems should be applied when combining the output from multi-model simulations (Giorgi & Mearns, 2002).

The converse of applying a weighting scheme is to treat the output from each model as being equally plausible - irrespective of their skill under present day conditions. Whilst also constituting a probabilistic approach, and thus representing an advance on the practice of taking a single scenario of future change, it comes with the caveat that a high level of confidence may be erroneously placed in poorly performing models, giving them an undue bearing on the ensemble projections. Whilst it is generally agreed that employing a multi-model ensemble is a more robust strategy for exploring potential changes in climate, there is yet to be a consensus on the issue of whether weighting schemes should be employed, and if so how they should be formulated.

By applying a weighting scheme an assumption is being made that the models will perform with a comparable level of skill under forcing conditions for which they have not been evaluated nor have any prior experience. Furthermore, there is a degree of subjectivity associated with which aspects of model performance to consider and the weighting different error types are given in the final scheme. Subjective choices are also associated with which metrics to employ and how to aggregate their results in order to formulate the final model or scenario weights (Kjellström & Giorgi, 2010). This brings into focus the fact that applying a weighting scheme may, rather than reducing uncertainty, simply add an additional layer of uncertainty which must be considered and made explicit in impact studies.

It is however argued that weighting schemes can be made more robust by using multiple diagnostics, considering different aspects of model performance and accounting for as much uncertainty as is possible (Tebaldi & Knutti, 2007). Furthermore, as argued by Sánchez *et al.* (2009), when employing an unweighted ensemble average - which is expected to be a closer fit to observed conditions than any individual model - the reduction in error experienced may be a result of error cancellation, whereby the model output is consistent with the observed data despite failing to correctly simulate the underlying processes governing system behaviour. Thus, while in some instances the weighted mean ensemble may appear to hold little advantage above simply taking the unweighted mean ensemble, it is a more defensible and robust strategy to apply model weights. This however comes with the caveat that the weighting scheme itself has been robustly formulated. In recent years a number of techniques have been employed to formulate weighting systems - based on various performance criteria and model diagnostics (e.g. Giorgi & Mearns, 2002, 2003; Murphy *et al.*, 2004; Tebaldi *et al.*, 2005; Piani *et al.*, 2007; Tebaldi & Knutti, 2007; Brekke *et al.*, 2008)

As part of the ENSEMBLES project a weighting scheme was used to formulate probabilistic climate projections based on the ensemble of participating RCMs. The skill of individual models was estimated based on a comparison between the simulated (driven using ERA-40 reanalysis data as unbiased lateral boundary conditions) and observed climate data (gridded E-OBS dataset). The weighting scheme was formulated based on a range of criteria used to evaluate model performance including: (1) a comparison between the probability distribution of modelled and observed climate data; (2) how well the annual cycle was reproduced; (3) accuracy at capturing extreme events; (4) the skill of competing models in simulating large-scale circulation and weather regimes; (5) ability to simulate the sub-GCM-grid scale mesoscale climate signal and (6) how well the RCMs captured linear trends in the observed series.

6.4.1 Formulation of a weighting scheme

Weighting schemes are applied on the basis that an accurate and reliable estimate of model performance under present-day climate conditions can be obtained. When evaluating downscaling models (either dynamical or statistical) a different methodological approach must be adopted depending on whether the models have been driven using large-scale GCM or reanalysis data. In the context of dynamical models

reanalysis data essentially provides unbiased quasi-observational boundary conditions. By using this data the effect of biases inherited from the driving GCM can be removed as a confounding factor, allowing the skill of individual regional models to be isolated and independently determined. Using reanalysis data also means that the models are able to reproduce the day-to-day variability and sequencing of weather events, allowing more precise model diagnostics to be applied at a higher temporal resolution (e.g. Table 6.12).

In contrast, downscaled GCM data represents a single realisation of climate; it does not follow the same temporal evolution as the observed system, but ideally reflects the climatology of the underlying domain. This precludes the use of verification metrics which require temporal coherence between the observed and modelled series. As highlighted by Maraun *et al.* (2010), the validation of downscaling models driven by GCM data is limited to assessing the spatial structure of the model climatology and the respective statistical distributions of the simulated climate variables. Evaluating the skill of a particular GCM-RCM model combination is complicated by biases inherited from the parent GCM as well as biases present in the downscaling model itself. Determining where in the model pathway bias in the output data accrues, is further obscured by the possibility of interactions between errors in the nested and parent model - which may act to amplify or dampen (i.e. cancel out) the total error in the downscaled series. As a result it may be a more defensible strategy to evaluate each component in the model chain independently, before determining how the accumulation of error in the driving and nested model affects the downscaled GCM data.

In developing a weighting scheme for use in this study a number of difficulties were encountered, the first of which was how an equitable weighting scheme could be formulated which considered both dynamically and statistically downscaled data. In the case of the statistical model a 15-year validation period existed for which the models could be independently assessed. In the interests of parity both the dynamical and statistical models would have to be evaluated using this common period; however, in previous studies a 40 year period (1961-2000) has generally been used to evaluate model performance. This is further complicated by the fact that a different set of reanalysis data (NCEP and ERA-40 respectively) was used as input to the statistical and dynamical models respectively; consequently differences in the performance of both approaches may be a result of the reanalysis data used rather than the downscaling model itself. Questions arose as to whether it was appropriate to weight models based

on performance over a 15-year period, and whether an equitable comparison of model skill could be made given that a different set of reanalysis data was used.

To produce the dynamically downscaled climate scenarios the regional models were forced using GCM simulations run under the A1B SRES scenario (with the exception of the C4I); however, the statistically downscaled GCM data relates to the A2 and B2 emission scenarios only. This creates problems when attempting to produce a single weighted PDF of projected climate for which all of the individual downscaled scenarios are considered. By virtue of the fact that a higher number of A1B type scenarios are included, it is likely that this emissions pathway would have an undue influence on the final probability distribution function - possibly overriding the influence of any climate change signal originating from the A2 and B2 scenarios respectively.

Difficulties also emerged regarding how to construct a weighting scheme whereby a set of weights could be formulated (following Déqué & Somot (2010)) for each GCM and downscaling model independently. Ideally the performance of each component (i.e. GCM-RCM) in a particular model pathway should be isolated and determined independently before being used to formulate the final weighting for that pathway. With respect to this it was important that an appropriate set of weights were formulated for each component in the model pathway. Questions arose as to whether an additional weight should be formulated based on the skill of the pathway itself (i.e. the output from the combined driving and downscaling model). This would allow for some consideration of the performance of both the driving and downscaling models when used together. It is possible that their respective skill, independent of one another, may hide an overall reduction in performance when errors in both models interact with one another. Similarly, formulating a weighting scheme based on the pathway alone, whereby the skill of each of its components has not been assessed independently, may mask the fact that error cancellation is occurring, resulting in a high weighting being erroneously assigned. For example, an undue weighting may be given in instances where a GCM with a cold bias is compensated for by a regional model with a warm bias. To overcome the difficulties outlined above the following steps were taken.

- It is unlikely that a robust set of weights could be derived based on a 15 year dataset; furthermore, the use of different reanalysis data may not provide an equitable basis for comparing the performance of individual downscaling models. Consequently an independently derived weighting scheme was developed for the dynamical and statistical model pathways respectively (Figure

6.11). This allowed for the use of the full 40 year period when evaluating RCM performance, it also provided for the fact that both the statistical and dynamical pathways are based on different emission scenarios. This approach however precludes the development of a single weighting scheme which could be applied to all of the data used in this study; it also meant that a single weighted probability distribution function of future change could not be produced.

- Weights were formulated for each regional model independently using the results from the model evaluation documented in the preceding sections. Here the performance of the ERA-40 driven models at simulating observed temperature and precipitation in the catchment was examined. Several metrics which variously describe each model's ability to simulate observed patterns of variability (across different time-scale), mean conditions and the climatology of the study areas were employed. Given that a single statistical downscaling model was used, no weighting was applied to it.
- Each GCM was assigned a weight; in the case of the dynamical model pathways these weights are taken from Déqué and Somot (2010) who formulated them as part of the ENSEMBLES weighting scheme. A different set of weights based on the Climate Prediction Index (CPI) (Murphy *et al.*, 2004) were applied to the three GCMs used in the statistical model pathways. These weights are taken from Fealy (2010) who developed them for use with in an Irish context with statistically downscaled scenarios from the SDSM data archive. The method used by Fealy (2010) follows that of Wilby and Harris (2006) who refined the methodological framework outlined by Murphy *et al.* (2004) for use in a statistical downscaling context.
- A weighting for each model pathway was also used as part of the overall weighting scheme. This was calculated based on how well a particular model pathway reproduced the empirical probability distribution of monthly mean and daily values. How well the individual model combinations reproduced the mean annual climatology of the catchment was also considered when formulating the scenario weights.

In summation two different sets of weights were used (Figure 6.24); each of which reflect the performance of the GCM and downscaling models independent of one another. A third weight was included which characterized the skill of the combined GCM and downscaling model (i.e. different climate realizations). The scenarios included in the dynamically downscaled weighting scheme are shown in Figure 6.11. Two of the 19 pathways are excluded as they either did not have a corresponding ERA-40 driven dataset, or were not based on the A1B emission scenario.

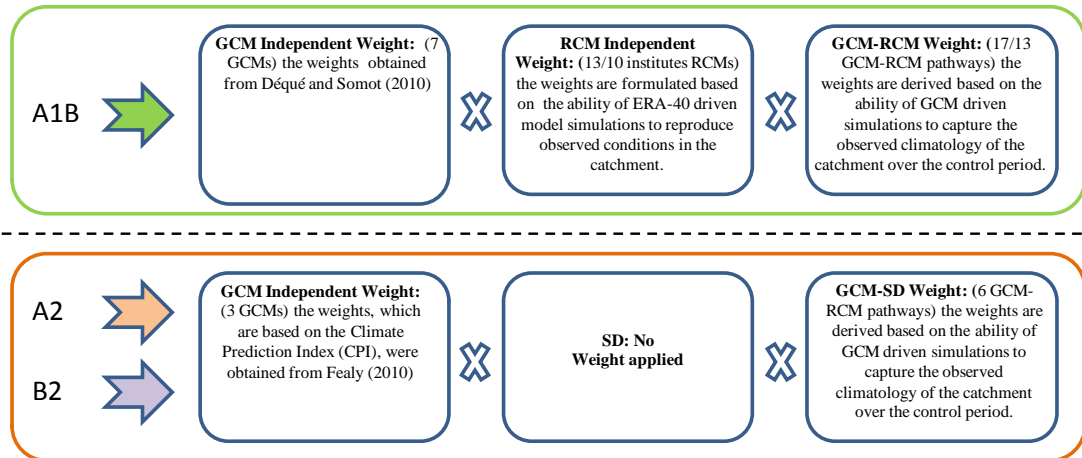


Figure 6.24 Schematic of the model weighting scheme. To ensure equitability when comparing all climate projections the data was collapsed based on the respective emission scenarios; thus a separate set of weights were developed for the dynamical (A1B) and statistical (A2 and B2) pathways independent of one another.

6.4.1.1 RCM weights

The independent RCM weights were derived based on how well each ERA-40 driven model reproduced observed temperature (minimum and maximum) and precipitation in the catchment. A separate set of weights were formulated for each variable on a seasonal basis. When selecting criteria with which to evaluate model skill it was important that the same aspect of performance were not considered multiple times (i.e. by different metrics) as this may introduce bias to the weighting scheme. Several of the metrics used to formulate the RCM weights are different to those used to evaluate model performance in the preceding section. This was due to the focus of the weighting scheme being much narrower and the need to avoid biasing the weights. In addition, given that spatial variability was not considered, it was important that the model's ability to capture temporal patterns of variability over a range of frequencies was considered (e.g. daily, seasonal, interannual). It was also desirable that the same metrics could be applied to evaluate model performance for both precipitation and temperature.

The Pearson's correlation coefficient was employed to quantify how well each model reproduced the observed day-to-day variability of temperature and precipitation in the catchment - the correlation is estimated on a seasonal basis. In addition the correlation coefficient was used to characterise how well each model captured the 'phase of seasonality' (e.g. Figure 6.19(a)) or the similarity between the observed and model simulated annual climatology (Brekke *et al.*, 2008). Pearson's r was used for the reason it provides a measure of association but has the advantage of being sensitive to outliers. Two additional metrics which examined each model's ability to reproduce trends and variability in the observed series were also employed.

Following Lorenz and Jacob (2010) a skill score was assigned to each model based on how well they reproduced both annual and seasonal trends in the observed data. The magnitude and direction of linear trends were estimated using the slope parameter from a regression between the annual/seasonal means and corresponding time step. The skill score (S) was calculated for each RCM using the following:

$$S = 1 - \frac{|\beta_{OBS} - \beta_{MOD}|}{\gamma + |\beta_{OBS} - \beta_{MOD}|}$$

where β_{MOD} and β_{OBS} are the linear trends estimated from the modelled and observed series respectively; γ is a scaling parameter for the S score which, in this case was set to 0.5. As it affects the magnitude of the score only and not the respective ranking of each RCM, the value of γ is not of critical importance. In addition to examining linear trends the coefficient of determination (R^2) was also used to calculate the covariance between the observed and model simulated inter-seasonal/interannual variability (e.g. Figure 6.20).

The skill scores obtained from the seasonal and annual values for each metric (S and R^2) were aggregated into a single skill score. Lorenz and Jacob (2010) suggest that the ability of a model to capture annual trends is more important than their ability to simulate seasonal trends; following this, the seasonal R^2 and S scores were given a lower weighting when the results were aggregated. A weight of 0.5 was given to the skill score estimated using the annual series whereas a weighting of 0.125 was given to each of the skill scores derived using the seasonal series. The final aggregated score for R^2 and S respectively is given by:

$$S_{combined} = 0.5 \cdot S_{annual} + 0.125 \cdot (S_{DJF} + S_{JJA} + S_{MAM} + S_{SON})$$

$$R^2_{combined} = 0.5 \cdot R^2_{annual} + 0.125 \cdot (R^2_{DJF} + R^2_{JJA} + R^2_{MAM} + R^2_{SON})$$

One of the drawbacks associated with the metrics employed here is that the models are weighted based on how well they simulate temporal rather than spatial patterns of variability. In addition, their ability to reproduce the large scale dynamics of atmospheric behaviour is not considered. However, given that the catchment is the sole focus of this study, and that the records used to quantify model performance cover a relatively long period, it was thought that model skill could be adequately described using these evaluation criteria alone.

The metrics employed focus on random rather than systematic error in the model simulations. As a result they do not allow for the fact that a model with a large systematic bias and low random error is given a similar weighting to models which perform well according to both criteria. However, given that a subjective decision would have to be made regarding the relative importance of random and systematic error (i.e. how each would be weighted), it was decided that random error would be used as the key criterion to assess model performance. In addition to selecting the various aspects of performance to assess, ample consideration must be given to how the scores from individual metrics are aggregated to produce the final RCM weights. In this study the skill scores from each metric were multiplied, this was to ensure that the models only received a high aggregated weighting if they performed well according to each of the various evaluation criterion employed (Christensen *et al.*, 2010). The weights generally reflect the findings of the in-depth analysis of RCM performance outlined in section 6.3.2.

Generally those models which were found to perform well for a particular season were found to perform well across all seasons. For both precipitation and temperature the ALADIN RCM run by Météo-France receives the lowest weighting; those RCM (HadRM3) simulations conducted by the UK Met Office are also assigned a low weighting. In contrast the regional model run by the Swedish Meteorological and Hydrological Institute (RCA) was assigned a high weighting for both variables, as were those models run by the C4I (RCA3), ETHZ (CLM), KNMI (RACMO2) and MPI-M (REMO) institutes. The model weights are more variable for precipitation when compared to both minimum and maximum temperature. Although the weights are formulated independently for each variable, generally those which are assigned a high weighting for precipitation are also assigned a high weighting for temperature - suggesting there is a degree of consistency across the models.

The individual skill scores indicate that those models which perform well at capturing pattern of variability in the inter-annual/seasonal temperature series do not always capture the linear trend. For example the ALADIN model run by Météo-France receives a low R^2 score but a high value for the S metric. In other instances high/low values for both measures were returned. In the case of precipitation, the Météo-France model receives a low score for both metrics, this is in contrast the CLM model run by the Swiss ETHZ institute which returned high scores for both the R^2 and S metrics.

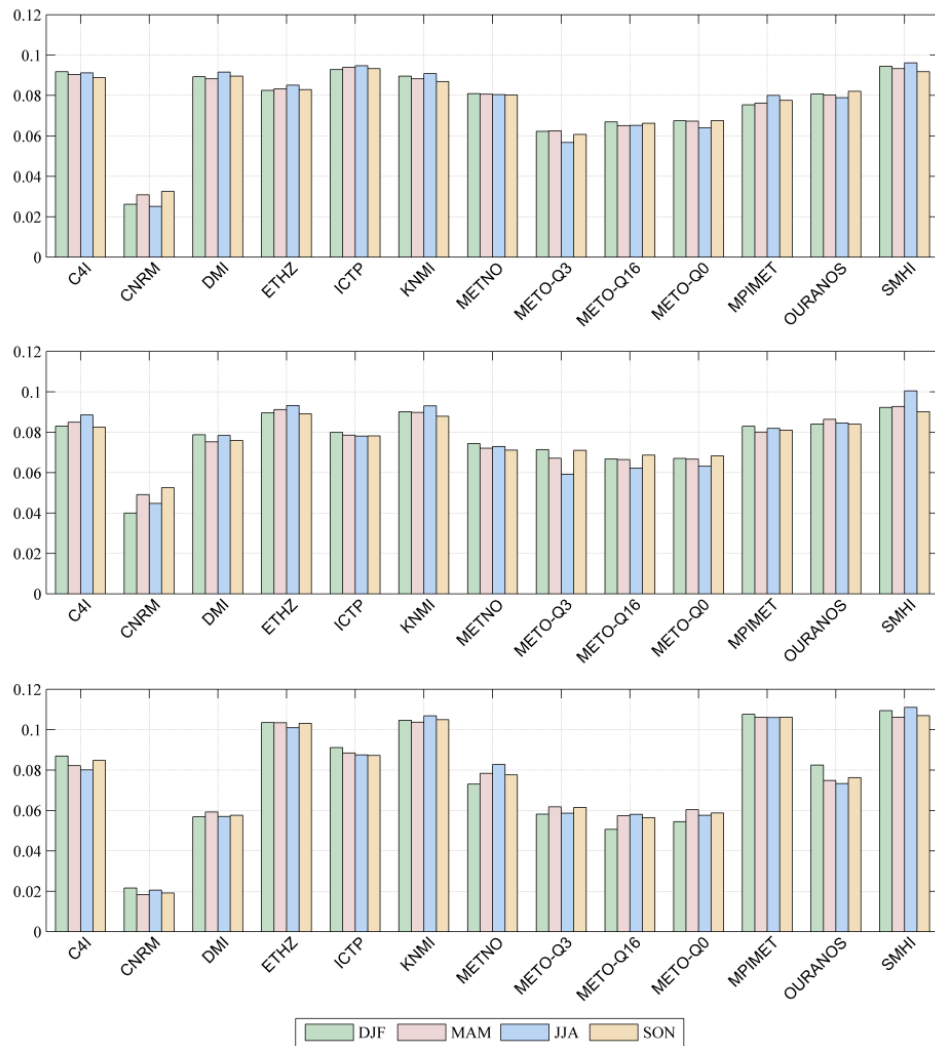


Figure 6.25 Aggregated seasonal weights formulated for each of the 13 RCMs used to downscale GCM data for the period 1961-2050. The seasonal weights for each variable are shown in the top (minimum temperature), middle (maximum temperature) and bottom (precipitation) panels. Prior to plotting the weights were normalized on a seasonal basis.

6.4.1.2 GCM weights

The GCM weights (Table 6.14) employed in this study are taken from Déqué and Somot (2010) who produced them for use as part of the ENSEMBLES weighting scheme. To derive weighted projections of future changes in climate for Europe Déqué

and Somot (2010) formulated two sets of weights which reflected the skill of the (ERA-40 driven) regional and global models used in the study when evaluated independently of one another. Here the weights for the nested and driving models were determined independently and subsequently combined to weight the output from each respective GCM-RCM model pathway.

The GCM weights were calculated based on how well each model reproduced large-scale circulation patterns over a common European domain. To calculate the weights Déqué and Somot (2010) applied a cluster analysis to ERA-40 500hPa geopotential height data on a daily time-step; based on this four circulation patterns were identified for each season. The time series from each GCM simulation was subsequently recoded depending on its similarity (distance criterion) to each respective pattern. Based on differences in the frequency of the ERA-40 and simulated patterns a skill score for each GCM was derived. The method used by Déqué and Somot (2010) follows that outlined by Sanchez-Gomez *et al.* (2008) who applied it to ERA-40 driven RCM data. Of note in Table 6.14 is the fact that the UK Met Office’s HadCM3 GCM is assigned a series of different weightings - irrespective of its sensitivity. As Table 6.14 indicates the high sensitivity (Q16) HadCM3 model, along with the ECHAM5 model from the Max-Planck Institute, are assigned a relatively high weighting. In contrast the HadCM3 low sensitivity (Q3) model is assigned a comparatively lower weighting.

Institute	Model	Weight
METO-HC	<i>HadCM3, Std (Q0)</i>	0.063
METO-HC	<i>HadCM3, Low (Q3)</i>	0.045
METO-HC	<i>HadCM3, High (Q16)</i>	0.081
MPIMET	<i>ECHAM5</i>	0.081
CNRM	<i>ARPEGE</i>	0.069
NERSC	<i>BCM</i>	0.069
CCCma	<i>CGCM3</i>	0.093

Table 6.14 GCM weights (Déqué & Somot, 2010)

6.7.1.3 Model pathway weighting scheme

In each model pathway the performance of the constituent regional and global model, when evaluated independently, may mask deficiencies in their overall skill when combined. Therefore quantifying the performance of the individual pathways as an entity independent of their components is considered important. Given the lack of temporal coherence between the observed and modelled data any comparison is limited

to examining how well the models simulate the baseline climatology or reproduce the statistical attributes of the observed climate series. In this study the same methods are used to formulate the weights for the both the statistical (SD-GCM) and dynamical (GCM-RCM) model pathways.

A number of the metrics used to estimate the weights for the ERA-40 driven regional models are also used to calculate the scenario weights. In both cases metrics which describe random model error are used. Previous studies have however included some measure of model bias in the weighting criteria for GCM data. For example the Reliability Ensemble Average (REA) method (Giorgi & Mearns, 2002) considers model bias over the control period as a measure of GCM performance. Given the limited ways in which climate scenarios can be assessed, and the difficulties associated with differentiating between different error types - particularly when constrained by the lack of temporal coherence between the observed and model simulated data - it was considered important to include some measure of model bias in the weighting scheme for the climate scenarios.

As in the case of the RCM weights the Pearson's correlation coefficient is used to quantify how well each pathway reproduces the observed annual climatology of the catchment ('phase of seasonality') (Brekke *et al.*, 2008) (Figure 6.26). In addition the metric proposed by Perkins *et al.* (2007) was used to compare the empirical probability distribution functions (PDFs) of the simulated and observed series. Here the PDFs are constructed by discretizing the data according to a predefined bin width; a dimensionless metric is then applied to estimate the propinquity of the PDF constructed using the observed and model simulated data. The metric can be written as:

$$SS = \sum_{bin=1}^{bin=N} \min(PDF_{Downscaled}, PDF_{Observed})$$

Both the maximum and minimum temperature series were discretized using a bin width of 0.5°C. In the case of precipitation, rainfall amounts on wet days only were considered. Following Kjellström (2010) a threshold of >1 mm was used to classify wet days. To discretize the precipitation series a bin width of 1 mm was used. This metric was applied on a seasonal basis to daily and monthly data (monthly mean) respectively. Figure 6.27 illustrates the concept of the *SS* metric using smoothed empirical distribution functions for monthly mean precipitation.

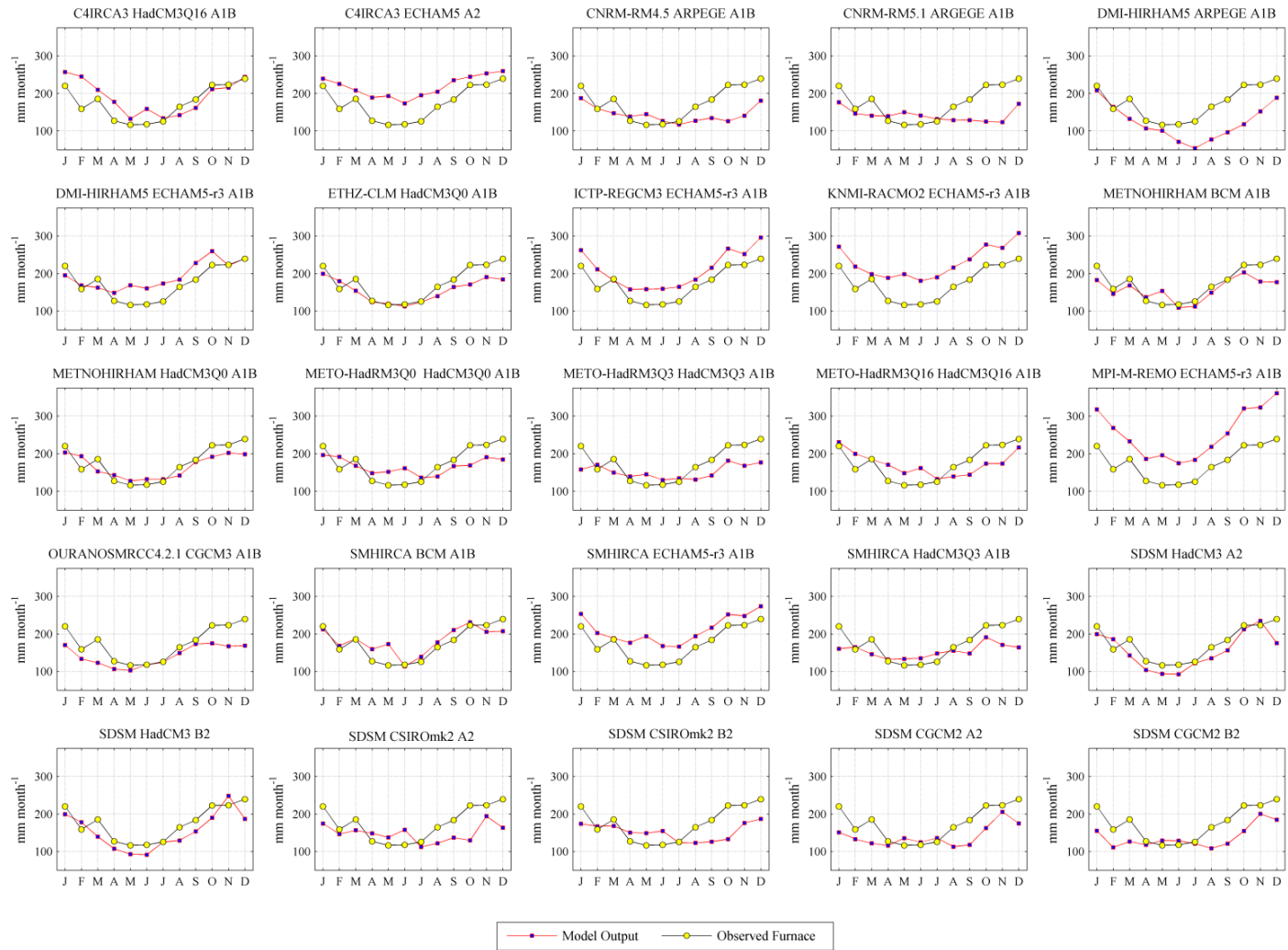


Figure 6.26 Observed and model simulated mean monthly precipitation receipts averaged over the 30 year control period (1961-1990). Climate scenarios from 25 model pathways (19 GCM-RCM; 6 GCM-SD) are compared to observed precipitation from the Furnace weather station.

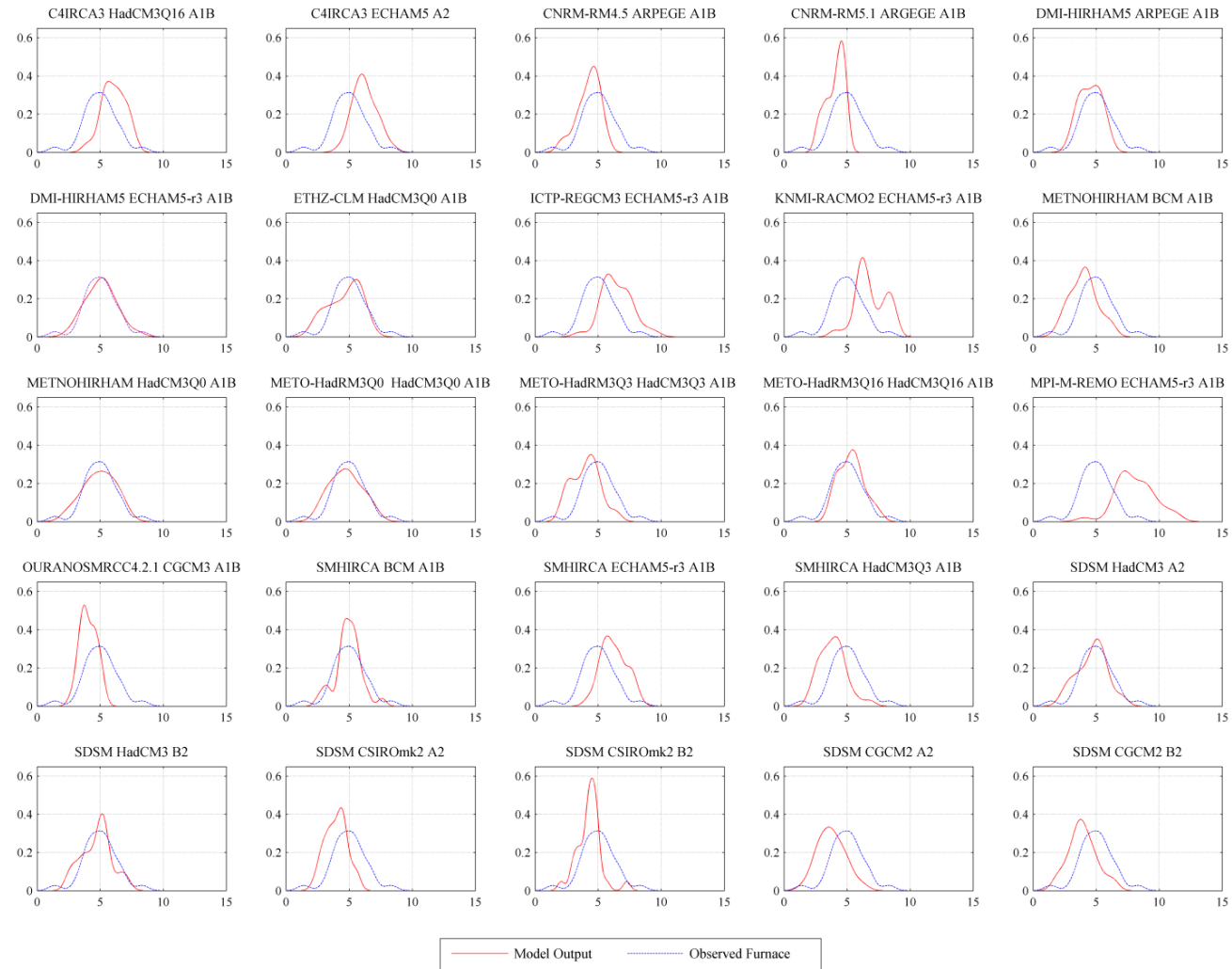


Figure 6.27 Smoothed empirical probability distribution functions of observed and model simulated monthly mean winter precipitation receipts for the control period (1961-1990). Climate scenarios from 25 model pathways (19 GCM-RCM; 6 GCM-SD) are compared to observed precipitation from the Furnace weather station.

According to Kjellström *et al.* (2010) - who employed the *SS* metric to evaluate the performance of the ERA-40 driven RCMs used in the ENSEMBLES project - daily data (i.e. high frequency, day-to-day variations) can be taken as largely representing regional scale forcings. Thus the results from the metric applied to the downscaled climate series (at this temporal resolution) provide an estimate of RCM performance. In contrast monthly data (i.e. low frequency variations) is more strongly related to the dynamics of the driving global model, thus the results from the metric applied at this resolution are more relevant to the GCM. The *SS* metric has the advantage of being able to compare the empirical PDF of the observed and model simulated climate series; however, it is sensitive to systematic bias in the model data. For example where the shape of the distribution is similar, but the location is different, a low score will be returned (e.g. Figure 6.27; MPI-M-REMO ECHAM5-r3); thus, whilst the model bias is not explicitly quantified by this metric, it does have a bearing on the estimated skill score.

Two additional metrics were used when formulating the scenario weights, one of which has previously been employed by Xu *et al.* (2010) in their proposed advancement of the REA method. Following Xu *et al.* (2010) the model pathways were assessed based on how well each reproduced the observed interannual variability. With respect to temperature, variability was quantified using the standard deviation of the inter-annual mean series. The inter-annual coefficient of variation (CV) (standard deviation divided by the mean) was applied to precipitation. An additional metric was used to examine the similarity of trends found in the observed and model simulated series. This is the same metric used to compare linear trends in the ERA-40 driven RCM simulations discussed above; however, the period of analysis was reduced to the 30 year control (1961-1990) and seasonal trends were not considered. Both the interannual variance and the similarity of trends in the annual data series are used by Brekke *et al.* (2007) to evaluate model performance. To ensure those models assigned a high weighting performed well according to all criteria, the individual skill scores were multiplied to produce the final weighting for each model pathway. Figure 6.28 shows the standardized seasonal weights formulated for each model pathway and variable.

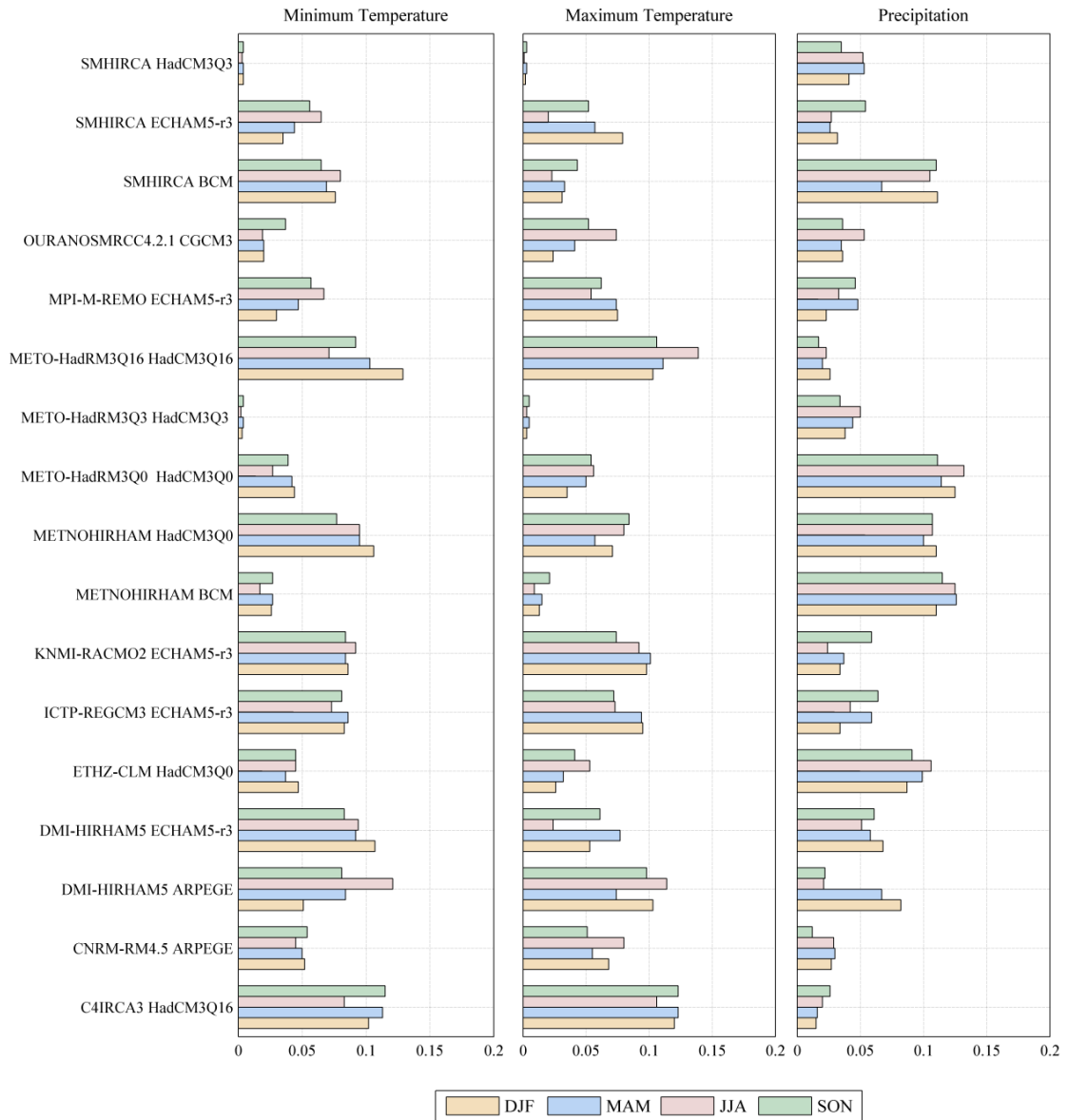


Figure 6.28 Aggregated seasonal weights formulated for each of the 17 GCM-RCMs pathways which run up until 2050. The weights are normalized on a seasonal basis for each variable.

Table 6.15 shows each GCM-RCM model pathway ranked based on their assigned weighting. Each pathway is colour coded according to the GCM used. It indicates that irrespective of the RCM (or institute) employed, the GCM has a considerable influence on the weightings assigned to individual pathways. With respect to downscaled temperature generally, in those instances where the HadCM3 Q3 GCM (indicative of low climate sensitivity) was used as the driving model, a low weighting has been assigned (e.g. SMHIRCA and METO-HadRM3Q3). In contrast where the HadCM3 Q16 GCM (indicative of high climate sensitivity) was used as boundary conditions the model pathways have been assigned a relatively higher weighting.

In contrast to temperature, the weightings assigned to the individual model pathways are much more variable for precipitation. The lowest weightings are assigned to those scenarios whereby the UK Met Office’s HadCM3 high sensitivity (Q16) GCM was used as the driving model (e.g. C4I RCA3 HadCM3Q16 and METO-HadRM3Q16 HadCM3Q16). In contrast, those pathways using the HadCM3 low sensitivity (Q3) GCM as boundary conditions (e.g. METO-HadRM3Q0 HadCM3Q0 and METNOHIRHAM HadCM3Q0) have generally been assigned a lower weighting.

Rank	Minimum Temperature	Maximum Temperature	Precipitation
1	C4IRCA3 HadCM3Q16	C4IRCA3 HadCM3Q16	METO-HadRM3Q0 HadCM3Q0
2	METO-HadRM3Q16 HadCM3Q16	METO-HadRM3Q16 HadCM3Q16	METNOHIRHAM BCM
3	DMI-HIRHAM5 ECHAM5-r3	DMI-HIRHAM5 ARPEGE	METNOHIRHAM HadCM3Q0
4	METNOHIRHAM HadCM3Q0	KNMI-RACMO2 ECHAM5-r3	SMHIRCA BCM
5	KNMI-RACMO2 ECHAM5-r3	ICTP-REGCM3 ECHAM5-r3	ETHZ-CLM HadCM3Q0
6	DMI-HIRHAM5 ARPEGE	METNOHIRHAM HadCM3Q0	DMI-HIRHAM5 ECHAM5-r3
7	ICTP-REGCM3 ECHAM5-r3	MPI-M-REMO ECHAM5-r3	ICTP-REGCM3 ECHAM5-r3
8	SMHIRCA BCM	CNRM-RM4.5 ARPEGE	DMI-HIRHAM5 ARPEGE
9	MPI-M-REMO ECHAM5-r3	DMI-HIRHAM5 ECHAM5-r3	SMHIRCA HadCM3Q3
10	SMHIRCA ECHAM5-r3	SMHIRCA ECHAM5-r3	METO-HadRM3Q3 HadCM3Q3
11	CNRM-RM4.5 ARPEGE	METO-HadRM3Q0 HadCM3Q0	OURANOSMRCC4.2.1 CGCM3
12	ETHZ-CLM HadCM3Q0	OURANOSMRCC4.2.1 CGCM3	KNMI-RACMO2 ECHAM5-r3
13	METO-HadRM3Q0 HadCM3Q0	ETHZ-CLM HadCM3Q0	MPI-M-REMO ECHAM5-r3
14	OURANOSMRCC4.2.1 CGCM3	SMHIRCA BCM	SMHIRCA ECHAM5-r3
15	METNOHIRHAM BCM	METNOHIRHAM BCM	CNRM-RM4.5 ARPEGE
16	SMHIRCA HadCM3Q3	METO-HadRM3Q3 HadCM3Q3	METO-HadRM3Q16 HadCM3Q16
17	METO-HadRM3Q3 HadCM3Q3	SMHIRCA HadCM3Q3	C4IRCA3 HadCM3Q16

Table 6.15 The 17 GCM-RCMs pathways which run up until 2050 ranked (highest to lowest) according to their assigned weighting - the weights are averaged across seasons. The pathways are colour coded according to the driving GCM used.

With respect to the statistically downscaled precipitation scenarios, the CSIROmk2 GCM pathways have been assigned the lowest weighting; in contrast those scenarios derived from the UK Met Office’s HadCM3 GCM are given a greater weighting. For the statistically downscaled temperature scenarios the highest weightings are assigned to the HadCM3 and CSIROmk2 pathways, whilst a low weighting is given to the CGCM2 pathways.

6.4.1.4 Final aggregated weights

The final scenario weights for the downscaled RCM data (Figure 6.11) were calculated by multiplying the ERA-40 RCM weights, independent GCM weights (from Déqué &

Somot (2010)) and scenario weights (model pathways) together. In the case of the statistically downscaled data the climate prediction index (CPI) from Fealy (2010) was multiplied by the scenario weightings discussed in the preceding section. The weights were variously adjusted depending on the number of ensemble members considered – for example 17 scenarios run up until the mid-century (2050), in contrast 13 scenarios cover the period up to 2100. With respect to the weights formulated for the 17 dynamically downscaled temperature (minimum and maximum) scenarios, the model projections provided by Met Éireann (C4I) are assigned the highest weighting. The scenarios from the Italian (ICTP) and Dutch (KNMI) institutes are also assigned a high weighting. Both were derived using the same ECHAM5 GCM as boundary conditions but are downscaled using different RCMs. In both instances where the UK Met Office’s HadCM3 low sensitivity (Q3) GCM was used as the driving model, a low weighting has been assigned. In contrast, where the standard (Q0) and high sensitivity (Q16) HadCM3 GCM was used a relatively greater weighting has been assigned. With respect to the statistically downscaled temperature series, those scenarios derived from the HadCM3 GCM have received a high overall weighting (Figure 6.30).

The weightings for precipitation are generally not consistent with those formulated for the temperature scenarios, highlighting that model performance is to a certain degree dependent on the variable considered. This is illustrated by the comparatively lower weighting assigned to the precipitation scenario downscaled by Met Éireann. The greatest weighting in the ensemble is assigned to the scenario provided by the Swedish Meteorological and Hydrological Institute (SMHI), who used the Bergen GCM in conjunction with the Rossby Center regional climate model (RCA). Despite being downscaled using the same RCM, the two additional precipitation scenarios provided by the SMHI receive a comparatively lower weighting. The scenario downscaled by the Norwegian Meteorological institute (METNO) - which also employed the Bergen climate model - is assigned the second highest weighting in the ensemble. Those ensemble members downscaled using the UK Met Office’s HadCM3 standard sensitivity (Q0) GCM have received a high weighting. Generally for those ensemble members where the HadCM3 (Q16) or ARPEGE models were used as the driving GCM, a low weighting has been assigned. In terms of the statistically downscaled precipitation scenarios, those series which are downscaled from the HadCM3 GCM have been given a much greater weighting when compared to the scenarios downscaled from the either the CGCM2 or CSIRO GCMs.

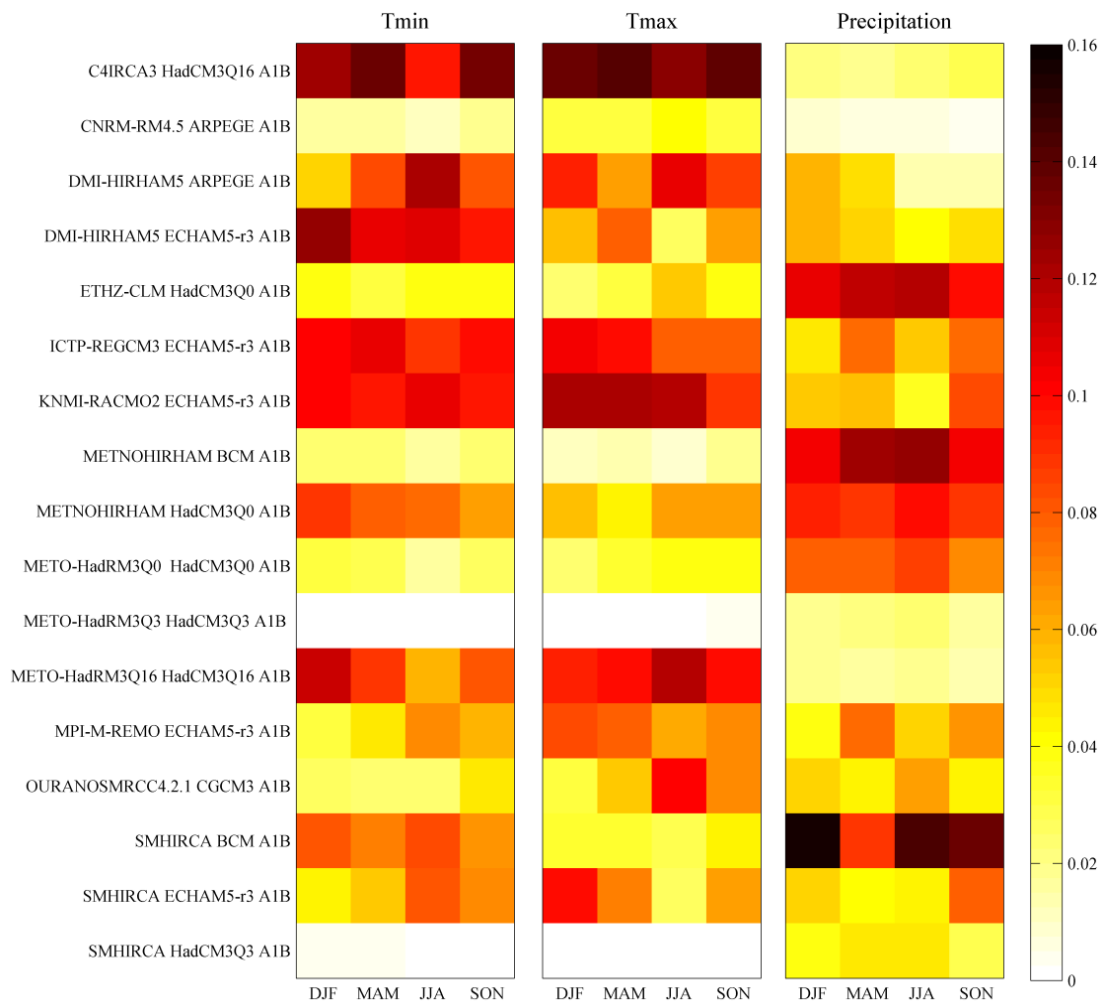


Figure 6.29 Aggregated seasonal weights for the dynamically downscaled temperature and precipitation scenarios. Darker/lighter shading denotes those scenarios assigned a higher/lower weighting.

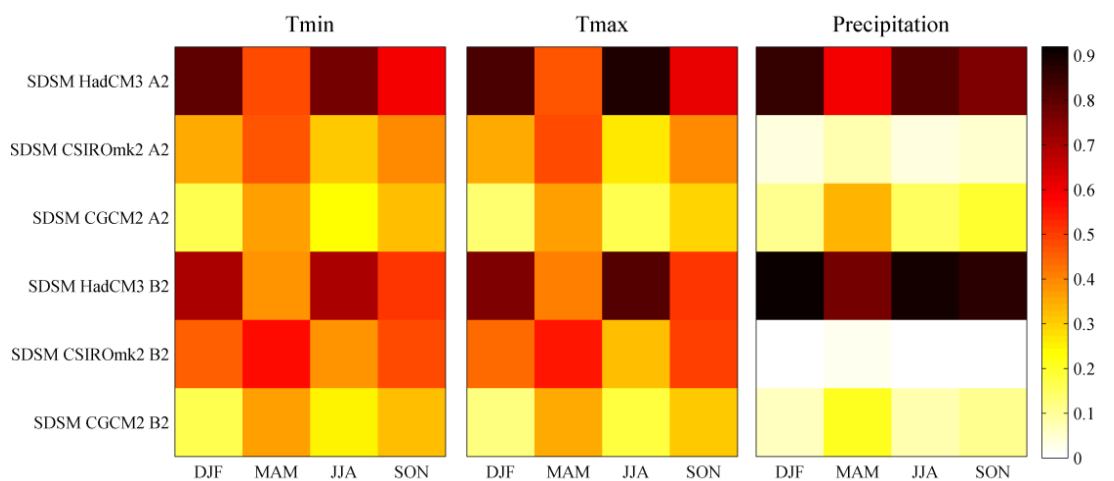


Figure 6.30 Aggregated seasonal weights for the statistically downscaled temperature and precipitation ensemble members. Darker/lighter shading denotes those scenarios assigned a higher/lower weighting.

6.5 Conclusion

In this study statistically downscaled scenarios are used alongside dynamically downscaled climate data obtained from the EU funded ENSEMBLES project (van der Linden & Mitchell, 2009). Although the ENSEMBLES dataset represents a valuable resource, and provides a means for addressing some aspects of model uncertainty, the dataset has a number of shortcomings which limits its usefulness, one of the most critical of which is that not all GCM-RCM model combinations in the dataset have been satisfied. Essentially the dataset constitutes an ‘ensemble of opportunity’ rather than a systematic sampling of the model space. This shortcoming is compounded by the datasets adherence to a single GHG emission scenario, which limits any exploration of uncertainty to the models only. In order to incorporate uncertainties relating to the emission scenario and downscaling method used, a number of statistically downscaled scenarios were included in the climate ensemble used in this study.

It was considered important that the models employed to generate the climate data could be evaluated with respect to how well they simulated observed conditions in the catchment. It was shown that model performance varied depending on the season and variable considered; in addition, no one model was found to outperform its competitors in all aspects of performance. The results highlighted that using the model bias as the sole performance criterion may be misleading with respect to how well the models capture observed patterns of variability. With respect to this it was found that disaggregating model error into its systematic and random components allowed for a greater understanding of model performance. Given that a correction can be applied to remediate systematic bias - although this requires an assumption in the constancy of model bias under altered forcing - random error may provide a better overall indicator of model skill.

Whilst it is universally recognized that employing a multi-model ensemble is a more robust approach for estimating the climate response to a change in forcing, the use of performance based weighting systems - whereby a likelihood value is assigned to each constituent ensemble member - is much more contentious. The arguments made against adopting such an approach highlight the implicit assumption of stationarity in model performance and point to the possibility of introducing bias by way of the weighting criteria employed. However, it is recognized that weighting ensemble members may be more defensible than treating each member as being equally plausible, irrespective of

how well they simulate present-day observed system behaviour. Where the use of model weighting is advocated, it comes with the caveat that the formulated weights are robust and account for as much uncertainty as is possible.

In this study some of the issues relating to the development of a weighting scheme which could be employed in the context of an impacts assessment were explored. Although the initial intention was to include both the statistically and dynamically downscaled scenarios in a single weighting system, differences in both datasets meant a separate set of weights had to be developed for each. As outlined above, the final aggregated scenario weights reflected how well each component in the model pathway (i.e. GCM-RCM) performed independently of one another. As it was considered important that the possible interaction of errors accruing from the downscaling and driving global model respectively were accounted for; thus a measure of how well each scenario reproduced observed climate over the control period was incorporated in the final weighting scheme. Developing a weighting system in this way is a complex task, and critically depends on employing three different approaches, each of which is tailored to provide a robust descriptor of performance. RCM model skill was gauged using daily data, which reflects the model's role in simulating local scale forcings and small scale climate variability not captured in large-scale GCM datasets. In contrast the assessment of downscaled GCM data was restricted to how well the models captured patterns of variability over longer timescales and reproduced the statistical distribution of the observed data. The final aggregated scores reflect the skill of a given pathway for a particular season. The metrics used are however not strictly seasonally based as the models were also required to capture annual, as well as interannual aspects of the observed climate series. This was to ensure that seasonal performance was linked with the model's ability to capture those climate and atmospheric processes which operate over longer timescales and are fundamental to determining the character of regional or local-scale climate.

The weighting scheme used in this study has a number of acknowledged shortcomings; this includes the fact it only considers a narrow range of climate parameters and that it is based solely on model performance at capturing observed conditions for the catchment – although this is not without precedent in other studies (e.g. Wilby & Harris, 2007). It was however outside the remit of this study to develop a more broadly based weighting system (i.e. considering other climate variables or alternative/larger domains), thus model performance with respect to the catchment and climate variables considered took

precedence. It is acknowledged however that a more in-depth analysis of model performance would provide additional support for the formulated weightings. Employing a weighting scheme was also a means of engaging in the current debate surrounding the use of performance based systems. It could be argued that one of the deficiencies in datasets like those made available through ENSEMBLES is the lack of information or meta-data provided on the reliability of the models used; such information would aid in the development and more widespread use of weighting schemes. The proceeding chapter examines projected changes in climate for the catchment using the downscaled climate projections discussed above.

Chapter 7

Projected changes in climate for the Burrishoole catchment

7.1 Introduction

In this study a series of high resolution climate scenarios are used to examine likely changes in the climate of the Burrishoole catchment; each scenario represents a plausible realization of future climate under perturbed forcing conditions. Model projections are examined both individually and on a collective basis using the ensemble average. To this end the weighting scheme described in the previous chapter - formulated based on the ability of each ensemble member to simulate present-day climate conditions - is used to calculate the weighted mean ensemble. Comparisons are subsequently drawn between projections derived from the weighted and unweighted ensemble average (i.e. where each ensemble member is assigned an equal weighting). The climate scenarios used represent different combinations of GHG-emission scenarios, driving GCMs and statistical/dynamical downscaling models. By considering multiple model pathways this study attempts to sample across the uncertainties encountered at each stage in the ‘cascade of uncertainty’ (Figure 4.2). Model projections are examined on the basis of three future time horizons: the 2020s (2010-2039), 2050s (2040-2069) and 2080 (2070-2099); the 30 year model control period (1961-1990) is used to represent baseline or reference conditions. Thirty years is the standard period over which climate is generally defined; in addition using a time slice of this length allows for inter-decadal variability to be considered when determining whether defined changes in the system are projected to occur.

7.2 Projected changes in temperature

The model projections suggest that over each successive time horizon air temperatures in the catchment are likely to increase (Figure 7.1) - with the summer and autumn months projected to experience the greatest increases. Although there is a general consensus between the individual model pathways regarding the direction of change, there is a high degree of inter-scenario variability regarding the exact magnitude and time evolution of projected change. Differences between the emission scenarios are noticeable from the 2050s onward, becoming particularly evident over the 2080s. In

general warming is greatest under the A2 emission scenario (e.g. SDSM-CSIROmk2-A2); however, when individual pathways are considered, those with a greater sensitivity suggest larger absolute increases. The influence of model sensitivity is evident in the climate projections made available by Met Éireann (C4I) and the UK Met Office for which the HadCM3 high sensitivity (Q16) GCM was used as the driving model. Despite being derived using different RCMs, those scenarios where the ECHAM5-r3 GCM was used as boundary conditions appear to follow a similar pathway (Figure 7.2). This highlights the role of the GCM in influencing the overall trend and inter-annual variability in the downscaled projections. Figure 7.2 shows the spread in the model projections, which appears to increase as a function of distance from the reference period. This spread reflects the degree to which the emission scenario becomes increasingly dominant in determining the climate response as the century progresses. When the model weights discussed in Chapter six are applied, there appears to be little divergence between the weighted and unweighted ensemble average for the A1B model pathways.

Listed in Appendix I are the projected changes in mean minimum and maximum temperature suggested by each of the twenty five climate scenarios. The downscaled scenario provided by Met Éireann - whereby the HadCM3 high sensitivity GCM was used as the driving model - suggests the largest absolute increases in both temperature variables. Over the 2080s this model pathway suggests an increase in average maximum temperature of $\sim 4.8^{\circ}\text{C}$ for the summer and autumn seasons respectively. It also suggests an increase of 7°C in average minimum temperature for August - the largest monthly increase projected by any individual ensemble member, even those run using the more carbon intensive A2 SRES scenario.

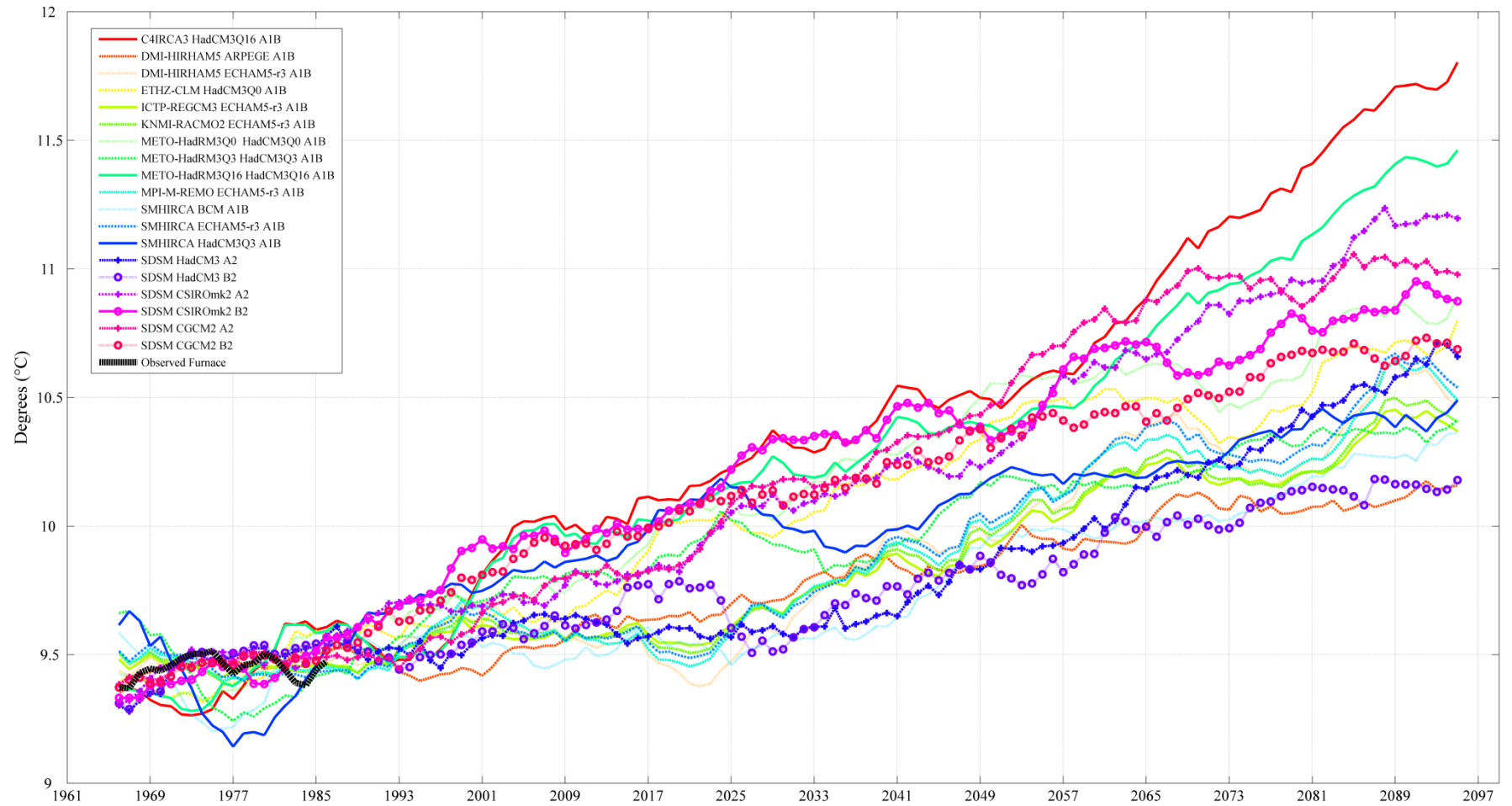


Figure 7.1 The projected 10-year moving average (mean) temperature for the Burrishoole catchment (1961-2100) plotted for each of the 19 ensemble members whose projections cover the period 1961-2099. Also shown is the 10 year moving average for mean temperature observed in the catchment. This is calculated using data from the Furnace weather station.

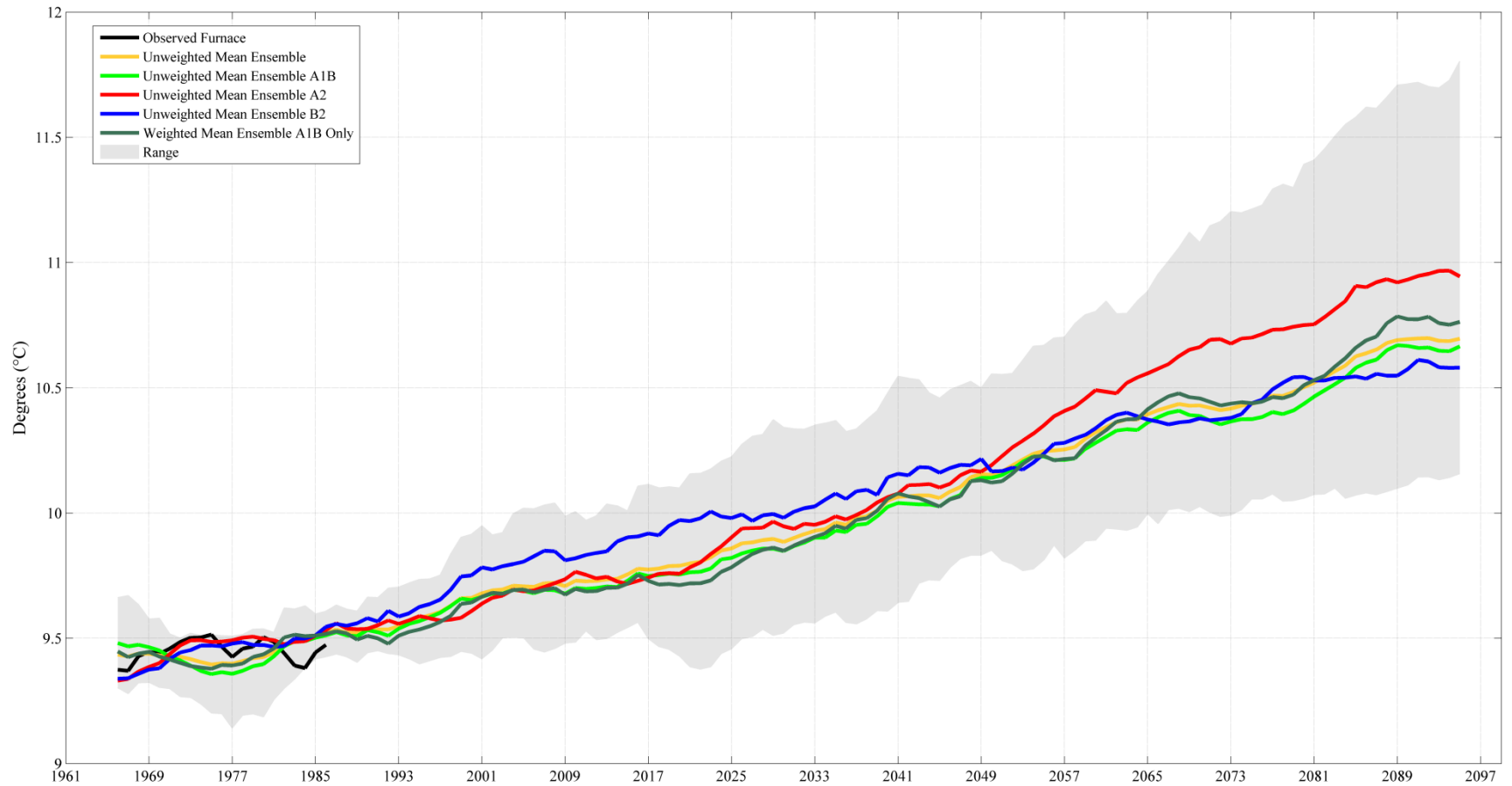


Figure 7.2 The projected 10-year moving average (mean) temperature for the Burrishoole catchment estimated based on the unweighted (A1B, A2, B2 and all scenarios) and weighted mean ensemble (A1B) for each SRES scenario. The plot includes the equally weighted mean ensemble calculated using all 19 ensemble members. The shaded area is used to illustrate the range in model response to perturbed forcing. Also shown is the 10 year moving average of the observed mean temperature in the catchment. This is calculated using data from the Furnace weather station.

When compared to the other model pathways, the statistically downscaled scenario from the HadCM3 model - run using the B2 emission scenario - generally suggests the lowest increases in temperature. For the 2080s horizon this pathway projects an increase in mean winter temperature of 0.85°C (minimum) and 0.61°C (maximum) respectively. An increase in summer temperature of 1.9°C (minimum) and 1.8°C (maximum) over the 2080s is also suggested by this ensemble member.

Figure 7.3 and 7.4 indicate that the greatest spread in the projected temperature response is associated with the 2080s, particularly the months of July, August and September. The plots also indicate that the statistically downscaled B2 and A2 scenarios generally lie within the projected range of the dynamically downscaled A1B scenarios. The wide response range of the dynamical pathways is due the inclusion of those scenarios generated using GCMs whose sensitivity has been enhanced (i.e. Q16). When the ensemble average is taken the overall response is much more conservative than the projected range suggests. There appears only to be a negligible difference between the unweighted and weighted ensemble average; however, differences between the two are evident during the summer months, particularly over the 2080s. Whilst the range in temperature projections increases over each horizon, by the 2050s all pathways are in agreement that monthly temperatures (both minimum and maximum) are likely to have increased relative to the control period.

Figure 7.5 shows the projected change in extreme summer and winter temperature defined using the 90th and 95th percentiles. For each successive horizon the models suggest an increase in both indices; however, there appears to be a high degree of inter-model variability regarding the exact magnitude of change. Generally the statistically downscaled CGCM2-A2 scenario, along with the scenarios downscaled by Met Éireann and the UK Met Office (high sensitivity) suggest the largest increases in both percentiles. In contrast the projections provided by Météo-France (ARPEGE) and the SMHI (BCM) suggest increases of a much lower magnitude. Given the divergence between individual ensemble members, it is difficult to determine a clear pattern of change; however, over each horizon the range widens and the models generally suggest an increase in extreme temperatures. Projected changes in both the mean and higher order statistics are indicative of a 'shift' in the probability distribution for temperature.

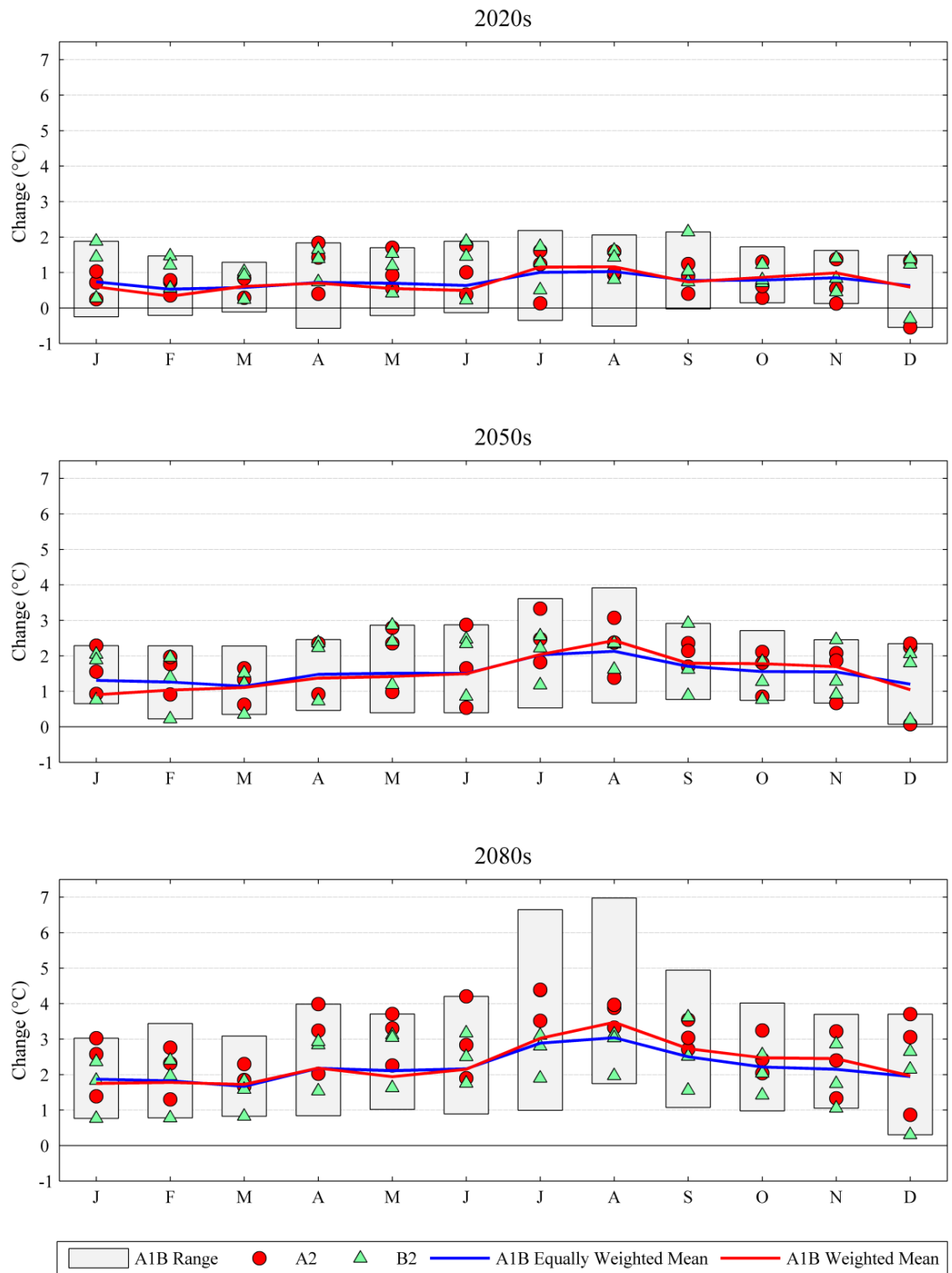


Figure 7.3 Projected changes in average monthly maximum temperature for the Burrishoole catchment. Changes are estimated relative to the 30 year control period (1961-1990) for the 2020s (top), 2050s (middle) and 2080s (bottom) respectively. The range in projected changes from the A1B model pathways are plotted using the grey bar; model projections relating to the A2 and B2 emission scenarios are plotted separately. Also shown is the equally weighted and weighted mean ensemble for the A1B ensemble members.

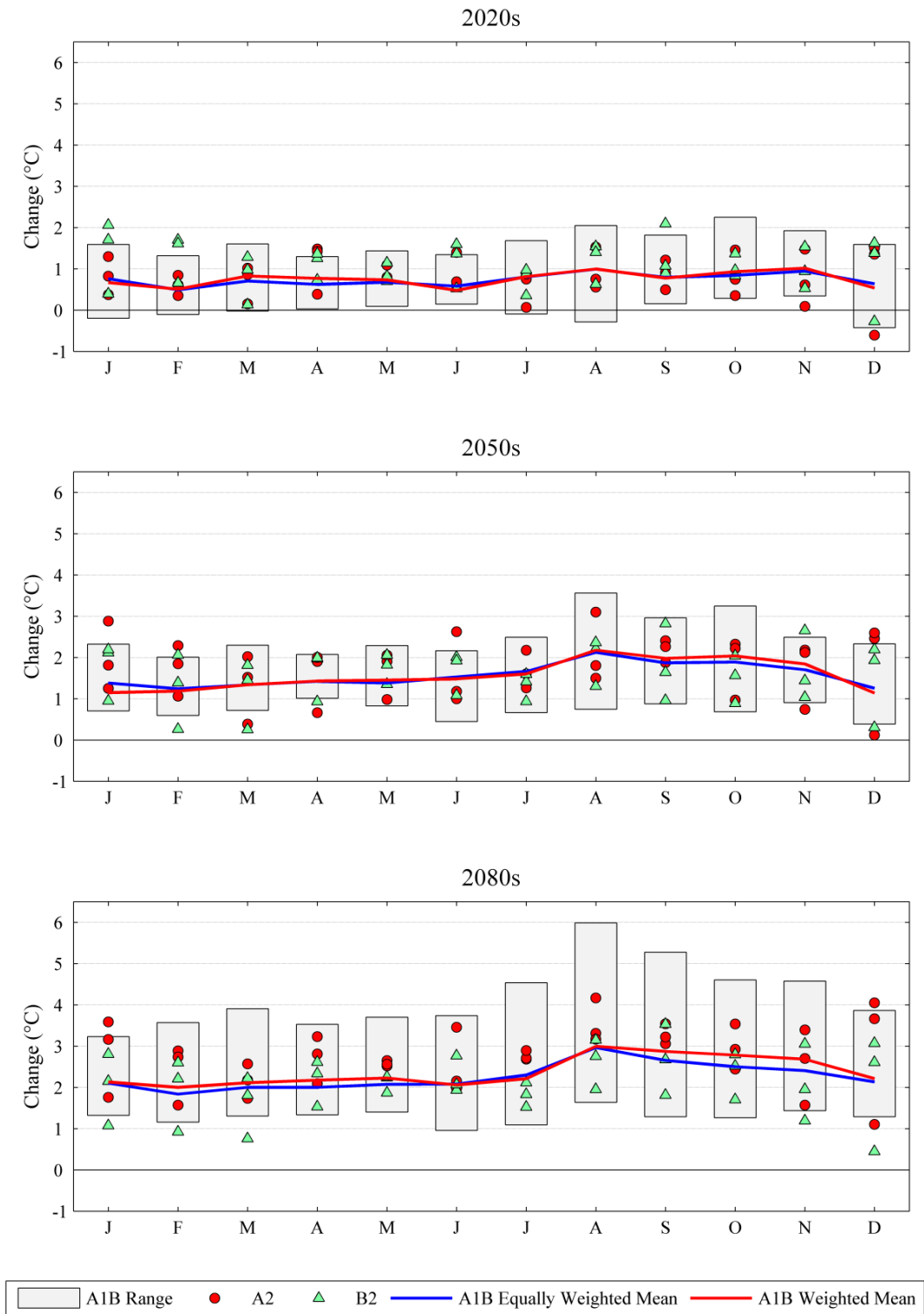


Figure 7.4 Projected changes in average monthly minimum temperature for the Burrishoole catchment. Changes are estimated relative to the 30 year control period (1961-1990) for the 2020s (top), 2050s (middle) and 2080s (bottom) respectively. The range in projected changes from the A1B model pathways are plotted using the grey bar; model projections relating to the A2 and B2 emission scenarios are plotted separately. Also shown is the equally weighted and weighted mean ensemble for the A1B ensemble members.

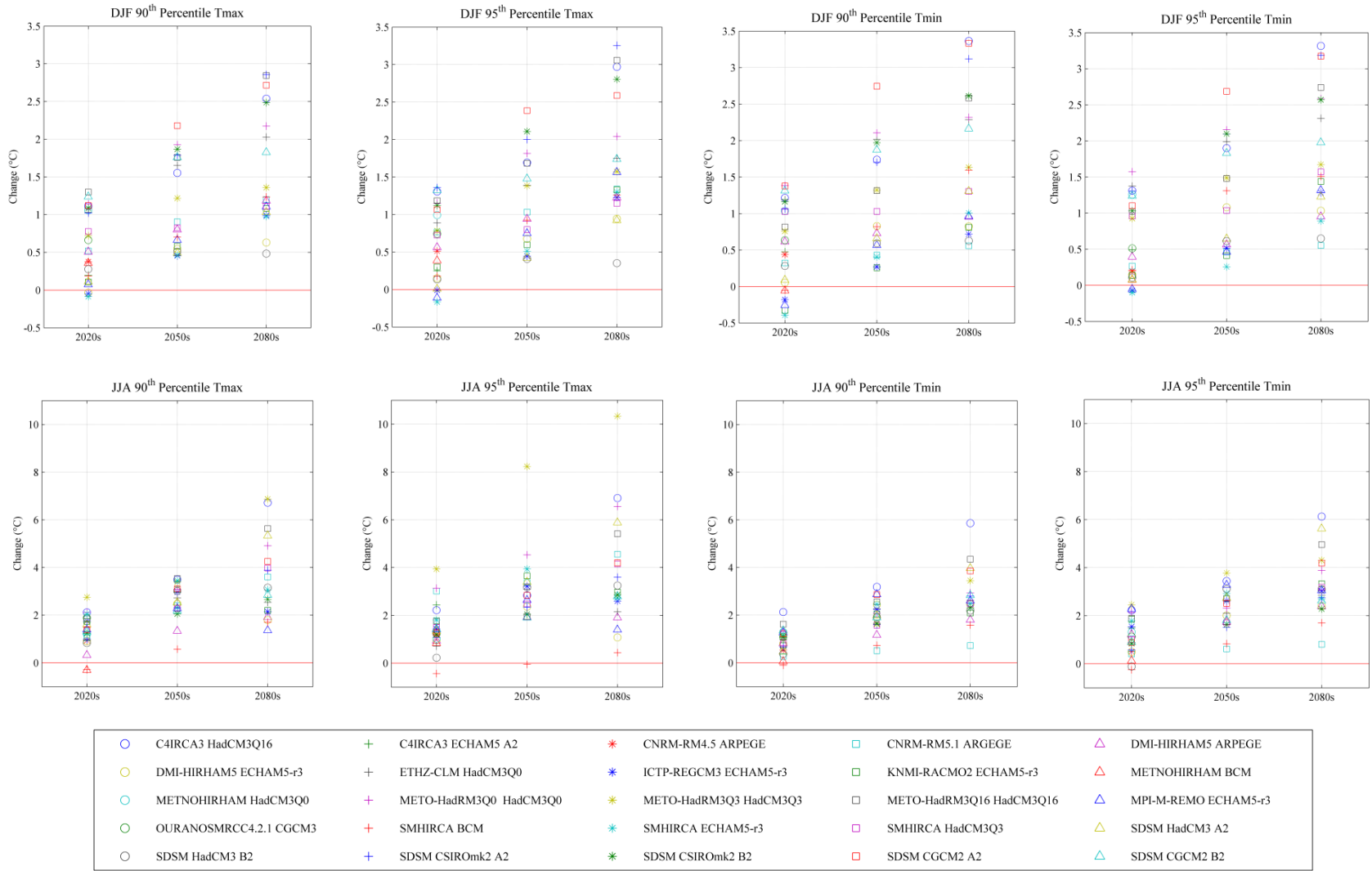


Figure 7.5 Projected changes in the 90th and 95th percentile of summer and winter temperature (minimum and maximum).

7.3 Projected changes in precipitation

Model projections suggest that under a warming climate the catchment's precipitation regime is likely to become increasingly seasonal in nature - with wetter winters and drier summers occurring. This trend is anticipated to become more pronounced as the century progresses. There is however a high degree of uncertainty regarding not only the magnitude but also the direction of change. This is particularly evident during the earlier half of the century and through the transition seasons of spring and autumn. Appendix II lists the projected change in mean monthly and seasonal precipitation receipts for each horizon; changes are presented as a percentage of the equivalent rainfall occurring over the 30 year control period.

Over the 2020s the scenario provided by the Swedish Meteorological and Hydrological Institute (SMHI) - whereby the HadCM3 low sensitivity (Q3) GCM was used as the driving model - suggests the largest increase in winter precipitation receipts (+21%). The scenario provided by Met Éireann (HadCM3-Q16) (-13%), as well as the statistically downscaled CGCM2 (A2 emission scenario) (-13%) ensemble member, suggest the largest decrease in summer rainfall amounts. The largest decrease for any month is suggested by the projection from the Norwegian Meteorological Institute (METNO) which suggests a 31% decrease in receipts for May. The largest monthly increase is suggested for December (+31%) by the low sensitivity SMHI HadCM3 model pathway. Over the 2050s an increase in winter receipts of between 3% (METO high sensitivity Q16 HadCM3 pathway) and 24% (statistically downscaled CSIROmk2 B2 pathway) is projected. With the exception of the scenario from the Danish Meteorological Institute (HIRHAM5-ECHAM5-r3-A1B) (+1%), all pathways indicate a decrease in summer rainfall of between 1% (ETHZ-CLM-HadCM3Q0) and 21% (CNRM-RM5.1-ARGEGE). There is much less convergence between ensemble members regarding changes in autumn. For this season each of the dynamically downscaled projections suggests an increase. This is in contrast to the statistically downscaled scenarios which indicate that a decrease in receipts is likely. The greatest monthly increase is suggested for February (+36%; SMHIRCA-BCM), while the largest decrease is projected for May (-32%; SDSM-CGCM2-A2). Over the 2080s there is a much stronger agreement between individual scenarios regarding increases in winter precipitation - the largest of which is associated with the SMHI-BCM pathway (+31%). The smallest increase is suggested by the scenario provided by the Max Plank Institute (+4.4%). The models are generally also in agreement about changing summer patterns

where all but one (DMI ECHAM5-r3) of the ensemble member projects sizeable decreases in receipts (range: -27% to +5.32%). The greatest reductions for the 2080s are projected by the UK Met Office's low sensitivity (Q3) scenario (-26%) and the scenario provided by Météo-France (CNRM-RM5.1-ARGEGE) (-26.4%). There is much less agreement between pathways regarding the exact nature of change in receipts for the spring and autumn seasons. It appears that some models suggest large increases, whilst others indicate that sizeable reductions are likely to occur. For instance the statistically downscaled CGCM2 A2 scenario suggests a 29% decrease in spring, while the SMHI HadCM3-Q3 pathway projects an increase of 24%. With the exception of the statistically downscaled scenarios a general increase in autumn receipts is suggested. In contrast to the 2020s and 2050s, much greater decreases/increases are returned on a monthly basis. Generally the largest increases are associated with the SMHI scenario; which is downscaled from the Bergen climate model (BCM) (February: 39.7%, March: 39.6% and December: 33.7%). Decreases of up to 35% are suggested by some model pathways for June, July and August respectively. The greatest decrease is however projected for May - for which the statistically downscaled CGCM2-A2 model pathway projects a 36% decrease.

Although the pathways generally exhibit a high level of agreement regarding the nature of change in the precipitation regime for summer and winter, it is obvious that a great deal of uncertainty is associated with model projections for spring. It is also difficult to differentiate between the respective emissions scenarios when assessing the magnitude of projected change. Similarly, it is difficult to draw a distinction between the models which are more or less sensitive to future forcing. Figure 7.6 shows the projected change in mean monthly precipitation receipts for each 30 year horizon relative to the control. The plot indicates the degree to which individual pathways diverge. The suggested increase in the seasonality of the catchment's precipitation regime is most pronounced over the 2080s; however, this is also the period when models tend to disagree most about likely changes in the transition seasons – as evidenced by differences between the statistically and dynamically downscaled scenarios. It appears that the emission scenario becomes increasingly important as the century progresses - indicated by the number of A2 and B2 based scenarios which fall outside the range of A1B projections. This however could be related to differences in the downscaling method used (i.e. dynamical versus statistical). Similarly to temperature, the weighted A1B ensemble average is shown to diverge little from the equally weighted mean ensemble (Figure 7.6).

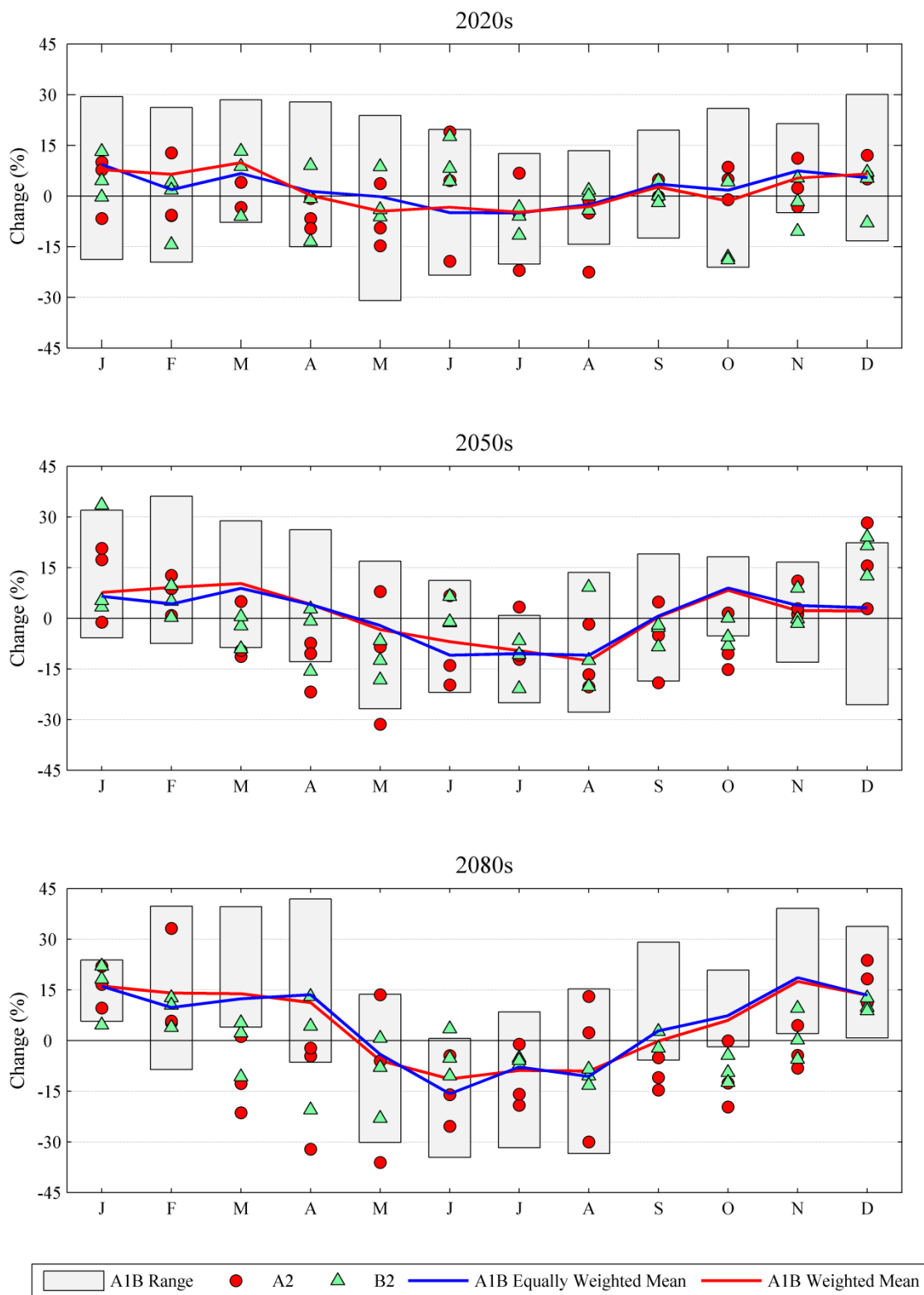


Figure 7.6 Projected changes in average monthly precipitation for the Burrishoole catchment. Changes are estimated relative to the 30 year control period (1961-1990) for the 2020s (top), 2050s (middle) and 2080s (bottom) respectively. The range in projected changes from the A1B model pathways are plotted using the grey bar; model projections relating to the A2 and B2 emission scenarios are plotted separately. Also shown is the equally weighted and weighted mean ensemble for the A1B ensemble members.

Figures 7.7(a) and 7.7(b) show the projected change in precipitation for a series of percentiles (20th, 40th, 50th, 60th, 80th, 90th and 95th) estimated for the winter and summer seasons respectively. The percentiles are calculated using precipitation amounts on wet days only (≥ 2 mm). The downscaled scenarios generally suggest an increase in the majority of percentiles during winter – particularly those more indicative of heavy or extreme rainfall events. This is consistent with the suggested increase in rainfall amounts for this season. Almost half of the model projections suggest at least a 10% increase in the 95th and/or 90th percentiles for the 2080s horizon. A number of model pathways indicate a greater relative increase in higher percentiles, while reductions or lesser increases are associated with the lower percentiles. For other ensemble members the suggested increase is relatively consistent across percentiles, suggesting a general shift in the distribution. In contrast to winter, the changes projected for summer are much less consistent. Generally a decrease in the lower percentiles is suggested (i.e. $\leq 80^{\text{th}}$ percentile), this is consistent with a reduction in receipts for this season. A number of scenarios suggest that a decrease in the lower percentiles will be accompanied by a concurrent increase in the higher percentiles (e.g. METNO HadCM3 standard sensitivity pathway); in general this is most evident over the 2080s. Therefore, although an overall reduction in precipitation amounts is projected to occur - highlighted by decreases in the 50th percentile - the frequency of more extreme events during this season may increase, particularly over the latter half of the century. The inconsistent changes across percentiles may indicate a change in the shape as well as the location of the distribution for this season.

Figure 7.8 shows projected changes (%) in the variance of precipitation for each model pathway and season respectively. It is suggested that an increase in the variability of wet-day precipitation is likely to occur under future forcing. For the 2080s, 18 of the 19 dynamically downscaled model pathways suggest an increase in the variability of wet-day amounts during winter. For autumn the spread of projected changes appears to increase over each successive horizon; here it is generally the statistically downscaled scenarios which suggest a decrease, in contrast the dynamically downscaled projections generally indicate that increases are likely to occur. There appears to be no one pathway which returns a consistent increase/decrease across all seasons and horizons. In addition there is no clear increase/decrease along the lines of emission scenario or model sensitivity. The uncertainty associated with changes in mean precipitation receipts is reflected in the projected changes in the higher order statistics.

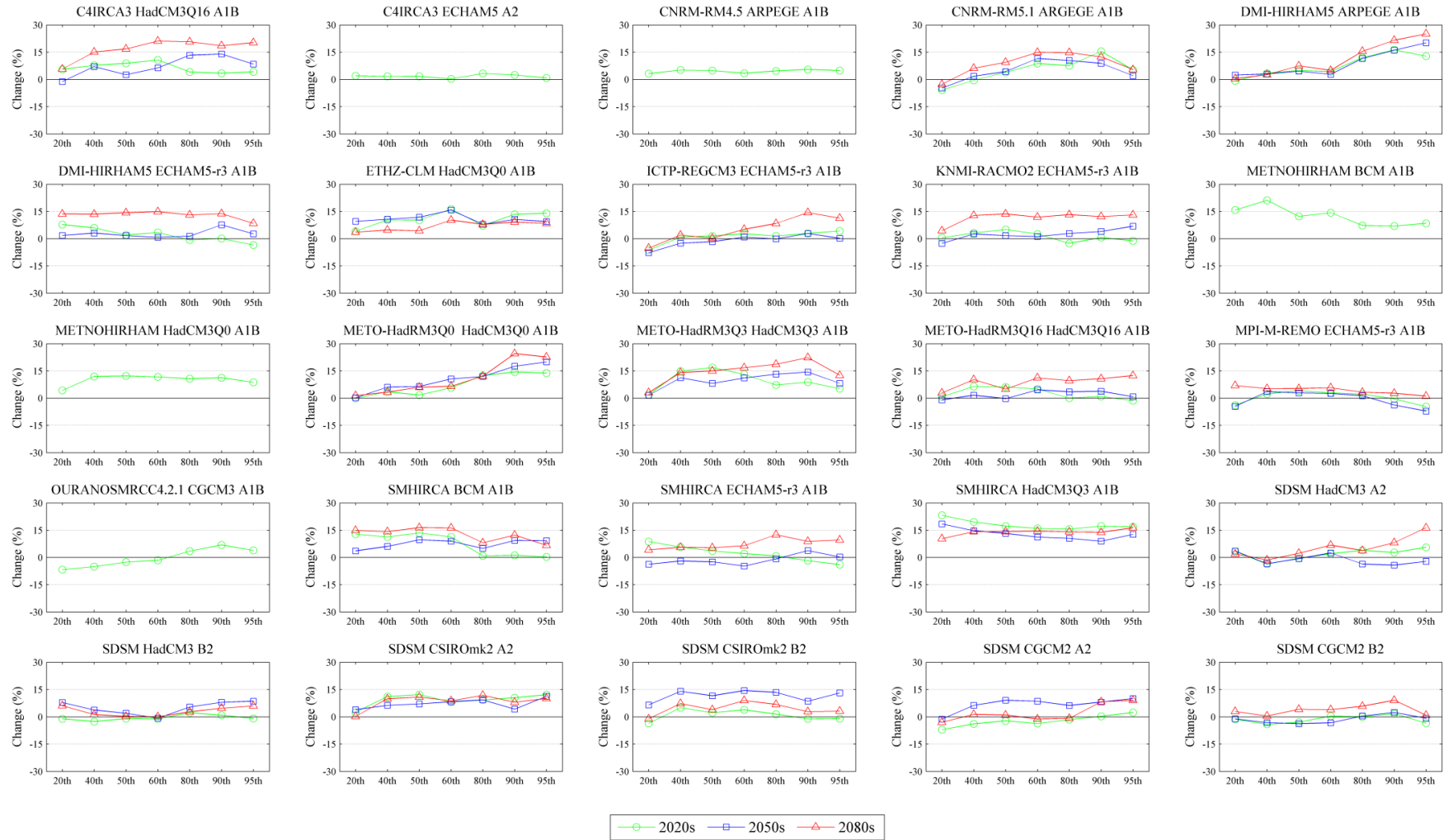


Figure 7.7(a) Projected changes in the 20th, 40th, 50th, 60th, 80th, 90th and 95th percentiles of winter rainfall amounts. A wet day threshold of ≥ 2 mm is used.

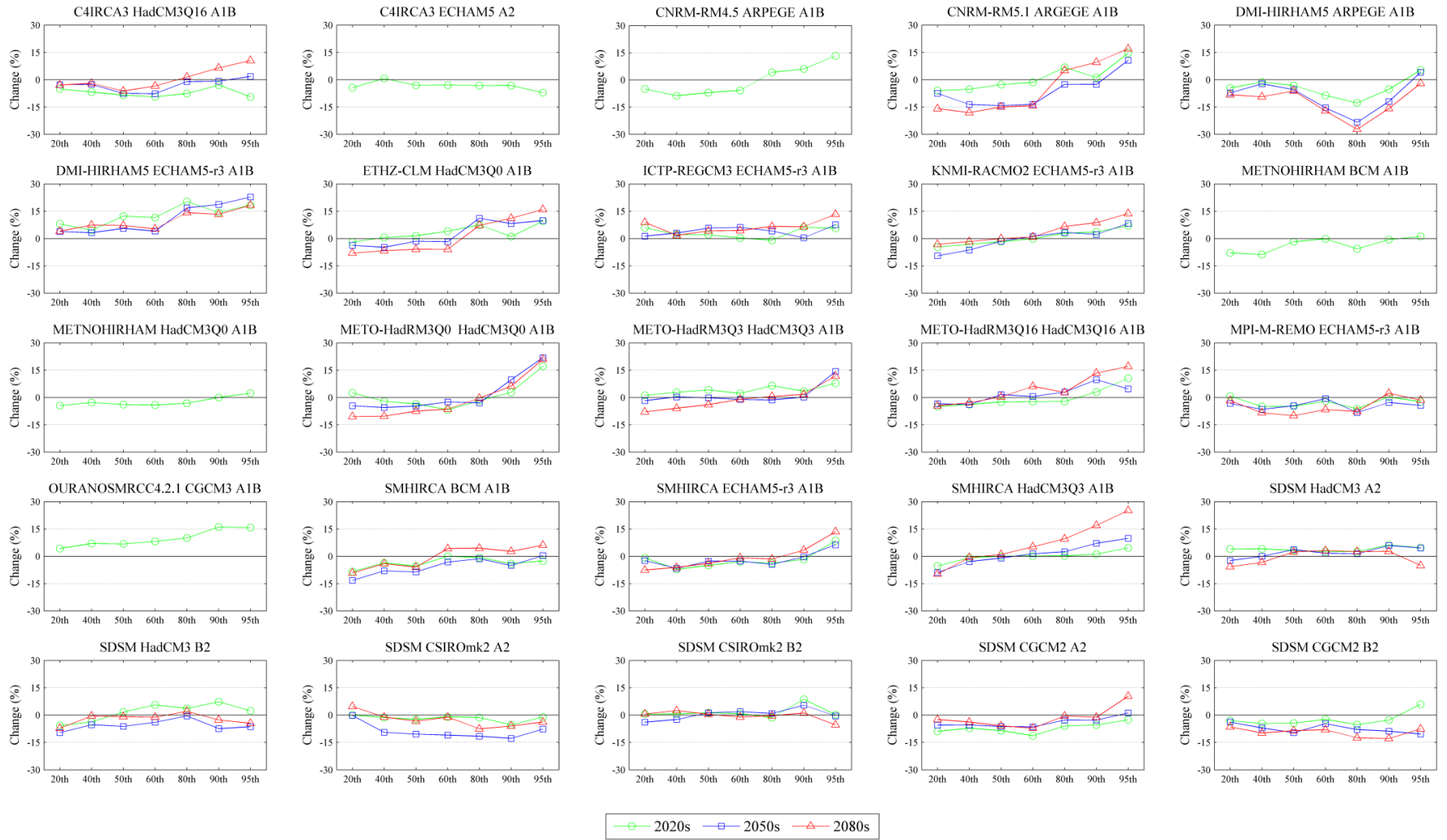


Figure 7.7(b) Projected changes in the 20th, 40th, 50th, 60th, 80th, 90th and 95th percentiles of summer rainfall amounts. A wet day threshold of ≥ 2 mm is used.

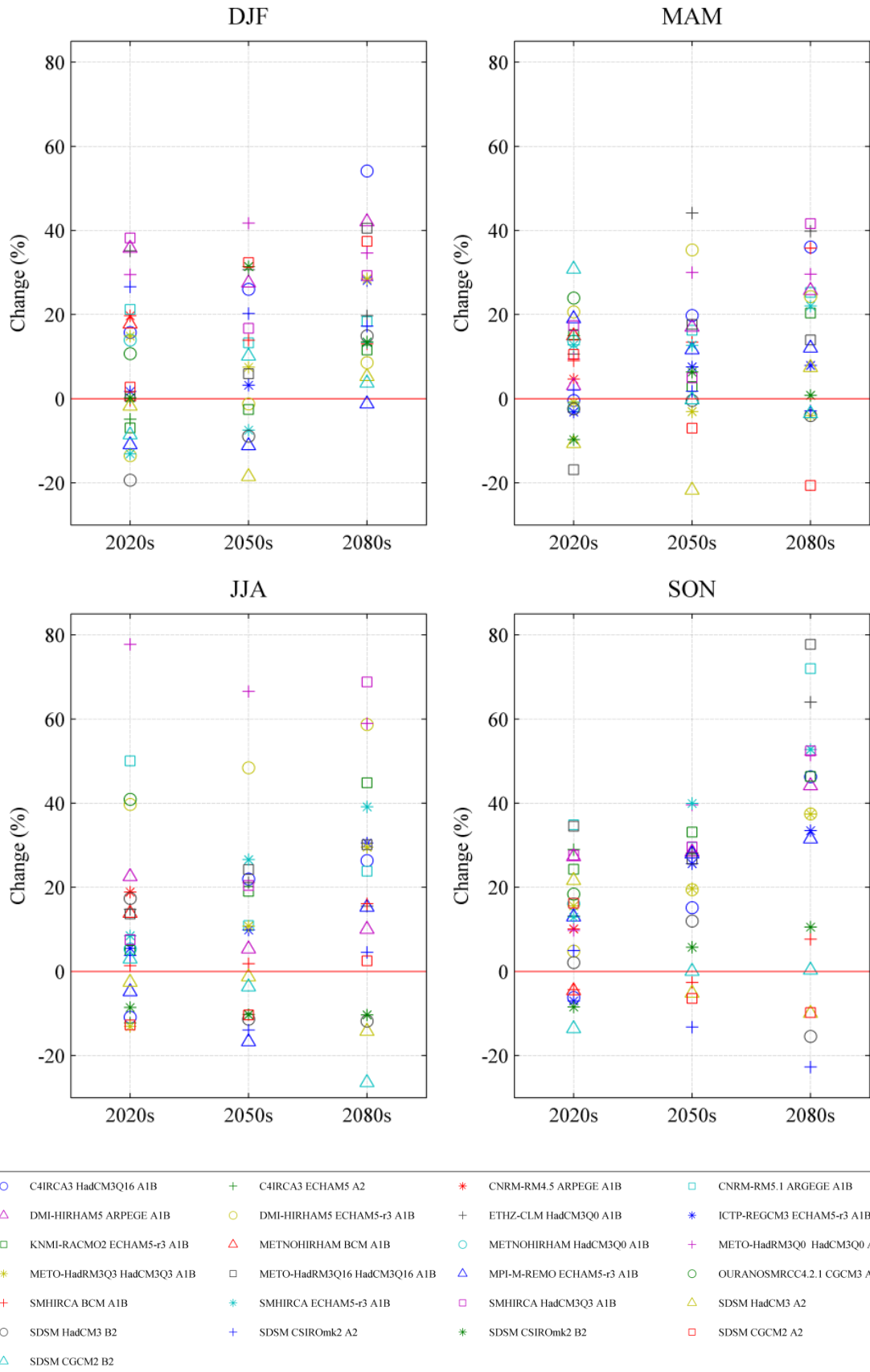


Figure 7.8 Projected changes in the seasonal variance of rainfall amounts (≥ 2 mm) for the Burrishoole catchment.

7.4 Probability distribution for reference period and climate scenarios

Shown in Figure 7.9 and 7.10 are a series of smoothed probability density functions (PDFs) plotted for summer (JJA) and winter (DJF) respectively. The plots show the PDF for each individual ensemble member along with the PDF for the weighted mean ensemble estimated for each emission scenario (averaged using the weighting scheme outlined in Chapter six). The PDF of observed temperature over the 30 year baseline period is also shown. Following Déqué and Somot (2010) and Déqué (2009) the PDFs were constructed by binning the data series for each variable and formulating the associated density; a bin resolution of 0.5°C and 0.25 mm was used when discretizing temperature and precipitation respectively. The weighted histograms were calculated using the following:

$$PDF(x) = \sum_{i=1}^n PDF_i(x)p_i$$

where $PDF_i(x)$ is the PDF of the variable x for a given model pathway i , n is the number of pathways considered and p_i is the probability or weight assigned to a particular ensemble member. For visual purposes each histogram was smoothed using a low pass filter with Gaussian kernels whose standard deviation was adjusted to maintain the density shape whilst smoothing the PDF outline.

Figure 7.9 and 7.10 show a clear distinction between the weighted ensemble average and the 30 year reference PDF. Over each successive horizon the PDFs appear to shift further from the reference towards warmer values without a discernible change in shape - this occurrence is common to both seasons. There does however appear to be a change in the shape of the PDF for summer maximum temperature, which is particularly evident over the 2080s. When the individual ensemble members are plotted as empirical cumulative distribution functions (Figure 7.11 and 7.12) the projected shift in the distribution over each successive horizon is more apparent. Also shown is the weighted mean ensemble. The plots indicate that differences in the SRES scenarios become more pronounced over each successive horizon - highlighting the greater influence which the emission scenario has on the climate response towards the end of the century. Figure 7.13 shows the weighted and non-weighted mean ensemble for minimum winter and summer temperature respectively. The plots indicate that the difference between the weighted and non-weighted mean PDFs for the A1B scenario is negligible, as are differences between the weighted and non-weighted A2 and B2 ensemble members.

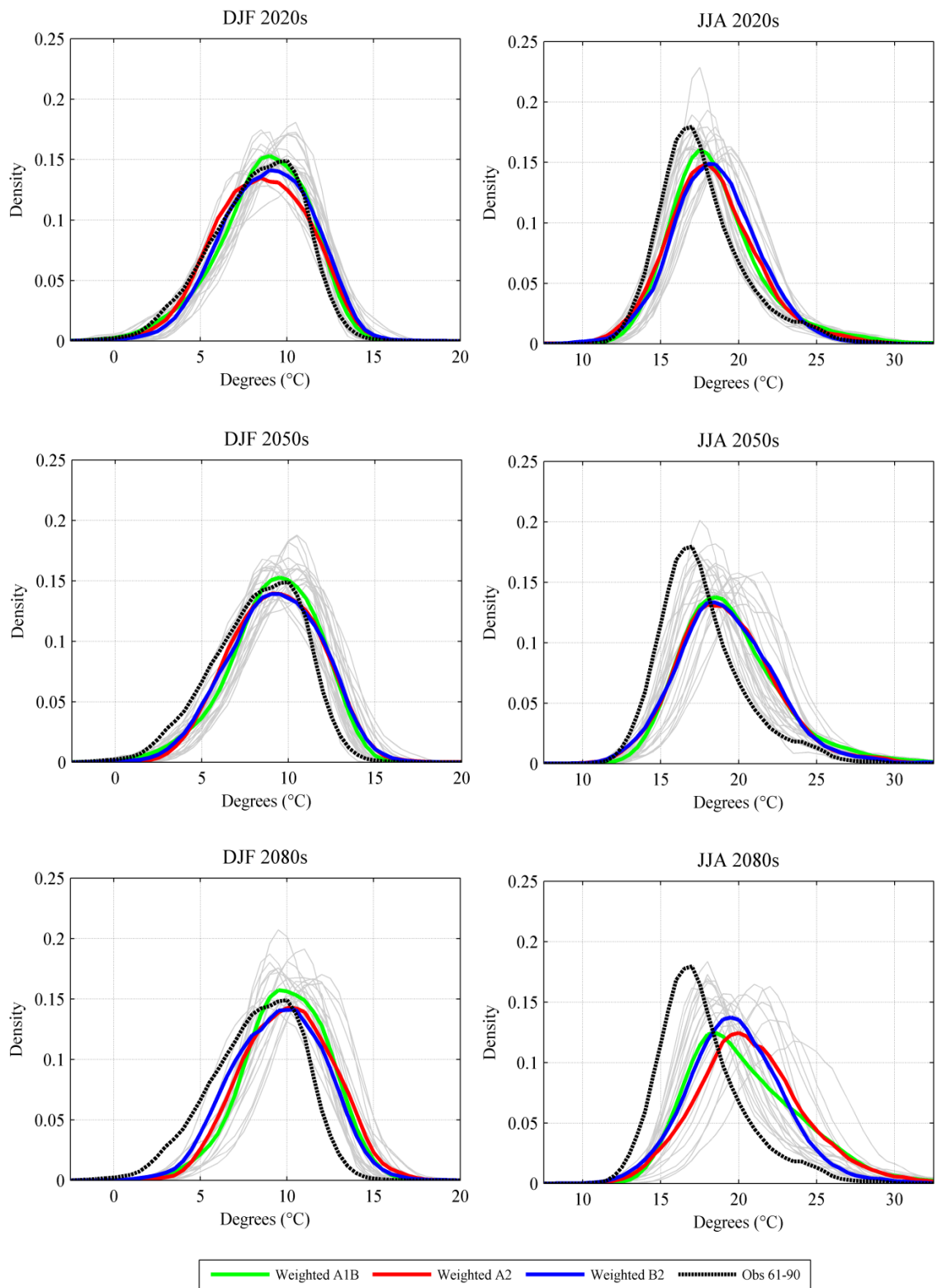


Figure 7.9 Smoothed probability distribution functions (PDFs) constructed using downscaled temperature (maximum) projections for the Burrishoole catchment. The PDFs for each ensemble member are shown (grey) along with the weighted mean PDF for each emission scenario (A1B, A2 and B2). The weighting scheme used is discussed in Chapter six. Also shown is the smoothed PDF of observed maximum temperature for the period 1961-1990. The PDFs for summer and winter only are shown.

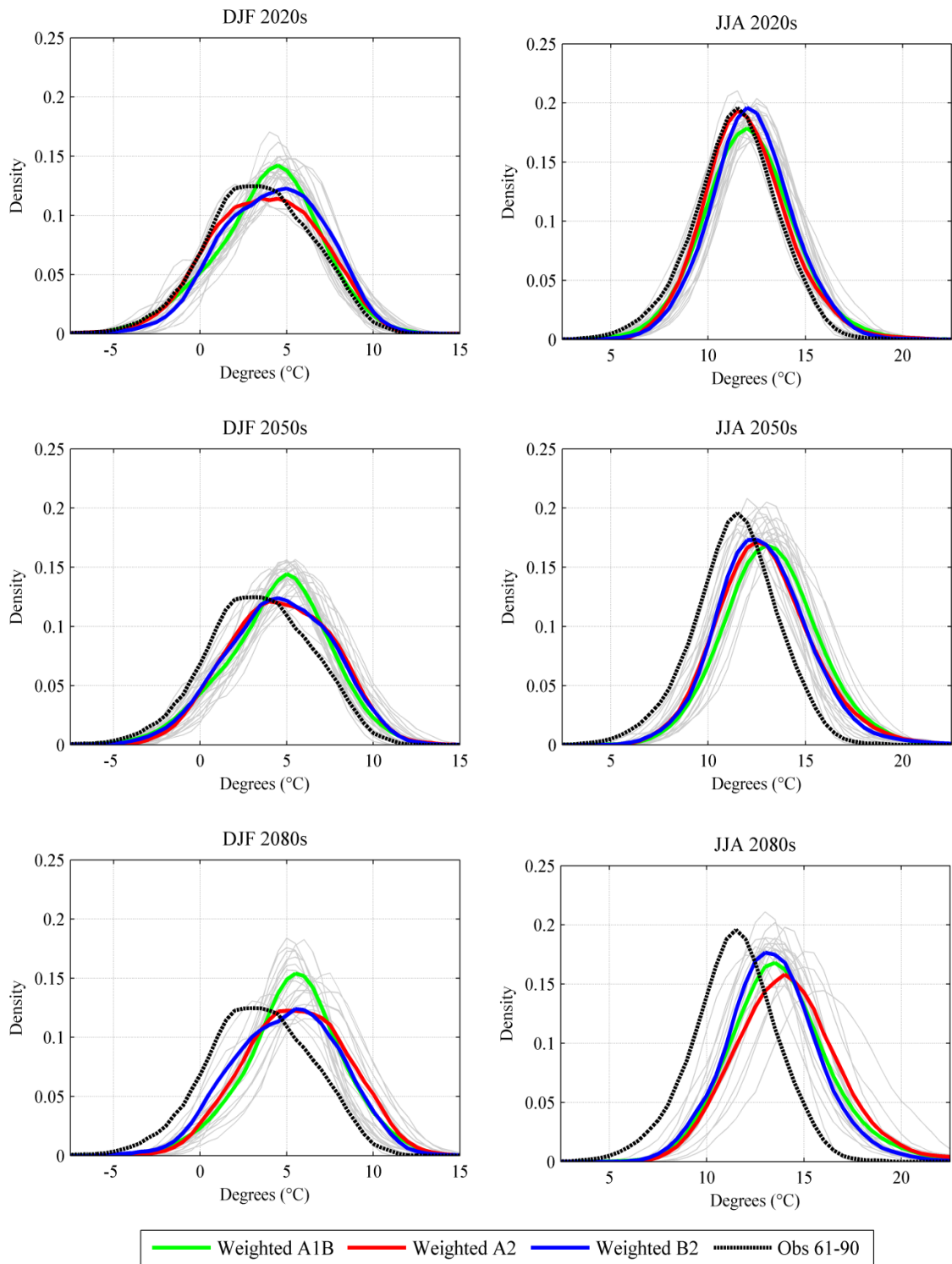


Figure 7.10 Smoothed probability distribution functions (PDFs) constructed using downscaled temperature (minimum) projections for the Burrisshoole catchment. The PDFs for each ensemble member and shown (grey) along with the weighted mean PDF for each emission scenario (A1B, A2 and B2). The weighting scheme used is discussed in Chapter six. Also shown is the smoothed PDF of observed maximum temperature for the period 1961-1990. The PDFs for summer and winter only are shown.

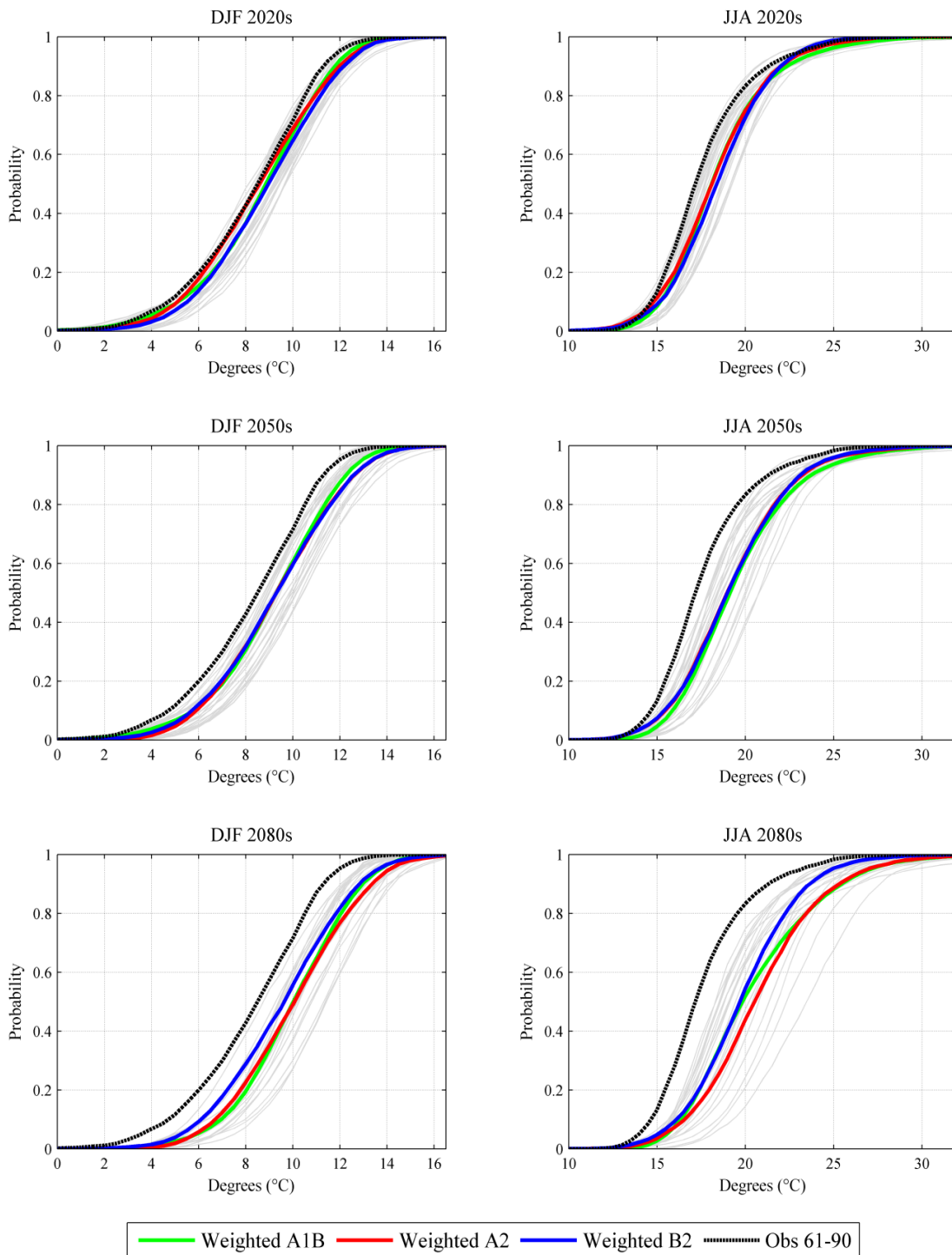


Figure 7.11 Empirical cumulative distribution functions (ECDFs) constructed using downscaled temperature (maximum) projections for the Burrishoole catchment. The ECDFs for each ensemble member and shown (grey) along with the weighted ensemble mean ECDF for each emission scenario (A1B, A2 and B2). The weighting scheme used is discussed in Chapter six. Also shown is the ECDF of observed maximum temperature for the period 1961-1990. The ECDFs for summer and winter only are shown.

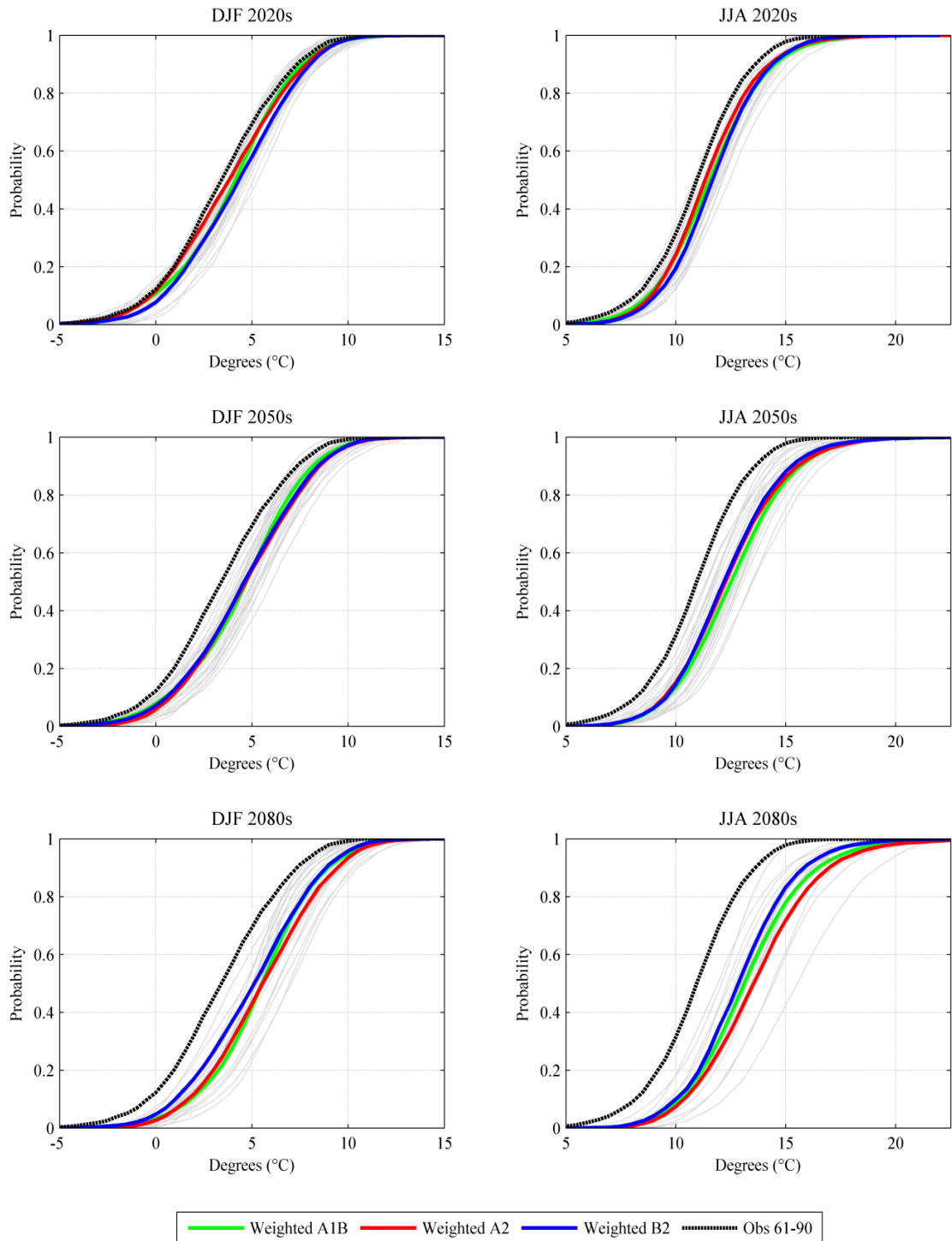


Figure 7.12 Empirical cumulative distribution functions (ECDFs) constructed using downscaled temperature (minimum) projections for the Burrishoole catchment. The ECDFs for each ensemble member and shown (grey) along with the weighted ensemble mean ECDF for each emission scenario (A1B, A2 and B2). The weighting scheme used is discussed in Chapter six. Also shown is the ECDF of observed maximum temperature for the period 1961-1990. The ECDFs for summer and winter only are shown.

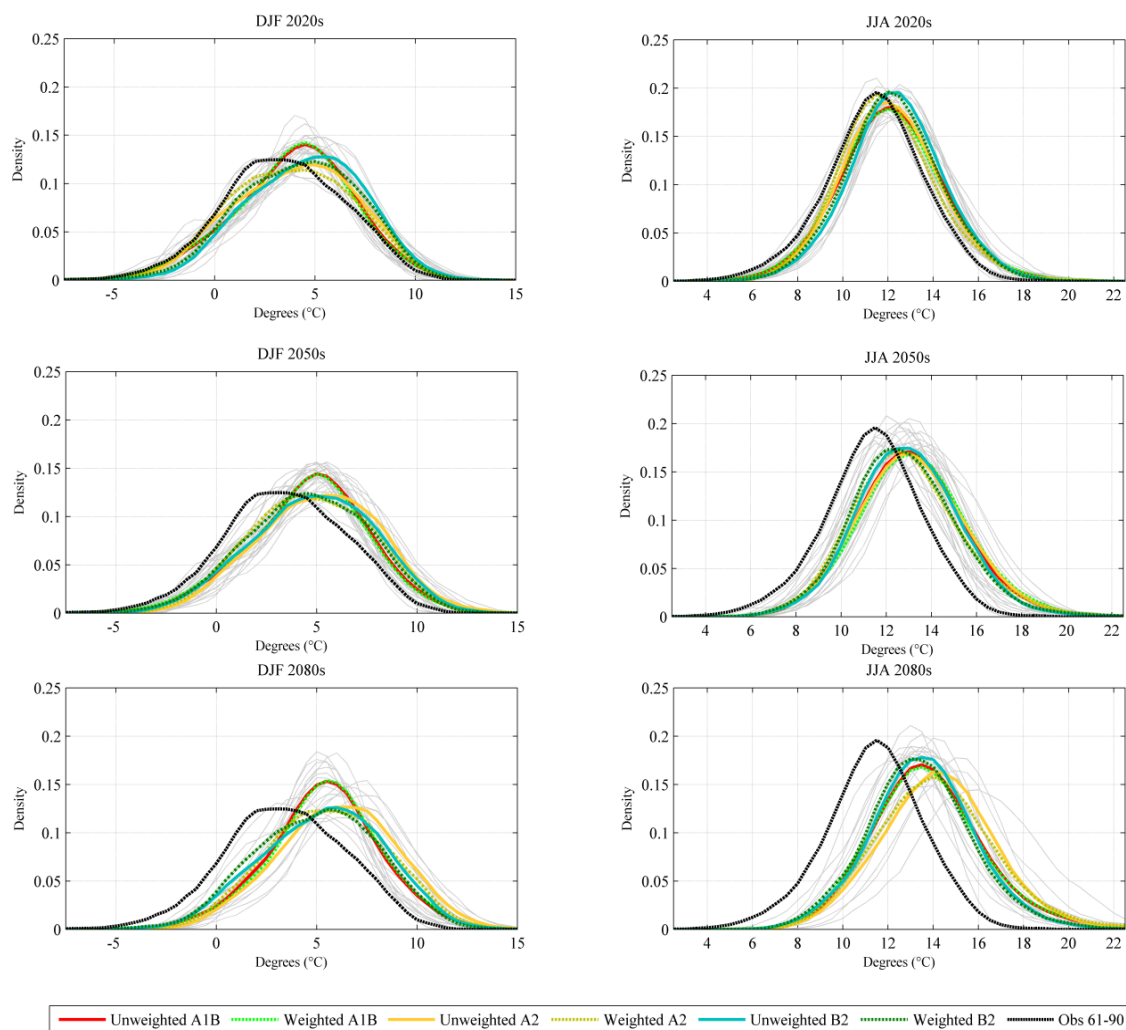


Figure 7.13 Smoothed probability distribution functions (PDFs) constructed using downscaled temperature (maximum) projections for the Burrishoole catchment. The PDFs for each ensemble member and shown (grey) along with the weighted mean PDF for each emission scenario (A1B, A2 and B2). The weighting scheme used is discussed in Chapter six. The equally weighted PDF for each emission scenario (A1B, A2 and B2) is also shown.

Differences in the equivalent smoothed PDFs for precipitation are difficult to determine visually; to address this, the weighted mean ensemble for this variable is explored using changes in the probability of occurrence for events a given magnitude - defined using a set threshold applied to wet days only (≥ 2 mm) (Table 7.1). This is the same approach adopted by Déqué and Somot (2010) when formulating probabilistic projections of future change in precipitation for several sites across Europe using the ENSEMBLES weighting scheme. For winter there is a suggested increase in the probability of heavy rainfall events, particularly those exceeding the 20 mm threshold. The projections indicate that the likelihood of such events occurring will increase over each successive horizon. With regards to the weighted and non-weighted mean ensemble the projected increase in heavy winter precipitation is of a similar magnitude. Generally the A1B and A2 scenarios suggest

DJF	$\geq 5\text{mm}$				$\geq 10\text{mm}$				$\geq 20\text{mm}$				$\geq 30\text{mm}$			
	Ctrl	2020s	2050s	2080s	Ctrl	2020s	2050s	2080s	Ctrl	2020s	2050s	2080s	Ctrl	2020s	2050s	2080s
Equally- weighted																
<i>A2</i>	0.524	0.545	0.547	0.562	0.256	0.276	0.280	0.300	0.052	0.060	0.061	0.073	0.011	0.014	0.013	0.016
<i>B2</i>	0.522	0.519	0.537	0.531	0.229	0.231	0.251	0.249	0.057	0.054	0.067	0.064	0.016	0.012	0.016	0.018
<i>A1B</i>	0.528	0.534	0.543	0.541	0.240	0.251	0.257	0.253	0.055	0.064	0.062	0.071	0.015	0.017	0.020	0.022
Weighted																
<i>A2</i>	0.540	0.528	0.536	0.536	0.243	0.257	0.242	0.252	0.058	0.064	0.054	0.071	0.015	0.017	0.015	0.023
<i>B2</i>	0.521	0.510	0.530	0.518	0.227	0.231	0.241	0.237	0.052	0.049	0.064	0.060	0.016	0.008	0.011	0.016
<i>A1B</i>	0.529	0.554	0.564	0.579	0.259	0.282	0.289	0.309	0.051	0.061	0.066	0.073	0.010	0.013	0.014	0.016
<i>Observed 1961-1990</i>	0.558				0.269				0.055				0.012			
JJA																
Equally- weighted																
<i>A2</i>	0.441	0.444	0.424	0.425	0.183	0.182	0.174	0.173	0.040	0.040	0.031	0.030	0.010	0.010	0.009	0.008
<i>B2</i>	0.444	0.429	0.424	0.435	0.181	0.179	0.176	0.179	0.039	0.038	0.035	0.038	0.011	0.010	0.009	0.010
<i>A1B</i>	0.434	0.431	0.434	0.432	0.181	0.186	0.188	0.193	0.035	0.042	0.044	0.049	0.008	0.011	0.012	0.015
Weighted																
<i>A2</i>	0.439	0.442	0.449	0.440	0.184	0.191	0.189	0.191	0.041	0.044	0.041	0.035	0.012	0.010	0.011	0.007
<i>B2</i>	0.447	0.465	0.423	0.439	0.185	0.196	0.179	0.185	0.040	0.044	0.033	0.036	0.010	0.011	0.010	0.011
<i>A1B</i>	0.441	0.439	0.456	0.452	0.186	0.191	0.196	0.203	0.036	0.042	0.044	0.050	0.008	0.010	0.012	0.014
<i>Observed 1961-1990</i>	0.449				0.182				0.042				0.011			

Table 7.1 The daily probability of precipitation estimated for different event thresholds (5mm, 10mm, 20mm, 30mm); probabilities are calculated using wet days only ($\geq 1\text{mm}$). The weighted and equally weighted mean ensemble for winter and summer is shown. Daily probabilities for the observed series are also shown (1961-1990).

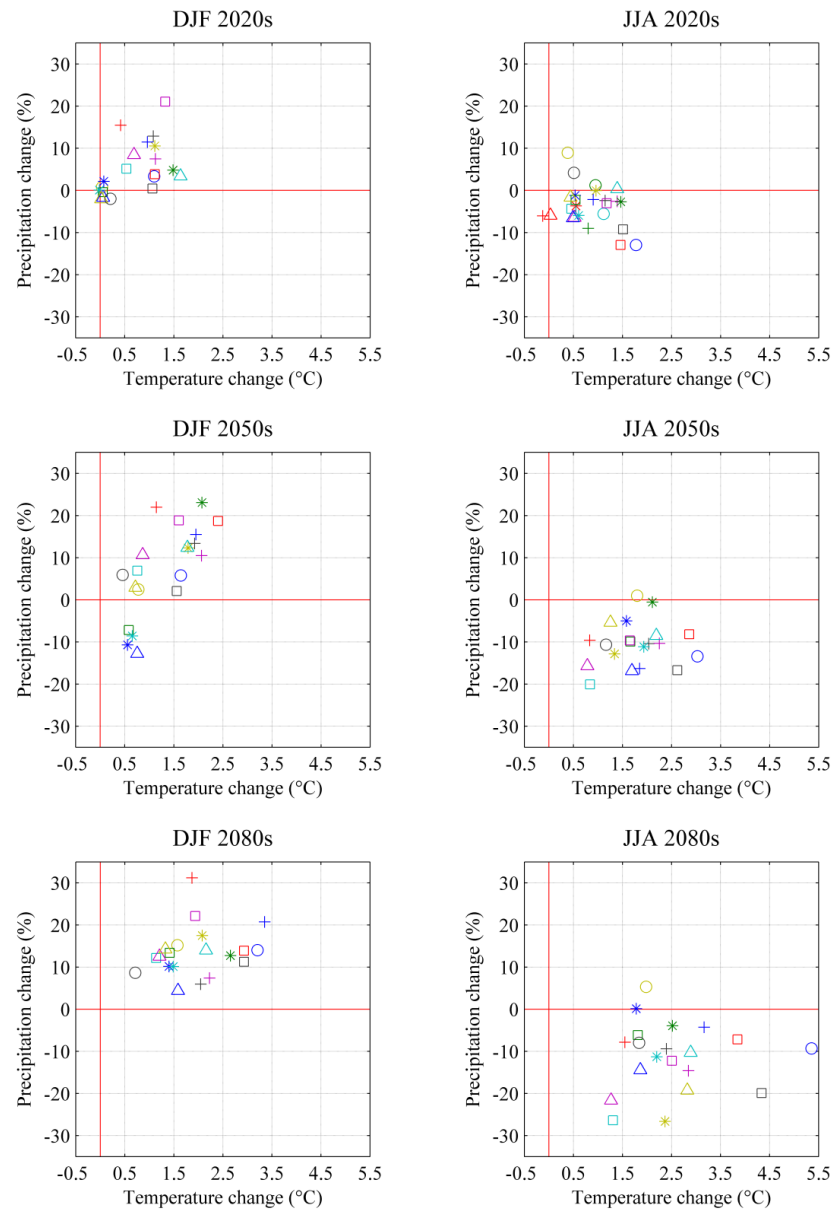
increases in heavy precipitation which are greater than those associated with the B2 scenario. The model projections for the A1B scenario indicate an increase in the probability of those rainfall events with a higher intensity threshold during summer. For both the B2 and A2 pathways a decrease in heavy summer precipitation is suggested. This is also the case for the probability of events with a lower magnitude. A degree of divergence between the weighted and non-weighted mean ensemble is evident for this season; despite this both reproduce the observed probabilities (1961-1990) with a high degree of skill.

7.5 Model response to climate forcing

Model projections generally indicate that the catchment is likely to experience wetter and warmer winters; whilst it is suggested that summers will become progressively warmer and drier. Figure 7.14 shows the degree to which the individual model pathways diverge over each successive horizon. It also highlights the heightened response of those model pathways for which the UK Met Office's high sensitivity HadCM3 GCM was used as the driving model - this is most evident for the summer season over the 2080s.

The bivariate probability distributions shown in Figure 7.15 are the smoothed equivalent of the individual pathway responses shown in Figure 7.14. To produce the plots the density surface of a 3-D histogram was smoothed using a 2-D Gaussian lowpass filter. Following this a contour plot was used to highlight regions with a high/low density. In this case density is a function of both the height of individual peaks (model response) and the proximity of the individual data points (convergence). By using this approach the response of each model pathway can be averaged, producing a (non-) weighted mean response for the multi-model ensemble. The plots are constructed using a similar approach as Déqué and Somot (2010). Figure 7.15 shows the smoothed data for each pathway plotted for winter and summer respectively; also plotted is the response of the individual model pathways. This provides a context for the overlying contours. In this instance each pathway is given an equal weighting irrespective of the emission scenario. Generally the plots are consistent with the individual model responses explored in Figure 7.14. The spread of the collective model response appears to increase over each successive horizon, particularly for the summer season where over the 2080s a number of points lie outside the smoothed surface. As a result their potential to appear as outliers lessens their contribution to the estimated ensemble response. What

is notable from the plots is that in a number of instances multi-modal regions of response are present. This is particularly evident for the winter season over the 2050s where both a decrease (-0.5mm d^{-1}) and increase in precipitation is projected - characterised by different degrees of warming. Generally the divergence in the multi-model response appears to be greatest over the 2080s.



○ C4IRCA3 HadCM3Q16 A1B	+ C4IRCA3 ECHAM5 A2	* CNRM-RM4.5 ARPEGE A1B	□ CNRM-RM5.1 ARGEGE A1B
△ DMI-HIRHAM5 ARPEGE A1B	○ DMI-HIRHAM5 ECHAM5-r3 A1B	+ ETHZ-CLM HadCM3Q0 A1B	* ICTP-REGCM3 ECHAM5-r3 A1B
□ KNMI-RACMO2 ECHAM5-r3 A1B	△ METNOHIRHAM BCM A1B	○ METNOHIRHAM HadCM3Q0 A1B	+ METO-HadRM3Q0 HadCM3Q0 A1B
* METO-HadRM3Q3 HadCM3Q3 A1B	□ METO-HadRM3Q16 HadCM3Q16 A1B	△ MPI-M-REMO ECHAM5-r3 A1B	○ OURANOSMRC4.2.1 CGCM3 A1B
+ SMHIRCA BCM A1B	* SMHIRCA ECHAM5-r3 A1B	□ SMHIRCA HadCM3Q3 A1B	△ SDSM HadCM3 A2
○ SDSM HadCM3 B2	+ SDSM CSIROmk2 A2	* SDSM CSIROmk2 B2	□ SDSM CGCM2 A2
△ SDSM CGCM2 B2			

Figure 7.14 Projected changes in temperature and precipitation for each respective model pathway. The plot illustrates the individual response of each model pathway to prescribed anthropogenic forcings.

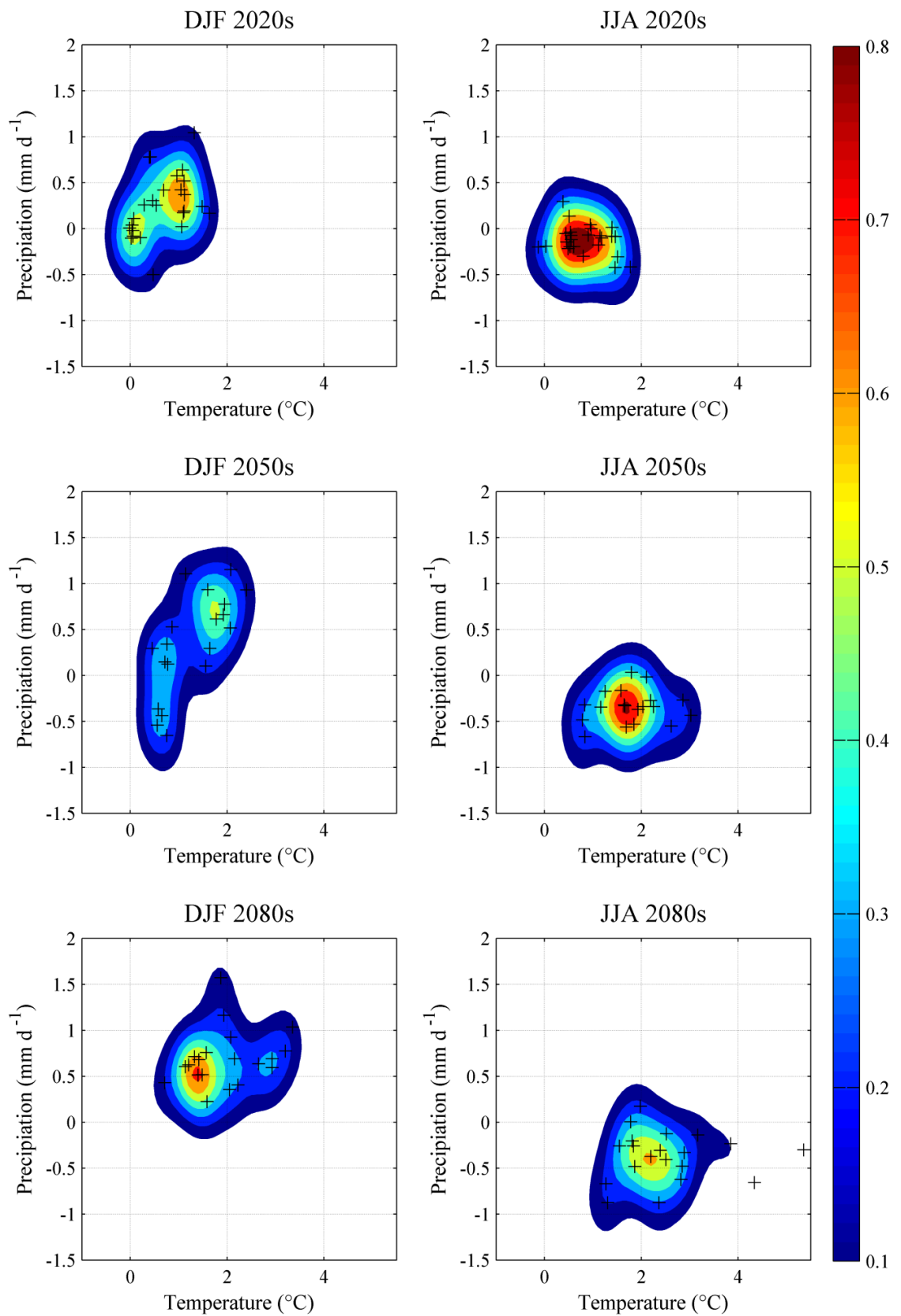


Figure 7.15 Bivariate probability density functions representing the multi-model response to future climate forcing. The contour plots overlay the response of individual model pathways (+). In this case each of the twenty five ensemble members is considered, and each is given an equal weighting when calculating the overall response.

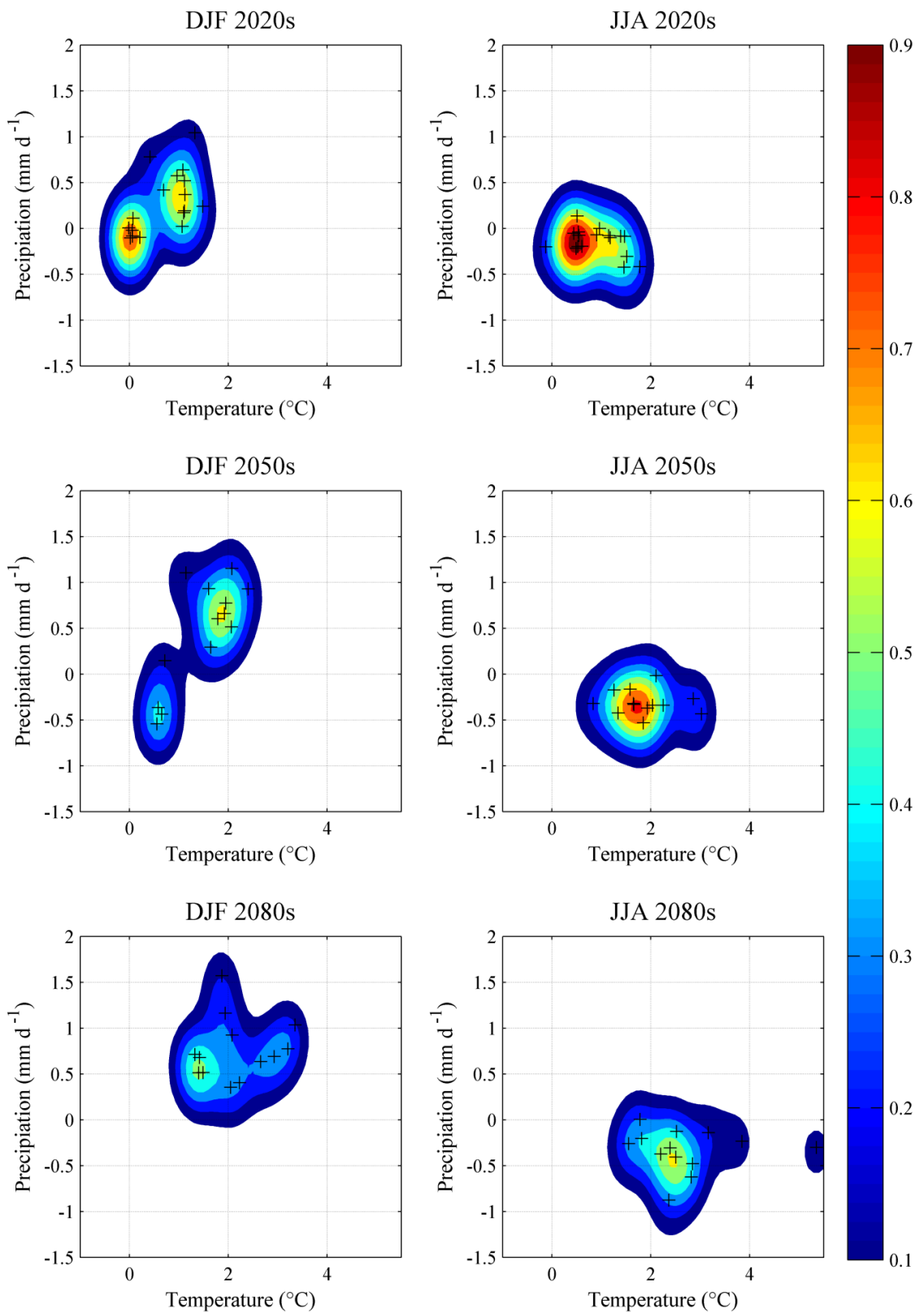


Figure 7.16 Bivariate probability density functions representing the response of the multi-model ensemble to future climate forcing. The contour plots overlay the response of individual model pathways (+). In this case the A1B ensemble members are considered. The weighting scheme discussed in Chapter 6 is used to weight the ensemble response.

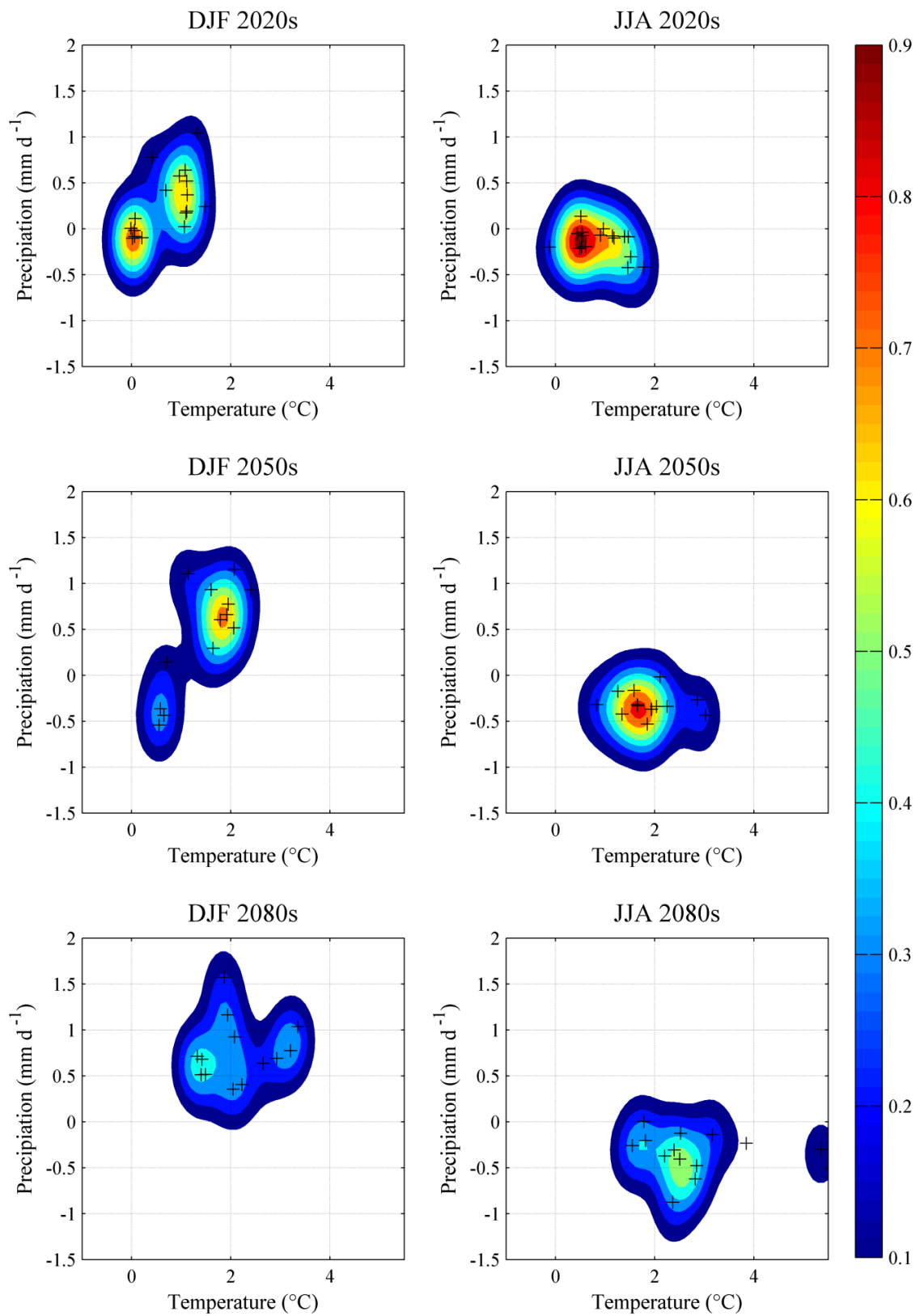


Figure 7.17 Bivariate probability density functions representing the response of the multi-model ensemble to future climate forcing. The contour plots overlay the response of individual model pathways (+). In this case the ensemble members relating to the A1B emission scenarios are considered - each is given an equal weighting when calculating the overall response.

Figures 7.16 and 7.17 show the weighted and unweighted smoothed multi-model response for those ensemble members relating to the A1B emission scenario only. Generally the plots appear similar to those shown in Figure 7.15; however, differences between the weighted and non-weighted plots are evident. This is particularly true for the 2050s where the unweighted plot (Figure 7.17) supports to a greater degree an increase rather than decrease in winter precipitation amounts. Similar plots were not constructed for the A2 and B2 based scenarios due to there being an insufficient number of data points (i.e. scenarios).

7.6 Other climate variables

Scenarios for a number of other climate variables were statistically downscaled using the output from three different GCMs (HadCM3, CSIROmk2 and CGCM2), each run using two different SRES scenarios (A2 and B2). This data was used as part of the RESCALE project discussed in Chapter one. Given that these variables were not used in the hydrological modelling, only a brief discussion of the results is provided. The SDSM statistical model (Wilby & Dawson, 2004) was used to downscale each variable; in addition both SDSM and a generalized linear model were used to downscale wind speed.

7.6.1 Wind speed

Over each future horizon there is an absence of any distinguishable change in local wind speed, a detail common to the projections from each GCM and emission scenario. This could be attributed to the absence of any thermal or moisture based variables in the downscaling predictor set. Such variables are sensitive to changes in radiative forcing and as such capture the underlying climate change ‘signal’. For each horizon and emission scenario deviations from the control are negligible, and it is possible that the projected changes listed in Table 7.2 could be attributed to natural variability rather than an anthropogenic forcing.

	Wind Speed SDSM				Wind Speed GLM				Relative Humidity				Solar Radiation SDSM				Potential Evaporation GLM			
	<i>DJF</i>	<i>MAM</i>	<i>JJA</i>	<i>SON</i>	<i>DJF</i>	<i>MAM</i>	<i>JJA</i>	<i>SON</i>	<i>DJF</i>	<i>MAM</i>	<i>JJA</i>	<i>SON</i>	<i>DJF</i>	<i>MAM</i>	<i>JJA</i>	<i>SON</i>	<i>DJF</i>	<i>MAM</i>	<i>JJA</i>	<i>SON</i>
HadCM3 A2																				
2020s	-0.19	-1.11	0.12	0.19	0.03	-1.35	-0.14	-0.15	-0.2	-0.35	-0.32	-0.44	0.6	0.0	1.1	1.2	-0.2	-0.1	1.2	1.6
2050s	-0.35	-4.51	-0.37	-1.50	-0.30	-4.88	-0.36	-1.41	-0.19	-0.94	-0.63	-0.52	-0.6	2.9	3.0	2.4	-0.1	2.8	3.3	3.0
2080s	2.52	1.33	-3.66	0.41	3.22	0.87	-3.93	0.48	-0.4	-1.51	-1.44	-1.48	-1.7	2.3	6.8	4.3	-1.1	2.0	7.6	4.7
HadCM3 B2																				
2020s	-0.46	-0.71	-0.05	0.22	-0.18	-0.98	-0.09	0.09	-0.2	-0.3	-0.3	-0.2	0.2	-0.1	1.8	0.2	-0.4	-0.3	1.7	0.6
2050s	1.97	1.51	-2.57	-0.56	2.58	1.37	-2.83	-0.62	-0.2	-0.8	-0.5	-0.5	-0.4	0.1	3.1	2.2	0	0.1	3.5	2.8
2080s	1.03	1.34	-2.07	0.26	1.43	1.27	-2.01	0.27	-0.4	-1.0	-0.9	-1.0	-0.1	1.0	4.3	2.5	-0.1	0.8	4.6	2.4
CSIROMk2 A2																				
2020s	4.67	0.81	-3.21	-0.90	0.97	-0.99	-1.89	-2.04	-0.15	0.49	0.08	0.12	0.2	0.1	1.5	-0.1	1.9	0.3	1.5	-0.1
2050s	1.86	0.35	-3.45	-0.35	5.24	-2.01	-1.72	0.98	-0.15	0.08	-0.13	-0.31	-1.1	2.0	2.4	0.4	-0.5	1.9	2.5	0.7
2080s	6.62	-2.29	-3.34	-0.11	7.47	-3.44	-2.75	-0.92	-0.35	0.36	0.08	-0.76	-1.8	3.5	3.9	2.5	-1.5	3.5	4.0	2.5
CSIROMk2 B2																				
2020s	0.46	-0.87	-1.74	-2.17	5.09	0.92	-3.17	-0.98	-0.13	0.06	0.07	-0.10	-2.1	0.8	2.1	-0.2	-4.6	1.1	1.8	-0.2
2050s	4.67	-1.68	-1.57	0.56	2.10	0.17	-3.46	-0.78	0.03	0.16	-0.07	0.16	-4.5	1.7	3.1	-0.3	-4.0	1.9	3.0	-0.1
2080s	6.61	-3.17	-2.65	-1.32	7.49	-2.37	-3.23	-0.29	-0.66	0.06	-0.16	-0.08	-2.4	3.6	4.3	0.1	-4.6	3.6	4.2	-0.2
CGCM2 A2																				
2020s	-1.04	1.21	-0.60	-1.43	-0.89	1.28	-0.53	-1.44	-0.41	-0.22	-0.50	-0.26	0.0	0.7	1.7	1.3	1.0	1.1	2.0	1.6
2050s	-0.73	5.30	-2.43	-0.10	-0.54	5.68	-2.58	0.05	-0.70	-0.92	-0.60	-0.78	-0.2	2.7	1.8	2.1	1.3	3.1	2.2	2.3
2080s	-0.44	6.07	-1.84	0.45	-0.48	6.17	-1.81	0.46	-0.51	-0.60	-0.87	-0.90	0.2	1.6	3.7	3.0	0.7	2.3	4.3	2.9
CGCM2 B2																				
2020s	-0.17	3.57	-2.59	-0.71	0.37	3.94	-2.65	-0.49	-0.16	-0.74	-0.28	-0.18	-0.9	2.1	2.3	1.3	-1.1	2.2	2.4	1.5
2050s	-3.2	3.13	-1.30	-1.93	-4.58	3.26	-1.39	-1.79	0.27	-0.38	-0.61	-0.56	-2.5	1.4	1.7	2.2	0.8	1.7	2.1	2.4
2080s	-2.14	4.02	-2.59	-1.42	-2.55	4.06	-2.67	-1.38	-0.22	-0.82	-0.63	-0.94	-0.2	2.7	3.4	3.2	1.4	3.0	3.7	3.0

Table 7.2 Model projected changes (%) in wind speed, relative humidity and potential evaporation. Scenarios for each variable are statistically downscaled from three GCMs (HadCM3, CSIROMk2 and CGCM2) - each run using both the A2 and B2 emission scenario. Both SDSM and a generalized linear model (GLM) were employed to downscale wind speed. The table is colour coded to highlight increases/decreases.

7.6.2 Relative humidity

With the exception of the scenarios downscaled from the CSIRO GCM, there is a general consensus between each GCM and emission scenario that relative humidity is likely to progressively decline over the course of the 21st century, with the greatest reductions being associated with the HadCM3 A2 scenario (Table 7.2). Suggested changes in relative humidity reflect projected increases in air temperature and the moisture holding capacity of the atmosphere.

7.6.3 Solar radiation & potential evaporation

Due to the influence which solar radiation has on evaporation rates, the changes projected to occur in each are relatively similar (Table 7.2). Model projections suggest that the greatest relative increases are likely to occur over summer, with deviations from reference conditions becoming more pronounced towards the end of the present century. The greatest increases for the summer season are projected by the HadCM3 A2 model pathway. An increase in both incoming solar radiation and evaporation rates is commensurate with enhanced air temperatures and projected reductions in rainfall receipts for this season. Model projections also suggest that winter reductions in both variables are likely to occur. The greatest decreases for the winter season are projected by the CSIROmk2 B2 model pathway.

7.7 Conclusion

Climate projections suggest that the Burrishoole catchment is likely to experience warmer and drier summers; it is suggested that this will be accompanied by the occurrence of wetter and warmer winters. The picture of change which emerges for the transition seasons of autumn and spring is much less clear. Each of the ensemble members agree that mean temperature is likely to increase, deviating further from reference conditions as the century progresses. Consistent with this trend is an increase in the warm extremes (e.g. 90th and 95th) for each season. The catchment's precipitation regime is anticipated to become increasingly seasonal in nature, with this trend becoming more pronounced as the century progresses. Heavy precipitation events are likely to increase during winter. With respect to the summer season a number of

ensemble members suggest an increase in heavy or extreme rainfall, despite the general trend for this season being one of a decline in total receipts. The uncertainty associated with changes in climate for autumn and spring are particularly significant in the context of this study, as both seasons coincide with critical periods in the life cycle of Atlantic salmon in the catchment.

The degree to which the model spread increases as the century progresses highlights the importance of adopting a multi-model approach. Generally differences between the emission scenarios do not become apparent until the 2080s, suggesting that up until the mid century the lack of convergence between individual ensemble members may be driven by the models used rather than the forcing scenario. While the emission scenario is important, particularly with respect to differences in the A2 and B2 scenarios, differences evident between individual ensemble members is noticeably influenced by the model sensitivity. The greatest absolute increases in temperature are associated with those model pathways whereby the UK Met Office's HadCM3 high sensitivity GCM was used as the driving model. Thus, despite being based on a less carbon intensive forcing scenario (i.e. A1B in contrast to the A2 based projections); greater increases in temperature are associated with those model pathways which have an enhanced response to GHG forcing. The response of the dynamically downscaled scenarios is largely controlled by the driving GCM, this is more apparent for temperature as opposed to precipitation, which is to a greater degree influenced by local scale forcings. Generally, in instances where the same GCM is used as boundary conditions, the pathways suggest temperature increases of a similar magnitude. In some cases the pathways have the same temporal evolution. This is most evident in cases where the ECHAM5-r GCM is employed. In contrast this pattern is less evident for precipitation, suggesting that the downscaling model may have a greater bearing on the projected regional scale response for this variable.

The changes in climate suggested by the statistically downscaled scenarios highlight the importance of including atmospheric predictors which capture the climate change signal. Both the statistical and dynamically modelled projections were found to be in agreement regarding likely changes in the catchment's precipitation regime. However, differences in the changes projected to occur in autumn receipts are noticeable. For this season, over both the 2050s and 2080s horizon, each of the regionally downscaled scenarios suggests an increase in receipts; this is in contrast to the statistically downscaled scenarios which indicate that a decrease is likely to occur. This general lack

of convergence may be due to the atmospheric predictors used to downscale precipitation for this season.

There appears to be a slight difference between the projections from the weighted mean ensemble and those from the unweighted mean ensemble, suggesting that there is little value added by employing the weighting scheme. This is a finding consistent with other studies, and may be related to the fact that no explicit consideration is given to systematic bias when formulating the scenario weights. Despite this, there are no suggestions that the application of a performance based weighting system is an invalid or less robust approach for combining the information contained in a multi-model ensemble. Indeed it could be argued that as the weights have been objectively formulated and reflect a model's ability to capture the most important aspects of local climate, it is a more defensible approach than assigning all ensemble members an equal weighting - irrespective of how well they simulate current day conditions. From a practical standpoint, employing a weighting system also offers an objective means for combining large amounts of often conflicting information with the aim of forming a coherent picture of future climate change. The proceeding chapter explores the various methodological approaches which can be adopted when assessing the potential hydrological response of river systems to projected changes in climate.

Chapter 8

Hydrological modelling and climate impact studies

8.1 Introduction

Previous research has found evidence for an intensification of the hydrological cycle at both a global and regional scale (e.g. Alexander *et al.*, 2006; Wentz *et al.*, 2007; Holland *et al.*, 2006; Holland *et al.*, 2007; Déry *et al.*, 2009; Zhang *et al.*, 2009a). A number of studies have indicated the existence of warming related trends in several hydroclimatic variables including precipitation (Dai *et al.*, 1997; Hulme *et al.*, 1998; New *et al.*, 2000), continental runoff (Groisman *et al.*, 2001; Labat *et al.*, 2004), atmospheric water vapour (New *et al.*, 2000; Dai, 2006), glacier mass balance (Oerlemans, 2005), the length of growing seasons (Cooter and LeDuc, 1995), evapotranspiration (Golubev *et al.* 2001) and soil moisture (Robock *et al.*, 2000). However, evidence for an intensification of the hydrological cycle must be prefaced with an acknowledgement that the findings from individual studies are found often not to be in agreement - an outcome which is due in part to the limitations of observational datasets and differences in the methods employed by individual researchers. It is argued that, when compared to observed changes in a number of variables, including precipitation, runoff and soil moisture patterns, trends evident in evaporation, evapotranspiration and atmospheric water vapor provide much stronger support for an intensification of the hydrological cycle (Huntington, 2006). A more in-depth discussion on observed changes in the hydrological cycle is provided in Section 2.1.

8.2 Global and regional scale impact studies

To date numerous model based studies have been conducted to assess climate change impacts on various aspects of the hydrologic environment including flow regimes, groundwater recharge rates, the availability of water resources and the nature of extreme flow events (Leavesley, 1994; Arnell, 1998). Given the significant implications which changes in the spatial and temporal variability of runoff have for the functioning of freshwater ecosystems, climate impact studies have become a key research area for freshwater ecologists.

Nijssen *et al.* (2001) employed climate projections from four GCMs (HCCPR-CM2, HCCPR-CM3, MPI-ECHAM4, and DOE-PCM3) to explore the hydrologic sensitivity of nine continental river basins to changed change conditions (Amazon, Amur, Mackenzie, Mekong, Mississippi, Severnaya Dvina, Xi, Yellow and Yenisei) using the variable infiltration capacity (VIC) macro-scale hydrological model. The GCM simulations suggested that each basin analysed is likely to experience an increase in both temperature and precipitation, with the greatest warming projected to occur at the highest latitudes during the winter months. Catchments which appeared most sensitive to a change in forcing were those in the mid to high latitudes, for which snow melt makes a greater contribution to the overall water balance. Here the largest changes were associated with mid and early spring when snow melt occurs. In snow dominated systems a warmer climate is likely to result in an earlier spring peak runoff, additionally warmer winters mean less snow accumulation and a reduction in the snow packs capacity to act as a store within the system. Nijssen *et al.* (2001) highlight inter-model variability as a key source of uncertainty in the projected hydrological response.

Arnell (1999) investigated the potential impact of climate change on hydrological regimes in Europe. For this study a macro-scale water balance model was run on a daily time-step at a spatial resolution of $0.5^{\circ} \times 0.5^{\circ}$; four different scenarios were used to represent potential climate pathways. Streamflow projections indicated a reduction in annual runoff in Southern Europe ($<50^{\circ}\text{N}$); the model simulations suggested that this would be accompanied by an increase in runoff across northern Europe. Changes in runoff were found to be reflective of projected changes in precipitation which follow a similar north-south divide. For western maritime Europe a reduction in flow during the summer months was suggested, as was an increase in winter runoff. Winter flows were also projected to increase across Eastern Europe. In snow dominated catchments - which are those highlighted as most sensitive to a change in climate - changes in the timing and volume of snowmelt are likely to result in an increase and decrease in winter and spring runoff respectively. The greatest percentage reductions in flow were associated with countries in southern and south-eastern Europe, additionally the intensity of drought events was found to increase in Western Europe, but decrease in northern and eastern regions.

Arnell and Reynard (1996) used a rainfall-runoff model in conjunction with equilibrium and transient climate change scenarios to investigate changes in river flow for 21 catchments across the UK. It was found that annual runoff was likely to

increase/decrease by approximately 20% according to the wettest/driest scenarios. The study highlighted that the catchment characteristics play a key role in determining the hydrological sensitivity of the catchment response to a change in forcing. Arnell (1998) explored the potential impacts of climate change on water resources across the UK. The study findings indicated that annual, summer and winter streamflow is likely to decrease in southern Britain. It is suggested this will be accompanied by a decrease in groundwater recharge and a reduction in water quality. In contrast model simulations suggested that runoff is likely to increase in northern Britain, particularly over the wetter winter months. Pilling and Jones (1999) employed a rainfall-runoff model (HYSIM) to examine changes in effective runoff across the UK under altered forcing. Model simulations were conducted using a 10 km × 10 km resolution grid in-conjunction with climate data from the Hadley Centre's high resolution equilibrium GCM (UKHI) for 2050 and transient GCM (UKTR) for 2065. Results from the UKHI scenario indicated that annual effective runoff is likely to increase across most of the UK. According to the UKTR scenario effective runoff is likely to decrease across much of England and Wales. Both scenarios agree that northern Britain is likely to become wetter and the south drier; the scenarios were also found to be in agreement regarding an increase in the seasonality of the flow regime. Fowler and Kilsby (2007) examined changes in the flow regime of eight study catchments located in northeast England using dynamically downscaled climate data. Based on the A2 emission scenario, a slight increase in annual runoff was indicated for those catchments at a higher elevation; in contrast for catchments at a lower elevation a decrease was suggested (~16%). On a seasonal basis, summer reductions in mean flow were projected (40–80%) to occur, as were increases in mean winter discharge (up to 20%). The results also suggested a change in the magnitude of seasonal high (winter increase in Q05 of up to 25%) and low flows (summer decrease in the magnitude of Q95 of 40-80%).

Pilling and Jones (2002) examined the impact of climate change on the Wye catchment (Wales) using the HYSIM rainfall-runoff model in-conjunction with statistically downscaled climate data from the HadCM2 GCM. The results indicated an increase in the seasonality of the flow regime - manifest in the occurrence of wetter winters and markedly drier summers. Also suggested was an increase in the frequency of extreme high and low flow events. Cameron (2006) examined the potential impact of climate change on the Lossie catchment (northeast Scotland) using a rainfall-runoff model (TOPMODEL) and the UKCIP02 climate scenarios. Cloke *et al.* (2010) examined

changes in river flow for the Medway catchment (UK) using the UKCP09 climate scenarios. The results indicated a reduction in mean daily river flows for all months and over each future time horizon considered. For the UK numerous other climate impact studies, which examine changes in catchment hydrology under projected climate conditions have been conducted (e.g. Wilby, 2005; Vidal & Wade, 2006; Wilby & Harris, 2006; Bell *et al.*, 2007; New *et al.*, 2007).

Several similar studies have been conducted in an Irish context. Murphy and Charlton (2008) used HYSIM to investigate the hydrologic response of nine catchment systems to projected climate change. The study employed statistically downscaled scenarios from three GCMs (HadCM3, CGCM2 and CSIROmk2) each run using both the A2 and B2 emission scenarios. Although the physical characteristics of each catchment were shown to influence their individual response - highlighting the need to conduct catchment specific modelling studies where the results are used to inform localised planning and adaptation - a number of general conclusions regarding changes in the hydrological regime under projected climate could be made. Model simulations suggest that the seasonality of the flow regime is likely to increase, with higher flows occurring during both the winter and spring seasons. For the majority of catchments model projections indicate that this will be accompanied by extended dry periods during the summer and autumn months. The frequency of both high (Q05) and low flows (Q95) is projected to increase during the winter and summer months respectively. Similarly the magnitude and frequency of flooding events is likely to increase, with the greatest relative increases being associated with those events which have a greater return period. The findings from Murphy and Charlton (2008) also suggest a reduction in groundwater recharge rates – with knock-on effects for groundwater levels at critical periods during the year when long term stores are required to sustain baseflow.

Similarly Steele-Dunne *et al.* (2008) assessed the potential impact of climate change on the hydrology of nine catchment systems located across Ireland. Here the HBV rainfall-runoff model was forced using dynamically downscaled (using the RCA3 regional climate model) data from the ECHAM5 GCM run under the A1B emission scenario. The results suggested an increase in the seasonality of the flow regime across all catchments - confirming the earlier findings of Murphy and Charlton (2008). Projected changes in flow were driven primarily by an increase/decrease in receipts of winter/summer rainfall. An increase in evaporation losses also contributed to changes in the seasonality of the flow regime. For the period October to April (2021-2060 relative

to 1961-2000) model simulations suggested an increase in discharge of up to 20%. The greatest monthly increase for the majority of catchments was suggested for the month of January. A decrease in runoff (up to 60%) was projected for the months of May to September inclusive. Bastola *et al.* (2011) investigated the impact of climate change on the hydrological regime of four Irish catchment systems (Boyne, Moy, Suck and Blackwater). This study explicitly considered uncertainty in both the forcing data and hydrological models used. The results indicated that future streamflow is likely to become increasingly seasonal in nature, with progressive increases in winter discharge being accompanied by a corresponding decrease in summer runoff.

Despite its importance for determining the full range of potential changes in the catchment hydrology, the majority of impact studies do not address the role of natural variability, which may act to dampen or exacerbate the effects of anthropogenic climate change on the hydrological regime of river systems. A number of studies have examined whether the suggested climate-driven changes in streamflow lie within or exceed the bounds of natural climate variability. Hulme *et al.* (1999) used two GCM simulations in conjunction with two environmental response models to examine the effects of unforced variability and climate change uncertainties on runoff across Europe. The results indicated that for some regions, the impact of anthropogenic climate change was undetectable relative to changes arising from multi-decadal natural variability. The authors argue that examining simulated changes in runoff under future climate change, independent from the effects of natural variability, may lead to an exaggeration in the importance of climate change - signalling that projected impacts may occur even in the absence of a change in radiative forcing. It is suggested that in order to develop robust adaptation strategies, climate-related changes in flow should be considered alongside those of multi-decadal natural variability.

Arnell (2003) considered changes in both the mean and 5th percentile of monthly flow in six catchments located across the UK. Projected changes were considered in the context of changes occurring as a result of multi-decadal unforced variability. Changes related to climate warming - where an amplification of the seasonal flow regime was suggested - appeared to have a different affect when compared to changes associated with natural variability. By the 2050s, for one season at least, the majority of model projected changes in runoff were found to lie outside the likely range of natural variability. It was found that including natural variability alongside anthropogenically mediated changes

in the hydrological regime led to a substantial increase in the range of potential monthly and seasonal changes projected to occur.

Prudhomme and Davies (2008b) examined changes in streamflow for four catchments in the UK using two variants of the same rainfall-runoff model (probability distributed moisture model; Moore, 1985). This study examined the runoff response to changes in climate in the context of natural variability. The authors highlight that projected changes in runoff may be the result of natural variability and therefore cannot be attributed to any discernible climate change signal. It was found that, at least up until the end of present century (2080s), projected changes in mean monthly flow did not generally lie outside the bounds of natural variability (estimated over the baseline period). According to the parameters set out in the study, changes could not be deemed to be significant if they were found to lie within the range of natural variability.

8.3 Approaches to hydrological modelling in impact studies

Fundamentally a hydrologic model is a numerical representation of the relationship between the inputs to a catchment system and the resulting discharge through its stream network - taking account of the various losses and stores which may exist. Essentially the models seek to partition water amongst the various components of the hydrological cycle; the key elements of this are illustrated using the water balance equation:

$$Q = P - ET \pm \Delta S$$

where Q is catchment discharge, P is precipitation, ET is evapotranspiration, and ΔS refers to changes in storage. Assuming that no groundwater flow occurs across the catchment boundary the equation remains valid (Leavesley, 1994). Many different models with various levels of complexity exist, ranging from empirical models based on transfer functions through to high resolution physically-based distributed models. These models allow sub-catchment scale processes to be modelled using immutable physical laws (e.g. Newton's law of the gravitation and the laws of conservation of mass, energy and momentum). This divergent spectrum of approaches in hydrological modelling also includes conceptual rainfall-runoff (CRR) models. CRR models are based on a series of simplifying assumptions about the working of the true system and are generally lumped at the catchment scale. Within this rather simplified classification of approaches in

hydrologic modelling, many variations or hybridized type models, representing different methodological approaches exist.

Given the range of approaches which can be taken it is possible to model runoff without necessarily considering the physical processes which contribute to, or influence runoff generation within the catchment system. This 'black box' type approach is however generally less favoured than those models which include some (quasi-) physical representation of important hydrologic processes, or which are based on some simplified conceptualisation of the system's true workings. However, the desire to increase the complexity of hydrological models, in terms of their structure, parameters and input requirements, with the expectant result of improved accuracy and a better representation of system dynamics, must be weighed against the intensive data and computing requirements of complex models, and the possibility that a more parsimonious approach may provide an equally plausible representation of system behaviour at the scales required. Xu (1999) states that the complexity of the model used must be commensurate with the scope of the study being undertaken, and it is only within this context that a judgement can be made regarding model suitability. As outlined by Leavesley (1994) models used in impact studies can be grouped into four categories depending on their level of complexity or structure, included in this are: (i) empirical models, (ii) water balance models, (iii) conceptual lumped parameter models and (iv) process based distributed-parameter models.

Water balance models have been employed in a resource management context to identify the regional scale hydrologic response to projected changes in climate (e.g. Gleick 1987a; 1987b; Schaake, 1990; Arnell, 1992; Kwadijk & Rotmans, 1995; Xu & Halldin, 1997; Xu & Singh, 1998; Guo *et al.*, 2002; Jiang *et al.*, 2007). Using the water balance equation outlined above the models account for fluxes of water between the various components of the hydrological cycle on a monthly time step (e.g. precipitation, runoff, soil moisture). Gleick (1987a; 1987b) used a water balance model to assess climate change impacts on water availability in the Sacramento River basin (California). It was found that the model was capable of reproducing both the timing and magnitude of observed monthly/seasonal runoff. In addition it was shown to accurately simulate soil moisture conditions - highlighting its applicability to regional scale impact studies. Gleick (1987b) used 18 different climate scenarios to investigate changes in runoff and soil moisture using the same model. Similarly Arnell (1992) employed a water balance model developed by Thornthwaite and Mather (1955) to study changes in monthly

discharge for 15 catchment systems located across the UK. This study also examined those factors which made catchments more or less sensitive to changes in climate. Arnell (1992) compared the projections from the water balance model to those from four different empirical models; in this case each was forced using the same climate data. Inter-model differences were found to be large, and the author states that projections derived using the empirical models should be treated with caution. Gleick (1986) argues that although water balance models offer advantages over alternative modelling approaches, they are unable to provide information at the temporal and spatial scales required for conducting in-depth impact assessments. This is reiterated by Leavesley (1994) who highlights their inability to capture changes in the characteristics of individual runoff events as a key limitation.

In cases where more detailed studies of changes in surface, subsurface or groundwater flow have been conducted, conceptual rainfall-runoff (CRR) models have generally been used (e.g. HBV (Bergström, 1976); the Sacramento Soil Moisture Accounting Model (Burnash *et al.*, 1973); the Stanford watershed model (Crawford & Linsey, 1966)). These models are a conceptual numerical representation of the key hydrologic processes (e.g. surface runoff, subsurface flow, evapotranspiration, capillary action, etc.), physical properties and outputs which characterise a catchment system. They represent the catchment as a simplified agglomeration of stores (e.g. groundwater, soil moisture) and (non-) linear transport or routing functions which trace the movement of water through the system taking account of various losses which may occur. Essentially the models implement the water balance equation set out above in much greater detail, taking a more explicit account of the various system components and complex relationships which exist between them.

Conceptual models incorporate a number of parameters which must be specified by the user so that the models may reproduce observed system behaviour accurately. Many of the parameter values may be estimated using field measurements however, the models may also include a number of parameters (i.e. process parameters) which do not represent directly measurable hydrological features - their values must be inferred using observed data (Wheater *et al.*, 1993). The requirement to optimize a number of parameters is necessary given the degree to which the models simplify the complexities of the true system. In addition, by optimizing the process parameters it allows errors or bias in the physically based parameter values - which arise from spatially aggregating the catchment characteristics - to be offset. As the parameters are typically lumped at

the catchment scale, the level of detail (spatial and temporal) with which the models are capable of representing the heterogeneous nature of the catchment system and the complexity of the localized hydrologic response is limited (Singh & Woolhiser, 2002).

Despite their acknowledged limitations, conceptual models are considered a key tool for conducting impact assessments, and have been successfully applied in a climate change context under a diverse range of geomorphic and climatic conditions across disparate temporal and spatial scales (e.g. Nemeč & Schaake, 1982; Bultot *et al.*, 1988; Keith, 1990; Vehviläinen & Lohvansuu, 1991; Panagoulia, 1992; Bultot *et al.*, 1994; Sefton & Boorman, 1997; Gellens & Roulin, 1998; Bergström *et al.*, 2001; Arnell, 2003; Booij, 2005; Vidal & Wade, 2006; New *et al.*, 2007; Steele-Dunne *et al.*, 2008; Andersson *et al.*, 2010; Boyer *et al.*, 2010; Driessen *et al.*, 2010).

Their ease of use, low computational requirements and ability to simulate the movement and storage of water in the system has led to the widespread use of CRR models in impact studies; however, the degree to which the models simplify the workings of the true system - whereby certain physical processes, system components and spatial characteristics are omitted or approximated in order to make the models workable with respect to the true system dynamics - along with the requirement to optimize a number of the model parameters, means their output will invariably be subject to some degree of uncertainty. In addition, their conceptual nature means that individual models have differing structures whereby both the processes and stores within the system are given more/less prominence (or omitted entirely) or represented using different numerical schemes. This ultimately gives rise to uncertainty in the model structure and the estimated hydrologic response. Water balance models are similar to CRR models in that they both represent the system as a simplified agglomeration of stores, consequently both model types are subject to many of the same uncertainties (Guo & Ying, 1997).

Parameter uncertainty relates primarily to model calibration and the optimization procedure whereby a numerical algorithm is typically used to search the n -dimensional parameter space for values which optimize a specified objective function. As it can mask errors in the model structure and input data, optimization may potentially lead to overconfidence in the adequacy of a model or its predictive reliability. The uncertainty inherent in hydrological modelling is manifest in the differential response of individual models to perturbed forcing conditions. It has been shown that different models (integrating across parameter sets and model structures), when run using the same

observed data may provide an equally good representation of system behaviour. However, when run using future climate scenarios - under forcing conditions for which the models may have no prior experience - each model may exhibit a significantly different hydrologic response (Harlin & Kung, 1992; Jiang *et al.*, 2007).

Deficiencies in the search procedure and the irregularities of the response surface lead to difficulties in determining a unique 'best' set of parameter values (Uhlenbrook *et al.*, 1999; Beven & Binley, 1992; Beven & Freer, 2001a). The idea that a global optimum parameter set can be identified has been challenged by the concept of 'equifinality' (Beven, 2006a) - whereby multiple parameter sets can be found, perhaps in vastly differing regions of the parameter space, all of which provide an equally plausible realisation of observed system behaviour (Duan *et al.*, 1992; Freer *et al.*, 1996). By logical extension the concept of equifinality also applies to the model structure. Thus in a broader sense the principle essentially suggests that there may be many representations of a catchment system, consisting of numerous combinations of competing model structures and parameter values, all of which are equally valid in terms of their ability to provide an acceptable simulation of observed behaviour. Parameter uncertainty is also linked to the level of interdependence between the parameter values and their identifiability in the model structure.

In order to minimize uncertainty in the model parameters, and as a means of increasing their spatial resolution, lumped conceptual models have been extended to represent the catchment system as a composite of constituent sub-catchments. One of the models which implement this approach is TOPMODEL (Beven *et al.*, 1979; Beven *et al.*, 1995). This model uses an index to delineate the catchment based on its topographical homogeneity. Alternatively the catchment may be subdivided into a series of sub-basins according to delineated catchment boundaries (e.g. ARNO; Todini, 1996); however, adopting such an approach necessitates optimizing a larger number of parameters. In addition, given that for each basin the same flow series may be used, a degree of intercorrelation among the parameters is likely to be introduced. To overcome the difficulties associated with spatially disaggregating conceptual models, it is possible to estimate all of the model parameters based on the physical attributes of the catchment using high resolution datasets - such an approach forms the basis of distributed, physically based hydrological modelling.

In studies where high resolution information on spatial patterns of variability in the hydrologic response is required, physically-based spatially-distributed hydrological models like SHE, MIKE SHE and SHETRAN have generally been employed (Beven, 1989; Bathurst & O'Connell, 1992; Parkin *et al.*, 1996; Walsh & Kilsby, 2007; Sultana & Coulibaly, 2011). These models are run at a high spatial resolution and take explicit account of the various hydrologic processes, system inputs and boundary conditions which characterise a catchment system. Their high resolution also means they allow for a better representation of the heterogeneity in the catchment characteristics and the localized hydrological response. By providing a more physically explicit account of the catchment system, these models overcome some of the limitations associated with their conceptual counterparts.

Whilst distributed models have proved useful for assessing the potential impacts of land-use changes on watershed hydrology (Walsh & Kilsby, 2007; Paudel *et al.*, 2010), their application in climate impact studies has been somewhat limited (Sultana & Coulibaly, 2011). This is due primarily to their intensive data requirements and significant computational costs. Their use has also been hampered by the difficulties associated with applying the models to more complex and/or larger catchment systems. Sultana and Coulibaly (2011) used a coupled MIKE SHE/MIKE 11 hydrologic model to examine the potential impact of climate change on the hydrology of the Spence Creek catchment located in southern Ontario Canada. The authors employed statistically downscaled data from the CGCM3 GCM to run the model. The study highlighted the advantage distributed models have, whereby the impacts of climate change on a range of hydrologic processes (e.g. streamflow, snow storage, ET, groundwater recharge) can be assessed within a single modelling framework. In addition, the authors highlight that the model was capable of simulating a complex catchment system with a high degree of skill. Dibike and Coulibaly (2007) employed both a conceptual (HBV-96) and physically-distributed model (WatFlood) to investigate the difficulties associated with using downscaled climate data to simulate hydrological behaviour under 'current' day and projected climate conditions. Their study showed that both models performed well in reproducing streamflow when run using observed data; however, the models responded differently and performed less well (over the control period) when driven using the downscaled climate data.

It could be argued that, due to their strong grounding in physical reality and their adherence to immutable physical laws, these models are more appropriate for

application in a climate change context, where they are required to extrapolate beyond known conditions (Beven, 2001a). With respect to CRR models this necessitates an assumption in the stationarity of the model as well as the optimized parameter values. Although fully-distributed physical models appear more ‘realistic’ when compared with conceptual models, the simplifications which they incorporate mean they are subject to some of the same uncertainties (e.g. parameterisation, spatial resolution) (Beven, 2001a; Blasone *et al.*, 2008b). Beven (1989) cites the lumping of sub-grid scale processes, the overparameterization of the models and our incomplete knowledge of the system as key limitations in physically based modelling. In addition, when applied in climate impact studies the models are subject to the same assumption of stationarity in the model response; albeit that given their physical grounding it may be argued that this assumption is somewhat more-well founded. At the opposite end of the modelling spectrum a number of studies have employed simple empirical and regression models to estimate changes in runoff using different climate scenarios (Revelle & Waggoner, 1983; Arnell & Reynard, 1989). These models make no attempt to take explicit account of the known physics or hydrological processes which govern runoff generation and flow processes.

8.4 Addressing stationarity

One of the foremost assumptions implicit in most climate change impact studies is that the models calibrated using historical data remain valid under the forcing conditions of possible future climates (Xu, 1999; Prudhomme *et al.*, 2002). Here an assumption is being made that the applicability of the model structure and the fitted parameter values are both time and state invariant; in addition, an assumption is being made about the stationarity of the catchment characteristics (e.g. land cover) as well as the physical processes which govern the system hydrology. An example of this is how the vegetation response to increasing temperatures and higher atmospheric concentrations of CO₂ may influence evapotranspiration rates and by extension the stationarity of the rainfall-runoff relationship.

For climate change studies to be robust with respect to these assumptions Klemes (1985) suggests that the models used should have a strong physical basis - whereby each of their structural components can be independently validated. According to this criterion, process-based distributed models provide the most appropriate approach for

conducting climate impact studies; however, as highlighted above, these models remain a simplified representation of reality, and as such are subject to the same assumptions regarding the stationarity of the estimated catchment response. According to Klemes (1985, 1986) stationarity can be assumed providing that a rigorous approach to model testing is adopted. This generally requires that model performance is assessed under contrasting climate conditions (Xu, 1999; Vaze *et al.*, 2010). Klemes (1985, 1986) suggests two separate split-sample type approaches for model validation which can be used in a climate change context. The first is the differential split-sample test and is employed to assess climate transferability (e.g. calibrated using a wet period and validated using a dry period); the second is the proxy-basin differential split-sample test used to assess both climatic and geographic transferability. Pilling and Jones (2002) employed a differential split-sample test in their study of the Wye catchment. As the observed data available for model calibration/validation was relatively short, and did not contain any easily identifiable prolonged periods of wet/dry conditions, they used extreme wet and dry spells lengths to test the transferability of the model parameters (following Gleick, 1987). In their study of climate change impacts on flood frequency in the UK, Prudhomme *et al.* (2003) indicate that the periods over which the hydrological models used were calibrated and tested contained enough information on both dry (1970s) and wet (1980s) conditions to ensure the model parameters were robust with respect to their validity under future climate.

Vaze *et al.* (2010) state that despite the fundamental importance of this assumption little work has been done to test its validity - a point reiterated by Li *et al.* (2011). Vaze *et al.* (2010) investigated the deterioration in the projections from a series of modelling experiments which arose when a model parameterized using a particular set of conditions was employed to simulate flow behaviour under future climate. This study was conducted using four lumped CRR models (SIMHYD, Sacramento, SMARG and IHACRES) and 61 catchments located across South-east Australia. The results suggested that when calibrated using more than 20 years of observed data, the models were reliably able to simulate future runoff, provided that mean annual rainfall was less than 15% drier or 20% wetter than the average annual rainfall experienced over the calibration period. In addition, the results suggested that it was more difficult for a model trained using a wet period to simulate runoff under dry conditions than if the reverse was considered.

More recently, Li *et al.* (2011) investigated the transferability of hydrological models under non-stationary conditions. For this study two different models were used to simulate streamflow behaviour in 30 Australian river catchments. The differential split sample test of Klemes (1986) was employed; in addition, Monte Carlo sampling was used to explore parameter stability. The findings suggested that models tuned to simulate runoff for a wet scenario should be calibrated using a wet period from the historical record and vice versa. In addition the model parameters were shown to be differentially sensitive to the choice of calibration period. Li *et al.* (2011) espouse the value of applying the differential split sample approach along with the Monte Carlo sampling procedure as a means of reducing uncertainties arising from parameter instability and non-uniqueness.

8.5 Uncertainty in hydrological modelling studies

The difficulties presented by the equifinality of different model structures and parameter sets, as well as the issues of parameter sensitivity and stability under altered conditions, have led to many researchers adopting a more pragmatic approach whereby the limitations of CRR models are recognized, and the associated uncertainty in their output is explicitly accounted for (Pappenberger & Beven, 2006). Being able to characterize and quantify uncertainty in the hydrological response is particularly important in the context of climate change impact studies, whereby the models may be required to extrapolate beyond conditions for which they were initially calibrated and tested.

The various simplifying assumptions on which hydrological models are based, along their differential interpretation of key hydrologic processes, force many distortions in the models and undermines their predictive capacity under altered forcing – an outcome which is exacerbated by the inherent complexities and random nature of the catchment system. However, despite the acknowledged limitations of hydrological models, Montanari (2004) states that most research in operational hydrology remains focused on finding the best estimate rather than on quantifying uncertainty in the model response. Walker *et al.* (2003) characterizes the uncertainty associated with hydrological models using two broad yet distinct categories:

- Uncertainty relating to imperfect knowledge of the system (epistemic uncertainty) - which is regarded as being reducible through a greater understanding and more accurate representation of system processes.

- Uncertainty due to the inherent variability and chaotic nature of the system (stochastic or ontological uncertainty). This type of uncertainty is regarded as being non-reducible.

There are four principal sources of uncertainty in hydrological modelling which include: (a) random or systematic errors in the input data (e.g. precipitation sampling and/or measurement errors); (b) random or systematic errors in the output data (e.g. imprecise rating curves); (c) errors due to an incomplete or biased model structure (d) errors arising from non-optimal parameter values (Refsgaard & Storm, 1996). In the context of climate impact assessments this widens to include uncertainty in the forcing scenarios used. In this case uncertainty stems from a wide range of factors including the choice of emissions scenario and driving GCM. In terms of local scale assessments the regionalization technique or downscaling model used is also a source of uncertainty. Error sources (a) and (b) above are related to the quality of available data whilst (c) and (d) are related to the models used. Achieving reductions in uncertainty relating to the model structure and parameters requires an improved understanding of the physical processes which govern the system and how accurately they are represented by the models. Typically model uncertainty is associated with (d), which can be minimized using parameter calibration; however, it is important that in doing so the errors in (a), (b) and (c) are not compensated for. In such cases the models may appear to simulate the observed flow regime, without necessarily capturing the underlying mechanisms which control system behaviour. This has consequences for the transferability of the model and its predictive reliability under altered forcing. Given that it is the parameters which are adjusted in order to optimize the model fit, parameter uncertainty is often used to address the combined effects of all uncertainty sources (i.e. total or global uncertainty), without necessarily acknowledging or quantifying the contribution from each in isolation.

Characterising uncertainty in hydrological models has become a key research area for hydrologists, with numerous studies being devoted to developing robust methods for dealing with and quantifying uncertainty, many of which focus on separating and treating all error sources independent of one another (e.g. Liu & Gupta, 2007). Montanari (2011) provides a comprehensive introduction to uncertainty in hydrological modelling, describing different sources of uncertainty along with the current methods employed to address, and where possible reduce them (Table 8.1).

Assessment Method	Classification	Type of Uncertainty Addressed	Reference
<i>AMALGAM</i>	Nonprobabilistic, parameter estimation	Parameter	Vrugt and Robinson (2007)
<i>BATEA</i>	Probabilistic, parameter estimation, uncertainty assessment, sensitivity analysis	Precipitation induced	Kavetski <i>et al.</i> (2006a, 2006b)
<i>BFS</i>	Probabilistic, Bayesian	Global	Krzysztofowicz (1999, 2001, 2002)
<i>BMA</i>	Probabilistic, multimodel	Global	Hoeting <i>et al.</i> (1999)
<i>DYNIA</i>	Nonprobabilistic, identifiability analysis	Parameter	Wagner <i>et al.</i> (2003)
<i>GLUE</i>	Nonprobabilistic (when an informal likelihood is used), parameter estimation, uncertainty assessment, sensitivity analysis	Global, parameter, data, structural	Beven and Binley (1992)
<i>IBUNE</i>	Probabilistic, parameter estimation, uncertainty assessment, sensitivity analysis	Global, precipitation induced, model structure induced	Ajami <i>et al.</i> (2007)
<i>Machine Learning</i>	Nonprobabilistic	Usually global, in principle all	Shrestha <i>et al.</i> (2009)
<i>Meta-Gaussian</i>	Probabilistic, data analysis	Global	Montanari and Brath (2004)
<i>MOSCEM-UA</i>	Nonprobabilistic, parameter estimation, sensitivity analysis	Parameter	Vrugt <i>et al.</i> (2003a)
<i>SCE-UA</i>	Probabilistic, parameter estimation	Parameter	Duan <i>et al.</i> (1992)

Table 8.1 Methods for addressing uncertainty in hydrological modelling studies (Source: Montanari, 2011). AMALGAM, a multialgorithm genetically adaptive method for multiobjective optimization; BATEA, Bayesian total error analysis; BFS, Bayesian forecasting system; BMA, Bayesian multimodel analysis; DYNIA, dynamic identifiability analysis; GLUE, generalized likelihood uncertainty estimation; IBUNE, integrated Bayesian uncertainty estimator; MOSCEM-UA, multiobjective shuffled complex evolution University of Arizona; SCE-UA, shuffled complex evolution university of Arizona.

As outlined by Renard *et al.* (2010) various methodological approaches exist for addressing uncertainty including, amongst others, frequentist approaches (Montanari & Brath, 2004), Bayesian Recursive Estimation (Thiemann *et al.*, 2001), Bayesian hierarchical models (Kavetski *et al.*, 2006a, 2006b; Kuczera *et al.*, 2006; Huard & Mailhot, 2008), instrumental-variable methods (Young, 1998), model averaging (Duan *et al.*, 2007; Marshall *et al.*, 2007a), the dynamic identifiability analysis framework (DYNIA) (Wagener *et al.*, 2003), the simultaneous optimization and data assimilation algorithm (SODA) (Vrugt & Gupta, 2006) and more standard Bayesian type approaches (Kuczera and Parent, 1998; Krzysztofowicz, 2002; Feyen *et al.*, 2007). Each method differs with respect to the assumptions made about different error types; they also differ with regards to what aspects of uncertainty they consider and whether different error sources are explicitly accounted for.

8.5.1 Data uncertainty

Deficiencies or errors in the observed data are regarded as a key source of uncertainty in hydrological modelling, and has received much attention in the context of uncertainty assessments. Data uncertainties arise from both the limitations of current monitoring techniques (e.g. instrumentation error, poor sampling, inaccurate rating curves) and the highly heterogeneous nature of hydro-climatological variables. Using erroneous data means hydrological models are optimized against an imperfect set of observations, thereby inducing errors in the fitted parameters and introducing uncertainty to the model output (Beven & Westerberg, 2011).

This is reiterated by MacMillan *et al.* (2011) who state that ignoring errors in the input data - introduced through sampling and measurement errors, as well as by the interpolation technique used - may lead to bias in the estimated parameters and compromise the reliability of the model output. Several studies have explored the sensitivity of hydrological models to errors in the input data (e.g. Xu & Vandewiele, 1994; Paturel, 1994; Kobold *et al.*, 2003; Hossain *et al.*, 2004; Xu, 2006; Das *et al.*, 2008). Generally these studies are in agreement that, irrespective of the model complexity there is an inherent sensitivity to the quality of the observed data. In addition they indicate that the models are generally more sensitive to errors in the precipitation as opposed to evaporation series (Xu & Vandewiele, 1994; Paturel *et al.*, 1995). Xu (2006) examined the spatial and seasonal affects of errors (both systematic

and random) in precipitation data on the performance of a conceptual monthly water balance model (NOPEX-6). In this case the model was used to simulate conditions in 26 catchments located in the Malaren basin (central Sweden). The study highlighted that the quality of the precipitation data affects the calibrated parameter values. In addition it was shown that using erroneous data can lead to the introduction of simulation errors in the model. Xu (2006) states that model performance was found to be dependent on the type as well as the magnitude of the error introduced to the input data; it was also found to be dependent on the individual catchment characteristics and season considered. The results indicated that the model used amplified initial errors in the precipitation data, and that those catchments with a lower runoff coefficient value were more sensitive to errors in the data. In addition the findings indicated that the model was more sensitive to systematic as opposed to random error; however, it was found that that as random error increased the estimated parameter values became more unstable.

A study by Andréassian *et al.* (2001) highlighted that errors in the rainfall data can be propagated through to errors in the simulated data as well as the calibrated model parameters. Chowdhury and Sharma (2007) examined the effects of uncertainty in the input data by artificially adding noise to the observed precipitation series; an empirical relationship between the resulting error in the simulated values and the noise added was subsequently derived. McMillan *et al.* (2011) assessed the suitability of different rainfall error models using instrumental records from a dense gauge and radar network in the Mahurangi catchment (New Zealand). The study indicated that multiplicative error is the most appropriate for correcting mean rainfall values during periods of high rainfall.

Accounting for errors in the output data is important in terms quantifying the total or global model uncertainty, with many studies highlighting the potential errors which can be introduced to streamflow series by way of inaccuracies in the stage–discharge rating-curve (e.g. cross section change, bed movement, vegetation growth, etc.) (Petersen-Øverleir, 2004; Moyeed & Clark, 2005; Reitan & Petersen-Øverleir, 2009; Di Baldassarre & Montanari, 2009; Liu *et al.*, 2009). McMillan *et al.* (2010) propose a method for quantifying uncertainties in discharge measurements relating to discrepancies in the rating curves used. The authors found that implementing a comprehensive assessment of uncertainty in the output data - including from sources such as changes in the cross-sectional channel form - led to a significant improvement in model skill. Similarly, Di Baldassarre and Montanari (2009) proposed a

methodological framework for quantifying uncertainty in flow series which focuses on deficiencies in the rating curves and the methods by which they are derived.

Uncertainty in the input data can be addressed by applying the GLUE procedure (Generalized Likelihood Uncertainty Estimation) (Beven & Bingley, 1992) in conjunction with an input error model to produce likelihood weighted model simulations. In the case of this methodological approach, errors in the input and output data are implicitly rather than explicitly addressed. Krzysztofowicz (1999; 2001; 2002) proposed the Bayesian Forecasting System (BFS) whereby a deterministic hydrological model is used along with a probabilistic quantitative precipitation forecast model to produce a probabilistic forecast for any hydrologic predictand (e.g. river stage, discharge volume). The method addresses uncertainty in the precipitation data as well as uncertainties stemming from other error sources (e.g. uncertainties in the model structure and parameters). In this case other sources of uncertainty are aggregated rather than being isolated and independently addressed. The method has the advantage of explicitly considering uncertainties in the input data; however, it treats errors in the precipitation data as the dominant uncertainty source, with all other sources assumed to be of lesser significance. To explicitly account for uncertainties in both the input and output data Kavetski *et al.* (2006a; 2006b) proposed the Bayesian total error analysis (BATEA) framework. The method incorporates an error model which allows uncertainties in both the input and output data to be considered. This methodological framework also addresses those other sources of uncertainty which contribute to the overall predictive uncertainty in hydrological models. Similarly Ajami *et al.* (2007) proposed a Bayesian type approach, IBUNE (Integrated Bayesian UNcertainty Estimator) which considers uncertainty in the precipitation data as part of a broader methodological framework - whereby all sources of uncertainty are explicitly accounted for. IBUNE uses the same approach as BATEA for addressing uncertainty in the precipitation data.

8.5.2 Model structure uncertainty

According to Refsgaard *et al.* (2007), model structure uncertainty is the conceptual uncertainty arising from an incomplete and simplified model description of the true system. Structural uncertainty may be a consequence of model choice, in which case this source of uncertainty is epistemic and can be reduced by selecting a model which is

more appropriate with respect to physical characteristics of the study catchment. However, the complexities and random nature of the catchment system mean that structural uncertainty is also in-part irreducible, as no one model is capable of replicating all aspects of system behaviour exactly (Beven, 2002). Refsgaard *et al.* (2007) state that although this is one of the key sources of uncertainty in model predictions (along with parameter and input data uncertainty) it is frequently neglected and no generic methodology with which to address it exists. Neuman (2003) also states that insufficient attention is paid to this error source, with most researchers focusing exclusively on uncertainty in the model parameters.

A robust and statistically rigorous assessment of structural uncertainty would only be possible if perfect input/output data were available; however, in reality no such dataset exists, and consequently such an assessment of structural uncertainty, whereby this error source is examined whilst all others (parameter and data) are extinguished and thus have no confounding influence, is not possible. Despite this it is possible to isolate structural uncertainty by reducing, or holding constant other uncertainty sources and comparing the performance of competing models. Montanari (2011) indicates that the variability shown in the range of responses from different models provides an approximate measure of the uncertainty introduced by structural error - providing that the influence of all other uncertainty sources is negligible.

Refsgaard *et al.* (2007) suggest that the more conventional approach of employing a single conceptual model leads to an inadequate sampling of the model space, giving rise to model bias and an underestimation of predictive uncertainty. Similarly, both Neuman (2003) and Neuman *et al.* (2012) highlight that the numerous ways in which hydrologic environments can be interpreted, both conceptually and numerically, mean that using a single model leads to an implicit underestimation of structural uncertainty. Neuman (2003) suggests that using a single model in isolation may lead to Type I model errors whereby alternative but equally valid models are rejected (by omission); this approach may also result in Type II model errors whereby an invalid model is adopted (fails to be rejected). Neuman (2003) indicates that uncertainty stemming from the model structure is typically much greater than that introduced by the model parameters.

Uhlenbrook *et al.* (1993) explored uncertainty relating to the model structure using the HBV CRR model. In this study the model was adjusted to reflect differing conceptualizations of the processes which govern runoff generation. In all three

different runoff routines available in the model were considered, the number of land-use and elevation zones were also varied. The results indicated that, irrespective of whether different or even unrealistic concepts were employed, it was possible to obtain good efficiency scores. This alludes to the compensatory role which the parameter estimates can play in concealing deficiencies in the model structure. Engeland *et al.* (2005) investigated uncertainties in both the model structure and parameters using the WASMOD rainfall-runoff model applied to 25 river catchments located across Sweden. The study indicated that, when total uncertainty in the model simulations was considered, the affect of structural uncertainty was greater than that stemming from parametric uncertainty.

Refsgaard *et al.* (2006) review a number of approaches for assessing structural uncertainties in conceptual models. Those approaches discussed include the use of a structural error term and a strategy based on increasing parameter uncertainty to reflect (but not explicitly account for) uncertainty in the model structure. To overcome the limitations of using a single model it is argued that the output from different model structures should be combined, and by allowing for a better assessment of predictive uncertainty, this constitutes a more robust approach to hydrological modelling (Marshall *et al.*, 2007b). Indeed Marshall *et al.* (2007b) go as far as to state that, (2007b: 848) “combining models can provide a model performance that is substantially better than any single model”. The argument for adopting a multi-model approach is based on the fact that each individual model provides a different representation of system processes, and by aggregating the information from each a more robust account of those hydrologic mechanisms which influence system behaviour can be obtained (Raftery *et al.*, 2005). It also represents a move away from implicitly assuming a particular ‘optimum’ model structure towards a better assessment of predictive uncertainty. The concept of using several different models - each with a different internal setup or architecture - is already a well-established approach in both weather forecasting and climate modelling; however, it is a relatively uncommon practice in a hydrological context (Butts *et al.*, 2004). The work of Butts *et al.* (2004) highlights the importance of addressing uncertainty in the model structure; it also underlines the need to employ multi-model ensembles when seeking to quantify both structural and parametric uncertainty in hydrological modelling.

A multi-model analysis is typically performed by employing some rigorous selection criteria to firstly identify suitable models; this may be based on expert judgement,

empirical testing or different model information criteria (e.g. Akaike Information Criterion, Bayesian Information Criterion) (Ye *et al.* (2008) provides a comprehensive review of these techniques). Subsequently a likelihood weight or probability is assigned to each model using some performance criteria or subjective interpretation of model importance. Based on this the statistics and predictions generated by multiple-models can be aggregated, with a higher weighting being applied to those models deemed to provide a better representation of system behaviour. This methodological approach is akin to the GLUE procedure typically used to assess parameter uncertainty, but can be applied in this context also (e.g. Rojas *et al.*, 2009).

Refsgaard *et al.* (2006) advocates a scenario based approach whereby a number of alternative or competing models are considered. In this study, for each model the input data and parameter uncertainties were estimated, differences between the respective model simulations were subsequently used to isolate the uncertainty attributable to the model structure. Butts *et al.* (2004) employed a multi-model approach to examine the impact which the model structure and complexity had on uncertainty in a flood forecasting study. The study findings indicated that model performance was strongly dependent on the model structure; the results also highlighted the benefits of utilizing multi-model ensembles as a means of improving hydrological simulations and identifying significant error sources.

Jiang *et al.* (2007) examined differences in the response of six water balance models to a change in climate forcing. It was found that each model had similar capabilities in terms of simulating historical water balance components; however, when driven using the same climate scenarios, inter-model differences became more pronounced. In terms of accounting for uncertainty in the differential response of individual models, this highlights the importance of employing multi-model ensembles in climate impact studies.

Whilst it is argued that aggregating the information from different model structures allows for a better estimation of future change, it must be acknowledged that by only considering a small number of models the possibly remains that the uncertainty space is being inadequately sampled. The lack of independence between models (i.e. some may have the same basic structure) is also of concern. With respect to this using models which lack independence may result in a particular region of the model space may be oversampled - leading to bias in the ensemble output and an underestimation of

uncertainty. Conversely, it could be argued that models from opposing regions of the model space may provide such divergent conceptualizations of the system that they may retain independence but lack physical realism - thereby introducing error and additional uncertainty to the ensemble.

Classical frequentist approaches generally provide modellers with few tools for explicitly addressing model uncertainty. In contrast Bayesian statistical theory provides a suitable methodological framework for addressing model uncertainty. Neuman (2003) propose the Maximum Likelihood Bayesian Model Averaging (MLBMA) framework to combine the output from several conceptual models and to assess their joint predictive probability – as part of this approach Neuman (2003) implements Bayesian Model Averaging (BMA). BMA is widely applied in areas such as climate modelling and weather forecasting (Raftery *et al.*, 2005; Sloughter *et al.*, 2007); it has also been employed in a hydrological context (e.g. Ajami *et al.*, 2006; Vrugt *et al.*, 2006, 2008; Duan *et al.*, 2007; Zhang *et al.*, 2009b; Bastola *et al.*, 2011; Neuman *et al.*, 2012). The basic premise of BMA is to make inferences using information from a multi-model ensemble based on a weighted average of the model space. According to the BMA approach the output from competing models is used to derive a predictive probability density function which represents a weighted average of each model's predictive probability. The weights used represent the posterior probabilities of the individual models and reflect their relative contribution to predictive skill over the training period (Hoeting *et al.*, 1999).

The MLBMA method is different to the more conventional BMA approach in that it is less computationally demanding and can be applied in cases where reliable prior information is not available. When implementing the MLBMA approach a model selection criterion (Kashyap Information Criterion) is firstly used to eliminate inadequate models from the ensemble. BMA is also employed as part of the Integrated Bayesian Uncertainty Estimator (IBUNE) framework proposed by Ajami *et al.* (2007). For the purposes of assessing the role of uncertainty in climate change impact studies Bastola *et al.* (2011) adopted a multi-model approach. As part of this study both BMA and the GLUE framework were employed. The results highlighted the importance of sampling different model structures when conducting climate change impact assessments. Similarly, in a climate change context, Najafi *et al.* (2011) employed BMA to combine the output from four hydrologic models.

Marshall *et al.* (2007a, 2007b) advances the ideas put forward in an earlier paper (Marshall *et al.*, 2006) which proposed the hierarchical mixtures of experts (HME) framework for addressing model uncertainty. This approach is based on combining the output from different models as a means of sampling structural uncertainty. The method allows individual models to be given a weighting based on the antecedent catchment conditions. For example, a model which is better at simulating a particular aspect of flow (e.g. low flows) is given a greater weighting when such conditions are encountered; conversely when opposing conditions are dominant (e.g. high flows) an alternative, more appropriate model may be given a higher weighting. The method therefore explicitly acknowledges the skill of competing models at simulating different parts of the hydrograph. Essentially the HME method allows the catchment to be modelled dynamically, whereby different models are dominant, and by extension different hydrological processes, depending on the prevalent catchment conditions. The HME method is implemented using a Bayesian approach which allows model and parameter uncertainty to be explicitly accounted for.

Rojas *et al.* (2008) explored the use of a multi-model approach for addressing structural and scenario uncertainties in groundwater modelling. The authors employ an ensemble based approach which combines the use of GLUE and BMA. Rojas *et al.* (2009) propose an advancement of the technique initially developed by Rojas *et al.* (2008) whereby Monte Carlo Markov Chain (MCMC) sampling is used. While the methodology addresses uncertainty in the model selection, it also accounts for uncertainty in the parameters and input data - albeit in an implicit manner.

8.5.3 Uncertainty in the model parameters

In addition to the model structure, uncertainty is also introduced by the requirement to calibrate a number of the model parameters, and the difficulties in inferring their respective values using observed data. Here uncertainty stems from the role of parameters in the model structure and issues specific to the optimization process itself, including the high-dimensionality of the parameter space, the inefficiency of search techniques and the equifinality of parameter sets (Beven, 1993; Wilby, 2005; Wagener *et al.*, 2006). Further uncertainties are introduced by way of errors in the input/output data used, the limitations associated with different objective functions and the level of interdependence between the model parameters. Uncertainty in the parameters is critical

to model reliability, particularly when the parameters are applied under conditions for which they had not initially been calibrated or tested. A number of studies provide evidence of the impact which parameter uncertainty can have on the model simulated data (e.g. Harlin & Kung, 1992; Uhlenbrook *et al.*, 1999; Sieber & Uhlenbrook, 2005; Huang & Liang, 2006).

Given that the optimization process may lead to other sources of error being compensated for or masked, the requirement to optimize some parameters, as well as the over-parameterization of the model itself, has wide ranging implications for model and predictive uncertainty. With respect to model calibration uncertainty is associated with those parameters which are estimated directly from field measurements as well as those (process) parameters whose values are inferred from observational data. The more conventional approach to reducing parameter uncertainty is to calibrate the model's process parameters using a robust optimization procedure; however, deficiencies in the various search techniques used and the irregularities of the response surface introduces uncertainty to the optimized parameter values. This has led to some rejecting the idea of an optimum parameter set in favour of the concept of equifinality (Spear & Hornberger, 1980; Hornberger & Spear, 1981; Beven, 1993; 2000). Equifinality refers to the existence of multiple parameter sets (and model structures) each of which provides a plausible representation of observed system behaviour. According to Beven (2006a) equifinality can be considered a manifestation of the combined effects of errors in the input/output data, the conceptualization of system processes and uncertainty in the model parameters.

With respect to determining an optimum parameter set, the challenge of calibrating a model's process parameters has been approached by developing more effective search techniques, including for example, the Shuffled Complex Evolution algorithm (Duan *et al.*, 1992), genetic algorithms (Wang 1991) and simulated annealing (Sumner *et al.*, 1997) - which are robust with respect to the difficulties presented by the response surface (e.g. roughness, discontinuous derivatives, parameter interaction, the presence of multiple-local optima and regions of attraction) (Duan *et al.* 1992; 1994). This approach to calibration assumes that an optimal parameter set exists and as such implicitly ignores any assessment of predictive uncertainty. Others have approached the problem by developing methods like GLUE (Beven and Binley, 1992) which forgo the concept of an optimum parameter set in favour of the concept of equifinality (Beven, 2006a).

The GLUE procedure allows model predictions to be given as ranges with some associated prediction interval, rather than as a single deterministic value based on an optimal parameter set. As it is the parameter sets rather than individual parameter values which are varied, this approach has the advantage of implicitly accounting for interdependence between the model parameters (Uhlenbrook *et al.*, 1999). Although GLUE is typically considered a methodological approach for addressing uncertainty in the parameters only, it technically provides an estimate of total uncertainty. The procedure assumes that global uncertainty can be characterized using uncertainty in the model parameters only, whereby all sources of uncertainty are mapped onto the parameter space. As such the uncertainties stemming from errors in the input/output data are not explicitly accounted for, nor are uncertainties in the model structure. The advantage of the procedure is that it allows all uncertainty sources to be considered (albeit implicitly); however, associated with this is the possibility that significant data errors or/and fundamental shortcomings in the model structure are being masked, resulting in overconfidence in the model and the possible propagation of unforeseen errors (Rojas *et al.*, 2010).

Not all of the proposed approaches for tackling parameter uncertainty are founded on the concept of equifinality. The Meta-Gaussian approach advocated by Montanari and Brath (2004) uses the model error to estimate confidence intervals – in this case the optimized parameter values are used. According to Montanari and Brath (2004) several other methods which employ confidence limits, including NLFIT (Kuczera, 1994), PEST (Brockwell & Davis, 1991) and Bayesian Recursive Estimation (BARE) (Thiemann *et al.*, 2001) exist.

Montanari (2011) divides the various approaches for addressing parameter uncertainty based on whether importance sampling (e.g. GLUE) or Markov chain Monte Carlo (MCMC) sampling is used. Similarly Xiaomeng *et al.* (2011) classify methods in uncertainty assessments into those implementing GLUE and those which employ a Bayesian framework. Feyen *et al.* (2007) state that the approaches taken to assess parameter uncertainty include those based on the use of multi-normal approximations (Kuczera and Mroczkowski, 1998), uniform sampling of the parameter space (Uhlenbrook *et al.*, 1999), Bayesian Recursive Estimation (Thiemann *et al.*, 2001) parametric bootstrapping and Markov Chain Monte Carlo (MCMC) models (Kuczera and Parent, 1998). Feyen *et al.* (2007) also include GLUE and the Meta Gaussian

approach; however, the authors suggest these methods provide an estimate of global rather than parametric uncertainty.

Feyen *et al.* (2007) and Vrugt *et al.* (2003b) offer similar criticisms of the various methodological approaches available. Both argue that traditional statistical theory based on first-order approximations and multinomial distributions are inadequate for dealing with the non-linearity and complexity of hydrological models; furthermore, both highlight the potential shortcomings of informal Bayesian approaches like GLUE which implement uniform random sampling of the parameter space. In contrast both Feyen *et al.* (2007) and Vrugt *et al.* (2003b) argue the merits of employing a formal Bayesian framework, emphasising the applicability of MCMC methods for complex inference and search problems. According to the formal Bayesian approach, the posterior distribution of the parameter values is estimated by updating the prior distribution on the basis of some likelihood measure. The posterior distribution reflects uncertainty in the parameter values and forms the basis of making probabilistic model predictions. Given that formal Bayesian methods and GLUE constitute the two most widely applied approaches for addressing parameter and model uncertainty, researchers have focused on highlighting the weaknesses and strengths associated with each. This has led to a rigorous debate in the hydrologic literature regarding the methodological and theoretical basis of both approaches – as well as their respective applicability in uncertainty assessments.

Uniform random sampling is typically conducted as part of the GLUE procedure; however, it is argued that the inefficiencies and potential pitfalls associated with randomly sampling the parameter space - particularly in the presence of high dimensionality - is an important weakness of GLUE and other methods which employ this sampling technique (Vrugt *et al.*, 2003b; Feyen *et al.*, 2007). Many researchers highlight other shortcomings associated with GLUE including the use of informal likelihood measures, the subjective way in which behavioural parameter sets are selected and that the method is not Bayesian in the strictest sense (Blasone *et al.*, 2008a, 2008b; Stedinger, 2008; McMillan & Clarke 2009; Jin *et al.*, 2010). The subjectivity of GLUE is not just related to the threshold value used to classify behavioural parameter sets, but also to the selected parameter ranges and the likelihood measures employed. Jin *et al.* (2010) state that the outcome of the GLUE procedure is conditional on the subjective elements which it incorporates; consequently its subjectivity is highlighted as one of its key shortcomings. Given the arguments advanced against GLUE there has

been a concerted effort by hydrologists to develop alternatives like MCMC methods, whereby a more targeted sampling of the parameter space is conducted in the context of a formal Bayesian framework.

Jin *et al.* (2010) indicate that although GLUE is less demanding computationally and easier to understand and implement, its lumped treatment of error sources means it is difficult to determine which error types are dominant. This is in contrast to formal Bayesian approaches which attempt to disaggregate the affect of data, parameter and structural error respectively, allowing those elements which contribute most to global uncertainty to be identified. Stedinger *et al.* (2008) conducted an in-depth appraisal of GLUE and criticised the use of informal likelihood functions - a shortcoming also highlighted by a number of other researchers (e.g. Christensen, 2004; Montanari, 2005; Mantovan & Todini, 2006; Gallagher *et al.*, 2007). Stedinger *et al.* (2008) state that the prediction limits derived using GLUE are not commensurate with those obtained using classical or Bayesian statistics and as such are not valid, the authors also criticise the poor treatment of errors in the input data. Montanari (2007) criticises GLUE on the basis that the rescaled likelihood measure is not a statistically consistent estimate of the probability density of the model output; as a result the derived prediction intervals do not reflect the true values of the prediction range. Montanari (2007) also states that GLUE should not be considered a probabilistic method but rather a weighted sensitivity analysis.

Criticisms of formal Bayesian approaches focus on the validity of the assumptions implicit in employing a formal error model. It is argued that, given the non-linearity of hydrological models and the complexities of runoff data, formal error structures are generally limited to providing only an approximate representation of errors in the model output. It is argued that the approximation of the model errors leads to bias in the estimated parameter values (Beven, 2006b; Beven *et al.*, 2006; 2008). Beven (2006b) expresses doubt that the assumptions implicit in formal Bayesian frameworks are valid with respect to the complexities of the catchment system, the level of interdependence between the model parameters and the interaction between different error types. Beven (2006b) also criticises the requirement to specify prior distributions for the model parameters and the assumptions which this entails.

Kuczera and Parent (1998) compared two Monte Carlo based approaches - importance sampling (implemented through the GLUE procedure) and the Metropolis-Hasting algorithm - for assessing parameter uncertainty. Based on the finding of this study the

authors state that, when conducting importance sampling unless a large number of random samples are drawn, the procedure may produce misleading results and introduce bias to the model output. In contrast it was found that the Metropolis algorithm is likely to produce reliable inferences for the posterior distribution of the model parameters with only modest sampling. Similarly, Yang *et al.* (2008) compared GLUE to a Bayesian framework implemented using MCMC. This study also considered a number of alternative approaches including Parameter Solution (ParaSol), the Sequential Uncertainty Fitting algorithm (SUFI-2) and importance sampling. The various methods considered were compared using the soil and water assessment tool (SWAT). The authors concluded that due to their solid conceptual and statistical basis, Bayesian approaches are most appropriate for addressing uncertainty in the model parameters. Jin *et al.* (2010) also compared GLUE to the Metropolis Hastings algorithm; the results indicated that, (a) GLUE is sensitive to the threshold value set whereby a lower value gives rise to wider uncertainty bounds; (b) similar estimates for parameter and model uncertainty were returned by both methods - but only when a relatively high threshold value was used (≥ 0.8 NS) to identify behavioural parameter sets; and (c) the posterior distributions generated by the Bayesian method were less scattered when compared to the equivalent distributions derived using the GLUE procedure.

Vrugt *et al.* (2009) compared GLUE to a formal Bayesian approach using the differential evolution adaptive metropolis (DREAM) MCMC scheme together with a likelihood function which explicitly considered uncertainty stemming from the input data, model structure and parameter values. The authors found that both GLUE and DREAM produced similar results in terms of the total uncertainty in model simulations; however, the Bayesian approach had the advantage of allowing the various error sources to be isolated. A number of advancements to the Metropolis Hastings algorithm - typically employed in more conventional MCMC approaches - have been proposed; for example Vrugt *et al.* (2003b) employed the Shuffled Complex Evolution Metropolis (SCEM-UA) (Duan, 1992) algorithm with the aim of improving MCMC sampling.

Given that one of the main criticisms of GLUE is that it handles all sources of uncertainty in an implicit manner, advances in uncertainty analysis have focused on quantifying the individual contribution which each constituent error source makes to the total predictive uncertainty in model simulations (i.e. errors in the input/output data, the model structural and parameter estimates). Typically methods for addressing uncertainty in this way adopt a Bayesian framework. Rojas *et al.* (2008; 2010) propose a

methodological approach which combines BMA (Hoeting *et al.*, 1999) and GLUE as a means for quantifying uncertainty in the parameters, input data and model structure respectively. This approach is based on the equifinality of different models - integrating across different parameter sets and competing model structures. Rojas *et al.* (2010) advance the method outlined in Rojas *et al.* (2008) by using MCMC. Renard *et al.* (2010) employed the Bayesian Total Error Analysis (BATEA) framework (Kavetski *et al.*, 2006a; Kuczera *et al.*, 2006), developed to explicitly account for each error source which induces uncertainty in the model output. BATEA allows total uncertainty to be assessed but treats different error sources independently. Renard *et al.* (2010) indicates that the BATEA approach offers improvements over more conventional methods which aggregate all uncertainties into a single error term. Similarly, Ajami *et al.* (2007) proposed the Integrated Bayesian Uncertainty Estimator (IBUNE) framework to explicitly account for different error sources. The method addresses uncertainties in the input data and model parameters using the Shuffled Complex Evolution Metropolis MCMC algorithm, but is extended to incorporate a precipitation error model. In addition BMA is used to address structural deficiencies by combining individual model simulations.

The identifiability of the model parameters is highlighted by a number of researchers as an important source of uncertainty, particularly in the context of land-use or climate change studies (Wagener, 2001). One approach to addressing this is to use a more parsimonious model structure (e.g. Wagener *et al.*, 2001) whereby only those components shown to be important for capturing the hydrological processes which regulate flow behaviour are included (e.g. Hornberger *et al.*, 1985; Jakeman & Hornberger, 1993; Young *et al.*, 1996). A sensitivity analysis is important for testing the suitability of a model concept and where possible improving the model structure (Sieber & Uhlenbrook, 2005). Additionally, the results of a sensitivity analysis can reduce uncertainty in a model's predictive capacity (Saltelli, 2000). In conducting the analysis it is important that the observed data used includes enough information about system behaviour to ensure that key structural components are not erroneously omitted on the basis that they appear non-identifiable; this may result in the model being unreliable when used to extrapolate beyond known conditions.

Uncertainty relating to parameter identifiability may also be addressed by optimizing how the information available for model calibration is used. Montanari (2011) highlights the importance of using multi-objective evaluation criteria to assess model

performance and reduce predictive uncertainty. This includes using multiple variables, response modes (e.g. different parts/sections of the hydrograph), data sites (different gauging points) and study catchments (e.g. basin proxy test whereby the model is tested on a similar catchment). Similarly, Wagener *et al.* (2001) advocate using additional output variables (e.g. groundwater levels, water quality data) and different data periods (e.g. wet/dry periods) to identify and test the model parameters. To further address uncertainty different objective functions can be used; adopting this approach also allows any bias introduced by way of the performance criteria employed to be removed (e.g. Pareto optimal solutions (Gupta, 1998)).

Wagener *et al.* (2003) propose the Dynamic Identifiability Analysis procedure (DYNIA) which, it is argued, is a more robust method for model parameter and structure identification. The method maximizes the information provided by the observed dataset and allows for any temporal variations which may exist in the identifiability of the model parameters. The multi-objective generalized sensitivity analysis (MOGSA) algorithm - discussed by Bastidas *et al.* (1999) and Arabi *et al.* (2007) - provides a more advanced approach for assessing parameter identifiability and performing multi-criteria optimization. This technique uses the Pareto ranking method to delineate behavioural from non-behavioural parameter sets; differences between both parameter sets are then used to estimate the parameter sensitivity. It is argued that this is a more robust approach which can reduce uncertainty in sensitivity assessments.

8.6 Uncertainty in climate change impact studies

Hydrological models constitute an additional link in the “cascade of uncertainty” (Schneider, 1983). Wilby (2005) highlights the importance of understanding the relative contribution of the individual uncertainty components to the total uncertainty in hydrological impact studies (e.g. Booij 2005; Wilby 2005; Cameron 2006; Wilby & Harris 2006; Bastola *et al.*, 2011). Kay *et al.* (2006) examined the relative contribution which six different sources of uncertainty made to the total uncertainty in the results of a study into climate change impacts on flood frequency in England. This study considered uncertainty stemming from the emission scenario, GCM structure, regionalization model and natural climate variability (explored by applying different GCM initial conditions). In addition, uncertainty in the hydrological model structure as well as the parameter values was examined. The results suggested that the largest

contribution to total uncertainty came from the driving GCM; however, it was found that this was largely due to a single model which skewed the results. When excluded from the analysis other sources of uncertainty became more significant. Despite this, the uncertainties relating to the GCM remained larger than those stemming from the hydrological models or the choice of emission scenario. The study also highlights the importance of considering natural climate variability when conducting uncertainty assessments.

Wilby (2005) explored the impact which uncertainty in the hydrological model parameters (CATCHMOD CRR) had on the results of a climate change impacts study conducted to examine changes in flow for the River Thames (UK). Statistically downscaled data from a single GCM, run using both the A2 and B2 emission scenarios, was used. The study employed a Monte Carlo sampling approach to investigate the identifiability, stability and non-uniqueness of parameters in the context of historic climate variability; also explored was the influence which the calibration period had on model projections. The study concluded that the identifiability of parameters was low, particularly over dry periods and in instances where a more complex model structure was employed. Wetter periods were found to offer more information for the purposes for model calibration, enhancing the transferability of parameters to drier periods for which the model had no prior experience. The study findings indicated that uncertainty relating to the training period used was equivalent to uncertainty arising from the choice of emission scenario. Similarly, uncertainty associated with the emission scenario was found to be comparable in magnitude to uncertainty stemming from the equifinality of parameter sets. The uncertainty due to equifinality was shown to be seasonally dependent, being of greater/lesser significance during winter/summer respectively. Given that only a single global model was used, the affect which uncertainty arising from the choice GCM had on the hydrological response was not considered.

Wilby *et al.* (2006) examined changes in daily flow for the Kennet river catchment (UK) using statistically downscaled data from three GCMs – each of which was run using two different emission scenarios (A2 and B2). The results indicated that uncertainty arising from the choice of GCM was greater than that stemming from the emission scenario used. In addition, it was found that uncertainty related to the GCM was greatest during the summer months. In their study of climate change impacts on the hydrology of a Nordic catchment (Chute-du-Diable, Quebec) Minville *et al.* (2008) found that the choice of GCM was the greatest contributing factor to uncertainty in the

projected hydrological response. This study used data from five different global models, each run using two different GHG emission scenarios. Climate data was downscaled using change factors for three 30 year horizons (2020s, 2050s and 2080s).

In a two part study Prudhomme and Davies (2008a, 2009b) examined uncertainty in baseline simulated and projected streamflow for four catchments in the UK. Two lumped CRR models were employed in the study; in addition climate scenarios downscaled using both a statistical (SDSM) and dynamical (HadRM3 RCM) approach were used. The climate data was downscaled from three GCMs (HadCM3, CCGCM2, and CSIRO-mk2), each run using both the A2 and B2 emission scenarios. In all, the study considered three different sources of uncertainty including: uncertainty in the GCMs, downscaling technique and hydrological models used. With respect to the hydrological component of the study, uncertainty stemming from both the model structure and parameter values was considered. In addition, model simulations were examined in the context of natural climate variability over the 30 year reference period (1961-1990) - estimated using a block resampling technique applied to the observed and downscaled climate data. Prudhomme and Davies (2009a) assessed uncertainties over the 30 year baseline period and concluded that for all four catchments considered, GCM uncertainty was greater than that arising from the choice of downscaling technique, and both were consistently greater in magnitude than the uncertainty stemming from the hydrological models or unforced climate variability. The authors state that the findings highlight the importance of considering more than one GCM and downscaling technique when conducting impact assessments. Using the same climate scenarios (in addition to the UKCIP02 scenarios), study catchments and hydrological models, Prudhomme and Davies (2009b) explored the relative contribution which different sources of uncertainty made to the total uncertainty in the projected hydrological response. Similar to their earlier study (Prudhomme & Davies, 2009a), the most dominant source of uncertainty was found to be the GCM, this was followed by the downscaling technique and emission scenario used – the uncertainty from both these sources was found to be of a similar magnitude.

Chen *et al.* (2011) focused specifically on the affect which uncertainty arising from the downscaling model used (six different models, including both statistical and dynamical models) had on the projected hydrological response of the Manicouagan river basin (central Canada). It was found that the uncertainty range originating from the choice of

28 climate projections (seven GCMs and three emissions scenarios) was slightly larger than the range associated with the downscaling model.

Wilby and Harris (2006) conducted an in-depth analysis of the contribution which each component in the 'cascade of uncertainty' made to the overall uncertainty in the results of a climate impacts assessment. This study used information from four GCMs, two emission scenarios and two statistical downscaling techniques. In addition Wilby and Harris (2006) considered two hydrological model structures (based on the CATCHMOD CRR model) along with two sets of model parameters. The study focused on climate change impacts on low flows in the River Thames for the 2080s only. The model projections were shown to be affected most by uncertainty in the climate change scenarios - specifically the choice of GCM. Uncertainties due to the emission scenario and hydrological model parameters were found to have a lesser impact. In order of the relative contribution each component made to the overall uncertainty (greatest to least), Wilby and Harris (2006) surmise their findings thusly: GCM > (empirical) downscaling method > hydrological model structure > hydrological model parameters > emission scenario. The projections were found to be most sensitive to the choice of GCM (manifested in abrupt changes in summer low flows), and in particular to the differential behaviour of atmospheric moisture amongst the GCMs employed. The study highlights the benefits of adopting a probabilistic framework when conducting impact studies.

Bastola *et al.* (2011) examined the affect which uncertainty in the hydrological models had on the results of an impacts study undertaken to assess the streamflow response of four Irish catchments to a change in climate forcing. To conduct the study four different hydrological models were used in conjunction with statistically downscaled data from three GCMs, each run using both the A2 and B2 emission scenario. The results suggested that the role of hydrological model uncertainty (considering both structural and parametric uncertainty) was remarkably high, and consequently efforts should be made to address it when conducting impact studies.

In a similar study Najafi *et al.* (2011) used the output from eight GCM simulations (based on two emission scenarios) as input to four hydrologic models (the Sacramento Soil Moisture Accounting (SAC-SMA) model, Conceptual HYdrologic MODel (HYMOD), Thornthwaite-Mather model (TM) and the Precipitation Runoff Modelling System (PRMS)) in order to estimate the hydrological response of the Tualatin River Basin (Oregon, USA) to altered climate conditions. The results indicated that - with the

exception of the dry season - GCM uncertainty was greater than the uncertainty stemming from the hydrologic model structure. In addition uncertainty arising from the choice of GCM was found to increase over successive future time horizons. In the study BMA was used as both a means for examining model uncertainty and combining the output from different model structures.

8.7 Conclusion

The extent to which the hydrological models used in impact studies simplify the inherent complexities and random nature of the catchment system means their output is invariably subject to some degree of uncertainty. This is compounded by uncertainties in the climate scenarios used as input to hydrological models and the assumptions implicit in modelling flow behaviour under altered forcing conditions. Given the potential consequences of maladaptation, there is an onus on those undertaking impact assessments to address the various sources of uncertainty which undermine the predictive reliability of hydrological models (Hulme & Carter, 1999). This necessitates employing a more rigorous methodological framework whereby uncertainty relating to both the model structure and parameter values is explicitly considered.

Various methodological approaches have been proposed for addressing uncertainty, not just in the model structure or parameters, but also in the observed input and output data used. Irrespective of the degree to which these approaches differ, and the various cases made for their suitability in uncertainty assessments, it is clear that a concerted effort must be made to address uncertainty in impact studies. This is a common theme in many of the studies referred to above. It is also clear that an assumption cannot be made as to where the dominant sources of uncertainty lie (e.g. GCM, emission scenario, model parameters), thus, with respect to the precautionary principle, a holistic approach for addressing each component in the chain of uncertainties must be applied on a catchment-by-catchment basis (Bastola *et al.*, 2011).

The proceeding chapter outlines the methodological framework adopted for modelling the selected sub-catchments of the Burrishoole system. A description of the models used is provided along with a discussion on their applicability for modelling the system hydrology – particularly with respect to their high peat content. The performance of the models in simulating observed flow behaviour is outlined; following this model

projected changes in key flow indices (Q05, Q50 and Q95) under future forcing are discussed.

Chapter 9

The hydrological response of the Burrishoole system to future climate change

9.1 Introduction

In this study a series of high resolution climate scenarios are used to assess the potential impacts of climate change on the hydrology of the Burrishoole catchment. To this end two sub-catchments, which comprise part of the greater catchment Burrishoole system were selected for conducting in-depth modelling analysis. Three different rainfall-runoff models (HBV, HYSIM and TOPMODEL) - each of which was shown to provide a plausible representation of observed system behaviour - were used to explore the hydrological response of each catchment to altered forcing conditions. Dynamically downscaled climate data made available through the ENSEMBLES project (van der Linden & Mitchell, 2009), in-conjunction with a series of statistically downscaled climate scenarios, were used as input to the hydrological models.

Although we can state with a high degree of certainty that the Earth's climate system is likely to change in response to further increases in atmospheric GHGs, due to our limited understanding of feedback mechanisms and the inherent limitations to the predictability of local or regional scale climate, a large amount of uncertainty (of which a large part is irreducible) is implicitly associated with projections of future climate change. In the context of hydrological impact studies this uncertainty is amplified through its interaction with uncertainty in the hydrological models used and the various simplifying assumptions which they incorporate. Uncertainty in the estimated hydrological response poses a major challenge for planners who are required to formulate robust adaptation strategies. Thus, when basing future planning decisions on the results from impact assessments a certain degree of confidence in the projected outcome is considered a prerequisite.

In order to address the various uncertainties which affect local scale climate projections, the output from multiple combinations of driving GCMs, GHG emission scenarios and regionalization techniques/models were considered. With respect to the impacts modelling a robust approach, based primarily on sampling the model space (integrating across both the model structure and parameter values) was used to address this aspect of

uncertainty in the projected hydrological response. To address both parameter and structural uncertainty the GLUE procedure of Beven and Bingley (1992) was employed. In addition the probabilistic framework proposed by Wilby and Harris (2006) was used to combine information from different climate pathways and projected flow series. Adopting this approach allowed the weighting scheme described in the chapter six - formulated based on the ability of competing models to simulate present-day climate conditions - to inform ensemble estimates of future changes in the catchment hydrology. Probability distribution functions are used to quantify the uncertainty stemming from both the climate and hydrological modelling components of the study. Changes in the flow regime are examined for each of three 30 year future horizons (the 2020s (2010-39), 2050s (2040-69) and 2080s (2070-99)) relative to the control period (1961-1990).

9.2 Data

Information on the physical characteristics of the study catchments and the observed datasets used is provided in section 3.5. In total twenty five different climate scenarios are considered, six of which have been downscaled using the SDSM statistical downscaling model. Dynamically downscaled climate projections made available as part of the EU funded ENSEMBLES project (van der Linden and Mitchell, 2009) were also used (see Figure 6.11). Supplementary information on the datasets employed in this study is provided in the proceeding sections; this includes a discussion on the method used to bias correct the RCM data. In addition the quantile mapping technique employed to transfer climate scenarios - corrected using data from the Furnace weather station located at the outlet of the Burrishoole catchment - to each upland catchment is outlined.

9.2.1 Bias correction of RCM data

The inherent limitations to the predictability of regional scale climate means that climate models often produce biased simulations which typically do not reflect the climatology of the study area or model domain; consequently their output may require correction prior to being employed in impact studies. As highlighted in previous chapters, bias may be manifest in the consistent over or under estimation of mean conditions; it can also be evident in other aspects of the modelled series (e.g. the

number of consecutive wet days) (Ines & Hansen, 2006). Correction requires an assumption in the stationarity of the model bias, and when applied care must be taken to ensure that the character and integrity of the climate change signal is maintained (Christensen *et al.*, 2008).

9.2.1.1 Background

As argued by Dosio & Paruolo (2011), bias in the driving data precludes hydrological models simulating a catchment's flow regime in any physically or ecologically meaningful way, consequently applying a bias correction to future climate scenarios is regarded as a necessary step for obtaining climatologically sensible input data. (Shabalova *et al.*, 2003; Wood *et al.*, 2004; Kleinn *et al.*, 2005; Leander & Buishand, 2007; Boé *et al.* 2007; Déqué *et al.*, 2007; Fowler & Kilsby, 2007; Ashfaq *et al.* 2010; Haerter *et al.*, 2011). The general methods used for bias correction include: (a) monthly correction factors (Durman *et al.*, 2001; Fowler & Kilsby, 2007); (b) linear/non-linear transformation functions (Horton *et al.*, 2006; Leander & Buishand, 2007; Leander *et al.*, 2008); (c) probability distribution transfer functions (Déqué, 2007; Block *et al.*, 2009; Piani *et al.*, 2010); and (d) empirical correction factors (Engen-Skaugen, 2007).

Leander and Buishand (2007) applied a power law transformation to correct bias in both the mean and variability of regionally downscaled precipitation data. It was found that this non-linear type correction led to a better representation of the observed extreme daily and multi-day precipitation amounts than the more widely employed linear scaling technique. As a means of preserving the day-to-day variability of the downscaled series, Terink *et al.* (2009) employed the same method used by Leander and Buishand (2007). The correction was applied to both temperature and precipitation downscaled from ERA-15 reanalysis data. Shabalova *et al.* (2003) also employed a power transformation in order to modify the mean and coefficient of variation in downscaled precipitation data.

Kleinn *et al.* (2005) used a seasonally dependent scaling factor to correct biases in precipitation and temperature data downscaled to the Rhine basin. This approach differs to that of Leander and Buishand (2007) in that no correction was applied to the variance of the downscaled series. The authors state that this was an adequate correction method as the mean bias in the regional model used (CHRM) accounted for a significant proportion of its overall bias in the frequency distribution. Their study found that by

using bias corrected data they were able to reproduce more accurately the observed annual flow regime of the study region. Similarly, Fowler and Kilsby (2007) used monthly correction factors to address the bias in dynamically downscaled climate data used to model changes in the hydrology of eight catchments in northwest England. Despite not employing any correction to the variance of the input precipitation series, Fowler and Kilsby (2007) state that the corrected control simulation reproduced the observed climate variability with a reasonable level of skill.

Hay *et al.* (2002) employed a gamma distribution to correct output from the RegCM2 regional model run for four catchments in the continental United States. It was found that when biases in the precipitation and temperature data used were redressed, the accuracy of the simulated runoff series improved significantly; however, despite applying a correction it was found that the modelled precipitation data did not capture the day-to-day variability of the observed series. Ashfaq *et al.* (2010) employed a quantile-based technique to correct dynamically downscaled GCM data. In this study hydrologic simulations conducted using both the corrected and non-corrected series were compared. The results indicated that biases present in the driving data not only affected the realism of hydrological simulations (over a control period of 1961-1990) but, where both the corrected and non-corrected data was used, statistically different hydrological responses to future climate forcing were elicited.

The correction technique employed by Ashfaq *et al.* (2010) follows the quantile mapping method set out by Wood *et al.* (2002, 2004), who applied a bias correction/spatial-disaggregation technique to correct model bias in the frequency distribution of climate data for the study area. The technique was also used to spatially disaggregate the corrected data to a higher resolution grid commensurate with the hydrologic model used. Whereas Wood *et al.* (2004) applied the quantile correction to monthly data; Boé *et al.* (2007) applied it to daily precipitation data. In this case the corrected climate scenarios were used to model the hydrological response of the Seine river basin to projected climate change. Déqué (2007) also employed a quantile mapping approach to bias correct downscaled climate projections; in this case the corrected scenarios were used to examine changes in the frequency of precipitation and temperature extremes over France.

Piani *et al.* (2010a) used quantile mapping to bias correct daily temperature and precipitation fields in climate scenarios obtained from the ENSEMBLES data archive.

The method was developed and tested on two different periods without distinguishing between seasons. The results indicated that the method improved the mean and higher order statistics of the distribution; improvements were also noted in the heavy precipitation and drought index of the corrected dataset. Piani *et al.* (2010b) refined the quantile method by applying more complex non-linear transfer functions to model the relationship between cumulative distribution functions fitted (for the control period) to the observed and model simulated data respectively - in this case the Gamma distribution was used to model rainfall intensity. The correction models were developed and tested over two independent time periods using precipitation and temperature data downscaled from the ECHAM5 GCM; the transfer functions were formulated and applied on a monthly basis. The corrected data was found to improve both the mean and variance of the downscaled data in all but a few regions. Rojas *et al.* (2011) applied the same correction technique as Piani *et al.* (2010b) to the datasets used in their impacts study of changing flood patterns in Europe using climate projections downscaled from the ECHAM5 GCM. Haerter *et al.* (2010) implement a quantile based bias correction technique referred to as the 'cascade bias correction method'. Haerter *et al.* (2010) make the point that the timescales on which corrections are applied impacts how patterns of variability across disparate timescales are represented in the corrected data. For example, daily data and monthly mean data can exhibit different statistical behaviour, and as a result should be adjusted using corrections derived for each independent of one another. The method proposed by Haerter *et al.* (2010) addresses this by generating a cascade of bias correction functions, each of which is formulated and applied on a different timescale.

Kleinn *et al.* (2005) argue that the quantile mapping approach is limited in its application as it requires datasets of a sufficient length to properly characterise the observed climatology. Jakob *et al.* (2011) evaluated seven different empirical-statistical methods used to correct biases in daily precipitation data for the Alpine region. This study found that quantile mapping was the best performing method - particularly with respect to the higher quantiles. Fowler and Kilsby (2007) highlight that quantile mapping assumes the distributions used to correct model bias are time and state invariant, the authors purposefully adopted a scaling type approach to avoid making this assumption. However, both Boé *et al.* (2007) and Déqué (2007) argue that using correction factors implicitly assumes that climate variability is well simulated, in

addition it assumes that systematic error in the variance is negligible and thus not likely to unduly affect results.

Van Pelt *et al.* (2009) investigated two different bias correction techniques applied to dynamically downscaled GCM data. The study focused on the use of bias correction in the context of changing precipitation and river discharge patterns in the Meuse river basin. The first method considered employed a two step approach whereby the proportion of wet days was corrected prior to the wet day average amounts being adjusted (WD bias correction). The second method used employed a power law transformation to correct both the mean and coefficient of variation (MV bias correction). The WD technique was found to perform well in correcting the average values but removed too many successive precipitation events from the series. In contrast the MV approach was found to be less skilful at reproducing the means, but captured the temporal precipitation pattern and standard deviation of the observed series more successfully. When each corrected precipitation series was used as input to a hydrological model, large differences in the projected flow series were found to occur. The authors state that this was due to different correction methods being applied. This study emphasizes the importance of selecting an appropriate correction technique; it also draws attention to the fact that bias correction adds another dimension to the uncertainties which already affect impact studies.

9.2.2.2 *Quantile mapping*

In this study the quantile mapping technique in Boé *et al.* (2007) was applied to the dynamically downscaled precipitation and temperature scenarios from the ENSEMBLES data archive. This method was chosen as over the control period the downscaled scenarios displayed disparate levels of skill in terms of how well each reproduced the observed climatology of the catchment. If a single or fewer number of relatively skilful models were used it may have allowed the application of a scaling approach; however, given the number of model pathways considered, and their often poor ability to simulate some aspect of observed conditions, a more holistic approach based on correcting the frequency distribution of the modelled series was deemed necessary. In addition, given that the mean and variance of the driving data were important in terms of realistically simulating all aspects of the catchment's flow regime, including the higher order statistics, it was important that a correction which considered

both aspects of the distribution was applied. A separate correction was developed for each scenario using data for the period 1961-1990. To ensure the annual cycle of the modelled data was commensurate with the observed climatology the correction was applied on a monthly basis. This was deemed necessary given the importance of accurately simulating both the volume and timing of flow through the catchment. Both these parameters are important for gauging the impact of changes in the hydrological regime on the various stages in the life history of salmonids. In addition applying such a correction was considered important for the hydraulic modelling conducted using the simulated flow data. As the statistical datasets were downscaled directly to the catchment's weather station, the correction was applied to the dynamically downscaled scenarios only.

To derive the correction a linear interpolation between the percentiles estimated for the observed series and each downscaled scenario (estimated over the model control period (1961-1990)) was firstly applied; the fitted transfer function was subsequently used to correct the full data series for each ensemble member (1961-2100). With respect to precipitation, the transfer function was fitted using rainfall amounts only. Figure 9.1

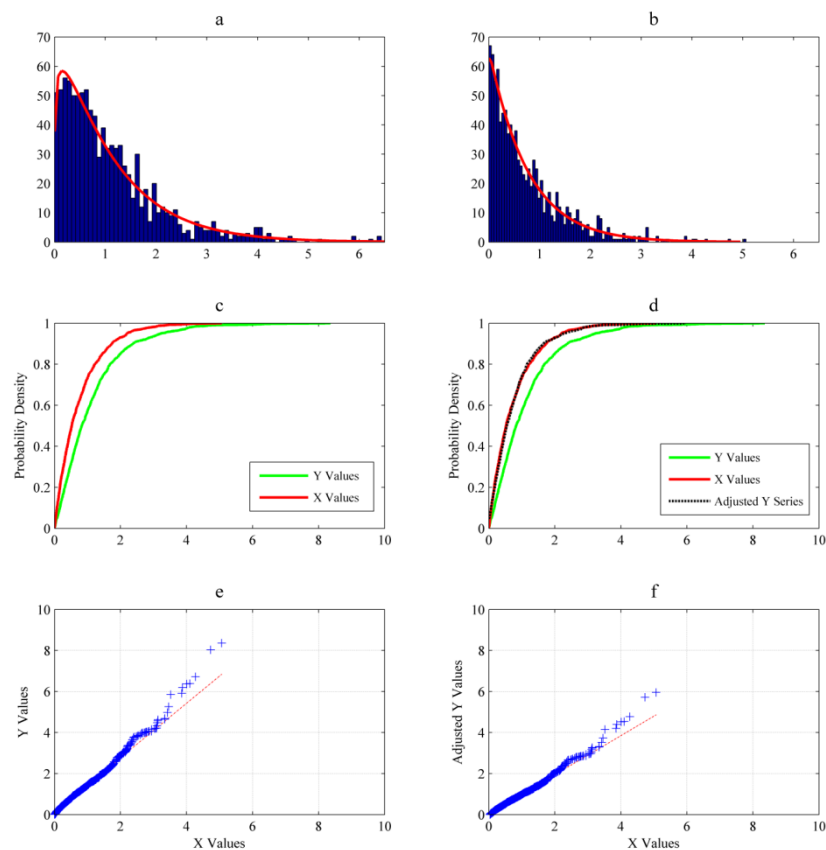


Figure 9.1 Quantile mapping applied to a synthetic dataset. Panels (a) and (b) show the respective differences in the probability distribution functions for each dataset. Shown in panel (c) are the equivalent cumulative distribution functions (cdfs) of the data shown in panels (a) and (b). Panel (d) illustrates how well the cdf of the corrected Y dataset conforms to the cdf of the X dataset. Panels (e) and (f) show the adjustment brought about by applying the correction.

outlines the steps involved in the quantile mapping procedure using two randomly generated sets of data (X and Y) which follow the Gamma distribution. Piani *et al.* (2010b) employ a different approach to quantile mapping whereby a fitted rather than empirical distribution is used. In this study it was found that employing a fitted distribution did not bring about any noticeable improvement in the corrected data above that achieved using the empirical distribution. Figure 9.2 and 9.3 highlight the improvement brought about in the mean and variance of the downscaled precipitation series when the quantile correction method was applied. In the overwhelming majority of cases the correction is successful at reducing the bias in both parameters; however, for some months it either fails to reduce the bias or increases it.

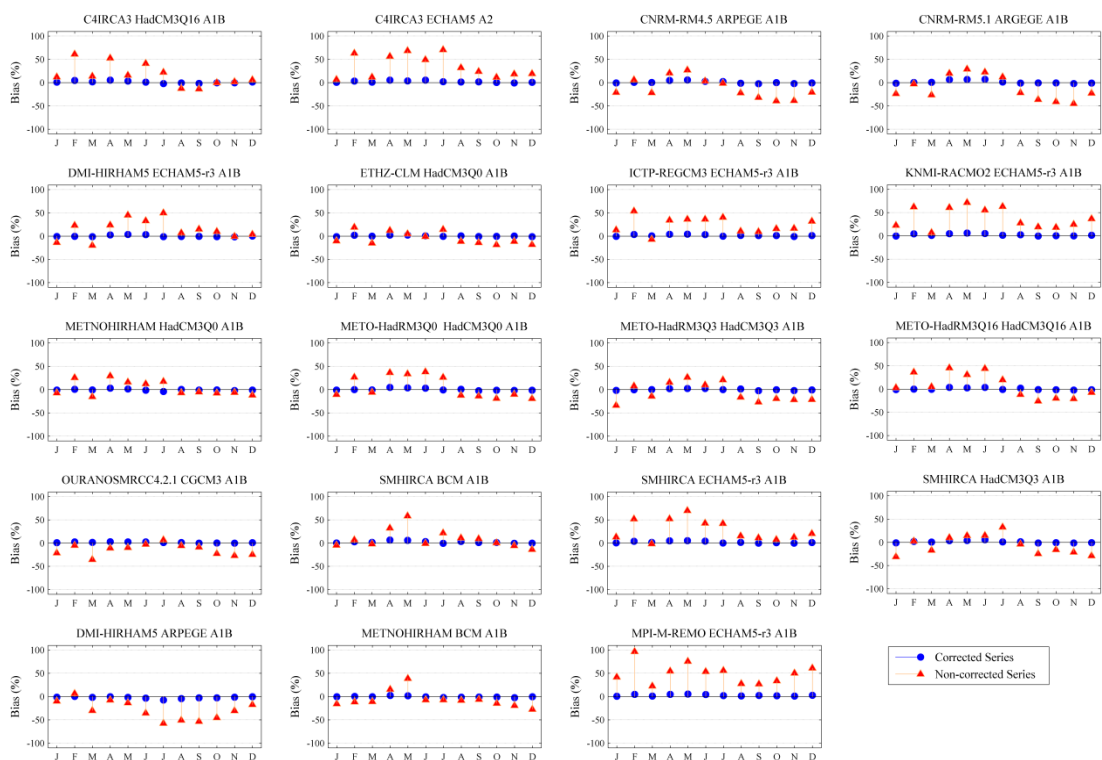


Figure 9.2 Percent bias in the mean of the corrected and non-corrected downscaled precipitation data. Quantile mapping is applied on a monthly basis.

A number of complications arose when applying this method to daily RCM data. Climate models tend to over-estimate the number of days for which rainfall occurs – commonly referred to as the ‘drizzle effect’. To account for this, for each non-rain day (i.e. zero-precipitation) in the modelled series, an observed value was randomly selected in the interval where the observed cumulative distribution function is less than or equal to the modelled probability of a non-rain day. Although this ensures the model simulated proportion of rain days is commensurate with the observations, the correction assumes that the probability of precipitation is the same under future climate forcing as it is under present-day climate. Although this is an important shortcoming of the

method, it is symptomatic of the difficulties associated with correcting both rainfall occurrence and amounts respectively.

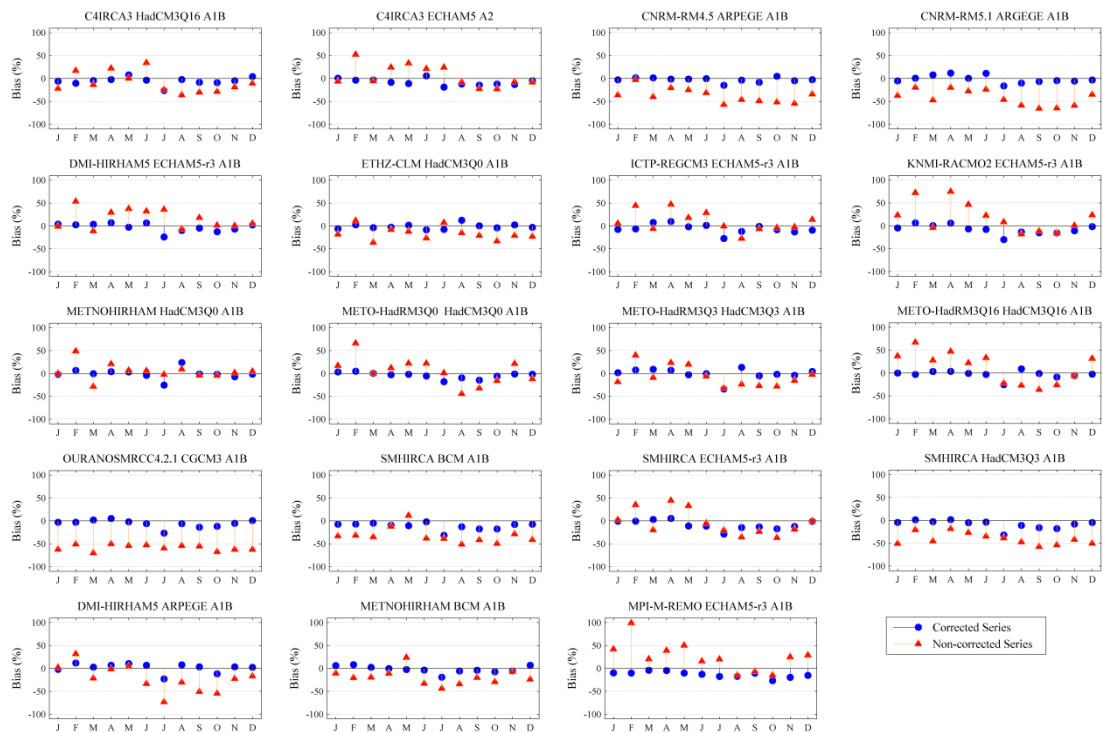


Figure 9.3 Percent bias in the variance of the corrected and non-corrected downscaled precipitation data. Quantile mapping is applied on a monthly basis.

Difficulties lie in balancing the degree to which both parameters are adjusted in order to reproduce the statistics of the observed series. In the case of the correction applied in this study greater emphasis was placed on capturing rainfall amounts. An additional shortcoming in the method arises due to values in the full downscaled series exceeding the largest values occurring over the control period. In accordance with the quantile correction method a simple extrapolation is used to correct these values; however, in doing so it is assumed that the linearly derived correction is applicable to values in the tails of the distribution for which the transfer function has not been calibrated. This may constrain higher values in an unrealistic way, affecting how extreme and higher quantile events are represented in the downscaled series.

9.2.2 Mapping of climate scenarios within the catchment

When developing the hydrological model for each catchment, model simulations which used the weighted average rainfall series (averaged across records from individual

upland gauging sites; see section 3.5.3) as their input data displayed far superior efficiency scores during calibration when compared to simulations which used observed precipitation from the Furnace weather station. This is due to the localized nature of precipitation within each sub-catchment - which is to a large extent driven by the complexities of the local terrain and the strong influence of topographic features (e.g. elevation, slope, aspect). Consequently the observed precipitation series from the Furnace station (situated on a lowland site at an altitude of ~14 m) does not fully reflect the true spatial variability of precipitation within each sub-catchment, nor does it capture the influence of orographic enhancement on the precipitation regime of upland areas.

Ideally, in order to capture locally specific conditions, precipitation scenarios would have been statistically downscaled for each individual sub-catchment; however, due to the length of the records available for upland gauging points, precipitation data could not be downscaled directly to these sites. Instead it was only possible to downscale rainfall to the Furnace station, for which records of a sufficient length were available to develop robust transfer functions. To overcome this, quantile mapping was employed to construct precipitation scenarios for each study catchment using data downscaled to the Furnace station.

As applied in this study, the technique establishes a relationship between the magnitude of a rainfall event recorded at Furnace and the 'same' event observed in an upland catchment. The method has previously been employed in a downscaling context as a bias correction technique (Wood *et al.*, 2004; Boé *et al.*, 2007; Déqué, 2007). To apply the method a linear transfer function (calculated using wet-day amounts only) was used to model the relationship between observed precipitation recorded at Furnace and the precipitation series (calculated based on a weighted average of the records from individual upland gauges) for each study catchment. In order to obtain the upland precipitation scenarios the formulated mapping function was then applied to the point scale scenarios downscaled to the Furnace weather station. The mapping function generally indicated that the magnitude of rainfall events recorded at Furnace were lower than those experienced in upland areas – this was particularly evident for higher quantile events.

Q-Q mapping was also applied to the dynamically downscaled climate scenarios. In this case the data had already been bias corrected using long-term records from the Furnace

station. Given the short length of the data series from each catchment it was not possible to determine a robust function whereby the RCM data could be corrected on a catchment-by-catchment basis. Thus the RCM data was firstly corrected using records from Furnace; following this the datasets were mapped to each sub-catchment using the same technique applied to the statistically downscaled scenarios.

Used in this context quantile mapping allows for some consideration of the influence which elevation is known to have on precipitation receipts - and by extension the hydrological regime of upland catchments. Other methods for translating the rainfall scenarios to upland areas, including correction factors, regression models and spatial interpolation techniques were examined; however, given the short length of the records available from upland gauges, as well as the large proportion of missing data in their records, these methods were considered unsuitable or were impractical for use. In addition, by using the Q-Q technique an adjustment could be applied to both the mean and variance of the rainfall series, thus overcoming some of the deficiencies associated with more conventional interpolation and scaling type approaches.

9.2.3 Evaporation Data

RCMs generally do not provide a direct measurement of evaporation from the land surface, consequently information on this parameter must be obtained using modelled data for other meteorological variables. In this study evaporation was estimated by applying the Hargreaves equation to the downscaled temperature series (Hargreaves & Samani, 1982; 1985). This equation can be written as:

$$ET_0 = 0.0023R_a(T + 17.8)\sqrt{T_{max} - T_{min}}$$

here ET_0 is the reference evapotranspiration rate (mm d^{-1}), R_a is the water equivalent of the total incoming extraterrestrial solar radiation (mm d^{-1}), T_{max} , T_{min} and T are daily maximum, minimum and mean air temperature respectively - where T is calculated as the average of T_{max} and T_{min} - finally 0.0023 is the empirical coefficient proposed by Hargreaves and Samani (1985).

It must be recognized that estimating evaporation using methods which employ temperature as the sole predictor may introduce bias to the driving data used in hydrological impact studies. This is related to the fact that temperature is only one of a

number of variables which determine evaporation rates (e.g. wind speed, relative humidity) (Ekström *et al.*, 2007). In catchments for which evaporation losses have a significant influence on the hydrological regime, the potential to introduce bias by using temperature driven evaporation scenarios is of particular importance. Given the suggested increases in air temperature, the potential for bias to be introduced in this way is likely to be enhanced when using model projected data. As noted by Kay and Davies (2008), it may be that changes in atmospheric variables other than temperature have a greater bearing on overall changes in PE. It is therefore desirable that the methods used for calculating evaporation should incorporate additional variables (e.g. wind speed, vapour pressure). By providing a better representation of the physical processes governing evaporation, formula which include additional parameters are likely to provide a closer approximation to the true rate of evaporation, and by extension its response to altered forcing conditions (Brandsma, 1995). Variations in the methods used to derive evaporation data from climate model output have been shown to be an important source of uncertainty in the results of hydrological impact studies (Arnell, 1999; Kay & Davies, 2008).

In this study the Hargreaves formula was favoured over more complex estimation methods (e.g. Penman-Monteith, 1965) which generally require a larger set of atmospheric variables - some of which may be less well simulated by climate models. The Hargreaves formula was thus employed to minimize the potential uncertainty in the evaporation data. It was also used in order to overcome the requirement to bias correct a larger set of climate parameters, which may have proved problematic given the lack of observed data for some variables.

9.3 Hydrological model selection

In this study an ensemble of three different CRR models was used to explore the hydrological response of the selected catchments to a change in climate forcing. The confounding influence which other sources of uncertainty (e.g. input/output, model parameters, etc.) have present difficulties when attempting to validate a given model structure; thus it is a more pragmatic approach to address structural and model concept uncertainty through the use of multi-model ensembles (e.g. Refsgaard *et al.*, 2006; Jiang *et al.*, 2007; Marshall *et al.*, 2007a, 2007b; Bastola *et al.*, 2011; Neuman *et al.*, 2012). Model choice depends on several factors including the research question posed and the

quality of available data (Ng & Marsalek, 1992; Xu, 1999a; 1999b). Furthermore, as the models constitute a simplified version of reality, it is important that the selected models capture those aspects (i.e. hydrologic processes or catchment properties) of the observed system which are most important for controlling runoff generation (Bronstert, 2004).

In this study model selection posed a number of difficulties relating primarily to the physical characteristics of the study catchments, their potential hydrological response to altered forcing and the limitations of the observed data. Models were required which could adequately simulate the 'flashy' nature of the catchment response and cope with the dearth of any real storage capacity. Consequently the model's ability to transition from dry to wet conditions and vice versa was important. Additionally, given the extensive coverage of blanket peat across the system, it was important that the models could adequately capture its influence on the catchment hydrology.

An analysis of observed data from the Glenamong catchment suggests that the rainfall-runoff relationship is essentially a linear one. Although this highlights the responsive nature of the system, it masks the complexities of the underlying processes controlling runoff generation. Research into the hydrology of peat dominated systems suggests that the responsiveness of the study catchments is most likely a product of their extensive peat coverage and steep topography (e.g. Burt *et al.*, 1990; Price, 1992; Evans *et al.*, 1999; Holden, 2000; Holden & Burt, 2002; 2003). Holden (2005) states that it is mistaken to assume peatlands (a) operate as a long-term store to sustain baseflow and (b) act as a soakage area to attenuate peak flows. Holden (2005) indicates that it is actually the opposite which is true, stating that peat systems are highly responsive to precipitation events; in addition their baseflows are typically discontinuous and poorly maintained (Price, 1992; Evans *et al.*, 1999; Holden & Burt, 2003). Holden (2005) highlights that the high water tables which characterise peatland systems mean there is little available storage capacity with which to attenuate flood events, thus peatlands are generally a source area for flooding.

In their study into runoff production in catchments covered predominantly by blanket peat - focusing on the Trout Beck catchment situated in the northern Pennines (UK) - Holden and Burt (2003) highlighted the importance of both saturation excess and near surface flow as runoff generating mechanisms, the authors also suggest that infiltration excess overland flow plays an important role in determining the runoff response. This is an assertion also made by Burt *et al.* (1990) who state that, given their low infiltration rates, blanket peatlands may be one of the only natural examples of areas which produce

Hortonian overland flow in the UK. Similarly Holden (2005) indicates that the responsiveness of peat systems can be attributed to the dominance of saturation excess overland flow together with the rapid throughflow of soil water in macropores and soil pipes in the upper peat layers. Holden & Burt (2003) state that, irrespective of the peat thickness, flow in the upper 5 cm of the matrix has a significant bearing on the runoff response. Similarly, Warburton *et al.* (2004) highlight that 93% of runoff occurs from the surface layer in peat systems, in contrast only 6% occurs from a depth of 1 to 5 cm - 0.05% occurs from a depth of 5 to 10 cm.

According to Holden and Burt (2003) most models of peatland hydrology are groundwater based and as such do not adequately capture runoff production and water movement at or close to the peat surface. With this in mind, it was important that the models used in this study were able to capture those hydrologic processes which occur in the uppermost soil and interception layers - particularly as groundwater plays a much less significant role in the hydrological regime of each catchment.

Climate change has the potential to significantly alter the peat matrix (e.g. enhanced summer drying and winter wetting), and by extension the hydrologic processes which characterise peatland systems (e.g. antecedent conditions, hydraulic conductivity, moisture retention, flow pathways, vegetation cover, etc.). Warburton *et al.* (2004) highlights the influence which cracking in the peat surface (under dry summer conditions) can have on the development of vertical pathways and the creation of permanent extensions to the pipe network. Consequently the issue of stationarity in the hydrologic processes governing system behaviour - as well as in the response of the hydrological models - under altered climate conditions may be of greater concern in the case of peatland catchments. Pilling and Jones (2002) make this point in their assessment of climate change impacts on the Wye catchment, whose soils are largely comprised of blanket peat and peaty podzols. Pilling and Jones (2002) state that given the possible non-linearity of the soil response - manifest in increased soil drying and the development of macropores in the peat matrix - the models may be at risk of underestimating high flow events. This is compounded by the fact that soil conditions under future climate forcing may only have been observed in the historical record under extreme conditions, and consequently little may be known about the long term catchment response or the potential validity of hydrological models when applied in a climate change context.

To address some of the issues discussed above, and as a means of addressing some of the wider issues relating to model structure and parameter uncertainty, three different CRR models were used in this study: HBV (Bergström, 1976; 1995), TOPMODEL (Beven and Kirkby, 1979; Beven *et al.*, 1995) and HYSIM (Manley, 2006). Each model represents a differing conceptualization of system processes; they also differ with respect to their level of complexity (i.e. the number of parameters) and data requirements. With regards to capturing those processes which contribute to runoff production, each model incorporates routines which account for soil moisture fluxes - acknowledged to be important in determining the hydrology of peatland systems. In addition the models appear to be robust with respect to the complex topography of the study area and the responsiveness of the flow regime. The influence of the soil layers and the importance of the soil moisture dynamics is reflected in the sensitivity analysis conducted for each model (see section 9.4).

9.3.1 HBV-light

HBV-light is a semi-distributed rainfall-runoff model which simulates catchment discharge on a daily time-step using precipitation, temperature and potential evaporation as input data. The basic concepts which underpin the model workings are discussed by Bergström (1991; 1992). HBV was developed by the Swedish Meteorological and Hydrological Institute (SMHI) for use in Nordic countries but has since been applied successfully in different regions under diverse climatological and geomorphic conditions (e.g. Lindström & Rodhe, 1986; Brandt *et al.*, 1988; Bergström *et al.*, 1992; Saelthun, 1996; Arheimer & Brandt, 1998; Bergström & Graham, 1998; Bergström *et al.*, 2001; Siebert & Beven, 2009; Steele-Dunne *et al.*, 2008; Konz & Seibert, 2010).

This study employs version 3.0.0.0 of HBV-light (Seibert, 1997, 1999, 2000, 2005). The model consists of three main components including: (i) subroutines for snow melt and accumulation, (ii) subroutines for soil moisture accounting and (iii) a response function and river routing subroutines (Figure 9.4). The soil box can be sub-divided into a series of 'zones' based either on elevation and/or vegetation type - for which the model makes calculations independently. Applying the model in a spatially disaggregated manner allows the heterogenous nature of the catchment and the influence which elevation has on the input variables and snow routine to be incorporated. Given the size of the catchments considered, the homogeneity of their

land cover and the redundancy of the snow routine, it was assumed that sub-dividing the catchments would add little to the model's predictive power and may introduce bias by way of the disaggregation process. Of the models considered HBV incorporates (with respect to the total number of model parameters) the greatest number of process parameters (Table 9.1); thus issues of parameter uncertainty and overfitting may be more relevant to this model.

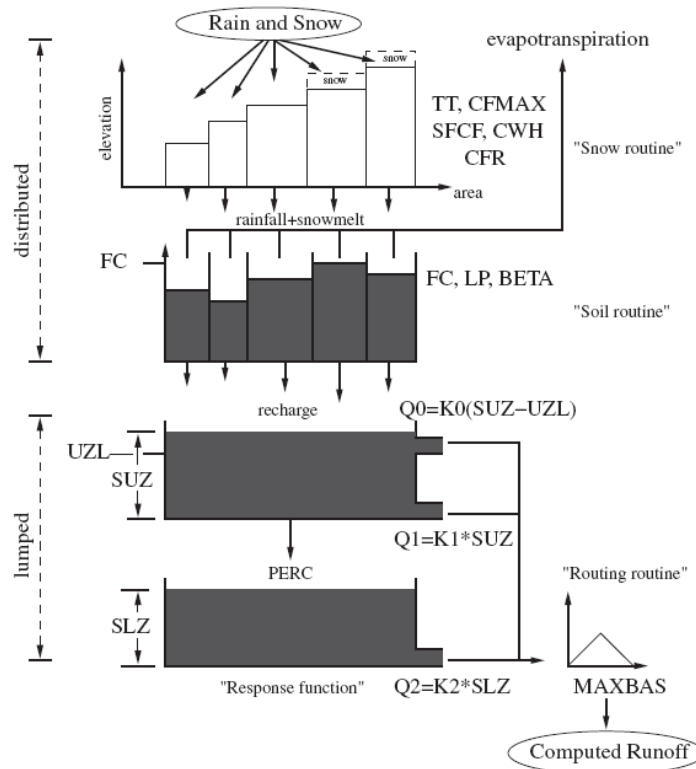


Figure 9.4 HBV-light model structure. (Source: Siebert, 2000)

Parameter	Explanation	Min	Max	Unit
<u>Snow Routine</u>				
<i>TT</i>	Threshold Temperature	-	-	°C
<i>CFMAX</i>	Degree-day factor	-	-	mm °C d ⁻¹
<i>SFCF</i>	Snowfall Correction factor	-	-	-
<i>CWH</i>	Water Holding Capacity	-	-	-
<i>CFR</i>	Refreezing Coefficient	-	-	-
<u>Soil and Evaporation Rate</u>				
<i>FC</i>	Maximum Soil Moisture (SM)	50	600	mm
<i>LP</i>	SM threshold for reduction of evaporation	0.3	1	-
<i>BETA</i>	Shape coefficient	0.5	6.0	-
<u>G.W. And Response Routine</u>				
<i>K₀</i>	Recession Coefficient	0.04	0.5	d ⁻¹
<i>K₁</i>	Recession Coefficient	0.01	0.4	d ⁻¹
<i>K₂</i>	Recession Coefficient	0.001	0.20	d ⁻¹
<i>UZL</i>	Threshold for K ₀ outflow	0	40	mm
<i>PERC</i>	Maximal flow from upper to lower GW-box	0	3	mm d ⁻¹
<i>MAXBAS</i>	Routing, base of weighting function	1	2	d

Table 9.1 HBV-light: model parameters and sampling ranges.

9.3.2 TOPMODEL

TOPMODEL (TOPography based hydrological MODEL) was initially developed with the aim of describing the spatial pattern of storm flow generation in upland catchments having a humid temperate climate (Beven & Kirkby, 1979; Beven *et al.*, 1984). The model has since has been employed under a diverse array of climate and hydrologic conditions. Many alterations have been made to the basic model by users to suit their individual requirements, highlighting its flexibility and usefulness as a modelling tool (e.g. Beven & Wood, 1983; Robson *et al.*, 1992; Band *et al.*, 1993; White & Running, 1994; Beven *et al.*, 1995; Duan & Miller, 1997; Scanlon *et al.*, 2000; Beven & Freer, 2001b; Walter *et al.*, 2002; Cameron, 2006). In this study the R package ‘topmodel’ was used (Buytaert, 2011); this package implements the 1995 FORTRAN version of TOPMODEL devised by Keith Beven. The theoretical basis of the model is outlined by Beven and Kirby (1979) and Beven (1997a, 1997b). TOPMODEL can be described as a quasi-distributed rainfall-runoff model based on the variable-source-area concept of streamflow generation, whereby the dynamics of surface and sub-surface contributing areas are explicitly modelled (Beven & Kirkby, 1979; Beven *et al.*, 1995; Choi & Beven, 2006). It uses rainfall and potential evapotranspiration to simulate streamflow on a daily or sub-daily time-step. The model combines the computational efficiency and data requirements of a conceptual model with the physical theory offered by a distributed model (Beven *et al.*, 1995). As the model parameters can be estimated from field measurements, it is frequently described as a ‘physically based’ model (Beven & Kirkby, 1979). However, according to Franchini *et al.* (1996), given that it is not fully distributed it may be optimistic to describe it in this manner; indeed Franchini *et al.* (1996) refer to it as a ‘variable contributing area conceptual model’ rather than a physical model, citing a number of reasons for this including its conceptual structure and the requirement to optimize a number of the model parameters.

The most important element in the application of TOPMODEL is the topographic index which is used to model how the catchment’s topography influences its hydrological behaviour. The index provides a basis for simulating sub-catchment scale variations in both soil moisture deficits and the localized water table response; from this it can be determined where saturated land surfaces conducive to overland flow are likely to develop. Total flow is calculated as the sum of surface runoff and flow in the saturated zone. Surface runoff is itself estimated as the sum of two components - infiltration excess (Hortonian runoff) and saturation excess overland flow (Dunne runoff). The

local topography has a significant influence on the hydrological regime of the study catchments. The suitability of TOPMODEL for use in this study is related to its inclusion of routines representing infiltration and saturation excess overland flow – both of which are known to be important for runoff generation in peat dominated systems (Holden & Burt, 2003). The structure of the 1995 version of TOPMODEL is shown in Figure 9.5.

Nine model parameters were included in the Monte Carlo simulation analysis (Table 9.2) - two of which (Sr0 and qs0) are initialisation parameters. As the model incorporates a relatively small number of parameters, it limits the risk of over parameterization and reduces the difficulties associated with sampling the parameter space (Franchini *et al.*, 1996).

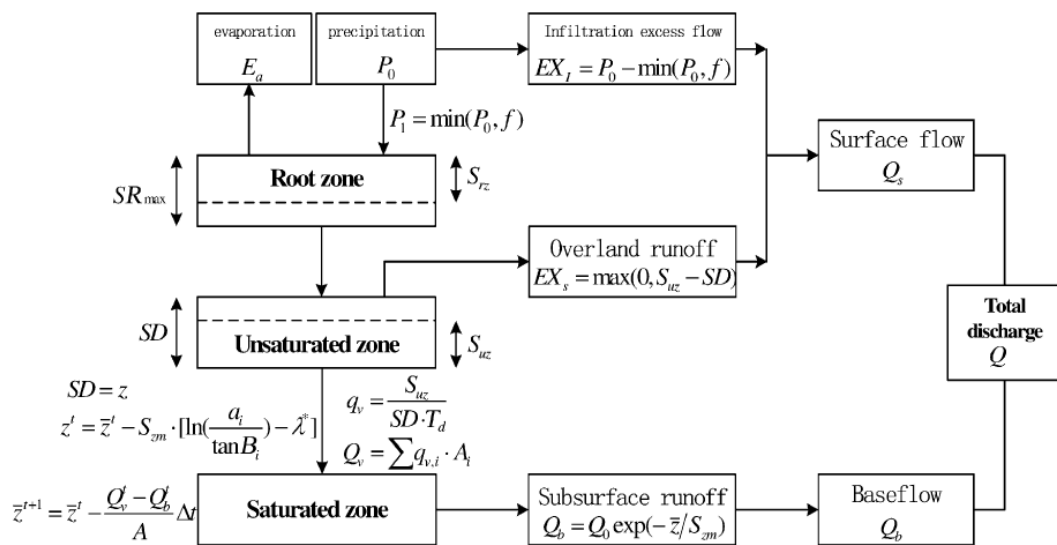


Figure 9.5 TOPMODEL: model structure (Source: Lin *et al.*, 2010)

Parameter	Explanation	Min	Max	Unit
$\ln(T0)$	The natural log of the effective transmissivity of the soil when just saturated. A homogenous soil throughout the catchment is assumed.	-2	1.5	m^2/h
m	Controls the rate of decline of transmissivity in the soil profile	0	0.2	m
$Srmax$	Maximum root zone storage deficit	0	2	m
td	Unsaturated zone time delay per unit storage deficit	0	3	$h\ m^{-1}$
vr	Channel flow inside catchment	100	1000	$m\ h^{-1}$
$K0$	Surface hydraulic conductivity	0	0.01	$m\ h^{-1}$
CD	Capillary drive (Morel-Seytoux and Khanji, 1974)	0	5	
$Sr0$	Initial storage deficit in the root zone (an initialisation parameter)	0	0.02	m
$qs0$	Initial subsurface flow per unit area (an initialisation parameter)	0	4e-5	m

Table 9.2 TOPMODEL: model parameters and sampling ranges.

It must be acknowledged that TOPMODEL has been the subject of some criticism. Siebert (1997) cites the assumptions on which the model is based - including steady state flow rates and the spatially uniform recharge of groundwater - as key shortcomings which prohibit the model from correctly simulating the temporal and spatial dynamics of movement in the water table. Siebert (1997) suggests that TOPMODEL should move towards incorporating a more spatially explicit consideration of water table dynamics. To derive the topographical index used by the model data from a Digital Elevation Model (DEM) is required (Quinn *et al.*, 1995); for this study a DEM with a resolution of 20m×20m was used.

9.2.3 HYSIM

HYSIM (Manley, 2006) is a lumped rainfall-runoff model which uses precipitation and potential evaporation as input data to simulate streamflow using parameters which describe the catchment hydrology and channel hydraulics in a realistic way. As it incorporates a number of physically based parameters HYSIM has previously been described as a 'physical-process based model' (Pilling & Jones, 1999). The suitability of the model for conducting impact assessments is reflected by the fact it has a long history of use by the UK Environment Agency. Pilling and Jones (1999) employed HYSIM to simulate effective runoff (based on a 10 km × 10 km grid) for the UK under baseline and projected climate conditions. In a separate study Pilling and Jones (2002) used the model to assess the impact of climate change on streamflow in the upper Wye catchment. As highlighted above, the Wye catchment is characterised as having a high peat content; thus the efficiency scores (NS score over validation period: 0.856) returned during model testing are suggestive of its applicability to upland peat systems. HYSIM has also been employed for conducting climate change impact studies in an Irish context (Murphy & Charlton, 2006, 2009). Importantly for this study HYSIM has already been applied to model the hydrology of the Glenamong catchment (Figure 3.2) (Linda *et al.*, 2005). Here the model was used as part of a study examining soil erosion and sediment transport. Although only an eight month period was available for model calibration, the results suggested that runoff was generated predominantly through quick overland flow; the model simulations also suggested the catchment possessed little storage capacity. This is commensurate with the assessment of peat dominated systems provided by Holden (2005).

In this study the most recent version of the HYSIM (HYSIM 5.00; build 2.13) was used. The model outputs data for a range of variables including streamflow, actual evapotranspiration, soil moisture and groundwater levels. Seven natural stores including: snow, interception, upper soil horizon, lower soil horizon, transitional groundwater, groundwater and minor channels, are conceptually represented in the model (Figure 9.3). The parameter values determine the holding capacity of each respective store and controls the rate at which transfer between them occurs.

The model incorporates several physically based parameters whose values must be estimated directly from the study area - albeit at a lumped scale. The model's physical grounding is one its strengths, particularly in a climate change context where stationarity in the model parameters is a key assumption. In this study the physical parameters were estimated using GIS analysis of soil type, land-use cover and the productivity of the catchment geology (see section 3.2). Using high resolution topographical datasets reduces the subjectivity associated with specifying the physical parameters (Schumann, 2000). Although the physical properties of the catchment must be aggregated to derive the final parameter values, given the uniformity of soil and land-cover type across the study catchments, it was thought that lumping the catchment characteristics would not affect model performance to such a degree that representative sub-catchments should be used. HYSIM includes a number of hydraulic parameters (listed below) which relate primarily to the dimensions of the stream channel. High resolution aerial photographs taken of the study area, along with a digital elevation model (DEM) were used to estimate the hydraulic parameters. The model also incorporates four process parameters (two interflow and two permeability parameters) each of which is associated with the soil texture and land-use.

The user manual provides values for the model parameters which should be used where peatland is present - suggesting the model's potential applicability to peat type systems. Seven of the model's parameters (Table 9.3) were considered in the subsequent Monte Carlo simulation analysis. Included in the analysis are the model's four identified process parameters. Those parameters representing the groundwater recession rate, rooting depth and Pore Size Distribution Index (PSDI) were also estimated using MC analysis. The sampling ranges were set based on preliminary simulations and are within the range of values specified by the HYSIM manual (Manley, 2006).

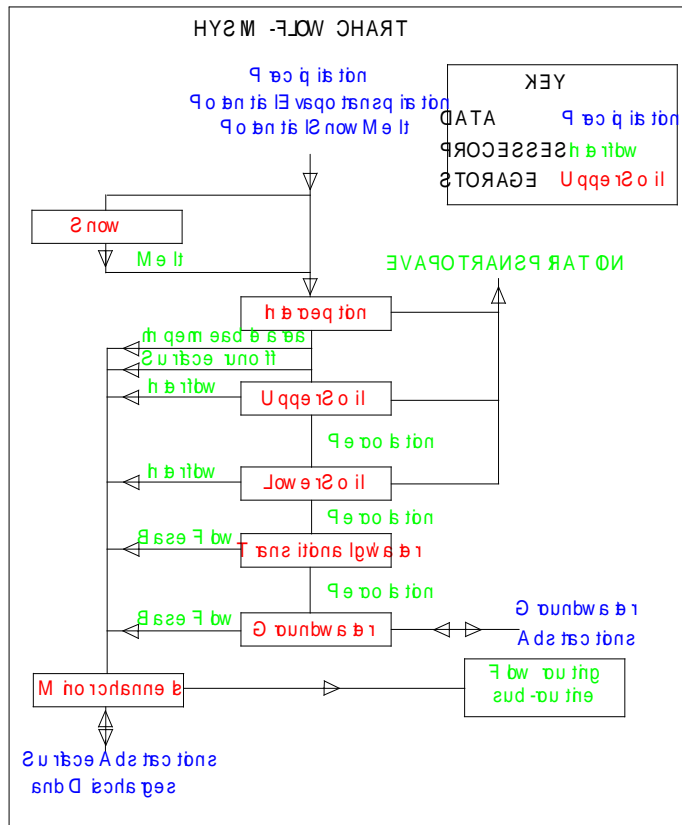


Figure 9.6 HYSIM: model structure (Source: Manley, 2006)

Parameter	Min	Max	Unit
Saturated Permeability at the Horizon Boundary	1	1000	mm h ⁻¹
Saturated Permeability at the Base of the Lower Horizon	1	100	mm h ⁻¹
Interflow Run-off from the Upper Horizon at Saturation	1	1000	mm h ⁻¹
Interflow Run-off from the Upper Lower at Saturation	1	100	mm h ⁻¹
Groundwater Recession	0.5	0.9	
Pore Size Distribution Index (PSDI)	.1	.9	
Rooting Depth	200	1000	mm

Table 9.3 HYSIM: model parameters and sampling ranges.

9.4 Sensitivity analysis

Conducting a sensitivity analysis is important for determining a model’s suitability to the physical and climatic conditions presented by the study catchment (Abebe *et al.*, 2010). It is also an important step in the calibration process. According to Sieber and Uhlenbrook (2005) a sensitivity analysis can: (i) identify the parameters which are most sensitive; (ii) highlight whether the model’s reaction to alterations in the parameter

values or boundary conditions are realistic; (iii) determine whether the conceptual outlay of the model is appropriate for realistically capturing system behaviour; and (iv) be used to reduce the model structure to its most elemental components. The Regional Sensitivity Analysis (RSA) (Spear & Hornberger, 1980; Hornberger & Spear, 1981) or Hornberger-Spear-Young method is a relatively simple way to qualitatively assess model sensitivity using Monte Carlo simulation. The method has the advantage of allowing parameter sensitivity to be examined without the requirement to hold parameter values constant between successive model runs. Sieber and Uhlenbrook (2005) compared the RSA method to a more complex regression-based sensitivity analysis which considered time-dependency as a factor affecting parameter sensitivity. The results of this study indicated that the parameter sensitivity was indeed temporally dependent. Whilst more complex methods than the RSA exist, Saltelli (2000) argues that, irrespective of the method employed, the most important issue is that some measure of parameter sensitivity is provided.

In this study the RSA method was used to assess parameter sensitivity. To conduct the analysis 10,000 parameter values were drawn at random from the pre-defined parameter space. The model parameters considered and their respective ranges are specified above (Tables 9.1 to 9.3). The NS (Nash-Sutcliffe) efficiency criterion was used to partition the parameter values into behavioural and non-behavioural groups; from this the cumulative distributions for each parameter and both groups were plotted (Figure 9.7 to 9.9). For the analysis a NS threshold value of 0.70 was used to identify behavioural parameter sets. A measure of parameter sensitivity is given by the degree to which the accumulated distribution functions from both groups converge/diverge. Where the model response is sensitive to a given parameter a divergence between the curves is evident; however, the absence of an overlap between the accumulated distributions is not necessarily a pre-requisite for deeming a parameter to be insensitive. This is because it is possible that intercorrelation may mask the true sensitivity of the model parameters. The Kolmogorov–Smirnov test (significance level 0.05) was applied to quantify the distance between the distribution functions of the behavioural and non-behavioural groups (Table 9.4 to 9.6). The sensitivity analysis was carried out using the Glenamong sub-catchment only and the full length of the observed data series was used. The dot plots for each model are shown in Appendix III; these plots are used to project the n -dimensional parameter space onto a single axis.

Figure 9.7 shows the empirical cumulative distribution function estimated for the nine parameters used in HBV-light. With the exception of *PERC* and *K2*, each of the parameters exhibits some degree of sensitivity. *PERC* determines the percolation rate from the upper to lower groundwater storage box and *K2* is the recession coefficient for the lower groundwater zone. The relative insensitivity of both parameters reflects the negligible contribution groundwater makes to catchment discharge. Those parameters relating to the soil moisture routine, including *FC*, *BETA* and *LP*, appear to be moderately sensitive; however, the analysis appears to suggest that the most sensitive parameters include the routing parameter (*MAXBAS*) and those relating to the upper groundwater zone (*K0*, *UZL* and *K1*). Both *K0* and *UZL* control flow peaks and the catchment's responsiveness to precipitation events; the sensitivity of these parameters is in keeping with the 'flashy' nature of the flow regime.

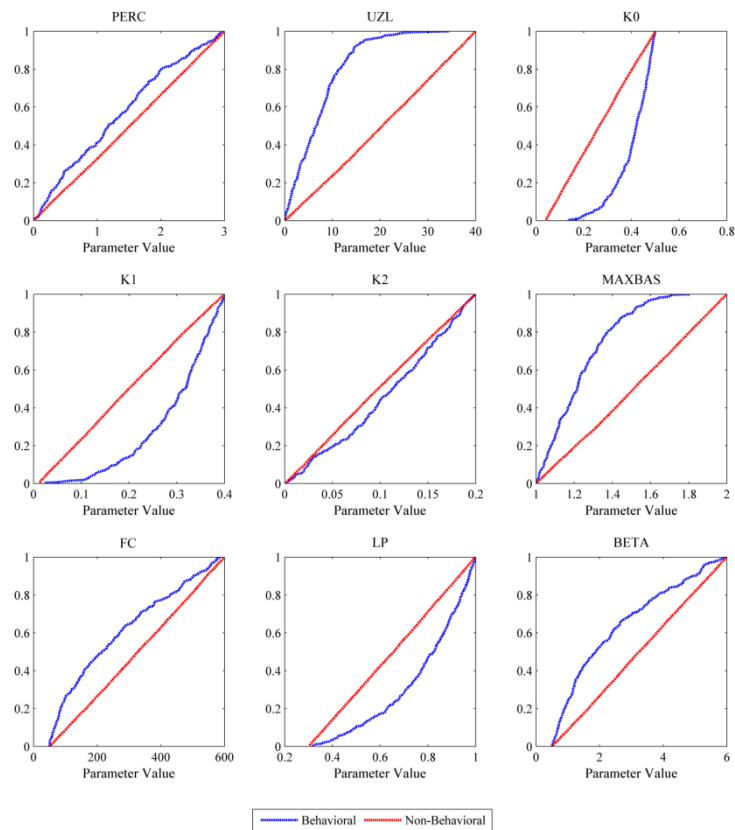


Figure 9.7 Results of the regional sensitivity analysis (RSA) conducted for the nine process parameters used in HBV-light. Parameter sensitivity is expressed by the accumulated distribution functions formulated using the Nash Sutcliffe (NS) efficiency scores returned for individual parameter sets (y-axis). Parameters are classified as behavioural if they attain a NS score of ≥ 0.7

Parameter	PERC	UZL	K0	K1	K2	MAXBAS	FC	LP	BETA
K-S Statistic	<u>0.14</u>	<u>0.57</u>	<u>0.48</u>	<u>0.37</u>	<u>0.11</u>	<u>0.45</u>	<u>0.22</u>	<u>0.29</u>	<u>0.27</u>

Table 9.4 Results of the Kolmogorov–Smirnov test (significance level 0.05) used to quantify differences between the accumulated distribution functions of the behavioural and non-behavioural parameter sets for the HBV-light model. Differences are highlighted as being significant if underlined.

Figure 9.8 plots the results of the sensitivity analysis conducted for TOPMODEL. Both $Sr0$ and $qs0$ are initialization parameters and the plots shown in Figure 9.8 are indicative of the model sensitivity to initial conditions. Of the remaining parameters $Srmax$ (K-S value of 0.73; Table 9.5) appears to be the most sensitive. This parameter controls the maximum allowable storage deficit and is important for the routing of precipitation through the upper soil horizon; it is also important for the generation of overland flow. The m and $lnTe$ parameters - which determine the rate of decline in the transmissivity of the soil profile and the effective transmissivity of the soil when saturated - also appear to be sensitive. In contrast the capillary drive and surface hydraulic conductivity are not sensitive; both these parameters are related to runoff generated through infiltration excess overland flow. Their low K-S score indicates that this runoff mechanism may not be important.

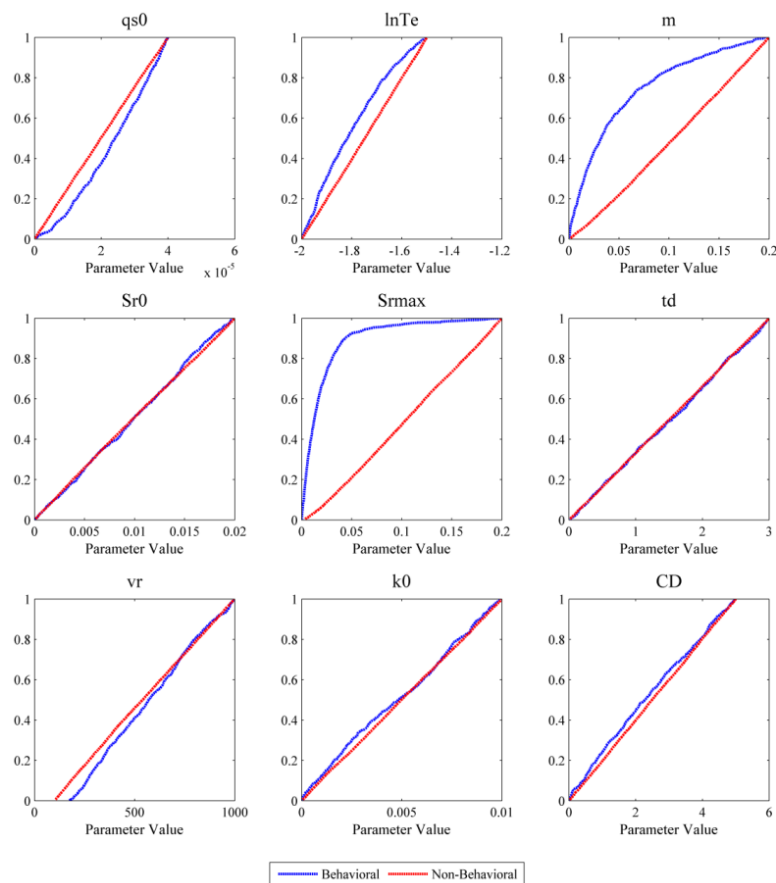


Figure 9.8 Results of the regional sensitivity analysis (RSA) conducted for TOPMODEL. Both $Sr0$ and $qs0$ are initialization parameters. . Parameter sensitivity is expressed by the accumulated distribution functions formulated using the Nash Sutcliffe (NS) efficiency scores returned for individual parameter sets (y-axis). Parameters are classified as behavioural if attaining a score ≥ 0.7

Parameter	qs0	lnT0	m	Sr0	Srmax	td	vr	k0	CD
K-S Statistic	<u>0.53</u>	<u>0.16</u>	<u>0.43</u>	0.04	<u>0.73</u>	0.02	<u>0.10</u>	<u>0.06</u>	<u>0.06</u>

Table 9.5 Results of the Kolmogorov–Smirnov test (significance level 0.05) used to quantify differences between the accumulated distribution functions of the behavioural and non-behavioural parameter sets for TOPMODEL. Differences are highlighted as being significant if underlined.

Figure 9.9 shows the empirical cumulative distribution functions of the seven parameters from HYSIM considered in the sensitivity analysis. Those parameters associated with the upper soil horizon, including the saturated permeability at the horizon boundary and interflow in the upper horizon are generally more sensitive than those associated with the lower soil horizon; in addition, the parameter controlling groundwater recession appears relatively insensitive. The sensitivity analysis suggests that both the PSDI and rooting depth are important parameters - the former determines the holding capacity of the upper and lower horizons respectively, whilst the latter controls the hydrological response of the soil matrix.

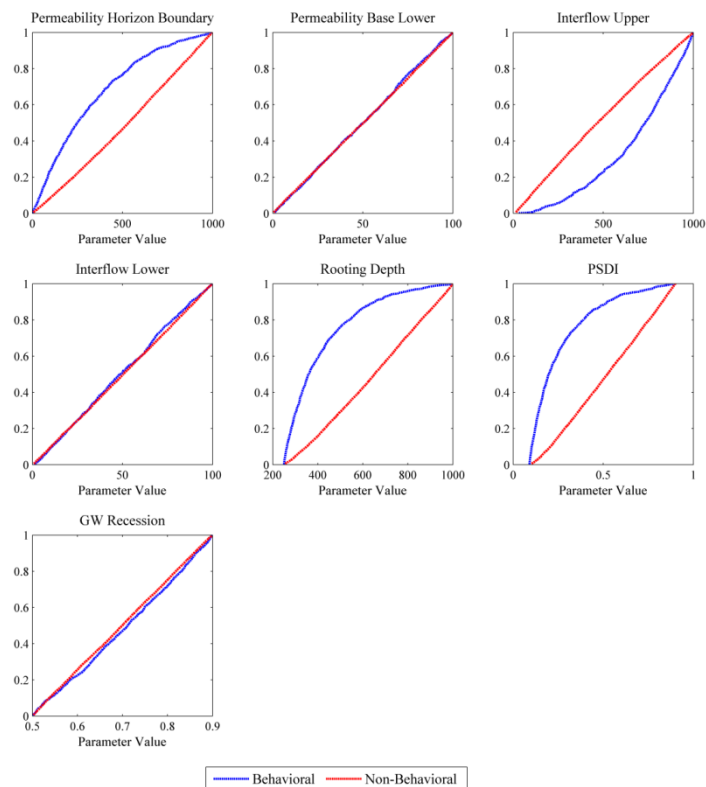


Figure 9.9 Results of the regional sensitivity analysis (RSA) conducted for HYSIM. Parameter sensitivity is expressed by the accumulated distribution functions formulated using the Nash Sutcliffe (NS) efficiency scores returned for individual parameter sets (y-axis). Parameters are classified as behavioural if attaining a score ≥ 0.7 .

Parameter	Permeability Horizon Boundary	Permeability Base Lower	Interflow Upper	Interflow Lower	Rooting Depth	PSDI	GW Recession
K-S Statistic	<u>0.32</u>	0.02	<u>0.32</u>	0.04	<u>0.46</u>	<u>0.49</u>	0.04

Table 9.6 Results of the Kolmogorov–Smirnov test (significance level 0.05) used to quantify differences between the accumulated distribution functions of the behavioural and non-behavioural parameter sets for HYSIM. Differences are highlighted as being significant if underlined.

The results of the sensitivity analysis are generally commensurate with the physical characteristics of the catchment and its observed hydrological behaviour. The catchment is extremely responsive to precipitation and can be characterised as a runoff dominated system, consequently those parameters relating to the soil horizon(s) (or in the case of HYSIM the uppermost soil layer) - particularly those related to storage and movement in the soil matrix (upper and lower) - are important; as are those parameters which control overflow from the saturated zone. The catchment has little groundwater storage or transmissive capacity, this is reflected in the relative insensitivity of parameters relating to groundwater recession. The results are generally in keeping with the hydrologic processes which are said to dominate peatland catchments; this includes both overland flow and lateral flow through the upper horizon. In addition the lack of sensitivity in the groundwater parameters is in keeping with the hydrologic nature of peatland systems (Price, 1992, Evans *et al.* 1999, Holden & Burt, 2003; Holden, 2005).

Given the similarity of both catchments considered in this study, the sensitivity analysis was conducted for the Glenamong only. Although the results shown are for the NS criterion, the results of the same analysis conducted using different goodness-of-fit measures produced similar results; however, with respect to the NS_{\log} , (logarithmic of the Nash-Sutcliffe criterion), the sensitivity shown for the NS criterion was much more pronounced. In addition, there were cases where the parameters appeared to be more/less sensitive to the volume criteria used (RVE). In some cases discharge volume was shown to be sensitive to the groundwater parameters, this is consistent with the role these parameters have in determining the volumetric flow rate, particularly during drier phases (i.e. when peak flows are not occurring). The fact that parameters which do not appear to be sensitive according to one criterion may be sensitive when assessed using another suggests that uncertainty may be introduced to the sensitivity analysis by way of the efficiency criteria employed. Additionally - as with the GLUE procedure - subjectivity in the sensitivity analysis arises by way of the parameter ranges used and the threshold employed to identify behavioural parameter values. It may also be introduced and the number of samples taken. Thus the findings of the RSA described above must be considered in the context of the subjective elements which the procedure incorporates.

9.5 Methodology

9.5.1 Generalized Likelihood Uncertainty Estimation (GLUE)

The Generalized likelihood Uncertainty Estimation (GLUE) procedure proposed by Beven and Binley (1992) is a general methodological framework for model calibration and uncertainty estimation based on the concept of equifinality (Beven, 2006a). The procedure can be considered an extension of the methodological blueprint set out by Hornberger and Spear (1981) in the Regionalised Sensitivity Analysis (RSA), or equally as a simplification of more computationally demanding formal Bayesian approaches. The procedure was developed to address uncertainties stemming from errors in the model structure and parameter values; it also provides a means for addressing uncertainty in the input and measurement data used (Beven & Binley, 1992). The steps involved in its application are outlined in Figure 9.10.

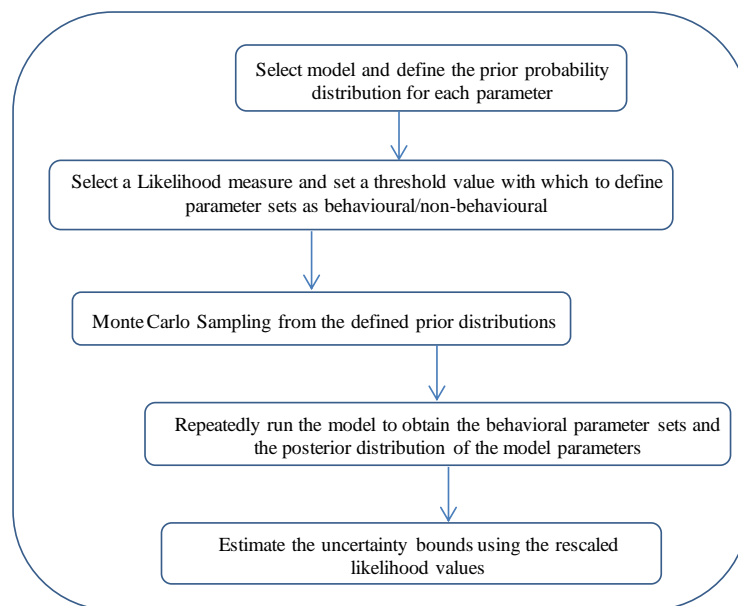


Figure 9.10 Steps involved in the application of the Generalized Likelihood Uncertainty Estimation (GLUE) method of Beven and Binley (1992).

The procedure was initially developed for addressing uncertainty in hydrological modelling but has since been successfully applied to studies of other environmental systems (e.g. Beven & Binley, 1992; Beven, 1993, 2009; Aronica *et al.*, 1998; Lamb *et al.*, 1998; Cameron *et al.*, 1999, 2000; Beven & Freer, 2001a, 2001b; Page *et al.*, 2004; Iorgulescu *et al.*, 2005; Beven, 2006a; Montanari, 2005, 2007; Jin *et al.*, 2010; Juston *et al.*, 2010; Jianqiang *et al.*, 2011; Ortiz *et al.*, 2011). In a hydrological context GLUE has been applied to groundwater modelling (Christensen, 2004), water quality analysis (Smith *et al.*, 2005; Freni *et al.*, 2008), urban drainage (Freni *et al.*, 2009), flood studies

(Aronica, 1998) and climate change impact assessments (Cameron, 2006; Cloke *et al.*, 2010).

As applied in this study the procedure aims to identify behavioural models based on a thorough exploration of the model space – encompassing different model structures and parameter sets. According to the GLUE procedure behavioural models are firstly identified from multiple model runs, whereby each successive simulation is conducted using a different parameter set. Each parameter set is selected using Monte Carlo sampling applied to a series of independent (typically) uniform distributions (Beven & Binley, 1992; Freer *et al.*, 1996). Model performance is subsequently determined using some efficiency criterion or likelihood measure which compares the similarity of the observed and model simulated data. Those parameter sets which return an efficiency score above a specified threshold are classified as ‘behavioural’ and retained. GLUE is typically applied without any prior knowledge of the respective parameter distributions; however, the parameter space must be delimited using feasible parameter ranges specified *a priori* (Beven & Freer, 2001b). In some instances importance sampling has been used to increase the efficiency with which the parameter space is sampled (e.g. Kuczera & Parent, 1998); however, this incurs an assumption regarding the likelihood of sampling behavioural sets from a particular region of the parameter space. The respective likelihood values of the retained parameter sets are rescaled so that the cumulative likelihood is equal to unity. The likelihoods are analogous to probabilities (Stedinger *et al.*, 2008); however, it is argued that the likelihood values are not true probabilities in the sense that only behavioural parameter sets are considered and a formal error model may not be employed. A cumulative likelihood weighted distribution function of the model simulations is constructed using the rescaled likelihoods as model weights. From this the uncertainty bounds (e.g. 90% confidence interval) and median simulation (i.e. 50th percentile) of the combined model output can be formulated. The posterior distribution of the model parameters can be examined using the retained parameter sets weighted according to their associated efficiency scores.

In applying the GLUE procedure subjective choices are made in both the setting of the sampling ranges and the threshold value used to identify behavioural parameter sets. A degree of subjectivity is also introduced by the choice of likelihood measure – although being able to select different efficiency criteria has the advantage of allowing the most relevant aspects of model performance (with respect to the modelling question posed) to be considered when estimating the model weights (e.g. modelling peak flows)

(Mantovan & Todini, 2006). Section 8.5.3 outlines the various shortcomings associated with the GLUE methodology.

In the case of the three models referred to above, an ensemble of 10,000 parameter sets were drawn independently from uniform distributions across the ranges specified for each parameter (see Tables 9.4 to 9.6). Parameter ranges were defined based on the results of the sensitivity analysis discussed above and values specified in published literature (e.g. Steele-Dunne *et al.*, 2008). Two independent evaluation periods (calibration & validation) were used to identify behavioural parameter sets and assess model performance. For each CRR model one hundred parameter sets were sampled from those parameters identified as being behavioural over both the calibration and validation periods (independent of one another) - as such the parameter sets used are assumed to be representative of the behavioural parameter space. This approach follows that of Cloke *et al.* (2010) who also used a sub-sample of one hundred parameter sets in their assessment of climate change impacts on the hydrology of the Medway catchment (UK). It also follows Pilling and Jones (2002) who used one hundred simulations of the HYSIM model to examine climate change impacts on the flow regime of the Wye catchment. The potential to introduce bias by way of not considering all behavioural sets is acknowledged; however, randomly selecting a sub-sample of the identified sets was necessary given the computational demands of running twenty five climate scenarios for a 100-150 year period.

Each behavioural parameter set is treated as a plausible realisation of the catchment system - despite being related to different model structures. When the likelihood values are rescaled it is done so using the three hundred likelihood values; similarly the associated prediction quantiles for the combined model simulations are estimated from the weighted cumulative distribution function formulated using all three hundred parameter sets. Essentially the catchment system space is defined as a collection of behavioural modelling solutions, obtained by varying both the model structure and parameter values (Refsgaard *et al.*, 2006; Montanari, 2007). Consequently no explicit consideration is given to the likelihood of the model structure itself. In this respect each CRR model is regarded as being equally plausible but the behavioural parameter sets are not. The constraints of this approach preclude a superior model structure contributing a greater number of parameter sets to the overall ensemble. However, GLUE stipulates that it is not the best performing models which are retained, only those which are shown to be behavioural. Thus the approach taken is consistent with the

criteria set out for implementing the GLUE procedure. Beven and Freer (2001a) advocate the extension of GLUE to competing model structures with the caveat that the same likelihood measure and set of observations is used.

By implementing the GLUE methodology in this way, uncertainty in the model structure, input data and parameters, as well as any effects of model non-linearity and covariation in the parameter values, is implicitly considered without recourse to their relative contribution to the overall predictive uncertainty – a point discussed in section 8.5.3. The GLUE procedure assumes that global uncertainty can be characterized using uncertainty in the model parameters only, whereby all sources of uncertainty are mapped onto the parameter space, albeit that in the case of this study different model structures are considered. As such the approach makes no attempt to isolate or explicitly treat the various components of uncertainty independently, which is an acknowledged shortcoming of the approach taken.

The only formal requirement of the likelihood measure used when applying GLUE is that it increases monotonically with increasing goodness of fit (Beven & Freer, 2001a). In this study three different efficiency measures were employed. Typically the Nash-Sutcliffe (NS) (Nash & Sutcliffe, 1970) efficiency criterion is used as the sole likelihood measure; however, the NS score is biased towards larger peak flows – an important consideration given the responsiveness of the study catchments (Wilby, 2005; Choi & Beven, 2007). To address this, two additional efficiency criteria, the volumetric error and the log of NS criterion were employed - the latter necessitates the logarithmic transformation of the flow series. When the NS metric is applied this transformation allows flow variations of a lower magnitude to have a similar bearing on the returned skill score. The relative volume error (RVE) was used to evaluate performance at simulating the quantity of flow. Using the metrics outlined here was considered important as the habitat assessment required that the simulated runoff data captured both the volume and timing of flow through a particular channel reach.

When the NS criterion was used as the sole likelihood measure it resulted in the models underestimating summer flows and inadequately capturing the transition from drier to wetter periods (based on the median of the multi-model simulation); by using additional efficiency measures these failings in the model performance were remediated. In addition, when the models were forced using the same climate data, there appeared to be a greater level of concordance between the projections from each individual model, but only when those parameters identified using the additional testing criteria were

employed. This was particularly evident over the summer months and during transitional phases. Montanari (2011) and Wagener *et al.* (2001) suggest that model uncertainty can be reduced by adopting stricter criteria for model testing (see section 8.5.3). In this sense using additional likelihood measures may be considered a means of addressing stationarity in the model parameters. The NS efficiency criterion expresses the fraction of observed variance which is accounted for by the model simulation, it can be written as:

$$NS = 1 - \left[\left(\sum_{i=1}^n Q_{obs} - Q_{sim} \right)^2 / \left(\sum_{i=1}^n Q_{obs} - \bar{Q}_{obs} \right)^2 \right]$$

where Q_{obs} and Q_{sim} are the observed and simulated flow series, \bar{Q}_{obs} is the average observed flow and n is the number of time steps. The inverse of the relative volumetric error (Inverse RVE) is written as:

$$Inverse\ RVE = 1 - \left[\left(\left| \sum Q_{sim} - \sum Q_{obs} \right| \right) / \sum Q_{obs} \right]$$

The inverse is taken so that a higher value denotes a more skilful model. The behavioural threshold for each efficiency criterion is set independently based on the range of values returned by the MC simulation. To account for differences in model performance, the thresholds are set on a catchment-by-catchment basis. The final likelihood values for the retained parameter sets were calculated as an average of the three efficiency scores over both evaluation periods. This approach is advocated by Beven (2001) and can be written as:

$$L_p(\underline{\theta}_i | \underline{Y}) = \frac{W_0 L_0(\underline{\theta}_i) + W_1 L_p(\underline{\theta}_i | \underline{Y}_1) + \dots + W_m L_p(\underline{\theta}_i | \underline{Y}_m)}{C}$$

where $L_p(\underline{\theta}_i | \underline{Y})$ is the posterior likelihood of the parameter set (θ), W_0 to W_m are the likelihood weights and \underline{Y}_1 to \underline{Y}_m are the evaluation periods used. The value of C is set to ensure the cumulative posterior likelihoods sum to unity. In this study each of the three efficiency scores are given an equal weighting. For a parameter set to be retained it had to return a score equal to or above the threshold set for each performance criterion over both evaluation periods independently. This removed the potential for compensation across efficiency scores when determining which parameters to retain. Alternative

methods for combining the values from individual likelihood measures include multiplication (e.g. Beven & Binley, 1992), Bayesian updating, fuzzy union, fuzzy interaction and weighted fuzzy combination (Aronica *et al.*, 1998; Beven, 2001).

Choi and Beven (2007) employed a similar approach to that adopted in this study whereby a series of likelihood measures (six in total) were used to assess model performance (over different time periods) and reduce uncertainty in the parameter estimates. Choi and Beven (2007) adopted a Bayesian approach for combining efficiency scores. This method was not employed in this study as it was important that the individual metrics were given a similar weighting when determining the final likelihood values. It should be noted that the choice of likelihood measure(s) and the method used for combining them are important sources of uncertainty - an issue explored by He *et al.* (2011).

In impact studies a fundamental assumption is being made that the parameter sets shown to be behavioural under observed conditions remain valid under the forcing conditions of possible future climates. It is acknowledged that having long term records which are sufficiently informative with respect to patterns of flow behaviour and extremes of conditions allow a more rigorous approach to model testing (Klemes, 1985). In such cases the validity of this assumption can be robustly addressed. However, in this study the observed records available for both catchments are relatively short (~ 6 years). In addition, there are no discernible prolonged periods of high or low flows with which to test the transferability of parameter sets - an issue which is complicated by shortcomings in the data quality. To compensate for this the additional efficiency criteria discussed above were applied and a high threshold value was set. Not testing the transferability of the model parameters is an acknowledged shortcoming which may undermine the final results of the study; however, it is one imposed by the datasets available and therefore was to a certain extent unavoidable.

As highlighted above, GLUE has a number of shortcomings related primarily to the random nature of the sampling procedure and the lack of a formal error model (Montanari, 2005; Mantovan & Todini, 2006; Blasone *et al.*, 2008). The procedure has also been criticised for the subjective elements it incorporates. It has been shown that the subjective nature of some steps taken when applying the procedure can influence the final results (Stedinger *et al.*, 2008; Cloke *et al.*, 2010; Jin *et al.*, 2010). Many researchers now favour the use of formal Bayesian approaches above GLUE which, it is argued, provide a more accurate representation of uncertainty bounds and a more

statistically coherent estimate of predictive uncertainty. The arguments against using formal Bayesian methods highlight their dependence on various simplifying statistical assumptions including normality, independence and homoscedasticity (Stedinger *et al.*, 2008). It is argued that these assumptions may be easily violated in the context of real world model applications (Ruark *et al.*, 2011). Beven (2008a) states that even slight departures from these assumptions may lead to bias in the parameter estimates.

Cloke *et al.* (2010) - who employed GLUE in a climate change context - state that although it is debatable whether a formal Bayesian approach provides a more robust and objective alternative, it may not be fundamentally important as long as some estimate of uncertainty is transparently provided. Beven (2006a) argues that the subjectivity of GLUE should be made explicit to ensure it is applied in a transparent and methodologically rigorous way. It is acknowledged that variations of the GLUE procedure exist, whereby various adjustments, advancements or additions have been made to the basic methodological framework (e.g. Rojas *et al.*, 2008; Bastola *et al.*, 2011); the use of such approaches were not explored in this study.

9.3.2 Monte Carlo simulation of probabilistic flow projections

Although the GLUE procedure allows uncertainty in hydrological models to be addressed, the method does not provide a means for producing probabilistic information on future changes in the flow regime whereby the uncertainty stemming from both the hydrological and climate modelling components can be incorporated. In addition, it does not allow the weighting scheme previously developed for the climate scenarios to be applied when estimating ensemble based projections of the hydrological response to altered forcing. To address both of these issues a broader methodological framework based on Monte Carlo simulation was employed. The method is similar to that used by Wilby and Harris (2006) to combine information about future changes in low flows for the River Thames based on an ensemble of different GHG emission scenarios, GCMs, downscaling techniques and hydrological model simulations (considering both model structure and parameter uncertainty). This methodological framework is implemented alongside GLUE for several reasons. Firstly applying GLUE facilitates an exploration of hydrological model uncertainty and allows for a comparison in the response of the study catchments to individual forcing scenarios. As the same parameter sets and likelihood values are used in both approaches, the probabilistic framework borrows

from the methodological blueprint set out in GLUE. In addition, both methods are similar in that they seek to produce a weighted distribution function with which to characterise uncertainty. Consequently the probabilistic framework is not implemented as a competing methodological approach, but rather as a complementary method which allows a single distribution function of future change to be produced conditional on all aspects of the uncertainty cascade.

Producing probabilistic projections of future changes in the flow regime requires that weights or likelihood values are assigned to the various components in the chain of uncertainty (i.e. emission scenario, GCM, downscaling technique, hydrological model structure and parameter sets). Monte Carlo simulation is then conducted whereby different combinations of climate pathways and hydrological model simulations are randomly selected based on the assigned weightings. Once a flow series has been sampled, projected changes (e.g. 2050s relative to the control) in the relevant flow statistic (e.g. Q50) are calculated. In this study a two step approach is taken whereby both the climate scenario and hydrological model (i.e. parameter set) are selected independently of one another (Figure 9.11). The weights assigned to the climate pathways are the same as those employed to estimate the weighted ensemble average for precipitation discussed in Chapter six.

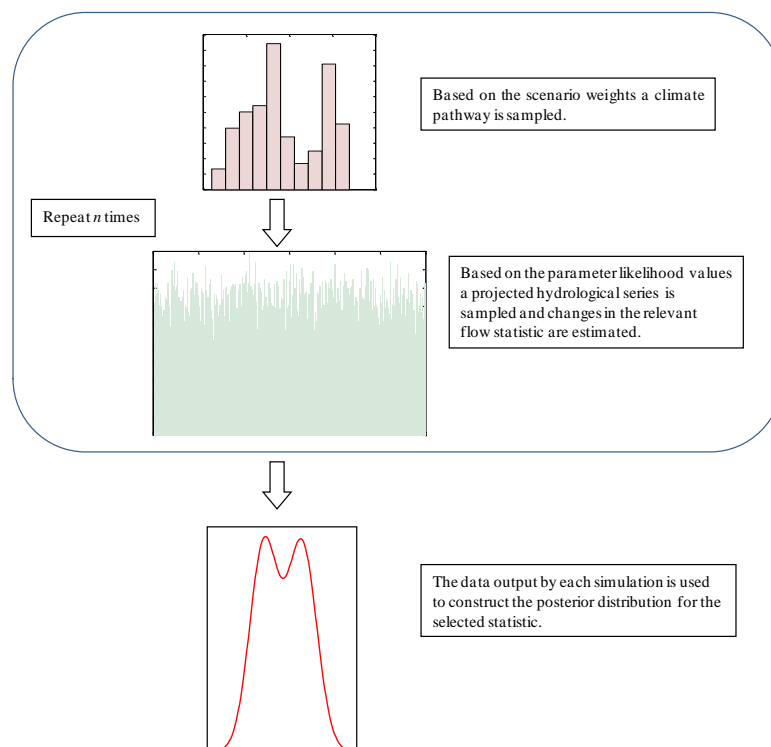


Figure 9.11 Schematic of the Monte Carlo sampling procedure used to formulate the posterior distribution for the selected flow statistic (Q50, Q05 or Q95).

The weights assigned to the individual hydrological simulations are the same (normalized) likelihood values used when applying the GLUE procedure. MC simulation is performed on the basis that those climate pathways and model parameters (implicitly including the hydrological model structure) which have been assigned a greater weighting are sampled more often. The estimated statistic from each sample is amalgamated to form the posterior distribution for each flow statistic. Given that the data is sampled according to some predefined weighting criteria, the central tendency of the distribution is representative of the most likely changes in the selected flow statistic - conditional on the model pathway considered (i.e. emission scenario, GCM, downscaling model, hydrological model structure and parameter set). The associated spread of the posterior distribution provides an estimate of uncertainty in the projected hydrological response.

Wilby and Harris (2006) indicate that a weighting scheme could be developed based on the ability of the individual GCM/downscaling/hydrological model combinations to reproduce the selected flow statistic over the model control period (e.g. 1961 - 1990). Adopting this approach however, means that the skill of each individual component in the modelling chain, independent of one another, remains unknown. Importantly it also means the assessor runs the risk of concealing instances where error cancellation has occurred. Here the various components of uncertainty may interact with one another in such a way that the modelled hydrological data provides an accurate estimate of flow without the underlying mechanisms necessarily being correct. This may potentially lead to overconfidence in a particular outcome. To avoid this, the likelihood values applied to the climate pathways are estimated independently of the hydrological models and vice versa. This approach comes with the caveat that no weighting is attached to the climate scenarios and hydrological models when combined (i.e. where the skill of each respective model structure/parameter set and climate pathway over the model control period is evaluated against observed flow conditions).

Given that uncertainties in the climate scenarios may be amplified when uncertainties in the hydrological models are encountered, this is an important potential weakness of this approach. However, in this study it was not possible to formulate such a weighting given the relatively short length (~6 years) of the observed flow data. This precludes any evaluation of the long term statistical similarity of the observed and simulated flow series over the model control period. The approach taken here does however follow that of Wilby and Harris (2006); in this case the weights employed were estimated and set

independently with respect to each component in the model chain. Thus no attention is given to the skill of the chain when considered in its entirety as an independent entity.

As previously indicated a different weighting scheme was formulated for the downscaled climate data relating each emission scenario (Figure 6.11). Consequently three different MC simulations were conducted - one for each of the emission scenarios considered (A1B, A2 and B2). In addition to this a further analysis was performed whereby both the A2 and B2 scenarios were included in a single MC simulation. In this case each emission scenario was assigned an equal weighting ($p=0.5$). Given that the number of potential climate pathways which may be sampled during the analysis is dependent on the emission scenario and whether the series covers the period up to 2050 or 2100, the number of samples taken during each simulation was altered (Table 9.7); this was to ensure an adequate sampling of the model space.

One of the main drawbacks of the MC sampling approach as implemented in this study is that there is no way of knowing the correct termination point for the procedure; i.e. whereby enough simulations have been conducted to ensure the posterior distribution has been fully characterised. This runs the risk of inadequately sampling the hydrological response space and may result in an underestimation of predictive uncertainty. In order to address this a relatively large number of simulations were conducted; in addition a number of descriptive statistics - including the median, IQR and 90% interval of the posterior distribution - were monitored during the procedure to ensure enough samples had been taken. This was indicated by the degree to which the statistics used stabilised or ceased to change over successive runs.

Emission Scenario	Number of associated climate pathways	Number of runs conducted
A2	3	22,500
B2	3	22,500
A2 and B2	6	45,000
A1B Until 2020s	17	127,500
A1B Until 2080s	13	97,500

Table 9.7 The number of Monte Carlo simulations conducted for each emission scenario. The MC simulation is used to estimate the posterior distribution of the selected flow indices over each successive horizon (2020s, 2050s and 2080s). The numbers of simulations is altered according to the number of climate pathways considered.

9.6 Model performance under observed conditions

The threshold values used to classify behavioural parameter sets were selected on the basis that a sufficient number of skillful sets were returned, but that the uncertainty bounds were wide enough to envelope a high proportion of the observed values. As strict criteria regarding the adequacy of parameter sets was applied (i.e. high thresholds, multiple performance criteria, split-sample approach) this was a difficult balance to achieve. Using high threshold values meant that behavioural sets were generally sampled from a similar region of the parameter space - yielding narrow uncertainty bounds. However, as it was essential that the retained parameters performed well in reproducing both the timing and volume of flow under different conditions, it is important that the models used and the weighting criteria applied reflected this.

9.6.1 Glenamong

A threshold value of 0.70 was set for both the NS and NS_{log} efficiency criteria. In addition a threshold of 0.90 was used for the relative bias; thus a parameter set was retained only if it either over or under simulated observed flow by no more than 10%. The parameter sets were tested using two different independent evaluation periods (calibration: Aug 2003 – Aug 2006; validation: Sept 2006 - Aug 2009). The efficiency scores returned for the 100 behavioural parameter sets sampled for each model are shown in Table 9.8.

Period	Calibration			Validation		
	NS (≥0.7)	NS _{log} (≥0.7)	Inverse RVE (≥0.9)	NS (≥0.7)	NS _{log} (≥0.7)	Inverse RVE (≥0.9)
Threshold set:						
<i>HBV</i>						
Min	0.70	0.70	0.95	0.70	0.62	0.95
Max	0.84	0.88	1.00	0.79	0.82	1.00
Mean	0.76	0.78	0.97	0.75	0.72	0.97
<i>HYSIM</i>						
Min	0.78	0.76	0.90	0.75	0.72	0.90
Max	0.82	0.85	0.96	0.78	0.84	0.95
Mean	0.81	0.82	0.92	0.77	0.78	0.92
<i>TOPMODEL</i>						
Min	0.70	0.70	0.90	0.70	0.70	0.90
Max	0.80	0.81	1.00	0.80	0.80	1.00
Mean	0.76	0.72	0.95	0.76	0.72	0.95

Table 9.8 Efficiency scores for the Glenamong catchment returned by the 100 behavioural parameter sets retained for each CRR model estimated over the calibration and validation periods respectively.

Table 9.9 displays the NS, NS_{log} and volumetric error calculated for the median of the multimodel simulation (estimated using GLUE); also shown is the mean width of the prediction interval (PI) for the 90% uncertainty bounds and the count efficiency (CE) indicating the percentage of observed points which lie within the 90% interval. Generally the median of the multimodel ensemble returns marginally higher NS and NS_{log} scores when compared to the median of each individual model. The combined model simulations also return a higher CE value; this is to be expected given that the prediction interval (PI) is also wider. Of the three rainfall-runoff models used HBV produced consistently high skill scores.

The estimated PI and CE values - along with the number of parameters sets returned as behavioral for each model - is dependent on the threshold value set. In this study, where a lower threshold was employed, the PI, CE and NBPS (number of behavioural parameter sets) increased; however, reducing the threshold value with the aim of increasing the CE and NBPS is done so at the expense of other measures of efficiency and model skill. This highlights the influence which the threshold value can have on the character of the multimodel ensemble. In addition it illustrates how subjectivity is introduced to the modelling process and the influence which it can have on the final results.

	NS	NS _{log}	Inverse RBIAS	CE (%)	PI (m ⁻³ s ⁻¹)
<i>Median Multimodel Simulation</i>					
Calibration	0.86	0.86	0.99	87.7	0.86
Validation	0.85	0.85	0.95	84.7	0.84
<i>HBV Median</i>					
Calibration	0.84	0.84	0.99	82.2	0.70
Validation	0.81	0.82	0.98	80.2	0.71
<i>HYSIM Median</i>					
Calibration	0.85	0.80	0.96	72.2	0.67
Validation	0.82	0.83	0.94	76.4	0.69
<i>TOPMODEL Median</i>					
Calibration	0.82	0.81	0.98	67.1	0.59
Validation	0.79	0.78	0.95	67.4	0.59

Table 9.9 Efficiency scores for the Glenamong catchment returned by the median series for each CRR model as well as the median of the multimodel simulation. The efficiency scores are estimated for the calibration and validation period respectively.

Figure 9.12(a) shows the 90% PI and median series of the multimodel simulation for the Glenamong over a 200 day period; the plot incorporates the largest flow event on record for this catchment ($\sim 12 \text{ m}^3 \text{ s}^{-1}$). Figure 9.12(b) shows the responsiveness of the flow regime and the degree to which the PI of the multi-model simulation envelopes the observed values. It can be seen that the flooding event is captured well, as are the recession curves and periods when flow is substantially lower. The responsiveness of the flow regime points to the significance of the observed precipitation series in terms of accurately simulating flow behaviour. Where the model simulation fails to capture a given flow event, the corresponding precipitation event is generally not present or underrepresented in the observed series. This highlights the influence which the observed data has on the final efficiency scores; it also suggests that setting a lower threshold value may not produce a corresponding increase in the CE value. As illustrated in Figure 9.12(a) there does appear to be a degree of skew in the median towards the lower bound - particularly during low flow phases; this is a recognized issue with the GLUE procedure (Bastola *et al.*, 2011). Plotted in Figures 9.12(c) and 9.12(d) are the 90% PI and median series for each of the rainfall-runoff models for the same 200 day period. The uncertainty bounds are slightly wider for HBV when compared to both HYSIM and TOPMODEL. The narrow width of the PI is due to the behavioral parameters being sampled from a similar region of the parameter space, leading to little variation in the simulated response. With regards to TOPMODEL the bounds appear to be particularly narrow during low flow periods; in contrast the bounds are much wider during storm events.

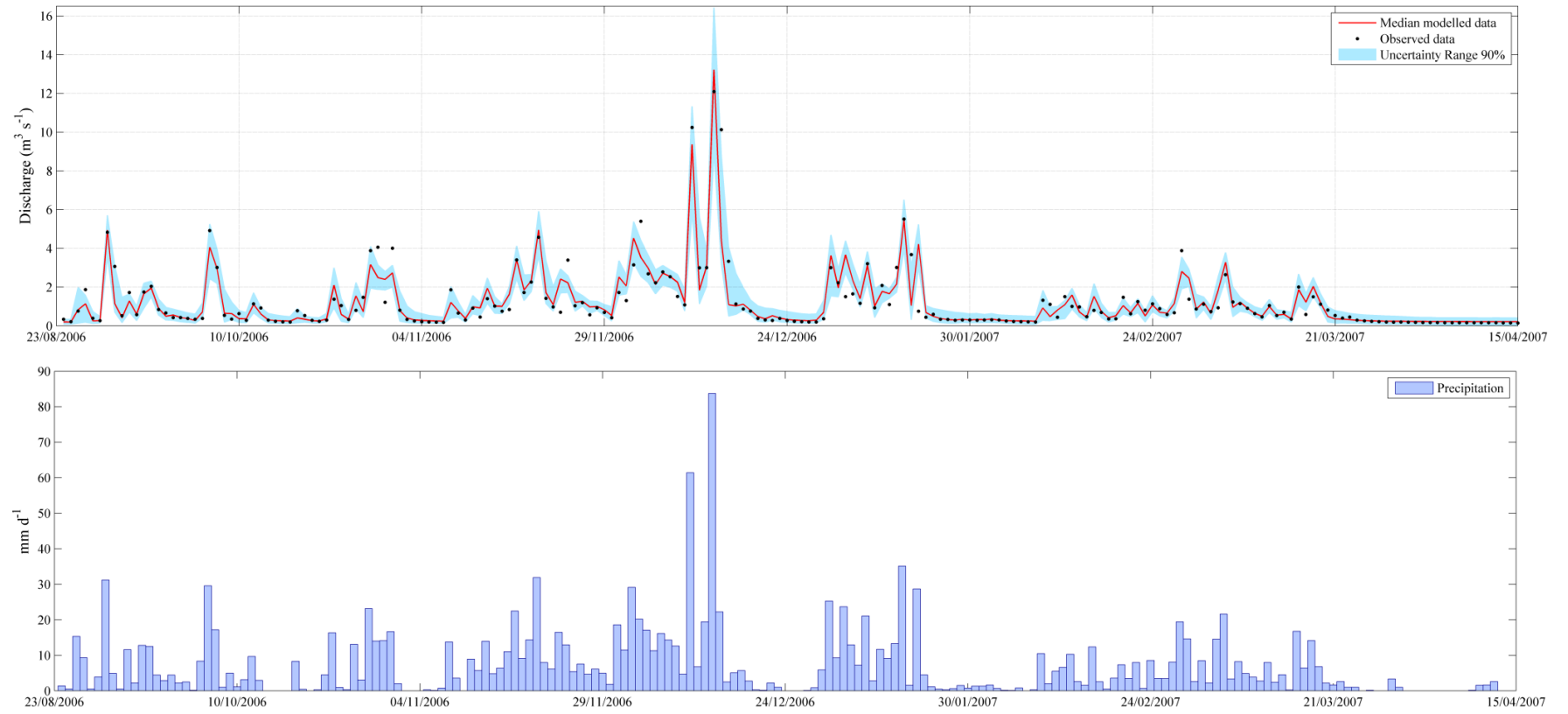


Figure 9.12(a) Shown in the top panel is the median and 90% confidence interval derived from the multimodel simulation for the Glenamang catchment (Aug 2006 to April 2007; 200 days); also shown are the observed data points for the same time period. The observed precipitation is shown in the lower panel.

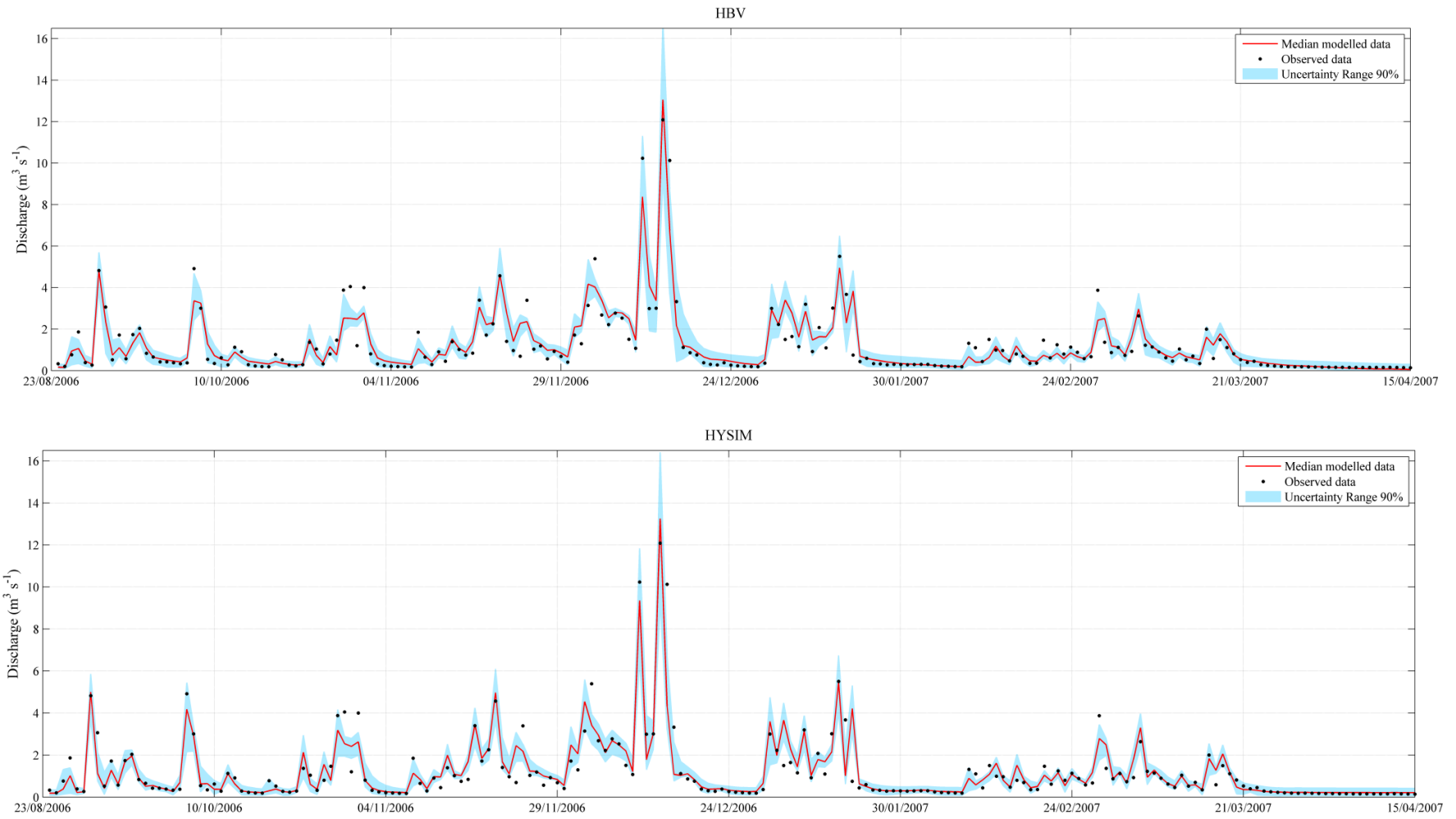


Figure 9.12(b) Shown in the top and lower panels is the median and 90% confidence interval (Aug 2006 to April 2007; 200 days) for the Glenamong catchment simulated using HBV and HYSIM respectively. Also shown are the observed data points for the same time period.

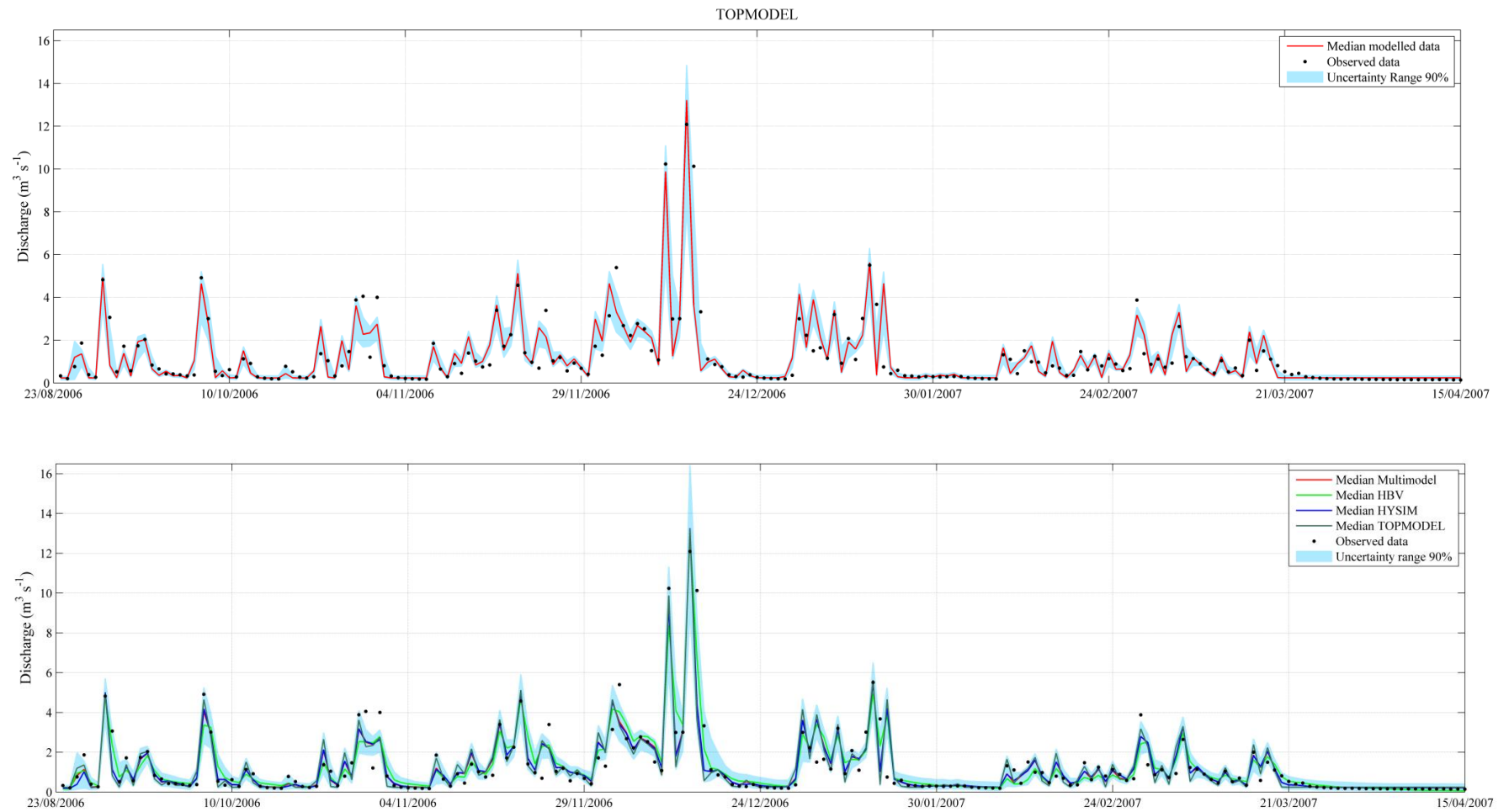


Figure 9.12(c) Shown in the top panel is the median and 90% confidence interval (Aug 2006 to April 2007; 200 days) for the Glenamong catchment simulated using TOPMODEL. Shown in the lower panel is the median series estimated for each CRR model (HBV, HYSIM and TOPMODEL). Also plotted are the median series and 90% confidence interval for the multimodel simulation.

Generally no single model outperforms the others in terms of capturing both the mean and variance of the annual flow regime (Figure 9.13). The greatest relative bias in the model simulated monthly mean values is associated with May and June; in contrast, the lowest bias is returned for November and January. With respect to the monthly variance TOPMODEL exhibits a lower bias for the majority of months; however, it also returns the greatest bias for any single month (August 81.4 %). The Q-Q plots shown in Figure 9.14 illustrate the skill of each model - as well as the multimodel simulation - at capturing observed events across a range of magnitudes. The plots indicate that the median series from both HYSIM and TOPMODEL provide a close fit to the observed values; this is in contrast to the median from both the multimodel simulation and HBV which approximate less well - albeit marginally so - to the observed series. Although TOPMODEL appears more skilful at capturing some aspects of flow behaviour, the PI for this model is narrower and its CE is lower. Thus its ability to reproduce the observed flow statistics may be a result of narrower uncertainty bounds rather than the model being superior with respect to how it conceptualizes hydrological processes in the catchment.

Although the multimodel simulation returns consistently high efficiency scores across all of the performance criteria employed, it is not clear where the added value exists in employing three different model structures (in contrast to employing a single model in isolation). This may be linked to the quality of the available datasets and the fact that the rainfall-runoff relationship is essentially a linear one, and as such is not that difficult for the models to capture. However, as discussed in the preceding sections, the value of the multimodel approach is not necessarily related to developing a modelling framework which is better able to capture observed flow behaviour, but is rather related to how the multimodel ensemble enables a greater sampling of the uncertainty space. Therefore, while the multimodel framework allows the strengths of individual rainfall-runoff models to be combined, it also provides a means for addressing uncertainty in the projected hydrological response.

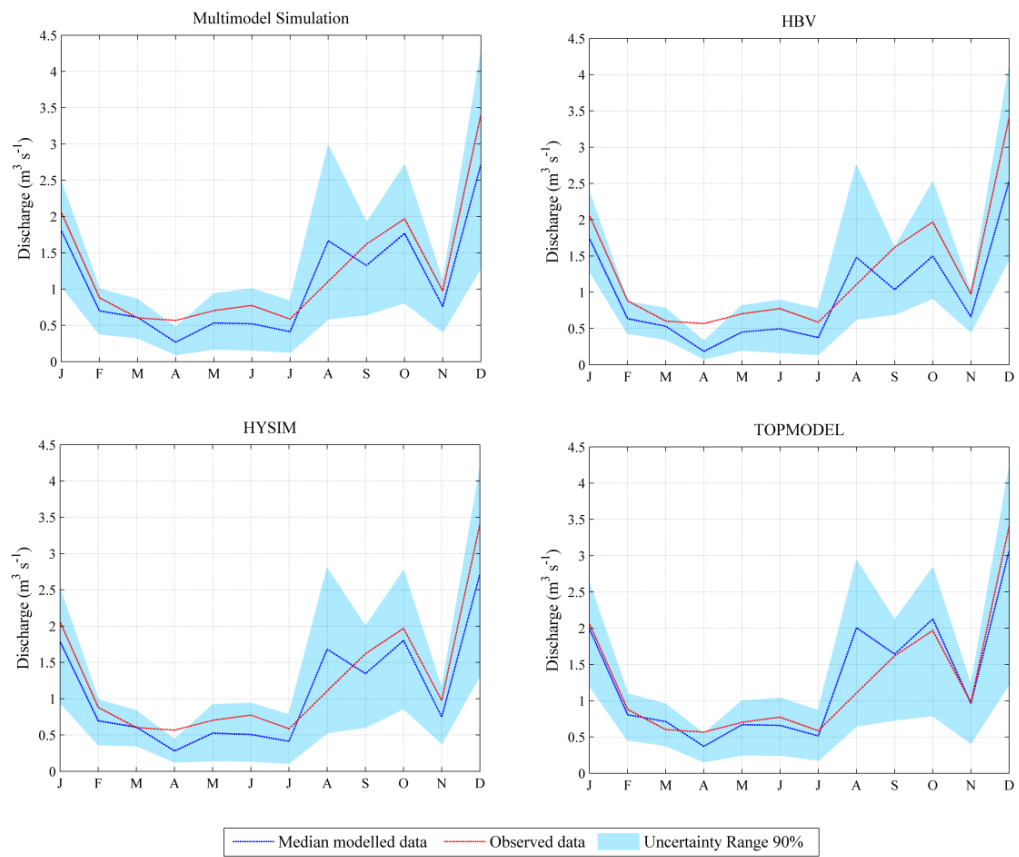
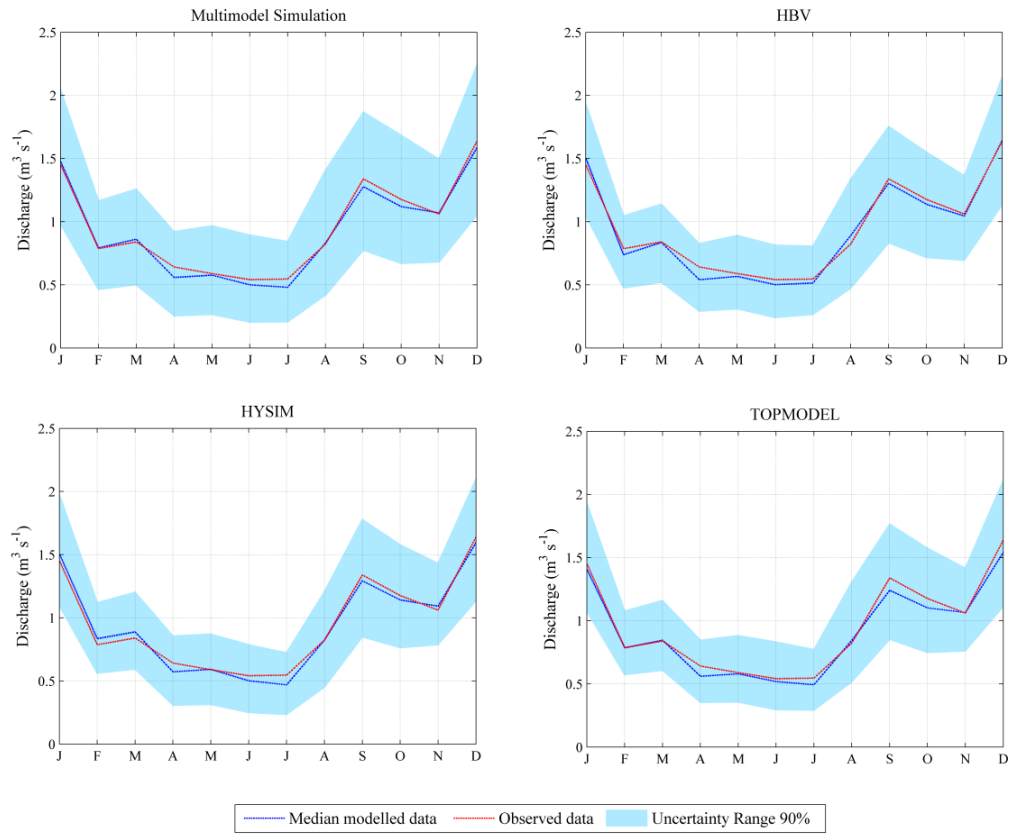


Figure 9.13 Observed and model simulated monthly mean (upper panel) and variance (lower panel) flow values for the Glenamang catchment plotted along with the median and 90% confidence interval for each CRR model (HBV, HYSIM and TOPMODEL). Also plotted are the median and 90% confidence interval for the multimodel simulation.

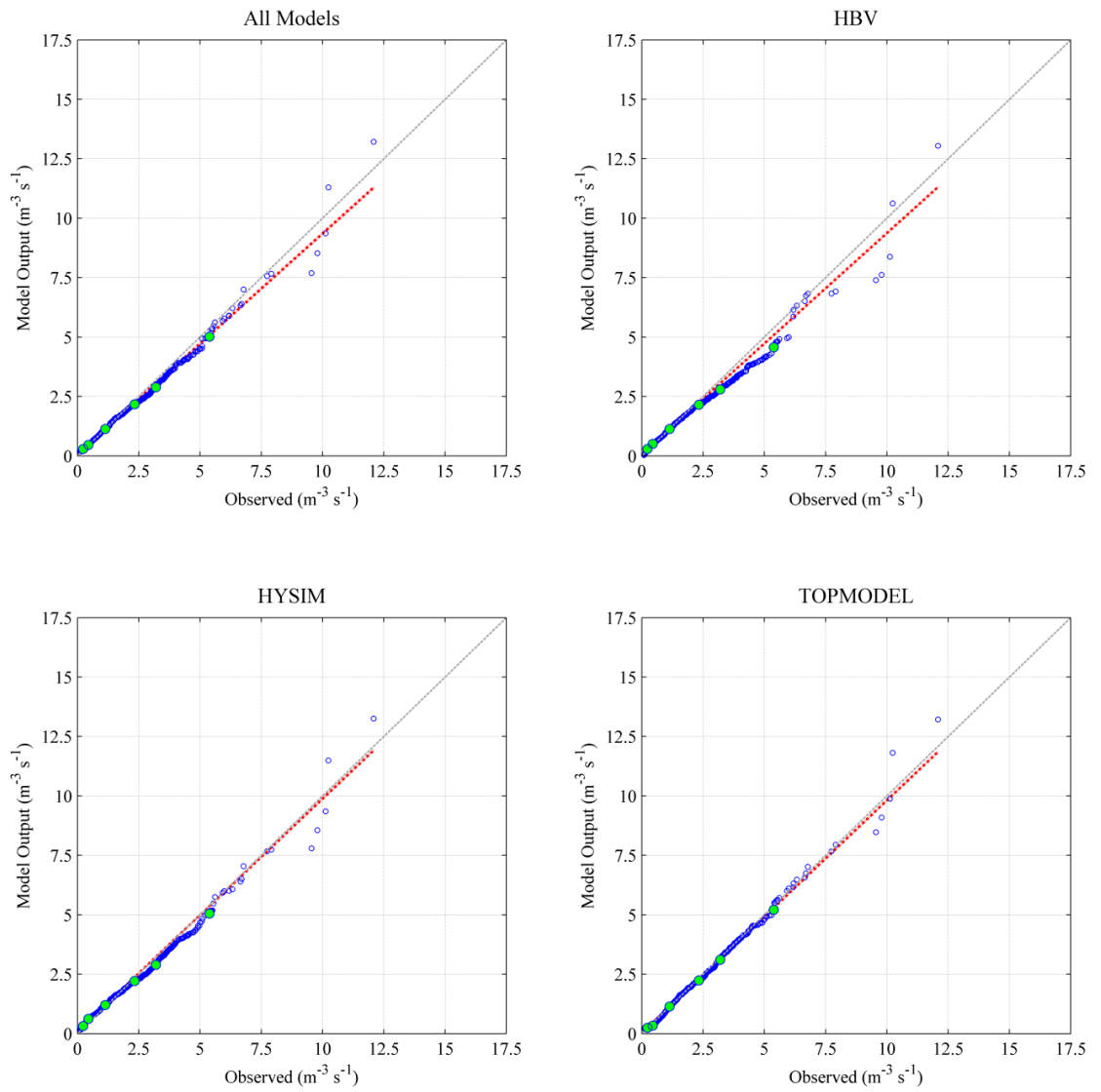


Figure 9.14 Q-Q plots of observed *versus* simulated flow values for the Glenamong catchment. The median series for each CRR model (HBV, HYSIM and TOPMODEL) as well as the multimodel simulation is plotted. The green dots are used to highlight those flow values relating to the following percentiles: 25th, 50th, 75th, 90th, 95th and 99th.

9.6.2 Srahrevagh

In contrast to the Glenamong, the models were less skillful when applied to model flow in the Srahrevagh catchment. An examination of its observed hydrometric and precipitation records suggests that the low skill scores are most likely related to the quality of the observed datasets rather than any fundamental structural deficiencies in the models used. Given that both the Glenamong and Srahrevagh were chosen on the basis that they presented better quality data, the performance scores are indicative of the difficulties which would have been encountered if other sub-catchments - which presented poorer quality datasets - had been considered (see section 3.3).

For the Srahrevagh a lower threshold value for each efficiency criteria was used (NS and $NS_{\log} \geq 0.65$; inverse RVE ≥ 0.80). The calibration and validation periods employed covered the dates Aug 2003 to Aug 2006, and Sept 2006 to June 2009 respectively. Table 9.10 provides a summary of the scores returned for the behavioral parameter sets retained for each CRR model. Generally for each model the parameters return similar scores over both evaluation periods; despite this, both HBV and TOPMODEL were found to have lower CE values (Table 9.11) when compared to HYSIM and the multimodel simulation. Less than half (~43%) of the observed points were found to lie within the 90% interval for HBV and TOPMODEL; in contrast for HYSIM and the multimodel simulation the CE ranges from 65-75%.

Period	Calibration			Validation		
	NS (≥ 0.65)	NS_{\log} (≥ 0.65)	Inverse RVE (≥ 0.8)	NS (≥ 0.65)	NS_{\log} (≥ 0.65)	Inverse RVE (≥ 0.8)
Threshold set:						
HBV						
Min	0.65	0.66	0.80	0.67	0.66	0.82
Max	0.76	0.83	0.85	0.71	0.72	1.00
Mean	0.71	0.78	0.83	0.70	0.67	0.97
HYSIM						
Min	0.67	0.65	0.83	0.67	0.65	0.85
Max	0.74	0.69	1.00	0.71	0.78	0.92
Mean	0.71	0.66	0.96	0.70	0.71	0.87
TOPMODEL						
Min	0.68	0.68	0.80	0.66	0.65	0.82
Max	0.73	0.81	0.83	0.70	0.68	1.00
Mean	0.71	0.74	0.81	0.68	0.67	0.98

Table 9.10 Efficiency scores for the Srahrevagh catchment returned by the 100 behavioural parameter sets retained for each CRR model estimated over the calibration and validation periods respectively.

	NS	NS _{log}	Inverse RBIAS	CE (%)	PI (m ³ s ⁻¹)
<i>Median Multimodel Simulation</i>					
Calibration	0.70	0.83	0.81	75.16	0.17
Validation	0.69	0.80	0.82	68.78	0.13
<i>HBV Median</i>					
Calibration	0.70	0.79	0.84	43.19	0.10
Validation	0.69	0.80	0.80	43.73	0.09
<i>HYSIM Median</i>					
Calibration	0.72	0.74	0.98	72.13	0.17
Validation	0.71	0.68	0.96	65.15	0.16
<i>TOPMODEL Median</i>					
Calibration	0.70	0.79	0.84	43.19	0.10
Validation	0.69	0.66	0.98	38.94	0.09

Table 9.11 Efficiency scores for the Shrevagh catchment returned by the median series for each CRR model as well as the median of the multimodel simulation. The efficiency scores are estimated for the calibration and validation period respectively

In contrast to the models when considered on an individual basis, the multimodel simulation produces consistently high efficiency scores across all metrics and over both evaluation periods. Figure 9.15(a) plots the 90% PI and median of the multimodel simulation for a continuous 300 day period. Figure 9.15(b) shows the median series for each model plotted over the 90% PI calculated based on the multimodel simulation. From in Figure 9.15(a) the responsive nature of the catchment, particularly with respect to precipitation events of a much lower magnitude is evident. With the exception of the autumn months, for which the mean monthly flow is generally underestimated, the models reproduce the annual flow regime (Figure 9.16); however, each model greatly underestimates the monthly variance - a fact which is particularly evident over the autumn months.

This may be due to deficiencies in the ability of each model to transition from drier to wetter periods; however, given that this is a failing which is common to all models, it is most likely linked to the quality of the observed data used. This is plausible given the potential for any shortcomings (e.g. missing values, under-recording of extreme events) in the data to be enhanced by its relatively short length. As shown in the Q-Q plots (Figure 9.17) the models generally capture the median and lower percentiles but tend to underestimate higher values, reflecting the degree to which the variance of the monthly values is underestimated.

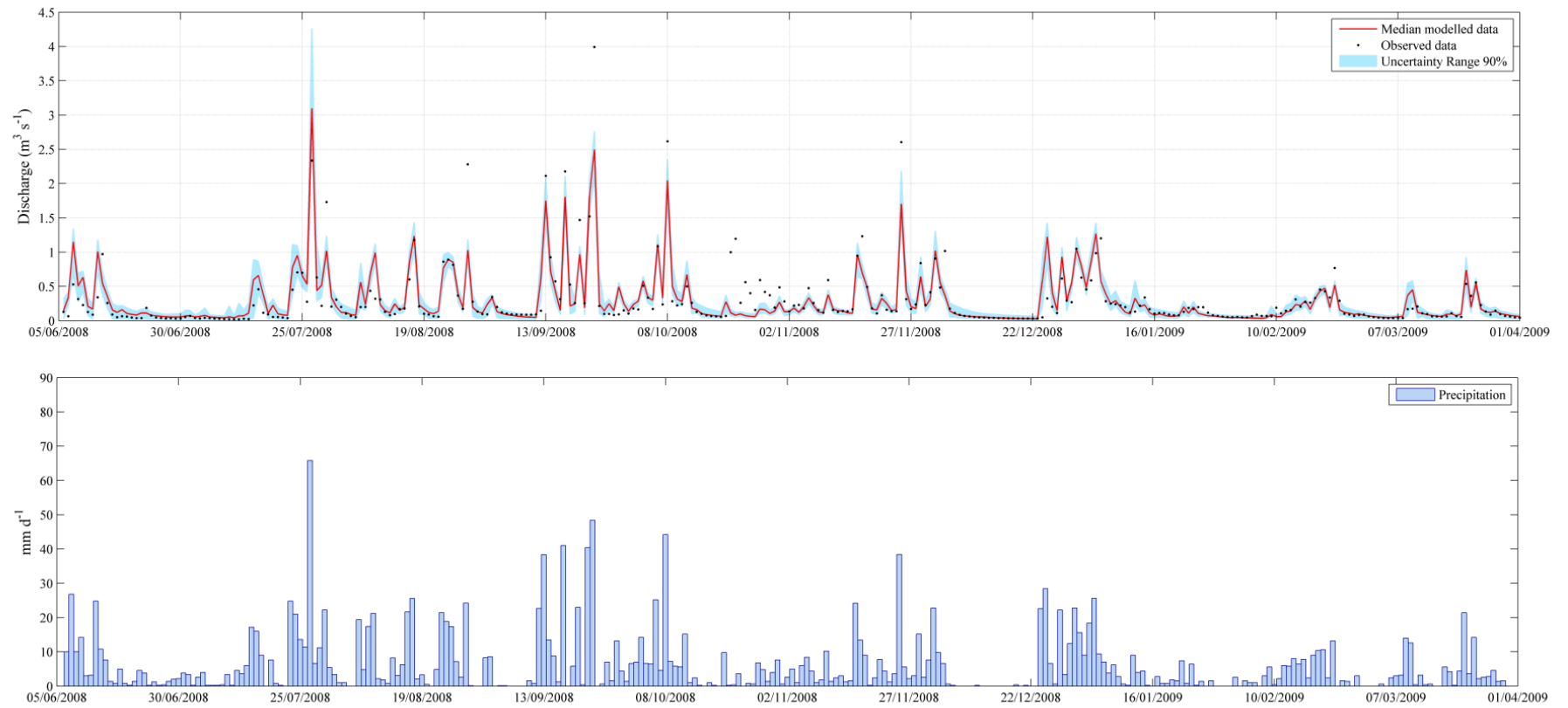


Figure 9.15(a) Shown in the top panel is the median and 90% confidence interval derived from the multimodel simulation for the Srahrevagh catchment (June 2006 to January 2007; 300 days); also shown are the observed data points for the same time period. The observed precipitation is shown in the lower panel.

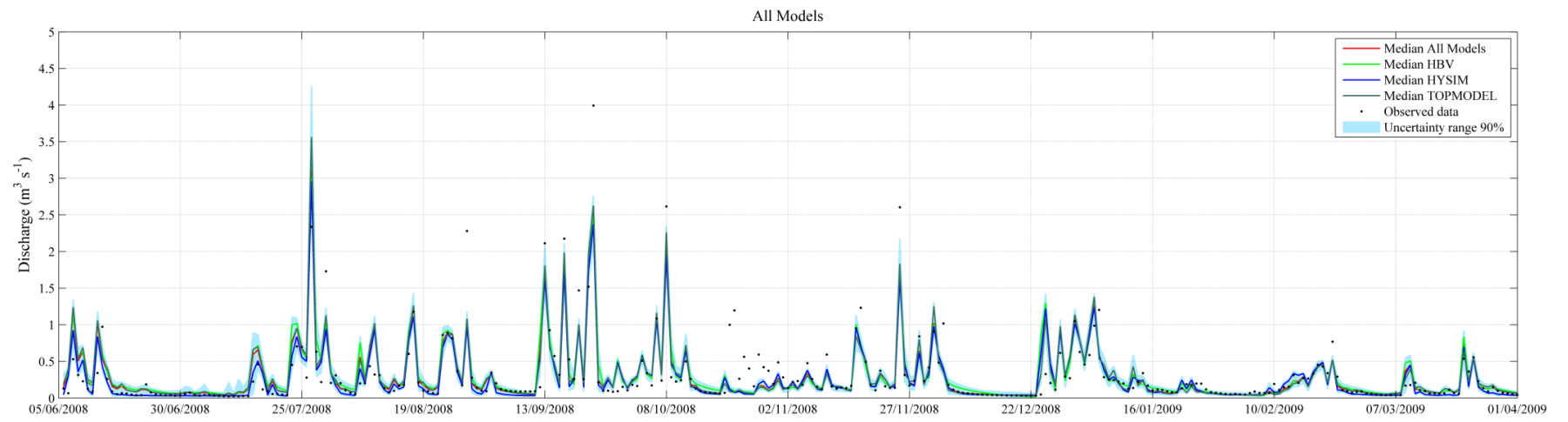


Figure 9.15(b) The median series derived for each CRR model (HBV, HYSIM and TOPMODEL) plotted over the median and 90% confidence interval from the multimodel simulation (June 2006 to January 2007; 300 day). Also shown are the observed data points for the same period.

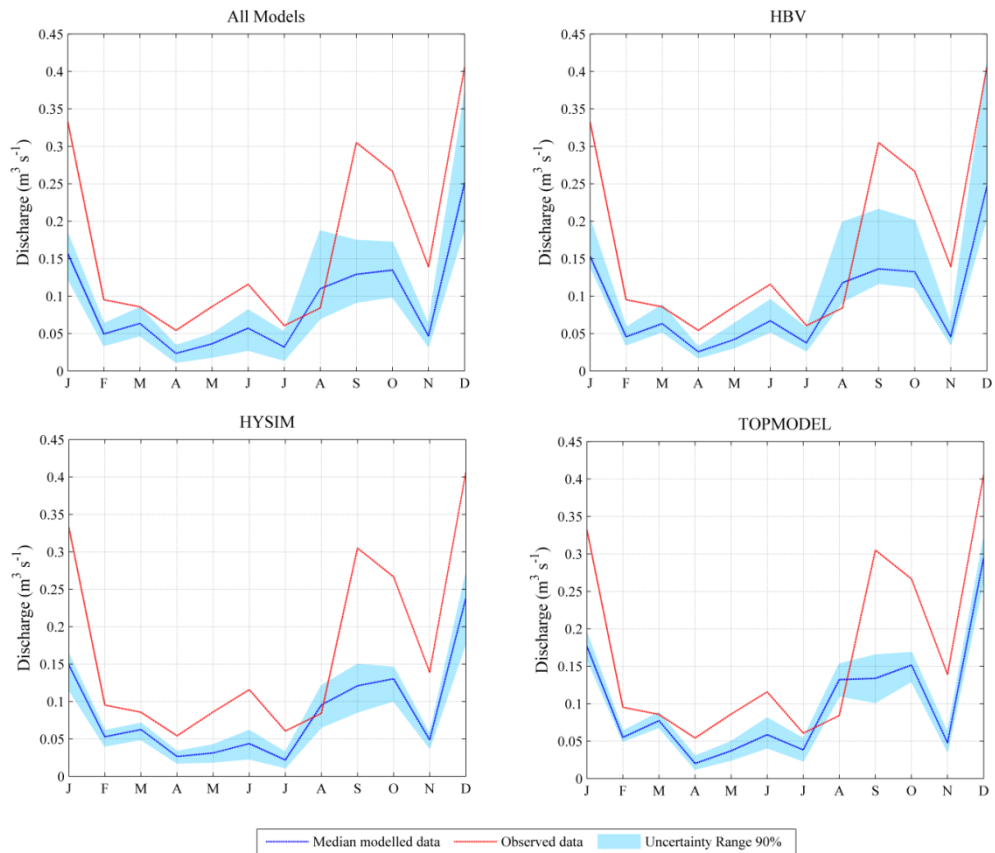
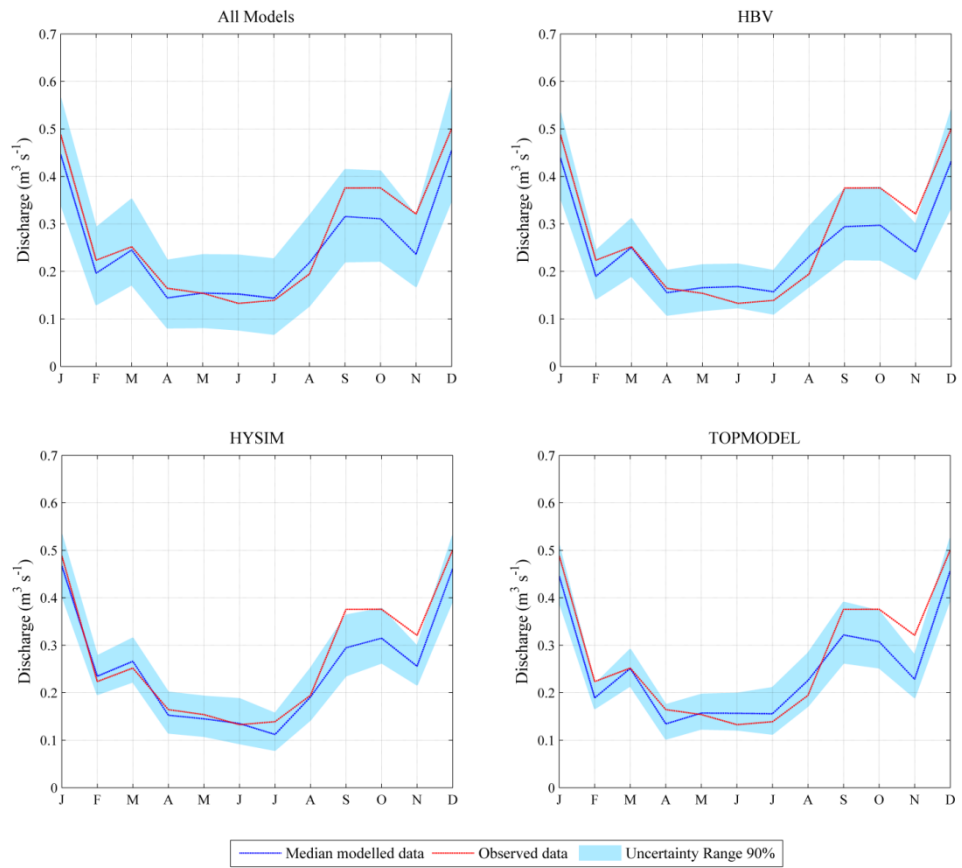


Figure 9.16 Observed and model simulated monthly mean (upper panel) and variance (lower panel) flow values for the Srahrevagh catchment, plotted along with the median and 90% confidence interval for each CRR model (HBV, HYSIM and TOPMODEL). Also plotted are the median and 90% confidence interval for the multimodel simulation.

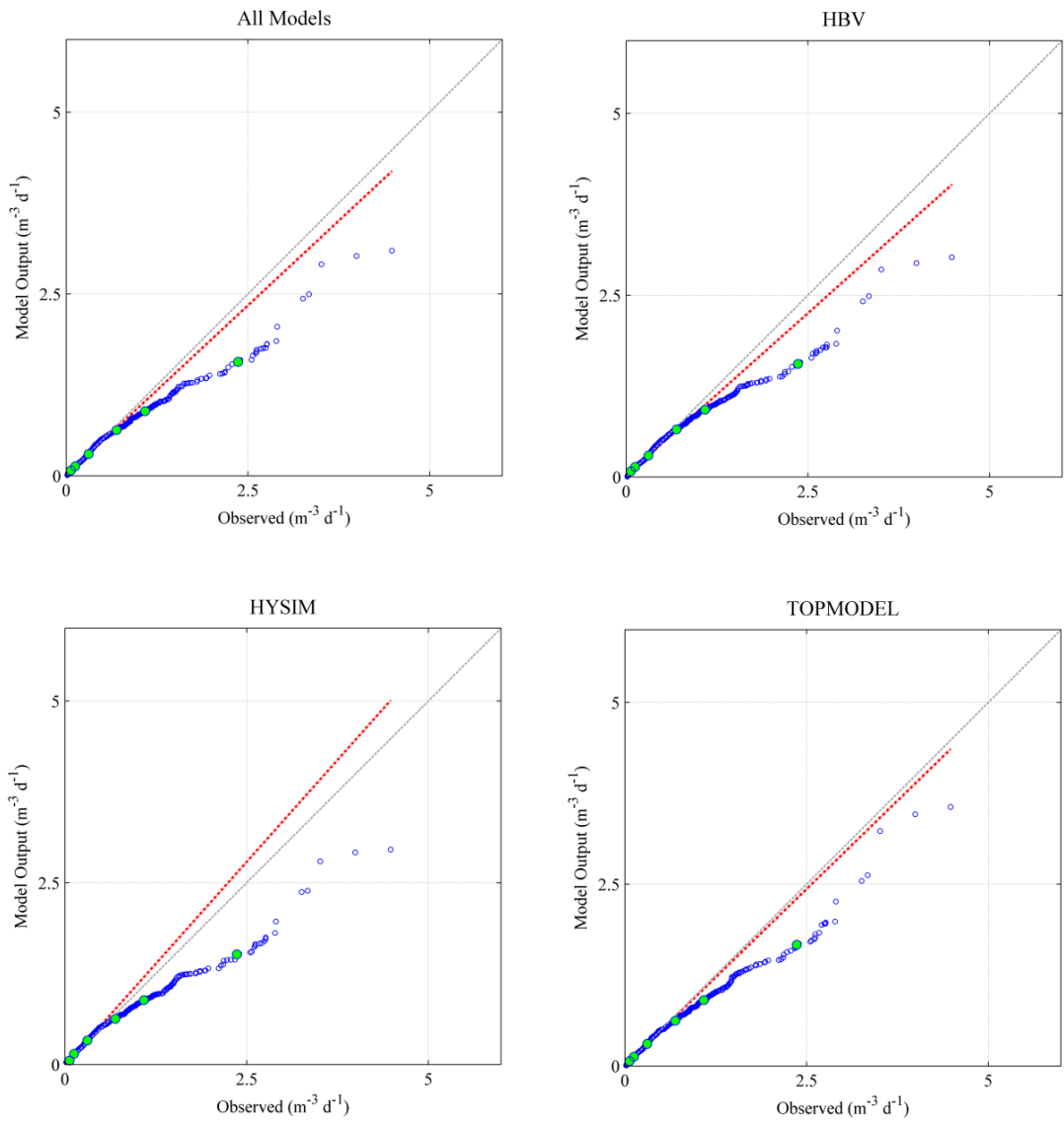


Figure 9.17 Q-Q plots of observed *versus* simulated flow for the Srahrevagh. The median series for each CRR model (HBV, HYSIM and TOPMODEL), as well as the multimodel simulation, is plotted. The green dots are used to highlight those flow values relating to the following percentiles: 25th, 50th, 75th, 90th, 95th and 99th.

The issue of the underestimation of variance may be related to precipitation events which are not fully captured in the observed precipitation records and as a result cannot be correctly represented in the simulated flow series. Given the localised nature of precipitation across the catchment, and the problem of malfunctioning rain gauges, some underestimation of precipitation is likely to have occurred. Thus this issue is not thought to be a problem with the models but rather linked to the quality of the observed data and the inherent responsiveness of the catchment.

On the basis of the results discussed above for both catchments, the multimodel approach appears to have two advantages over using any single model in isolation. Firstly, the multimodel simulation exhibits a consistently high level of skill across each of the performance criteria employed. This is in contrast to the performance of the models on an individual basis which is more variable - albeit that in some cases this is only marginally so. Secondly, where a single model performs better than the multimodel simulation it is typically linked to the model having narrower uncertainty bounds. In contrast the bounds of the multimodel ensemble are generally wider than any individual model - reflected in the CE and PI values for each. Thus the multimodel ensemble has the advantage of being consistently skillful (with respect to the metrics employed) but it also has wider bounds allowing it to capture a larger proportion of the uncertainty space.

9.7 The contribution of rainfall-runoff models to uncertainty

Figure 9.18 is used to highlight the contribution which the rainfall-runoff models make to the envelope of projected changes in the annual flow regime. Here the climate scenario provided by the Danish Meteorological Institute (DMI-HIRHAM5-ARPEGE) is used to explore the contribution which both model structure and parameter uncertainty make to the overall uncertainty in the projected hydrological response. Figure 9.18 shows the average width of the 90% PI simulated using the retained behavioral parameter sets for each of the three rainfall-runoff models used; also shown is the average width of the 90% PI for the multimodel simulation. The PI is reported on a monthly basis for each horizon (as well as the control period) as a percentage of the mean monthly flow value from the median simulation for that period - this removes any bias for months with greater/lesser absolute values.

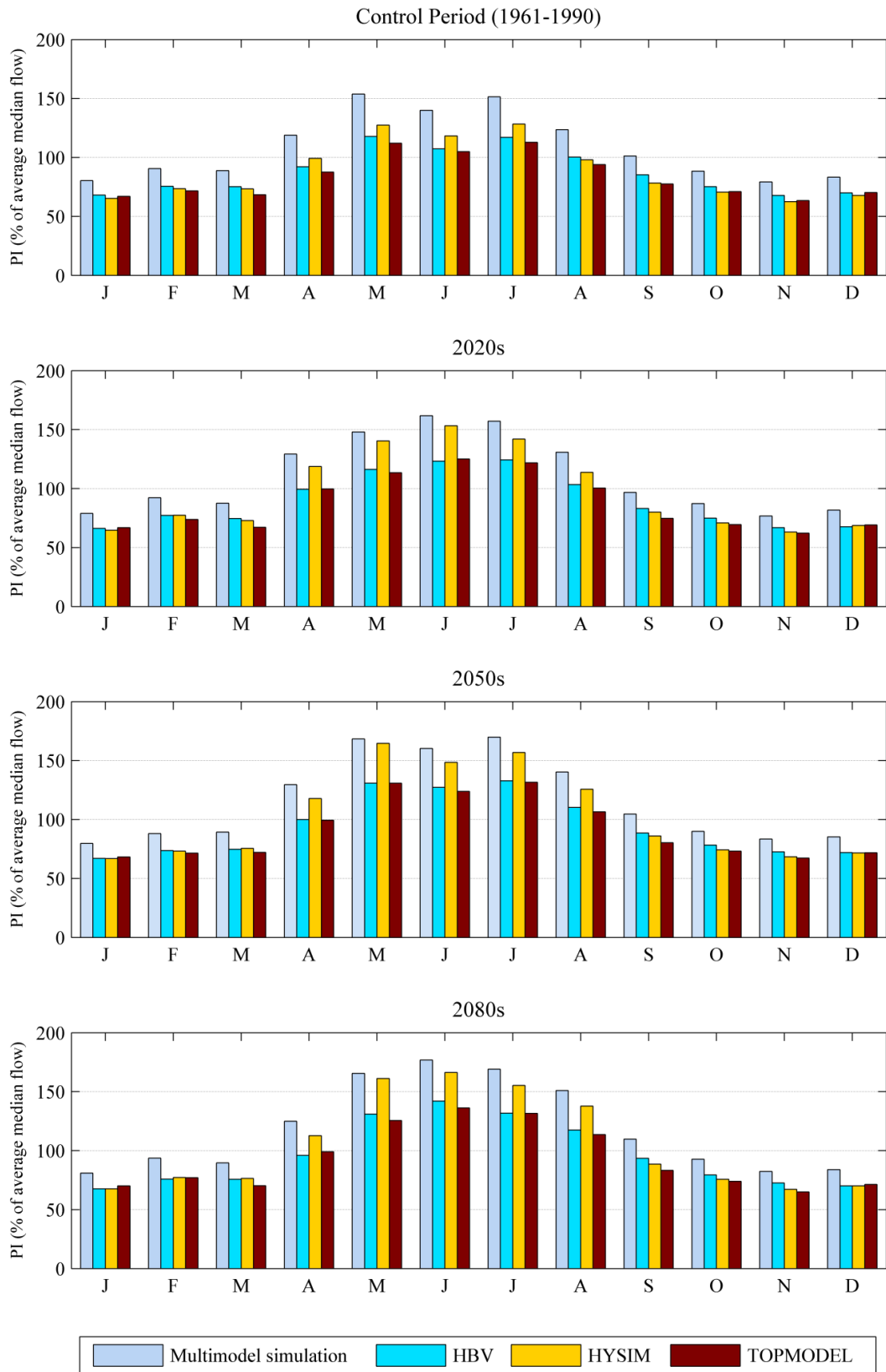


Figure 9.18 Average width of the 90% prediction interval (PI) simulated using the retained behavioral parameter sets for each of the three CRR (HBV, HYSIM and TOPMODEL); also shown in the average width of the 90% PI for the multimodel simulation. The PI is shown as a percentage of the mean monthly flow value calculated using the median simulation for that period.

The plots show that the bounds are greatest for the multimodel simulation as opposed to the models when considered on an individual basis. As such it highlights the value of combining the output from different model structures in terms of capturing uncertainties which GLUE, when applied to any single model in isolation, cannot account for. In such cases uncertainty in the model parameters is being considered without recourse to uncertainty in the model structure, thus resulting in an underestimation of the potential uncertainty in the hydrological response. The degree to which the PI of the multimodel ensemble increases over the PI of the models on an individual basis is indicative of the influence which the model structure has on the uncertainty bounds. The relatively marginal increase in the multimodel PI above that of each model independently does not indicate that the role of structural uncertainty is of a lesser magnitude than parametric uncertainty. This is because uncertainties cannot be disaggregated and independently quantified given that there is no true value for the model parameters or structure. Thus the interaction between uncertainties stemming from both sources masks the contribution which each makes on an independent basis to the overall predicative uncertainty.

In general the bounds are widest for summer and narrowest over the winter months; in addition the rainfall-runoff model with the widest/narrowest bounds varies depending on the month considered. The greater and more variable width of the bounds for the summer season is symptomatic of the difficulties encountered by the models when transitioning from wetter to drier periods - and vice versa. In addition, it is most likely that as conditions become more removed from those experienced over the observed period - on which the models have been trained - that a greater variation in the model response would be experienced. This is typified by the projections for the summer months whereby the width of the PI increases over each successive future horizon (relative to the control period) - an outcome which is particularly noticeable for the HYSIM model. The same analysis conducted using alternative input data indicated that irrespective of the driving scenario used, similar results regarding differences in the PI of the individual model and multimodel response were returned.

9.8 Components of uncertainty

To highlight the importance of considering each component in the cascade of uncertainty estimated changes in the mean annual flow regime (both on a seasonal and monthly basis) of the Glenamong catchment are further explored. Specifically, the range in the projected hydrological response is examined, whereby the affects of each component in the cascade is considered in isolation by holding all others constant. Table 9.12 demonstrates that irrespective of which component is considered, there are no noticeable increases/decreases in the range associated with each; however, given that the range fluctuates on both a seasonal and monthly basis, this is difficult to conclusively determine, and would require further analysis. A number of studies have indicated that typically the choice of emission scenario and/or GCM contributes most to the overall uncertainty in the hydrological response (e.g. Wilby & Harris, 2006; Prudhomme & Davies, 2009b; Kay *et al.*, 2009; Chen *et al.*, 2011); however, others have pointed to the downscaling technique or the hydrological model (structure or parameter set) used as being equally important in terms of their contribution to the uncertainty envelope (e.g. Bastola *et al.*, 2011).

In Table 9.12 the largest absolute ranges are associated with instances where the GCM is varied (e.g. 57.5% August; 36.5% summer). Irrespective of whether the input data is statistically or dynamically downscaled, the choice of GCM is shown to be important in determining the hydrological response. It is also shown that different RCMs (when run using the same GCM data) return similar ranges as in cases where both the GCM and emission scenario are altered. Thus, the downscaling method - or more specifically the RCM used - has a comparable affect on differences in the hydrological response as the choice of GCM or emission scenario. Table 9.12 also highlights the range in projected changes when each of the three hydrological models is run using the same driving data. In this instance the median series calculated for each model is considered. The CRR model used appears to affect the hydrological response to a similar degree as when other components in the uncertainty cascade are examined. The influence of climate sensitivity is also explored in Table 9.12. It is shown that the estimated range when the climate sensitivity is altered (e.g. for April 34.8%) is comparable to the ranges obtained when other components are considered.

	Jan	Feb	Mar	Apr	May	Jun	Jul	Aug	Sept	Oct	Nov	Dec	Winter	Spring	Summer	Autumn
<u>Altered Emission Scenario</u>																
SDSM HadCM3 A2	12.6	2.3	-4.2	-11.3	-10.3	-10.3	-20.9	-35.1	-19.7	-23.0	-0.5	14.6	11.0	-7.6	-24.5	-13.9
SDSM HadCM3 B2	2.4	10.1	-1.1	5.5	-4.3	-6.1	-11.5	-15.8	-3.9	-12.0	-7.1	7.2	6.0	0.1	-11.9	-8.0
Range	10.1	7.8	3.2	16.8	5.9	4.3	9.4	19.4	15.8	11.0	6.6	7.4	4.9	7.7	12.5	5.9
<u>Altered GCM: statistical downscaling</u>																
SDSM HadCM3 A2	12.6	2.3	-4.2	-11.3	-10.3	-10.3	-20.9	-35.1	-19.7	-23.0	-0.5	14.6	11.0	-7.6	-24.5	-13.9
SDSM CGCM2 A2	16.6	2.3	-24.5	-34.7	-44.2	-39.7	-34.8	6.4	-12.0	-16.3	-10.9	7.2	9.7	-31.8	-18.3	-13.1
Range	4.0	0.0	20.3	23.4	33.9	29.4	13.9	41.6	7.7	6.7	10.4	7.5	1.3	24.2	6.2	0.7
<u>Altered GCM: dynamical downscaling</u>																
DMI-HIRHAM5 ARPEGE A1B	11.1	1.6	1.8	-1.8	-20.4	-31.0	-5.5	-42.2	-6.9	-3.0	-1.1	12.4	9.4	-4.0	-29.6	-3.4
DMI-HIRHAM5 ECHAM5-r3 A1B	21.4	3.4	18.4	24.4	8.5	1.3	-2.1	15.4	-3.0	6.3	18.1	11.8	13.6	17.9	6.8	7.8
Range	10.3	1.8	16.6	26.2	28.9	32.3	3.4	57.5	3.9	9.3	19.2	0.7	4.1	21.9	36.5	11.2
<u>Altered RCM</u>																
ICTP-REGCM3 ECHAM5-r3 A1B	14.1	1.1	9.3	6.8	1.3	-7.6	4.1	0.5	-7.0	-2.0	12.6	7.8	8.7	6.8	-1.0	1.7
DMI-HIRHAM5 ECHAM5-r3 A1B	21.4	3.4	18.4	24.4	8.5	1.3	-2.1	15.4	-3.0	6.3	18.1	11.8	13.6	17.9	6.8	7.8
Range	7.3	2.3	9.1	17.6	7.2	8.9	6.2	14.9	4.0	8.3	5.5	3.9	4.9	11.2	7.9	6.1
<u>Altered Climate Sensitivity</u>																
METO-HadRM3Q0 HadCM3Q0 A1B	7.0	-1.7	-0.6	-2.3	6.2	-26.8	-17.7	-19.0	-8.6	12.3	9.9	7.6	5.2	0.4	-21.1	5.5
METO-HadRM3Q3 HadCM3Q3 A1B	11.7	10.7	5.9	32.6	-4.5	-21.8	-19.7	-30.9	9.3	6.1	12.2	24.6	16.2	11.5	-25.6	9.2
METO-HadRM3Q16 HadCM3Q16 A1B	12.3	2.5	-0.4	3.3	11.6	-35.2	-20.6	-24.3	3.6	17.5	32.5	10.2	9.2	3.4	-26.7	18.9
Range	5.3	12.4	6.6	34.8	16.1	13.4	2.9	11.9	17.9	11.4	22.5	17.1	11.0	11.0	5.7	13.4
<u>Altered Hydrological Model</u>																
HBV: C4IRCA3 HadCM3Q16 A1B	17.5	6.4	2.2	1.9	18.2	-26.0	-1.7	-14.2	1.4	15.3	33.8	22.4	24.6	7.4	-14.0	16.8
HYSIM: C4IRCA3 HadCM3Q16 A1B	13.2	3.9	0.8	-6.9	4.0	-31.7	-18.6	-24.5	-4.1	10.5	28.2	16.5	19.3	-0.7	-24.9	11.5
TOPMODEL: C4IRCA3 HadCM3Q16 A1B	13.4	3.3	1.2	-3.8	6.3	-27.1	-9.5	-18.0	-2.6	9.6	28.2	16.8	19.5	1.3	-18.2	11.7
Range	4.3	3.1	1.4	8.8	14.2	5.7	16.9	10.3	5.5	5.7	5.6	5.9	5.2	8.1	11.0	5.3

Table 9.12 Projected changes (%) in mean flow for the 2080s horizon (2070-2099) relative to the 30 year control period (1961-1990). Changes in flow are estimated for the Glenamong catchment. The range in projected mean monthly and seasonal flow for each uncertainty component is shown. The range is taken as the difference in the projected flow suggested when each component in the uncertainty chain is altered whilst the others are held constant. The cells are colour coded to highlight higher/lower values.

Table 9.12 offers only a superficial assessment of uncertainty, for example parameter uncertainty is not examined nor is the affect of natural variability. Furthermore, basing it on monthly/seasonal changes in mean flow, where only a sub-sample of the full range of climate data is used, means that no clear findings can be provided. Despite this, Table 9.12 does highlight the importance of sampling right across the uncertainty cascade, and although it cannot be said what the dominant source(s) of uncertainty are, it can be inferred that omitting any one component may result in the under estimation of uncertainty. It also highlights that uncertainty stemming from the climate sensitivity and choice of RCM, both of which are sources of uncertainty which are typically not addressed in impact assessments, should be considered in studies that seek to quantify or explore all aspects of the uncertainty cascade.

9.9 Projected changes in flow

The results from climate impact studies are underpinned by an assumption in the stationarity of the model parameters. In the interests of reducing uncertainty in the projected response it is important that the validity of this assumption is addressed (e.g. Booij 2005; Dibike & Coulibaly 2005; Maurer & Duffy 2005; Wilby, 2005; Fowler & Kilsby 2007; Vaze *et al.*, 2010). Due to the short length of the hydro-climatological records available for use in this study, and that no prolonged period of extreme wet or dry conditions were represented in the observed series, stationarity was dealt by imposing additional efficiency criteria (model bias and NS_{log}), setting relatively high threshold values and using a split-sample approach to model calibration/validation - albeit that the samples did not represent contrasting hydrological or climate conditions. The shortcomings of such an approach are acknowledged; however, given the constraints of the observed data the options available for model testing were limited.

Projected changes in the flow regime of each catchment are examined on the basis of three future time horizons: the 2020s (2010-2039), 2050s (2040-2069) and 2080 (2070-2099); the 30 year model control period (1961-1990) is used to represent baseline or reference conditions. The first set of results are derived using GLUE (Beven & Bingley, 1992) and are discussed with respect to each of the twenty five climate scenarios considered (Figure 6.11). When the results from individual climate pathways are reported the median of the multimodel simulation is used. The results from the Monte Carlo simulation discussed above are also given. Appendix IV lists the projected

changes in the flow regime of both catchments estimated using each individual ensemble member. Changes in the annual flow regime (examined both on a seasonal and monthly basis) are explored using three key flow indices relating to high (Q05), low (Q95) and median (Q50) flow conditions.

9.9.1 Glenamong

Generally the model projections suggest that the catchment's flow regime is likely to become increasingly seasonal in nature, with higher winter and lower summer flows occurring. There is however a high degree of inter-scenario variability regarding the exact magnitude, timing and direction of change, particularly over the transition seasons of spring and autumn.

9.9.1.1 Median Flow (Q50): Individual Climate Pathways

Figure 9.19 shows projected changes in the monthly median (Q50) flow statistic for the Glenamong catchment. Over the 2020s the greatest relative increase is suggested for March (+57.5%) by the climate scenario from the Swedish Meteorological and Hydrological Institute (SMHI). In this case the low sensitivity HadCM3 model was used as the driving GCM. Over this horizon the largest decrease is projected for the month of February (-31%) by the statistically downscaled CGCM2 A2 pathway.

Over the 2050s the single largest increase in Q50 is associated with March for which the SMHI scenario (using the Bergen Climate Model) suggests an increase of 61%. The greatest decrease is suggested for December (-42.6%) by the ensemble member provided by the Max-Planck Institute. In this case the ECHAM5-r3 GCM was used as the driving model. On a seasonal basis all of the pathways suggest a decrease in summer Q50 (ranging from -23.8% to -8.4%).

Over the 2080s the greatest relative increase is again suggested for March by the SMHI (BCM) pathway (+72%); the greatest decrease is projected for August by the Météo-France (CNRM-RM5.1 ARGEGE) climate scenario (-38.8%). In terms of the prediction range the greatest difference in projected changes is associated with March (97.9%); in contrast the narrowest prediction range is associated with July (24.2%). The increased

seasonality of the flow regime is most pronounced over the 2080s (as is evident from the A1B ensemble average in Figure 9.19), indicating that for this period a much clearer climate change signal is present. Over this time horizon each of the pathways suggest a decrease in summer Q50 (range -3.3% to -29.3%); whilst the majority of pathways suggest an increase in median flow for the winter season (range -3.2% to 54.6%).

9.9.1.2 Median Flow (Q50): Probabilistic Flow Projections

Figure 9.20 shows the posterior distribution derived from the MC analysis of the A1B pathways for the Q50 flow statistic (see Figure 6.11). The distribution is represented as a boxplot constructed for each month and future horizon. The plots suggest an increase in the seasonality of the flow regime, with this trend projected to become increasingly pronounced over each successive horizon. The greatest reductions are associated with the months of June and August over the 2080s; for this horizon the median of the posterior distribution suggests a ~20% decrease in Q50 for both months. The greatest increases are projected for the months of January and March over the 2080s and 2050s respectively. The widest uncertainty bounds (based on the 90% confidence interval) are generally associated with the months of March, February and December.

Results from the MC simulation conducted for the A2 and B2 based model pathways are shown in Figure 9.21; in addition the results of the MC simulation carried for both the A2 and B2 scenarios is shown. As the HadCM3 GCM is the most heavily weighted, it is sampled most often during the analysis and therefore has a greater bearing on the projected response. The suggested increase in the seasonality of the flow regime is most pronounced under the more carbon intensive A2 SRES scenario. Changes relating to the both the B2 and A2/B2 based projections are of a lesser magnitude. The largest decreases in Q50 are projected for the summer and to a greater extent autumn months. Under the A2 scenario, for the 2080s horizon the greatest decrease in Q50 is suggested for the months of August (-29.9%), September (-27%) and October (-29.4%). Under the B2 scenario a lesser decrease of 16%, 9% and 17.2% is suggested for the same months. Under the B2 scenario the greatest increase in Q50 is associated with December over the 2050s; for this month Q50 is projected to increase by 19.3%. An increase of a similar magnitude is suggested for February over the 2080s horizon. The uncertainty bounds are generally widest for August, April and March.

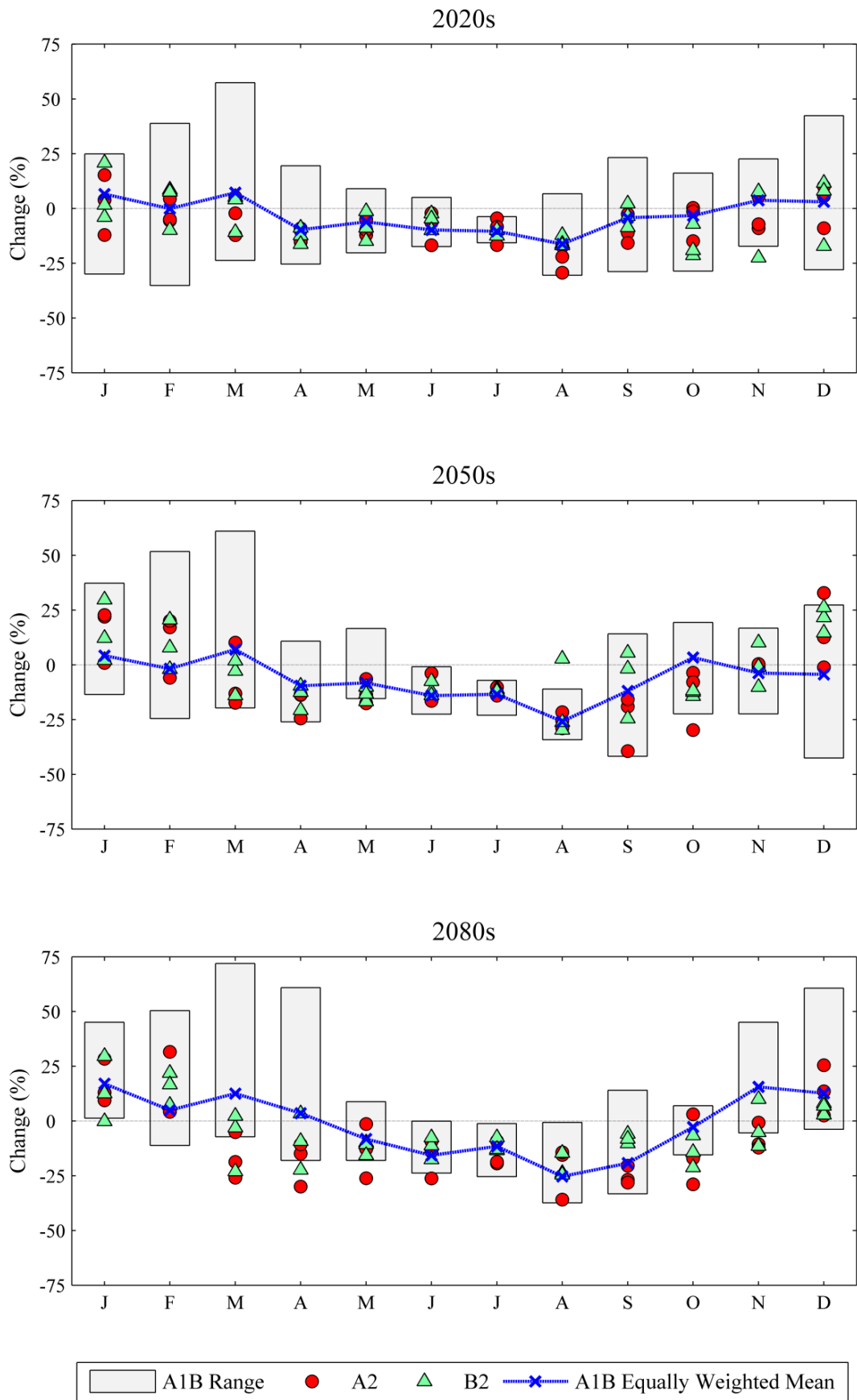


Figure 9.19 Percentage change in the Q50 flow statistic for the Glenamong catchment calculated relative to the 30 year control (1961-1990) period for the 2020s (top), 2050s (middle) and 2080s (bottom) respectively. The range in projected changes from the A1B model pathways are plotted using the grey bar; model projections relating to the A2 and B2 emission scenarios are plotted separately. Also shown is the weighted mean ensemble for the A1B ensemble members

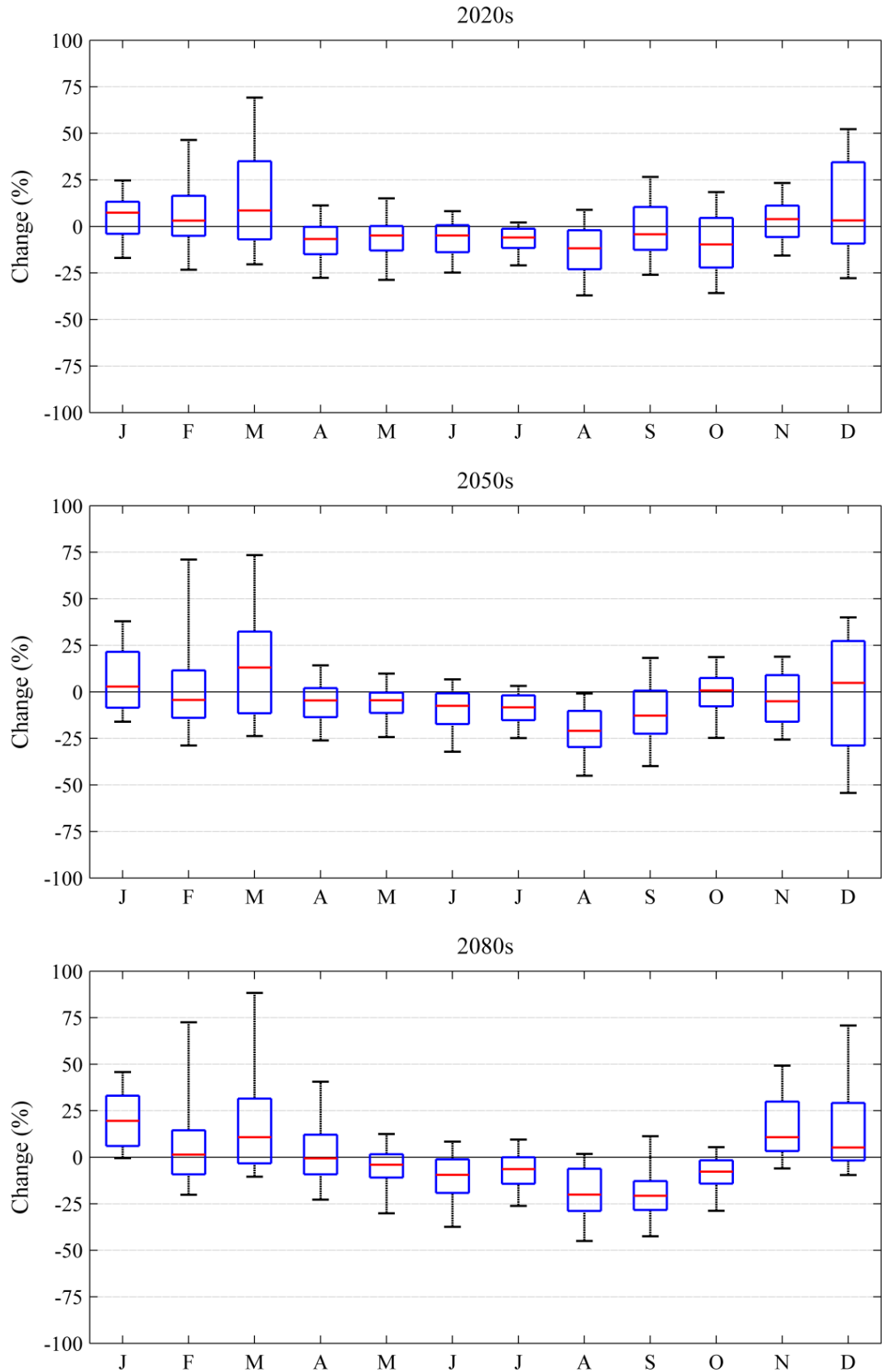


Figure 9.20 Monthly boxplots of the percent change in the Q50 median flow statistic for the Glenamong catchment. Changes are estimated relative to the 30 year control (1961-1990) period for the 2020s (top), 2050s (middle) and 2080s (bottom) respectively. The plots are formulated based on the posterior distribution of the Monte Carlo simulation conducted for the AIB based climate scenarios. On each box the central mark represents the median, the edges represent the 25th and 75th percentiles and the whiskers represent the 90% confidence interval.

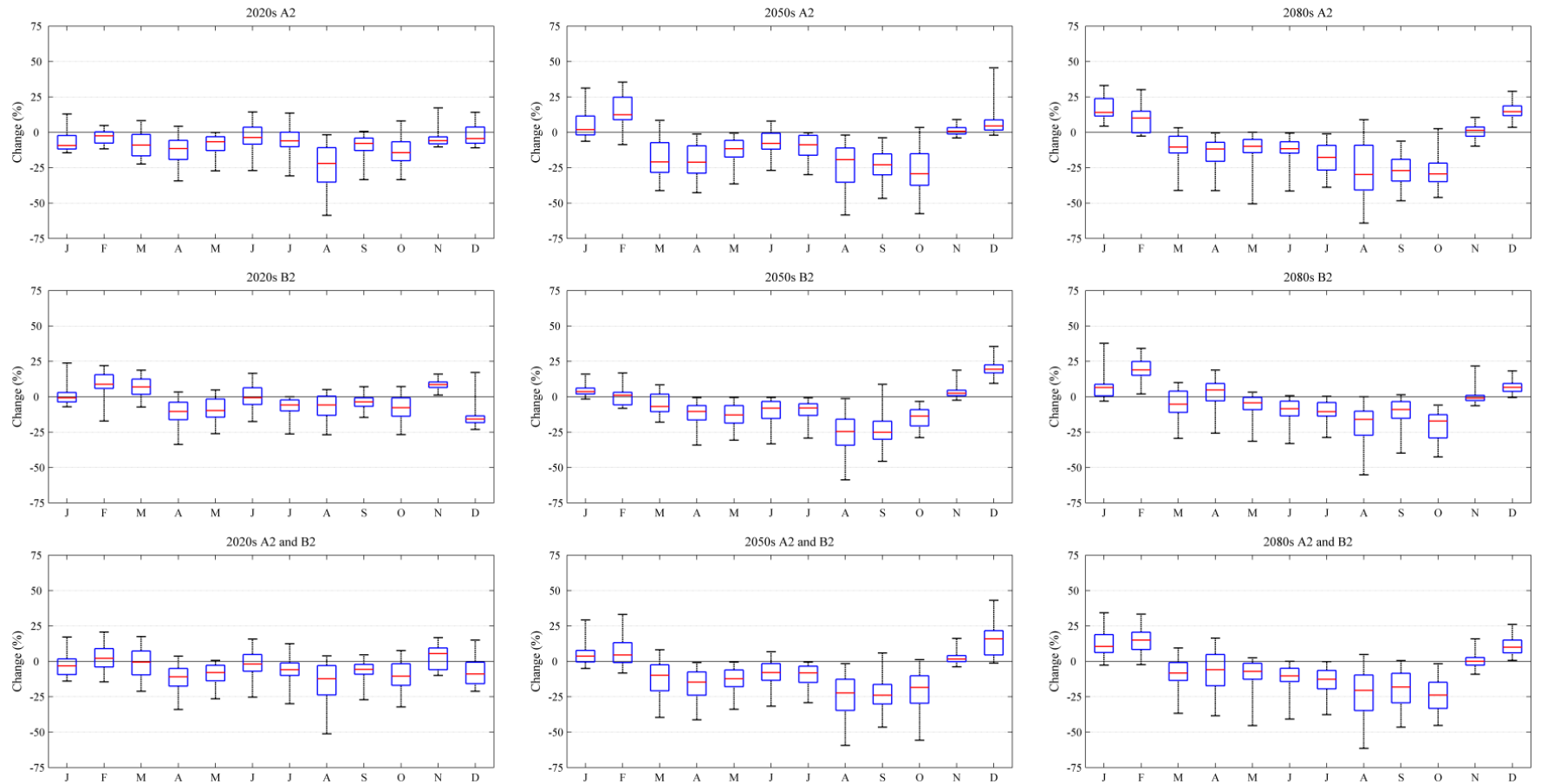


Figure 9.21 Monthly boxplots of the percent change in the Q50 median flow statistic for the Glenamiong catchment. Changes are estimated relative to the 30 year control (1961-1990) period for the 2020s (left), 2050s (middle) and 2080s (right) respectively. The plots are formulated based on the posterior distribution of the Monte Carlo simulation conducted for the A2 (top), B2 (middle) and A2/B2 based climate scenarios (bottom). On each box the central mark represents the median; the edges represent the 25th and 75th percentiles and the whiskers represent the 90% confidence interval.

9.9.1.3 High Flows (Q05): Individual Climate Pathways

Figure 9.22 shows the projected changes in Q05 (i.e. the flow that is equally or exceeded 5% of the time) for the Glenamong catchment. In accordance with the suggested increase in the seasonality of the flow regime, the model projections generally indicate that high flows are likely to increase over the winter months and decrease during summer. Over the 2020s the greatest increase (+46.1%) is suggested for June under the climate scenario provided by the Danish Meteorological Institute (DMI) - for which the ECHAM5-r3 was used as the driving GCM. Of the winter months the largest increase in Q05 is suggested for January (+26.8%) by the SMHI low sensitivity (Q3) HadCM3 GCM pathway. For the winter season the same pathway suggests an increase of 22.5%.

Over the 2050s the greatest increase is projected for December (+38.4%) by the DMI-ARPEGE climate scenario. The greatest relative increase for the winter season (+18.8%) is also suggested by this climate pathway. For the 2080s horizon all projections indicate an increase in high flows during the winter season - this increase ranges from 2.5% (MPI-M ECHAM5-r3 scenario) to 23.8% (DMI-ARPEGE scenario).

9.9.1.4 High Flows (Q05): Probabilistic Flow Projections

Based on the median of the posterior distribution for the A1B based climate scenarios (Figure 9.23) the greatest increases in Q05 are associated with February (+15%) and December (+14%) over the 2080s. The greatest decrease is projected for July (-10%) over the same horizon. The 90% confidence interval is generally largest for May over the 2020s; in contrast the interval is narrowest for September and October over the 2050s. What is apparent from Figure 9.23 is that the width of the plots increases as the century progresses, indicating a greater degree of divergence between the individual model projections.

Projected changes in Q05 suggested by the results of the MC analysis conducted using the statistically downscaled scenarios are shown in Figure 9.24. Generally the greatest increases in high flows are suggested for the winter months over the 2080s. Under the A2 SRES scenario an increase of 16.4% and 21.8% is suggested for January and December respectively. Under the B2 SRES scenario for the same months an increase of 9.2% and 17.3% is suggested.

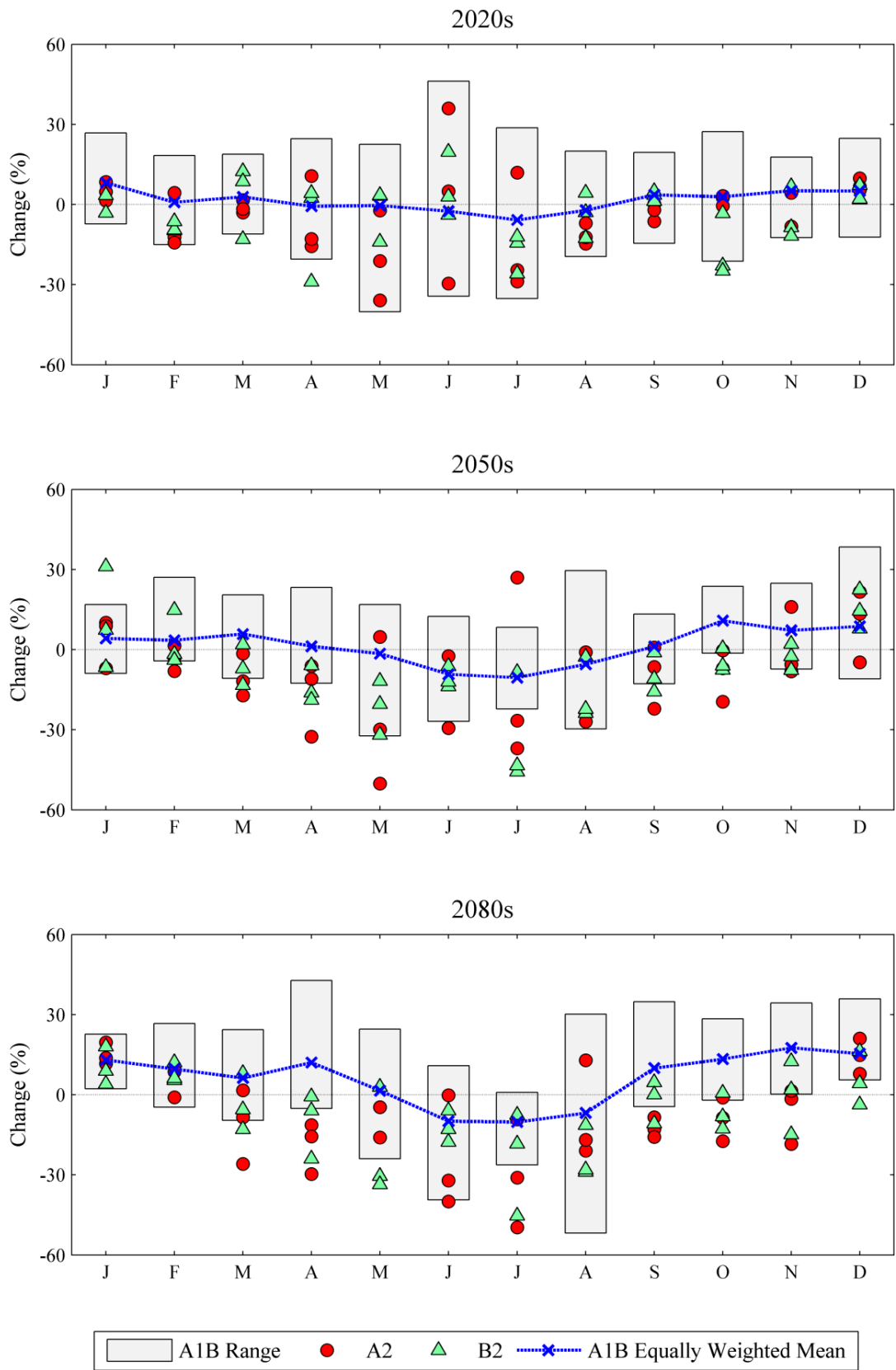


Figure 9.22 Percentage change in the Q05 flow statistic for the Glenamong catchment calculated relative to the 30 year control (1961-1990) period for the 2020s (top), 2050s (middle) and 2080s (bottom) respectively. The range in projected changes from the A1B model pathways are plotted using the grey bar; model projections relating to the A2 and B2 emission scenarios are plotted separately. Also shown is the weighted mean ensemble for the A1B ensemble members.

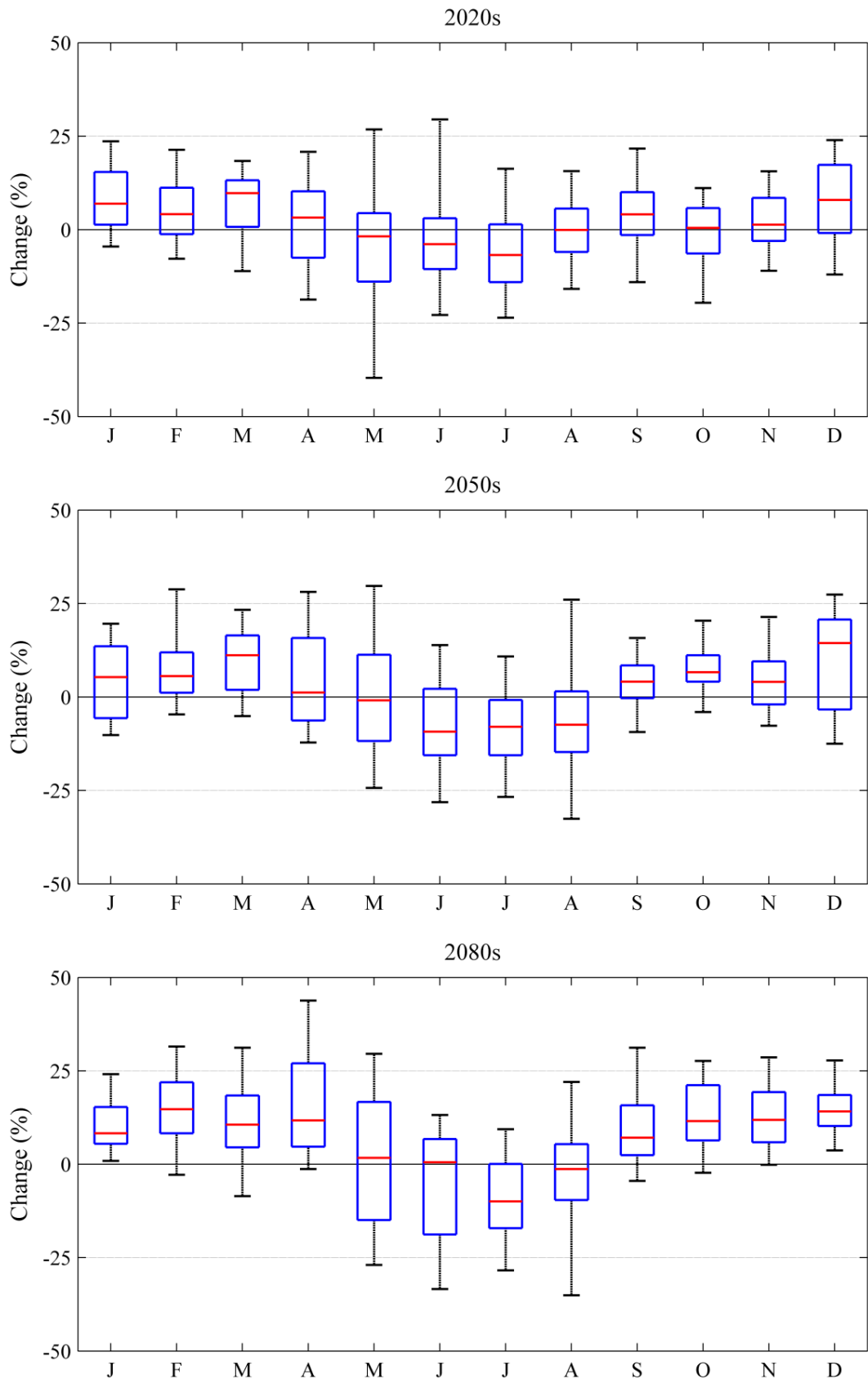


Figure 9.23 Monthly boxplots of the percent change in the Q05 median flow statistic for the Glenamong catchment. Changes are estimated relative to the 30 year control (1961-1990) period for the 2020s (top), 2050s (middle) and 2080s (bottom) respectively. The plots are formulated based on the posterior distribution of the Monte Carlo simulation conducted for the A1B based climate pathways. On each box the central mark represents the median, the edges represent the 25th and 75th percentiles and the whiskers represent the 90% confidence interval.

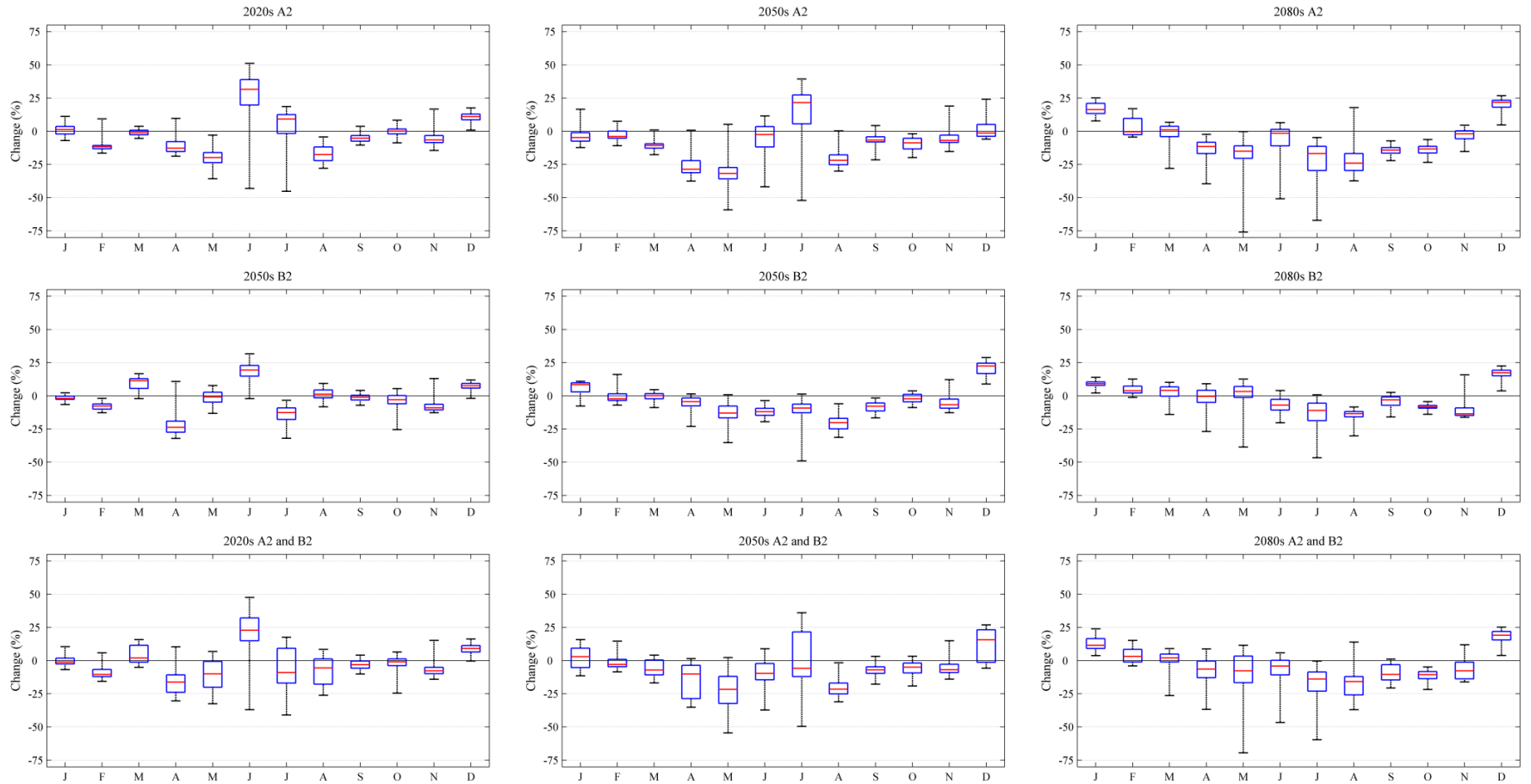


Figure 9.24 Monthly boxplots of the percent change in the Q05 median flow statistic for the Glenamong catchment. Changes are estimated relative to the 30 year control (1961-1990) period for the 2020s (left), 2050s (middle) and 2080s (right) respectively. The plots are formulated based on the posterior distribution of the Monte Carlo simulation conducted for the A2 (top), B2 (middle) and A2/B2 based climate scenarios (bottom). On each box the central mark represents the median; the edges represent the 25th and 75th percentiles and the whiskers represent the 90% confidence interval.

9.9.1.5 Low Flows (Q95): Individual Climate Pathways

Low flows are calculated using the Q95 flow threshold, denoting the flow which is equalled or exceeded 95% of the time. Over the 2020s the greatest decrease in Q95 is projected for October (-26.8%) by the climate scenarios provided by the Norwegian Meteorological Institute (METNO). In this case the HadCM3 standard sensitivity (Q0) model was used as the driving GCM. The range in projected changes for Q95 is generally narrowest during the summer months and greatest during the winter months (Figure 9.25). For the 2050s, the greatest reduction in monthly low flows is projected for October (-23.3%) by the Météo-France ARGEGE scenario. The greatest decrease in summertime Q95 for this horizon is suggested by the statistically downscaled HadCM3 A2 climate pathway (-12.3%). The statistically downscaled HadCM3 A2 pathway also returns the greatest decrease in monthly flow for the 2080s (October; -22.5%). The largest increase in monthly Q95 over the same horizon is suggested for January (+43.3%). On a seasonal basis the greatest reduction in low flows is projected for summer by the statistically downscaled HadCM3 A2 scenario (-15.7%).

9.9.1.6 Low Flows (Q95): Probabilistic Flow Projections

In contrast to both the median and high flow statistics, projected changes in Q95 under the A1B scenario are much less apparent. However, as Figure 9.26 suggests, the uncertainty associated with future estimates is an important factor in terms of interpreting probabilistic projections. Based on the median of the posterior distribution the greatest decrease associated with any month or time horizon is suggested for November over the 2050s (-6.5%). For Q50 and Q05 differences relative to the control generally increase over each successive horizon; however, in the case of low flows, the reverse is true - most notably over the summer months. This is not in keeping with a general reduction in flow for this period; however, the width of the boxplots suggests there is a large degree of uncertainty associated with how low flows may change in response to altered forcing. The results from the MC simulation are generally in agreement with the analysis conducted for the individual pathways (Figure 9.25).

Boxplots of projected changes in monthly low flows for the A2 and B2 based pathways are shown in Figure 9.27. Generally the projections suggest a reduction in Q95 for the majority of months, particularly during the summer and autumn. The greatest reductions are returned by the A2 based pathways for October (-18.5%) and September (-12.6%)

over the 2050s. With respect to the B2 scenario over the 2080s, a reduction of 2.6%, 8.9% and 8.15% is suggested for June, July and August respectively.

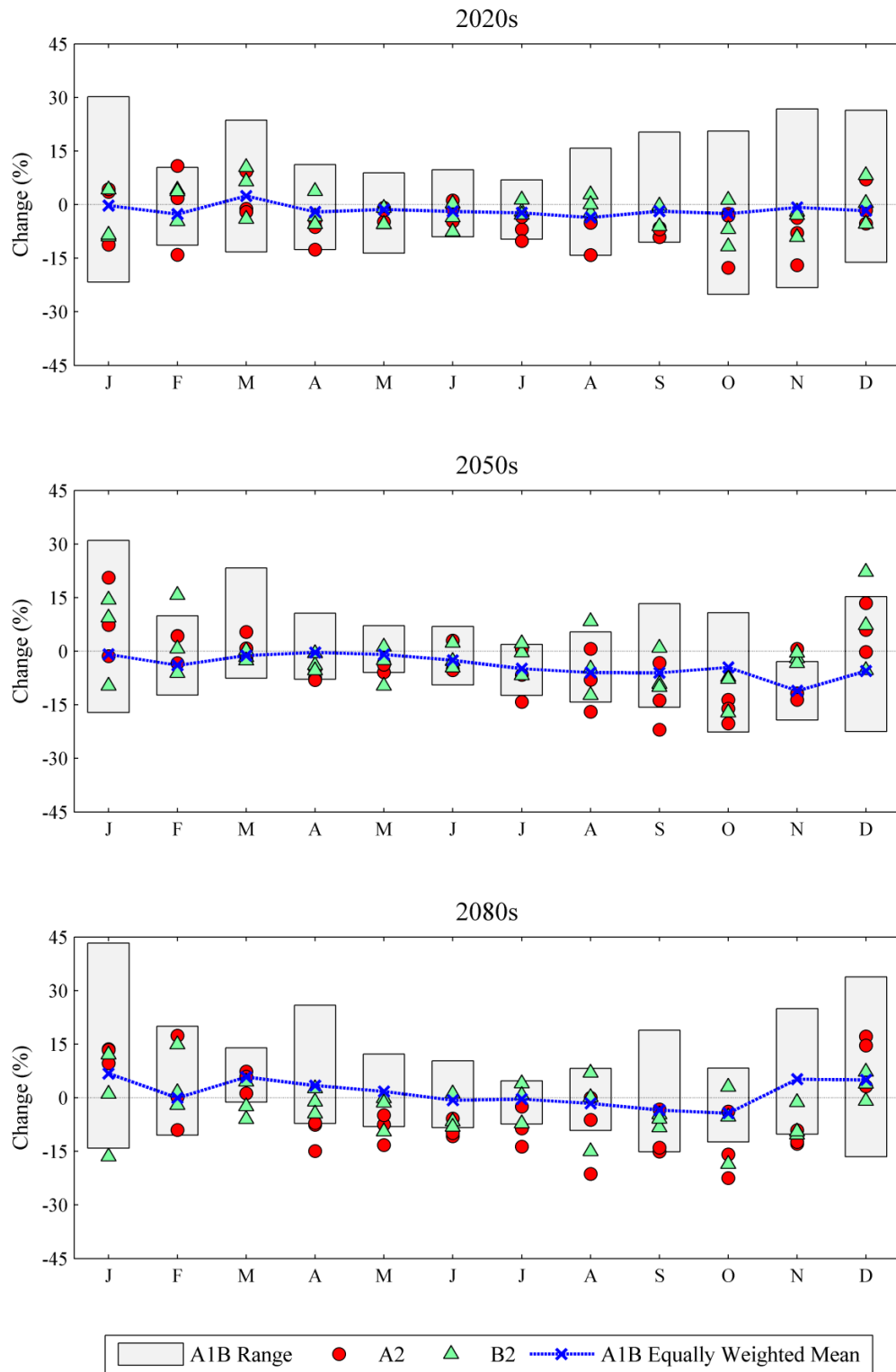


Figure 9.25 Percentage change in the Q95 flow statistic for the Glenamiong catchment calculated relative to the 30 year control (1961-1990) period for the 2020s (top), 2050s (middle) and 2080s (bottom) respectively. The range in projected changes according to the A1B dynamically downscaled climate pathways are plotted using the grey bar; model projections relating to the A2 and B2 emission scenarios are plotted separately. Also shown is the weighted mean ensemble for the A1B ensemble members.

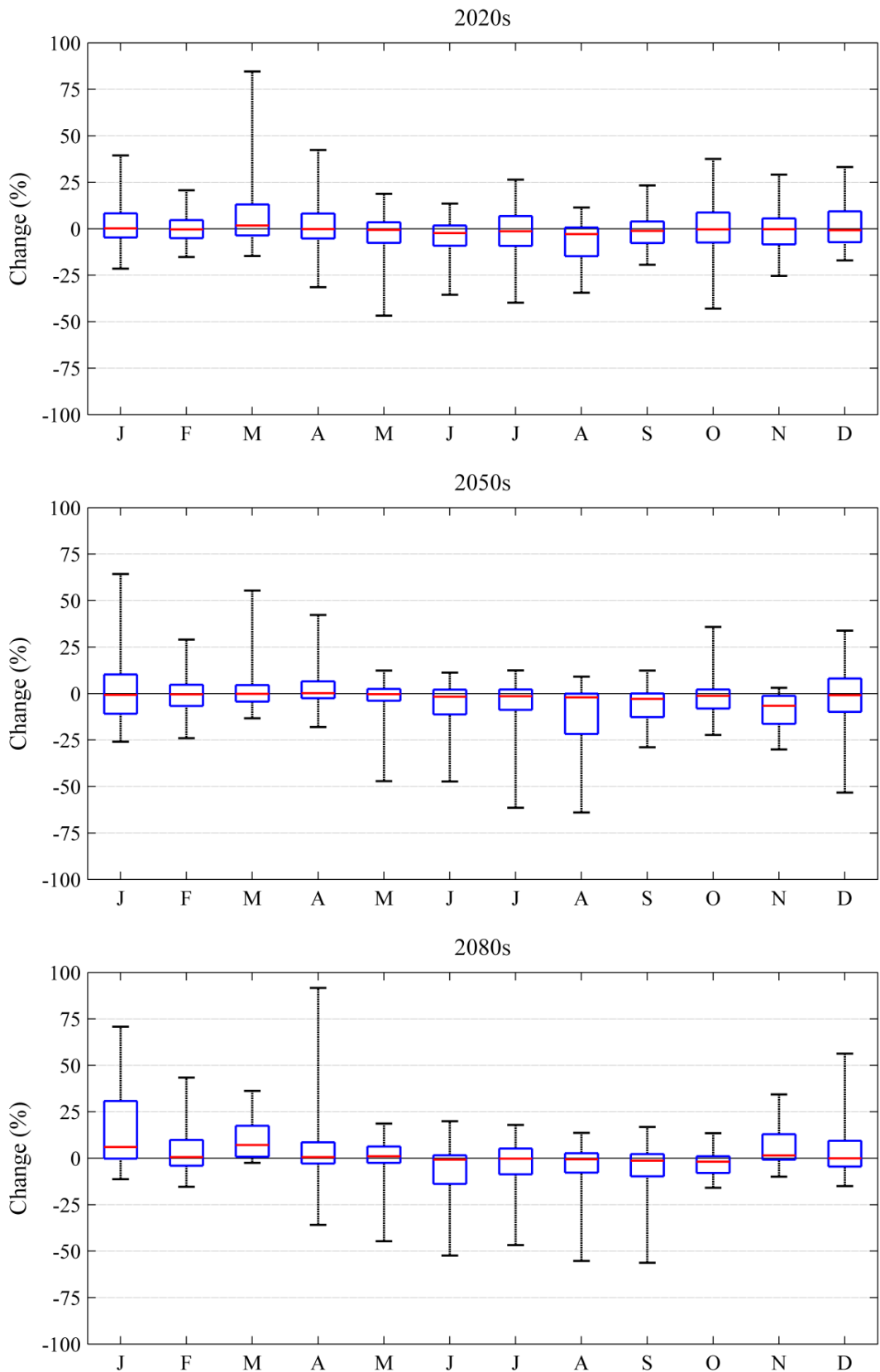


Figure 9.26 Monthly boxplots of the percent change in the Q95 median flow statistic for the Glenamong catchment. Changes are estimated relative to the 30 year control (1961-1990) period for the 2020s (top), 2050s (middle) and 2080s (bottom) respectively. The plots are formulated based on the posterior distribution of the Monte Carlo simulation conducted for the A1B based climate scenarios. On each box the central mark represents the median, the edges represent the 25th and 75th percentiles and the whiskers represent the 90% confidence interval.

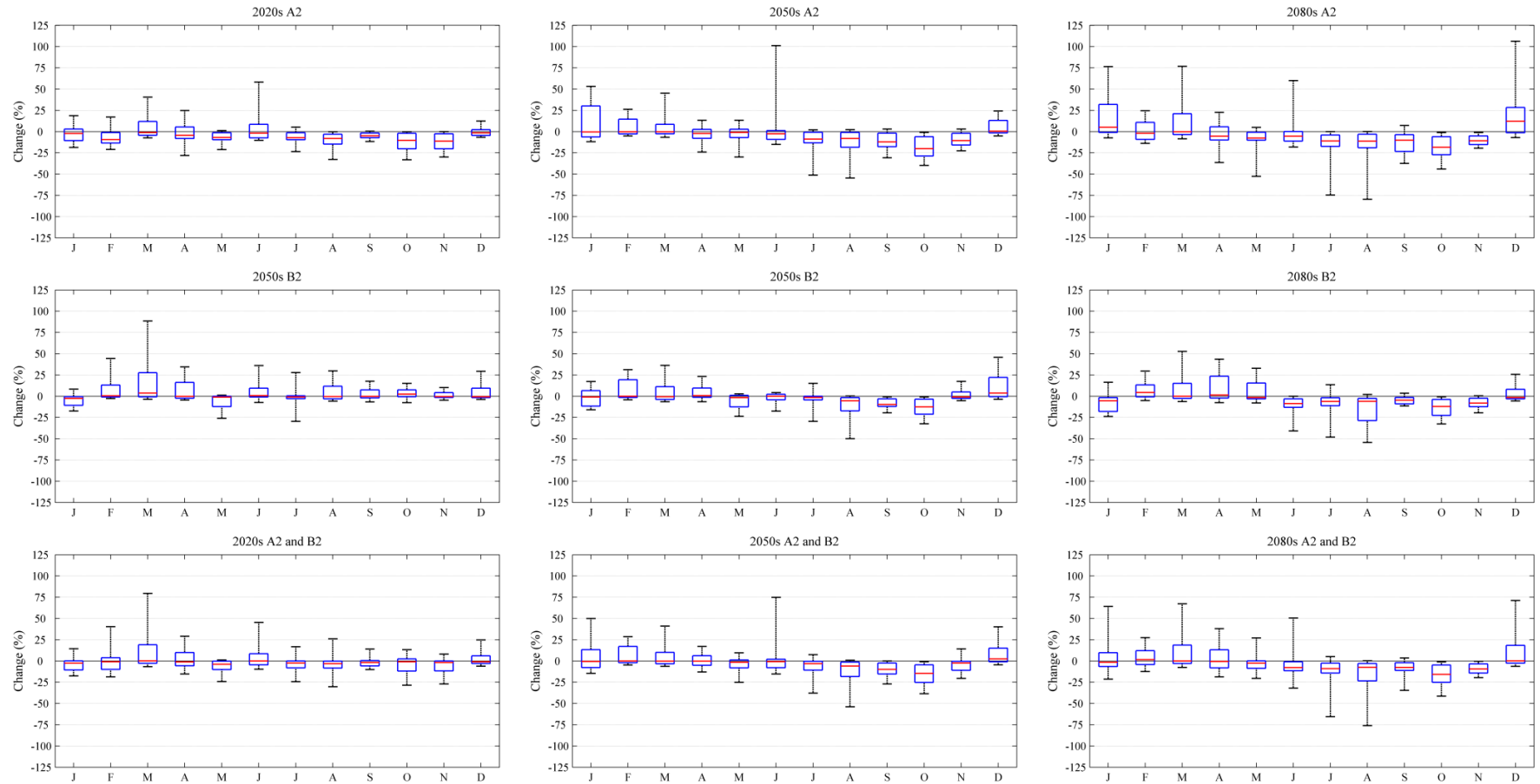


Figure 9.27 Monthly boxplots of the percent change in the Q95 median flow statistic for the Glenamong catchment. Changes are estimated relative to the 30 year control (1961-1990) period for the 2020s (left), 2050s (middle) and 2080s (right) respectively. The plots are formulated based on the posterior distribution of the Monte Carlo simulation conducted for the A2 (top), B2 (middle) and A2/B2 based climate scenarios (bottom). On each box the central mark represents the median; the edges represent the 25th and 75th percentiles and the whiskers represent the 90% confidence interval.

9.9.2 Srahrevagh

Given that that the same scenarios used to examine changes in the flow regime of the Glenamong catchment are used when modelling the Srahrevagh (although quantile mapping was applied to the downscaled data for each), and as the catchment has the same physical characteristics as the Glenamong, the results relating to the probabilistic flow projections only are examined for this catchment.

9.9.2.1 Median Flows (Q50): Probabilistic Flow Projections

Projected changes in Q50 for the A1B SRES scenario suggest an increase in the seasonality of the catchment's flow regime, with this pattern becoming more pronounced as the century progresses (Figure 9.28). The largest decreases in Q50 are associated with the 2080s for the months of August (-19.3%), June (-13.6%), July (-9.4%) and September (-14.7%). For the same horizon the greatest increases suggested by the MC simulation are returned for January (+17.5%), November (+9%), December (+4.4%) and March (+8.5%).

For the A2 based climate pathways over the 2080s the greatest monthly decreases are associated with August (-32.5%), July (-21.9%), September (-16.3%) and October (-21.6%) (Figure 9.29); the greatest increases are associated with December (+14.4%), January (+18.7%) and February (+10.3%) for the same horizon.

9.10.1.2 High Flows (Q05): Probabilistic Flow Projections

Results from the MC simulation (Figure 9.30) based on the A1B climate pathways suggest an increase in Q05 for December (~15%) over both the 2050s and 2080s. For the 2080s increases in high flows of 14.3%, 12.9% and 13.5% are suggested for the months of February, October and November respectively; in contrast a reduction of 10% is projected for the month of July. Projected changes in Q05 under the A2 and B2 based climate pathways are shown in Figure 9.31. The greatest increase in high flows is suggested under the A2 emissions pathway for the months of February (21.5%) and December (23%) over the 2080s horizon.

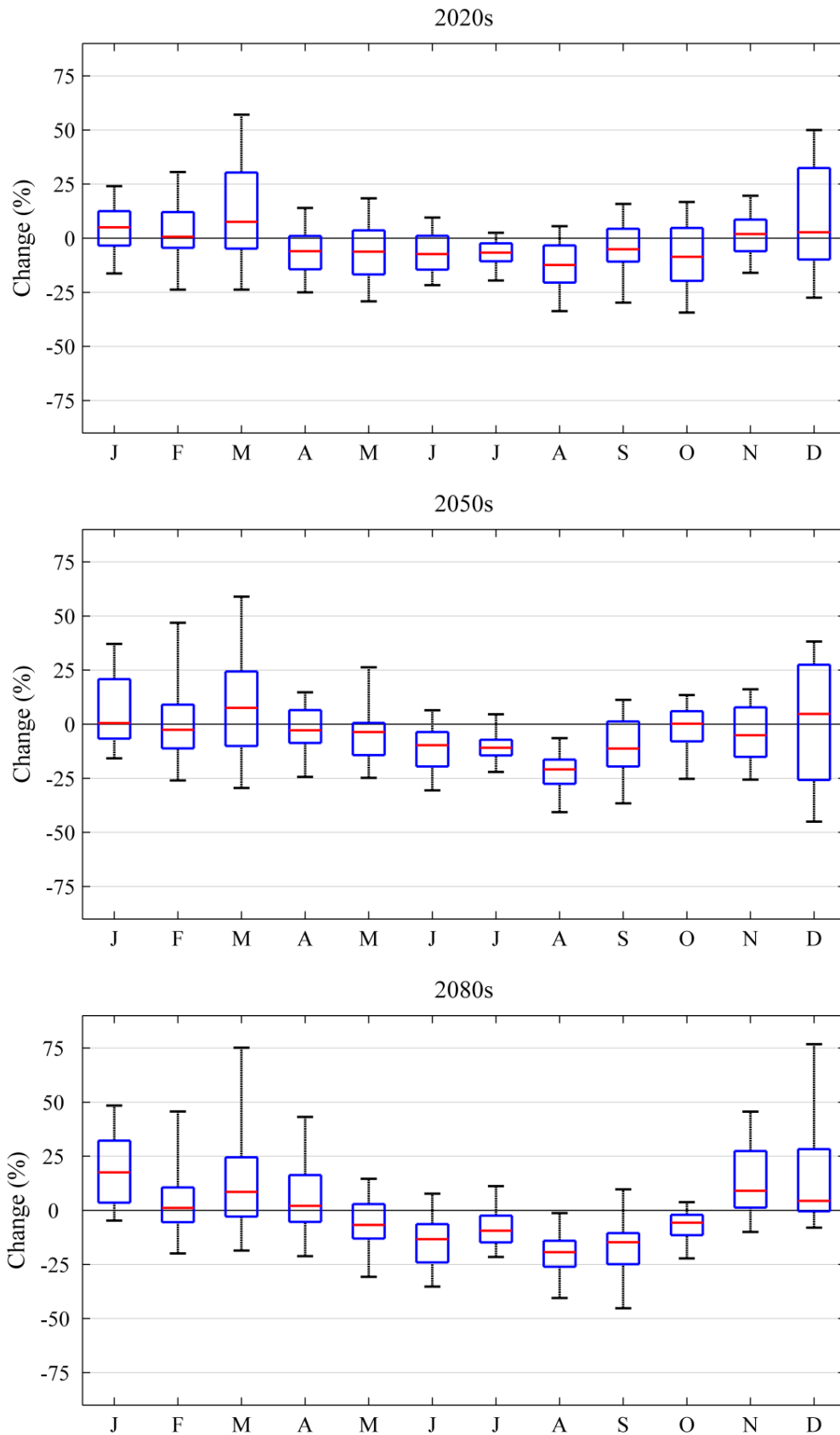


Figure 9.28 Monthly boxplots of the percent change in the Q50 median flow statistic for the Srahrevagh catchment. Changes are estimated relative to the 30 year control (1961-1990) period for the 2020s (top), 2050s (middle) and 2080s (bottom) respectively. The plots are formulated based on the posterior distribution of the Monte Carlo simulation conducted for the A1B based climate scenarios. On each box the central mark represents the median, the edges represent the 25th and 75th percentiles and the whiskers represent the 90% confidence interval.

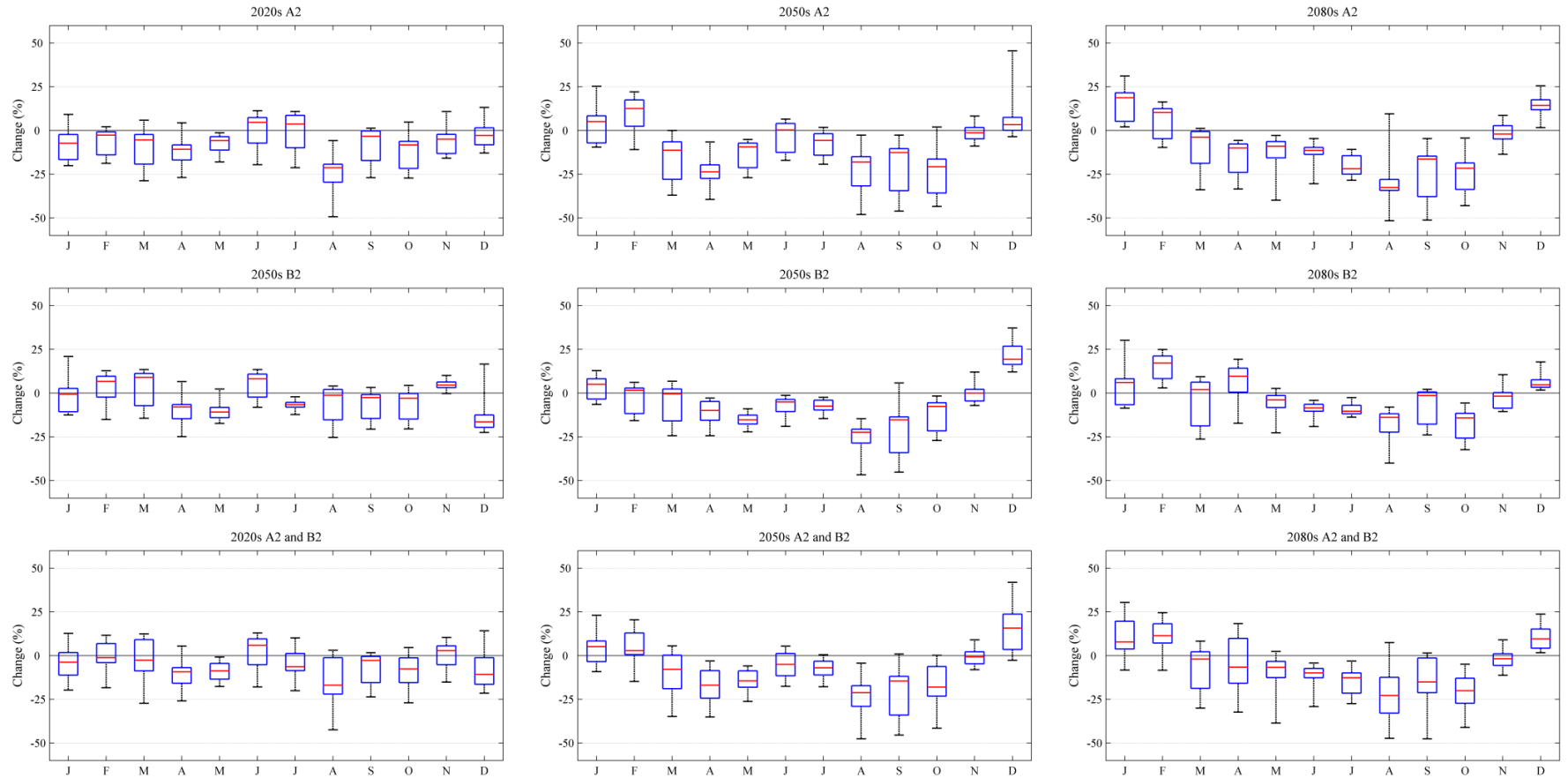


Figure 9.29 Monthly boxplots of the percent change in the Q50 median flow statistic for the Srahrevagh catchment. Changes are estimated relative to the 30 year control (1961-1990) period for the 2020s (left), 2050s (middle) and 2080s (right) respectively. The plots are formulated based on the posterior distribution of the Monte Carlo simulation conducted for the A2 (top), B2 (middle) and A2/B2 based climate scenarios (bottom). On each box the central mark represents the median; the edges represent the 25th and 75th percentiles and the whiskers represent the 90% confidence interval.

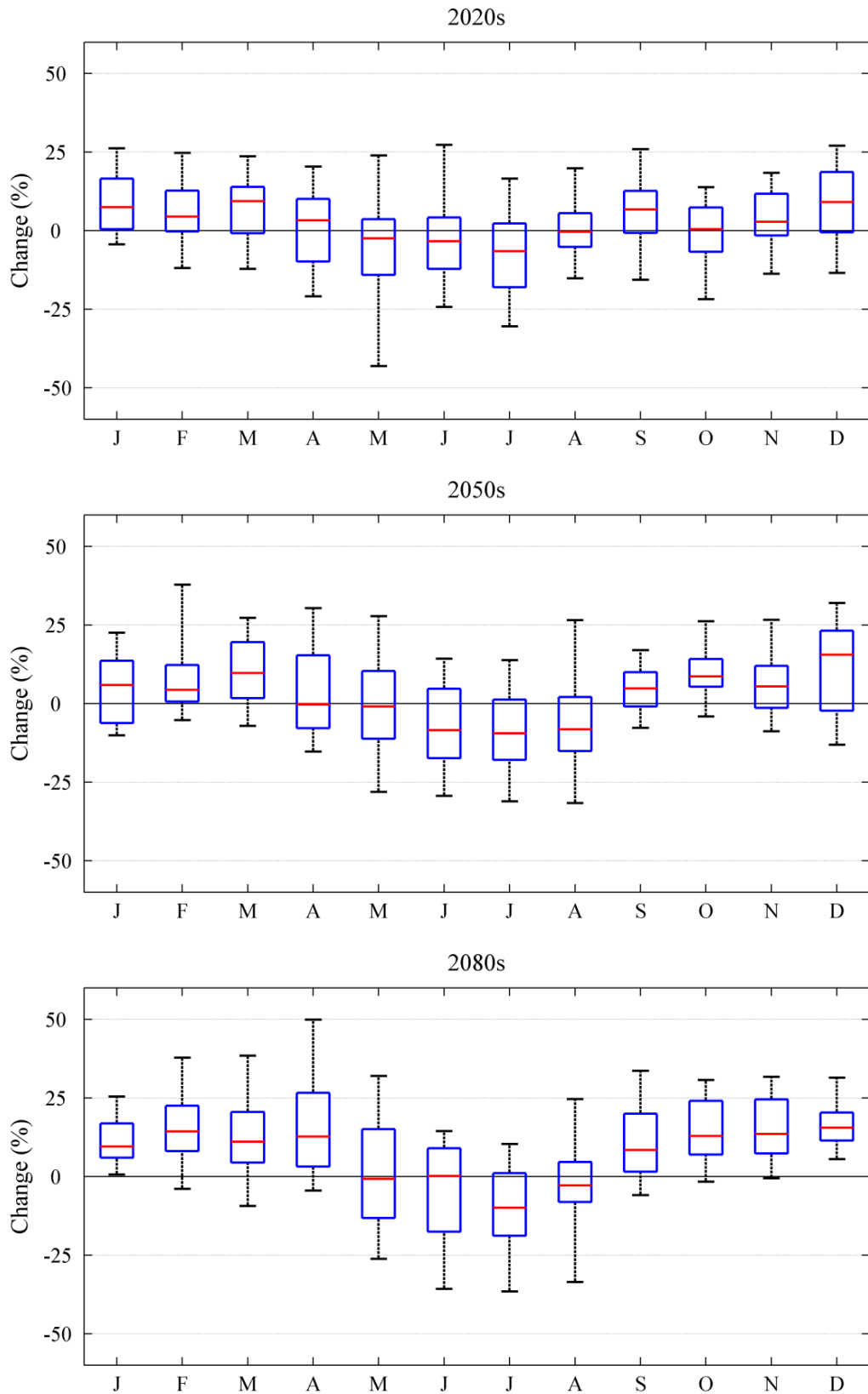


Figure 9.30 Monthly boxplots of the percent change in the Q05 median flow statistic for the Srahrevagh catchment. Changes are estimated relative to the 30 year control (1961-1990) period for the 2020s (top), 2050s (middle) and 2080s (bottom) respectively. The plots are formulated based on the posterior distribution of the Monte Carlo simulation conducted for the A1B based climate scenarios. On each box the central mark represents the median, the edges represent the 25th and 75th percentiles and the whiskers represent the 90% confidence interval.

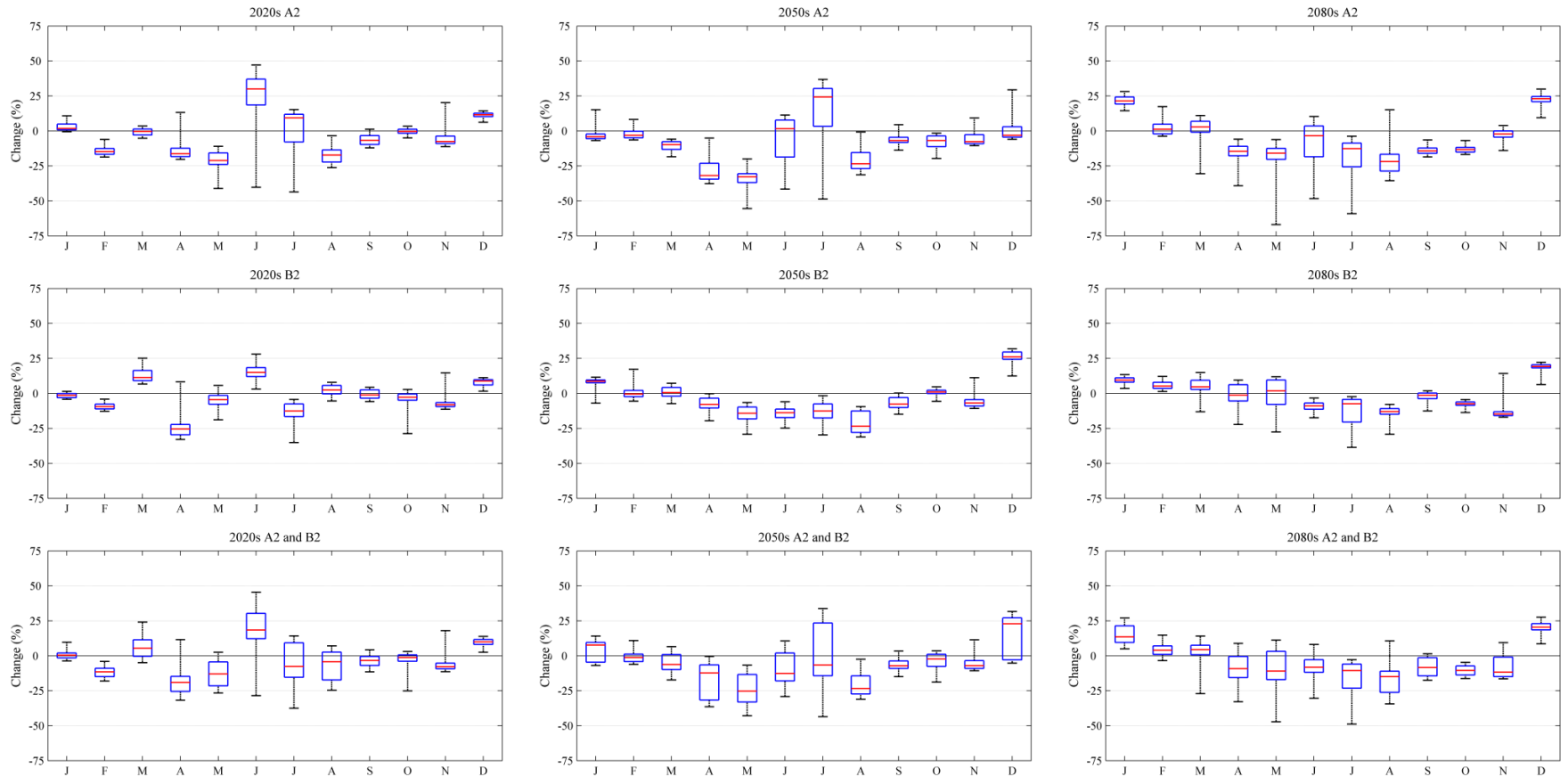


Figure 9.31 Monthly boxplots of the percent change in the Q05 median flow statistic for the Srahrevagh catchment. Changes are estimated relative to the 30 year control (1961-1990) period for the 2020s (left), 2050s (middle) and 2080s (right) respectively. The plots are formulated based on the posterior distribution of the Monte Carlo simulation conducted for the A2 (top), B2 (middle) and A2/B2 based climate scenarios (bottom). On each box the central mark represents the median; the edges represent the 25th and 75th percentiles and the whiskers represent the 90% confidence interval.

Low Flows (Q95): Probabilistic Flow Projections

In comparison to both the Q50 and Q05 flow statistics, clearly defined patterns of change in Q95 are much more difficult to determine (Figure 9.32). The results of the MC simulation suggest that the greatest reduction in summer Q95 is likely to occur over the 2050s. For this time horizon the largest projected monthly decrease is suggested for August (+20%). Similarly a reduction of 12% and 9.8% is suggested for June and July respectively over the same horizon.

Projected changes in monthly low flows under the A2 and B2 pathways are shown in Figure 9.33. For a number of summer months, particularly July and August over the 2080s, a clear reduction in Q95 is suggested. Analysis of the A2 based scenarios indicates a decrease in Q95 for August (+37%) over the 2080s. Notable reductions are also suggested for June (8.1%), July (32%) and October (26%). Decreases of a lesser magnitude are suggested for the same months (June: 9.8%, July: 16.6%, August: 31.9% October: 20.8%) under the B2 scenario.

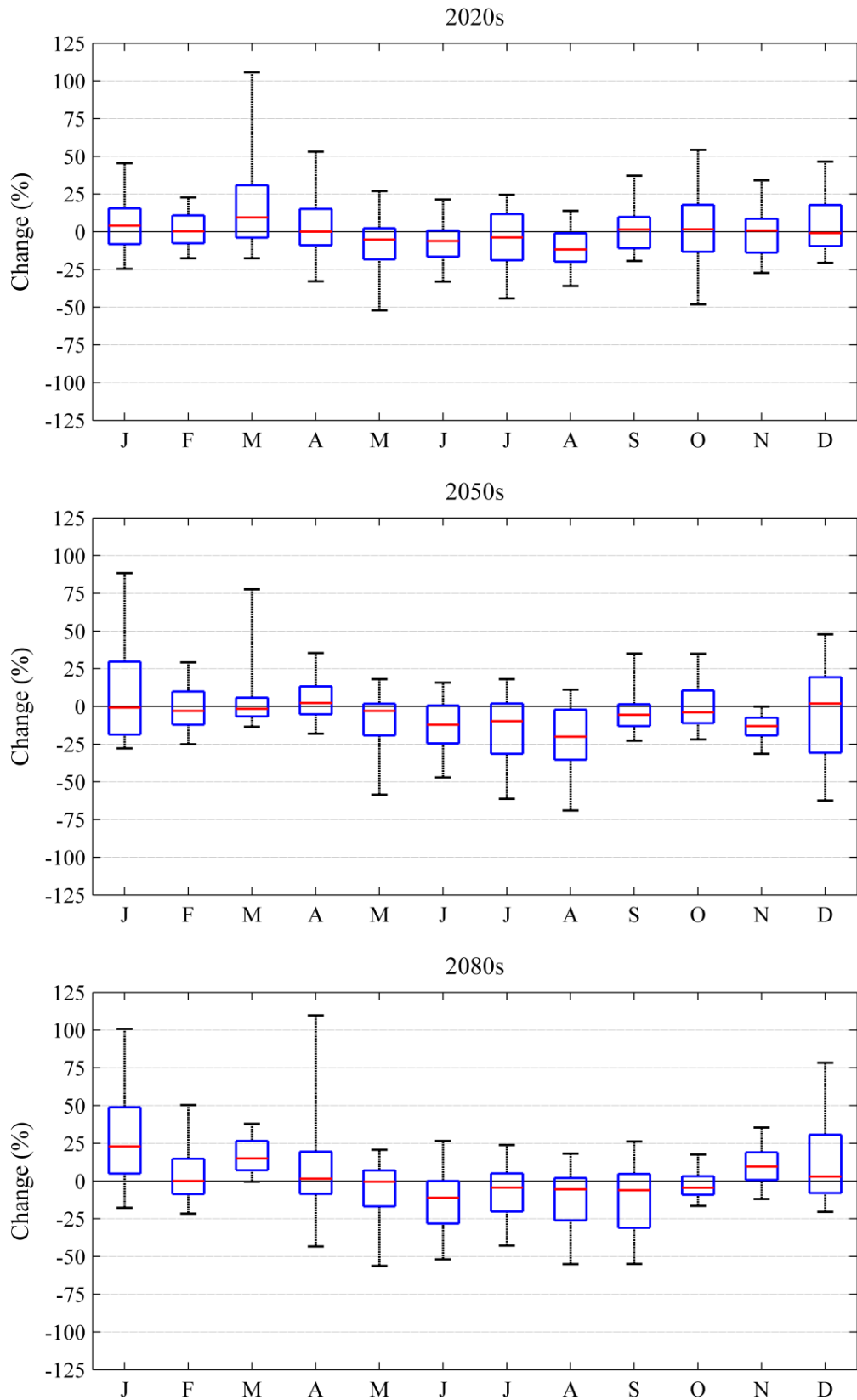


Figure 9.32 Monthly boxplots of the percent change in the Q95 median flow statistic for the Srahrevagh catchment. Changes are estimated relative to the 30 year control (1961-1990) period for the 2020s (top), 2050s (middle) and 2080s (bottom) respectively. The plots are formulated based on the posterior distribution of the Monte Carlo simulation conducted for the AIB based climate pathways. On each box the central mark represents the median, the edges represent the 25th and 75th percentiles and the whiskers represent the 90% confidence interval.

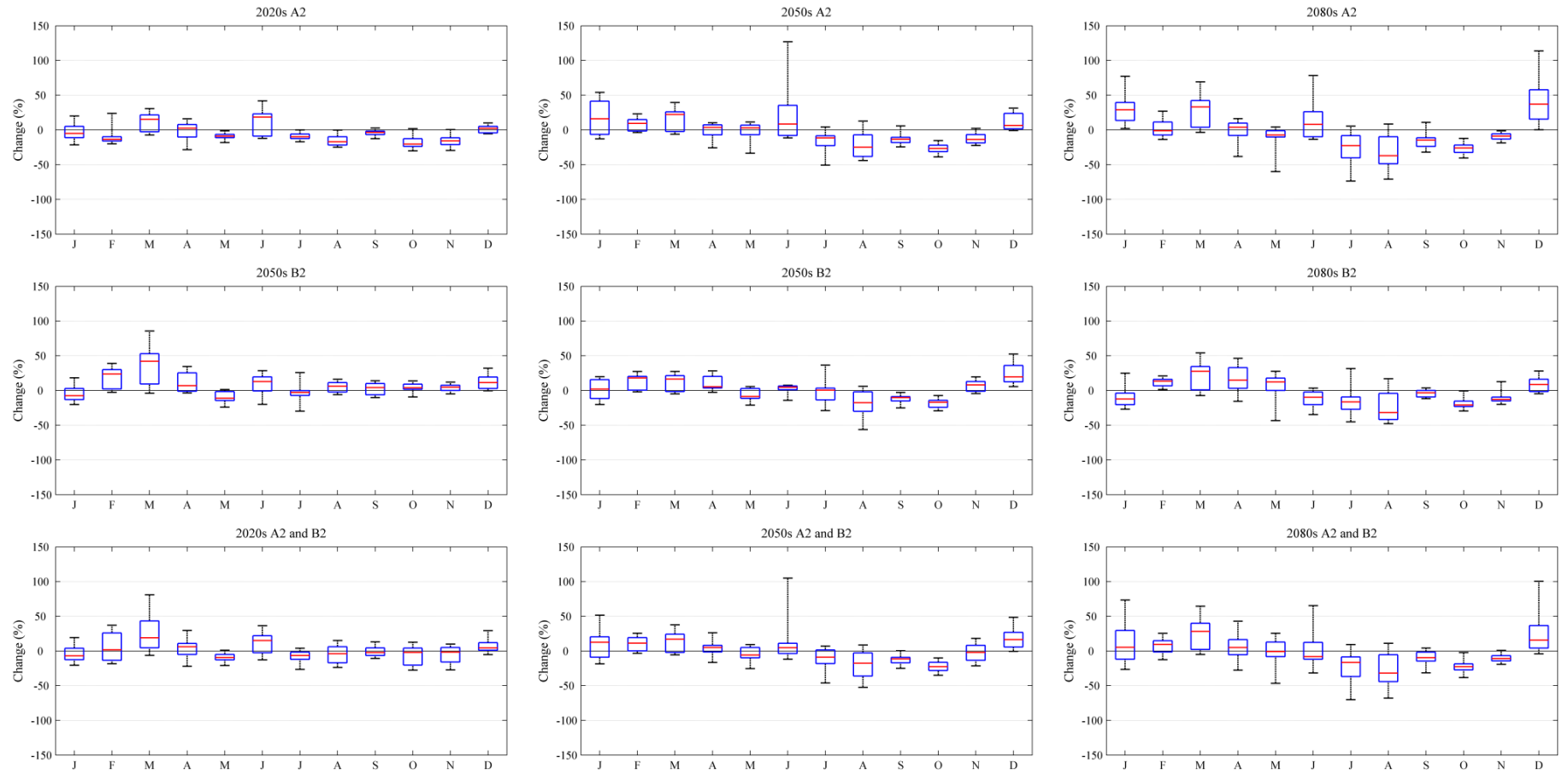


Figure 9.33 Monthly boxplots of the percent change in the Q95 median flow statistic for the Srahrevagh catchment. Changes are estimated relative to the 30 year control (1961-1990) period for the 2020s (left), 2050s (middle) and 2080s (right) respectively. The plots are formulated based on the posterior distribution of the Monte Carlo simulation conducted for the A2 (top), B2 (middle) and A2/B2 based climate scenarios (bottom). On each box the central mark represents the median; the edges represent the 25th and 75th percentiles and the whiskers represent the 90% confidence interval.

9.10 Conclusion

The potential impacts of climate change on the hydrological regime of two constituent sub-catchments of the greater Burrishoole system were explored. Monte Carlo simulation was used to estimate changes in key flow statistics conditional on a weighted sampling of the uncertainty space. The components of uncertainty which were considered included the emissions scenario, driving GCM, downscaling method/RCM and hydrological model - accounting for both model structure and parameter uncertainty. The results suggested that the seasonality of the flow regime in both catchments is likely to increase, with this trend becoming more pronounced as the century progresses. Increases in Q50 (median flow) and Q05 (high flow) are suggested for winter, whilst reductions in both flow statistics are projected for the summer months. In the case of low flows (Q95), under the A1B SRES scenario, the models suggest slight reductions for the majority of months over the 2050s; however, over the 2080s horizon low flows return to a level commensurate with the reference period. In contrast, under the A2 SRES scenario, decreases in Q95 are projected to occur over each future time horizon; it is also suggested that reductions will be most acute over the 2080s.

The GLUE procedure of Beven and Bingley (1992) was used to explore uncertainty in the hydrological models. In this study an ensemble approach was taken whereby multiple model structures and parameter sets were employed to explore changes in the hydrology of both catchments. With respect to model skill, the multimodel ensemble was found not to be superior to any single CRR model when taken in isolation; however, the added value in its application lies in the fact it allows a greater sampling of the uncertainty space (i.e. both structural and parameter uncertainty).

The various shortcomings associated with the GLUE procedure are well documented, and it is acknowledged that the findings of this study are conditional on the subjective elements it incorporates. To address uncertainty in the model parameters multiple evaluation criteria were applied and high threshold values were used. This acted to constrain the region of the parameter space from which behavioural sets were sampled, leading to little variation in the model response and narrow uncertainty bounds. Using multiple efficiency criteria was necessary given the importance of accurately simulating both the timing and volume of flow through the river channels.

One of the weaknesses of the GLUE methodology - as implemented in this study - is that no likelihood value is explicitly attached to the respective model structures;

however, given that no true model can be identified this was considered a valid approach. As the methodological framework for the MC simulation incorporates several steps from the GLUE procedure, many of the caveats associated with GLUE also underpin the probabilistic projections. In addition the limitations of the observed data restricted how the assumption of stationarity in the models could be addressed - which must be considered when interpreting the final results. Despite the various shortcomings of the methodology and datasets employed, this study adopts a robust and transparent approach for addressing uncertainty - whereby each of the subjective elements have been made explicit. In addition, although GLUE as a procedure for addressing uncertainty has its detractors, it remains a widely applied and accepted approach for addressing uncertainty which, in the case of this study, has been exemplified as a means for addressing both structural and parametric uncertainty. Thus this study serves to highlight its flexibility and importance as a method for addressing uncertainty in hydrological impact assessments.

The importance of sampling all components in the cascade of uncertainty is highlighted. Although this study attempts to consider the main aspects of uncertainty, as the full range of GHG emission scenario and GCM sensitivities are not considered, the study offers only an insight into the range of uncertainties associated with modelling the hydrological response to future climate change. In this sense the study findings are strictly conditional on, and to a degree biased by, the uncertainty which is sampled. One of the key uncertainties in hydrological impact assessments is natural variability; however, in this study it is not explicitly addressed - even though it is to some extent represented in the ensemble of downscaled climate scenarios. This was due to the computational demands of running enough stochastically generated scenarios to sample natural variability whilst addressing uncertainty in both the model structure and parameter values. Whilst it is important that natural variability is addressed, this study has made a contribution by examining those aspects of uncertainty which are typically not considered in impact assessments – including the climate sensitivity and the effect which the choice of RCM has. The proceeding chapter explores how the changes suggested to occur in the flow regime may impact the long-term viability of salmonid populations in the Burrishoole catchment.

Chapter 10

Climate change impacts on Atlantic salmon (*Salmo salar*): linking projected changes in flow to habitat requirements

10.1 Introduction

Climate may be considered a ‘master variable’ (Power *et al.*, 1995) which, over geological time has influenced the distribution, form and elemental composition of habitats, affecting in turn the productivity, dispersal, phenology and localised adaptation of freshwater biota (Cox & Moore, 1993; Harrod & Graham, 2004). It is therefore logical to expect that any change in such a core determining variable would have a significant impact on in-stream habitat and ecosystem functions, with resultant consequences for the behaviour, growth, distribution and survival of some freshwater and anadromous fish species, including Atlantic salmon (*Salmo salar*) (Graham & Harrod, 2009; Clews *et al.*, 2010; Wenger *et al.*, 2011).

Climate constitutes a single if critical component in a vast interacting hierarchy (Figure 10.1) (Armstrong *et al.*, 1998); as a result determining a direct causal link between recent climate change and observed alterations in the population structure or phenotypic response of salmonids is a complex task. However, there is a growing body of evidence which suggests that the recent warming of freshwaters and the associated change in water quality has affected the physiology (Fry, 1971; Stefansson *et al.*, 2003), phenology (Zydlewski *et al.*, 2005; Mc Ginnity *et al.*, 2009), distribution (Friedland, 2003; Juanes *et al.*, 2005) and survival of some salmonid species (Daufresne *et al.*, 2004; King *et al.*, 2007; McGinnity *et al.*, 2009; Clews *et al.*, 2010). By altering primary variables like precipitation and temperature, climate change may reduce the availability of habitats preferred by salmonids and limit access to exploitable resources - thereby undermining the local carrying capacity of river systems (Riley *et al.*, 2009; Clews *et al.*, 2010; Wenger *et al.*, 2011).

Different aspects of the flow regime, including the seasonality, interannual variability and the timing as well as volume of high flow events are important for the successful completion of each stage in the life history of salmonids (Dudgeon *et al.*, 2006).

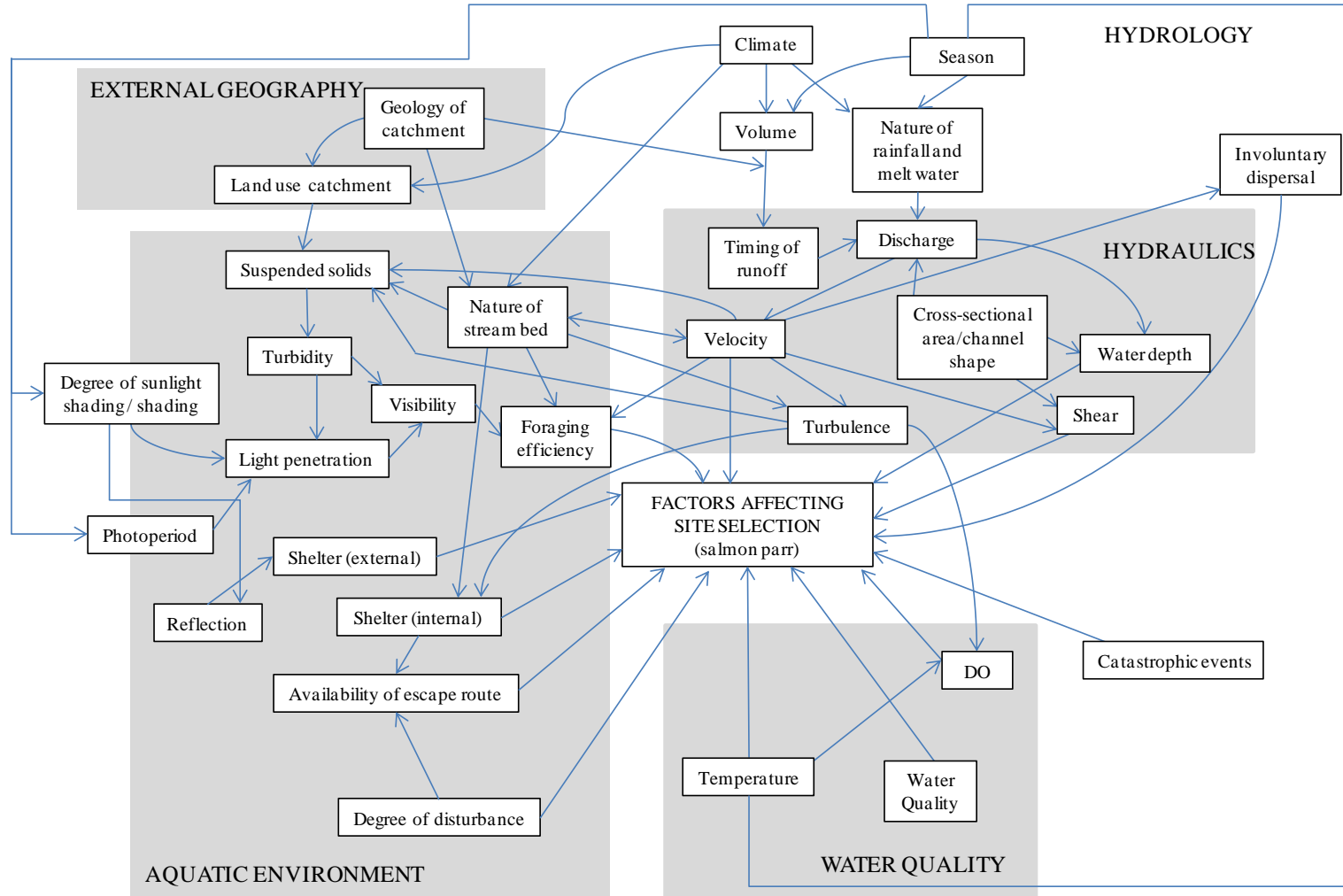


Figure 10.1 Schematic illustrating the interaction between those abiotic factors known to affect salmon and trout parr (Source: Armstrong *et al.*, 2003)

Consequently changes in climate may lead to a loss in the synchrony established between patterns of flow behaviour and the evolved life history strategy of salmonids. It is likely this would reduce the ‘*window of opportunity*’ during which the physiological requirements of salmonids coincide with optimal environmental conditions. A balance exists between those more extreme or high flow events which are beneficial to salmon and those which can have deleterious consequences. While spates are necessary for migration, under perturbed forcing a change in the magnitude or timing of high flows may lead to the outwash of eggs and fry or promote the earlier migration of smolts to sea. Similarly an increase in the incidence or duration of low flows may act to delay migration or, by reducing the quantity and diversity of available habitat, negatively impact growth with knock on effects for success during subsequent life stages.

This chapter examines the potential impact of climate change on flow behaviour and habitat availability in two sub-catchments which comprise part of the greater Burrishoole system. Changes in flow are explored with respect to the known habitat and flow requirements of Atlantic salmon at two key stages in their life cycle – spawning and migration. Methods for quantifying the uncertainties which pervade the translation of emission scenarios and coarse scale GCM projections into habitat conditions at the reach scale are adopted.

10.2 The potential impacts of changing flow regimes on salmonids

Climate-related changes in river flow have wide ranging and multifaceted implications for the behaviour, growth and distribution of salmonids in the freshwater environment (Clews *et al.*, 2010). Hydrological regimes are regarded as a key driver of lotic ecosystems, critical for determining the availability of preferred habitat and the phenology of freshwater species (Wenger *et al.*, 2011). The principles outlined by Bunn and Arthington (2002) (Figure 2.3) - which summarize how hydrological regimes influence aquatic biodiversity - are particularly applicable to diadromous species like Atlantic salmon which, over the course of their life cycle require access to diverse habitats and rely on flow for migration and connectivity across freshwater systems. Poff *et al.* (1997) outline five components of the flow regime which affect physical habitat and regulate ecological processes in lotic ecosystems. They include the magnitude, predictability and duration of flows; they also include the frequency of flow events and the rate of change in hydrologic conditions. As shown in Figure 10.2 the full range of

flow behaviour is important for providing habitat diversity, facilitating migration and maintaining/restoring the form as well as structure of in-stream habitats.

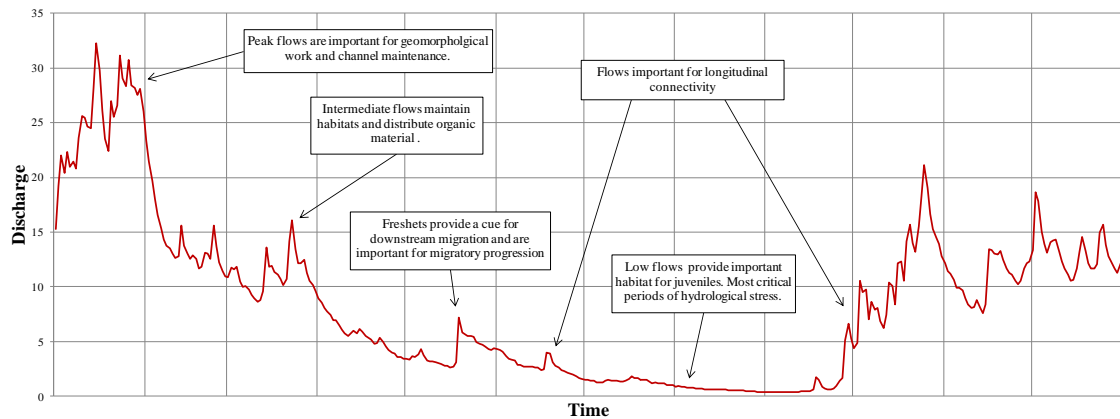


Figure 10.2 The significance which different components of the hydrograph have for freshwater ecosystems and salmonid species (Source: Poff *et al.*, 1997)

By providing food, oxygen, refuge and migratory cues, flow constitutes one of the most basic requirements for survival in the freshwater environment. It is a major determinant of the quality, quantity and diversity of available habitat across diverse spatial and temporal scales (e.g. catchment, reach and patch). At the finest scales flow may affect energy intake and swimming costs, whilst at larger scales it influences the channel morphology and determines longitudinal connectivity. Clews *et al.* (2010) indicate that at the reach scale the quality of available habitat directly affects the abundance of salmonids by influencing the provision of refugia and food resources. Importantly the flow regime must be sufficiently diverse so that habitat requirements at different life stages can be met (Nislow & Armstrong, 2011). This also applies more generally to their evolved life history strategies (e.g. use of refugia, feeding and resting patterns) for which access to a varied range of micro-habitats is required.

Fish species respond to a range of variables which vary with flow including, for example, temperature, food availability, turbidity, dissolved oxygen and olfactory cues. The level of interdependence between these variables makes it difficult to isolate how climate-related changes in the hydrological regime may impact salmonid populations - either directly or indirectly (e.g. low flows may amplify the effect of higher water temperatures). Armstrong *et al.* (2003) indicate that the quality and quantity of available habitat is influenced by a range of both abiotic and biotic factors as well as the complex interactions which occur between them (Figure 10.1). Those abiotic factors which affect salmonids include, amongst others, water temperature (Crisp, 1993, 1996; Armstrong *et al.*, 2003), the substrate composition (Moir *et al.*, 1998; Vadas & Orth,

2001), channel cover (Heggenes, 1990) water depth and velocity (Heggenes, 1990; Hendry & Cragg-Hine, 1997; Moir, 1998; Geist *et al.*, 2000; Guay *et al.*, 2000; Beecher *et al.*, 2002; Armstrong, 2003; Linnansaari *et al.*, 2010), dissolved oxygen (Crisp, 1993; Armstrong *et al.*, 2003), water quality (Crisp, 1993; Armstrong *et al.*, 2003) and the various elements of streamflow behaviour including high and low flows, average flow conditions and the timing of flow events (Lytle & Poff, 2004).

The salmon's life cycle has evolved in response to, and is largely attuned with the localised flow regime (Beechie *et al.*, 2006; Tetzlaff *et al.*, 2008). Lytle and Poff (2004) outline how the timing of life-history events - such as spawning and migration - are optimized with respect to the time at which particular flow events or seasonal changes in hydrological conditions occur. The importance of river-flow regimes means any alteration in the long-term pattern of flow behaviour (e.g. an increase in seasonality, changes in the timing of spates or extreme events) may lead to a loss in the synchronicity established between streamflow, habitat conditions and the physiological requirements of salmonids at different life stages (Figure 2.3) (Bunn & Arlington, 2002; Lytle & Poff 2004).

Alterations in the timing of flow events have wider implications for the evolved life history strategies of salmonids. For example, changing patterns of flow behaviour may result in salmonids becoming decoupled from their food sources; in addition it may disrupt their evolved facilitative relationships or interaction with other aquatic species (e.g. interspecific competition, exposure to predation, etc.) (Burkett *et al.*, 2005). It may also affect their interaction with, and exposure to, other biotic and abiotic drivers which also vary with flow and are likely to change in response altered forcing (Figure 10.1). This picture is complicated by warming related changes in the phenology and behaviour of salmonids which may further disturb the relationship between the timing of life events and the occurrence of optimal in-stream conditions; thus, the interaction between flow and other drivers may be as important as changes in the flow regime when considered in isolation.

By influencing fish movement and the connectivity of exploitable habitats, water flow can affect migration, respiration, energy expenditure, feeding and spawning; each of which are important for recruitment and year class success (Armstrong *et al.*, 1998, 2003; Bowen *et al.*, 2003; Berland *et al.*, 2004; Jonsson, 2009; Clews *et al.*, 2010). For example, spates may be required to ascend artificial or natural obstacles and thus are essential for migratory progression (Bjorn & Reiser, 1991). Similarly migration may be

delayed during prolonged low flow periods, potentially limiting access to suitable spawning areas and increasing exposure to thermal stress. The ability to move freely within a river system is important in terms of determining its overall carrying capacity. Under altered conditions the inability of individuals to distribute across the system may lead to density-dependence having a greater influence on the population dynamics. In cases where fish are unable to access different parts of the system, an increase in competition for territory and resources (e.g. food, channel cover, instream refugia) may occur; by limiting access to refugia it may also enhance vulnerability to predation. Armstrong *et al.* (1998) highlight the importance of population density at critical times as a limiting factor for growth and survival in Atlantic salmon.

10.2.1 Salmonid eggs and fry

Under future climate conditions enhanced winter and spring high flows are likely to increase the vulnerability of nests and gravel beds to the effects of erosion and sediment deposition. By mobilizing larger substrate materials, high flows may increase the exposure of salmonid eggs and fish larvae to mechanical shock. It may also result in alevins becoming physically trapped in the gravel substrate thereby preventing emergence (Jensen & Johnsen, 1999). In addition, by increasing turbidity the greater erosion and movement of finer materials may act to reduce the intra-gravel flow of oxygen for developing embryos. Furthermore higher winter flows may lead to an increase in the washout or scouring of eggs and spawning gravels, thereby adversely affecting the survival rates of salmonid embryos and alevins (Cunjak *et al.*, 1998).

Crisp (1989) studied the washout depth and drift distance of salmonid eggs using artificial eggs as a surrogate. It was found that the burial depth and recorded flow level determined whether, and to what extent washout occurred. Gilvear *et al.* (2002) report that a large flash flood event which occurred in the River Ettrick - a tributary to the River Tweed (Scotland) - had the effect of washing out the majority of salmon eggs laid in spawning beds along the river. The authors highlight the causal link between this event and a reduction in the number of recorded spring salmon returning to the catchment five years later (the average life span of salmon in the catchment). Gilvear *et al.* (2002) also attribute a reduction in the number of juvenile salmon observed in the River Bloom (north-west Scotland) to a significant flow event which occurred several

years previous to this where a large proportion of the egg stock for that year was washed out.

Along the southern limits of their distributional range climate change may result in an increase in the frequency and duration of low flows during the winter and spring seasons. This may enhance the vulnerability of redds to drying and force juveniles to move into areas of higher predation risk. In addition, an increase in low flows would have the effect of reducing the flow of oxygen enriched water through the gravel substrate, thereby reducing the potential for hatching success during embryonic development and adversely affecting survival rates. It would also limit the flushing of silt and detritus from gravel beds which is important for the well-being of salmonid embryos.

The period between emergence and the establishment of feeding territories is considered critical for the success of year classes; indeed Thorstad *et al.* (2011) identifies this phase as one of the critical 'mortality bottlenecks' in the life history of Atlantic salmon. The survival and growth potential of salmonid fry is closely linked with flow conditions during and subsequent to emergence from the gravel substrate. The potential impacts of climate change on this life stage are generally linked with an alteration in the timing of emergence and changes in the flow regime. Increased water temperatures are likely to enhance the rate of embryonic development, resulting in a mismatch in the time at which 'swim-up' occurs and the periods when flows are conducive to sustaining and nurturing fry (Todd *et al.*, 2011). Earlier emergence - brought on by reduced incubation times - may expose fry to more hostile flow conditions, leading to involuntary displacement into unfavourable habitats or mortality through mechanical shock. This may be compounded by climate-mediated changes in both the magnitude and timing of peak winter and spring flow events. Extreme high flows during this life stage have been implicated in significant year-class losses (e.g. Jensen *et al.*, 1991; Nislow, 2004; Warren *et al.*, 2009; Nislow & Solomon, 2011). Thus any increase in the frequency of extreme high flows or flooding events which coincide with the time of emergence - whereby successive year classes may be affected - has the potential to significantly undermine the future viability of some populations.

A study by Ottaway and Clarke (1981) into the vulnerability of juvenile trout (*Salmo trutta*) and salmon to higher flow velocities found that, when periods with increased discharge coincided with fry emergence, significant losses due to displacement downstream occurred. Similarly, in a study on populations of Atlantic salmon and

brown trout in the River Saltdalselva (northern Norway), Jensen and Johnsen (1999) found that during years when high flows coincided with the alevin stage or the first week proceeding fry emergence, salmon mortality increased significantly. In contrast high flows during the egg stage were found to have a lesser impact on mortality rates. It was also found that for fish of age 1+ and older, peak spring flows did not influence mortality significantly, highlighting the increased resilience of older juveniles to washout by higher flow events. In addition, when compared with the effects of high spring flows, temperature was found only to have a minor impact on alevin mortality.

The findings of Jensen and Johnsen (1999) are consistent with those of Elliott (1987) who found that the timing and magnitude of high flow events, relative to the time at which fry emergence occurred, strongly affected year-class strength (i.e. spawning and survival success). This study examined populations of brown trout inhabiting two streams located in the Lake District of north-west England. Similarly, the results of a study by Lobon-Cervia (2004), which focused on river catchments in northwest Spain, found that discharge during or just after the period of trout emergence was a major determinant of recruitment success. In the case of this study it was found that the survival to emergence of salmon fry was low in instances where emergence coincided with the occurrence drought conditions. Wenger *et al.* (2011) state that the vulnerability of trout to high flows during the time proceeding spawning is due to the capability of high flows to disturb nests and displace newly emerged fry. The authors suggest that, under future climate conditions, trout spawning in autumn are vulnerable to an increase in winter flooding; similarly, trout which spawn in the spring are sensitive to increases in high summer flows.

The findings of Jensen *et al.* (1991) suggest that the timing of fry emergence may be sufficiently 'tuned' to ensure that the most deleterious flows are avoided. Tetzlaff *et al.* (2005) and Tetzlaff *et al.* (2008) also suggest that the time at which juvenile salmon emerge is locally adapted to coincide with the time when winter spates become less frequent - thereby reducing the vulnerability of fry to downstream displacement and the possibility of being cut-off from food resources. Similarly Thorstad *et al.* (2011) state that the spawning time of Atlantic salmon is sufficiently adapted to ensure eggs hatch during the period most favourable for fry survival. Under future climate conditions changes in the flow regime and increases in water temperatures are likely to determine any shift in the time of emergence and whether this coincides with more hostile flow

and habitat conditions; consequently the interaction and response of both variables to future forcing is important.

Nislow and Armstrong (2011) state that during the post-emergence phase the affect of flow on salmonids is manifest more in terms of growth rather than survival. Under future climate change a reduction in summer flows may increase interspecific competition and reduce habitat availability for fry, it may also result in increased mortality from predation and a reduction in growth opportunities (Nislow *et al.*, 2004; Nislow & Armstrong, 2011). Riley *et al.* (2009) examined the impact of low summer flows - considering both habitat use and survival - on juvenile salmon, trout and grayling (*Thymallus thymallus*) in a groundwater fed chalk stream (River Itchen, Hampshire, UK). In this study flow was artificially reduced to simulate conditions associated with low summer discharge. Riley *et al.* (2009) found that a reduction in flow resulted in an increase in the mortality of each species. It is suggested that the higher mortality experienced by age-0 salmon was due to an increased vulnerability to predation. In the case of trout and grayling it was linked to a reduction in water depth and velocity over their preferred sheltering habitats on the stream margins (i.e. near shore). Milner *et al.* (2010) argue that the availability of suitable low velocity areas during the early fry stage is a critical limiting factor for survival and productivity. Milner *et al.* (2010) also highlight water depth and the wetted area as important for providing cover and reducing vulnerability to predation. In addition the authors highlight that, by limiting habitat availability, a reduction in flow may affect juvenile productivity.

Clews *et al.* (2010) examined whether the effects of recent climate change on juvenile Atlantic salmon and trout in the Wye catchment could be linked with a long-term decline in the population of both species. It was found that the observed decreases in the population numbers of both species (over the 20 year period of record) was more strongly linked to climatic factors than any other variable considered. The noted decrease in populations was most pronounced during periods when low summer flows coincided with enhanced water temperatures. An increase in the occurrence of more prolonged periods of drought could lead to further losses of both species in the catchment.

Climate-mediated changes in flow and water temperature which coincide with the period of embryonic development may also have knock-on effects for parr growth and the success of year-classes during subsequent life stages. This is supported by Jonsson

et al. (2005) who analysed populations of Atlantic salmon in the river Imsa (southern Norway); in this case the authors found that higher water temperatures and increased discharge during the time of embryonic development (February–April) resulted in faster parr growth and an advance in the age of smoltification.

10.2.2 Salmonid parr and smolt production

The increased size and swimming ability of salmonids during the parr stage mean they are less vulnerable to outwash or short term changes in the flow environment (Nislow *et al.*, 2002). Climate change impacts on this phase are more complex, being characterised primarily by changes in the population dynamics and growth opportunities. Although less vulnerable to the effects of short term disturbances in the hydrologic environment, their long residence time in rearing habitats mean they are exposed to the full range of potential changes in the flow regime (i.e. higher winter and lower summer flows) (Jonsson & Jonsson, 2009; Armstrong & Nislow, 2011). Climate related changes in flow are likely to affect the parr stage principally by altering growth rates and disrupting interspecific relationships. Survival during this stage is largely density-dependent (providing adequate egg deposition), related to this is the fact that growth and productivity are directly linked to the availability of exploitable resources and access to preferred habitats.

An increase in water velocity generally leads to a greater abundance of drifting food and increased growth rates (Fausch, 1984); however, the positive relationship between discharge and growth must be weighed against the greater metabolic costs associated with inhabiting higher flow environments. Thus a net gain in body mass under high energy conditions is predicated on their being a sufficient increase in the availability of food resources (Nislow *et al.*, 2000; Hayes *et al.*, 2007); however, this caveat does not generally hold in winter when food is in short supply. Therefore higher flows during this season are likely to increase metabolic costs, without the corresponding increase in food availability - as a result forcing fish to use up their energy reserves (Huusko *et al.*, 2007). Based on the same reasoning an increase in low summer flows has the potential to reduce feeding and growth opportunities (Nislow *et al.*, 2004).

Xu *et al.* (2010) examined the potential effects of climate change on the growth of brook trout (*Salvelinus fontinalis*) in a stream reach located in western Massachusetts

(north-east USA). The findings indicated that during the spring, summer and autumn seasons, increases in streamflow lead to a corresponding increase in growth; however, the study suggested that during winter an increase in flow was linked to a decrease in growth rates. The authors attribute this to the reduced availability of prey and the greater metabolic costs associated with higher flows during this season.

Davidson *et al.* (2010) examined the contribution various abiotic (e.g. water temperature) and biotic (e.g. interspecific population density) factors made to the rate of growth in juvenile Atlantic salmon in the West Brook - a tributary to the Connecticut River located in north-east Massachusetts. It was found that variations in flow had a greater influence on growth than any other factor considered. Increased stream discharge was found to be the most important determinant of juvenile body size at the end of their age 1+ winter. Davidson *et al.* (2010) indicate that growth during the parr stage has important implications for subsequent life stages, particularly the age at which smoltification occurs.

Although a general increase in flow velocity may enhance growth, an increase in the incidence of extreme high flow events is likely to have a negative impact on salmon parr. Jensen and Johnsen (1999) found that the observed growth of Atlantic salmon parr (1+, 2+ and 3+) was diminished in years during which high peak flows were more frequent. One of the reasons proposed for this was the washout and scouring of invertebrate communities which, it is argued, lead to a reduction in the abundance of available food. In this study flood events did not appear to have the same impact on the growth of juvenile brown trout. The competitive advantage trout hold over salmon is offered as one explanation for the differences in the growth response of each species.

In a study conducted to assess the long-term effects of drought on populations of trout (*Salmo trutta*) in the UK, Elliott *et al.* (1997) found that summer droughts led to increased mortality of 1+ parr. This study covered a 30-year period and considered the most extreme drought events on record (e.g. 1976, 1993). It is likely that drought events such as these will occur with greater frequency and for more prolonged periods under future forcing. As such they provide an insight into the potential impacts of climate change on salmonids during this life stage. Elliott *et al.* (1997) concluded that a reduction in the density of returning females and an associated decline in egg production were linked to the long term effects of 1+ parr being subjected to a prolonged drought event. The authors highlight a causal link between the occurrence of

summer droughts, retarded parr growth and the development of smaller smolts. It is argued that smaller smolts are subject to higher mortalities at sea (Elliott, 1994), leading to the observed reduction in the number of returning adults. The study indicated that summer droughts have the most deleterious impact on parr growth; however, if spring and/or autumn droughts occurred in the same year, the long-term effects of drought occurring during the summer season were found to be amplified.

As discussed by Elliott *et al.* (1997), growth during the juvenile and parr phases have long term implications for population success. The link between growth during the juvenile stage and the success of year-classes during subsequent life stages is important. This is particularly true with respect to the age at which smoltification occurs and survival during the post-smolt phase. The age at smolting in salmonids is regulated by past growth performance and parr size (Jonsson & Jonsson, 2009). Members of the same age-class which grow faster tend to smolt at an earlier age and a smaller size; this is in contrast to more slow-growing individuals of the same age-class (Strothotte *et al.*, 2005). Changes in the time at which smoltification occurs has implications for the survival and success of post-smolts in the marine environment (Elliott, 1994). An increase in mortality during the marine stage has been linked to salmon smolts migrating at a younger age and smaller size (Økland *et al.*, 1993).

As highlighted by Jonsson *et al.* (2005) first year growth affects survival and performance during subsequent life stages. For example, salmon which grow faster during the parr stage may produce smaller eggs upon returning to their home rivers as mature adults. In addition, a shortening in the length of time spent in freshwater - as may occur in cases where parr grow faster and smolt at an earlier age - may reduce the breeding success of returning adults (Jonsson *et al.*, 2005). Thus changes in growth during the parr stage which result from changes in the flow regime have long term implications for the population structure and recruitment success of Atlantic salmon.

Davidson *et al.* (2010) highlight that good growth opportunities during the juvenile phase result in a greater proportion of the population maturing and undergoing smoltification at an earlier age. In contrast a reduction in growth delays the time of migration – an outcome which may benefit salmon by allowing them to exploit freshwater resources for an additional year, thereby producing larger smolts with a greater potential for success in the marine environment. An increase in the rate of parr growth may therefore lead to a decline in smolt age and ultimately a reduction in the

size of returning adults - potentially undermining reproductive success (e.g. reduced egg size and early survival) (Moffett *et al.*, 2006). According to Todd *et al.* (2011), under future climate conditions, the growth of salmon parr is on balance likely to increase, leading to a corresponding decrease in the age of smoltification. Davidson *et al.* (2010) also indicates that climate change may alter the relationship between growth and the time of smoltification, possibly resulting in smaller older smolts migrating to sea.

During the parr stage salmonids display sheltering behaviour and the availability of exploitable refugia is considered a significant determinant of growth and survival during this life stage. As a result changes in the occurrence of bed-mobilizing flows (~ bankful discharge), which may alter the form and composition of the channel substrate, are important in terms of the potential impacts they may have on the availability of preferred habitats. Nislow and Armstrong (2011) indicate that an increase in winter flooding may lead to the more frequent scouring of the channel substrate and an associated loss of sheltering habitat. Conversely a reduction in flow (particularly the magnitude of freshets) may lead to interstitial spaces in the substrate becoming infilled by smaller materials - typically out-washed during high flow events - resulting in a similar reduction in the availability of sheltering habitat.

10.2.3 Smolt migration

Along with water temperature, streamflow is considered an important modulator for the process of smolt migration, particularly with respect to the downstream progression of smolts and the period during which they enter marine waters (Byrne *et al.*, 2004). Thus changes in the flow regime have the potential to disrupt migration patterns, possibly altering the time at which smolts leave the freshwater environment. In doing so changes in flow can affect whether the timing of migration coincides with (un)favourable marine conditions. Being exposed to more hostile conditions in the marine environment reduces the likelihood of survival and the potential for success during the post-smolt phase (Hansen & Jonsson, 1989, 1991; Zydlewski *et al.*, 2005; Nislow & Armstrong, 2011). As mortality in post-smolts can significantly influence the productivity of breeding returns and alter the population dynamics, it is important that the time of migration coincides with optimal marine conditions.

It is known that the timing of outward migration is locally adapted to the flow regime of river systems, with smolts generally moving downstream on the recession limb of the spring hydrograph (McCormick *et al.*, 1998; Nislow & Armstrong, 2011). Nislow and Armstrong (2011) indicate that the magnitude of flow and the occurrence of freshets influences the speed at which smolts can move downstream, and it is this which determines whether salmon enter marine waters within a favourable timeframe. Thus reductions in flow during the period which smolt runs occur may have the effect inhibiting or deterring smolt migration. McCormick *et al.* (1998) point to the existence of a ‘*smolt window*’ during which the timing of migration coincides with favourable marine conditions. Entering coastal waters before or after this period may mean water temperatures are outside the optimal range for growth and survival; it may also have implications for food abundance, metabolic costs and exposure to predation (Todd *et al.*, 2011). For example, a delay in spring migration may expose salmonids to lower summer flows and more hostile estuarine conditions (i.e. when water quality and DO levels are generally reduced). A reduction in peak spring flows may also lead to a more dispersed smolt run and an associated reduction in shoal sizes; this brings with it an increase in the vulnerability of smolts to predation (Milner *et al.*, 2010; Todd *et al.*, 2010). As a result of enhanced sea surface temperatures - as would be expected under projected climate conditions - the likelihood of sub-optimal marine conditions coinciding with the time at which smolts leave freshwaters is likely to increase. This highlights the importance of the flow regime in ensuring that downstream progression and marine migration occurs within a favourable timeframe.

Any delay in entering coastal waters may also result in a loss of smolt characteristics - a process referred to as ‘desmoltification’ or parr revision (McCormick *et al.*, 1998). The period of time for which smolts retain the physiological attributes that adapt them to life in the marine environment is thought to be temperature and/or time dependent (McCormick *et al.*, 1999). This underlines the importance of avoiding any delay in entering coastal waters. McCormick *et al.* (1998) state it is likely that the smolt window will increasingly narrow under future climate, thus the occurrence of high spring flows (spates) which facilitate downstream migration will be of increasing importance. Cross and Piggins (1980) examined the affect of a spring drought which occurred in the year 1980 on the migration of salmon and sea trout smolts in the Burrishoole catchment. It was found that low flow conditions delaying migration which, the authors attribute to a depleted smolt run and poor marine survival for that year.

Smolt migration is triggered by a combination of the actual water temperature as well as temperature increases during the months preceding migration (Byrne *et al.*, 2004); however, in some cases smolt runs have been found to be prompted by increases in water flow. A study by Carlsson *et al.* (2004), which focused on the River Hals (Norway), found that the migration rate of salmon smolts increased concurrently with increases in flow; in contrast the migration of sea trout smolts was found to correlate with temperature only. As freshets may act as a migratory cue, changes in the timing of spring flow events may be as important for the success of smolt runs as changes in the magnitude and frequency of high flow events.

Whilst changes in spring flows are important for smolt migration, increases in extreme flows are likely to have more immediate effects. For example, an increase in high flows may lead to pre-smolts being involuntarily displaced downstream into brackish waters without being sufficiently physiologically adapted to conditions in a saline environment (osmotic shock). In such cases the outwash of pre-smolts has consequences for survivorship and subsequent success in the marine environment (Jonsson & Jonsson, 2009).

10.2.4 Migration into and through river systems

River flow is one of the most important variables for controlling the upstream migration of returning adult salmon. High flows are known to stimulate the movement of salmon from coastal waters into river systems; in addition returning fish only move into freshwaters when flow conditions are conducive to upstream progression. Indeed variations in the timing of adult returns are thought to (at least in part) reflect locally adapted phenotypic responses specific to the flow regime of their home rivers (Jonsson & Jonsson, 2009; Todd *et al.*, 2011).

Generally at the southernmost limits of their distributional range summer runs of Atlantic salmon are much rarer. This is due to the occurrence of lower summer flows which do not facilitate movement upstream. In these areas the majority of salmon generally migrate before June, when estuarine temperatures are lower and there is sufficient flow for them to undertake migration. An increase in the seasonality of the flow regime, as is anticipated to occur under altered climate conditions, may result in spring runs becoming more prevalent. Similarly, more prolonged low summer flows

may result in salmon altering the timing of migration to coincide with higher flows which occur during the wetter autumn months. Breeding adults who return earlier are likely to encounter lower flows and higher water temperatures during the months prior to spawning (Jonsson & Jonsson, 2009; Todd *et al.*, 2011; Reed *et al.*, 2011). It is argued this could lead to an increased risk of mortality and exposure to heat stress - particularly in reaches where access to deeper pools is restricted or where fish are obstructed from exploiting thermal refugia in the upland reaches of river systems.

A study by Juanes *et al.* (2004) suggests that Atlantic salmon may respond to lower summer flows by altering the time of return migration. This study found that when stock was introduced to the Connecticut River - a river system at a more southerly location in relation to the origin of the stocked fish, and which is characterised by lower summer flows - it responded by advancing the time at which upstream migration occurred (~ 0.5 day year⁻¹ over a 23 year period). Juanes *et al.* (2004) indicate that a shift towards earlier peak migration was not exclusive to the Connecticut system, the same trend was also found to occur in populations at more northerly locations. The detected shift in migration patterns was found to be consistent with long-term trends evident in both temperature and streamflow records; as a result the authors suggests that observed changes in migration may be a response to recent climate change.

Hendry and Cragg-Hine (2003) highlight the importance of there being sufficient flow for salmon to navigate upstream successfully to spawning and nursery habitats in the higher reaches of river systems. In addition they draw attention to the availability of holding areas and deep pool refugia as critical for migratory progression - particularly during the intermediate quiescent phase. By limiting access to preferred spawning habitats, changes in flow may force salmon to use sub-optimal spawning sites. This has the potential to affect survival rates during the embryonic phase and has longer-term implications for recruitment success. In addition the inability of returning adults to access all parts of a river system (which are suitable for spawning) may alter the dynamics of density-dependence and its impact on survival and growth during the early juvenile stage (Johnsen & Jensen, 1994; Garcia de Leaniz, 2008). Elliott (1984a, 1984b, 1985, 1989) found that the survival of newly emerged brown trout was density-dependent in a stream which was extensively utilized for spawning. Milner *et al.* (2010) highlight the importance of autumn and early winter flow as critical for determining spawning location and success. It is argued that during years which are characterized by the occurrence of low flow conditions, spawning distribution and upstream penetration

may be limited, resulting in poor parr production (Solomon *et al.*, 1999). For example, using the results of a radio-tagging study conducted on a sample of returning adult salmon, Solomon *et al.* (1999) found that the distribution of spawning activity was severely constrained during two dry autumns when low flows were prevalent (1989 and 1990). Moir *et al.* (1998) conducted a study on the Grinock Burn (Scotland) and found that, during years when high flows coincided with the spawning period salmon were able to penetrate further upstream - resulting in spawning activity being more evenly distributed across the river network. The authors identify the ability to progress upstream as critical for regulating the population-density of salmon. Changes in flow may also limit access to spawning areas in higher reaches. Such areas provide a thermal refuge during periods with elevated water temperatures. Under altered climate conditions being able to access such habitats is likely to be of increasing importance for returning salmon.

Spates are a key component of the flow regime and are important for regulating upstream migration. Higher flows are critical for ascending obstacles and overcoming increases in gradient as fish progress through the higher stream reaches (Bjorn & Reiser, 1991). As a result any change in the magnitude or timing of spates may delay upstream progression and limit the degree to which fish can distribute evenly across river systems (Milner, 1990). Along with a reduction in spates, extended low flow periods and enhanced water temperatures may delay migration; thus the interaction between changes in both the flow and thermal regimes of river systems will be important (Jonsson & Jonsson, 2009).

It has been found that when large numbers of salmon are confined below obstacles - as is the case when flows are too low to facilitate progression - it increases the possibility for disease and parasitic transmission (Johnsen & Jensen, 1994). It also enhances vulnerability to predation and increases the risk of mortality during low flow and/or high temperature events. Hari *et al.* (2006) found that water temperatures in alpine rivers located across Switzerland had increased over a 25 year period. This study attributed the long-term decline in the catch of trout (*Salmo trutta*) across the region to the more widespread occurrence of Proliferative Kidney Disease (PKD) (a disease whose proliferation is temperature-dependent). It is argued that the inability of fish to progress upstream to more favourable thermal habitats at higher altitudes had contributed to the spread of the disease and the resulting decline in population numbers. The study points out that the occurrence of lower flows had prevented fish ascending

natural obstacles and thus limited the degree to which they could access the higher reaches of river systems.

Due to the role they have in both facilitating and stimulating (e.g. olfactory cues) river entry (Solomon *et al.*, 1999; Solomon & Sambrook, 2004), high flow conditions are important for longitudinal connectivity and the upstream mobility of returning salmon. Solomon *et al.* (1999) employed radio-tracking to determine those periods when salmon were most likely to enter their home rivers and initiate upstream migration. The study was conducted using six river systems located in south-east England. The findings indicated that spates presented optimal conditions during which flows exceeded the thresholds required for movement into river systems. It was found that fish which could not avail of this opportunity either failed to enter the system or delayed entry until later in the year. It was also found that those who did not enter river systems within a ten day period did not progress into freshwaters until the proceeding autumn. The study by Solomon *et al.* (1999) indicated that the flow required for initiating movement into river systems varied between 101% and 284% of Q95.

The results of a subsequent study by Soloman and Sambrook (2004) indicated that, during periods of reduced flow, salmon tended to remain in tidal waters. This was in contrast to high flow periods (which may have been episodic in nature) during which it was found that the majority of adults passed into river systems without delay. When river flows were low most fish remained in coastal waters or returned to sea for several months, many subsequently failed to enter river systems despite flow conditions being conducive to do so. It is argued this may be due to a loss of 'physiological opportunity', whereby fish are optimally conditioned to undertake upstream migration. It is therefore important that spates coincide with the period during which fish enter coastal waters. Soloman and Sambrook (2004) suggest this is similar to the 'smolt window' (McCormick *et al.*, 1998) but applied to the case of return migration. It is argued that during a hot dry summer significant losses may be incurred as a result of fish delaying migration into river systems (Solomon & Sambrook, 2004). Prompt entry to freshwaters reduces mortality and allows populations to distribute appropriately across the river network. Fish who delay migration are likely to be subject to less favourable conditions in the lower reaches of the river systems than those who migrate upstream earlier and can exploit thermal refugia at higher elevations.

Jonsson and Jonsson (2009) state that under the right conditions discharge acts as a control on the population structure. This is due to the capacity of flow to limit the

number and size of individuals which can access river systems (e.g. larger individuals require higher flows to enter river systems). As a result variations in flow have knock-on effects for the composition of the spawning stock and the associated mean body size of subsequent year classes. Tetzlaff *et al.* (2008) found that during dry as opposed to wet years fewer Atlantic salmon entered the spawning grounds of the Girnock Burn River (Scotland). During wet years fish entered the river system early and consistently throughout the season; this is in contrast to dry years where returning salmon entered later and typically in response to smaller, incremental or episodic increases in flow. Increases of an equivalent magnitude were found not to have a similar effect on entry during wet years. This highlights the greater importance of spates for facilitating river entry under low flow conditions. Although it is acknowledged that flow is of critical importance for regulating the movement of salmonids into river systems, the correlation between flow and temperature means it is difficult to isolate the exact affect each variable has (Milner *et al.*, 2010).

10.2.5 Impacts on habitat maintenance

Climate mediated changes in the hydrological regime of river systems may impact salmonids by altering the processes of erosion and deposition, both of which are vital to the maintenance of in-stream features and key for determining the availability of preferred habitat – particularly micro-habitats (e.g. riffles, undercut banks). For example, spates are necessary for removing accumulated sediment and debris, maintaining the channel form and distributing organic material (Verdonschot *et al.*, 2010); they are also important for homogenizing water chemistry. Importantly for salmonids high flows - or so called ‘flush flows’ - are vital for removing silt from spawning gravels and thus play an important role in the maintenance of in-stream habitat. However, an increase in the magnitude or a change in the timing of high flow (or flooding) events may lead to increased losses resulting from the scouring of gravel beds. It may also promote the displacement of individuals and have a damaging effect on riparian zones; which are themselves an essential food source and a key determinant of in-stream conditions. Thus, whilst high flows are important in terms of the fluvial geomorphological properties of a river system and the diversity of available habitat, a fine balance exists between those flows which are beneficial and those which are detrimental to salmonids as well as the wider functioning of lotic ecosystems.

Linked with changes in the flow regime are altered patterns of deposition and sediment transport in river systems. An increase in the intensity of rainfall events, as is projected to occur as a result of altered climate forcing, is likely to result in greater rates of soil erosion. This would have the effect of subjecting river channels to increased siltation, smothering spawning gravels and damaging habitats important for benthic communities. By altering those fluvial processes which influence erosion and sedimentation rates, changes in precipitation and flow are likely to have knock-on effects for the overall productivity of river systems and the quality of available habitat.

10.2.6 Adaptation

Despite their inherent sensitivity to environmental conditions, salmonid species have successfully adapted to past fluctuations (occurring over varying time-scales) in climate, and any changes in freshwater ecosystems which occurred as a result. Under perturbed forcing the rate at which changes in climate are projected to occur (manifested in the hydrological and ecosystem response), with respect to the ecological or genetic adaptability of salmonids, is critical for determining their vulnerability to climate change. As highlighted by Graham and Harrod (2009), several studies have indicated that Atlantic salmon may not be adapting at a quick enough rate to recent climate change, as a result of which localised extinctions are likely to occur (Friedland *et al.*, 2003; Ottersen *et al.*, 2004; Fealy *et al.*, 2010; Elliott & Elliot, 2010). Indeed it is argued that the loss of some populations along the southern edge of their distribution may be driven by recent climate change (Friedland *et al.*, 2003).

Lytle and Poff (2004) outline the importance of species adaptation in the context of changing hydrological regimes; the authors point to the mode of adaptation (i.e. life history, behavioural and morphological) as critical for determining the resilience of aquatic biota to changes in climate. In salmonid species adaptations may involve altering some aspects of their behaviour (e.g. deepening nests to avoid scouring) and life history strategy (e.g. fry emergence optimized to avoid flood mortality, earlier migration).

With respect to the potential for adaptation to occur, changes in the seasonal timing of flow events are of particular importance. Lytle and Poff (2004) state that those species which respond to changes in flow through life history adaptations may be most affected

by changes in the timing of extreme events. The capacity of salmonids to adapt to altered flow conditions is dependent on how finely tuned they are to established patterns of flow behaviour. It will also depend on whether the rate at which change occurs provides sufficient time for populations to adapt. The manner in which hydrologic change occurs is therefore considered critical (e.g. more variable, less predictable, step-change, etc.).

The exceedance of critical thresholds which determine mortality in a particular age-class is important, particularly with regards to changes in the nature of extreme events under future climate forcing. It is likely that populations will face collapse if these thresholds (e.g. thermal tolerances, minimum depth requirements) are continuously breached - particularly if they relate to those life stages which are most sensitive to environmental conditions or which are already considered 'mortality bottlenecks' (e.g. fry emergence, smolt migration). The frequency with which these thresholds may be exceeded under altered climate may be of greater significance than a species capacity to adapt to progressive changes in the flow regime. Todd *et al.* (2010) indicate that extreme abiotic disturbances (e.g. prolonged high temperatures, extreme flood events) may have long-term consequences for juvenile salmon which are beyond those associated with changes in (seasonal or annual) mean conditions. In this context a species capacity to adapt to progressive changes may be outweighed by a short term increase in the frequency of more extreme events.

10.3 Methodology

The methodology used in this study follows that employed by Walsh and Kilsby (2007) who examined climate-related changes in flow and habitat conditions in the Eden catchment - an upland system located in North West England. In their study a hydrological model was employed to simulate streamflow using the UKCIP02 climate change scenarios. The simulated flow data was subsequently used to model changes in the hydraulics of four selected stream reaches.

Streamflow, when considered in terms of volumetric discharge (e.g. $\text{m}^{-3} \text{s}^{-1}$), may only be considered a proxy for variables such as water depth and velocity which are more closely identified with the habitat and physiological requirements of salmonids at different life-stages (Hendry & Cragg-Hine, 2003). According to Milner *et al.* (2010) it

is not flow *per se* which fish generally require, nor what they detect and respond to, but rather those hydraulic parameters including water depth and velocity, which depend on the interaction between volumetric flow and the channel morphology. Therefore in order to model the impacts of climate change on habitat availability, it is more appropriate to translate changes in flow into changes in more relevant hydraulic parameters.

In this study flow data obtained from hydrological model simulations was used to examine changes in four hydraulic variables including, water depth (m), velocity ($m s^{-1}$), Froude number (Fr) and discharge per metre width (q). Based on the known habitat requirements of Atlantic salmon conclusions could be drawn as to the potential impact of climate change on the availability of suitable in-stream habitat. Changes in each variable were estimated from the simulated flow data using information on the physical properties of the selected stream reaches and Manning's equation for open channel flow - which can be written as:

$$Q = \left(\frac{A}{n}\right) R^{2/3} S_0^{1/2}$$

where n represents Manning's coefficient, A is the cross-sectional area of flow, Q is volumetric discharge, S_0 is the slope of the stream reach and R is the hydraulic radius. The physical properties of each study channel were estimated over a 50 metre reach. To conduct the hydraulic modelling measurements for the width of the channel base and the channel slope were required, as was a value for Manning's n coefficient. To calculate these variables an idealized version of the stream reach was used. To this end each channel was standardized based on the assumption that its form approximated to that of a trapezoidal shape, whereby the stream banks have a 1 in 2 gradient. Walsh and Kilsby (2007) highlight that by adopting this approach important in-stream features (e.g. gravel bars, riffle-pool sequence), along with the non-uniformity of the channel form and structure - which are key for characterising channel systems in their natural state - are not considered. The nuanced physical features of a channel are important for the availability of diverse habitats across a range of scales (e.g. Moir *et al.*, 2004). It may be the ability to exploit micro-habitats formed by these features which are important for habitat availability - particularly with respect to sheltering habitats and the availability deep pool refugia - and the local carrying-capacity of river systems.

To conduct the type of analysis which would account for such features, a more in-depth mapping of the selected reaches would be required – this would lend itself to the use of a habitat simulation model such as PHABSIM (Bovee, 1996) or CASiMiR (Jorde *et al.*, 2000; Schneider, 2001). Such models are essentially higher resolution hydraulic rating curves which simulate how - with respect to the physiological requirements of the target species - changes in flow affect the availability of usable habitat (Box 9.1). Despite not incorporating high resolution physical data, the methodological approach adopted in this study does allow for an assessment of habitat availability under projected climate conditions. In addition employing a habitat model - which requires information on the geometry of the stream channel and detailed mapping of any in-stream features - in the context of a climate change impacts study such as this would require a more explicit assumption regarding the stationarity of the channel form. This may be difficult to justify given that the channel, in a geomorphological sense, is likely to change in response to alterations in the flow regime. Adopting such an approach would therefore require a more in-depth exploration of the issues involved - which is beyond the scope of this study. It is also possible that employing a dedicated habitat model would add little value over using the hydraulic rating approach adopted here.

Box 10.1

As a result of the environmental degradation brought about by the extensive alterations made to natural flow regimes, there has been a more widespread recognition of the importance they hold for the sustainability of freshwater ecosystems (Poff *et al.*, 1997, 2010; Jowett, 1997, 2010; Tharme, 2000, 2003). Environmental flow assessments (EFAs) are used to determine the quantity of flow (e.g. minimum ecological flow) required to maintain the ecological integrity of lotic ecosystems. While EFAs are generally used to assess the effects of water abstraction or channel modification, it is possible to apply the same methods in the context of climate change impact studies. Tharme (2003) identifies four broad methodological approaches for conducting EFAs, which include: hydrological assessments, hydraulic rating, habitat simulation and holistic methods. As highlighted by Jowett (1997) the common element of each approach is that the stream environment is maintained; however, each focuses on different aspects of the river system or hydraulic environment (e.g. flow statistics, wetted perimeter, physical habitat).

Hydrological index methods - also referred to as fixed-percentage or look-up tables - include the Tennant Method (Tennant, 1976), the Median Monthly Flow (Q50) (USFWS, 1981) and Aquatic Base Flow methods (Kulik, 1990). The approach requires setting a threshold value denoting the minimum flow required to sustain ecosystem functions and aquatic biota (e.g. 10% of mean annual flow provides minimum protection, whilst 30% is satisfactory). Such thresholds may be set using commonly adopted indices of flow or may be determined based on a detailed analysis of historical runoff data. This approach may be considered more holistic as it does not consider any one species in isolation, but rather considers the flow required to maintain the overall ecological well-being of river systems. The approach can be criticised for the *ad hoc* manner in which flow thresholds may be set (e.g. Q95 used to maintain critical levels of habitat). In this case it is possible that the use of generic indices may not reflect the actual flow required to service the unique physical, ecological and habitat requirements of a specific catchment system. Hydrological assessments also include methods which consider the whole range of flow behaviour, rather than pre-specified flow thresholds. This approach acknowledges that each component of the flow regime (e.g. 'flush flows'; Figure 10.2) is important to the ecological health of lotic systems.

Hydraulic rating methods assess those hydraulic parameters (e.g. wetted perimeter, minimum depth) which are known to affect the target species. This approach considers those variables which vary with flow, but are - in contrast to flow indices - more closely linked to the physiological requirements of aquatic biota (Caissie & El-Jabi, 2003). According to this approach an empirical relationship is established between each hydraulic parameter and river discharge. This relationship is formulated based on a survey of channel cross-sections, typically at points where habitat may already be limited (i.e. at points where habitats decrease more rapidly with decreasing flow) or along sections which are of particular significance for the target species (e.g. spawning areas). Based on this relationship and the known habitat requirements of the target species a flow threshold is set (i.e. minimum environmental flow); when flows fall below this it is assumed that the quality/quantity of available habitat is significantly degraded. As the application of this approach requires field measurements it is more complex than historic flow methods (Jowett, 1997). The hydraulic approach may be referred to as 'hydraulic rating' and can be considered a precursor to more complex habitat simulation methods. In contrast to using flow indices this approach may be considered more physically sensible; however, one of its key weaknesses is that it does not consider the ecosystem as a whole but rather focuses on a single species. The Wetted Perimeter Method (Reiser *et al.*, 1989) is one of the most commonly employed hydraulic rating methods (Tharme, 2003).

Habitat models explicitly consider the hydraulic conditions required to meet the specific physiological needs of the target species; this is in contrast to hydraulic rating curves which examine changes in the hydraulic parameters only (Jowett, 1997). Models like PHABSIM (Physical Habitat Simulation Model; Bovee, 1982; Stalnaker *et al.*, 1995) and CASiMiR (Computer Aided Simulation Model for Instream Flow Requirements; Jorde *et al.*, 2000, Schneider *et al.*, 2001) estimate how changes in flow affect the availability of suitable habitat. Model simulated data, describing the relationship between flow and the relevant habitat parameters (e.g. depth, velocity, substrate, cover), are combined with a habitat preference curve formulated specifically for the target species. Based on this an index (weighted usable area) describing the quantity of suitable habitat available over a range of flows can be formulated. This approach considers both the hydrologic and hydraulic factors which affect habitat availability; it also considers the biological requirements of the target species. Despite their widespread application, habitat simulation models are the subject of some criticism. It is argued that by not considering interspecific relationships or accounting for the various interactions between different life stages, the model's ability to provide a true description of habitat availability is limited (Gore & Nestler, 1988; Jowette 1997; Gore *et al.*, 1998; Holm *et al.*, 2001; Ahmadi-Nedushan, 2006). This approach has also been criticised for the assumption that the habitat preference curves are transferable between populations which may be locally adapted to specific environmental conditions. In addition, as highlighted by Caissie and El-Jabi (2003), very few studies have found a strong relationship between the simulated and observed data (Orth & Maughan, 1982; Bourgeois *et al.*, 1996). The models have generally been limited by their ability to provide information on changes in the availability of suitable habitats at larger spatial scales (e.g. entire river system). However, the development of models like the Mesohabitat Simulation Model (Meso-HABSIM) has allowed this issue to be somewhat redressed (Parasiewicz, 2001). Despite the limitations of habitat simulation models they still represent an important tool for conducting EFAs.

The holistic framework is the final methodological approach identified by Tharme (2003) (e.g. Arthington *et al.*, 1992; King *et al.*, 2003). According to King *et al.* (2003) this approach was developed in response to the various shortcomings associated with habitat models. Rather than being narrowly focused on the flow/hydraulic requirements of a specific species, holistic approaches consider the flow required to sustain each of the various elemental components which comprise the overall ecology of river systems. The approach requires that all system components, processes and biological community interactions - each of which is essential for sustaining optimal habitat conditions for the target biota - are considered. As a result holistic approaches require utilizing a range of modelling tools which enable different aspects (e.g. biological, hydraulic, hydrologic, etc.) of the system to be examined.

Holistic approaches are based on linking changes in the flow regime to changes in other aspects of the biophysical environment. They consider each species whose habitat is sensitive to flow, including invertebrates and other aquatic biota; in addition, all components of the flow regime and hydraulic environment, as well as various water quality parameters are considered. A key principle of holistic methods is the maintenance of natural flow regimes (encompassing long-term patterns of flow behaviour and natural variability) - which are understood to be critical with regards to preserving the ecological well-being of lotic systems. As the flow required for sustaining the entire ecosystem is considered, the flow indices approach discussed above could be interpreted as being holistic - albeit that it is implicitly rather than explicitly holistic.

In the case of this study the stream reaches which could be selected for hydraulic modelling were limited to those locations where the outlet point for each catchment is sited. This is because the hydrological models can only provide reliable flow data - particularly with respect to the volume of flow - at those points from which the observed long term gauge records used to calibrate the models were obtained. As a result only two stream reaches were considered when conducting the hydraulic modelling. Figure 10.3 and Table 10.1 provide information on the geometry of each study reach; the location of the Glenamong and Srahrevagh gauging points are shown in Figure 10.4, 10.5 and 3.2.

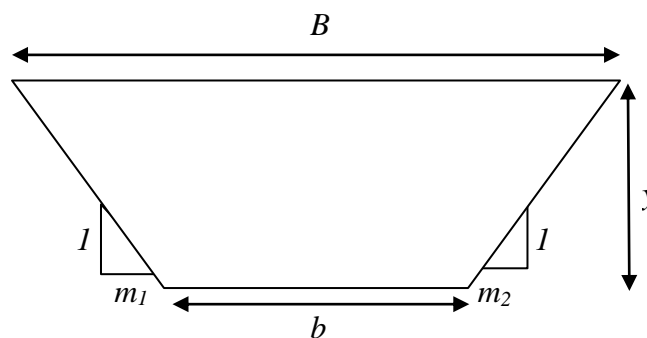


Figure 10.3 Idealized trapezoidal shape used to model the hydraulics of study reaches

Channel Properties	Glenamong	Srahrevagh
Channel base width (m) (b)	8.25	3.74
Manning's n	0.025	0.035
Slope (m/m)	0.012	0.015

Table 10.2 Dimensions of the 50 m Glenamong and Srahrevagh study reaches.

Being constrained to focus on those reaches or cross sections along the network where flow gauges are sited precludes the objective selection of strategically important sites. Despite this the data from these sites is sufficient to establish a relationship between the specified hydraulic parameters and the volumetric flow rate - which is the central tenet of hydraulic rating methods (Jowett, 1997; Caissie & El-Jabi, 2003; Tharme, 2003). Furthermore, as shown by Figures 10.4 and 10.5, both study reaches are highlighted as locations which have been used for spawning in the past. This information has been provided by the Marine Institute who conducted a survey of spawning areas across the catchment.

Following Walsh and Kilsby (2007) the Reliability, Resilience and Vulnerability (RRV) methodology was used to assess changes in three key flow statistics: Q05 (high), Q95 (low) and Q50 (median). The RRV analysis has been previously employed in a water

management context to assess the capabilities of water supply systems in meeting demand (Hashimoto *et al.*, 1982a, 1982b; Fowler *et al.*, 2003). Ajami *et al.* (2007) used a similar method to examine resource management and planning in the context of uncertainties in hydrological modelling. The central tenant of the RRV methodology is that the system being examined can at any given time be in either a satisfactory or unsatisfactory state – identified using a set threshold. The three parameters which comprise the RRV criteria are applied on this basis.

Reliability refers to the likelihood that a given flow value lies within the range of values which are deemed to be satisfactory, it is calculated using the following:

$$\left(\frac{\text{series length} - \text{the number of days for which the system is in an unsatisfactory state}}{\text{series length}} \right) \times 100.$$

Resilience is based on the persistence of unfavourable flow conditions and is a measure of the rate at which flow moves from an unsatisfactory to a satisfactory state. Resilience is estimated using:

$$\left(\frac{\text{the number of times a satisfactory flow value follows an unsatisfactory value}}{\text{number of unsatisfactory values}} \right) \times 100.$$

Finally *vulnerability* refers to the maximum length of time for which an unsatisfactory flow value occurs and is calculated using:

$$\left(\frac{\text{maximum number of days for which an unsatisfactory value occurs}}{\text{maximum number of successive days for which an unsatisfactory value occurs when each of the ensemble members are considered}} \right).$$

Habitat modelling was conducted using flow projections derived from an ensemble of twenty five climate scenarios, six of which were downscaled using the SDSM statistical downscaled model. Dynamically downscaled climate projections made available as part of the EU funded ENSEMBLES project (van der Linden and Mitchell, 2009) were also used (Figure 6.11).

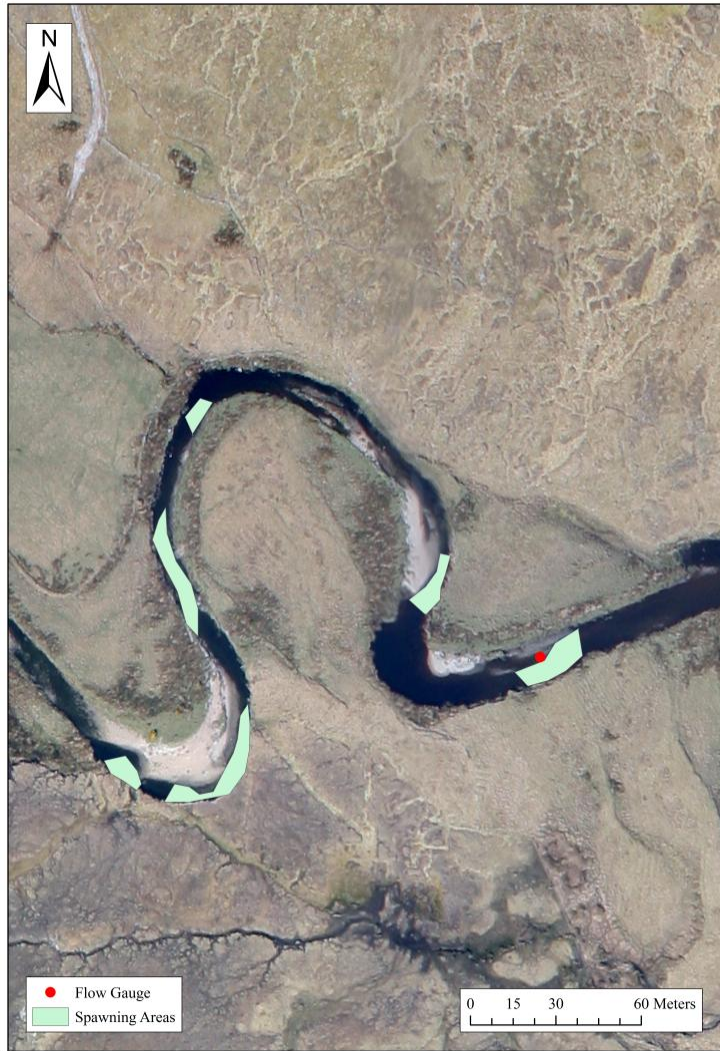


Figure 10.4 Aerial photograph of the Glenamong study reach

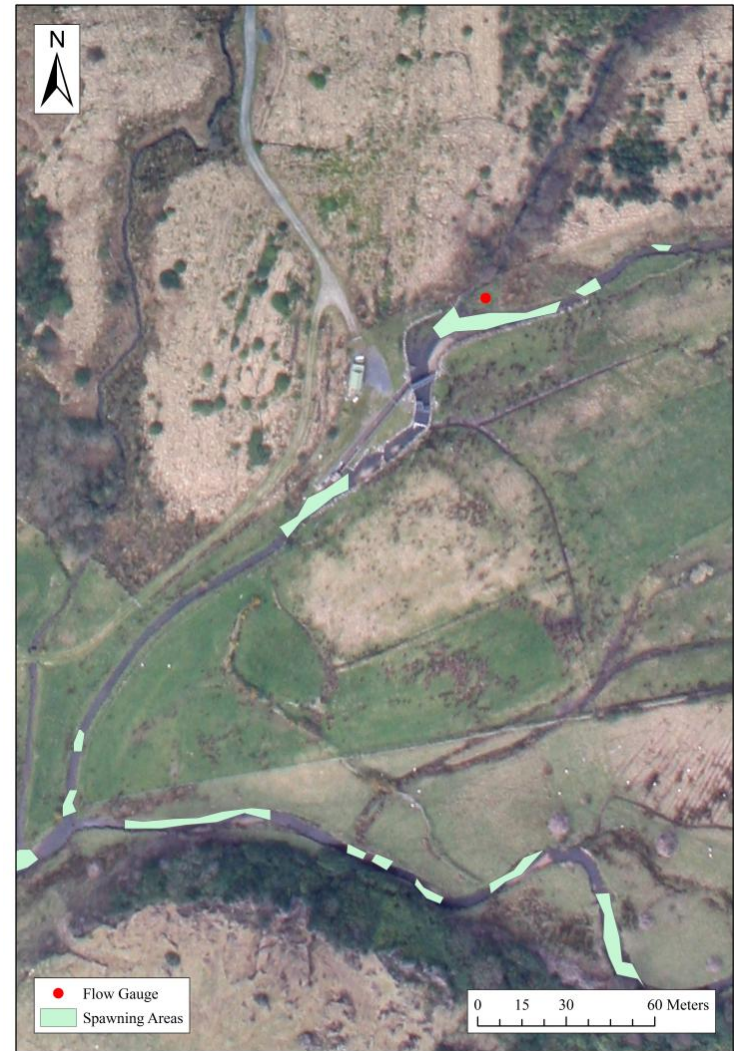


Figure 10.5 Aerial photograph of the Srahrevagh study reach

For each scenario three hundred hydrological simulations were conducted - integrating across three model structures and one hundred parameter sets. The hydraulic modelling and RRV assessment were conducted using the Monte Carlo simulation method previously applied to model the hydrological response of the study catchments to projected changes in climate (Wilby & Harris, 2007) (see section 9.3.2). Employing this approach allowed the formulated scenario weights to be incorporated when estimating future changes in habitat availability. The results are examined for each of three 30 year future horizons (2020s (2010-39), 2050s (2040-69) and 2080s (2070-99)) relative to the control period (1961-1990).

10.4 Ideal Flow Parameters

Numerous studies have provided evidence that fish actively seek particular combinations of water depth, velocity and substrate cover; each of which are considered key descriptors of available habitat and can be linked to the physiological requirements of salmonids at different life stages (Heggenes & Saltveit, 1990; Armstrong *et al.*, 1998; Hendry & Cragg-Hine, 2003). In this study the parameters used to describe habitat availability under altered flow conditions are the same as those employed by Walsh and Kilsby (2007). These parameters have been sourced from published studies (e.g. Hendry & Cragg Hine, 1997; Moir *et al.*, 2002) and relate to habitat requirements during the stages of spawning, juvenile development and upstream migration.

Based on the measurements taken from both study reaches, Manning's equation for open channel flow and the minimum ideal habitat values (i.e. Froude number, depth, velocity and discharge per unit width), the equivalent volumetric discharge value for each parameter and life stage was calculated. In this way the hydraulic parameters were translated into the corresponding discharge values for each study channel. Using the output from the hydrological modelling documented in the previous chapter, the percentage of time for which these flow values were equalled or exceeded under projected climate conditions was calculated. By comparing the values for each future horizon to that of the control period changes in the length of time for which the minimum habitat requirements are satisfied under projected climate could be estimated. For each respective life stage, only those periods during the year when habitat conditions are deemed to be important were examined. Thus, when examining changes in habitat for spawning fish, the period from October to December was considered; this

equates to the period when spawning in the catchment predominantly occurs. Similarly, the period from June to September was examined when assessing changes in the availability of habitat during upstream migration. In terms of juvenile salmon the study of changes in habitat is not confined to any specific period.

The first parameter used to describe habitat requirements is discharge per unit width (q) (Table 10.3); in this case it applies to adult fish only. The values for q are the same as those employed by Walsh and Kilsby (2007) and have been sourced from the Lancaster River Authority (Stewart, 1969). They are also reported in a number of published studies (e.g. Crisp, 1993; Hendry & Cragg-Hine, 2003) as established flow parameters for adult salmon. A q value of $0.03 \text{ m}^3 \text{ s}^{-1}$ is regarded as ‘survival flow’; this represents the flow for which adult fish are generally inactive and do not attempt to move upstream.

Life-stage	Ideal minimum ($\text{m}^3 \text{ s}^{-1} \text{ m}^{-1}$)
Survival Flow	$0.03 \text{ m}^3 \text{ s}^{-1} \text{ m}^{-1}$
Start of migration	$0.08 \text{ m}^3 \text{ s}^{-1} \text{ m}^{-1}$
Peak intensity of migration	$0.20 \text{ m}^3 \text{ s}^{-1} \text{ m}^{-1}$

Table 10.2 Ideal minimum values of discharge per metre width (q) for adult Atlantic salmon (Source: Stewart, 1969).

The second hydraulic parameter used is the Froude number. This was initially proposed as a descriptor of hydraulic habitat by Moir *et al.* (2002). As it is a dimensionless parameter, it provides a comparable measure of hydraulic conditions across river systems of contrasting sizes. In addition it can be used as a standard measure to compare the hydraulic requirements of different fish species (Moir *et al.*, 2002). In a study of the river Dee located in north-east Scotland Moir *et al.* (2002) found that favourable hydraulic conditions for spawning occurred when the water depth was above 0.15 m and the Froude number ranged between 0.30 and 0.44 - with a mean of 0.38. The findings of Moir *et al.* (2002) indicated that salmon in the River Dee utilized a wide range of water depths (0.12 to 0.66 m) and velocities (0.22 to 1.29 m s^{-1}) during spawning.

Values representing the ideal water depth and flow velocity for juvenile as well as spawning salmon are taken from Hendry and Cragg-Hine (1997). These values are based on a review of the findings from other studies. It is indicated that the water velocity which is most preferred for spawning ranges between 0.25 and 0.90 m s^{-1} . With respect to water depth the ideal minimum value ranges from 0.17 to 7.6 m (Hendry &

Cragg-Hine 1997). For fry and underyearling parr it is indicated that 0.20 m is the minimum water depth required; whilst the ideal value for current velocity ranges between 0.50 and 0.65 m s⁻¹. Similar ranges for water depth (0.20-0.40 m) and velocity (0.60-0.75 m s⁻¹) are required by yearling and older parr.

Life Stage	Ideal Minimum Velocity (m s ⁻¹)	Ideal Minimum Depth (m)
Spawning	0.25	0.17
Fry and underyearling parr	0.5	0.2
Yearling and older parr	0.6	0.2

Table 10.3 Ideal minimum flow depth and velocity values for juvenile Atlantic salmon (Hendry & Cragg-Hine, 1997)

10.5 Results

10.5.1 Reliability Resilience and Vulnerability (RRV Analysis)

The RRV analysis was conducted using the probabilistic framework outlined in section 9.3.2. According to this procedure, Monte Carlo simulation was used to estimate the respective posterior distribution for each of the RRV measures. The analysis was conducted for three flow statistics - Q50, Q95 and Q05 - representing median, low and high flows respectively. To examine differences between the model pathways the RRV parameters were also applied to each ensemble member independently - the results of which are provided in Appendix V. In this case the median series from the multi-model simulation derived using GLUE was used (see section 9.3.1).

The results of the RRV analysis for both catchments are shown in Table 10.4. In this case the median of the posterior distribution from the MC simulation is reported; the scenario weights discussed in chapter six were used when conducting the analysis. The similarity evident in the response of both catchments reflects the fact that they possess similar hydrologic properties. Under the A1B and A2 SRES scenarios the reliability analysis suggests an increase in high flows. This is in contrast to both the B2 and combined A2/B2 scenarios which suggest a general decrease in Q05. When the individual climate projections are considered the scenario provided by the Swedish Meteorological and Hydrological Institute (SMHI) - whereby the low sensitivity (Q3) HadCM3 was used as the driving model - suggests the greatest increase in Q05 (~7.3% by 2080s for the Srahrevagh). In contrast a number of the ensemble members, including the statistically downscaled CGCM2-A2 scenario suggest a decrease in high flows. Resilience provides a measure of the system's tendency to remain in an unsatisfactory

state. With respect to high flows the results for this metric are similar to those returned for the reliability criterion. According to the A1B scenario high flows are likely to persist for longer; this is in contrast to the other emission scenarios which suggest that resilience to high flows is likely to increase.

Each of the emission scenarios (Table 10.4) suggest a decrease in median flows (Q50); the greatest reduction in which is associated with the more carbon intensive A2 SRES scenario. Under this emissions pathway it is suggested that Q50 is likely to become ~Q45 by the 2080s, a finding common to both catchments. Generally reductions in the median flow statistic are greatest over the 2050s, suggesting that flows somewhat recover towards the end of the century. In terms of the individual model pathways, the greatest decrease is suggested by the statistically downscaled CGCM2 A2 scenario (Q43.3 over the 2080s); in contrast, increases are suggested by a number of ensemble members including the scenario provided by the SMHI – for which the Bergen Climate Model was used as the driving GCM. According to this pathway Q50 is likely to increase by 3% over the 2080s. Results for the resilience criterion suggest that, irrespective of the emission scenario considered, flows below the Q50 threshold are likely to persist for longer - a finding which is most evident under the A2 SRES scenario.

Results of the reliability test for the Q95 statistic suggest that over each successive horizon, a decrease in low flows is likely to occur. In general reductions are greatest for the 2050s (~Q89); however, the largest decrease is projected for the 2080s under the A2 SRES scenario (Q86). With respect to the individual ensemble members the greatest reduction is suggested by the statistically downscaled CGCM2 A2 scenario (~Q85 over the 2080s). A number of ensemble members do however suggest an increase in the reliability criterion for this flow statistic under projected climate conditions (e.g. UK Met Office HadCM3 low sensitivity (Q3); Q98 over the 2080s).

In contrast to the other flow indices considered, there are greater differences in the magnitude of projected changes in Q95 when the two study catchments are compared. In terms of resilience the results from the MC simulation suggest that unfavourable low flows (i.e. below the Q95 threshold) are likely to persist for longer. Vulnerability measures the maximum number of consecutive days for which the system is in an unfavourable state. For all scenarios there is a suggested increase in the maximum length of time that flow falls below the Q95 threshold (estimated for the control period). Generally the flow regime appears to be most vulnerable to low flows over the 2050s.

In contrast model simulations suggest that low flows may recover somewhat over the 2080s. The statistically downscaled CGCM2 B2 scenario suggests the greatest increase in vulnerability for the Q95 flow statistic.

	Glenamong				Srahrevagh			
	<i>Ctrl</i>	<i>2020s</i>	<i>2050s</i>	<i>2080s</i>	<i>Ctrl</i>	<i>2020s</i>	<i>2050s</i>	<i>2080s</i>
<i>Q05 Reliability (%)</i>								
A1B	5.00	5.49	5.74	6.50	5.00	5.49	5.79	6.40
B2	5.00	4.93	4.90	4.95	5.00	4.93	4.89	4.89
A2	5.00	4.86	4.53	5.10	5.00	4.85	4.53	5.04
A2 and B2	5.00	4.88	4.84	4.94	5.00	4.95	4.85	4.94
<i>Q05 Resilience</i>								
A1B	4.19	4.54	4.67	5.24	4.14	4.55	4.80	5.36
B2	4.21	4.15	3.99	3.92	4.21	4.13	3.98	3.92
A2	4.17	3.96	3.78	3.96	4.17	3.96	3.78	3.94
A2 and B2	4.18	4.03	3.86	3.93	4.15	4.05	3.95	3.96
<i>Q50 Reliability (%)</i>								
A1B	50.00	48.57	46.99	48.27	50.00	49.04	47.40	48.34
B2	50.00	48.52	46.56	48.06	50.00	48.52	46.57	48.06
A2	50.00	46.27	45.79	45.48	50.00	46.27	45.77	45.47
A2 and B2	50.00	47.93	46.28	47.53	50.00	48.07	47.81	47.42
<i>Q50 Resilience</i>								
A1B	18.90	18.35	17.55	17.93	18.55	18.02	17.31	17.73
B2	19.19	19.27	17.43	17.62	19.19	19.24	17.43	17.62
A2	18.90	17.98	17.19	17.05	18.90	17.99	17.19	17.05
A2 and B2	19.03	18.47	17.38	17.47	18.52	18.21	17.01	17.15
<i>Q95 Reliability (%)</i>								
A1B	95.00	93.74	92.68	93.68	95.00	94.01	92.63	93.54
B2	95.00	93.17	89.49	91.68	95.00	93.16	89.49	91.68
A2	95.00	91.76	89.34	86.11	95.00	91.63	88.88	86.05
A2 and B2	95.00	92.80	89.49	90.52	95.00	92.05	89.49	91.97
<i>Q95 Resilience</i>								
A1B	20.46	19.58	18.57	19.66	21.70	19.97	18.18	20.02
B2	22.26	23.54	20.20	18.46	22.26	23.54	20.15	18.44
A2	23.21	19.32	19.83	16.05	23.40	19.35	19.83	16.16
A2 and B2	22.83	21.03	20.05	17.64	22.45	22.16	20.10	17.04
<i>Q95 Vulnerability</i>								
A1B	0.58	0.71	0.80	0.62	0.48	0.56	0.71	0.58
B2	0.69	0.71	1.00	0.77	0.69	0.71	1.00	0.77
A2	0.54	0.80	0.90	0.85	0.54	0.79	0.90	0.85
A2 and B2	0.67	0.73	0.98	0.83	0.58	0.75	0.96	0.81

Table 10.4 Results of the Reliability, Resilience and Vulnerability (RRV) analysis for the Glenamong and Srahrevagh catchments. The analysis is conducted for three flow statistics representing median (Q50), low (Q95) and high flows (Q05); four different time periods including the control (1961-1990), 2020s (2010-2039), 2050s (2040-2069) and 2080s (2070-2099) are considered in the analysis. The results represent the median of the posterior distribution estimated using the MC simulation approach discussed in section 9.3.2. The ensemble weighting scheme outlined in chapter six was used when estimating changes in the RRV criteria

10.5.2 Changes in flow and habitat availability

10.5.2.1 Survival and upstream migration: adult salmon

Table 10.5(i) shows the percentage of time for which the discharge through each study channel exceeds the flow threshold corresponding to the ideal discharge per metre width (q ; $\text{m}^3 \text{s}^{-1} \text{m}^{-1}$) (Stewart, 1969). Projected changes are estimated based on the median of the posterior distribution derived using the MC simulation procedure; the scenario weights discussed in chapter six were employed when conducting the analysis. Over the control period the minimum ‘survival’ flow for adult salmon was attained for a greater proportion of time in the Glenamong (~75%) as opposed to the Srahrevagh (~65%); this is due to the channel reach from the Glenamong having a greater hydraulic radius and draining runoff from a larger catchment area.

The results suggest a progressive decrease in the proportion of time for which minimum survival flow is attained. Reductions in this parameter are mirrored in the results of the RRV analysis discussed above (specifically the reliability of Q50 and Q95 under future forcing). The greatest decrease in survival flow is associated with the A2 SRES scenario; in addition reductions for the Glenamong (~9% over the 2080s) are projected to be greater than the Srahrevagh (~3%). Decreases in this flow parameter are of a lesser magnitude under the A1B scenario. Model simulations generally indicate that the availability of in-stream habitat required by adult salmon is likely to be reduced under future climate conditions.

In both study channels a decrease in the flow required for upstream migration (June-September) is suggested. Under the A2 scenario, over the 2080s horizon, a reduction in the flow required for migration is projected in both channel reaches (Glenamong: -6.6%; Srahrevagh: -4.8%). Suggested reductions in this parameter reflect model projected changes in the Q05 high flow statistic - which is indicative of those (spate) flows necessary for upstream migration (Figure 9.26-9.27; 9.32-9.33). The results of the hydrological modelling suggest decreases in Q05 for June, July and August; while increases are projected for September. Suggested changes in Q05 during the period which upstream migration occurs are reflected in the reduction in ‘peak flows’ (Table 10.5(i)).

	Ctrl	2020s	2050s	2080s	Ctrl	2020s	2050s	2080s
<i>(i) Percentage time that discharge equivalent to the minimum ideal q is exceeded</i>								
Survival flow	Glenamong				Srahrevagh			
A1B	76.77	72.99	71.14	72.79	66.70	66.04	64.42	65.45
B2	75.53	71.72	67.94	69.65	65.59	65.82	63.76	64.76
A2	75.86	69.08	67.05	66.53	65.45	63.53	63.21	62.10
A2 and B2	75.56	70.43	67.45	68.54	65.62	64.76	63.61	63.77
Start of migration (June-September)								
A1B	26.31	23.42	21.64	21.12	17.81	15.71	14.18	13.80
B2	23.72	23.22	19.07	21.15	16.07	15.14	12.21	13.61
A2	24.26	21.39	20.46	17.65	16.31	14.37	13.72	11.55
A2 and B2	23.96	22.38	19.70	19.56	16.22	14.78	12.45	12.45
Peak migration (June-September)								
A1B	9.04	8.72	8.06	8.28	4.10	4.18	3.74	4.02
B2	8.22	8.58	6.50	7.51	3.99	3.99	3.01	3.42
A2	8.63	7.84	7.35	6.23	4.04	3.57	3.33	2.78
A2 and B2	8.44	8.22	6.94	6.91	4.01	3.77	3.14	3.11
<i>(ii) Percentage time that discharge equivalent to the minimum ideal depth and Froude number are exceeded</i>								
Spawning: Minimum Depth (October-December)	Glenamong				Srahrevagh			
A1B	82.21	80.25	78.48	81.97	55.33	53.30	53.19	56.59
B2	82.61	81.34	81.41	78.80	55.14	51.12	53.80	51.12
A2	82.64	77.39	77.90	80.14	54.96	51.44	50.94	51.74
A2 and B2	82.61	79.24	79.49	79.24	55.04	51.10	52.89	51.30
Spawning: Froude Number (October-December)								
A1B	76.59	75.14	73.01	75.89	50.07	47.97	47.75	51.15
B2	77.03	74.93	75.54	73.30	49.24	45.80	48.51	45.91
A2	77.10	71.52	71.63	73.84	49.38	45.76	45.47	46.19
A2 and B2	77.03	73.37	73.70	73.55	49.27	45.69	47.79	46.01
<i>(iii) Percentage time that discharge equivalent to the minimum ideal depth is exceeded</i>								
Ideal Depth: Spawning (October-December)	Glenamong				Srahrevagh			
A1B	76.59	75.14	73.01	75.89	50.07	47.97	47.75	51.15
B2	77.03	74.93	75.54	73.30	49.24	45.80	48.51	45.91
A2	77.10	71.52	71.63	73.84	49.38	45.76	45.47	46.19
A2 and B2	77.03	73.37	73.70	73.55	49.27	45.69	47.79	46.01
Ideal Depth: Fry and Yearling Parr/Yearling and older Parr								
A1B	46.73	43.89	42.68	44.00	28.63	27.94	27.18	27.93
B2	45.04	42.45	40.55	42.48	28.35	27.04	26.53	27.57
A2	44.96	40.33	39.87	39.85	28.52	26.26	26.18	26.29
A2 and B2	44.97	41.39	40.25	40.94	28.36	26.69	26.32	26.91
<i>Percentage time the discharge equivalent to the minimum ideal depth is exceeded</i>								
Ideal velocity: Fry and Yearling Parr								
A1B	53.48	51.59	46.63	47.58	26.97	27.47	26.59	27.91
B2	50.91	50.63	47.66	50.17	25.65	25.53	24.85	26.07
A2	50.76	47.02	46.80	47.05	25.87	24.39	24.32	24.92
A2 and B2	50.84	48.83	47.23	48.61	25.76	24.96	24.58	25.50
Ideal velocity: Yearling and older Parr								
A1B	46.09	43.39	42.24	43.51	20.62	20.93	19.78	21.33
B2	44.46	41.92	40.10	41.97	18.72	17.89	17.61	18.17
A2	44.40	39.86	39.44	39.44	19.18	17.65	17.45	17.14
A2 and B2	44.41	40.88	39.82	40.41	18.97	17.82	17.53	17.76

Table 10.5 Results of the habitat modelling conducted using the hydraulic parameters outlined for each life stage. 10.5(i) Percentage of time that flow corresponding to the minimum ideal discharge per metre width (q) is exceeded. 10.5(ii) Percentage of time that flow corresponding to the minimum ideal water depth and Froude number is exceeded. 10.5(iii) Percentage of time that flow corresponding to the minimum ideal water depth and velocity is exceeded. Four different time periods including the control, 2020s, 2050s and 2080s are considered. The results represent the median of the posterior distribution estimated using the MC sampling approach discussed in section 9.3.2. The ensemble weighting scheme outlined in chapter six was used when estimating changes in each parameter.

10.5.2.2 Changes in the availability of ideal spawning habitat

Results for the combined minimum depth and Froude number proposed by Moir *et al.* (2004) are shown in Table 10.5(ii). Both parameters are used as a measure of the habitat available for spawning in each channel under different flow conditions. Figure 10.4 and 10.5 highlight that the study channels from both the Glenamong and Srahrevagh catchments have been used for spawning in the past. Anecdotal evidence suggests that the Goulan sub-catchment (Figure 3.2) is the most heavily used area for spawning in the Burrishoole system. This may be because it is the only sub-catchment with a significant surface water body with which to moderate streamflow throughout the year. In contrast no other sub-catchment possesses surface or groundwater stores of any significance with which to moderate flows in this way. It is likely that salmon would favour spawning reaches which are less vulnerable to fluctuations in streamflow. As shown in Table 10.5(ii), the percentage of time that those flows corresponding to the minimum ideal depth and Froude number are exceeded is greater in the Glenamong. Under future climate forcing it is suggested that the proportion of time for which the minimum spawning requirements are satisfied is likely to decline – albeit that under the A1B scenario a marginal increase over the 2080s is suggested (~2%). Based on projected changes in patterns of flow behaviour, both sites are likely to be less suitable for spawning under future climate. With respect to the months when spawning predominantly occurs, results from the hydrological modelling suggest a decrease in Q50 (Figure 9.20-9.21; 9.28-9.29) for October; however, increases are suggested for November and December. This is commensurate with the results of the hydraulic modelling outlined in Table 10.5.

10.5.2.3 Habitat availability for spawning and juvenile salmon

Table 10.5(iii) shows the proportion of time for which the parameters relating to the ideal minimum velocity and water depth for juvenile salmon are attained in each catchment (Hendry & Cragg-Hine, 1997). Estimated values for velocity and depth suggest that the study reach from the Glenamong is more suitable as a rearing habitat when compared to that from the Srahrevagh. Over the control period flow corresponding to the ideal depth for juvenile salmon is attained 44% of the time; this is in contrast to 25% for the Srahrevagh. The percentage of time that flow fails to satisfy the minimum ideal velocity and depth for salmon fry and older parr is likely to increase

under future climate. This is most evident for the Srahrevagh channel, for which the velocity required for salmon parr (0+, 1+) is suggested to decrease by ~2% over the 2080s. These findings are commensurate with those of the RRV analysis - which is also representative of changes in flow estimated on an annual basis. Under future climate conditions the percentage of time for which the minimum water depth required for spawning is satisfied is likely to decrease – albeit that under A1B scenario, over the 2080s horizon, an increase is suggested. Results relating to the flow velocity required for spawning salmon are not reported as it was found that flow did not fall below the level required to sustain minimum ideal conditions.

10.6 Discussion of Results

The possible impact which projected changes in flow and habitat availability may have on each stage in the life cycle of salmon are explored using the results of both the hydrological and hydraulic modelling. With respect to the hydrological modelling conclusions are drawn based on the median of the MC simulation conducted for each of the three flow indices - the results of which are shown in Figures 9.19 to 9.33.

It is widely acknowledged that spates are important for entry to river systems - particularly during drier years when river flow is much lower. As a result the projected reduction in summer spates (Q05) may act to delay the entry of salmon returning to the Burrishoole system. This has potential consequences for survivorship, recruitment and breeding success in the catchment (Solomon *et al.*, 1999; Solomon & Sambrook, 2004). In addition, the inability to access their home rivers may result in salmon returning to sea or entering alternative river systems. The projected decline in median (Q50) and high flows (Q05) may have the effect of inhibiting the migratory progression of adults to preferred spawning sites in the higher reaches of the catchment. This is supported by the results of the hydraulic modelling which suggest a reduction in the flow required for upstream migration – particularly with respect to ‘peak’ migratory flows.

Any delay in upstream progression may enhance the potential for disease and parasitic transmission to occur between individuals corralled in the lower stream reaches or below obstacles. It also increases their vulnerability to predation and thermal stress. By limiting the degree to which upstream penetration can occur, the suggested increase in lower flows may result in the use of sub-optimal spawning areas. This has implications for recruitment levels and mortality during the alevin stage. In addition the potential

inability of salmon to distribute evenly across the stream network may result in density-dependence during the fry stage having a greater influence on survival and growth. This is supported by the results of the hydraulic modelling which suggest that the percentage of time for which ideal spawning conditions are attained under future climate is likely to decline, suggesting a reduction in the availability of suitable spawning areas across the stream network.

An increase in the seasonality of the flow regime (Q50) suggests that the time when salmon can enter the catchment and migrate upstream may be narrowed, consequently they may advance their time of entry to earlier in the year, in which case they would be exposed to lower summer flows (Q50 and Q05) and higher water temperatures during the months preceding spawning – potentially increasing their exposure to temperatures outside their thermal range. On the other hand salmon may change the time of migration to coincide with higher autumn flows. This may limit their ability to distribute evenly along the stream network and prohibit their progression to spawning areas in higher reaches where more suitable rearing habitats may exist. Indeed as water temperatures increase the ability to access thermal refugia at higher elevations in the catchment is likely to become increasingly important.

High flows (Q05) are projected to increase over the 2050s and 2080s, with the greatest increases being suggested for the months of December (22% under the A2 scenario) and January (16% under the A2 scenario) - both of which are important for spawning and embryonic development. Although high flows are beneficial for flushing silt from spawning gravels and are necessary for channel maintenance, an increase in the magnitude of higher flows may lead to the scouring of redds and the out wash of salmon eggs. In addition the projected increase in high flows may result in the greater mobilization of finer sediment, which has the potential to smother nests and trap alevins in the gravel substrate.

The projected increase in the seasonality of the flow regime suggests that during the fry and parr stage salmon are likely to be exposed to higher winter and lower summer (Q50) flows. In addition their exposure to more extreme high (Q05) and low (Q95) flow conditions is likely to increase. As it is subject to high mortality rates the fry stage is considered a significant ‘mortality bottleneck’, consequently the time of emergence is regarded as being critical for determining the success of year-classes. As embryonic development is dependent on degree-days, it is likely that increased water temperatures would advance the time of emergence, as a result coinciding with higher winter flows.

In addition, given the projected increase in high flows (Q05) during March and April (2080s) – as is suggested by the A1B scenario – it is possible that the period when fry emergence and dispersal occurs will coincide with the occurrence of more hostile flow and habitat conditions. Earlier emergence and increased high flows could thus lead to the more frequent wash-out or displacement of fry, as a result increasing mortality and negatively impacting growth during this critical life stage. Lower summer flows are likely to increase the risk of fry to predation; particularly given that they utilize the shallower waters along the stream margins.

As salmon parr (age 1+) have greater swimming ability they are considered less vulnerable to the direct effects of changes in flow or episodic disturbances of the hydrologic environment. For this life stage the impacts of climate mediated changes in the flow regime are thought to be manifest primarily through alterations in bioenergetics and growth patterns. With respect to this the suggested decrease in summer flows (Q50 and Q05) may lead to increased competition for resources and a reduction in growth during this season. However, increases in flow during autumn and spring (accompanied by increases in the availability of drifting food) may offset this - leading to an overall increase in growth.

The more frequent occurrence of summer drought has the potential to increase mortality and undermine the long-term success of year classes. Increases in Q95 are generally suggested for June to October inclusive, in addition projected reductions are greatest for the Srahrevagh (e.g. A2 scenario over the 2080s -37%) as opposed to the Glenamong (e.g. A2 scenario over the 2080s -18.5%). The results from the hydraulic modelling support the conclusions drawn from the hydrological projections alone. In general the percentage of time for which the ideal water depth for salmon fry and older parr is equalled or exceeded is likely to be reduced under future climate - this is more pronounced for the Srahrevagh when compared to the Glenamong catchment.

Peak spring flows (spates) are a key component of the flow regime as they facilitate - and in some cases provide an environmental cue for - the outward migration of smolts, which generally move downstream on the recession limb of storm events. Results from the hydrological modelling, conducted using the statistically downscaled A2 and B2 scenarios, suggest a decrease in high spring flows (Q05); the greatest reduction in which is associated with April (-28.6% under the A2 scenario over the 2050s) and March (-31.8% under the A2 scenario over the 2050s). A decrease in the median flow (Q50) is also suggested for these months by a number of climate scenarios. Median flows are

important for ensuring the availability of adequate refugia and reducing vulnerability to predation. This suggests that increased losses during outward migration may be incurred as a result of changes in spring flow. In general the results indicate that the high and median spring flows necessary for overcoming obstacles and allowing unimpeded progression to marine waters is likely to be reduced. A change in the flow regime may thus have the effect of narrowing the 'smolt window' - whereby the time of migration coincides with optimal marine conditions. The possibility for this to occur is amplified when climate-mediated changes in the marine environment are considered (e.g. increased sea-surface temperatures, reduced DO). This highlights the importance of flow for facilitating entry to coastal waters within a favourable timeframe. As discussed above the time at which smolts enter coastal waters is critical for post-smolt survival and success during the marine phase.

10.7 Conclusion

Changes in the flow regime and the availability of suitable habitat under future climate forcing are examined with respect to the habitat requirements of Atlantic salmon at different stages in their life cycle. Two constituent sub-catchments of the greater Burrishoole system were considered, and a series of flow indices (Q05, Q50 and Q95) were used to assess changes in their hydrology under projected climate conditions. In addition the RRV criteria were employed to describe each catchment's hydrological response to climate change. The results suggest that a decrease in the annual median flow (Q50) is likely to occur. Model projections also indicate that winter high flows (Q05) are likely to increase, accompanied by which is a decrease in low summer flows (Q95). The results of the RRV analysis also suggests that a reduction in the occurrence (Reliability) and persistence (Resilience) of flows equivalent to the Q50 and Q95 flow thresholds is likely, in addition the vulnerability to low flows (Q95) is suggested to increase.

Hydraulic modelling was used to provide an estimate of available habitat across two 50 metre stream reaches. Based on the results from this, changes in the availability of suitable habitat under future climate conditions were examined. Over the control period the results indicated that the stream reach from the Glenamong is more suitable as a rearing and spawning habitat when compared to the site from the Srahrevagh. Jowett (1997) indicates that small rivers are more 'at risk' to a change in flow than larger rivers

as they require a higher proportion of the average flow to maintain similar levels of habitat protection. The hydraulic modelling suggests that the projected changes in the availability of habitat are of a similar magnitude in both channels; however, the Srahrevagh may be more vulnerable given that habitat availability is comparably lower under 'current' climate. The results of the hydraulic modelling indicate that, for each parameter considered, the percentage of time that ideal habitat conditions may be attained under future climate is likely to decrease. Reductions are generally of a greater magnitude under the more carbon intensive A2 SRES scenario. The greatest decreases for any parameter considered are associated with 'survival' (-9.3%) and migration flows (-6.6%) (q ; $\text{m}^3 \text{s}^{-1} \text{m}^{-1}$) for adult salmon in the Glenamong. The hydrological projections highlight that the flows required for upstream migration (particularly spates) may be significantly reduced – particularly during the months of August and September. This may result in salmon migrating upstream later in the year when flows are suggested to remain conducive to river entry and movement upstream.

Changes in water depth, velocity and the Froude number all suggest that habitat availability may not be reduced significantly during the period when spawning predominantly occurs (October to December); however, the hydrological projections suggest that flow is likely to decrease in October and November, but increase substantially in December, thereby narrowing the window when conditions are favourable for spawning. The percentage of time that the minimum depth and velocity required for age 0+ (underyearlings and fry) and age 1+ salmon parr is attained is projected to decline. A reduction in habitat has implications for inter-specific competition, food availability, growth and access to sheltering habitats – the latter of which is critical for survival during the juvenile phase. Projected changes in the hydrological regime have implications for fry and older parr which may be exposed to more hostile winter (increase in Q05) and summer (decrease in Q95) conditions. It is likely this would have consequences for growth and lead to increases in mortality during this critical life stage. An advance in the time of hatching - resulting from enhanced water temperatures - may expose newly emerged fry to high spring/winter flows, possibly increasing the losses incurred through mechanical shock and involuntary displacement. Furthermore, given the suggested increases in high flows (Q05) during late spring, it is likely that fry will be exposed to more hostile flow conditions during the period preceding emergence.

Higher water temperatures and changes in the flow regime are likely to increase the growth of juvenile salmon, leading to younger, smaller smolts migrating to sea. This has potential implications for post-smolt survival and the number of returning adults – ultimately affecting the productivity of the catchment and altering the population dynamics. Changes in the flow regime may also alter the timing of outward migration; in addition the suggested reduction in spring peak flows may delay the time at which smolts enter coastal waters.

The capacity for flooding events to impact salmonids at all life stages, means an increase in the occurrence of extreme events may potentially result in successive year-classes experiencing significant losses. In this respect adaptation to progressive changes in mean flow conditions (e.g. altering the time of return migration), occurring over successive time horizons, may be of lesser importance for the viability of salmon stocks when considered in the context of more short-term increases in the frequency or magnitude of extreme events.

It is recognized that flow constitutes a single component in the vast interconnected hierarchy of both abiotic and biotic factors which affect salmon populations and determine the local carrying capacity of river systems (Figure 10.2). Consequently one of the shortcomings of this study is that it does not consider climate-mediated changes in other variables, nor does it consider their interaction with changes in the hydrological regime and how this may impact salmon in the catchment. Additionally, it does not seek to quantitatively relate changes in flow to alterations in the population structure or numbers. It may be beneficial in future studies to consider the interaction between different drivers and how they may to impact the population dynamics. The main conclusions of the study as they relate to each life stage are presented below.

Embryonic development and the Alevin stage

- The projected decreases in autumn flows (particularly Q95) are likely to reduce the proportion of time for which ideal spawning conditions occur. In addition lower flows during early autumn may limit spawning activity to later in the season and result in the use of sub-optimal spawning sites.
- The suggested increase in high winter flows may heighten the susceptibility of eggs and larvae to wash-out and mechanical shock.
- Higher flows may also lead to the erosion of spawning gravels and a loss of sheltering habitats.

- The interaction between lower spring/summer flows and higher water temperatures may increase mortality from thermal stress.

Salmon fry

- Changes in flow during the early juvenile phase may be of particular importance given that the period proceeding emergence it is one of the most critical for determining the success of year-classes - particularly given that this stage is already regarded as a critical 'mortality bottleneck'.
- A decrease in flow (Q50) is likely to reduce the percentage of time for which the minimum ideal habitat (depth, velocity) conditions for fry and underyearling parr are attained.
- A reduction in flow has implications for density-dependent survival and the diversity of available (micro-) habitats.
- The timing of emergence is critical and thought to be 'tuned' to avoid the most deleterious flows; thus, a change in the flow regime may result in the synchrony established between the timing of emergence and the occurrence of optimal habitat conditions being disrupted.
- An advance in the timing of emergence - as would be expected given the effect of higher water temperatures on embryonic development - would leave fry exposed to more hostile flow conditions. It is likely this would increase vulnerability to washout and negatively impact growth.
- The projected alterations in flows may lead to a reduction in the availability of resources; this has implications for survival, interspecific competition and the population dynamics of the catchment.
- By reducing access to sheltering habitats the projected decrease in summer flows is likely to increase vulnerability to predation.

Salmon parr

- Their long residency times in freshwater mean salmon parr are exposed to climate mediated changes in the full range (i.e. interannual, interseasonal) of flow and habitat conditions.
- The proportion of time for which the minimum habitat (depth and velocity) conditions required by age 1+ and older parr are attained is likely to be reduced.
- The suggested change in the annual flow regime may increase the vulnerability of salmon parr to wash-out, particularly given the projected increase in high winter flows. Their exposure to the affects of lower summer flows is also likely

to increase. However, their greater size and swimming ability mean they are better placed than younger fry to survive a decrease in available habitat or periodic disturbances of the hydrologic environment.

- The impacts of climate-mediated alterations in flow are likely to be manifest through changes in the dynamics of parr growth (e.g. poor growth associated with summer droughts).
- It is likely an increase in growth would lead to smaller smolts migrating to sea, with potential consequences for post-smolt survival and the number of breeding returns - ultimately undermining the catchment's productivity and altering the population structure.
- The suggested changes in Q05 and Q95 may affect patterns of erosion and deposition; potentially reducing the availability of sheltering habitats which are critical for growth and survival during this life stage.

Smoltification and outward migration

- The projected decrease in spring flows may narrow the 'smolt window' - when the timing of migration coincides with the occurrence of optimal marine conditions.
- The suggested reduction in spates (Q05) and median flows (Q50) may delay the migration of smolts to sea, resulting in the possible loss of smolt characteristics (desmoltification).
- By increasing their exposure to predation and adverse estuarine conditions a delay in outward migration may negatively impact post-smolt survival and subsequent success in the marine environment.
- The projected increase in low spring flows may result in more dispersed smolt runs - leading to an increase in the vulnerability of smolts to predation.

Adult Returns

- The projected decrease in high flows may delay the entry of salmon returning to the catchment, forcing them to return to sea or use other alternative river systems. During dry years a reduction in spates is likely to be of particular importance.
- The suggested decrease in high flows may act as a limiter on the size of individuals which can access the catchment, thereby altering the population dynamics of salmon stocks.

- The reduction in summer flows may result in upstream migration becoming increasingly seasonal, whereby spring runs occur earlier in the year and autumn runs later. In addition it is likely summer runs will become less prevalent.
- Lower summer flows and higher water temperatures are likely to expose adult fish which migrate upstream earlier in the year to more hostile conditions (i.e. higher temperatures, lower flows) prior to spawning.
- The projected decrease in summer flows may limit upstream progression, resulting in the use of sub-optimal spawning areas. Under future climate any impediment to migration is likely to be of particular importance given that it may limit access to thermal refugia in higher reaches of the system.
- Confining returning adults to the lower reaches or below obstacles may increase the potential for disease and parasitic transmission.

Chapter 11

Conclusion

11.1 Introduction

The link between observed changes in the Earth's climate system and anthropogenic emissions of carbon dioxide and other GHGs is now well established - both in the historical record and from model experiments. It is likely that if emissions continue on their current upward trajectory the climate will undergo further changes, with many, possibly unforeseen and long-term consequences for the ecological integrity of riverine ecosystems and their capacity to sustain viable populations of some freshwater and anadromous fish species - including Atlantic salmon (*Salmo salar*) (Walsh & Kilsby, 2007; Adrian *et al.*, 2009; Woodward *et al.*, 2010). Their sensitivity to changing environmental conditions (i.e. cold-adapted species requiring high oxygen environments), and the possibility that climate change may amplify the effects of any current anthropogenic stressors, underlines the importance of exploring the potential impacts of climate change on this ecologically significant species. In an Irish context, this is further underlined by the notable decline in native stocks experienced over the past several decades (Stefansson *et al.*, 2003; Peyronnet *et al.*, 2007).

Recent climate change has been detected in freshwaters primarily through alterations in the thermal regime of river and lake systems - changes in which reflect long-term trends evident in regional air temperatures. Changes in climate have also been detected through the response of various biological indicators; this includes observed changes in the distribution, phenology and abundance of some freshwater biota. In addition, recent climate change has had the effect of altering the structure of freshwater communities - manifest through the localised extinctions of some species and the ingress of other, non-native or exotic taxa. Several studies have provided evidence that warm-adapted species are replacing cold-adapted species in regions at higher latitudes; this is also the case in areas at higher altitudes which historically had provided a thermal niche for more sensitive species (Daufresne *et al.*, 2003; Parmesan, 2006).

As highlighted by Döll and Zhang (2010), the majority of climate impact studies conducted on freshwater ecosystems have focused exclusively on changes in temperature (Millennium Ecosystem Assessment, 2005; Fischlin *et al.*, 2007). Although this parameter is of critical importance, it cannot be considered in isolation as the sole

driver of change in lotic ecosystems. Given the significant influence it has on water quality, resource abundance and the availability/diversity of in-stream habitat, as well as its role in providing refugia, migratory cues and connectivity across freshwater systems, hydrology is as important as water temperature for determining the ecological status of river ecosystems and their long-term capacity to support viable, self-sustaining populations of Atlantic salmon and other salmonid species (Walsh & Kilsby, 2007; Graham & Harrod, 2009).

This study was undertaken with the aim of exploring the potential impacts of climate change on the freshwater habitat of Atlantic salmon - focusing primarily on how changes in hydrology may affect flow conditions and the availability of suitable in-stream habitat at different life stages. The study focused on the Burrishoole catchment, a relatively small but productive catchment system (~90 km²) located on Ireland's west coast. The Burrishoole is regarded as an internationally important 'sentinel' system for monitoring the status of anadromous fish stocks in Ireland and the north Atlantic region. The availability of detailed observational records for a range of environmental and climate variables, along with fish census data and extensive empirical knowledge of the catchment, means it provides an ideal basis for studying the potential impacts of climate change on salmonid species. Although the findings of this study are specific to the Burrishoole catchment, its similarity to many catchment systems found right along Ireland's west coast - in terms of its ecology, hydrology and geomorphological characteristics - means its suggested response to future forcing provides an indication of the impacts climate change is likely to have more generally. Understanding the potential hydrological response is essential when formulating catchment management plans which are robust with respect to the possible impacts of future climate change.

By affecting aspects of their phenology, physiology and life history strategy, as well as by reducing the availability of physical habitat, altering growth patterns and limiting movement across river systems, climate-mediated changes in flow may directly impact the processes of migration, reproduction and recruitment - each of which is critical for the long-term viability of salmon populations in the Burrishoole catchment. Changes in the flow regime may also affect salmon stocks by altering food web-dynamics, disrupting interspecific relationships and impacting those fluvial processes which are critical for the maintenance of in-stream habitat (Gilvear *et al.*, 2002; Walsh & Kilsby, 2007; Jonsson & Jonsson, 2009; Nislow & Armstrong, 2011).

The life history strategy of salmonids has evolved largely in response to, and is attuned with, established patterns of flow behaviour (Bunn & Arthington, 2002). With respect to this, changes in the hydrological regime of river systems may result in a disruption of the evolved synchrony between the occurrence of optimal habitat conditions and the time at which different life stages occur (Tetzlaff *et al.*, 2008). Essentially this would narrow the ‘*window of opportunity*’ during which the primary ecological and physiological requirements of local populations are met (McCormick *et al.*, 1998; Nislow & Armstrong, 2011).

Projected changes in high/low flows are important for the long-term viability of salmon stocks, particularly if changes in their timing of occurrence mean they coincide with those life stages which are already subject to high mortality or which are important for the success of year-classes. Changes in the flow regime which affect these life stages have a greater potential to impact the overall population dynamics and productivity of the catchment (Thorstad *et al.*, 2011). In addition, changes in the flow regime are likely to reduce the level of connectivity across the catchment’s river system and limit periods when water levels are conducive to river entry (Bunn & Arthington, 2002; Jonsson & Jonsson, 2009). Given the potential for extreme events to significantly disrupt ecosystem functions (e.g. scouring of benthic communities, erosion of spawning gravels) and result in high mortalities, the changing nature of extreme events (i.e. frequency, duration and magnitude) under future climate is of particular significance.

By influencing the provision of refugia and food resources, the quantity of in-stream habitat available directly affects the abundance and productivity of salmonid populations (Clews *et al.*, 2010). In general the results of the hydraulic and hydrological modelling indicate that the availability of suitable habitat is likely to be reduced under future climate - suggesting an overall decline in the carrying capacity of the Burrishoole system. This is highlighted by the projected decrease in the annual median flow (Q50) and the suggested reductions in the quantity of habitat available at critical periods during the year (e.g. time of spawning, upstream migration). An increase in the seasonality of the flow regime, along with changes suggested to occur in the timing, frequency and magnitude of both low and high flow events, means that exposure to more hostile flow and habitat conditions is likely to increase. Most significantly changes in the flow regime appear to coincide with those periods which are most important for the success of year-classes - including fry emergence and smolt migration.

Following from the work presented in this thesis a number of conclusions can be drawn as to the likely changes in the catchment hydrology and the impacts this may have on Atlantic salmon. Given the methodological approach adopted, one of the additional outcomes of this study is that it allowed for a wider exploration of uncertainty and the issues associated with developing an ensembles weighting system which could be employed in an impacts assessment. This chapter summarizes the key findings and recommendations from this study; it also highlights areas that could benefit from further research.

11.2 Summary of key findings

Any alterations in long-term patterns of flow behaviour or changes in the variability of habitat conditions are likely to impact the productivity of the Burrishoole catchment and undermine its capacity to nurture viable, self-sustaining populations of Atlantic salmon. It is known that each component in the hydrological regime (e.g. high, mean and low flows) is critical for the completion of different stages in the life history of salmonids. Spates are essential for both upstream and outward migration, whilst flooding events are beneficial for de-silting spawning gravels and contribute to the overall maintenance of the stream network. Low and median flows determine the amount of physical habitat available at any given time and have a significant influence on exposure to predation and the availability of drifting food resources.

For this study two constituent sub-catchments of the greater Burrishoole system were selected for conducting in-depth modelling studies. In order to assess their potential hydrological response to future climate forcing, an ensemble of high resolution climate scenarios was used to drive a series of rainfall-runoff models - each of which was shown to provide a plausible representation of observed system behaviour. The projected changes in hydrology were examined based on the known habitat and flow requirements of Atlantic salmon at key stages in their life cycle (e.g. spawning, migration).

An analysis of air temperature records from the Burrishoole catchment indicate that its climate has warmed significantly over the past several decades (1.48°C increase in mean temperature over the period 1960-2009) (Fealy *et al.*, 2010). Climate projections indicate a continuation of this warming trend, with changes in the catchment's precipitation regime also projected to occur. The ensemble projections suggest that the

catchment is likely to experience warmer and drier summers, and that this will be accompanied by warmer and wetter winters. A lack of convergence between ensemble members means it is much less clear how climate is likely to change during the transition seasons of spring and autumn.

The individual ensemble members generally agree that all seasons are likely to experience an increase in temperature - with increases being most pronounced towards the end of the present century. Projected changes are more acute under the A2 SRES scenario when compared to the less carbon-intensive B2 scenario; however, the ensemble members which suggest the greatest absolute increases are those derived using the UK Met Office's high sensitivity HadCM3 GCM as the driving model. Projected changes in temperature can be summarized as follows:

- Over the 2080s the weighted ensemble average for each SRES scenario suggests an increase in winter (DJF) maximum temperatures of 1.4°C (B2), 1.9°C (A2) and 1.8°C (A1B); for summer (JJA), over the same horizon, an increase of 2.4°C (B2), 2.9°C (A1B) and 3.3°C (A2) is projected.
- The weighted mean ensemble suggests an increase of 1.7°C (B2), 2.2°C (A2) and 2.1°C (A1B) in winter minimum temperature over the 2080s; for the summer season over the same horizon an increase of 2.1°C (B2), 2.4°C (A1B) and 2.8°C (A2) is suggested.
- When each respective ensemble member is considered the dynamically downscaled climate scenario provided by Met Éireann suggests the greatest absolute increase in temperature. In this case the HadCM3 high sensitivity GCM - run under the A1B SRES scenario - was used as the driving model. For the 2080s horizon this ensemble member suggests an increase in autumn minimum and summer maximum temperature of 4.8°C and 5.9°C respectively.
- For all seasons extreme maximum temperatures (90th and 95th percentiles) are projected to increase - as are extreme minimum temperatures.

Although a high degree of inter-model variability exists, the downscaled scenarios generally suggest an increasing tendency towards a more seasonal rainfall regime (i.e. higher winter and lower summer precipitation receipts) - with this trend becoming more pronounced as the century progresses. Heavy precipitation events during winter are likely to increase (90th and 95th percentiles); in addition a number of ensemble members suggest an increase in heavy or extreme rainfall during summer - despite the general

trend for this season being one of a reduction in total receipts. Key changes in the catchment's precipitation regime are summarized below:

- Over the 2080s the weighted ensemble average for each SRES scenario suggests an increase in winter precipitation receipts of 9.1% (B2), 14.5% (A2) and 15.1% (A1B) respectively; for summer (JJA) a decrease of 8.1% (B2), 9.7% (A1B) and 16.9% (A2) is suggested.
- The greatest seasonal decrease in rainfall amounts is associated with the statistically downscaled CGCM2 ensemble member (under the A2 SRES scenario). This scenario suggests a 29% reduction in spring receipts over the 2080s. The greatest increase (+31%) is projected for winter over the same horizon by the dynamically downscaled ensemble member provided by the Swedish Meteorological and Hydrological Institute (SMHI). In this case the Bergen Climate Model, run using the A1B emission scenario was used to provide boundary conditions.

The results of the hydrological modelling generally suggest that the flow regime of both study catchments is likely to become increasingly seasonal in nature, with deviations from reference conditions becoming more pronounced over each successive time horizon. Both catchments exhibit a similar hydrological response to projected changes in climate - underlining the fact that both have relatively similar physical and hydrologic characteristics. By extension, given the uniformity of the Burrishoole catchment, the model projections for each sub-catchment can be considered representative of changes in the hydrology of the Burrishoole system as a whole. Key results from the hydrological modelling can be summarized as follows:

- Over the 2080s the weighted ensemble average for each SRES scenario suggests an increase in the median winter flow (Q50) of 10.5% (B2), 14.6% (A2) and 8.1% (A1B) respectively; for summer (JJA) a decrease in Q50 of 10.7% (B2), 20.2% (A2) and 11.9% (A1B) is suggested.
- The greatest seasonal increase in Q50 is suggested by the statistically downscaled CGCM2 ensemble member (under the A2 scenario); in this case a 30.8% reduction in spring Q50 is suggested for the 2080s horizon. The greatest increase (54.6%) is projected for winter over the same horizon by the dynamically downscaled scenario provided by the SMHI (using the Bergen Climate Model under the A1B SRES scenario).

- The suggested increase in the seasonality of the flow regime is accompanied by a reduction in the percentage of time for which the Q50 flow threshold (estimated over the control period) is reached. It is suggested that by the 2080s, under the A2 scenario, Q50 is likely to be equalled or exceeded only 45% of the time (i.e. Q45).
- Model projections indicate an increase in high winter flows (Q05), with deviations from the control period becoming most pronounced from the 2050s onwards. Generally the ensemble projections suggest a decrease in Q05 during the summer months.
- With respect to low flows (Q95), under the A1B SRES scenario the models suggest a slight reduction in the majority of months over the 2050s; however, for the 2080s low flows are projected to return to a level similar to that experienced over the control period. This is in contrast to the A2 SRES scenario, for which incremental decreases in Q95 over each successive horizon are projected. Generally reductions are greatest during the autumn months; in addition, for all SRES scenarios, an increase in winter Q95 is projected.
- On an annual basis there is a projected decrease in the percentage of time for which the Q95 flow threshold (estimated over the control period) is attained; in addition, the persistence of flows lower than the Q95 threshold is suggested to increase.
- A greater degree of uncertainty is associated with changes in streamflow during the spring and autumn months; however, it is likely that discharge will increase in early spring but decrease later in the season. For the autumn season flows are projected to be lower during September but increase during the months of October and November.

In catchments which have a greater storage potential, higher recharge rates during winter could allow for the maintenance of baseflows during drier periods, thereby moderating the impact of an increasingly seasonal precipitation regime. However, the dearth of any real storage capacity across the Burrishoole system means it does not possess the physical attributes required to mitigate the impacts of an increasingly seasonal rainfall regime. This is illustrated by the projected increase in low flows during the summer/autumn months when baseflow is generally required to sustain river levels. The catchment's flow regime can be characterized as one which is runoff dominated and highly responsive to storm events. This can be attributed to a number of factors including its topography, poor storage capacity and high peat content. The presence of

peatlands is particularly significant given that they are conducive to the rapid transmission of runoff and are considered a source area for flooding (Burt *et al.*, 1990; Holden & Burt, 2003). This highlights the sensitivity of the catchment to an increase in the intensity or occurrence of heavy rainfall events, a fact underlined by the projected increase in high flows - particularly during the wetter winter months. As both study catchments are typical of many catchment systems found along the west coast (i.e. upland, spatey catchments, with a high peat content and poor groundwater potential), the results of the hydrological modelling point to an inherent vulnerability to climate change which is present more generally across the region.

11.3 The potential impacts on Atlantic salmon (*Salmo salar*)

Spawning, embryonic development and the fry stage

The projected decrease in autumn flows is likely to reduce the proportion of time over which the minimum ideal spawning conditions for salmon occur. In addition, the suggested increase in low flows (Q95) during early autumn may limit spawning activity to later in the season and result in the use of sub-optimal spawning areas. Projected decreases in the quantity of habitat available for spawning is likely to result in density-dependence having a greater influence on survival and growth during the period proceeding emergence. The suggested increase in high winter flows (Q05) is likely to enhance the susceptibility of eggs and larvae to wash-out from spawning gravels. Additionally, under higher flows the greater mobilization of larger bed materials is likely to heighten the vulnerability of nests to mechanical shock and result in the scouring/removal of spawning gravels; it may also lead to alevins becoming trapped in interstitial spaces, thereby preventing emergence. Similarly, more intense storm events carry the risk of increased sediment loads and the possible siltation of gravel beds. If gravels become clogged by fine sediment it can have the effect of reducing the flow of oxygen enriched water through salmon redds (Merz *et al.*, 2004).

Changes in the flow regime coinciding with the period during which fry emergence and dispersal occurs are particularly important. This is due to the sensitivity of salmon to changes in flow during this period and its importance for determining year-class success. Indeed this life stage is already considered a critical ‘mortality bottleneck’ (Thorstad *et al.*, 2011). Jensen *et al.* (1991) indicates that the timing of emergence is ‘tuned’ to avoid the most deleterious flows, highlighting how a ‘shift’ in the flow

regime has the potential to expose salmonids to more hostile environmental conditions. The results of the hydrological modelling suggest that high flows are likely to increase during winter and early spring, but decrease relative to the reference period in other seasons. This indicates that under future climate the time of emergence is more likely to coincide with adverse flow conditions (Jensen & Jonsson, 1999) - an outcome which is complicated by an advance in the time of hatching (as would be expected given the affect of higher water temperatures on the rate of embryonic development) (Jonsson & Jonsson, 2009; McGinnity *et al.*, 2009). It is likely this would further reduce the period when favourable flow and habitat conditions coincide with the time of emergence and fry dispersal. This would increase the vulnerability of salmon fry to involuntary displacement and the effects of mechanical stress - with the result that growth and survival during this stage is likely to be adversely affected.

The results of the hydraulic modelling indicate that the proportion of time for which the minimum habitat (depth, velocity) requirements of fry and underyearling parr are attained is likely to be reduced. The projected decrease in summer flows have implications for density-dependent survival and are likely to increase the vulnerability of fry to predation. In addition the more prolonged occurrence of low summer flows is likely to impact survivorship and growth, with long-term implications for the population dynamics of salmon within the catchment. The more frequent occurrence of drought events - as is suggested by model projections – may potentially result in population collapse if successive year-classes were to be affected. This is underlined not just by the direct effects low flows can have on juvenile salmon, but also by the impact they have on the overall ecological integrity of riverine ecosystems and the length of time they require to recover from such disturbances.

Parr and juvenile salmon

The long residence time of juvenile and older salmon parr in freshwaters mean they are exposed to climate-mediated changes in the full range of (inter-seasonal, inter-annual, seasonal extremes, episodic disturbances) flow and habitat conditions (Jonsson & Jonsson, 2009; Armstrong & Nislow, 2011). Their increased size and swimming ability mean parr are better placed than younger juveniles to survive and adapt to short-term disturbances in the hydrologic environment. However, projected changes in the flow regime (i.e. higher winter and lower summer flows) suggest that the vulnerability of

parr to wash-out and involuntary displacement is likely to increase during winter, as is their exposure to the effects of low summer flows (e.g. reduced growth, increased competition, exposure to heat stress and predation). In a study of the impact which drought conditions had on trout (*Salmo trutta*) populations in the UK, Elliott *et al.* (1997) found that a reduction in the density of returning females, and an associated decline in egg production, were linked to the long term effects of 1+ parr being subjected to a prolonged drought event. Similarly Elliott (1994) highlights a causal link between summer droughts, retarded parr growth and the development of smaller smolts. Given the impact which low flows can have on salmon parr, the more frequent occurrence of reduced flow years is likely to have long-term impacts on salmon stocks and recruitment levels in the catchment. The results of the hydraulic modelling suggest a decline in the availability of habitat required by age 1+ and older parr.

The suggested decrease in summer flows is also likely to increase the vulnerability of parr to predation and reduce the availability of sheltering habitats. This is of particular significance given that parr actively seek such habitats, and access to them is critical for determining growth and survival during this life stage (Armstrong & Nislow, 2011). Fealy *et al.* (2010) highlight that under future forcing conditions the number of days for which river water temperatures exceed 22°C is likely to increase. This is the temperature threshold at which salmon cease feeding and seek refuge. Such a change in the thermal regime suggests that sheltering habitats - and thermal refugia in particular - are likely to become increasingly important under future climate.

During the parr stage changes in the flow regime are likely to be manifest primarily through alterations in bioenergetics and changes in the dynamics of fish growth. For example, the projected increase in low summer flows is likely to reduce parr growth (primarily by limiting the abundance of drifting food); in contrast higher winter flows are anticipated to enhance growth potential. On balance it is likely that future changes in the flow regime would contribute to an increase in growth - leading to a larger proportion of smaller smolts migrating to sea (Todd *et al.*, 2011). As smaller smolts are generally understood to have a lower survival potential during the marine phase, increasing growth rates are likely to reduce the number of spawning salmon returning to the catchment. If this were to occur it would diminish recruitment levels and alter the population dynamics of the catchment (Nislow *et al.*, 2000; 2004; Hayes *et al.*, 2007; Davidson *et al.*, 2010).

Smoltification and migration

The projected decrease in spring flows, as is suggested by the majority of ensemble members, may result in a narrowing of the ‘*smolt window*’ - a limited period when the physiological and behavioural conditioning of smolts coincides with optimal marine conditions (McCormick *et al.*, 1998). The projected reduction in flow (particularly spates and median flows) during the latter months of the spring season may impede the downstream progression of smolts and alter the time at which outward migration occurs. Entering coastal waters later in the year exposes smolts to more hostile conditions (e.g. higher water temperatures, reduced DO levels), thereby impacting post-smolt survival rates and reducing the potential for success during the marine phase. This is complicated by projected increases in sea-surface temperatures which are likely to narrow the smolt window even further. This suggests that spring flows are likely to become increasingly important for ensuring smolts enter coastal waters within a favourable timeframe. A spring drought which occurred during 1980 in the Burrishoole catchment provides an indication of the impact which lower spring flows are likely to have on smolt migration. It was found that during this event the migration of both salmon and sea trout smolts was delayed; this had the effect of reducing smolt runs and increasing mortality for that year class (Cross & Piggins, 1980).

A delay in entering coastal waters may also result in ‘de-smoltification’, whereby salmon lose their smolt characteristics and are forced to remain in freshwaters. A reduction in spring flows (and spates in particular) is likely to result in more dispersed smolt runs - leading to an increase in vulnerability to predation (Milner *et al.*, 2010; Todd *et al.*, 2010). Given that spates can act as a migratory cue, wetter springs may induce the earlier migration of smolts to sea. This may also adversely affect the potential for survival in the marine environment (Carlsen *et al.*, 2004).

Adult Returns

The projected increase in the seasonality of the flow regime may result in the timing of river entry and upstream migration being altered, whereby, in order to avoid lower summer flows which impede migration, both spring and autumn runs would become more prevalent (Juanes *et al.* 2004; Todd *et al.*, 2011). For salmon which enter the catchment earlier in the year lower summer flows and higher water temperatures would

expose them to more physiologically stressful conditions in the months prior to spawning (Jonsson & Jonsson, 2009; Todd *et al.*, 2011; Reed *et al.*, 2011).

The projected decrease in high summer flows (Q05) may delay the entry of salmon returning to the catchment, forcing them to either remain in the marine environment or enter alternative catchment systems; consequently significant losses may be incurred in cases where salmon are forced to delay river entry (Solomon & Sambrook, 2004). In addition, lower summer flows may act as a limiter on the size of individuals which can enter the catchment, thereby negatively impacting recruitment and altering the population structure (Jonsson & Jonson, 2009).

Projected decreases in summer flows (and in particular spate events) are likely to impede progression upstream to more favourable spawning and rearing habitats. It is likely this will also limit the distribution of salmon along the catchment's stream network, leading to density-dependence having a greater influence on survival during the fry/parr stage. This is supported by the results of the hydraulic modelling which suggest a decline in the flows - particularly 'peak' migratory flows - required for upstream migration. The more regular occurrence of prolonged low flow periods, which restrict upstream progression to spawning areas, is likely to reduce recruitment success and limit stock productivity in the catchment (Jonsson & Jonsson, 2009). In addition, by reducing upstream penetration, changes in flow are likely to prevent salmon accessing thermal refugia in the uppermost reaches of the catchment. Given the anticipated increases in water temperature, exploiting such habitats is likely to become increasingly important for population success. The projected reduction in summer flows may temporarily confine adults below obstacles and in the lower reaches of the catchment, thereby enhancing the potential for disease and parasitic transmission. This also has the potential to increase exposure to thermal stress, particularly under low flow conditions (Hari *et al.*, 2006).

11.4 Points of discussion and scope for further work

11.4.1 Addressing uncertainty

It is critical that the initial point of departure for impact studies is that their results are sufficiently robust to form a solid foundation for the development of long-term planning and policy decisions. As a result it is of fundamental importance that the uncertainties

arising at each step in the process of translating future socio-economic storylines of human development into climate change impacts at a local scale are addressed. Indeed, there is now an onus on impact modellers to produce probabilistic rather than deterministic projections of future change which actively seek to quantify the various sources of uncertainty and incorporate them constructively in any assessment of the risk climate change poses to human and environmental systems.

As evidenced throughout this study efforts were made to capture as much uncertainty as was possible; however, given the context of the study and the limitations of the datasets/methods employed, there remain critical uncertainties which were not addressed (e.g. natural variability). In relation to this it must be acknowledged that the results of any probabilistic type approach - such as that employed in this study - which is based on sampling the various components of uncertainty must be prefaced with the caveat that their results are strictly conditional on, and are somewhat biased by the uncertainties which are considered.

Based on the contribution which each component in the modelling chain makes to uncertainty in the hydrological response, this study highlighted (Table 9.12) the importance of sampling across right across the uncertainty cascade. Although it did not illustrate what the dominant uncertainties were, it was highlighted that neglecting to address any one component may lead to an underestimation in the full range of uncertainty – potentially altering the final outcome. This study also highlighted that those sources of uncertainty, such as the climate sensitivity and the choice of downscaling RCM (including the use of the same RCMs run by different institutes), which in the past have generally not been (explicitly) considered in impact studies, should be recognized as potentially significant sources of uncertainty. In addition, those studies whose principal aim is to explore the theme of uncertainty and characterise the dominant contributing sources should endeavour to consider these aspects of uncertainty alongside those which are more typically addressed (e.g. choice of emission scenario). Given that this study provided only a superficial account of uncertainty and its potential impact on the projected hydrological response, a possible area for further research would be a more explicit exploration of uncertainty, whereby the contribution each source made to the final results could be quantified.

Access to datasets such as that provided through the ENSEMBLES project (van der Linden & Mitchell, 2009) and the requirement to address uncertainty in impact studies leads onto one of the bigger questions posed by employing climate ensembles - that is at

what point has the uncertainty space been sufficiently sampled, and whether it can be assumed that by considering additional climate scenarios (e.g. GHG emission scenario, different GCM/RCM combinations) or methodological approaches (e.g. downscaling technique) a different outcome would not be arrived at. This is a difficult if not impossible question to answer as it would require that all available climate projections, model combinations, etc. were considered - essentially necessitating an exploration of the entire uncertainty space. As a result it can only be assumed that the climate data and range of modelling techniques used provide an adequate characterisation of uncertainty in the final results.

The assumption that the uncertainty space has been sufficiently characterised can be made more robust by conducting a systematic sampling of all potential uncertainty sources. However, given the limitations of available data and the practical difficulties associated with impacts modelling (e.g. the number of model simulations required), implementing such an approach is an onerous and complex task. A more pragmatic approach may be to focus on sampling those sources of uncertainty which make a greater contribution to the overall uncertainty in the final results (e.g. sampling additional GCMs). With respect to this, conducting a sensitivity analysis could be beneficial when trying to establish what the dominant sources of uncertainty are, and how best to sample them so as to ensure that the uncertainty space is sufficiently characterised - without necessarily having to consider all potential uncertainty sources. Adopting a more strategic approach to sampling uncertainty would therefore allow the modelling process to be streamlined whilst ensuring that the most important aspects of uncertainty were addressed.

In this study one of the areas which would have benefitted from such an approach was the hydrological modelling. With respect to the methodological approach adopted the number of parameter sets considered presented a critical bottleneck (in terms of computing time and data generated) and was one of the impediments to considering natural variability alongside other sources of uncertainty. Conducting a sensitivity analysis may have indicated whether a fewer number of parameter sets would have sufficed in terms of addressing this aspect of uncertainty.

Based on the level of disagreement exhibited between the individual members of the climate ensemble used in this study, and the assessment of uncertainty presented in Table 9.12, it would appear that it is better to err on the side of caution and consider as much uncertainty as is practical to do so. However, based on the discussion above there

are limits to what can be achieved in terms of addressing uncertainty. Furthermore, as came to light during this study, the practical difficulties associated with considering a large number of climate projections means more emphasis needs to be placed on sampling those aspects of uncertainty which have a greater potential to influence the overall study findings. On the basis that larger climate ensembles may be available in future, a more strategic and less *ad hoc* approach to addressing uncertainty may ultimately be more productive when conducting impact assessments - particularly in cases where computing time and financial resources are limited.

11.4.2 The ENSEMBLES dataset

Multi-model ensembles have the advantage of allowing the predictive strength of different climate models to be combined; in addition, their use by impact assessors is important for addressing uncertainty and thus providing a more robust basis for adaptation and planning decisions. In this study a multi-model ensemble compiled as part of the EU funded ENSEMBLES project (van der Linden & Mitchell, 2009) was used. Although the advantages of employing the dataset were highlighted throughout this study, there are a number of deficiencies associated with it which limits its overall usefulness in impact assessments and restricts which aspects of uncertainty it allows the user to explore.

One of the key shortcomings of the dataset is due to the GCM-RCM matrix being incomplete. The absence of some model combinations introduces an element of bias into any probabilistic projections of future change which are derived from it. For example, the disproportionate representation of a particular GCM is likely to skew the results in its favour. In this sense the ensemble does not represent a systematic sampling of the model space. It could be argued that it is more akin to a collection of model pathways - or 'ensemble of opportunity' (Stone *et al.*, 2007) - which are included simply by virtue of their availability rather than because they meet some predefined criteria. The ensemble is also limited by the fact that most ensemble members are based on the A1B SRES scenario. This restricts the potential range of uncertainties which the ensemble can be used to address. Given the difficulties associated with producing such a dataset its limitations are to a certain degree unavoidable; however, attempts should be made to address these shortcomings in any similar studies which are undertaken,

particularly as it would improve the applicability of their output to impact assessments and allow for a more in-depth exploration of uncertainty.

11.4.3 Natural variability and extreme events

One of the shortcomings of this study is it did not consider the influence of natural variability when modelling projected changes in the catchment hydrology. This was due to several factors including the large number of model simulations required and the difficulties in considering the full range of data provided by the ENSEMBLES archive. As it can have the effect of dampening or amplifying the response to anthropogenic climate change, natural variability is an important source of uncertainty and one which should be addressed in hydrological impact studies (Hulme *et al.*, 1999; Arnell, 2003). In addition, contextualizing projected changes based on the range of natural variability - both under current and projected forcing conditions - has been shown to aid in determining whether a clearly defined climate change signal is present (Prudhomme & Davies, 2008a; 2008b).

Considering natural variability may also be beneficial for gauging the potential impacts which changes in the flow regime may have on salmon in the catchment. When assessing the impacts of climate change, natural variability (as determined over the control/baseline period) should provide an indication of the range in habitat and flow conditions for which salmonid populations are locally adapted - thus providing a measure of their potential resilience (through adaptive responses) to future change. Therefore it may be more appropriate to frame projected changes in the flow regime using natural variability. Given the importance of variability, both as a source of uncertainty and as a means for contextualizing the projected hydrological response, it is important that future studies seek to incorporate it.

Floods can cause major disruptions to lotic ecosystems (which may take years to fully recover) and have the potential to impact salmon at all life stages - both directly (e.g. outwash of fry) and indirectly (e.g. scouring of spawning gravels and benthic communities). Anecdotal evidence indicates that the large flooding event which occurred in the Burrishoole catchment on the 2nd of July 2009 (see section 3.3) led to the mobilization and outwash of significant amounts of substrate material; in addition a number of juvenile fish were found washed into traps downstream. Given their capacity to severely disrupt ecosystem functions and degrade in-stream habitats (e.g. filling in

holding pools, changing channel hydraulics) a change in the nature (magnitude, frequency) of flooding events under future forcing may result in significant population losses. If the return period for extreme events were to decrease, it could reduce productivity and limit recruitment levels, thereby inhibiting the recovery of salmon stocks and potentially resulting in population collapse (Jensen *et al.*, 1991; Riley *et al.*, 2009). In this respect the capacity of salmonids to adapt to progressive changes in mean flow conditions may be made redundant by more short-term increases in the frequency of extreme flows. In this study shortcomings in the observed data meant that an assessment of changes in extreme flows could not be undertaken (e.g. extreme value analysis). This relates primarily to the estimation of return periods using flow series of such a short length (~6 years), where higher flows were often under recorded or missing from the series. Given their potential impact, it is important that this aspect of the flow regime is considered when conducting similar studies.

11.4.4 The development and application of a weighting scheme

Whilst employing a multi-model ensemble is now generally regarded as a prerequisite for conducting robust impact studies, the use of performance based weighting systems - whereby a likelihood value is attached to individual ensemble members - is more contentious. This is primarily due to the assumption that the performance of individual models, as determined under present-day climate, remains the same under altered forcing conditions - an assumption which is essentially non-verifiable. Of critical importance when employing a weighting system is providing a robust measure of model skill. This is highlighted as a key potential weakness in weighting schemes, and is complicated by the fact that no universally accepted methodological approach or set of performance criteria exists (Weigel *et al.*, 2010).

It has been shown that the use of performance based weighting systems can bring about an improvement in the overall ensemble skill, and when employed in a climate change context, has the potential to reduce the uncertainty range associated with future projections. Those advocating the use of model weights premise their argument on the fact that a model which performs poorly at simulating current day conditions is also less likely to be reliable when used to model future climate; consequently its contribution to the ensemble should be constrained to reflect this. The counter argument to this is that a model's ability to simulate observed climate may in no way be indicative of its skill

when applied under altered forcing. As a result all models should be treated as being equally plausible, irrespective of how well they simulate present day conditions.

An alternative approach has been proposed whereby poorly performing models are simply omitted from the ensemble (Weigel *et al.*, 2010). As this would reduce the number of models sampled, adopting such an approach may lead to an underestimation of uncertainty. In addition, as with weighting schemes, this approach is predicated on providing an accurate estimate of model skill. It also assumes that a poorly performing model is less reliable than its competitors in all aspects of performance and thus cannot add any value to the overall ensemble. Given the difficulties associated with generating model projections, it may be a more pragmatic approach to include a larger number of models with disparate skill levels, but which may contain the true outcome, rather than to include a smaller number of better performing models which may not (Foley, 2010a; 2010b).

In this study the difficulties associated with formulating a weighting system which could be employed in the context of an impacts study were explored. The weighting scheme used was based on assigning a likelihood value to each respective component in the model pathway (i.e. driving GCM and downscaling RCM independently); in addition a weight was assigned to each individual climate scenario. Adopting this approach ensured error cancellation did not play a role in masking deficiencies in the performance of the driving and downscaling model independent of one another. Throughout this study the benefits of employing a more balanced approach towards the assessment of model skill, using a range of evaluation metrics was highlighted.

A number of issues came to light when developing the weighting scheme used in this study, the first of which was the importance of quantifying each aspect of performance without biasing the final weights. In this case the weights may be skewed if the same aspect of performance is considered multiple times using different metrics. It was found that deconstructing model error into its constituent random and systematic components allowed for greater understanding of model skill. In addition it was shown that basing performance on systematic bias alone is likely to mask shortcomings in a model's ability to capture patterns of variability - thereby providing an incomplete picture of model skill. In this respect it is important that the weighting scheme used is not based solely on this aspect of performance.

In this study the criteria used to assess performance focused primarily on the models ability to simulate temporal patterns of variability in observed precipitation and temperature for the catchment only. Consequently, how well they reproduced spatial patterns of variability in either variable - or indeed other variables - was not considered, nor was their skill at simulating different modes of variability or large-scale patterns of circulation. The failure to address these aspects of performance is recognized as a potential shortcoming; however, given that the catchment was the sole focus of this study an emphasis was placed on how well the models performed at capturing observed climate conditions for it.

Given that the weighting scheme used focused on temporal rather than spatial aspects of performance, the ability of individual models to capture both low and high frequency variations in climate was considered important. The ability of an ensemble member to simulate low-frequency variations is reflective of how well large-scale climate processes are captured. In contrast a model's ability to reproduce high-frequency variations is indicative of how well local-scale forcings are simulated. In this study it was found that the weighting scheme used appeared to add little value over simply taking the unweighted ensemble average. Despite this the argument remains that employing a weighting system is a more defensible approach, which acknowledges that not all models are equally skillful and as a result should not be given the same weighting in the ensemble.

Weighting schemes have the potential to benefit impact assessors, and it could be argued that their application represents the next logical step in addressing uncertainty. In this respect the development of methodological approaches for model weighting has great potential for further research - particularly given that this area is currently the subject of such debate, and that as yet no consensus has been reached regarding what constitutes best practice in this area. The advancement of techniques for evaluating model performance is also a key area for further research, particularly as providing a robust estimate of model skill is likely to be critical for the more widespread acceptance and use of weighting schemes. Whilst previous studies have largely explored the performance of RCMs when driven using reanalysis data, or have applied weighting schemes to produce probabilistic projections based on the output from multiple GCM simulations, it is important that methods for weighting the model pathway as an independent entity are developed (i.e. GCM-RCM model combination).

From the perspective of an impacts assessor the formulation of a weighting system is a difficult task, and the potential to introduce uncertainty to the final results means that providing an accurate assessment of model skill is of critical importance. In this respect it would be beneficial if climate modellers provided information on the skill of the models used to generate climate projections. Providing a measure of how well a model simulates a particular surface variable or captures some aspect of large-scale circulation would provide users with the meta-data required to develop study specific weighting schemes. In future such information would add value to the climate data made available through projects like ENSEMBLES.

11.4.5 Hydrological modelling

In this study it was highlighted that the various uncertainties stemming from the hydrological modelling made a notable contribution to the overall ‘uncertainty cascade’. As a result it was important that they were given due consideration when quantifying uncertainty in the projected hydrological response. Whilst a concerted effort was made throughout this study to address uncertainty, particular aspects of the methodological framework adopted - such as the parameter sampling ranges and threshold value used to identifying behavioural models - necessarily introduced a certain degree of subjectivity to the results. Given that the uncertainty relating to these subjective elements is difficult to quantify, in future studies it is important that efforts are made to remove or redress them. This would require a more in-depth assessment and development of competing methodological approaches, including for example the use of formal Bayesian methods. Although this was beyond the scope of this study, it does offer an opportunity for further research and should be explored as a means of reducing uncertainty.

It is common practice when conducting impact studies to address uncertainty in the model parameters, without recourse to the contribution which uncertainty in the model structure makes. In this study the value of employing a multi-model ensemble was examined. The results indicated that this approach allows for a greater sampling of the uncertainty space - beyond that which can be achieved by altering the model parameters alone - and that this is where the ‘added value’ in its application lies. In addition, employing a multi-model ensemble allows the strengths of competing model structures to be combined, thus providing a more reliable estimate of the potential hydrological response to perturbed forcing. This is in contrast to cases where a single ‘optimum’

model structure is employed. Uncertainty also stems from deficiencies in the observed data used, which may undermine the validity of the parameter values and force distortions in the model set-up. Given its potential to undermine the model reliability, this aspect of uncertainty warrants further study - particularly in relation to how it can be incorporated as part of a wider methodological framework for addressing uncertainty in climate impact studies.

11.4.6 Habitat modelling

The hydraulic rating method used to model changes in habitat availability under altered climate conditions is based on an idealized representation of the channel reaches. As a result the heterogeneity of their shape and structure is not considered, nor is the influence of important in-stream features (e.g. riffle-pool sequence). In addition the model used is only representative of habitat conditions over a relatively small proportion of the actual stream network - albeit that the variability of hydraulic conditions at these points should be indicative of changes in habitat further upstream. As a result the hydraulic rating approach employed only provides an approximate estimate of the actual habitat available under altered flow conditions. Despite its shortcomings this approach does allow for a physically sensible linkage to be made between changes in flow, habitat availability and the physiological requirements of salmon at different life stages.

In this study changes in the channel hydraulics were considered alongside projected alterations in the flow regime. Examining changes in patterns of flow behaviour provided support for the results of the habitat/hydraulic modelling. It also allowed inferences to be drawn regarding the impacts which changes in the flow regime may have at critical stages in the life history of Atlantic salmon. The next logical step in improving the hydraulic rating approach used is to implement a high resolution 2/3-D habitat model (e.g. PHABSIM (Bovee, 1996) or CASiMiR (Jorde *et al.*, 2000; Schneider, 2001)). Such models allow important reach scale geomorphological and fluvial features to be incorporated when examining habitat availability. In addition they have the advantage of utilizing biological information on the target species to estimate the availability of suitable habitat (habitat suitability criteria). A potential area for future research is to explore the applicability of such models to climate impact studies, and

following from this, to determine whether they would add any value over methodological approaches which may be considered less complex.

11.5 Addressing the potential impacts of climate change

Based on the findings of this study there are a number of general aspects to catchment management which are important for reducing the potential impacts of climate change on Atlantic salmon. Firstly, it is important that water quality is protected, particularly as an increase in low flows will amplify the effects of any pollutants originating from point or diffuse sources. Doing so will require limiting industrial discharges and regulating land-use - particularly agricultural practices (e.g. regulating the use of herbicides, pesticides and fertilizers) - more closely. Where necessary it will also require that the capacity of wastewater treatment works is improved and nutrient removal is implemented (i.e. tertiary treatment). Changes in flow are likely to limit connectivity across river systems, thereby reducing access to exploitable resources (e.g. food, thermal refugia, etc) and preferred habitats (e.g. spawning sites, nursery areas). To limit the extent to which this may occur, catchment managers should ensure artificial barriers (e.g. dams, weirs, flood gates, etc.) remain navigable under projected flow conditions. In some cases it may be more beneficial to remove barriers in order to ensure movement remains unimpeded. Greater emphasis will need to be placed on protecting the environmental flows required to maintain ecosystem functions and sustain salmonid stocks. This may be achieved by regulating abstractions, limiting water-transfers and making legal provisions for the protection of resources during periods of environmental stress. Although it is important that flows are managed with the aim of maintaining a minimum level of protection for salmon fisheries (e.g. Q95), greater emphasis will need to be placed on preserving natural flow regimes - both as a means for avoiding habitat loss and safeguarding the integrity of freshwater ecosystems. It is thus essential that the natural flow regime is adopted as the cornerstone for flow management in salmon catchments.

In order to mitigate the most deleterious impacts of climate change catchment managers will need to focus on preserving, and where necessary restoring, those in-stream and bankside features which are important for habitat diversity. Habitats which are important for salmonids include the stream margins and channel substrate; it also includes habitats formed by in-stream features such as gravel bars, riffle/pool sequences

and the channel bank. Additionally, given its role in providing shade, woody debris and food resources, the riparian zone is an important aspect of in-stream habitat (O'Grady, 1993). Riparian vegetation is also critical for preserving the integrity of the stream bank and reducing the potential effects of erosion. Maintaining habitat diversity will thus require management at both the reach (e.g. protection from livestock, preserving riparian vegetation and the removal of non-native riparian species) and catchment scale (e.g. preventing channelization, removing flow regulations and limiting flood protection works). Given that they are of such significance for salmon, it is important that spawning gravels are protected from siltation; thus, activities such as mining and forestry should be limited – the latter of which is of particular relevance to the Burrishoole catchment given its history as a site for commercial forestry.

How salmon stocks are managed in the future will also affect the potential impacts climate change may have. It is important that fishery managers consider how the supplementation of wild populations with hatchery fish may impact the adaptive capacity and the innate resilience of indigenous stocks. The interbreeding of farmed salmon with wild stocks also has the potential to undermine the genetic fitness of indigenous offspring. In this case the cross-breeding of wild and farmed fish may result in the genetic diversity of indigenous populations being reduced; as a result of which their capacity to adapt to environmental changes is likely to be undermined. It is thus important that farmed stocks are managed to ensure that the potential for cross-breeding to occur is minimized. This may be achieved through the implementation of stricter regulations on the salmon farming industry. In addition, stocks will need to be protected from overfishing. This may require more stringent controls on the number of salmon which can be caught; it may also require greater surveillance of inland fisheries and enhanced powers for protection officers.

11.6 Final Conclusion

The principal aim of this study was to explore the potential impacts of climate change on the freshwater habitat of Atlantic salmon in the Burrishoole catchment (~90 km²) - a relatively small but productive system located on Ireland's west coast. Although changes in climate are likely to affect all aspects of riverine systems, this study focused primarily on how the hydrological regime of the catchment is likely to change in

response to altered climate conditions; in addition, changes in the availability of habitat preferred by Atlantic salmon at different life stages were examined.

Model projections suggest that the catchment will become warmer, with wetter winters and drier summers occurring. It is likely this will be accompanied by an increase in the seasonality of its flow regime - manifest in a projected increase in high winter and low summer flows. The impacts which changes in the hydrological regime may have on salmon populations can be broadly characterised as a reduction in the availability of suitable habitat, a loss in connectivity across the catchment system and a disruption to the evolved synchrony between the occurrence of optimal in-stream conditions and the time at which certain life history events occur. Each of these factors is likely to impact the processes of migration, reproduction and recruitment - each of which is critical for the long-term viability of self-sustaining salmon stocks in the catchment.

While Atlantic salmon may be able to adapt to gradual changes in environmental conditions (Mc Ginnitty *et al.*, 2009; Graham & Harrod, 2009) - albeit that changes in the extremes may undermine the long-term viability of some populations - climate change represents an additional pressure on stocks which are already subject to numerous anthropogenic stressors. The results of the hydrological modelling highlight the sensitivity of smaller spatey catchments to changes in climate. Given that the Burrishoole system is typical of many catchments found along Ireland's western seaboard, the results highlight a vulnerability to climate change which is present more generally across the region. This is of particular significance given that many of Ireland's most productive salmon rivers are located along the west coast. It is therefore vital that the study findings are used more generally to inform catchment management and fish stocking strategies where, in order to guard against further population declines and to secure the viability of native stocks, a strong emphasis will need to be placed on mitigating the most deleterious impacts of climate change.

With respect to this catchment management plans will need to consider the potential impact of future climate change, not just in terms of its direct affects on the ecological integrity of freshwater systems, but also in terms of its capacity to amplify the effects of any human-induced pressures (e.g. land use or land-use change, eutrophication, commercial exploitation of stocks, impact of hatchery fish and commercial fish farming) (Fealy *et al.*, 2010). With this in mind, an approach to catchment management based on treating individual river systems as the management unit (Collins *et al.*, 2006), may be more appropriate (Fealy *et al.*, 2010). This would allow the impact of human

stressors unique to a given catchment to be considered alongside the environmental pressures arising from climate change. Adopting such an approach is also sympathetic to the fact that - at the catchment or even reach scale - salmon exist in locally adapted populations; therefore, it may be more appropriate to manage them on a catchment-by-catchment basis as an individual species (Freidland *et al.*, 2009).

Whilst addressing climate change is important in terms of stock management and habitat conservation, it also needs to be considered as part of any restocking or restoration projects undertaken. The long-term success of such projects will in-part depend on the whether the potential impacts of climate change are incorporated from the outset. This is of particular relevance to river systems which are already heavily degraded or have experienced significant declines in productivity.

Despite the potential for climate change to exacerbate the effects of any anthropogenic stressors, both the EU Habitats Directive (Directive 92/43/EEC) and EU Water Framework Directive - two of the most important pieces of EU legislation relating to the conservation and the restoration of freshwater habitats, the former of which makes specific reference to Atlantic salmon - do not explicitly address the additional pressures arising from climate change. As climate change has the capacity to undermine any efforts made to meet the criteria set out in these Directives, it is important that it is given high priority when developing catchment management plans.

One of the most conspicuous means of addressing the potential impacts of climate change is through a reduction in GHG emissions. At an international level the Kyoto Protocol 1997 (United Nations, 1998) established binding targets for reducing global GHG emissions. However, in the national context, no regulatory framework currently exists for achieving the national targets established under the protocol as part of the EU burden-sharing agreement. It is important that at a national level this failing is addressed.

Bibliography

- Abaurrea, J. & Asín, J. (2005) Forecasting local daily precipitation patterns in a climate change scenario. *Climate Research*, 28(3), 183-197.
- Abebe, N.A., Ogden, F.L. & Pradhan, N.R. (2010) Sensitivity and uncertainty analysis of the conceptual HBV rainfall–runoff model: Implications for parameter estimation. *Journal of Hydrology*, 389(3-4), 301-310.
- Adrian, R., Wilhelm, S. & Gerten, D. (2006) Life-history traits of lake plankton species may govern their phenological response to climate warming. *Global Change Biology*, 12(4), 652-661.
- Adrian, R., O'Reilly, C.M., Zagarese, H., Baines, S.B., Hessen, D.O., Keller, W., Livingstone, D.M., Sommaruga, R., Straile, D., Van Donk, E., Weyhenmeyer, G.A., Winder, M. (2009) Lakes as sentinels of climate change. *Limnology and Oceanography*, 54(6), 2283-2297.
- Ahmadi-Nedushan, B., St-Hilaire, A., Bérubé, M., Robichaud, É., Thiémonge, N. & Bobée, B. (2006) A review of statistical methods for the evaluation of aquatic habitat suitability for instream flow assessment. *River Research and Applications*, 22(5), 503-523.
- Ajami, N.K., Duan, Q. & Sorooshian, S. (2006) An Integrated Hydrologic Bayesian Multi-Model Combination Framework: Confronting Input, parameter and model structural uncertainty in Hydrologic Prediction. *Water Resources Research*, 43(1), 1-19.
- Ajami, N.K., Hornberger, G.M. & Sunding, D.L. (2008) Sustainable water resource management under hydrological uncertainty. *Water Resources Research*, 44(11), 1-10.
- Alexander, L.V., Zhang, X., Peterson, T.C., Caesar, J., Gleason, B., Klein Tank, A.M.G., Haylock, M., Collins, D., Trewin, B., Rahimzadeh, F., Tagipour, A., Rupa Kumar, K., Revadekar, J., Griffiths, G., Vincent, L., Stephenson, D.B., Burn, J., Aguilar, E., Brunet, M., Taylor, M., New, M., Zhai, P., Rusticucci, M. & Vazquez-Aguirre, J.L. (2006) Global observed changes in daily climate extremes of temperature and precipitation. *Journal of Geophysical Research*, 111(D5), 1-22.
- Allan, D.J. & Flecker, A.S. (1993) Biodiversity conservation in running waters. *BioScience*, 43(1), 32–43.
- Allan, R.P. & Soden, B.J. (2007) Large discrepancy between observed and simulated precipitation trends in the ascending and descending branches of the tropical circulation. *Geophysical Research Letters*, 34(18), 1-6.
- Allen, M.R., Stott, P.A., Mitchell, J.F.B., Schnur, R. & Delworth, T.L. (2000) Quantifying the uncertainty in forecasts of anthropogenic climate change. *Nature*, 417(6804), 617–620.
- Allen, M.R. & Ingram, W.J. (2002) Constraints on future changes in climate and the hydrologic cycle. *Nature*, 418, 224–232.

- Allen, M.R., Kettleborough, J.A. & Stainforth, D.A. (2003) *Model error in weather and climate forecast*. In: Proceedings of the 2002 European Centre for Medium Range Weather Forecasting, Predictability Seminar. European Centre for Medium Range Weather Forecasting: Reading, UK, 275-294.
- Andersson, L., Samuelsson, P. & Kjellström, E. (2011) Assessment of climate change impact on water resources in the Pungwe river basin. *Tellus A*, 63(1), 138-157.
- Andréassian, V., Perrin, C., Michel, C., Usart-Sanchez, I., & Lavabre, J. (2001) Impact of imperfect rainfall knowledge on the efficiency and the parameters of watershed models. *Journal of Hydrology*, 250(1-4), 206–223.
- Anon. (2005) *Annual Assessment of Salmon Stocks and Fisheries in England and Wales 2004*. Lowestoft: The Centre for Environment, Fisheries and Aquaculture Science, Cardiff: Environment Agency, 82.
- Arabi, M., Govindaraju, R.S., Engel, B., & Hantush, M. (2007) Multiobjective sensitivity analysis of sediment and nitrogen processes with a watershed model. *Water Resources Research*, 43(6), 1-11.
- Arheimer, B. & Brandt, M. (1998) Modelling nitrogen transport and retention in the catchments of southern Sweden. *Ambio*, 27(6), 471-480.
- Armitage, P.D. & Pardo, I. (1997) Impact assessment of regulation at the reach level using macroinvertebrate information from mesohabitats. *Regulated Rivers Research Management*, 10(2-4), 147-158.
- Armstrong, J.D., Braithwaite, V.A & Fox, M. (1998) The response of wild Atlantic salmon parr to acute reductions in water flow. *Journal of Animal Ecology*, 67(2), 203-211.
- Armstrong, J.D., Kemp, P.S., Kennedy, G.J.A., Ladle, M., & Milner, N.J. (2003) Habitat requirements of Atlantic salmon and brown trout in rivers and streams. *Fisheries Research*, 62(2), 143-170.
- Arnell, N. & Reynard, N., (1996) The effects of climate change due to global warming on river flows in Great Britain. *Journal of hydrology*, 183(3-4), 397–424.
- Arnell, N. (1992) Impacts of Climatic Change on River Flow Regimes in the UK. *Water and Environment Journal*, (6)5, 432–442.
- Arnell, N. (1998) Climate change and water resources in Britain. *Climatic Change*, 39(1), 83-110.
- Arnell, N. (1999) The effect of climate change on hydrological regimes in Europe: a continental perspective. *Science*, 9(19), 5-23.
- Arnell, N. (2003) Relative effects of multi-decadal climatic variability and changes in the mean and variability of climate due to global warming: future streamflows in Britain. *Journal of Hydrology*, 270(3-4), 195-213.

- Aronica, G., Hankin, B.G. & Beven, K.J. (1998) Uncertainty and equifinality in calibrating distributed roughness coefficients in a flood propagation model with limited data. *Advances in Water Resources*, 22(4), 349–365.
- Arvola, L., George, G., Livingstone, D., Jarvinen, M., Dokulil, M., Jennings, E., Noges, P., Noges, T. & Weyhenmeyer, G. (2010) The impact of the changing climate on the thermal characteristics of lakes. In: D.G. George ed. (2010) *The Impact of Climate Change on European Lakes*. Aquatic Ecology Series, 4, Springer. 85-101.
- Ashfaq, M., Bowling, L.C., Cherkauer, K., Pal, J.S. & Diffenbaugh N.S. (2010) Influence of climate model biases and dailyscale temperature and precipitation events on hydrological impacts assessment—a case study of the United States. *Journal of Geophysical Research*, 115(D14116), 1-15.
- Band, L.E., Patterson, P. & Nemani, R. (1993) Forest ecosystem processes at the watershed scale: incorporating hillslope hydrology. *Simulation*, 63(1-2), 93-126.
- Bárdossy, A., Stehlík, J. & Caspary, H-J. (2002) Automated objective classification of daily circulation patterns for precipitation and temperature downscaling based on optimized fuzzy rules. *Climate Research*, 23, 11–22
- Bárdossy, A., Bogardi, I. & Matyasovszky, I. (2005) Fuzzy rule-based downscaling of precipitation. *Theoretical and Applied Climatology*, 82(1-2), 119-129.
- Barnett, T.P., Adam, J.C. & Lettenmaier, D.P. (2005) Potential impacts of a warming climate on water availability in snow-dominated regions. *Nature*, 438(7066), 303–309.
- Barnston, A. G. (1992) Correspondence among the correlation, RMSE and Heidke forecast verification measures - Refinement of the Heidke score. *Weather and Forecasting*, 7(4), 699-709.
- Bastidas, L.A., Gupta, H.V., Sorooshian, S., Shuttleworth, W. J. & Yang, Z.L. (1999) Sensitivity analysis of a land surface scheme using multicriteria methods. *Journal of Geophysical Research*, 104(D16), 481-490.
- Bastola, S., Murphy, C. & Sweeney, J. (2011) The role of hydrological modelling uncertainties in climate change impact assessments of Irish river catchments. *Advances in Water Resources*, 34(5), 562-576.
- Bates, B.C., Kundzewicz, Z.W., Wu, S. & Palutikof, J.P., eds. (2008) *Climate Change and Water*. Technical Paper of the Intergovernmental Panel on Climate Change. IPCC Secretariat, Geneva.
- Bathurst, J.C. & O'Connell, P.E. (1992) Future of distributed modelling: the Système Hydrologique Européen. *Hydrological Processes*, 6(3), 265-277.

- Battarbee, R.W., Kernan, M., Livingstone, D., Nickus, U., Verdonshot, P., Hering, D., Moss, B., Wright, R., Evans, C., Grimalt, J., Johnson, R., Maltby, E., Linstead, L. & Skeffington, R. (2008) Freshwater ecosystem responses to climate change: the Euro-limpacs project. In: Quevauviller, P., Borchers, U., Thompson, C. & Simonart, T., eds. (2008) *The Water Framework Directive - Ecological and Chemical Status Monitoring*. London, UK: John Wiley & Sons. 313 - 515.
- Battin, J., Wiley, M.W., Ruckelshaus, M.H., Palmer, R.N., Korb, E., Bartz, K.K. & Imaki, H. (2007) *Projected impacts of climate change on salmon habitat restoration*. Proceedings of the National Academy of Sciences of the United States of America, 104(16), 6720–6725.
- Beaugrand, G. & Reid, P.C. (2003) Long-term changes in phytoplankton, zooplankton and salmon related to climate. *Global Change Biology*, 9(6), 801–817.
- Beaugrand, G. (2005) Monitoring pelagic ecosystems using plankton indicators. *ICES Journal of Marine Science*. 62(3), 333-338.
- Beaugrand, Grégory, Reid, P.C., Ibañez, F., Lindley, J.A., Beaugrand, G., Ibanez, F. & Edwards, M. (2011) Reorganization of Atlantic Copepod Climate Biodiversity. *Science*, 296(5573), 1692-1694.
- Beckmann, B.R. & Buishand, T. (2002) Statistical downscaling relationships for precipitation in the Netherlands and North Germany. *International Journal of Climatology*, 22(1), 15-32.
- Beecher, H.A., Caldwell, B.A. & Demond, S.B. (2002) Evaluation of depth and velocity preferences of juvenile coho salmon in Washington streams. *North American Journal of Fisheries Management*, 22(3), 785–795.
- Beechie, T., Buhle, E., Ruckelshaus, M., Fullerton, A. & Holsinger, L. (2006) Hydrologic regime and the conservation of salmon life history diversity. *Biological Conservation*, 130(4), 560–572.
- Bell, V.A., Kay A.L., Jones R.G. & Moore R.J. (2007) Use of a gridbased hydrological model and regional climate model outputs to assess changing flood risk. *International Journal of Climatology*, 27(12), 1657–1671.
- Bell, J., Duffy, P., Covey, C. & Sloan, L. (2000) Comparison of temperature variability in observations and sixteen climate model simulations. *Geophysical Research Letters*, 27(2), 261–264.
- Benestad, R. (2004) Tentative probabilistic temperature scenarios for northern Europe. *Tellus*, 56(2), 89-101.
- Benestad, R.E. (2001) A comparison between two empirical downscaling strategies. *International Journal of Climatology*, 21(13),1645-1668.
- Benestad, R.E. (2004) Empirical-Statistical Downscaling in Climate Modeling. *EOS Transactions American Geophysical Union*, 85(42), 417.

- Berglund, I., Hansen, L.P., Lundqvist, H., Jonsson, B., Eriksson, T., Thorpe & J.E., Eriksson, L.O. (1991) Effects of Elevated Winter Temperature on Seawater Adaptability, Sexual Rematuration, and Downstream Migratory Behaviour in Mature Male Atlantic Salmon Parr (*Salmo salar*). *Canadian Journal of Fisheries and Aquatic Sciences*, 48(6), 1041-1047.
- Bergström, S. (1976) *Development and application of a conceptual runoff model for Scandinavian catchments*. Report number 7, Swedish Meteorological and Hydrological Institute, Norrköping, Sweden.
- Bergström, S. (1991) Principles and Confidence in Hydrological Modelling, *Nordic Hydrology*, 22(2), 123-136.
- Bergström, S., Harlin, J. & Lindström, G. (1992) Spillway design floods in Sweden: I. New guidelines. *Hydrological Sciences*, 37(5), 505-519
- Bergström, S. (1992) *The HBV Model – its structure and applications*. Report number 4, Swedish Meteorological and Hydrological Institute, Norrköping, Sweden.
- Bergström, S. (1995) The HBV model. In: Singh, V.P., ed. (1995) *Computer models of watershed hydrology*. Littleton, Colorado, USA: Water Resources Publications. 443-476.
- Bergström, S. & Graham, L.P. (1998) On the scale problem in hydrological modelling. *Journal of Hydrology*, 211(1-4), 253-265.
- Bergström, S., Carlsson, B., Gardelin, M., Lindstrom, G., Pettersson, A. & Rummukainen, M. (2001) Climate change impacts on runoff in Sweden—assessments by global climate models, dynamical downscaling and hydrological modelling. *Climate Research*, 16(2), 101–112.
- Berland, G., Nickelsen, T., Heggenes, J., Økland, F., Thorstad, E.B. & Halleraker, J. (2004) Movements of wild Atlantic salmon parr in relation to peaking flows below a hydropower station, *River Research and Applications*, 20(8), 957– 966.
- Beven, K. & Kirkby, M.J. (1979) A physically based, variable contributing area model of basin hydrology. *Hydrological Sciences Journal*, 24(1), 43-69.
- Beven, K. & Wood, E.F. (1983) Catchment Geomorphology and the Dynamics of Runoff Contributing Areas, *Journal of Hydrology*, 65(1-3), 139-158.
- Beven, K. (1984) Infiltration into a class of vertically non-uniform soils. *Hydrological Sciences Journal*, 29(4), 425–434.
- Beven, K., Kirkby, M.J., Schoffield, N. & Tagg, A. (1984) Testing a Physically-based Flood Forecasting Model (TOPMODEL) for Three UK Catchments. *Journal of Hydrology*, 69(1-4), 119-143.
- Beven, K. (1989) Changing ideas in hydrology – The case of physically based models. *Journal of Hydrology*, 105(1-2), 157-172.

- Beven, K. (1993) Prophecy, reality and uncertainty in distributed hydrological modelling. *Advances in Water Resources*, 16(1), 41–51.
- Beven, K., Lamb, R., Quinn, P.F., Romanowicz, R. & Freer, J. (1995) TOPMODEL. In: Singh, V.P., ed. (1995) *Computer models of watershed hydrology*. Littleton, Colorado, USA: Water Resources Publications. 627-668.
- Beven, K. (1997a) TOPMODEL: a critique. *Hydrological Processes*, 11(9), 1069–1085.
- Beven, K., eds. (1997b) *Distributed modelling in hydrology: Applications of the TOPMODEL concepts*. UK: Wiley.
- Beven, K. (2001a) How far can we go in distributed hydrological modelling? *Hydrological Processes*, 5(1), 1-12.
- Beven, K. (2001b) Rainfall-runoff modelling-the primer. UK: Wiley.
- Beven, K. & Freer, J. (2001a) Equifinality, data assimilation, and uncertainty estimation in mechanistic modelling of complex environmental systems using the GLUE methodology. *Journal of Hydrology*, 249(1-4), 11-29.
- Beven, K. & Freer, J. (2001b) A dynamic TOPMODEL. *Hydrological Processes*, 15(10), 1993-2011.
- Beven, K. (2002). Towards a coherent philosophy for modelling the environment. *Proceedings of the Royal Society A: Mathematical, Physical and Engineering Sciences*, 458(2026), 2465-2484.
- Beven, K. (2006a) A manifesto for the equifinality thesis. *Journal of Hydrology*, 320(1-2), 18-36.
- Beven, K. (2006b) On undermining the science? *Hydrological Processes*, 20(14), 3141-3146.
- Beven, K. Smith, P. & Freer, J. (2008) So just why would a modeller choose to be incoherent? *Journal of Hydrology*, 354(1-4), 15-32.
- Beven, K. (2008a) On doing better hydrological science. *Hydrological Processes*, 22(17), 3549-3553.
- Beven, K. & Westerberg, I. (2011) On red herrings and real herrings: disinformation and information in hydrological inference. *Hydrological Processes*, 25(10), 1676-1680.
- Bjorn, T.C. & Reiser, D.W. (1991) *Habitat requirements of salmonids in streams*. In: Meehan, W.R., ed. (1991) *Influences of forest management on salmonid fishes & their habitats*. Bethesda, Maryland, USA. American Fisheries Society Special Publication 19. 83–138.
- Blasone, R., Vrugt, J., Madsen, H., Rosbjerg, D., Robinson, B. & Zyvoloski, G. (2008a) Generalized likelihood uncertainty estimation (GLUE) using adaptive Markov Chain Monte Carlo sampling. *Advances in Water Resources*, 31(4), 630-648.

- Blasone, R., Madsen, H. & Rosbjerg, D. (2008b) Uncertainty assessment of integrated distributed hydrological models using GLUE with Markov chain Monte Carlo sampling. *Journal of Hydrology*, 353(1-2), 18-32.
- Blazkova, S. & Beven, K. (2009) A limits of acceptability approach to model evaluation and uncertainty estimation in flood frequency estimation by continuous simulation: Skalka catchment, Czech Republic. *Water Resources Research*, 45(W00B16), 1-12.
- Blazkova, S. & Beven, K. (2004) Use of distributed data to reduce uncertainty in flood runoff predictions. [Online] 1-11. Available at: http://www.actif-ec.net/Workshop2/papers/ACTIF_S3_02.pdf (accessed 1st February 2011).
- Block, P., Filho, F., Sun, L., & Kwon, H. (2009) A streamflow forecasting framework using multiple climate and hydrological models. *Journal of the American Water Resources Association*, 45(4), 828–843.
- Boé, J., A. Hall, & Qu, X. (2009) September sea-ice cover in the Arctic Ocean projected to vanish by 2100. *Nature Geoscience*, 2(5), 341–343.
- Boé, J., Terray, L., Habets, F. & Martin, E. (2007) Statistical and dynamical downscaling of the Seine basin climate for hydro-meteorological studies. *International Journal of Climatology*, 27(12), 1643-1655.
- Böhm, U., Kücken, M., Ahrens, W., Block, A., Hauffe, D., Keuler, K., Rockel, B. & Will, A. (2006) CLM—the climate version of LM: brief description and long-term applications. *COSMO newsletter No. 6*, German Weather Service. 225-235.
- Booij, M. (2005) Impact of climate change on river flooding assessed with different spatial model resolutions. *Journal of Hydrology*, 303(1-4), 176-198.
- Bourgeois, G., Cunjak, R.A., Caissie, D. & El-Jabi, N. (1996) A spatial and temporal evaluation of PHABSIM in relation to measured density of juvenile Atlantic salmon in a small stream. *North American Journal of Fisheries Management*, 16(1), 154-166.
- Bovee, K.D. (1982) *A Guide to Stream Habitat Analysis Using the Instream Flow Incremental Methodology*. Instream Flow Information Paper 21, Washington D.C., U.S.A: Department of Fisheries and Wildlife Services.
- Bowen, Z.H., Bovee, K.D. & Waddle, T.J. (2003) Effects of flow regulation on shallowwater habitat dynamics and floodplain connectivity. *Transactions of the American Fisheries Society*, 132(4), 809–823.
- Boyer, C., Chaumont, D., Chartier, I. & Roy, A.G. (2010) Impact of climate change on the hydrology of St. Lawrence tributaries. *Journal of Hydrology*, 384(1-2), 65-83.
- Brandsma, T., 1995. Hydrological impact of climate change, a sensitivity study for the Netherlands. Unpublished PhD thesis, Delft University of Technology.
- Brandt, M., Bergström, S. & Gardelin, M. (1988) Modelling the effects of clearcutting on runoff - Examples from Central Sweden. *AMBIO*, 17(5), 307–313.

- Brekke, L.D., Dettinger, M.D., Maurer, E.P. & Anderson, M. (2008) Significance of model credibility in estimating climate projection distributions for regional hydroclimatological risk assessments. *Climatic Change*, 89(3-4), 371–394.
- Brinkmann, W.A.R. (1999) Within-type variability of 700 hPa winter circulation patterns over the Lake Superior basin. *International Journal of Climatology*, 19(1), 41–58.
- Brinkmann, W.A.R. (2000) Modification of a correlation-based circulation pattern classification to reduce within-type variability of temperature and precipitation. *International Journal of Climatology*, 20(8), 839–852.
- Brinkmann, W.A.R. (2002) Local versus remote grid points in climate downscaling. *Climate Research*, 21, 27–42.
- Bristow, K.L. & Campbell, G.S. (1984) On the relationship between incoming solar radiation and daily maximum and minimum temperature. *Agricultural and Forest Meteorology*, 31(2), 159-166.
- Brockwell, P.J. & Davis, R.A. (1991) *Time Series: Theory and Method*. 2nd ed. New York, USA: Springer-Verlag.
- Bronstert, A. (2004) Rainfall-runoff modelling for assessing impacts of climate and land-use change. *Hydrological Processes*, 18(3), 567-570.
- Brown, P.J. & Zidek, J.V. (1980) Adaptive multivariate ridge regression. *Annals of Statistics*, 8(1), 64–74.
- Brunetti, M., Colacino, M., Maugeri, M., & Nanni, T. (2001) Trends in the daily intensity of precipitation in Italy from 1951 to 1996. *International Journal of Climatology*, 21(3), 299-316.
- Bürger, G. (1996) Expanded downscaling for generating local weather scenarios. *Climate Research*, 7(2), 111–128.
- Bürger, G. (2002) Selected precipitation scenarios across Europe. *Journal of Hydrology*, 262(1–4), 99–110.
- Buffoni, L., Maugeri, M. & Nanni, T. (1999) Precipitation in Italy from 1833 to 1996. *Theoretical and Applied Climatology*, 63(1-2), 33–40.
- Buishand, T.A. (1978) Some remarks on the use of daily rainfall models. *Journal of Hydrology*, 36(3-4), 295–308.
- Buishand, T.A., Shabalova, M.V. & Brandsma, T. (2004) On the choice of the temporal aggregation level for statistical downscaling of precipitation. *Journal of Climate*, 17(9), 1816–1827.
- Bultot, F. & Gellens, D. (1994) Effects of climate change on snow accumulation and melting in the Broye catchment (Switzerland). *Climatic change*, 28(4), 339-363.

- Bultot, F., Dupriez, G.L. & Gellens, D. (1988) Estimated Regime of Energy-Balance Components, Evapotranspiration and Soil Moisture for a Drainage Basin the Case of a CO₂ Doubling. *Climatic Change*, 2(10), 39–56.
- Burgmer, T., Hillebrand, H. & Pfenninger, M. (2007) Effects of climate-driven temperature changes on the diversity of freshwater macroinvertebrates. *Oecologia*, 151(1), 93–103.
- Burkett, V.R., Wilcox, D. A., Stottlemeyer, R., Barrow, W., Fagre, D., Baron, J., Price, J., Nielsen, J.L., Allen, C.D., Peterson, D.L., Ruggerone, G. & Doyle, T. (2005) Nonlinear dynamics in ecosystem response to climatic change: Case studies and policy implications. *Ecological Complexity*, 2(4), 357-394.
- Burnash, R.J. Ferral, R.L. & McGuire, R.A. (1973) *A generalized streamflow simulation system conceptual modeling for digital computers*. California, USA: Joint Federal and State River Forecast Center, U.S. National Weather Service and California Department of Water Resources.
- Burt, T.P., Heathwaite, A.L. & Labadz, J.C. (1990) Runoff production in peat-covered catchments. In: Anderson, M.G. & Burt, T.P., eds. (1990) *Process Studies in Hillslope Hydrology*. UK: Wiley. 463-500.
- Burton, A., Kilsby, G.C., Fowler, H.J., Cowpertwait, P.S.P., O'Connell, P.E. (2008) RainSim: A spatial–temporal stochastic rainfall modelling system. *Environmental Modelling and Software*, 23(12), 1356-1369.
- Burton, A., Fowler, H.J., Blenkinsop, S. & Kilsby, C.G. (2010) Downscaling transient climate change using a Neyman–Scott Rectangular Pulses stochastic rainfall model. *Journal of Hydrology*, 381(1-2), 18-32.
- Buser, C.M., Künsch, H.R., Lüthi, D., Wild, M. & Schär, C. (2009) Bayesian multi-model projection of climate: bias assumptions and interannual variability. *Climate Dynamics*, 33(6), 849-868.
- Butts, M., Payne, J., Kristensen, M. & Madsen, H. (2004) An evaluation of the impact of model structure on hydrological modelling uncertainty for streamflow simulation. *Journal of Hydrology*, 298(1-4), 242-266.
- Buytaert, W. (2011) Implementation of the hydrological model TOPMODEL in R. [Online]. Available at: <http://cran.r-project.org/web/packages/topmodel/index.html> (accessed 10th October 2011).
- Byrne, C.J., Poole, R., Dillane, M., Rogan, G. & Whelan, K.F. (2004) Temporal and environmental influences on the variation in sea trout (*Salmo trutta*) smolt migration in the Burrishoole system in the west of Ireland from 1971 to 2000. *Fisheries Research*, 66(1), 85–94.
- Caissie, D. & El-Jabi, N. (2003) Instream flow assessment: from holistic approaches to habitat modelling. *Canadian Water Resources Journal*, 28(2), 173–183.
- Caldeira, K., Jain, A.K. & Hoffert, M.I. (2003) Climate Sensitivity Uncertainty and the need for Energy Without CO₂ Emission. *Science*, 299(March), 2052-2054.

- Cameron, D.S., Beven, K.J., Tawn, J., Blazkova, S. & Naden, P. (1999) Flood frequency estimation by continuous simulation for a gauged upland catchment (with uncertainty). *Journal of Hydrology*, 219(3-4), 169-187.
- Cameron, D.S. (2006) An application of the UKCIP02 climate change scenarios to flood estimation by continuous simulation for a gauged catchment in the northeast of Scotland, UK (with uncertainty). *Journal of Hydrology*, 328(1-2), 212-226.
- Cannon, A.J. (2009) Negative ridge regression parameters for improving the covariance structure of multivariate linear downscaling models. *International Journal of Climatology*, 29(5), 761-769.
- Carlsen, K.T., Berg, O.K., Finstad, B. & Heggberget, T.G. (2004) Diel periodicity and environmental influence on the smolt migration of Arctic charr, *Salvelinus alpinus*, Atlantic salmon, *Salmo salar*, and brown trout, *Salmo trutta*, in northern Norway. *Environmental Biology of Fishes*, 70(4), 403-413.
- Casati, B., Wilson, L.J., Stephenson, D.B., Nurmi, P., Ghelli, A., Pocerich, M., Damrath, U., Ebert, E.E., Brown, B.G. & Mason, S. (2008) Forecast verification: current status and future directions. *Meteorological Applications*, 15(1), 3-18.
- Cavazos, T. & Hewitson, B.C. (2005) Performance of NCEP-NCAR reanalysis variables in statistical downscaling of daily precipitation. *Climate Research*, 28(16), 95-107.
- Chandler, R.E. (2002) *GLIMCLIM: Generalised Linear Modelling for Daily Climate Series (Software and User Guide)*. Department of Statistical Science, University College London
- Chandler, R.E. & Wheeler, H.S. (2002a) Analysis of rainfall variability using Generalized Linear Models — a case study from the West of Ireland. *Water Resources Research*, 38(10), 674- 689.
- Chandler, R.E. & Wheeler, H.S. (2002b) Analysis of rainfall variability using generalized linear models: A case study from the west of Ireland. *Water Resources Research*, 38(10), 674-689.
- Chandler, R.E. (2005) On the use of generalized linear models for interpreting climate variability. *Environmetrics*, 16(7), 699-715.
- Chang, H.J. & Jung, I.W. (2010) Spatial and temporal changes in runoff caused by climate change in a complex large river basin in Oregon. *Journal of Hydrology*, 388(3-4), 186-207.
- Charles, S.P., Bates, B.C., Whetton, P.H. & Hughes, J.P. (1999) Validation of a downscaling model for changed climate conditions: case study of southwestern Australia. *Climate Research*, 12(1), 1-14.
- Charles, S.P., Bates, B.C, Smith, I.N. & Hughes, J.P. (2004) Statistical downscaling of daily precipitation from observed and modelled atmospheric fields. *Hydrological Processes*, 18(8), 1373-1394.

- Charlton, R. & Moore, S. (2003) *The Impact of Climate Change on Water Resources in Ireland*. In: Sweeney, J. *et al.* eds. (2003) *Climate Change: Scenarios and Impacts for Ireland*. ERTDI Report Series No. 15, Environmental Protection Agency, Johnstown Castle, Wexford, Ireland. 81-102.
- Chen, H., Guo, J., Xiong, W., Guo, S.L. & Xu, C.Y. (2010) Downscaling GCMs using the Smooth Support Vector Machine method to predict daily precipitation in the Hanjiang Basin. *Advances in Atmospheric Sciences*, 27(2), 274-284.
- Chen, J., Brissette, F.P. & Leconte, R. (2011) Uncertainty of downscaling method in quantifying the impact of climate change on hydrology. *Journal of Hydrology*, 401(3-4), 190-202.
- Chiew, F.H.S., Kirono, D.G.C., Kent, D.M., Frost, A.J., Charles, S.P., Timbal, B., Nguyen, K.C. & Fu., G. (2010) Comparison of runoff modelled using rainfall from different downscaling methods for historical and future climates. *Journal of Hydrology*, 387(1-2), 10-23.
- Choi, H. & Beven, K. (2007) Multi-period and multi-criteria model conditioning to reduce prediction uncertainty in an application of TOPMODEL within the GLUE framework. *Journal of Hydrology*, 332(3-4), 316-336.
- Christensen, J.H. & Christensen, O.B. (2003) Climate Modelling: Severe summertime flooding in Europe. *Nature*, 421(February), 2002-2003.
- Christensen, O.B., Drews, M., Christensen, J.H., Dethloff, K., Ketelsen, K., Hebestadt, I., Rinke, A. (2006) *The HIRHAM Regional Climate Model Version 5 (β)*. Technical report 06-17. Copenhagen, Denmark: Danish Meteorological Institute. 1399-1388.
- Christensen, J.H., Hewitson, B., Busuioc, A., Chen, A., Gao, X., *et al.* (2007b). Regional climate projections. In: Solomon, S., Qin, D., Manning, M., Chen, Z., Marquis M., *et al.*, eds. (2007a) *Climate Change 2007: The Physical Science Basis. Contribution of Working Group I to the Fourth Assessment Report of the Intergovernmental Panel on Climate Change*. Cambridge, UK & New York, NY, USA: Cambridge University Press.
- Christensen, J.H., Carter, T.R. & Rummukainen, M. (2007b) Evaluating the performance and utility of regional climate models: the PRUDENCE project. *Climate Change*, 81(S1), 1-6.
- Christensen, J.H., Boberg, F., Christensen, O. & Lucas-Picher, P. (2008) On the need for bias correction of regional climate change projections of temperature and precipitation. *Geophysical Research Letters*, 35(20), L20709.
- Christensen, J.H., Kjellström, E., Giorgi, F., Lenderink, G. & Rummukainen, M. (2010) Weight assignment in regional climate models. *Climate Research*, 44(2-3), 179-194.
- Christensen, S. (2004) A synthetic groundwater modeling study of the accuracy of GLUE uncertainty intervals. *Nordic Hydrology*, 35(1), 45-59.

- Chu, J.L. & Yu, P.S. (2010) A study of the impact of climate change on local precipitation using statistical downscaling. *Journal of Geophysical Research*, 115(D10), D10105.
- Church, J.A. & White, N.J. (2006) A 20th century acceleration in global sea level rise. *Geophysical Research Letters*, 33(1), 94-97.
- Clews, E., Durance, I., Vaughan, I.P. & Ormerod, S.J. (2010) Juvenile salmonid populations in a temperate river system track synoptic trends in climate. *Global Change Biology*, 16(12), 3271-3283.
- Cloke, H.L., Jeffers, C., Wetterhall, F., Byrne, T., Lowe, J. & Pappenberger, F. (2010) Climate impacts on river flow: projections for the Medway catchment, UK, with UKCP09 and CATCHMOD. *Hydrological Processes*, 24(24), 3476-3489.
- Coats, R., Perez-Losada, J., Schladow, G., Richards, R. & Goldman, C. (2006) The Warming of Lake Tahoe. *Climatic Change*, 76(1-2), 121-148.
- Coe, R. & Stern R.D. (1982) Fitting models to daily rainfall data. *Journal of Applied Meteorology*, 21(7), 1024-1031.
- Collins, M., Booth, B.B., Harris, G.R., Murphy, J.M., Sexton, D.M.H. & Webb, M.J. (2006) Towards quantifying uncertainty in transient climate change. *Climate Dynamics*, 27(2-3), 127-147.
- Collins, M. (2007) Ensembles and probabilities: a new era in the prediction of climate change. *Philosophical transactions. Series A, Mathematical, physical, and engineering sciences*, 365(1857), 1957-1970.
- Collins, M., Booth, B.B., Bhaskaran, B., Harris, G.R., Murphy, J.M., Sexton, D.M.H. & Webb, M.J. (2010) Climate model errors, feedbacks and forcings: a comparison of perturbed physics and multi-model ensembles. *Climate Dynamics*, 36(9-10), 1737-1766.
- Conway, D., Wilby, R.L. & Jones, P.D. (1996) Precipitation and air flow indices over the British Isles. *Climate Research*, 7(1-4), 169-183.
- Cooter, E.J. & Leduc, S.K. (1995) Recent frost date trends in the north-eastern USA. *International Journal of Climatology*, 15(1), 65-75.
- Coppola, E., Giorgi, F., Rauscher, S. & Piani, C. (2010) Model weighting based on mesoscale structures in precipitation and temperature in an ensemble of regional climate models. *Climate Research*, 44(2-3), 121-134.
- Corte-Real, J., Zhang, X. & Wangm, X. (1995) Downscaling GCM information to regional scales: a non-parametric multivariate regression approach. *Climate Dynamics*, 11(7), 413-424.
- Corte-Real, J., Qian, B. & Xu, H. (1998) Regional climate change in Portugal: precipitation variability associated with largescale atmospheric circulation. *International Journal of Climatology*, 635(6), 619-635.

- Corte-Real, J. & Hu, H. (1999) A weather generator for obtaining daily precipitation scenarios based on circulation patterns. *Climate Research*, 13, 61-75.
- CORINE (2003) CORINE Land Cover database, M. Krynitz, European Topic Center on Land Cove (ETC/LC).
- Côté, J., Gravel, S., Methot, A., Patoine, A., Roch, M. & Staniforth, A. (1998) The operational CMC/MRB Global Environmental Multiscale (GEM) model. I. design considerations and formulation. *Monthly Weather Review*, 126(6), 1373–1395.
- Cox, C.B. & Moore, P.D. (1993) *Biogeography: An Ecological and Evolutionary Approach*. 5th edition. Oxford, UK: Blackwell Science.
- Cox, P.M., Betts, R.A., Jones, C.D., Spall, S.A. & Totterdell, I.J. (2000) Acceleration of global warming due to carbon-cycle feedbacks in a coupled climate model. *Nature*, 408(November), 184-187.
- Cox, P. & Stephenson, D. (2007) Climate change: A changing climate for prediction. *Science*, 317(5835), 207– 208.
- Crane, R.G. & Hewiston, B.C. (1998) Doubled CO₂ precipitation changes for the Susquehanna Basin: down-scaling from the Genesis general circulation model. *International Journal of Climatology*, 18(1), 65-76.
- Crawford, N.H. & Linsley, R.K. (1966) *Digital simulation in hydrology, Standford watershed model IV*. Technical Report number 39, Department Civil Engineering, Standford University, USA.
- Crisp, D.T. (1981) A desk study of the relationship between temperature and hatching time for the eggs of five species of salmonid fishes. *Freshwater Biology*, 11(4), 361–368.
- Crisp, D.T. (1989) Use of artificial eggs in studies of washout depth and drift distance for salmonid eggs. *Hydrobiologia*, 178(2), 155-163.
- Crisp, D.T. (1993) The environmental requirements of salmon and trout in fresh water. *Freshwater Forum*, 3(3), 176– 202.
- Crisp, D.T. (1996) Environmental requirements of common riverine European salmonid fish species in fresh water with particular reference to physical and chemical aspects. *Hydrobiologia*, 323(3), 201-221.
- Crisp, D.T. (2000) *Trout and Salmon Ecology Conservation and Rehabilitation*. Oxford, UK: Blackwell Science.
- Cross, T.F. & Piggins, D.J. (1982) The effect of abnormal climate conditions on the smolt run of 1980 and subsequent returns of Atlantic salmon and sea trout. ICES CM:M26:8.
- Cubasch, U., Von Storch, H., Waszkewitz, J. & Zorita, E. (1996) Estimates of climate change in Southern Europe derived from dynamical climate model output. *Climate Research*, 7(2), 129–149.

- Cunjak, R.A., Prowse, T.D. & Parrish, D.L. (1998) Atlantic salmon in winter: “the season of parr discontent”? *Canadian Journal of Fisheries and Aquatic Sciences*, 55(S1), 161–180.
- Dai, A., Fung, I.Y. & Del Genio, A.D. (1997) Surface observed global land precipitation variations during 1900-88. *Journal of Climate*, 10(11), 2943–2962.
- Dai, A., Karl, T.R., Sun, B. & Trenberth, K.E. (2006) Recent Trends in Cloudiness over the United States: A Tale of Monitoring Inadequacies. *Bulletin of the American Meteorological Society*, 87(5), 597-606.
- Dankers, R. & Feyen, L. (2008) Climate change impact on flood hazard in Europe: An assessment based on high-resolution climate simulations. *Journal of Geophysical Research*, 113(D19105), 1-17.
- Das, T., Bardossy, A, Zehe, E., & He, Y. (2008) Comparison of conceptual model performance using different representations of spatial variability. *Journal of Hydrology*, 356(1-2), 106-118.
- Daufresne, M., Roger, M.C., Capra, H. & Lamouroux, N. (2004) Long-term changes within the invertebrate and fish communities of the Upper Rhône River: effects of climatic factors. *Global Change Biology*, 10(1), 124-140.
- Davidson, I.C. & Hazlewood, M.S. (2005) *Effect of Climate Change on Salmon Fisheries*. Science Report: W2-047/SR. Environment Agency, Bristol, UK.
- Davidson, R.S., Letcher, B.H. & Nislow, K.H. (2010) Drivers of growth variation in juvenile Atlantic salmon (*Salmo salar*): an elasticity analysis approach. *The Journal of animal ecology*, 79(5), 1113-1121.
- Dehn, M. & Buma, J. (1998) A method for predicting the impact of climate change on slope stability. *Environmental Geology*, 35(2-3), 190-196.
- Dehn, M. & Buma, J. (1999) Modelling future landslide activity based on general circulation models. *Geomorphology*, 30(2-3), 175–187.
- DelGenio, A.D., Lacis, A.A. & Ruedy, R.A. (1991) Simulations of the effect of a warmer climate on atmospheric humidity. *Nature*, 351(6325), 382–385.
- Déqué, M., Rowell, D.P., Lüthi, D., Giorgi, F., Christensen, J.H., Rockel, B., Jacob, D., Kjellström, E., de Castro, M. & van den Hurk, B. (2007) An intercomparison of regional climate simulations for Europe: assessing uncertainties in model projections. *Climatic Change*, 81(S1), 53-70.
- Déqué, M. (2009) *Temperature and precipitation probability density functions in ENSEMBLES regional scenarios*. ENSEMBLES Technical Report 5. Meteorological Office Hadley Centre, Exeter, UK.
- Déqué, M. & Somot, S. (2010) Weighted frequency distributions express modelling uncertainties in the ENSEMBLES regional climate experiments. *Climate Research*, 44 (2-3), 195-209.

- Déry, S.J., Hernández-Henríquez, M.A., Burford, J.E. & Wood, E.F. (2009) Observational evidence of an intensifying hydrological cycle in northern Canada. *Geophysical Research Letters*, 36(13), 1-5.
- Dessai, S., O'Brien, K. & Hulme, M. (2007) Editorial: On uncertainty and climate change. *Global Environmental Change*, 17(1), 1-3.
- Dettinger, M.D., Mo, K., Cayan, D.R. & Jeton, A.E. (1999) *Global to local scale simulations of streamflow in the Merced, American, and Carson Rivers, Sierra Nevada, California*. Preprints, American Meteorological Society's, 14th Conference Hydrology. Dallas, Texas, USA, January, 1999. 80–82.
- Di Baldassarre, G. & Montanari, A. (2009) Uncertainty in river discharge observations: a quantitative analysis. *Hydrology and Earth System Sciences*, 13(6), 913–921.
- Diaz-Nieto, J. & Wilby, R.L. (2005) A comparison of statistical downscaling and climate change factor methods: impacts on low flows in the River Thames, United Kingdom. *Climatic Change*, 69(2), 245–268.
- Dibike, Y.B. & Coulibaly, P. (2005) Hydrologic impact of climate change in the Saguenay watershed: comparison of downscaling methods and hydrologic models. *Journal of Hydrology*, 307(1-4), 145-163.
- Dibike, Y.B. & Coulibaly, P. (2007) Validation of hydrological models for climate scenario simulation: the case of Saguenay watershed in Quebec. *Civil Engineering*, 21(23), 3123-3135.
- Dibike, Y.B., Gachon, P., St-Hilaire, A., Ouarda, T.B.M.J. & Nguyen, V.T.V. (2007) Uncertainty analysis of statistically downscaled temperature and precipitation regimes in Northern Canada. *Theoretical and Applied Climatology*, 91(1-4), 149-170.
- Döll, P. & Zhang, J. (2010) Impact of climate change on freshwater ecosystems: a global-scale analysis of ecologically relevant river flow alterations. *Hydrology and Earth System*, 7(1), 1305-1342.
- Donatelli, M., Carlini, L. & Bellocchi, G. (2006) A software component for estimating solar radiation. *Environmental Modelling & Software*, 21(3), 411-416.
- Doney, S.C., Balch, W.M., Fabry, V.J. & Feely, R.A. (2009) Ocean acidification: A critical emerging problem for the ocean sciences. *Oceanography*, 22(4), 16–25.
- Dore, J.E., Lukas, R., Sadler, D.W., Church, M.J. & Karl, D.M. (2009) Physical and biogeochemical modulation of ocean acidification in the central North Pacific. *Proceedings of the National Academy of Sciences of the United States of America*, 106(30), 12235-12240.
- Dore, M.H.I. (2005) Climate change and changes in global precipitation patterns: what do we know? *Environment international*, 31(8), 1167-81.

- Dosio, A. & Paruolo P. (2011) Bias correction of the ENSEMBLES high-resolution climate change projections for use by impact models: Evaluation on the present climate. *Journal of Geophysical Research*, 116(D16), 1-22.
- Douglas, E.M., Vogel, R.M. & Kroll, C.N. (2000) Trends in floods and low flows in the United States: impact of spatial correlation. *Journal of Hydrology*, 240(1-2), 90-105.
- Douville, H., Chauvin, F., Planton, S., Royer, J.F., Salas-Melia, D. & Tyteca, S. (2002) Sensitivity of the hydrological cycle to increasing amounts of greenhouse gases and aerosols. *Climate Dynamics*, 20(1), 45-68.
- Driessen, T.L.A., Hurkmans, R.T.W.L., Terink, W., Hazenberg, P., Torfs, P.J.J.F. & Uijlenhoet, R. (2010) The hydrological response of the Ourthe catchment to climate change as modelled by the HBV model. *Earth*, 14(4), 651-665.
- Duan, J. & Miller, N.L. (1997) A generalized power function for the subsurface transmissivity profile in TOPMODEL. *Water Resources*, 33(11), 2559-2562.
- Duan, Q., Ajami, N.K., Gao, X. & Sorooshian, S. (2007) Multi-model ensemble hydrologic prediction using Bayesian model averaging. *Advances in Water Resources*, 30(5), 1371-1386.
- Duan, Q., Sorooshian, S. & Gupta, V. (1992) Effective and efficient global optimization for conceptual rainfall-runoff models. *Water Resources Research*, 28(4), 1015-1031.
- Duan, Q., Sorooshian, S. & Gupta, V.K. (1994) Optimal use of the SCE-UA global optimization method for calibrating watershed models. *Journal of Hydrology*, 158(3-4), 265-284.
- Dubrovsky, M., Buchtele, J. & Zalud, Z. (2004) High-frequency and low-frequency variability in stochastic daily weather generator and its effect on agricultural and hydrologic modelling. *Climate Change*, 63(1-2), 45-179.
- Dudgeon, D., Arthington, A. H., Gessner, M. O., Kawabata, Z.I., Knowler, D.J., Lévêque, C., Naiman, R.J., Prieur-Richard, A.H., Soto, D., Stiassny, M.L. & Sullivan, C.A. (2006) Freshwater biodiversity: importance, threats, status and conservation challenges. *Biological reviews of the Cambridge Philosophical Society*, 81(2), 163-82.
- Dufresne, J., Friedlingstein, P., Berthelot, M., Bopp, L. & Ciais, P. (2002) On the magnitude of positive feedback between future climate change and the carbon cycle. *Geophysical Research Letters*, 29(10), 0-3.
- Durman, C.F., Gregory, J.M., Hassell, D.C., Jones, R.G. & Murphy, J.M. (2001) A comparison of extreme European daily precipitation simulated by a global and a regional climate model for present and future climates. *Quarterly Journal of the Royal Meteorological Society*, 127(573), 1005-1015.

- Easterling, D.R., Horton, B., Jones, P.D., Peterson, T.C., Karl, T.R., Parker, D.E., Salinger, M.J., Razuvayev, V., Plummer, N., Jamason, P., Folland, C.K. (1997) Maximum and minimum temperature trends for the globe. *Science*, 277(5324), 364–367.
- Easterling, D.R. (1999) Development of regional climate change scenarios using a downscaling approach. *Climatic Change*, 41(3), 615–634.
- Easterling, D.R., Evans, J.L., Groisman, P.Y.A, Karl, T.R., Kunkel, K.E. & Ambenje, P. (2000) Observed variability and trends in extreme climate events. *Bulletin of the American Meteorological Society*, 81(3), 417– 25.
- Edwards, M. & Richardson, A.J. (2004) Impact of climate change on marine pelagic phenology and trophic mismatch. *Nature*, 430(7002), 881-4.
- Edwards, T.L., Crucifix, M. & Harrison, S.P. (2007) Using the past to constrain the future: how the palaeorecord can improve estimates of global warming. *Progress in Physical Geography*, 31(5), 481-500.
- Ekström M., Jones, P.D., Fowler H. J., Lenderink, G., Buishand, T.A., Conway, D. (2007) Regional climate model data used within the SWURVE project? 1: projected changes in seasonal patterns and estimation of PET. *Hydrology and Earth System Sciences*, 11(3), 1069-1083
- Elliott, J.M. (1984a) Numerical changes and population regulation in young migratory trout *Salmo trutta* in a Lake District stream, 1966-83. *The Journal of Animal Ecology*, 53(1), 327–350.
- Elliott, J.M. (1984b) Growth, size, biomass and production of young migratory trout *Salmo trutta* in a Lake District stream, 1966-83. *The Journal of Animal Ecology*, 53(3), 979-994.
- Elliott J.M. (1985) Population Regulation for Different Life-Stages of Migratory Trout *Salmo trutta* in a Lake District Stream, 1966-83. *Journal of Animal Ecology*, 54(2), 617-638.
- Elliott, J.M. (1987) Population regulation in contrasting populations of trout *Salmo trutta* in two lake district streams. *Journal of Animal Ecology*, 56(1), 83–98.
- Elliott, J.M. (1989) Mechanisms responsible for population regulation in young migratory brown trout, *Salmo trutta*. I. The critical time for survival. *Journal of Animal Ecology*, 58(3), 45–58.
- Elliott, J.M. (1991) Tolerance and resistance to thermal stress in juvenile Atlantic salmon, *Salmo salar*. *Freshwater Biology*, 25(1), 61–70.
- Elliott, J.M. (1994) *Quantitative Ecology and the Brown Trout*. Oxford, UK: Oxford University Press.
- Elliott, J.M., Hurley, M.A. & Elliott, J.A. (1997) Variable effects of droughts on the density of a sea-trout *Salmo trutta* over 30 years population. *Journal of Applied Ecology*, 34(5), 1229-1238.

- Elliott, J.M. & Elliott, J.A. (2010) Temperature requirements of Atlantic salmon *Salmo salar*, brown trout *Salmo trutta* and Arctic charr *Salvelinus alpinus*: predicting the effects of climate change. *Journal of fish biology*, 77(8), 1793-817.
- Engeland, K., Xu, C.Y. & Gottschalk, L. (2005) Assessing uncertainties in a conceptual water balance model using Bayesian methodology. *Hydrological sciences journal*, 50(1), 45-63.
- Engen-Skaugen, T., Haugen, J.E. & Tveito, O.E. (2007) Temperature scenarios for Norway: From regional to local scale. *Climate Dynamics*, 29(5), 441–453.
- Enke, W. & Spekat, A. (1997) Downscaling climate model outputs into local and regional weather elements by classification and regression. *Climate Research*, 8(1991), 195-207.
- Erlandsson, M., Buffam, I., Fölster, J., Laudon, H., Temnerud, J., Weyhenmeyer¹, G.A. & Bishop, K. (2008) 35 years of synchrony in the organic matter concentrations of Swedish rivers explained by variation in flow and sulphate. *Global Change Biology*, 14(5), 1191-1198.
- Footirt, A. McKenzie, M. Kristinzen, P. Leipprand, A. Dwosak, T. Huntingdon, J. Minnen, J.van Swart, R. (2007) Climate change and water adaptation issues. Technical report number 2, European Environment Agency, Copenhagen, Denmark.
- European Environment Agency (2010) Global and European temperature (CSI 012) – Assessment. [online], June, 2010. Available at: <http://www.eea.europa.eu/data-and-maps/indicators/global-and-european-temperature/global-and-european-temperature-assessment-3> (accessed, 23 October 2010).
- Evans, C.D., Monteith D.T. & Cooper D.M. (2005) Long-term increases in surface water dissolved organic carbon: observations, possible causes and environmental impacts. *Environmental Pollution*, 137(1), 55–71.
- Evans, C.D., Chapman, P.J., Clark, J.M., Monteith, D.T. & Cresser, M.S., (2006). Alternative explanations for rising dissolved organic carbon export from organic soils. *Global Change Biology*, 12(11), 2044–2053.
- Evans, M.G., Burt, T.P., Holden, J. & Adamson, J.K. (1999) Runoff generation and water table fluctuations in blanket peat: evidence from UK data spanning the dry summer of 1995. *Journal of Hydrology*, 221(3-4), 141-160.
- Evans, N., Baierl, A., Semenov, M.A., Gladders, P. & Fitt, B.D.L. (2008) Range and severity of a plant disease increased by global warming. *Journal of the Royal Society Interface the Royal Society*, 5(22), 525–531.
- Farda, A., Déqué, M., Somot, S., Horanyi, A., Spiridonov, V. & Toth, H. (2010) Model ALADIN as regional climate model for central and eastern Europe. *Studia Geophysica et Geodaetica*, 54(2), 313–332.
- Fausch K.D. (1984) Profitable stream positions for salmonids: relating specific growth rate to net energy gain. *Canadian Journal of Zoology*, 62(3), 441–452.

- Daly, K. & Fealy, R. (2006) *Digital Soil Information System for Ireland –Scoping Study*, Environmental Protection Agency, Johnstown Castle, Wexford, Ireland.
- Fealy, R. & Sweeney, J. (2007) Statistical downscaling of precipitation for a selection of sites in Ireland employing a generalised linear modelling approach. *International Journal of Climatology*, 27(15), 2083-2094.
- Fealy, R. & Sweeney, J. (2008) Statistical downscaling of temperature, radiation and potential evapotranspiration to produce a multiple GCM ensemble mean for a selection of sites in Ireland. *Irish Geography*, 41(1), 1-27.
- Fealy, R. (2010) *An Assessment of Uncertainties in Climate Modelling at the Regional Scale: The Development of Probabilistic Based Climate Scenarios for Ireland*. STRIVE Report Series No. 48, Environmental Protection Agency, Johnstown Castle, Wexford, Ireland.
- Fealy, R., Allott, N., Broderick, C., de Eyto, E., Dillane, M., Erdil, R.M., Jennings, E., McCrann, K., Murphy, C., O'Toole, C., Poole, R., Rogan, G., Ryder, E., Taylor, D., Whelan, K. & White, J. (2010) *RESCALE: Review and Simulate Climate and Catchment Responses at Burrishoole, Final Summary Report*. Marine Institute, Oranmore, Co. Galway, Ireland.
- Feeley, R.A., Doney, S.C. & Cooley, S.R. (2009) Ocean acidification: Present conditions and future changes in a high-CO₂ world. *Oceanography*, 22(4), 36–47.
- Feyen, L., Vrugt, J., Nuallain, B., Vanderknijff, J. & Deroo, A. (2007) Parameter optimisation and uncertainty assessment for large-scale streamflow simulation with the LISFLOOD model. *Journal of Hydrology*, 332(3-4), 276-289.
- Fischlin, A., Midgley, G.F., Price, J.T., Leemans, R., Gopal, B., Turley, C., Rounsevell, M.D. A., Dube, O.P., Tarazona, J., & Velichko, A.A., eds. (2007) Ecosystems, their properties, goods, and services. In: Parry, M.L., Canziani, O.F., Palutikof, J.P., van der Linden, P. J., & Hanson, C.E., eds. (2007) *Climate Change 2007: Impacts, Adaptation and Vulnerability. Contribution of Working Group II to the Fourth Assessment Report of the Intergovernmental Panel on Climate Change*. Cambridge, UK and New York USA: Cambridge University Press. 211–272.
- Foley, A.M. (2010a) Quantifying sources of uncertainty in regional climate model scenarios for Ireland. Unpublished PhD thesis, National University of Ireland Maynooth.
- Foley, A.M. (2010b) Uncertainty in regional climate modelling: A review. *Progress in Physical Geography*, 34(5), 647-670.
- Fowler, H.J., Kilsby, C.G. & O'Connell (2000) A stochastic rainfall model for the assessment of regional water resource systems underchanged climatic conditions. *Hydrology and Earth System Sciences*, 4(2), 261–280.
- Fowler, H.J. & Kilsby, C.G. (2002) Precipitation and the North Atlantic Oscillation: a study of climatic variability in Northern England. *International Journal of Climatology*, 22(7), 843–866.

- Fowler, H.J. & Kilsby, C.G. (2003) A regional frequency analysis of United Kingdom extreme rainfall from 1961 to 2000. *International Journal of Climatology*, 23(11), 1313-1334.
- Fowler, H.J., Kilsby, C.G. & O'Connell, P.E. (2003) Modeling the impacts of climatic change and variability on the reliability, resilience, and vulnerability of a water resource system. *Water Resources Research*, 39(8), 1-11.
- Fowler, H.J., C.G., Kilsby, O'Connell, P. & Burton, A. (2005) A weather-type conditioned multi-site stochastic rainfall model for the generation of scenarios of climatic variability and change. *Journal of Hydrology*, 308(1-4), 50-66.
- Fowler, H.J., Ekström, M., Kilsby, C.G. & Jones, P.D. (2005) New estimates of future changes in extreme rainfall across the UK using regional climate model integrations. 1. Assessment of control climate. *Journal of Hydrology*, 300(1-4), 212–233.
- Fowler, H.J., Blenkinsop, S. & Tebaldi, C. (2007) Linking climate change modelling to impacts studies: recent advances in downscaling techniques for hydrological. *International Journal of Climatology*, 27(12), 1547-1578.
- Fowler, H.J. & Kilsby, C.G. (2007) Using regional climate model data to simulate historical and future river flows in northwest England. *Climatic Change*, 80(3-4), 337-367.
- Fowler, H.J. & Ekström, M. (2009) Multi-model ensemble estimates of climate change impacts on UK seasonal precipitation extremes. *International Journal of Climatology*, 416(3), 385-416.
- Franchini, M., Wendling, J., Obled, C. & Todini, E. (1996) Physical interpretation and sensitivity analysis of the TOPMODEL. *Journal of Hydrology*, 175(1-4), 293–338.
- Freeman, C., Evans, C.D., Monteith, D.T., Reynolds, B. & Fenner, N. (2001) Export of organic carbon from peat soils. *Nature*, 412(6849), 785.
- Freer, J., Beven, K.J. & Ambrose, B. (1996). Bayesian estimation of uncertainty in runoff prediction and the value of data: an application of the GLUE approach. *Water Resources Research*, 32(7), 2161–2173.
- Frei, C. & Schär, C. (2001) Detection probability of trends in rare events: theory and application of heavy precipitation in the Alpine region. *Journal of Climate*, 14(7), 1568–1584.
- Frei, C., Christensen, J.H., Déqué, M., Jacob, D., Jones, R.G. & Vidale, P.L. (2003) Daily precipitation statistics in regional climate models: evaluation and intercomparison for the European Alps. *Journal of Geophysical Research*, 108(D3), 4124.
- Frei, C., Schöll, R., Fukutome, S., Schmidli, J. & Vidale, P.L. (2006) Future change of precipitation extremes in Europe: an intercomparison of scenarios from regional climate models. *Journal of Geophysical Research-Atmospheres*, 111(D6), D06105.

- Freni, G., Mannina, G. & Viviani, G. (2008) Uncertainty in urban stormwater quality modelling: The effect of acceptability threshold in the GLUE methodology. *Water Research*, 42(8-9), 2061-2072.
- Freni, G., Mannina, G., & Viviani, G. (2009) Uncertainty assessment of an integrated urban drainage model. *Journal of Hydrology*, 373(3-4), 392-404.
- Frich, P., Alexander, L.V., Della, Marta, P., Gleason, B., Haylock, M., Klein Tank, A. & Peterson, T. (2002) Global changes in climatic extremes during the 2nd half on the 20th century. *Climate Research*, 19(3), 193–212.
- Fried, J.S., Torn, M.S. & Mills, E. (2004) The impact of climate change on wildfire severity: a regional forecast for northern California. *Climate Change*, 64(1-2), 169–191.
- Friedland, K. (2000) Linkage between ocean climate, post-smolt growth, and survival of Atlantic salmon (*Salmo salar* L.) in the North Sea area. *ICES Journal of Marine Science*, 57(2), 419-429.
- Friedland, K.D., Reddin, D.G., McMenemy, J.R. & Drinkwater, K. (2003) Multi-decadal trends in North American Atlantic salmon stocks and climate trends relevant to juvenile survival. *Canadian Journal of Fisheries and Aquatic Sciences*, 60(5), 563–583.
- Friedlingstein, P., Cox, P., Betts, R., Bopp, L., Von Bloh, W., Brovkin, V., Cadule, P., Doney, S., Eby, M., Fung, I. & *et al.* (2006) Climate-carbon cycle feedback analysis: Results from the C4MIP model intercomparison. *Journal of Climate*, 19(14), 3337–3353.
- Frost, A.J., Charles, S.P., Timbal, B., Chiew, F.H.S., Mehrotra, R., Nguyen, K.C., Chandler, R.E., *et al.* (2011) A comparison of multi-site daily rainfall downscaling techniques under Australian conditions. *Journal of Hydrology*, 408(1-2), 1-18.
- Fry, F.E.J. (1971) The effect of environmental factors on the physiology of fish. In: Hoar, W.S. & Randal, D.J., eds. (1971) *Fish Physiology Volume VI: Environmental Relations and Behaviour*. New York, NY, USA: Academic Press. 1–98.
- Furevik, T., Bentsen, M., Drange, H., Kindem, I.K.T. & Kvamstø, N.G. (2003) Description and evaluation of the bergen climate model: ARPEGE coupled with MICOM. *Climate Dynamics*, 21(1), 27–51.
- Furrer, R., Sain, S.R., Nychka, D. & Meehl, G.A. (2007) Multivariate Bayesian analysis of atmosphere–ocean general circulation models. *Environmental and Ecological Statistics*, 14 (3), 249-266.
- Gallagher, M., & Doherty, J. (2007) Parameter estimation and uncertainty analysis for a watershed model. *Environmental Modelling & Software*, 22(7), 1000-1020.
- Garcia de Leaniz, C. (2008) Weir removal in salmonid streams: implications, challenges and practicalities. *Hydrobiologia*, 609(1), 83-96.

- Gardiner, M.J. & Radford, T. (1980) Ireland, General Soil Map. National Soil Survey, Dublin.
- Geist, D.R., Jones, J., Murray, C.J. & Dauble, D.D. (2000) Suitability criteria analyzed at the spatial scale of redd clusters improved estimates of fall Chinook salmon spawning habitat use in the Hanford Reach, Columbia River. *Canadian Journal of Fisheries and Aquatic Sciences*, 57(8), 1636–1646.
- Gellens, D. & Roulin, F. (1998) Streamflow Response of Belgian Catchments to IPCC Climate Change Scenarios. *Journal of Hydrology*, 210(1-4), 242–258.
- Gerten, D. & Adrian, R. (2002) Effects of climate warming, North Atlantic oscillation, and El Niño-Southern oscillation on thermal conditions and plankton dynamics in Northern Hemispheric lakes. *The Scientific World Journal*, 2, 586–606.
- Gibelin, A.L. & Déqué, M. (2003) Anthropogenic climate change over the Mediterranean region simulated by a global variable resolution model. *Climate Dynamics*, 20(4), 327–339.
- Gilvear, D.J., Heal, K.V. & Stephen, A. (2002) Hydrology and the ecological quality of Scottish river ecosystems. *Science of the Total Environment*, 294(1-3), 131-159.
- Giorgi, F. & Mearns, L.O. (1991) Approaches to the simulation of regional climate change: a review. *Reviews of Geophysics*, 29(2), 191–216.
- Giorgi, F. & Mearns, L.O. (1999) Introduction to special section: Regional climate modeling revisited. *Journal of Geophysical Research*, 104(D6), 6335–6352.
- Giorgi, F. & L.O. Mearns, (2002) Calculation of average, uncertainty range, and reliability of regional climate changes from AOGCM simulations via the “reliability ensemble averaging” (REA) method. *Journal of Climate*, 15(10), 1141–1158.
- Giorgi, F., Hewitson, B., Christensen, J., Hulme, M., Von Storch, H., Whetton, P., Jones, R., Mearns, L. & Fu, C. (2001) Regional Climate Information: Evaluation and Projections. In: Houghton, J.T., Ding, Y., Griggs, D.J., Noguer, M., van der Linden, P.J., Dai, X., Maskell, K. & Johnson, C.A., eds. (2001) *Climate Change 2001: The Scientific Basis, Contribution of Working Group I to the Third Assessment Report of the IPCC*. Cambridge, UK: Cambridge University Press. 739-768.
- Giorgi, F. & Mearns, L.O. (2003) Probability of regional climate change based on the Reliability Ensemble Averaging (REA) method. *Geophysical Research Letters*, 30(12), 2-5.
- Giorgi, F. (2005) Climate Change Prediction. *Climatic Change*, 73(3), 239-265.
- Giorgi, F., Im, E.-S., Coppola, E., Diffenbaugh, N.S., Gao, X.J., Mariotti, L. & Shi, Y. (2011) Higher hydroclimatic intensity with global warming. *Journal of Climate*, 24(20), 5309–5324.

- Gleick, P.H. (1986) Methods for evaluating the regional hydrologic impacts of global climatic changes. *Journal of Hydrology*, 88, 97–116.
- Gleick, P.H. (1987a) The Development and Testing of a Water Balance Model for Climate Impact Assessment: The Sacramento Basin. *Water Resources Research*, 23(6), 1049–1061.
- Gleick, P.H. (1987b) Regional Hydrologic Consequences of Increases in Atmospheric CO₂ and Other Trace Gases. *Climatic Change*, 10(2), 137–161.
- Golubev, V.S., Lawrimore, J.H., Groisman, P.Ya., Speranskaya, N.A., Zhuravin, S.A., Menne, M.J., Peterson T.C. & Malone, R.W. (2001) Evaporation changes over the contiguous United States and the former USSR: A reassessment. *Geophysical Research Letters*, 28(13), 2665-2668.
- Goodess, C.M. & Palutikof, J.P. (1998) Development of daily rainfall scenarios for southeast Spain using a circulation-type approach to downscaling. *International Journal of Climatology*, 18(10), 1051-1083.
- Goodess, C.M. & Jones, P.D. (2002) Links between circulation and changes in the characteristics of Iberian rainfall. *International Journal of Climatology*, 22(13), 1593–1615.
- Gordon, C., Cooper, C., Senior, C.A., Banks, H., Gregory, J.M., Johns, T.C., Mitchell, J.F.B. & Wood, R.A. (2000) The simulation of SST, sea ice extents and ocean heat transports in a version of the Hadley Centre coupled model without flux adjustments. *Climate Dynamics*, 16(2-3), 147–168.
- Gore, J.A. & Nestler, J.M. (1988) Instream flow studies in perspective. *Regulated Rivers: Research and Management*, 2(2), 93-101.
- Gore, J.A., Crawford, D.J. & Addison, D.S. (1998) An analysis of artificial riffles and enhancement of benthic community diversity by physical habitat simulation (PHABSIM) and direct observation. *Regulated Rivers: Research and Management*, 14(1), 69–77.
- Graham, L.P., Andreasson, J., Carlsson, B. (2007a) Assessing climate change impacts on hydrology from an ensemble of regional climate models, model scales and linking methods - A case study on the Lule River basin. *Climatic Change*, 81(1), 293–307.
- Graham, L.P., Hagemann, S., Jaun, S. & Beniston, M. (2007b) On interpreting hydrological change from regional climate models. *Climatic Change*, 81(1), 97–122.
- Graham, C.T. & Harrod, C. (2009) Implications of climate change for the fishes of the British Isles. *Journal of Fish Biology*, 74(6), 1143-1205.
- Greene, A.M., Goddard, L. & Lall, U. (2006) Probabilistic multimodel regional temperature change projections. *Journal of Climate*, 19(17), 4326–4343.

- Griffies, S.M. & Bryan, K. (1997) A predictability study of simulated North Atlantic multidecadal variability. *Climate Dynamics*, 13(7-8), 459-487.
- Grimalt, J.O., Catalan, J., Fernandez, P., Piña, B. & Munthe, J. (2010) Distribution of Persistent Organic Pollutants and Mercury in Freshwater Ecosystems Under Changing Climate Conditions. In: Kernan, M., Battarbee, R.W. & Moss, B., eds. (2010) *Climate Change Impacts on Freshwater Ecosystems*. Oxford, UK: Wiley-Blackwell. 181-202.
- Groisman, P. & Knight, R. (2001) Heavy precipitation and high streamflow in the contiguous United States: Trends in the twentieth century. *Bulletin of the American Meteorological Society*, 82(2), 219–246.
- Groisman, P.Y., Karl, T.R., Easterling, D.R., Knight, R.W., Jamason, P.F., Hennessy, K.J., Suppiah, R., *et al.* (1999) Changes in the probability of heavy precipitation: Important indicators of climatic change. *Climatic Change*, 42(1), 243-283.
- Groisman, P.Y., & Knight, R. (2001) Heavy precipitation and high streamflow in the contiguous United States: Trends in the twentieth century. *Bulletin of the American*, 82(2), 219-246.
- Groisman, P.Y., Knight, R.W., Easterling, D.R., Karl, T.R., Hegerl, G.C. & Razuvaev, V.N. (2005) Trends in intense precipitation in the climate record. *Journal of Climate*, 18(9), 1326–1350.
- Grotch, S.L. & MacCracken, M.C. (1991) The use of general circulation models to predict regional climatic change. *Journal of Climate*, 4(3), 286-303.
- Gruza, G., Rankova, E., Razuvaev, V. & Bulygina, O., (1999) Indicators of climate change for the Russian Federation. *Climatic Change*, 42(1), 219–42.
- GSI (2003) Geological Survey of Ireland, Draft National Aquifer Map.
- Guay, J.C., Boisclair, D., Rioux, D., Leclerc, M., Lapointe, M. & Legendre, P. (2000) Development and validation of numerical habitat models for juveniles of Atlantic salmon (*Salmo salar*). *Canadian Journal of Fisheries and Aquatic Sciences*, 57(10), 2065–2075.
- Guo, S. & Ying, A. (1997) Uncertainty analysis of impact of climate change on hydrology and water resources. In: Rosbjerg, D., Bontayeb, N-E, Gustard, A., Kundzewicz, Z.W. & Rasmussen, P.F., eds. (1997) *Sustainability of Water Resources Under Increasing Uncertainty*. IAHS, Publication No. 241, Wallingford, UK. 331–338.
- Guo, S., Wang, J., Xiong, L., Ying, A. & Li, D. (2002) A macro-scale and semi-distributed monthly water balance model to predict climate change impacts in China. *Journal of Hydrology*, 268(1-4), 1-15.
- Gupta, H.V., Sorooshian, S. & Yapo, P.O. (1998) Toward improved calibration of hydrologic models: Multiple and noncommensurable measures of information. *Water Resources*, 34(4), 751-763.

- Haerter, J.O., Hagemann, S., Moseley, C., & Piani, C. (2011) Climate model bias correction and the role of timescales. *Hydrology and Earth System Sciences*, 15(3), 1065–1079.
- Hagemann, S., Machenhauer, B., Jones, R., Christensen, O.B., Déqué, M., Jacob, D. & Vidale, P.L. (2004) Evaluation of water and energy budgets in regional climate models applied over Europe. *Climate Dynamics*, 23(5), 547–567.
- Hamlet, A.F. & Lettenmaier, D.P. (2000) Effects of climate change on hydrology and water resources in the Columbia river basin. The basin covers portions of seven western states. *Journal of the American Water Resources Association*, 35(6), 1597-1623.
- Hammond, D. & Pryce, A.R. (2007) *Climate change impacts and water temperature*. Science Report SC060017/SR, Environment Agency, Bristol, UK.
- Hampton, S.E., Izmet'Eva, L.R., Moore, M.V., Katz, S.L., Dennis, B., & Silow, E.A. (2008) Sixty years of environmental change in the world's largest freshwater lake - Lake Baikal, Siberia. *Global Change Biology*, 14(8), 1947-1958.
- Hanna, E., Huybrechts, P., Steffen, K., Cappelen, J., Huff, R., Shuman, C., Irvine-Fynn, T., *et al.* (2008) Increased Runoff from Melt from the Greenland Ice Sheet: A Response to Global Warming. *Journal of Climate*, 21(2), 331-341.
- Hänsel, S., Petzold, S., Matschullat, J. (2008) Precipitation trend analysis for central eastern Germany 1851–2006. In: Strelcova, K., Matyas, C., Kleidon, A., Lapin, M., Matejka, F., Blaenecy, M., Skvarenina, J., Holecý & J., eds. (2008) *Bioclimatology and Natural Hazards*. New York, NY, USA: Springer-Verlag New York Inc. 29–38.
- Hansen, L.P. & Jonsson, B. (1989) Salmon ranching experiments in the River Imsa: effect of timing of Atlantic salmon (*Salmo salar*) smolt migration. *Aquaculture*, 82(1-4), 367–373.
- Hansen, L.P. & Jonsson, B. (1991) The effect of timing of Atlantic salmon smolt and postsmolt release on the distribution of adult return. *Aquaculture*, 98(1-3), 61–67.
- Hansen, J., Sato, M., Kharecha, P., Beerling, D., Masson-delmotte, V., Pagani, M., Raymo, M., Royer, D.L. & Zachos, J.C. (2008) Target Atmospheric CO₂: Where Should Humanity Aim? *The Open Atmospheric Science Journal*, 2, 217-231.
- Hansen, J., Ruedy, R., Sato, M. & Lo, K. (2010) Global surface temperature change. *Reviews of Geophysics*, 48(4), 1-29.
- Hanson, C.E., Palutikof, J.P., Livermore, M.T.J., Barring, L., Bindi, M., Corte-Real, J., *et al.* (2007) Modelling the impact of climate extremes: An overview of the MICE project. *Climatic Change*, 81(S1), 163–177.
- Hare, W. (2006) Relationship between global mean temperature and impacts on ecosystems, food production, water and socioeconomic systems. In: Schellnhuber, H.J., Cramer, W., Nakicenovich, N., Wigley, T. & Yohe, G., eds. (2006) *Avoiding dangerous climate change*. Cambridge, UK: Cambridge University Press. 177-185.

- Hargreaves, G.H. & Samani, Z.A. (1982) Estimating potential evapotranspiration. *Journal of the Irrigation and Drainage Division*, 108(3), 225–230.
- Hargreaves, G.H. & Samani, Z.A. (1985) Reference crop evapotranspiration from temperature. *Applied Engineering in Agriculture*, 1(2), 96-99.
- Hari, R.E., Livingstone, D.M., Siber, R., Burkhardt-Holm, P. & Guettinger, H. (2006) Consequences of climatic change for water temperature and brown trout populations in Alpine rivers and streams. *Global Change Biology*, 12(1), 10–26.
- Harley, C.D.G., Randall Hughes, A., Hultgren, K.M., Miner, B.G., Sorte, C.J.B., Thornber, C. S., Rodriguez, L.F., *et al.* (2006) The impacts of climate change in coastal marine systems. *Ecology letters*, 9(2), 228-41.
- Harpham, C. & Wilby, R.L. (2005) Multi-site downscaling of heavy daily precipitation occurrence and amounts. *Journal of Hydrology*, 312(1-4), 235-255.
- Harrington, R., Woiwod, I. & Sparks, T. (1999) Climate change and trophic interactions. *Trends in Ecological Evolution*, 14, 146–150.
- Hashimoto, T., Loucks, D.P. & Stedinger, J.R. (1982a) Robustness of water resources systems. *Water Resources Research*, 18(1), 21-26.
- Hashimoto, T., Stedinger, J.R. & Loucks, D.P. (1982b) Reliability, resiliency, and vulnerability criteria for water resource system performance evaluation. *Water Resources Research*, 18(1), 14-20.
- Hashmi, M., Shamseldin, A. & Melville, B. (2009) *Downscaling of future rainfall extreme events: a weather generator based approach*. In: Proceedings of the 18th World Imacs Congress and MODSIM09 International Congress on Modelling and Simulation: Interfacing Modelling and Simulation with Mathematical and Computational Sciences. Cairns, Queensland, Australia, 3-17 July 2009. Christchurch, New Zealand: Modelling and Simulation Society of Australia and New Zealand. 3928–3934.
- Hashmi, M.Z., Shamseldin, A.Y. & Melville, B.W. (2010) Comparison of SDSM and LARS-WG for simulation and downscaling of extreme precipitation events in a watershed. *Stochastic Environmental Research and Risk Assessment*, 25(4), 475-484.
- Hassan, H., Aramaki, T., Hanaki, K., Matsuo, T., Wilby, R.L., (1998) Lake stratification and temperature profiles simulated using downscaled GCM output. *Journal of Water Science and Technology*, 38(11), 217–226.
- Hauer, F. R., Baron, J. S., Campbell, D. H., Fausch, K. D., Hostetler, S. W., Leavesley, G. H., Leavitt, P. R., *et al.* (1997) Assessment of Climate Change and Freshwater Ecosystems of the Rocky Mountains, USA and Canada. *Ecosystems*, 11(8), 903-924.
- Haugen, J.E. & Haakensatd, H. (2006) *Validation of HIRHAM version 2 with 50 and 25 km resolution*. RegClim general technical report, No. 9. 159–173.

- Hawkins, E. & R. Sutton (2009) The potential to narrow uncertainty in regional climate predictions. *Bulletin of the American Meteorological Society*, 90(8), 1095–1107.
- Hay, L.E., McCabe, G.J., Wolock, D.M. & Ayers, M.A. (1991) Simulation of precipitation by weather type analysis. *Water Resources Research*, 27(4), 493–501.
- Hay, L.E., Wilby, R.L. & Leavesley, G.H. (2000) A comparison of delta change and downscaled GCM scenarios for three mountainous basins in the United States. *Journal of the American Water Resources Association*, 36(2), 387–397.
- Hay, L.E., Clark M.P., Wilby R.L, Gutowski, W.J., Leavesley, G.H., Pan Z., Arritt R.W. & Takle, E.S. (2002) Use of regional climate model output for hydrologic simulations. *Journal of Hydrometeorology*, 3(5), 571-590.
- Hay, L.E. & Clark, M.P. (2003) Use of statistically and dynamically downscaled atmospheric model output for hydrologic simulations in three mountainous basins in the western United States. *Journal of Hydrology*, 282(1-4), 56–75.
- Hayes, J.W., Hughes N.F. & Kelly L.H. (2007) Process-based modelling of invertebrate drift transport, net energy intake and reach carrying capacity for drift-feeding salmonids. *Ecological Modelling*, 207(2-4), 171–188.
- Hayhoe, K., Wake, C.P., Huntington, T.G., Luo, L., Schwartz, M.D., Sheffield, J., Wood, E., *et al.* (2006) Past and future changes in climate and hydrological indicators in the US Northeast. *Climate Dynamics*, 28(4), 381-407.
- Haylock, M.R., Peterson, T.C., Alves, L.M., Ambrizzi, T., Anunciação, Y.M.T., Baez, J., Barros, V.R., *et al.* (2006a) Trends in Total and Extreme South American Rainfall in 1960 – 2000 and Links with Sea Surface Temperature. *Journal of Climate*, 19(8), 1490-1512.
- Haylock, M.R., Cawley, G.C., Harpham, C., Wilby, R.L. & Goodess, C.M. (2006b) Downscaling heavy precipitation over the United Kingdom: a comparison of dynamical and statistical methods and their future scenarios. *International Journal of Climatology*, 26(10), 1397–1415.
- Haylock, M.R., Hofstra, N., Klein, Tank, A.M.G, Klok, E.J., Jones, P.D. & New, M.A. (2008) European daily high-resolution gridded data set of surface temperature and precipitation for 1950–2006. *Journal of Geophysical Research*, 113(D20), D20119.
- Hays, G.C., Richardson, A.J. & Robinson, C. (2005) Climate change and marine plankton. *Trends in ecology & evolution*, 20(6), 337-44.
- He, J., Jones, J.W., Graham, W.D. & Dukes, M.D. (2010) Influence of likelihood function choice for estimating crop model parameters using the generalized likelihood uncertainty estimation method. *Agricultural Systems*, 103(5), 256-264.
- He, Y., Pu, T., Li, Z., Zhu, G., Wang, S., Zhang, N., Wang, S., *et al.* (2010) Climate change and its effect on annual runoff in Lijiang Basin-Mt. Yulong Region, China. *Journal of Earth Science*, 21(2), 137-147.

- Heggenes, J. (1990) Habitat utilization and preferences in juvenile Atlantic salmon (*Salmo salar*) in streams. *Regulated Rivers: Research & Management*, 5(4), 341–354.
- Heggenes, J.A.N., Saltveit, S.J. & Lingaas, O.L.A. (1996) Predicting fish habitat use to changes in water flow: Modelling critical minimum flows for Atlantic salmon, *Salmo salar*, and brown trout, *S. trutta*. *Regulated Rivers Research Management*, 12(2-3), 331-344.
- Heino, J., Virkkala, R. & Toivonen, H. (2009) Climate change and freshwater biodiversity: detected patterns, future trends and adaptations in northern regions. *Biological reviews of the Cambridge Philosophical Society*, 84(1), 39-54.
- Held, I.M. & Soden, B.J. (2000) Water vapor feedbacks and global warming. *Annual Review of Energy and the Environment*, 25(1), 441-475.
- Held, I.M. & Soden, B.J., (2006) Robust responses of the hydro-logical cycle to global warming. *Journal of Climate*, 19(21), 5686–5699.
- Hellström, C., Chen, D., Achberger, C. & Räisänen, J. (2001) Comparison of climate change scenarios for Sweden based on statistical and dynamical downscaling of monthly precipitation. *Climate Research*, 19, 45-55.
- Henderson-Sellers, A. (1993) An Antipodean Climate of Uncertainty. *Climate Change*, 25(3-4), 203–224.
- Hendry, K. & Cragg-Hine, D. (1997) *Restoration of riverine salmon habitats*. Fisheries Technical Manual 4, Environment Agency, Bristol, UK.
- Hendry, K. & Cragg-Hine, D. (2003) *Ecology of the Atlantic Salmon*. Conserving Natura 2000 Rivers Ecology Series No.7, English Nature, Peterborough, UK.
- Hennessy, K.J., Suppiah, R. & Page, C.M. (1999) Australian rainfall changes, 1910–1995. *Australian Meteorological Magazine*, 48(1), 1-13.
- Hering, D., Haidekker, A., Schmidt-Kloiber, A., Barker, T., Buisson, L., Graf, W., Grenouillet, G., Lorenz, A., Sandin, L. & Stendera, S. (2010) Monitoring the Responses of Freshwater Ecosystems to Climate Change, in *Climate Change Impacts on Freshwater Ecosystems*. In: Kernan, M., Battarbee, R.W. & Moss, B., eds. (2010) *Climate Change Impacts on Freshwater Ecosystems*. Oxford, UK: Wiley-Blackwell. 84-118.
- Hess, P. & Brezowsky, H. (1952) Katalog der Großwetterlagen Europas, Ber. Dt. Wetterd. in der US-zone 33, Bad Kissingen, Germany.
- Hess, P. & Brezowsky, H. (1977) Katalog der Großwetterlagen Europas, 3. Aufl. Ber. Dt. Wetterd., 113.
- Hewitson, B.C. & Crane, R.G. (1996) Climate downscaling: techniques and application. *Climate Research*, 7(2), 85–95.

- Hewitson, B.C. & Crane, R.G. (2006) Consensus between GCM climate change projections with empirical downscaling: precipitation downscaling over South Africa. *International Journal of Climatology*, 26, 1315–1337.
- Hickling, R., Roy, D.B., Hill, J.K., & Thomas, C.D. (2005) A northward shift of range margins in British Odonata. *Global Change Biology*, 11(3), 502-506.
- Hickling, R., Roy, D.B., Hill, J.K., Fox, R., & Thomas, C.D. (2006) The distributions of a wide range of taxonomic groups are expanding polewards. *Global Change Biology*, 12(3), 450-455.
- Hirabayashi, Y., Kanae, S. & Emori, S. (2009) Global projections of changing risks of floods and droughts in a changing climate. *Atmospheric Environment*, 53(4), 54-772.
- Hoerl, A.E. & Kennard, R.W. (1970) Ridge regression: biased estimation for nonorthogonal problems. *Technometrics*, 12(1), 55–67.
- Hoeting, J.A., Madigan, D., Raftery, A.E., & Volinsky, C.T. (1999) Bayesian Model Averaging: A Tutorial. *Statistical Science*, 14(4), 382-417.
- Hofstra, N., New, M. & McSweeney, C. (2010) The influence of interpolation and station network density on the distribution and extreme trends of climate variables in gridded data. *Climate Dynamics*, 35(5), 841–858.
- Holbrook, S.J., Schmitt, R.J. & Stephens, J.S. Jr. (1997) Changes in an assemblage of temperate reef fishes associated with a climatic shift. *Ecological Applications*, 7(4), 1299–310.
- Holden, J. (2000) Runoff production in blanket peat covered catchments. Unpublished Ph.D. thesis, University of Durham.
- Holden, J., Burt, T.P. & Cox, N.J. (2001) Macroporosity and infiltration in blanket peat: the implications of tension disc infiltrometer measurements. *Hydrological Processes*, 303(2), 289-303.
- Holden, J., & Burt, T.P. (2002) Infiltration, runoff and sediment production in blanket peat catchments: implications of field rainfall simulation experiments. *Hydrological Processes*, 16(13), 2537-2557.
- Holden, J. & Burt, T.P. (2003) Hydrological studies on blanket peat: the significance of the acrotelm-catotelm model. *Journal of Ecology*, 91(1), 86-102.
- Holden J. (2005) Controls of soil-pipe frequency in upland blanket peat. *Journal of Geophysical Research*, 110(F01002).
- Holland, M.M., Bitz, C.M. & Tremblay, B. (2006) Future abrupt reductions in the summer Arctic sea ice. *Geophysical Research Letters*, 33(23), 1-5.
- Holland, M.M., Finnis, J., Barrett, A.P. & Serreze, M.C. (2007) Projected changes in Arctic Ocean freshwater budgets. *Journal of Geophysical Research*, 112(G4), 1-13.

- Holm, C.F., Armstrong, J.D. & Gilvear, D.J. (2001) Investigation a major assumption of predictive instream habitat models: is water velocity preference of juvenile Atlantic salmon independent of discharge? *Fish Biology*, 59(6), 1653–1666.
- Hondzo, M. & Stefan, H. (1993) Regional water temperature characteristics of lakes subjected to climate change. *Climatic Change*, 24(3), 187-211.
- Hornberger, G.M. & Spear, R.C. (1981) An approach to the preliminary analysis of environmental systems. *Journal of Environmental Management*, 12(1), 7–18.
- Hornberger, G.M., Beven, K.J., Cosby, B.J. & Sappington, D.E. (1985) Shenandoah watershed study: calibration of the topography-based, variable contributing area hydrological model to a small forested catchment. *Water Resources Research*, 21(12), 1841–1850.
- Horton, P., Schaefli, B., Mezghani, A., Benoît, H. & Musy, A. (2006) Assessment of climate-change impacts on alpine discharge regimes with climate model uncertainty. *Hydrological Processes*, 20(10), 2091–2109.
- Horton, R., Herweijer, C., Rosenzweig, C., Liu, J., Gornitz, V., & Ruane, A.C. (2008) Sea level rise projections for current generation CGCMs based on the semi-empirical method. *Geophysical Research Letters*, 35(2), 1-5.
- Hossain, F., Anagnostou, E.N., Dinku, T., & Borga, M. (2004) Hydrological model sensitivity to parameter and radar rainfall estimation uncertainty. *Hydrological Processes*, 18(17), 3277-3291.
- Houghton, J.T., Ding, Y., Griggs, D.J., Noguera, M., van der Linden, P.J., Dai, X., Maskell, K. & Johnson, C.A., eds. (2001) *Climate Change 2001: the Scientific Basis. Contribution of Working Group I to The Third Assessment Report of the Intergovernmental Panel on Climate Change*. Cambridge, UK and New York, USA: Cambridge University Press.
- Hua, T.A., & Gunst, R.F. (1983) Generalized ridge regression: a note on negative ridge parameters. *Communications in Statistics Part A Theory and Methods*, 12(9), 37–45.
- Huang, M. & Liang, X. (2006) On the assessment of the impact of reducing parameters and identification of parameter uncertainties for a hydrologic model with applications to ungauged basins. *Journal of Hydrology*, 320(1-2), 37-61.
- Huard, D. & Mailhot, A. (2008) Calibration of hydrological model GR2M using Bayesian uncertainty analysis. *Water Resources Research*, 44(2),1-9.
- Hudson, J.J., Keith, M., Hudson, J. J., Dillon, P. J., & Somers, K.M. (2003) Long-term patterns in dissolved organic carbon in boreal lakes: the role of incident radiation , precipitation , air temperature , southern oscillation and acid deposition. *Hydrology and Earth System Science*,7(3), 390-398.
- Hughes, J.P., Guttorp, P. & Charles, S.P. (1999) A nonhomogeneous hidden Markov model for precipitation occurrence. *Journal of the Royal Statistical Society, Series C – Applied Statistics*, 48(1), 15–30.

- Hughes, L. (2000) Biological consequences of global warming: is the signal already apparent? *Trends in Ecology & Evolution*, 15(2), 56-61.
- Hulme, M., Osborn, T.J. & Johns, T.C. (1998) Precipitation sensitivity to global warming: comparisons of observations with HadCM2 simulations. *Geophysical Research Letters* 25(17), 3379–3382.
- Hulme, M. & Carter, T. (1999) Representing Uncertainty in Climate Change Scenarios and Impact Studies. *Global Environmental Change*, 1(3), 14-16.
- Hulme, M., Barrow, E.M., Arnell, N.W., Harrison, P.A. & Johns, T.C. (1999) Relative impacts of human- induced climate change and natural climate variability. *Geology*, 397(February), 688-691.
- Hundecha, Y. & Bardossy, A. (2005) Trends in daily precipitation and temperature extremes across western Germany in the second half of the 10th century. *International Journal of Climatology*, 25(9), 1189–1202.
- Huntington, T. (2006) Evidence for intensification of the global water cycle: Review and synthesis. *Journal of Hydrology*, 319(1-4), 83-95.
- Huth, R. (1997) Potential of continental-scale circulation for the determination of local daily surface variables. *Theoretical and Applied Climatology*, 56(3-4), 165–186.
- Huth, R. (1999) Statistical downscaling in central Europe: evaluation of methods and potential predictors. *Climate Research*, 13(2), 91-101.
- Huth, R. (2004) Sensitivity of local daily temperature change estimates to the selection of downscaling models and predictors. *Journal of Climate*, 17(3), 640–652.
- Huth, R. & Kliegrov, S. (2008) Non-linearity in statistical downscaling: does it bring an improvement for daily temperature in Europe? *International Journal of Climatology*, 477, 465-477.
- Huth, R., Beck, C., Philipp, A., Demuzere, M., Ustrnul, Z., Cahynová, M., Kyselý, J., *et al.* (2008) Classifications of atmospheric circulation patterns: recent advances and applications. *Annals of the New York Academy of Sciences*, 1146, 105-52.
- Huusko, A., Greenberg, L., Stickler, M., Linnansaari, T., Nykanen, M., Vehanen, T. *et al.* (2007) Life in the ice lane: the winter ecology of stream salmonids. *River Research and Applications*, 23(5), 469–491.
- Hyvarinen, V. (2003) Trends and characteristics of hydrological time series in Finland. *Nordic Hydrology*, 34(1-2), 71–90.
- Ines, A.V.M. & Hansen, J.W. (2006) Bias correction of daily GCM rainfall for crop simulation studies. *Agricultural and Forest Meteorology*, 138(1-4), 44–53.
- Inman, M. (2011) Opening the future. *Nature Climate Change*, 1, 7-9.

- Iorgulescu, I., Beven, K.J., & Musy, A. (2005) Data-based modelling of runoff and chemical tracer concentrations in the Haute-Mentue research catchment (Switzerland). *Hydrological Processes*, 19(13), 2557-2573.
- IPCC (2001) Climate change 2001: the scientific basis. In: Houghton, J.T., Ding, Y., Griggs, D.J., Noguer, M., van der Linden, P.J., Dai, X., Maskell, K. & Johnson, C.A., eds. (2001) *Contribution of Working Group I to the Third Assessment Report of the Intergovernmental Panel on Climate Change*. Cambridge, UK and New York, USA: Cambridge University Press.
- IPCC (2007a) Climate Change 2007: The Physical Science Basis. In: Solomon, S., Qin, D., Manning, M., Chen, Z., Marquis, M., Averyt, K.B., Tignor, M., Miller, H.L., eds. (2007) *Contribution of Working Group I to the Fourth Assessment Report of the Intergovernmental Panel on Climate Change*. Cambridge, UK and New York, USA: Cambridge University Press.
- IPCC (2007b) Climate Change 2007: Impacts, Adaptation and Vulnerability. In: Parry, M.L., Canziani, O.F., Palutikof, J.P., van der Linden, P.J. & Hanson, C.E., eds. (2007) *Contribution of Working Group II to the Fourth Assessment Report of the Intergovernmental Panel on Climate Change*. Cambridge, UK and New York, USA: Cambridge University Press.
- Irvine, K., Allott, N., de Eyto, E., Free, G., White, J., Caroni, R., Kennelly, C., Keaney, J., Lennon, C., Kemp, A., Barry, E., Day, S., Mills, P., O'Riain, G., Quirke, B., Twomey, H. & Sweeney, P. (2000) *Ecological Assessment of Irish Lakes – The development of a new methodology suited to the needs of the EU Directive for Surface Waters*. Irish Environmental Protection Agency, Johnstown Castle, Wexford, Ireland.
- Jacob, D., Bärring, L., Christensen, O.B., Christensen, J.H., Castro, M., Déqué, M., Giorgi, F., *et al.* (2007) An inter-comparison of regional climate models for Europe: model performance in present-day climate. *Climatic Change*, 81(S1), 31-52.
- Iwashima, T. & Yamamoto, R. (1993) A statistical analysis of the extreme events: Long-term trend of heavy daily precipitation. *Journal of the Meteorological Society of Japan*, 71(5), 637-640.
- Jacob, D. (2001) A note to the simulation of the annual and interannual variability of the water budget over the Baltic Sea drainage basin. *Meteorology and Atmospheric Physics*, 77(1-4), 61-73.
- Jakeman, A.J. & Hornberger, G.M. (1993) How much complexity is warranted in a rainfall-runoff model? *Water Resources Research*, 29(8), 2637-2649.
- Jakob Themeßl, M., Gobiet, A. & Leuprecht, A. (2011) Empirical-statistical downscaling and error correction of daily precipitation from regional climate models. *International Journal of Climatology*, 31(10), 1530-1544.
- James, P.M. (2006) Second Generation Lamb Weather Types – A New Generic Classification method with Evenly Tempered Type Frequencies. In: 6th Annual Meeting of the EMS/6th ECAC, EMS2006A00441, Ljubljana, Slovenia.

- Janzen, F.J. (1994) Climate change and temperature-dependent sex determination in reptiles. *Proceedings of the National Academy of Sciences of the United States of America*, 91(16), 7487-90.
- Jenkins, G. & Lowe, J. (2003) *Handling Uncertainties in the UKCIP02 Scenarios of Climate Change*. Hadley Centre Technical Note 44. Meteorological Office, Exeter, UK.
- Jenkinson, A.F. & Collison, F.P. (1977) *An Initial Climatology of Gales over the North Sea*. Synoptic Climatology Branch, Memorandum No. 62, Meteorological Office, Bracknell, UK.
- Jennings, E., Allott, N., Pierson, D., Schneiderman, E., Lenihan, D., Samuelsson, P. & Taylor, D. (2009) Impacts of climate change on phosphorus loading from a grassland catchment – implications for future management. *Water Research*, 43(17), 4316–4326.
- Jensen, A.J., Johnsen, B.O., & Heggberget, T.G. (1991) Initial feeding time of Atlantic salmon, *Salmo salar*, alevins compared to river flow and water temperature in Norwegian streams. *Environmental Biology of Fishes*, 30(4), 379–385.
- Jensen, A.J. & Johnsen, B. (1999) The functional relationship between peak spring floods and survival and growth of juvenile Atlantic salmon (*Salmo salar*) and brown trout (*Salmo trutta*). *Functional Ecology*, 13(6), 778–785.
- Jiang, T., Chen, Y., Xu, C., Chen, X., Chen, X. & Singh, V.P. (2007) Comparison of hydrological impacts of climate change simulated by six hydrological models in the Dongjiang Basin, South China. *Journal of Hydrology*, 336(3-4), 316-333.
- Jin, X., Xu, C.-Y., Zhang, Q. & Singh, V.P. (2010) Parameter and modeling uncertainty simulated by GLUE and a formal Bayesian method for a conceptual hydrological model. *Journal of Hydrology*, 383(3-4), 147-155.
- Johnsen, B.O., Arnekleiv, J.V., Asplin, L., Barlaup, B.T., Næsje, T.F., Rosseland, B.O., Saltveit, S.J. & Tvede, A. (2010) Hydropower Development – Ecological Effects. In: Aas, Ø., Einum, S., Klemetsen, A. & Skurdal, J., eds. (2010) *Atlantic Salmon Ecology*. Oxford, UK: Wiley-Blackwell. 409-432.
- Johnsen, B.O. & Jensen, A.J. (1994) The spread of furunculosis in salmonids in Norwegian rivers. *Journal of Fish Biology*, 45(1), 47-55.
- Jolliffe, I.T & Stephenson, D.B. (2003) *Forecast Verification: A Practitioner's Guide in Atmospheric Science*. Chichester, UK: Wiley.
- Jones, P.D. & Hulme, M. (1996) Calculating regional climatic time series for temperature and precipitation: methods and illustrations International. *Journal of Climatology*, 16(4), 361-377.
- Jones, P.D., New, M., Parker, D.E., Martin, S. & Rigor, I.G. (1999) Surface air temperature and its variations over the last 150 years. *Reviews of Geophysics*, 37, 173-199.

- Jones, R.N. (2000) Analysing the risk of climate change using an irrigation demand model. *Climate Research*, 14(2), 89-100.
- Jones, C.G., Willen, U., Ullesrtig, A. & Hansson, U. (2004) The Rossby Centre regional atmospheric climate model part I: model climatology and performance for the present climate over Europe. *Ambio*, 33(4-5), 199-210.
- Jonsson, B., Forseth, T., Jensen, A.J. & Naesje, T.F. (2001) Thermal performance of juvenile *Salmo salar* L. *Functional Ecology*, 15(6), 701-711.
- Jonsson, B., & Jonsson, N. (2009) A review of the likely effects of climate change on anadromous Atlantic salmon *Salmo salar* and brown trout *Salmo trutta*, with particular reference to water temperature and flow. *Journal of fish biology*, 75(10), 2381-447.
- Jonsson, N., Jonsson, B. & Hansen, L.P. (2005) Does climate during embryonic development influence parr growth and age of seaward migration in Atlantic salmon (*Salmo salar*)? *Canadian Journal of Fisheries and Aquatic Sciences*, 62(11), 2502-2508.
- Jorde, K., Schneider, M. & Zollner, F. (2000) Analysis of Instream Habitat Quality - Preference Functions and Fuzzy Models. Stochastic Hydraulics 2000, Wang, Z.-Y. & Hu, S.-H., eds. (2000). Balkema, Rotterdam, the Netherlands. 671 - 680.
- Jowett, I.G. (1992) Models of the Abundance of Large Brown Trout in New Zealand Rivers. *North American Journal of Fisheries Management*, 12(3), 417-432.
- Jowett, I.G. (1997) Instream flow methods: a comparison of approaches. *Regulated Rivers: Research & Management*, 13(2), 115-127.
- Juanes, F., Gephard, S. & Beland, K. (2004) Long-term changes in migration timing of adult Atlantic salmon (*Salmo salar*) at the southern edge of the species distribution. *Canadian Journal of Fisheries and Aquatic Sciences*, 61(12), 2392-2400.
- Jun, M., Knutti, R. & Nychka, D. (2008) Spatial analysis to quantify numerical model bias and dependence: how many climate models are there? *Journal of the American Statistical Association*, 103(483), 934-947.
- Juston, J., Andrén, O., Kätterer, T., & Jansson, P.-E. (2010) Uncertainty analyses for calibrating a soil carbon balance model to agricultural field trial data in Sweden and Kenya. *Ecological Modelling*, 221(16), 1880-1888.
- Kalnay, E., Kanamitsu, M., Kistler, R., Collins, W., Deaven, D., Gandin, L., Iredell, M., Saha, S., White, G., Woollen, J., Zhu, Y., Chelliah, M., Ebisuzaki, W., Higgins, W., Janowiak, J., Mo, K.C., Ropelewski, C., Wang, J., Leetmaa, A., Reynolds, R., Jenne, R., Joseph, D. (1996) The NCEP/NCAR 40-year reanalysis project, *Bulletin of the American Meteorological Society*, 77(3), 437-471.
- Karl, T.R., Wang, W.C., Schlesinger, M.E., Knight, R.W. & Portman, D. (1990) A method of relating general circulation model simulated climate to observed local climate. Part I: seasonal statistics. *Journal of Climate*, 3(10), 1053-1079.

- Karl, T.R., & Knight, R.W. (1998) Secular trends of precipitation amount, frequency, and intensity in the United States. *Bulletin of the American Meteorological Society*, 79(2), 231-241.
- Katz, R.W. (1977) Precipitation as a chain-dependent process. *Journal of Applied Meteorology*, 16(7), 671-676.
- Katz, R.W. (1996) Use of conditional stochastic models to generate climate change scenarios. *Climatic Change*, 32(3), 237-255.
- Katz, R.W. (1999) Extreme value theory of precipitation: sensitivity analysis for climate change. *Advances in Water Resources*, 23(2), 133-139.
- Kavetski, D., Kuczera, G. & Franks, S.W. (2006a) Bayesian analysis of input uncertainty in hydrological modeling: 1. Theory. *Water Resources Research*, 42(W03407).
- Kavetski, D., Kuczera, G. & Franks, S.W. (2006b) Bayesian analysis of input uncertainty in hydrological modeling: 2. Application. *Water Resources Research*, 42(W03408).
- Kay, A.L., Davies, H.N. (2008) Calculating potential evaporation from climate model data: a source of uncertainty for hydrological climate change impacts. *Journal of Hydrology*, 358(3-4), 221-239.
- Kay, A.L., Davies, H.N., Bell, V.A. & Jones, R.G. (2008) Comparison of uncertainty sources for climate change impacts: flood frequency in England. *Climatic Change*, 92(1-2), 41-63.
- Keeling, C.D. (1960) The concentration and isotopic abundances of carbon dioxide in the atmosphere. *Tellus*, 2(12), 322-334.
- Keith, R.C. (1990) Effects of CO₂-induced climatic changes on snowpack and streamflow. *Hydrological Sciences Journal*, 35(5), 511-522.
- Kendon, E.J., Rowell, D.P., Jones, R.G. & Buonomo, E. (2008) Robustness of future changes in local precipitation extremes. *Journal of Climate*, 21(17), 4280-4297.
- Kennedy, J., Morice, C. & Parker, D. (2010). Global and regional climate in 2010. *Weather*, 66(7), 188-194.
- Kernan, M., Battarbee, R.W. & Moss, B., eds. (2010) *Climate Change Impacts on Freshwater Ecosystems*. Oxford, UK: Wiley-Blackwell.
- Khan, M.S., Coulibaly, P. & Dibike, Y. (2006) Uncertainty analysis of statistical downscaling methods. *Journal of Hydrology*, 319(1-4), 357-382.
- Kidson, J.W. & Thompson, C.S. (1998) A comparison of statistical and model-based downscaling techniques for estimating local climate variations. *Journal of Climate* 11(4), 735-753.

- Kidson, J.W. & Watterson, I.G. (1995) A synoptic climatological evaluation of the changes in the CSIRO nine-level model with doubled CO₂ in the New Zealand region. *International Journal of Climatology*, 15(11), 1179–1194.
- Kilsby, C., Jones, P., Burton, A., Ford, A., Fowler, H., Harpham, C., James, P., Smith, A. & Wilby, R. (2007) A daily weather generator for use in climate change studies. *Environmental Modelling & Software*, 22(12), 1705-1719.
- Kilsby, C., Jones, P., Burton, A., Ford, A., Fowler, H., Harpham, C., James, P., Smith, A. & Wilby, R. (2007) A daily weather generator for use in climate change studies. *Environmental Modelling Software*, 22 (12), 1705–1719.
- King, H.R., Pankhurst, N.W. & Watts, M. (2007) Reproductive sensitivity to elevated water temperatures in female Atlantic salmon is heightened at certain stages of vitellogenesis. *Journal of Fish Biology*, 70(1), 190–205.
- King, J., Brown, C. & Sabet, H. (2003) A scenario-based holistic approach to environmental flow assessments for rivers. *River Research and Applications*, 19(5-6), 619–639.
- King, W.P., Pethica, J.B., Cross, G.L. W., Krauss, P.R., Renstrom, P.J., Guo, L.J., Tobolsky, A.V., *et al.* (2008) Physiology and climate change. *Science*, 322(5902), 690-692.
- Kite, G.W. (1997) Simulating Columbia River flows with data from regional scale climate models. *Water Resources Research*, 33(6), 1275–1285.
- Kjellström, E., Barring, L., Gollvik, S., Hansson, U., Jones, C., Samuelsson, P., Rummukainen, M., Ullersig, A., Willen, U., Wyser, K. (2005) *A 140-year simulation of European climate with the new version of the Rossby Centre regional atmospheric climate model (RCA3)*. Reports meteorology and climatology, 108, SMHI, Norrköping, Sweden.
- Kjellström, E. & Giorgi, F. (2010) Regional climate model evaluation and weighting. *Climate Research*, 44(2-3), 117-119.
- Kjellström, E., Boberg, F., Castro, M., Christensen, J., Nikulin, G. & Sánchez, E. (2010) Daily and monthly temperature and precipitation statistics as performance indicators for regional climate models. *Climate Research*, 44(2-3), 135-150.
- Kleinn, J. (2005) Hydrologic simulations in the Rhine basin driven by a regional climate model. *Journal of Geophysical Research*, 110(D4), 1-18.
- Klemes, V. (1985) *Sensitivity of Water-Resource Systems to Climate Variations*. WCP-98, World Climate Program, World Meteorological Organization, Geneva.
- Klemes, V. (1986) Operational Testing of Hydrological Simulation Models. *Hydrological Science*, 31(1), 13-24.
- Knowles, N., Dettinger, M., & Cayan, D. (2006) Trends in snowfall versus rainfall for the eastern United States. *Journal of Climate*, 19(18), 4545–4559.

- Knutti, R. & Hegerl, G.C. (2008) The equilibrium sensitivity of the Earth's temperature to radiation changes. *Nature Geoscience*, 1(11), 735-743.
- Knutti, R., Allen, M.R., Friedlingstein, P., Gregory, J. M., Hegerl, G. C., Meehl, G. A., Meinshausen, M., *et al.* (2008) A Review of Uncertainties in Global Temperature Projections over the Twenty-First Century. *Journal of Climate*, 21(11), 2651-2663.
- Knutti, R., Furrer, R., Tebaldi, C., Cermak, J. and Meehl, G.A. (2010) Challenges in Combining Projections from Multiple Climate Models. *Journal of Climate*, 23(10), 2739-2758.
- Konz, M., & Seibert, J. (2010) On the value of glacier mass balances for hydrological model calibration. *Journal of Hydrology*, 385(1-4), 238-246.
- Kostopoulou, E. & Jones, P.D. (2005) Assessment of climate extremes in the Eastern Mediterranean. *Meteorology and Atmospheric Physics*, 89(1-4), 69-85.
- Krzysztofowicz, R. (1999) Bayesian theory of probabilistic forecasting via deterministic hydrologic model. *Water Resources*, 35(9), 2739-2750.
- Krzysztofowicz, R. (2001) The case for probabilistic forecasting in hydrology. *Journal of Hydrology*, 249(1-4), 2-9.
- Krzysztofowicz, R. (2002) Bayesian system for probabilistic river stage forecasting. *Journal of Hydrology*, 268(1-4), 16-40.
- Kuczera, G. (1994) NLFIT: A Bayesian nonlinear regression program suite, Users manual. Dept. of Civil, Surveying and Environmental Engineering, University of Newcastle, UK.
- Kuczera, G. & Mroczkowski, M. (1998) Assessment of hydrologic parameter uncertainty and the worth of data. *Water Resources Research*, (34)6, 1481-1489.
- Kuczera, G. & Parent, E. (1998) Monte Carlo assessment of parameter uncertainty in conceptual catchment models: the Metropolis algorithm. *Journal of Hydrology*, 211(1-4), 69-85.
- Kuczera, G., Kavetski, D., Franks, S. & Thyer, M. (2006) Towards a Bayesian total error analysis of conceptual rainfall-runoff models: Characterising model error using storm-dependent parameters. *Journal of Hydrology*, 331(1-2), 161-177.
- Küttel, M., Luterbacher, J. & Wanner, H. (2010) Multidecadal changes in winter circulation-climate relationship in Europe: frequency variations, within-type modifications, and long-term trends. *Climate Dynamics*, 36(5-6), 957-972.
- Kulik, B.H. (1990) A Method to Refine the New England Aquatic Base Flow Policy. *Rivers*, 1(1), 8-22.
- Kundzewicz, Z.W., Graczyk, D., Maurer, T., Przymusińska, I., Radziejewski, M., Svensson, C. & Szwed, M. (2005) Trend detection in river flow time-series: 1. annual maximum flow. *Hydrological Sciences Journal*, 50(5), 797-810.

- Kundzewicz, Z., Radziejewski, M. & Pińskwar, I. (2006). Precipitation extremes in the changing climate of Europe. *Climate Research*, 31(1), 51-58.
- Kunkel, K.E., Andsager, K. & Easterling, D.R. (1999) Long-term trends in extreme precipitation events over the conterminous United States and Canada. *Journal of Climate*, 12(8), 2515–2527.
- Kwadijk, J. & Rotmans, J. (1995) The impact of climate change on the river Rhine: a scenario study. *Climatic Change*, 30(4), 397–425.
- Kysely, J. (2002) Comparison of extremes in GCM-simulated, downscaled and observed central-European temperature series. *Climate Research*, 20(3), 211–222.
- Labat, D. (2004) Evidence for global runoff increase related to climate warming. *Advances in Water Resources*, 27(6), 631-642.
- Labat, D. Godd ris, Y., Probst, J.L. & Guyot, J.L. (2004). Evidence for global runoff increase related to climate warming. *Advances in Water Resources*, 27(6), 631–642.
- Labat, D. Godd ris, Y., Probst, J.L. & Guyot, J.L. (2005) Reply to comment of Legates *et al.* *Advances in Water Resources*, 28(12), 1316-1319.
- Lake, P., Palmer, M., Biro, P., Cole, J., & Covich, A. (2000) Global change and the biodiversity of freshwater ecosystems: impacts on linkages between above-sediment and sediment biota. *BioScience*, 50(12), 1099-1107.
- Lamb, H.H. (1950) Types and spells of weather around the year in the British Isles: Annual trends, seasonal structure of the year, singularities. *Quarterly Journal of the Royal Meteorological Society*, 76, 393-438.
- Lamb, H.H. (1972) British Isles weather types and a register of daily sequence of circulation patterns, 1861–1971. *Geophysical Memoirs*, 116, HMSO, London, UK.
- Lamb, R., Beven, K., & Myrab , S. (1998) Use of spatially distributed water table observations to constrain uncertainty in a rainfall – runoff model. *Advances in Water Resources*, 22(4), 305-317.
- Lambert, S.J. & Boer, G.J. (2001) CMIP1 evaluation and intercomparison of coupled climate models. *Climate Dynamics*, 17(2-3), 83–106.
- Laprise, R., Caya, D., Frigon, A. & Paquin, D. (2003) Current and perturbed climate as simulated by the second-generation Canadian Regional Climate Model (CRCM-II) over northwestern North America. *Climate Dynamics*, 21(5-6), 405-421.
- Lassalle, G., Beguer, M., Beaulaton, L., & Rochard, E. (2008) Diadromous fish conservation plans need to consider global warming issues: An approach using biogeographical models. *Biological Conservation*, 141(4), 1105-1118.
- Le Qu r , C., Raupach, M.R., Canadell, J.G., Marland, G. *et al.* (2009) Trends in the sources and sinks of carbon dioxide. *Nature Geoscience*, 2(12), 831 – 836.

- Leander, R. & Buishand, T. (2006) Resampling of regional climate model output for the simulation of extreme river flows. *Journal of Hydrology*, 332(3-4), 487–496.
- Leander, R., Buishand, T.A., van den Hurk, B.J.J.M. & de Wit, M.J.M. (2008) Estimated changes in flood quantiles of the river Meuse from resampling of regional climate model output. *Journal of Hydrology*, 351(3-4), 331–343.
- Leavesley, G.H. (1994) Modelling the effects of climate change on water resources – a review. *Climatic Change*, 28(1), 159–177.
- Legates, D.R., Lins, H.F. & McCabe, G.J. (2005) Comments on “Evidence for global runoff increase related to climate warming” by Labat *et al.* *Advances in Water Resources*, 28(12), 1310-1315.
- Lehner, B., Döll, P., Alcamo, J., Henrichs, T. & Kaspar, F. (2006) Estimating the impact of global change on flood and drought risks in Europe: a continental, integrated analysis. *Climatic Change*, 75(3), 273-299.
- Lenderink, G. (2010) Exploring metrics of extreme daily precipitation in a large ensemble of regional climate model simulations. *Climate Research*, 44(2-3), 151-166.
- Lenderink, G., van Ulden, A., van den Hurk, B. & Keller, F. (2007) A study on combining global and regional climate model results for generating climate scenarios of temperature and precipitation for the Netherlands. *Climate Dynamics*, 29(2-3), 157–176.
- Letcher B.H. & Terrick T.D. (1998) Maturation of male age-0 Atlantic salmon following a massive, localized flood. *Journal of Fish Biology*, 53, 1243–1252.
- Letcher, B. & Terrick, T. (1998) Maturation of male age-0 Atlantic salmon following a massive, localized flood. *Journal of Fish Biology*, 53(6), 1243–1252.
- Lettenmaier, D.P. & Gan, T.Y. (1990) Hydrologic sensitivities of the Sacramento–San Joaquin river basin, California, to global warming. *Water Resources Research*, 26 (1), 69–86.
- Leung, L.R., Hamlet, A.F., Lettenmaier, D.P. & Kumar, A. (1999) Simulations of the ENSO Hydroclimate Signals in the Pacific Northwest Columbia River Basin. *Bulletin of the American Meteorological Society*, 80(11), 2313-2329.
- Levitus, S. (2000) Warming of the World Ocean. *Science*, 287(5461), 2225-2229.
- Levitus, S. (2005) Warming of the world ocean, 1955–2003. *Geophysical Research Letters*, 32(2), 1-4.
- Levitus, S., Antonov, J.I., Boyer, T.P., Locarnini, R.A., Garcia, H.E. & Mishonov, A.V. (2009) Global ocean heat content 1955–2008 in light of recently revealed instrumentation problems. *Geophysical Research Letters*, 36(7), 1-5.

- Li, C.Z., Zhang, L., Wang, H., Zhang, Y.Q., Yu, F.L. & Yan, D.H. (2011) The transferability of hydrological models under nonstationary climatic conditions. *Hydrology and Earth System Sciences Discussions*, 8(5), 8701-8736.
- Lin, K., Zhang, Q. & Chen, X. (2010) An evaluation of impacts of DEM resolution and parameter correlation on TOPMODEL modeling uncertainty. *Journal of Hydrology*, 394(3-4), 370-383.
- Lindström, G. & Bergström, S. (2004) Runoff trends in Sweden 1807–2002. *Hydrological Sciences Journal*, 49(1), 69–83.
- Lindström, G. & Rodhe, A. (1986) Modelling water exchange and transit times in till basins using oxygen-18. *Nordic Hydrology*, 17(4), 325-334.
- Lindström, G., Gardelin, M., Johansson, B., Persson, M., Bergström, S. (1997) Development and test of the distributed HBV-96 hydrological model. *Journal of Hydrology*, 201(1-4), 272-288.
- Linnansaari, T., Keskinen, A., Romakkaniemi, A., Erkinaro, J. and Deep, O.P. (2010) Deep habitats are important for juvenile Atlantic salmon *Salmo salar* L. in large rivers. *Ecology of Freshwater Fish*, 19(4), 618-626.
- Lins, H.F. & Slack, J.R. (1999) Streamflow trends in the United States. *Geophysical Research Letters*, 26(2), 227–230.
- Liu, B., Xu, M., Henderson, M. & Qi, Y. (2005) Observed trends of precipitation amount, frequency, and intensity in China, 1960 – 2000. *Journal of Geophysical Research*, 110(D08103).
- Liu, X., Coulibaly, P. & Evora, N. (2008) Comparison of data-driven methods for downscaling ensemble weather forecasts. *Hydrology and Earth System Sciences*, 12(2), 615–624.
- Liu, Y. & Gupta, H.V. (2007) Uncertainty in hydrologic modeling: Toward an integrated data assimilation framework. *Water Resources Research*, 43(7), 1-18.
- Liu, Y., Freer, J., Beven, K., & Matgen, P. (2009) Towards a limits of acceptability approach to the calibration of hydrological models: Extending observation error. *Journal of Hydrology*, 367(1-2), 93-103.
- Liu, Z., Xu, Z., Charles, S.P., Fu, G. & Liu, L. (2011) Evaluation of two statistical downscaling models for daily precipitation over an arid basin in China. *International Journal of Climatology*, 31(13), 2006–2020.
- Livingstone, D.M. (1999). *Ice break-up on southern Lake Baikal and its relationship to local and regional air* Ice break-up on southern Lake Baikal and its relationship in Siberia and to the North Atlantic Oscillation temperatures. *Limnology*, 44(6), 1486-1497.
- Livingstone, D.M. (2003) Impact of secular climate change on the thermal structure of a large temperate central European lake. *Climatic Change*, 57(1), 205-225.

- Loaciga, H.A., Valdes, J.B., Vogel, R., Garvey, J. & Schwarz, H. (1996) Global warming and the hydrologic cycle. *Journal of Hydrology*, 174(1-2), 83–127.
- Lobon-Cervia, J. (2004) Discharge-dependent covariation patterns in the population dynamics of brown trout (*Salmo trutta*) within a Cantabrian river drainage. *Canadian Journal of Fisheries and Aquatic Sciences*, 61(10), 1929–1939.
- Loeb, N.G. & Su, W. (2010) Direct Aerosol Radiative Forcing Uncertainty Based on a Radiative Perturbation Analysis. *Journal of Climate*, 23(19), 5288–5293.
- Long, C.B., MacDermot, C.V., Morris, J.H., Sleeman, A.G., Tietzsch-Tyler, D., Aldwell, C.R., Daly, D., Flegg, A.M., McArdle, P.M. & Warren, W.P. (1992) Geology of North Mayo. Geological Survey of Ireland, Dublin.
- Lopez, A., Tebaldi, C., New, M., Stainforth, D. Allen, M. & Kettleborough, J. (2006) Two approaches to quantifying uncertainty in global temperature changes, *Journal of Climate*, 19(19), 4785–4796.
- Lorenz, P. & Jacob, D. (2010) Validation of temperature trends in the ENSEMBLES regional climate model runs driven by ERA40. *Climate Research*, 44(2-3), 167-177.
- Lorius, C., Jouzel, J., Raynaud, D. & Hansen, J. (1990) The ice-core record: climate sensitivity and future greenhouse warming. *Nature*, 347(6289), 139-145.
- Lüthi, D., Le Floch, M., Bereiter, B., Blunier, T., Barnola, J.-M., Siegenthaler, U., Raynaud, D., *et al.* (2008) High-resolution carbon dioxide concentration record 650,000–800,000 years before present. *Nature*, 453(7193), 379-82.
- Lund, S.G., Caissie, D., Cunjak, R.A., Vijayan, M.M. & Tufts, B.L. (2002) The effects of environmental heat stress on heat-shock mRNA and protein expression in Miramichi Atlantic salmon (*Salmo salar*) parr. *Canadian Journal of Fisheries and Aquatic Sciences*, 59(9), 1553–1562.
- Lytle, D.A. & Poff, N.L. (2004) Adaptation to natural flow regimes. *Trends in ecology & evolution*, 19(2), 94-100.
- MacCrimmon, H.R. & Gets, B.L. (1979) World distribution of Atlantic salmon, *Salmo salar*. *Journal of the Fisheries Research Board of Canada*, 36(4), 422-457.
- Magnuson, J.J. (2000) Historical Trends in Lake and River Ice Cover in the Northern Hemisphere. *Science*, 289(5485), 1743-1746.
- Manley, R.E. (1993) *HYSIM Reference Manual*. R.E. Manley Consultancy, Cambridge, UK.
- Manton, M.J., Della-Marta, P.M., Haylock, M.R., Hennessy, K.J., Nicholls, N., Chambers, L.E., Collins, D.A., *et al.* (2001) Trends in extreme daily rainfall and temperature in Southeast Asia and the South Pacific: 1961-1998. *International Journal of Climatology*, 21(3), 269-284.

- Mantovan, P. & Todini, E. (2006) Hydrological forecasting uncertainty assessment: Incoherence of the GLUE methodology. *Journal of Hydrology*, 330(1-2), 368-381.
- Maraun, D., Wetterhall, F., Ireson, A.M., Chandler, R.E., Kendon, E.J., Widmann, M. Brienen, S., Rust, H.W., Sauter, T., Themeßl, M. (2010) Precipitation downscaling under climate change. Recent developments to bridge the gap between dynamical models and the end user. *Reviews of Geophysics*, 48,(3), 1-38.
- Marshall, L., Sharma, A. & Nott, D. (2006) Modeling the catchment via mixtures: Issues of model specification and validation. *Water Resources Research*, 42(11), 1-14.
- Marshall, L., Nott, D. & Sharma A. (2007a) A single model ensemble versus a dynamic modeling platform: semi-distributed rainfall runoff modeling in a Hierarchical Mixtures of Experts framework. *Geophysical Research Letters*, 34(L01404).
- Marshall, L., Nott, D. & Sharma A. (2007b) Towards dynamic catchment modelling: a Bayesian hierarchical mixtures of experts framework. *Hydrological Processes*, 21(7), 847-861.
- Martin, J.H.A. & Mitchell, K.A. (1985) Influence of sea temperature upon the numbers of grilse and multi-sea-winter Atlantic salmon (*Salmo salar*) caught in the vicinity of the River Dee (Aberdeenshire). *Canadian Journal of Fisheries and Aquatic Sciences*, 42(9), 1513–1521.
- Mavromatis, T. & Hansen, J.W. (2001) Interannual variability characteristics and simulated crop re-sponse of four stochastic weather generators. *Agricultural and Forest Methodology*, 109(4), 283-296.
- May, L., Place, C, O’Hea, B., Lee, M., Dillane, M. & McGinnity, P. (2005) Modelling soil erosion and transport in the Burrishoole catchment, Newport, Co. Mayo, Ireland. *Freshwater Forum*, 23(1), 139-154.
- McCabe, G.J. & Wolock, D.M. (2002) A step increase in streamflow in the conterminous United States. *Geophysical Research Letters*, 29 (24), 2185.
- McCarthy, I.D. & Houlihan, D.F. (1997) The effect of temperature on protein synthesis in fish: the possible consequences for wild Atlantic salmon (*Salmo salar L.*) stocks in Europe as a result of global warming. In: Wood, C.M. & McDonald, G., eds. (1997) *Global Warming: Implications for Freshwater and Marine Fish*. Cambridge, UK: Cambridge University Press. 51–77.
- McCarty, J.P. (2001) Ecological consequences of recent climate change. *Conservation Biology*, 15(2), 320-331.
- McCormick S.D., Cunjak R.A., Dempson B., O’Dea M.F. & Carey J. (1999) Temperature-related loss of smolt characteristics in Atlantic salmon in the wild. *Canadian Journal of Fisheries and Aquatic Sciences*, 56(9), 1648–1649.
- McCormick, S.D., Hansen, L.P., Quinn, T.P. & Saunders, R.L. (1998) Movement, migration, and smolting of Atlantic salmon (*Salmo salar*). *Canadian Journal of Fisheries and Aquatic Sciences*, 55 (S1), 77-92.

- McCullagh, P. & Nelder, J.A. (1989) *Generalized Linear Models*. 2nd edition, London, UK: Chapman and Hall.
- McElwain, L. & Sweeney J. (2003) Climate change in Ireland-recent trends in temperature and precipitation. *Irish Geography*, 36(2), 97–111.
- McGinnity, P., Jennings, E., DeEyto, E., Allott, N., Samuelsson, P., Rogan, G., Whelan, K., *et al.* (2009) Impact of naturally spawning captive-bred Atlantic salmon on wild populations: depressed recruitment and increased risk of climate-mediated extinction. *Proceedings. Biological sciences / The Royal Society*, 276(1673), 3601–10.
- McGuffie, K., Henderson-Sellers, A., Holbrook, N., Kothavala, Z., Balachova, O. & Hoekstra, J. (1999) Assessing simulations of daily temperature and precipitation variability with global climate models for present and enhanced greenhouse climates. *International Journal of Climatology*, 19(1), 1–26.
- Mckee, A.D., Atkinson, D., Collings, S.E., Eaton, J.W., Gill, A.B., Harvey, I., Hatton, K., *et al.* (2003) Response of freshwater microcosm communities to nutrients, fish, and elevated temperature during winter and summer. *Limnology and Oceanography*, 48(2), 707–722.
- McMillan, H., & Clark, M. (2009) Rainfall-runoff model calibration using informal likelihood measures within a Markov chain Monte Carlo sampling scheme. *Water Resources Research*, 45(4), 1–12.
- McMillan, H., Jackson, B., Clark, M., Kavetski, D., & Woods, R. (2011) Rainfall uncertainty in hydrological modelling: An evaluation of multiplicative error models. *Journal of Hydrology*, 400(1–2), 83–94.
- Mearns, L.O., Giorgi, F., McDaniel, L. & Shields, C. (1995) Analysis of daily variability of precipitation in a nested regional climate model: comparison with observations and doubled CO₂ results. *Global Planet Change*, 10(49), 55–78.
- Mearns, L.O., Bogardi, I., Giorgi, F., Matyasovsky, I. & Palecki, M. (1999) Comparison of climate change scenarios generated daily temperature and precipitation from regional climate model experiments and statistical downscaling. *Journal of Geophysical Research*, 104(D6), 6603–6621.
- Mearns, L.O., Giorgi, F., Whetton, P., Hulme, M., Lal, M. & Pabon, D. (2003) *Guidelines for the Use of Climate Scenarios Developed from Regional Climate Model Experiments*. Data Distribution Centre of the Intergovernmental Panel on Climate Change.
- Mearns, L.O., *et al.* (2006) Overview of the North American Regional Climate Change Assessment Program. In NOAA RISA-NCAR Meeting, Tucson, AZ, March 2006.
- Meehl, G.A., Washington, W.M., Santer, B.D., Collins, W.D., Arblaster, J.M., Hu, A., Lawrence, D.M., *et al.* (2006) Climate change projections for the twenty-first century and climate change commitment in the CCSM3. *Journal of climate*, 19(11), 2597–2616.

- Mehrotra, R. & Sharma, A. (2011) Impact of atmospheric moisture in a rainfall downscaling framework for catchment-scale climate change impact assessment. *International Journal of Climatology*, 31(3), 431-450.
- Mekis, E. & Hogg, W.D. (1999) Rehabilitation and analysis of Canadian daily precipitation time series. *Atmosphere Ocean*, 37(1), 53– 85.
- Menzel, A. & Fabian, P. (1999) Growing season extended in Europe. *Nature*, 397(6721), 1996-1996.
- Menzel, A., Estrella, N. & Fabian, P. (2001) Spatial and temporal variability of the phenological seasons in Germany from 1951–1996. *Global Change Biology*, 7(6), 657–666.
- Menzel, A., Sparks, T.H., Estrella, N., Koch, E., Aasa, A., Ahas, R., Alm-Kübler, K., *et al.* (2006) European phenological response to climate change matches the warming pattern. *Global Change Biology*, 12(10), 1969-1976.
- Merz, J.E., Setka, J.D., Pasternack, G.B., & Wheaton, J.M. (2004) Predicting benefits of spawning habitat rehabilitation to salmonid (*Oncorhynchus* spp.) fry production in a regulated California river. *Canadian Journal of Fisheries and Aquatic Sciences*, 61(8), 1433–1446.
- Michaelides, S.C., Liassidou, F. & Schizas, C.N. (2007) Synoptic classification and establishment of analogues with artificial neural networks. *Pure and Applied Geophysics*, 164(6-7), 1347–1364.
- Milner, N.J., Dunbar, M.J., Newson, M.D., Potter, E.C.E., Solomon, D.J., Armstrong, J.A., Mainstone C.P., & Llewelyn, C.I. eds. (2010) *Managing river flows for salmonids: evidence-based practice. Pitlochry, 9-11th March, 2010*. Atlantic Salmon Trust Flows Workshop March 2010.
- Millennium Ecosystem Assessment (2005) *Ecosystems and human well-being: wetlands and water synthesis*. World Resources Institute, Washington, DC, USA: World Resources Institute.
- Milly, P.C.D., Wetherald, R.T., Dunne, K.A. & Delworth, T.L. (2002) Increasing risk of great floods in a changing climate. *Nature*, 415(6871), 514–517.
- Milly, P.C.D., Dunne, K.A. & Vecchia, A.V. (2005) Global pattern of trends in streamflow and water availability in a changing climate. *Nature*, 438(7066), 347–350.
- Min, S.-K., Legutke, S., Hense, A. & Kwon, W.-T. (2005) Internal variability in a 1000-yr control simulation with the coupled climate model ECHO-G – II . El Niño Southern Oscillation and North Atlantic Oscillation. *Tellus*, 57(4), 622-640.
- Min, S.-K. & Hense, A. (2007) Hierarchical evaluation of ipcc ar4 coupled climate models with systematic consideration of model ncertainties. *Climate Dynamics*, 29(7-8), 853–868.

- Min, S.-K., Zhang, X. & Zwiers, F. (2008) Human-Induced Arctic Moistening. *Science* 320(5875), 518-520.
- Min, S.-K., Zhang, X., Zwiers, F.W., & Hegerl, G.C. (2011) Human contribution to more-intense precipitation extremes. *Nature*, 470(7334), 378-81.
- Minville, M., Brissette, F., & Leconte, R. (2008) Uncertainty of the impact of climate change on the hydrology of a nordic watershed. *Journal of Hydrology*, 358(1-2), 70-83.
- Moffett, I.J.J., Allen, M., Flanagan, C., Crozier, W.W. & Kennedy, G.J.A. (2006) Fecundity, egg size and early hatchery survival for wild Atlantic salmon, from the River Bush. *Fisheries Management and Ecology*, 13(2), 73–79.
- Moir, H.J., Soulsby, C. & Youngson, A. (1998) Hydraulic and sedimentary characteristics of habitat utilized by Atlantic salmon for spawning in the Girnock Burn, Scotland. *Fisheries Management and Ecology*, 5(3), 241–254.
- Moir, H.J., Soulsby, C. & Youngson, A.F. (2002) Hydraulic and sedimentary controls on the availability and use of Atlantic salmon (*Salmo salar*) spawning habitat in the River Dee system, north-east Scotland. *Geomorphology*, 45(3-4), 291–308.
- Montanari, A. & Brath, M. (2004) A stochastic approach for assessing the uncertainty of rainfall-runoff simulations. *Water Resources Research*, 40(1), 1-11.
- Montanari, A. (2005) Large sample behaviors of the generalized likelihood uncertainty estimation (GLUE) in assessing the uncertainty of rainfall-runoff simulations. *Water Resources Research*, 41(8), 1-13.
- Montanari, A. (2007) What do we mean by “uncertainty”? The need for a consistent wording about uncertainty assessment in hydrology. *Hydrological Processes*, 21(6), 841-845.
- Montanari, A. (2011) Uncertainty of Hydrological Predictions. In: Wilderer, P. ed. *Treatise on Water Science*. Oxford Academic Press. Vol. 2, 459-478.
- Monteith, D., Stoddard, J.L., Evans, C.D., de Wit, H.A., Forsius, M., Høgåsen, T., Winander, A., Skjelkvåle, B.L., Jeffries, D.S., Vuorenmaa, J., Keller, B., Kopáček, J. and Vesely, J. (2007) Dissolved organic carbon trends resulting from changes in atmospheric deposition chemistry. *Nature*, 450(7169), 537-540.
- Monteith, J.L. (1965) Evaporation and environment. *Symposia of the Society for Experimental Biology*, 19, 205–234.
- Montoya, J.M. & Raffaelli, D. (2010) Climate change, biotic interactions and ecosystem services. *Philosophical transactions of the Royal Society of London. Series B, Biological sciences*, 365(1549), 2013-2018.
- Mooij, W.M., Hülsmann, S., De Senerpont Domis, L.N., Nolet, B.A., Bodelier, P.L.E., Boers, P.C.M., Pires, L.M.D., *et al.* (2005) The impact of climate change on lakes in the Netherlands: a review. *Aquatic Ecology*, 39(4), 381-400.

- Morrison, B.R.S. (1989) The growth of juvenile Atlantic salmon, *Salmo salar*, and brown trout, *Salmo trutta*, in a Scottish river system subject to cooling-water discharge. *Journal of Fish Biology*, 35(4), 539–556.
- Moss, B., Mckee, D., Atkinson, D., Collings, S.E., Eaton, J.W., Gill, A.B., Hatton, K., *et al.* (2003) How important is climate? Effects of warming, nutrient in shallow lake addition and fish on phytoplankton microcosms. *Journal of Applied Ecology*, 40(5), 782-792.
- Moss, R. & Schneider, S. (2000) *Uncertainties*. In: Pachauri, R., Taniguchi T., & Tanaka, K., eds. (2000) *Guidance Papers on the Cross Cutting Issues of the Third Assessment Report of the IPCC*. Intergovernmental Panel on Climate Change, Geneva.
- Moss, R.H., Edmonds, J.A, Hibbard, K.A, Manning, M.R., Rose, S.K., van Vuuren, D.P., Carter, T.R., *et al.* (2010) The next generation of scenarios for climate change research and assessment. *Nature*, 463(7282), 747-56.
- Mote, P.W. (2003) Trends in snow water equivalent in the Pacific Northwest and their climatic causes. *Geophysical Research Letters*, 30(12), 1601-1604.
- Moyeed, R.A. & Clarke, R.T. (2005) The use of Bayesian methods for fitting rating curves, with case studies. *Advances in Water Resources*, 28(8), 807-818.
- Mudelsee, M., Borngen, M., Tetzlaff, G. & Grunewald, U. (2003) No upward trends in the occurrence of extreme floods in central Europe. *Nature*, 425(6954), 166–169.
- Müller-Wohlfeil, D.I., Bürger, G. & Lahmer, W. (2000) Response of a river catchment to climatic change: application of expanded downscaling to Northern Germany. *Climatic Change*, 47(1), 61–89.
- Murphy, A.H. (1988) Skill scores based on the mean square error and their relationships to the correlation coefficient. *Monthly Weather Review*, 116(12), 2417-2424.
- Murphy, A.H. (1993) What is a “good” forecast? An essay on the nature of goodness in weather forecasting. *Weather Forecasting*, 8(2), 281–293.
- Murphy, A.H. & Wilks, D.S. (1998) A case study of the use of statistical models in forecast verification: Precipitation probability forecasts. *Weather and Forecasting*, 13(3), 795-810.
- Murphy, C. & Charlton, R. (2008) *Climate Change and Water Resources in Ireland*. In: Sweeney, J.S., ed. (2008) *Climate Change: Refining the Impacts*. Environmental Protection Agency, Johnstown Castle, Wexford, Ireland.
- Murphy, C., Fealy, R., Charlton, R. & Sweeney, J.S. (2006) The reliability of an “off the shelf” Conceptual Rainfall-Runoff model for use in climate impact assessment: uncertainty quantification using Latin Hypercube Sampling. *Area*, (38)1, 65-78.
- Murphy, J. (1999) An evaluation of statistical and dynamical techniques for downscaling local climate. *Journal of Climate*, 12(8), 2256-2284.

- Murphy, J. (2000) Predictions of climate change over Europe using statistical and dynamical downscaling techniques. *International Journal of Climatology*, 20(5), 489-501.
- Murphy, M.M., Sexton, D.M.H., Barnett, D.N., Jones, G.S., Webb, M.J., Collins M., & Stainforth, D.A. (2004) Quantification of modelling uncertainties in a large ensemble of climate change simulations. *Nature*, 430, 768–772.
- Murphy, J.M., Sexton, D.M.H., Barnett, D.N., Jones, G.S., Webb, M.J., Collins, M., *et al.* (2011) Quantification of modelling uncertainties in a large ensemble of climate change simulations. *Nature*, 430(7001), 768-772.
- Naden, P., Allott, N., Arvola, L., Jarvinen, M., Jennings, E., Moore, K., Nic Aongusa, C., Pierson, D. and Schneiderman, E. (2010) Modelling the impacts of climate change on dissolved organic carbon, Aquatic Ecology Series, 4. In: D.G. George ed. (2010) *The Impact of Climate Change on European Lakes*. Aquatic Ecology Series, 4, Springer. 221-252.
- Najafi, M.R., Moradkhani, H. & Jung, I.W. (2011). Assessing the uncertainties of hydrologic model selection in climate change impact studies. *Hydrological Processes*, 25(18), 2814-2826.
- Nakicenovic, N., Alcamo, J., Davis, G. *et al.*, eds. (2000) *Special Report on Emissions Scenarios (SRES)*. Cambridge, U.K: Cambridge University Press.
- Nash, L.L. & Gleick, P.H. (1991) The sensitivity of streamflow in the Colorado Basin to climatic changes. *Journal of Hydrology*, 125(3-4), 221-241.
- Nemec, J. & Schaake, J. (1982) Sensitivity of water resources systems to climate variation. *Hydrological Sciences Journal*, 27(3), 327–43.
- Neuman, S.P. (2003) Maximum likelihood Bayesian averaging of uncertain model predictions. *Stochastic Environmental Research and Risk Assessment (SERRA)*, 17(5), 291-305.
- Neuman, S.P., Xue, L., Ye, M. & Lu, D. (2012) Bayesian analysis of data-worth considering model and parameter uncertainties. *Advances in Water Resources*, 36(0), 75-85.
- New, M. & Hulme, M. (2000) Representing uncertainty in climate change scenarios: a Monte-Carlo approach. *Integrated Assessment*, 1(3), 203-213.
- New, M., Hulme, M. & Jones, P.D. (2000) Representing Twentieth-Century Space – Time Climate Variability Part II: Development of 1901 – 96 Monthly Grids of Terrestrial Surface Climate. *Journal of Climate*, 13(13), 2217-2238.
- New, M., Lopez, A., Dessai, S. & Wilby, R. (2007) Challenges in using probabilistic climate change information for impact assessments: an example from the water sector. *Philosophical transactions. Series A, Mathematical, physical, and engineering sciences*, 365(1857), 2117-31.

- Ng, H.Y.F. & Marsalek, J. (1992) Sensitivity of streamflow simulation to changes in climatic inputs. *Nordic Hydrology*, 23(4), 257–72.
- Nickus, U., Bishop, K., Erlandsson, M., Evans, C.D., Forsius, M., Laudon, H., Livingstone, D. M., Monteith, D. and Thies, H. (2010) Direct Impacts of Climate Change on Freshwater Ecosystems. In: Kernan, M., Battarbee, R.W. & Moss, B., eds. (2010) *Climate Change Impacts on Freshwater Ecosystems*. Oxford, UK: Wiley-Blackwell. 38-64.
- Nijssen, B., O'Donnell, G.M., Lettenmaier, D.P., Lohmann, D. & Wood, E.F. (2010) Predicting the discharge of global rivers. *Journal of Climate*, 14(15), 3307-3323.
- Nislow K.H., Folt C.L. & Parrish D.L. (2000) Spatially explicit bioenergetic analysis of habitat quality for age-0 Atlantic salmon. *Transactions of the American Fisheries Society*, 129(5), 1067–1081.
- Nislow, K.H., Einum, S. & Folt, C.L. (2004) Testing predictions of the critical period for survival concept using experiments with stocked Atlantic salmon. *Journal of Fish Biology*, 65(SupplementA), 188–200.
- Nislow, K.H. & Armstrong, J.D. (2011) Towards a life-history-based management framework for the effects of flow on juvenile salmonids in streams and rivers. *Fisheries Management and Ecology*, [in press].
- Nislow, K.H., Magilligan, F.J., Folt C.L. & Kennedy, B.P. (2002) Within-basin variation in the short-term effects of major flood on stream fishes and invertebrates. *Journal of Freshwater Ecology*, 17(2), 305–318.
- O'Grady, M.F. (1993) Initial observations on the effects of various levels of deciduous bankside vegetation on salmonid stocks in Irish waters. *Aquaculture and Fisheries Management*, 24(4), 563–573.
- O'Sullivan, A. (1993) Site synopsis, Owenduff/Nepin complex, ASI survey. National Parks and Wildlife service. Unpublished.
- Oberkampf, W.L., DeLand, S.M., Rutherford, B.M., Diegert, K.V. & Alvin, K.F. (2002) Error and uncertainty in modeling and simulation. *Reliability Engineering & System Safety*, 75(3), 333-357.
- Oerlemans, J. (2005) Extracting a climate signal from 169 glacier records. *Science*, 308(5722), 675-677.
- Olden, J.D., & Naiman, R.J. (2010) Incorporating thermal regimes into environmental flows assessments: modifying dam operations to restore freshwater ecosystem integrity. *Freshwater Biology*, 55(1), 86-107.
- Orr, J.C., Fabry, V.J., Aumont, O., Bopp, L., Doney, S.C., Feely, R.A, Gnanadesikan, A., *et al.* (2005) Anthropogenic ocean acidification over the twenty-first century and its impact on calcifying organisms. *Nature*, 437(7059), 681-6.

- Orth, D.J. & Maughan, O.E. (1982) Evaluation of the incremental methodology for recommending instream flows for fishes. *Transactions of the American Fisheries Society*, 111(4), 113-145.
- Ortiz, C., Karlton, E., Stendahl, J., Gärdenäs, A.I., & Ågren, G.I. (2011) Modelling soil carbon development in Swedish coniferous forest soils—An uncertainty analysis of parameters and model estimates using the GLUE method. *Ecological Modelling*, 222(17), 3020-3032.
- Osborn, T.J., Hulme, M., Jones, P.D. & Basnett, T.A. (2000) Observed trends in the daily intensity of United Kingdom precipitation. *International Journal of Climatology*, 20(4), 347–364.
- Osborn, T.J. & Hulme, M. (2002) Evidence for trends in heavy rainfall events over the UK. *Philosophical transactions. Series A, Mathematical, physical, and engineering sciences*, 360(1796), 1313-25.
- Ottaway, E.M. & Clarke, A. (1981) A preliminary investigation into the vulnerability of young trout (*Salmo trutta L.*) and Atlantic salmon (*S. salar L.*) to downstream displacement by high water velocities. *Journal of Fish Biology*, 19(2), 135–145.
- Ottersen, G., Planque, B., Belgrano, A., Post, E., Reid, P., & Stenseth, N. (2001) Ecological effects of the North Atlantic Oscillation. *Oecologia*, 128(1), 1-14.
- Ottersen, G., Alheit, J., Drinkwater, K. F., Friedland, K. D., Hagen, E. & Stenseth, N. C. (2004). The response of fish populations to ocean climate fluctuations. In: Stenseth, N.C., Ottersen, G., Hurrell, J.W. & Belgrano, A., eds. (2004) *Marine Ecosystems and Climate Variation*. Oxford, UK: Oxford University Press. 73–94.
- Page, T., Whyatt, J.D., Beven, K.J., & Metcalfe, S.E. (2004) Uncertainty in modelled estimates of acid deposition across Wales: a GLUE approach. *Atmospheric Environment*, 38(14), 2079-2090.
- Palmer, T.N. & Räisänen, J. (2002) Quantifying the risk of extreme seasonal precipitation events in a changing climate. *Nature*, 415(6871), 512-4.
- Palmer, T.N., Doblas-Reyes, F.J., Hagedorn, R., Alessandri, A., Gualdi, S., Andersen, U., Feddersen, H., *et al.* (2004) Development of a European Multimodel Ensemble System for Seasonal-To-Interannual Prediction (Demeter). *Bulletin of the American Meteorological Society*, 85(6), 853-872.
- Panagoulia, D. (1992) Hydrological modelling of a medium-size mountainous catchment from incomplete meteorological data. *Journal of Hydrology*, 137(1-4), 279-310.
- Panofsky, H.W. & Brier, G.W. (1968) *Some Applications of Statistics to Meteorology*. Philadelphia, USA: The Pennsylvania State University Press.
- Pappenberger, F. & Beven, K.J. (2006) Ignorance is bliss: Or seven reasons not to use uncertainty analysis. *Water Resources Research*, 42(5), 1-8.

- Parasiewicz, P. (2001) MesoHABSIM: a concept for application of instream flow models in river restoration planning. *Fisheries*, 26(9), 6–13.
- Parker, M.M. (1977) *Lough Furnace, County Mayo; physical and chemical studies of an Irish saline lake, with reference to the biology of Neomysis integer*. Unpublished Ph.D. thesis, Trinity College, Dublin.
- Parkin, G., O'Donnell, G., Ewen, J., Bathurst, J.C., O'Connell, P.E. & Lavabre, J., (1996) Validation of catchment models for predicting land-use and climate change impacts. 1. Case study for a Mediterranean catchment. *Journal of Hydrology*, 175(1-4), 595–613.
- Parmesan, C. & Yohe, G. (2003) A globally coherent fingerprint of climate change impacts across natural systems. *Nature*, 421(6918), 37–42.
- Parmesan, C. (2006) Ecological and Evolutionary Responses to Recent Climate Change. *Annual Review of Ecology, Evolution, and Systematics*, 37(1), 637-669.
- Parrish, D.L., Behnke, R.J., Gephard, S.R., McCormick, S.D. & Reeves, G.H. (1998) Why aren't there more Atlantic salmon (*Salmo salar*)? *Canadian Journal of Fisheries and Aquatic Sciences*, 55(S1), 281-287.
- Parry, M.L., ed. (2000) *Assessment of potential effects and adaptations for climate change in Europe*. The Europe ACACIA Project. Jackson Environment Institute, University of East Anglia, Norwich, UK.
- Paturel, J.E., Servat, E. & Vassiliadis, A. (1995) Sensitivity of conceptual rainfall-runoff algorithms to errors in input data - case of the GR2M model. *Journal of Hydrology*, 168(1-4), 111-125.
- Paudel, M., Nelson, E.J., Downer, C.W. & Hotchkiss, R. (2011) Comparing the capability of distributed and lumped hydrologic models for analyzing the effects of land use change. *Journal of Hydroinformatics*, 13(3), 461.
- Perkins, D.M., Reiss, J., Yvon-Durocher, G. & Woodward, G. (2010) Global change and food webs in running waters. *Hydrobiologia*, 657(1), 181-198.
- Perkins, S.E., Pitman, A.J., Holbrook, N.J. & McAneney, J. (2007) Evaluation of the AR4 climate models' simulated daily maximum temperature, minimum temperature, and precipitation over Australia using probability density functions. *Journal of Climate*, 20(17), 4356–4376.
- Perry, A.L., Low, P.J., Ellis, J.R. & Reynolds, J.D. (2005) Climate change and distribution shifts in marine fishes. *Science*, 308(5730), 1912–1915.
- Petersen-Øverleir, A. & Reitan, T. (2009) Accounting for rating curve imprecision in flood frequency analysis using likelihood-based methods. *Journal of Hydrology*, 366(1-4), 89-100.
- Petit, J., Jouzel, J., Raynaud, D. & Barkov, N. (1999) Climate and atmospheric history of the past 420,000 years from the Vostok ice core, Antarctica. *Nature*, 399(6735), 429-436.

- Petrow, T. & Merz, B. (2009) Trends in flood magnitude, frequency and seasonality in Germany in the period 1951–2002. *Journal of Hydrology*, 371(1-4), 129-141.
- Peyronnet, A., Friedland, K. D., Maoileidigh, N.Ó., Manning, M., & Poole, W.R. (2007) Links between patterns of marine growth and survival of Atlantic salmon *Salmo salar*, L. *Journal of Fish Biology*, 71(3), 684-700.
- Philipp, A., Della-Marta, P.M., Jacobeit, J., Fereday, D.R., Jones, P.D., Moberg, A. & Wanner, H. (2007) Long-Term Variability of Daily North Atlantic–European Pressure Patterns since 1850 Classified by Simulated Annealing Clustering. *Journal of Climate*, 20(16), 4065-4095.
- Piani, C., Frame, D.J., Stainforth, D.A. & Allen, M.R. (2005) Constraints on climate change from a multi-thousand member ensemble of simulations. *Geophysical Research Letters*, 32 (23), 1-5.
- Piani, C., Haerter, J. & Coppola, E. (2010a) Statistical bias correction for daily precipitation in regional climate models over Europe. *Theoretical and Applied Climatology*, 99(1-2), 187–192.
- Piani, C., Weedon, G., Best, M., Gomes, S., Viterbo, P., Hagemann, S. & Haerter, J. (2010b) Statistical bias correction of global simulated daily precipitation and temperature for the application of hydrological models. *Journal of Hydrology*, 395(3-4), 199–215.
- Pilling, C.G. & Jones, J.A.A. (1999) High resolution climate change scenarios: implications for British runoff. *Hydrological Processes*, 13(17), 2877–2895.
- Pilling, C.G. & Jones, J.A.A., (2002). The impact of future climate change on seasonal discharge, hydrological processes and extreme flows in the Upper Wye experimental catchment, Mid-Wales. *Hydrological Processes*, 16(6), 1201-1213.
- Plummer, D., Caya, D., Coté, H., Frigon, A., Côté, H., Giguère, M., *et al.* (2006) Climate and climate change over North America as simulated by the Canadian regional climate model. *Journal of Climate*, 19(13), 3112–3132.
- Poff, N.L. & Ward, J.V. (1989) Implications of stream flow variability and predictability for lotic community structure: a regional analysis of stream flow patterns, *Canadian Journal of Fisheries and Aquatic Sciences*, 46(10), 1805–1818.
- Poff, N.L. Allan, J.D., Bain, M.B., Karr, J.R., Prestegard, K.L., Richter, B.D., Sparks, R.E., *et al.* (1997) The Natural Flow Regime. *BioScience*, 47(11), 769-784.
- Poff, N.L. & Zimmerman, J.K.H. (2010) Ecological responses to altered flow regimes: a literature review to inform the science and management of environmental flows. *Freshwater Biology*, 55(1), 194-205.
- Poff, N.L., Richter, B.D., Arthington, A.H., Bunn, S.E., Naiman, R.J., Kendy, E., Acreman, M., *et al.* (2010) The ecological limits of hydrologic alteration (ELOHA): a new framework for developing regional environmental flow standards. *Freshwater Biology*, 55 (1), 147-170.

- Polyak, L., Alley, R.B., Andrews, J.T., Brigham-Grette, J., Cronin, T.M., Darby, D.A., Dyke, A.S., *et al.* (2010) History of sea ice in the Arctic. *Quaternary Science Reviews*, 29(15-16), 1757-1778.
- Pörtner, H.O. & Knust, R. (2007) Climate change affects marine fishes through the oxygen limitation of thermal tolerance. *Science*, 315(5808), 95-7.
- Power M.E., Sun A., Parker G., Dietrich W.E. & Wootton J.T. (1995) Hydraulic food-chain models. *BioScience*, 45(3), 159–167.
- Price, J.S. (1992) Blanket bog in Newfoundland: Part 2. Hydrological processes. *Journal of Hydrology*, 135(1-4), 103–119.
- Pringle, C. (2003) What is hydrologic connectivity and why is it ecologically important? *Hydrological Processes*, 17(13), 2685-2689.
- Prudhomme, C., Reynard, N. & Crooks, S. (2002) Downscaling of global climate models for flood frequency analysis: where are we now? *Hydrological Processes*, 16(6), 1137–1150.
- Prudhomme, C., Jakob, D. & Svensson, C. (2003) Uncertainty and climate change impact on the flood regime of small UK catchments. *Journal of Hydrology*, 277(1-2), 1-23.
- Prudhomme, C. & Davies, H. (2008a) Assessing uncertainties in climate change impact analyses on the river flow regimes in the UK. Part 1: baseline climate. *Climatic Change*, 93(1-2), 177-195.
- Prudhomme, C. & Davies, H. (2008b) Assessing uncertainties in climate change impact analyses on the river flow regimes in the UK. Part 2: future climate. *Climatic Change*, 93(1-2), 197-222.
- Quinn, P.F., Beven, K.J. & Lamb, R. (1995). The $\ln(a/\tan b)$ index: how to calculate it and how to use it within the TOPMODEL framework. *Hydrological Processes*, 9(2) 161–182.
- Racsko, P., Szeidl, L. & Semenov, M. (1991) A serial approach to local stochastic weather models. *Ecological Modelling*, 57(1-2), 27–41.
- Radu, R., Déqué, M. & Somot, S. (2008) Spectral nudging in a spectral regional climate model. *Tellus A*, 60(5), 898–910.
- Raftery, A.E., Gneiting, T., Balabdaoui, F. & Polakowski, M. (2005) Using Bayesian model averaging to calibrate forecast ensembles. *Monthly Weather Review*, 133(5), 1155–1174.
- Rahel, F.J. & Olden, J.D. (2008) Assessing the effects of climate change on aquatic invasive species. *Conservation biology*, 22(3), 521-33.
- Räisänen, J. & Palmer, T.N. (2001) A probability and decision-model analysis of a multimodel ensemble of climate change simulations. *Journal of Climate*, 14(15), 3212–26.

- Räisänen, J. (2007) How reliable are climate models? *Tellus A*, 59(1), 2-29.
- Reed, T.E., Schindler, D.E., Hague, M.J., Patterson, D. a, Meir, E., Waples, R.S. & Hinch, S.G. (2011) Time to evolve? Potential evolutionary responses of Fraser river sockeye salmon to climate change and effects on persistence. *PLoS one*, 6(6),1-13.
- Refsgaard, J.C., van der Sluijs, J.P., Brown, J., & van der Keur, P. (2006) A framework for dealing with uncertainty due to model structure error. *Advances in Water Resources*, 29(11), 1586-1597.
- Refsgaard, J.C, Vandersluijs, J., Hojberg, A. & Vanrolleghem, P. (2007) Uncertainty in the environmental modelling process – A framework and guidance. *Environmental Modelling & Software*, 22(11), 1543-1556.
- Refsgaard, J.C. & Storm, B. (1996) Construction, calibration and validation of hydrological models. In: Abbot, M.B., Refsgaard, J.C., eds. (1996) *Distributed Hydrological Modelling*. Kluwer, Dordrecht, The Netherlands: Springer.19-39.
- Reiser, D.W., Wesche, T.A., Estes, C. (1989) Status of instream flow legislation and practise in North America. *Fisheries*, 14(2), 22–29.
- Reist, J.D., Wrona, F.J., Prowse, T.D., Power, M., Dempson, J.B., King, J.R. & Beamish, R.J. (2006) An overview of effects of climate change on selected Arctic freshwater and anadromous fishes. *Ambio*, 35(7), 381–387.
- Renard, B., Kavetski, D., Kuczera, G., Thyer, M. & Franks, S.W. (2010) Understanding predictive uncertainty in hydrologic modeling: The challenge of identifying input and structural errors. *Water Resources Research*, 46(W05521).
- Revelle, R.R. & Waggoner, P.E. (1983) Effect of a carbon dioxide-induced climatic change on water supplies in the western United State. In:*Changing Climate*. The Carbon Dioxide Assessment Committee National Academy Report 8211, Washington, D.C., USA. 419-432.
- Richardson, C.W. (1981) Stochastic simulation of daily precipitation, temperature, and solar radiation. *Water Resources Research*, 17(1), 182–90.
- Rignot, E. (2011) Is Antarctica melting? *Wiley Interdisciplinary Reviews Climate Change*, 2(3), 324-331.
- Rijnsdorp, A.D., Peck, M.A., Engelhard, G.H., Möllmann, C. & Pinnegar, J.K. (2009) Resolving the effect of climate change on fish populations. *ICES Journal of Marine Science*, 66(7), 1570–1583.
- Riley, W.D., Ibbotson, A.T., Lower, N., Cook, A.C., Moore, A., Mizuno, S., Pinder, A. C. *et al.* (2008) Physiological seawater adaptation in juvenile Atlantic salmon (*Salmo salar*) autumn migrants. *Freshwater Biology*, 53(4), 745-755.
- Riley, W.D., Maxwell, D.L., Pawson, M.G. & Ives, M.J. (2009) The effects of low summer flow on wild salmon (*Salmo salar*), trout (*Salmo trutta*) and grayling (*Thymallus thymallus*) in a small stream. *Freshwater Biology*, 54(12), 2581-2599.

- Robock, A., Konstantin, Y.V., Srinivasan, J.K., Entin, J.K., Hollinger, N.A., Speranskaya, N.A., Liu, S. & Nampkai, A. (2000) The global soil moisture data bank. *Bulletin of the American Meteorological Society*, 81(6), 1281–1299.
- Robson, A.J., Whitehead, P.G. & Johnson, R.C. (1993) An application of a physically based semi-distributed model to the Balquhiddy catchments. *Journal of Hydrology*, 145(3-4), 357-370.
- Robson, A.J., Jones, T.K., Reed, D.W. & Bayliss, A.C. (1998) A study of national trend and variation in UK floods. *International Journal of Climatology*, 18(2), 165–182.
- Robson, A.J. (2002) Evidence for trends in UK flooding. *Transactions of the Royal Society - Series A: Mathematical, Physical and Engineering Sciences*, 360(1796), 1327–1343.
- Roe, G.H. & Baker, M.B. (2007) Why is climate sensitivity so unpredictable? *Science* 318(5850), 629–632.
- Roeckner, E., Bäuml, G., Bonaventura, L., Brokopf, R., Esch, M., Giorgetta, M., Hagemann, S., Kirchner, I., Kornblueh, L., Manzini, E., Rhodin, A., Schlese, U., Schulzweida, U., Tompkins, A., (2003) *The Atmospheric General Circulation Model ECHAM5 Part I: Model Description*. Max-Planck Institute for Meteorology, Report No. 349, Hamburg, Germany, 1-127.
- Rojas, R., Feyen, L., & Dassargues, A. (2008) Conceptual model uncertainty in groundwater modelling: Combining generalized likelihood uncertainty estimation and Bayesian model averaging. *Water Resources Research*, 44(12), 1-16.
- Rojas, R. & Dassargues, A. (2009) Sensitivity analysis of prior model probabilities and the value of prior knowledge in the assessment of conceptual model uncertainty in groundwater modelling. *Hydrological Processes*, 23(8), 1131-1146.
- Rojas, R., Kahunde, S., Peeters, L., Batelaan, O., Feyen, L., & Dassargues, A. (2010) Application of a multimodel approach to account for conceptual model and scenario uncertainties in groundwater modelling. *Journal of Hydrology*, 394(3-4), 416-435.
- Root, T.L., Price, J.T., Hall, K.R., Schneider, S.H., Rosenzweig, C. & Pounds, J.A. (2003) Fingerprints of global warming on wild animals and plants. *Nature* 421(6918), 57–60.
- Rougier, J., Sexton, D.M.H., Murphy, J.M. & Stainforth, D. (2009) Analyzing the Climate Sensitivity of the HadSM3 Climate Model Using Ensembles from Different but Related Experiments. *Journal of Climate*, 22(13), 3540-3557.
- Rowell, D.P. (2006) A Demonstration of the Uncertainty in Projections of UK Climate Change Resulting from Regional Model Formulation. *Climatic Change*, 79(3-4), 243-257.
- Roy, D.B. & Sparks, T.H. (2000) Phenology of British butterflies and climate change. *Global Change Biology*, 6(4), 407–16

- Royer, D.L. (2006) CO₂-forced climate thresholds during the Phanerozoic. *Geochimica et Cosmochimica Acta*, 67(12), 665–5675.
- Ruark, M.D., Niemann, J.D., Asce, M., Greimann, B.P. & Arabi, M. (2011) Method for Assessing Impacts of Parameter Uncertainty in Sediment Transport Modeling Applications. *Journal of Hydraulic Engineering*, 137(6), 623-636.
- Rummukainen, M. (2010) State-of-the-art with regional climate models. *Wiley Interdisciplinary Reviews Climate Change*, 1(1), 82-89.
- Sala, O.E. (2000) Global Biodiversity Scenarios for the Year 2100. *Science*, 287(5459), 1770-1774.
- Salinger, D.H. & Anderson, J.J. (2006) Effects of water temperature and flow on adult salmon migration swim speed and delay. *Transactions of the American Fisheries Society*, 135(1), 188–199.
- Saltelli, A. (2000) Fortune and future of sensitivity analysis. In: Saltelli, A., Chan, K., Scott, E.M., eds. (2000) *Sensitivity Analysis*. Chichester, UK: Wiley. 421–426.
- Samuelsson, P., Jones, C., Willén, U., Ullerstig, A., Gollvik, S., Hansson, U., Kjellström, E., Nikulin, G., and Wyser, K. (2011) The Rossby Centre Regional Climate Model RCA3: Model description and performance. *Tellus*, 63A(1), 4-23.
- Sánchez, E., Romera, R., Gaertner, M.A., Gallardo, C., Castro, M. (2009) A weighting proposal for an ensemble of regional climate models over Europe driven by 1961–2000 ERA40 based on monthly precipitation probability density function. *Atmospheric Science Letters*, 10(4), 241–248.
- Sanchez-Gomez, E., Somot, S. & Déqué, M. (2009) Ability of an ensemble of regional climate models to reproduce weather regimes over Europe–Atlantic during the period 1961–2000. *Climate Dynamics*, 33(5), 723–736.
- Sanderson, B.M., Knutti, R., Aina, T., Christensen, C., Faull, N., Frame, D.J., Ingram, W.J., *et al.* (2008) Constraints on Model Response to Greenhouse Gas Forcing and the Role of Subgrid-Scale Processes. *Journal of Climate*, 21(11), 2384-2400.
- Scanlon, T.M., Ruffensperger, J.P., Hornberger, G.M., & Clapp, R.B. (2000) Shallow subsurface storm flow in a forested headwater catchment: Observations and modeling using a modified TOPMODEL. *Water Resources*, 36(9), 2575-2586.
- Schaake, J.C. (1990) From Climate to Flow. In: P.E. Waggoner, ed. (1990) *Climatic Change and U.S. Water Resources*. New York, USA: Wiley & Sons. 177–206.
- Schindler, D.W., Bayley, S.E., Parker, B.R., Beaty, K.G., Dana, R., Fee, E.J., Schindler, E.U., *et al.* (1990) The Effects of Climatic Warming on the Properties of Boreal Lakes and Streams at the Experimental Lakes Area, Northwestern Ontario. *Limnology and Oceanography*, 41(5), 1004-1017.
- Schindler, D. (2001) The cumulative effects of climate warming and other human stresses on Canadian freshwaters in the new millennium. *Canadian Journal of Fisheries and Aquatic Sciences*, 58(1) 18-29,

- Schmidli, J., & Frei, C. (2005) Trends of heavy precipitation and wet and dry spells in Switzerland during the 20th century. *International Journal of Climatology*, 25(6), 753-771.
- Schmidli, J., Frei, C. & Vidale, P.L. (2006) Downscaling from GCM precipitation: a benchmark for dynamical and statistical downscaling methods. *International Journal of Climatology*, 26(5), 679–689.
- Schmidli, J., Goodess, C.M. & Frei, C. (2007) Statistical and Dynamical Downscaling of Precipitation: An Evaluation and Comparison of Scenarios for the European Alps. *Journal of Geophysical Research*, 112(D4), 1-20.
- Schmittner, A., Urban, N.M., Shakun, J.D., Mahowald, N.M., Clark, P.U., Bartlein, P.J., Mix, A.C., *et al.* (2011) Climate Sensitivity Estimated from Temperature Reconstructions of the Last Glacial Maximum. *Science*, 334(6061), 1385-1388.
- Schneeberger, C., Blatter, H., Abe-Ouchi, A. & Wild, M. (2003) Modelling changes in the mass balance of glaciers of the northern hemisphere for a transient 2×CO₂ scenario. *Journal of Hydrology*, 282(1–4), 145–163.
- Schneider, M., Jorde, K., Zollner, F. & Kerle, F. (2001) *Development of a user-friendly software for ecological investigations on river systems, integration of a fuzzy rule-based approach.* In: Proceedings Environmental Informatics 2001, 15th International Symposium, Informatics for Environmental Protection, ETH Zurich, Switzerland.
- Schneider, S.H. & Lane, J. (2006) What Is ‘Dangerous’ Climate Change? *Nature*, 41(6833), 1-6.
- Schneider, S.H. (1983) CO₂, Climate and Society: A Brief Overview. In: Chen, R.S., Boulding, E. & Schneider, S.H., eds. (1983) *Social Science Research and Climate Change: An Interdisciplinary Appraisal.* Dordrecht, The Netherlands: D. Reidel Publishing. 9–15.
- Schönwiese, C.D. & Rapp, J. (1997). *Climate Trend Atlas of Europe Based on Observations 1891 –1990.* Dordrecht, The Netherlands: Kluwer Academic Publishers.
- Schoof, J.T. & Pryor, S. (2001) Downscaling temperature and precipitation: A comparison of regression-based methods and artificial neural networks. *International Journal of Climatology*, 21(7), 773–790.
- Schumann, A., Funke, R., & Schultz, G. (2000) Application of a geographic information system for conceptual rainfall-runoff modeling. *Journal of Hydrology*, 240(1-2), 45–61.
- Scinocca, J.F., McFarlane, N.A., Lazare, M., Li, J. & Plummer, D. (2008) The CCCma third generation AGCM and its extension into the middle atmosphere. *Atmospheric Chemistry and Physics*, 8(2), 7883–7930.
- Scott, P.S. & Kettleborough, J.A. (2002) Origins and estimates of uncertainty in predictions of twenty-first century temperature rise. *Nature*, 416(6882), 723–726.

- Sefton, C.E.M. & Boorman, D.B. (1997). A regional investigation into climate change impacts on UK streamflows. *Journal of Hydrology*, 195(14), 26-44.
- Seibert, J. (1997) Estimation of parameter uncertainty in the HBV model. *Nordic Hydrology*, 28(4-5), 247-262
- Seibert, J. (1997) *On TOPMODEL's ability to simulate groundwater dynamics*. In: ed. Dickkrüger, B., Kirkby, M.J. & Schröder, U. (1997) *Regionalization in Hydrology*. IAHS Publication, 254, 211-220.
- Seibert, J. (1999) Regionalisation of parameters for a conceptual rainfall-runoff model. *Agricultural and Forest Meteorology*, 98(1), 279-293
- Seibert, J. (2000) Multi-criteria calibration of a conceptual rainfall-runoff model using a genetic algorithm. *Hydrology and Earth System Sciences*, 4(2), 215-224.
- Seibert, J. & Beven, K.J. (2009) Gauging the ungauged basin: how many discharge measurements are needed? *Hydrology and Earth System Sciences*, 13(6), 883-892.
- Semenov, M.A. & Barrow, E.M. (1997) Use of a stochastic weather generator in the development of climate change scenarios. *Climatic Change*, 35(4), 397-414.
- Semenov, M.A. Brooks, R.J. Barrow, E.M. & Richardson, C.W. (1998) Comparison of the WGEN and LARS-WG stochastic weather generators for diverse climates, *Climate Research*, 10(2), 95–107.
- Semenov, M.A. & Brooks, R.J. (1999) Spatial interpolation of the LARS-WG stochastic weather generator in Great Britain. *Climate Research*, 11(2), 137–148.
- Semenov, M.A. (2007) Development of high-resolution UKCIP02-based climate change scenarios in the UK. *Agricultural and Forest Meteorology*, 144, (1-2), 127-138.
- Semenov, M.A. (2009) Impacts of climate change on wheat in England and Wales. *Journal of the Royal Society Interface the Royal Society*, 6(33), 343–350
- Semenov, M.A. & Halford, N.G. (2009) Identifying target traits and molecular mechanisms for wheat breeding under a changing climate. *Journal of Experimental Botany*, 60(10), 2791-2804.
- Semenov, M.A. & Stratonovitch, P. (2010) Use of multi-model ensembles from global climate models for assessment of climate change impacts. *Climate Research*, 41(1), 1-14.
- Senerpont Domis, L.N., Mooij, W.M. & Huisman, J. (2007) Climate-induced shifts in an experimental phytoplankton community: a mechanistic approach. *Hydrobiologia*, 584(1), 403-413.
- Senior, C.A. (1999) Comparison of mechanisms of cloud-climate feedbacks in GCMs. *Journal of Climate*, 12(5), 1480–1489.

- Shabalova, M., van Deursen, W., & Buishand, T. (2003) Assessing future discharge of the river Rhine using regional climate model integrations and a hydrological model. *Climate Research*, 23, 233–246.
- Sheffield, J., & Wood, E.F. (2007) Projected changes in drought occurrence under future global warming from multi-model, multi-scenario, IPCC AR4 simulations. *Climate Dynamics*, 31(1), 79-105.
- Shepherd, A. & Wingham, D. (2007) Recent Sea-Level Contributions of the Antarctic and Greenland Ice Sheets. *Science*, 315(5818), 1529-1532.
- Shrestha, D.L., Kayastha, N., & Solomatine, D.P. (2009) A novel approach to parameter uncertainty analysis of hydrological models using neural networks. *Hydrological Earth System Science*, 6(2), 1235-1248.
- Sieber, A. & Uhlenbrook, S. (2005) Sensitivity analyses of a distributed catchment model to verify the model structure. *Journal of Hydrology*, 310(1-4), 216-235.
- Siebert, J. (2005) *HBV Light Version 2 User's Manual*. University of Stockholm.
- Singh, V.P. & Woolhiser, D.A. (2002) Mathematical Modeling of Watershed Hydrology. *Journal of Hydrologic Engineering*, 7(4), 270-292.
- Slonosky, V.C., Jones, P.D., Davies, T.D. (2001) Atmospheric circulation and surface temperature in Europe from the 18th century to 1995. *International Journal of Climatology*, 21(1), 63–75.
- Sloughter, J.M.L., Raftery, A.E., Gneiting, T. & Fraley, C. (2007) Probabilistic quantitative precipitation forecasting using Bayesian model averaging. *Monthly Weather Review*, 135(9), 3209-3220.
- Smith, R.M.S., Evans, D.J. & Wheater, H.S. (2005) Evaluation of two hybrid metric-conceptual models, for simulating phosphorus transfer from agricultural land in the river enborne, a lowland UK catchment, *Journal of Hydrology*, 304(1-4), 366–380.
- Solomon, D.J., Sambrook, H.T. & Broad, K.J. (1999) *Salmon migration and river flow. Results of tracking radio tagged salmon in six rivers in South West England*. Research & Development Publication 4, Environment Agency, Almondsbury.
- Solomon, D.J. & Sambrook, H.T. (2004) Effects of hot dry summers on the loss of Atlantic salmon, *Salmo salar*, from estuaries in South West England. *Fisheries Management and Ecology*, 11(5), 353–363.
- Solomon, S., Rosenlof, K. H., Portmann, R. W., Daniel, J. S., Davis, S. M., Sanford, T. J. & Plattner, G.-K. (2010) Contributions of stratospheric water vapor to decadal changes in the rate of global warming. *Science*, 327(5970), 1219-23.
- Song, X., Zhan, C., Kong, F., & Xia, J. (2011) Advances in the study of uncertainty quantification of large-scale hydrological modeling system. *Journal of Geographical Sciences*, 21(5), 801-819.

- Souvignet, M. & Heinrich, J. (2011) Statistical downscaling in the arid central Andes: uncertainty analysis of multi-model simulated temperature and precipitation. *Theoretical and Applied Climatology*, 106(1-2), 229-244.
- Spak, S., Holloway, T. & Lynn, B. (2007) A comparison of statistical and dynamical downscaling for surface temperature in North America. *Journal of Geophysical Research*, 112(D08101), 1-37.
- Spear, R.C. & Hornberger, G.M. (1980) Eutrophication in Peel Inlet, II, Identification of critical uncertainties via generalized sensitivity analysis. *Water Research*, 14(1), 43–49.
- Stainforth, D.A., Aina, T., Christensen, C., Collins, M., Faull, N., Frame, D.J., Kettleborough, J., Knight, S., Martin, A., Murphy, J., Piani, C., Sexton, D., Smith, L.A., Spicer, R.A., Thorpe, A.J., Allen, M.R. (2005) Uncertainty in predictions of the climate response to rising levels of greenhouse gases. *Nature*, 433(7024), 403–406
- Stalnaker, C. B., Lamb, B. L., Henriksen, J., Bovee, K. & Bartholow, J. (1995) *The Instream Flow Incremental Methodology: a Primer for IFIM*. United States Geological Survey Biological Report 29, Washington, DC, USA.
- STARDEX (2005) *Statistical and Regional dynamical Downscaling of Extremes for European regions final report*. [online]. Available at: http://www.cru.uea.ac.uk/projects/stardex/reports/STARDEX_FINAL_REPORT.pdf. (accessed May 2011).
- Stedinger, J.R., Vogel, R.M., Lee, S.U., & Batchelder, R. (2008) Appraisal of the generalized likelihood uncertainty estimation (GLUE) method. *Water Resources Research*, 44(W00B06), 1-17.
- Steele-Dunne, S., Lynch, P., Mcgrath, R., Semmler, T., Wang, S., Hanafin, J. & Nolan, P. (2008) The impacts of climate change on hydrology in Ireland. *Journal of Hydrology*, 356(1-2), 28-45.
- Stefan, H., Fang, X. & Hondzo, M. (1998) Simulated climate change effects on year-round water temperatures in temperate zone lakes. *Climatic Change*, 40(3-4), 547-576.
- Stefansson, S., McGinnity, P., Björnsson, B.T., Schreck, C.B. & McCormicke, S.D. (2003) The importance of smolt development to salmon conservation, culture, and management: perspectives from the 6th International Workshop on Salmonid Smoltification. *Aquaculture*, 222(1-4), 1-14.
- Stern, R. & Coe, R. (1984) A model fitting analysis of rainfall data. *Journal of the Royal Statistical Society Series A*, 147(1), 1–34.
- Stewart, L. (1969) *Criteria for safeguarding fisheries, fish migration and angling in rivers*. Yearbook of the Association of River Authorities, 134-149.
- Stillman, J.H. (2003) Acclimation capacity underlies susceptibility to climate change. *Science*, 301(5629), 65.

- Stone, D.A., Weaver, A.J. & Zwiers, F.W. (1999) Trends in Canadian precipitation intensity. *AtmosphereOcean*, 38(2), 321 – 47.
- Stone, D.A., Allen, M.R., Selten, F., Kliphuis, M, & Stott, P.A. (2007) The detection and attribution of climate change using an ensemble of opportunity. *Journal of Climate*, 20(3), 504–516.
- Straile, D., Jöhnk, K., Rossknecht, H., Strailel, D. & Johnk, K. (2012) Complex effects of winter warming on the physicochemical characteristics of a deep lake. *Limnology*, 48(4), 1432-1438.
- Strothotte, E., Chaput, G.J. & Rosenthal, H. (2005) Seasonal growth of wild Atlantic salmon juveniles and implications on age at smoltification. *Journal of Fish Biology*, 67(6), 1585–1602.
- Sultana, Z. & Coulibaly, P. (2011) Distributed modelling of future changes in hydrological processes of Spencer Creek watershed. *Hydrological Processes*, 25(8), 1254-1270.
- Sumner, N.R., Fleming, P.M. & Bates, B.C. (1997) Calibration of a modified SFB model for twenty-five Australian catchments using simulated annealing. *Journal of Hydrology* 197(1-4), 166–188.
- Swansburg, E., Chaput, G., Moore, D., Caisse, D. & El-Jabi, N. (2002) Size variability of juvenile Atlantic salmon: links to environmental conditions. *Journal of Fish Biology*, 61(3), 661–683.
- Tans, P. (2009) An accounting of the observed increase in oceanic and atmospheric CO₂ and an outlook for the future. *Oceanography* 22(4), 26–35.
- Tao, F., Yokozawa, M., Hayashi, Y. & Lin, E. (2003) Changes in agricultural water demands and soil moisture in China over the last half-century and their effects on agricultural production. *Agriculture and Forest Meteorology*, 118(3-4), 251–261.
- Taylor, K.E. (2001) Summarizing multiple aspects of model performance in a single diagram. *Journal of Geophysical Research*, 106(D7), 7183–7192.
- Tebaldi, C. (2004) Regional probabilities of precipitation change: A Bayesian analysis of multimodel simulations. *Geophysical Research Letters*, 31(24), 1-5.
- Tebaldi, C. Smith, D. Nychka, & L.O. Mearns, (2005) Quantifying uncertainty in projections of regional climate change: A Bayesian approach to the analysis of multimodel ensembles. *Journal of Climate*, 18(10), 1524–1540.
- Tebaldi, C. & Knutti, R. (2007) The use of the multi-model ensemble in probabilistic climate projections. *Philosophical Transactions of the Royal Society a-Mathematical Physical and Engineering Sciences*, 365(1857), 2053-2075.
- Tennant, D.L. (1976) Instream flow regimes for fish, wildlife, recreation and related environmental resources. *Fisheries*, 1(4), 6-10.

- Tetzlaff, D., Soulsby, C., Gibbins, C.N., Bacon, P.J & Youngson, A.F. (2005) An approach to assessing hydrological influences on feeding opportunities of juvenile Atlantic salmon (*Salmo salar*): a case study of two contrasting years in a small, nursery stream. *Hydrobiologia*, 549(1), 65–77.
- Tetzlaff, D., Gibbins, C., Bacon, P., Youngson, A. and Soulsby, C. (2008) Influence of hydrological regimes on the pre-spawning entry of Atlantic salmon (*Salmo salar* L.) into an upland river. *River Research and Applications*, 24(5), 528–542.
- Teutschbein, C. & Seibert, J. (2010) Regional Climate Models for Hydrological Impact Studies at the Catchment Scale: A Review of Recent Modeling Strategies. *Geography Compass*, 4(7), 834-860.
- Teutschbein, C., Wetterhall, F. & Seibert, J. (2011) Evaluation of different downscaling techniques for hydrological climate-change impact studies at the catchment scale. *Climate Dynamics*, 37(9-10), 2087-2105.
- Tharme, R.E. (2000) An overview of environmental flow methodologies, with particular reference to South Africa. In: King, J.M., Tharme, R.E., De Villiers, M.S., eds. (2000) *Environmental Flow Assessments for Rivers: Manual for the Building Block Methodology*. Water Research Commission Technology Transfer Report No. TT131/00. Water Research Commission, Pretoria, South Africa. 15–40.
- Tharme, R.E. (2003) A global perspective on environmental flow assessment: emerging trends in the development and application of environmental flow methodologies for rivers. *River Research and Applications*, 19(5-6), 397-441.
- Thiemann, M., Trosset, M., Gupta, H. & Sorooshian, S. (2001) Bayesian recursive parameter estimation for hydrologic models. *Water Resources Research*, 37(10), 2521–2536.
- Thomas, C.D., Cameron, A., Green, R.E., Bakkenes, M., Beaumont, L.J., Collingham, Y.C., Erasmus, B.F.N., *et al.* (2004) Extinction risk from climate change. *Nature*, 427(6970), 145-8.
- Thompson, L.C., Cocherell, S. a., Chun, S.N., Cech, J.J. and Klimley, A.P. (2010) Longitudinal movement of fish in response to a single-day flow pulse. *Environmental Biology of Fishes*, 90(3), 253-261.
- Thornthwaite, C.W. & Mather, J.R. (1955) The Water Balance. *Publications in Climatology*, 8(1), 1-86.
- Thorstad, E.B., Whoriskey, F., Rikhardsen, A.H. & Aarestrup, K. (2010) Aquatic Nomads: The Life and Migrations of the Atlantic Salmon. In: Kernan, M., Battarbee, R.W. & Moss, B., eds. (2010) *Climate Change Impacts on Freshwater Ecosystems*. Oxford, UK: Wiley-Blackwell. 1-32.
- Timbal, B., Hope, P. & Charles, S. (2008) Evaluating the Consistency between Statistically Downscaled and Global Dynamical Model Climate Change Projections. *Journal of Climate*, 21(22), 6052-6059.

- Tockner, K., Pusch, M., Borchardt, D. & Lorang, M.S. (2010) Multiple stressors in coupled river-floodplain ecosystems. *Freshwater Biology*, 55(Suppl. 1), 135-151.
- Todd, C.D., Hughes, S.L., Marshall, C.T., MacLean, J.C., Lonergan, M.E., & Biuw, E.M. (2008) Detrimental effects of recent ocean surface warming on growth condition of Atlantic salmon. *Global Change Biology*, 14(5), 1–13.
- Todd, C.D., Friedland, K.D., MacLean, J.C., Hazon, N. & Jensen, A.J. (2010) Getting into Hot Water? Atlantic salmon Responses to Climate Change in Freshwater and Marine Environments. In: Aas, Ø., Einum, S., Klemetsen, A. & Skurdal, J., eds. *Atlantic Salmon Ecology*. Oxford, UK: Wiley-Blackwell. 409-432.
- Todini, E. (1996) The ARNO rainfall-runoff. *Journal of Hydrology*, 175(1-4), 339-382.
- Tomozeiu, R., Cacciamani, C., Pavan, V., Morgillo, A. & Busuioc, A. (2006) Climate change scenarios for surface temperature in Emilia-Romagna (Italy) obtained using statistical downscaling models. *Theoretical and Applied Climatology*, 90(1-2), 25-47.
- Trenberth, K.E., (1999) Conceptual framework for changes of extremes of the hydrological cycle with climate change. *Climatic Change*, 42(1), 327–339.
- Trenberth, K.E., Jones, P.D., Ambenje, P., Bojariu, R., *et al.* (2007) Observations: surface and atmospheric climate change. In: Solomon, S., Qin, D., Manning, M., Chen, Z., *et al.*, eds. (2007) *Climate Change 2007: The Physical Science Basis. Contribution of Working Group I to the Fourth Assessment Report of the Intergovernmental Panel on Climate Change*. Cambridge, UK & New York, NY, USA: Cambridge University Press.
- Trenberth, K.E., Dai, A., Rasmussen, R.M., & Parsons, D.B. (2003) The Changing Character of Precipitation. *Bulletin of the American Meteorological Society*, 84(9), 1205-1217.
- Trenberth, K.E., Fasullo, J.T. & Kiehl, J. (2009) Earth's Global Energy Budget. *Bulletin of the American Meteorological Society*, 90(3), 311-323.
- Trenberth, K.E. (2011) Changes in precipitation with climate change. *Climate Research*, 47(1), 123-138.
- Trigo, R.M. and Palutikof, J.P. (1999) Simulation of daily temperatures for climate change scenarios over Portugal: a neural network model approach. *Climate Research*, 13(1), 45-59.
- Trigo, R.M. & Palutikof, J.P. (2001) Precipitation scenarios over Iberia: A comparison between direct GCM output and different downscaling techniques. *Journal of Climate*, 14(23), 4422-4446.
- Tumbo, S.D., Mpeti, E., Tadross, M., Kahimba, F.C., Mbillinyi, B.P. and Mahoo, H.F. (2010) Application of self-organizing maps technique in downscaling GCMs climate change projections for Same, Tanzania. *Physics and Chemistry of the Earth*, 35(13-14), 608-617.

- U.S. Fish and Wildlife Service (USFWS) (1981). *Interim Regional Policy for New England Stream Flow; Recommendations*. Memorandum from H.N. Larsen, Director, Region 5 of U.S. Fish and Wildlife Service, Newton Corner, MA.
- Uhlenbrook, S., Seibert, J., Leibundgut, C. & Rhode, A. (1999) Prediction uncertainty of conceptual rainfall-runoff models caused by problems in identifying model parameters and structure. *Hydrological Sciences*, (44)5, 779-797.
- Uppala, S.M., Kllberg, P.W., Simmons, A.J., Andrae, U., Bechtold, V.D.C., Fiorino, M., Gibson, J.K., *et al.* (2005) The ERA-40 re-analysis. *Quarterly Journal of the Royal Meteorological Society*, 131(612), 2961-3012.
- Vadas, R.L. & Orth, D.J. (2001) Formulation of habitat suitability models for stream fish guilds: do the standard methods work? *Transactions of the American Fisheries Society*, 130(2), 217–235.
- van der Linden, P., & Mitchell, J., eds. (2009) *ENSEMBLES: Climate Change and its Impacts: Summary of research and results from the ENSEMBLES project*. Met Office Hadley Centre, FitzRoy Road, Exeter EX1 3PB, UK.
- van Pelt, S. C., Kabat, P., ter Maat, H.W., van den Hurk, B.J.J.M., & Weerts, A.H. (2009) Discharge simulations performed with a hydrological model using bias corrected regional climate model input. *Hydrology and Earth System Sciences*, 6(3), 4589-4618.
- van Vuuren, D.P., Feddema, J., Lamarque, J.F., Riahi, K., Rose, S., Smith, S. Hibbard, K. (2008) Work plan for data exchange between the Integrated Assessment and Climate Modeling community in support of Phase-0 of scenario analysis for climate change assessment (Representative Community Pathways). [online]. Available at: http://www.aimes.ucar.edu/docs/RCP_handshake.pdf (accessed 1st May 2011).
- Vaze, J., Post, D.A., Chiew, F.H.S., Perraud, J.-M., Viney, N.R. & Teng, J. (2010) Climate non-stationarity – Validity of calibrated rainfall–runoff models for use in climate change studies. *Journal of Hydrology*, 394(3-4), 447-457.
- Vehviläinen, B., & Lohvansuu, J. (1991) The effects of climate change on discharges and snow cover in Finland. *Hydrological Sciences Journal*, 36(2), 109–121.
- Velicogna, I. (2009) Increasing rates of ice mass loss from the Greenland and Antarctic ice sheets revealed by GRACE. *Geophysical Research Letters*, 36(19), 5-8.
- Verdonschot, P.F.M., Hering, D., Murphy, J., Jähnig, S.C., Rose, N.L., Graf, W., Brabec, K. & Sandin, L. (2010) Climate Change and the Hydrology and Morphology of Freshwater Ecosystems. In: Kernan, M., Battarbee, R.W. & Moss, B., eds. (2010) *Climate Change Impacts on Freshwater Ecosystems*. Oxford, UK: Wiley-Blackwell. 65-83.
- Vidal, J.P. & Wade, S. (2006) *Effects of Climate Change on River Flows and Groundwater Recharge: synthesis report*. UK Water industry Research Limited.

- Visser, M.E. & Both, C. (2005) Shifts in phenology due to global climate change: the need for a yardstick. *Proceedings. Biological sciences / The Royal Society*, 272(1581), 2561-9.
- Vogel, R., Zafirakou-Koulouris, A., Matalas, N.C. (2002) Frequency of record-breaking floods in the United States. *Water Resources. Research*, 37(6), 1723–1731.
- von Storch, H. (1999) On the Use of ‘Inflation’ in Statistical Downscaling. *Journal of Climate*, 12 (12), 3505–3506.
- von Storch, H., Zorita, E. & Cubasch, U. (1993) Downscaling of global climate change estimates to regional scale: An application to Iberian rainfall in wintertime, *Journal of Climate*, 6(6), 1161–1171.
- Vrac, M., Stein, M.L., Hayhoe, K. & Liang, X.-Z. (2007) A general method for validating statistical downscaling methods under future climate change. *Geophysical Research Letters*, 34(18), 1-5.
- Vrugt, J.A. (2003a) Effective and efficient algorithm for multiobjective optimization of hydrologic models. *Water Resources Research*, 39(1214), 1-19.
- Vrugt, J.A., (2003b) A Shuffled Complex Evolution Metropolis algorithm for optimization and uncertainty assessment of hydrologic model parameters. *Water Resources Research*, 39(1201), 1-16.
- Vrugt, J.A., Diks, C.G.H., Gupta, H.V., Bouten, W. & Verstraten, J.M. (2005) Improved treatment of uncertainty in hydrologic modeling: Combining the strengths of global optimization and data assimilation. *Water Resources Research*, 41(1), 1-17.
- Vrugt, J.A. & Gupta, H. (2006) Real-time data assimilation for operational ensemble streamflow forecasting. *Journal of Hydrometeorology*, 7(3), 548-565.
- Vrugt, J.A., Clark, M.P., Diks, C.G.H., Duan, Q. & Robinson, B.A. (2006) Multi-objective calibration of forecast ensembles using Bayesian model averaging. *Geophysical Research Letters*, 33(19), 2-7.
- Vrugt, J.A. & Robinson, B.A. (2007) Improved evolutionary optimization from genetically adaptive multimethod search. *Proceedings of the National Academy of Sciences of the United States of America*, 104(3), 708-11.
- Vrugt, J.A., Diks, C.G.H. & Clark, M.P. (2008) Ensemble Bayesian model averaging using Markov Chain Monte Carlo sampling. *Environmental Fluid Mechanics*, 8(5-6), 579-595.
- Vrugt, J.A., Braak, C.J.F., Gupta, H.V. & Robinson, B.A. (2009) Equifinality of formal (DREAM) and informal (GLUE) Bayesian approaches in hydrologic modeling? *Stochastic Environmental Research and Risk Assessment*, 23(7), 1011-1026.
- Wagener, T., & Wheater, H. (2006) Parameter estimation and regionalization for continuous rainfall-runoff models including uncertainty. *Journal of Hydrology*, 320(1-2), 132-154.

- Wagener, T., Boyle, D.P., Lees, M.J., Wheater, H.S., Gupta, H.V. & Sorooshian, S. (2001) A framework for development and application of hydrological models. *Hydrology and Earth System Sciences*, 5(1), 13-26.
- Wagener, T., McIntyre, N., Lees, M.J., Wheater, H.S., & Gupta, H.V. (2003) Towards reduced uncertainty in conceptual rainfall-runoff modelling: dynamic identifiability analysis. *Hydrological Processes*, 17(2), 455-476.
- Walker, K.F., Sheldon, F. & Puckridge, J.T. (1995) A perspective on dryland river ecosystems. *Regulated Rivers: Research & Management*, 11(1), 85–104.
- Walker, W.E., Harremoes, P., Rotmans, J., Van der Sluijs, J., Van Asselt, M., Janssen, P. & Von Krauss, M.P.K. (2003) Defining uncertainty: a conceptual basis for uncertainty management in model-based decision support. *Integrated Assessment*, 4(1), 5–17.
- Walsh, C.L. & Kilsby, C.G. (2007) Implications of climate change on flow regime affecting Atlantic salmon. *Civil Engineering*, 11(3), 1127-1143.
- Walter, M.T., Steenhuis, T.S., Mehta, V.K., Thongs, D., Zion, M., & Schneiderman, E. (2002) Refined conceptualization of TOPMODEL for shallow subsurface flows. *Hydrological Processes*, 16(10), 2041-2046.
- Walter, M.T., Wilks, D.S., Parlange, J.-Y. & Schneider, R.L. (2004) Increasing evapotranspiration from the conterminous United States. *Journal of Hydrometeorology*, 127(3), 405–408.
- Walther, G.R., Post, E., Convey, P., Menzel, A., Parmesan, C., Beebee, T.J.C., Fromentin, J.M., Hoegh-Guldberg, O. & Bairlein, F. (2002) Ecological responses to recent climate change. *Nature*, 416(6879), 389–395
- Warburton, J., Holden, J., & Mills, A. J., (2004). Hydrological controls of surficial mass movements in peat. *Earth-Science Reviews*, 67(1-2), 139-156.
- Warren, D., Ernst, A. & Baldigo, B. (2009) Influence of Spring Floods on Year-Class Strength of Fall- and Spring-Spawning Salmonids in Catskill Mountain Streams. *Transactions of the American Fisheries Society*, 138 (1), 200-210.
- Warren, R., Price, J., Fischlin, A., Nava Santos, S., & Midgley, G. (2010) Increasing impacts of climate change upon ecosystems with increasing global mean temperature rise. *Climatic Change*, 106(2), 141-177.
- Arnekk, N. & Reynard, N. (1989) *Estimating the impacts of climatic change on river flows: Some examples from Britain*. In: Proceedings of the Conference on Climate and Water, Helsinki, 1, 413-425.
- Watson, A.J. (2008) Certainty and uncertainty in climate change predictions: What use are climate models? *Environmental and Resource Economics*, 39(1), 37–44.

- Verspoor, E., Stradmeyer, L. & Nielsen, J. (2007) The Atlantic Salmon. In: Webb, J., Verspoor, N. Aubin-Horth, N., Romakkaniemi, A. & Amiro, P., eds. (2007) *The Atlantic Salmon: Genetics, Conservation, and Management*. Oxford, UK: Blackwell. 17-56.
- Weichert, A. & Bürger, G. (1998) Linear versus nonlinear techniques in downscaling. *Climate Research*, 10(2), 83-93.
- Weigel, A.P., Knutti, R., Liniger, M. A. & Appenzeller, C. (2010) Risks of Model Weighting in Multimodel Climate Projections. *Journal of Climate*, 23(15), 4175-4191.
- Weigel, A.P., Liniger, M.A. & Appenzeller, C. (2008) Can multi-model combination really enhance the prediction skill of probabilistic ensemble forecasts? *Quarterly Review of the Royal Meteorological Society*, 134(630), 241-260.
- Weir, G. (1996) 'Sheep overgrazing in the Nephin Bogs', MSc. thesis, Trinity College, Dublin.
- Wenger, S.J., Isaak, D.J., Luce, C.H., Neville, H.M., Fausch, K.D., Dunham, J B., Dauwalter, D.C., *et al.* (2011) Flow regime, temperature, and biotic interactions drive differential declines of trout species under climate change. *Proceedings of the National Academy of Sciences*, 108(34), 14175-14180.
- Wentz, F. J., Ricciardulli, L., Hilburn, K., & Mears, C. (2007) How much more rain will global warming bring? *Science*, 317(5835), 233–235.
- Wetterhall, F., Halldin, S. & Xu, C.-Y. (2007) Seasonality properties of four statistical-downscaling methods in central Sweden. *Theoretical and Applied Climatology*, 87 (1-4), 123-137.
- Wetterhall, F., Bárdossy, A., Chen, D., Halldin, S. & Xu, C.-Yu. (2008) Statistical downscaling of daily precipitation over Sweden using GCM output. *Theoretical and Applied Climatology*, 96(1-2), 95-103.
- Weyhenmeyer, G., Blenckner, T. & Pettersson, K. (1999) Changes of the plankton spring outburst related to the North Atlantic Oscillation. *Limnology and Oceanography*, 44(7), 1788–1792.
- Wheater, H.S., Jakeman, A.J. & Beven, K.J. (1993) Progress and directions in rainfall-runoff modelling. In: Jakeman, A.J., Beck, M.B., McAleer, M.J., eds. (1993) *Modelling Change in Environmental Systems*. Chichester, UK: Wiley. 101–132.
- Whelan, K.F., Poole, W.R., McGinnity, P., Rogan, G. and Cotter, D. (1998) The Burrishoole System. In: Moriarty, C., ed. (1998) *Studies of Irish Rivers and Lakes, Essays on the occasion of the XXVII Congress of Societas Internationalis Limnologiae (SIL)*, Dublin, 1998. 191-212.
- White, J.D. & Running, S.W. (1994) Testing scale dependent assumptions in regional ecosystem simulations. *Journal of Vegetation Science*, 5(5), 687-702.

- Whitehead, P.G., Wilby, R.L., Battarbee, R.W., Kernan, M. & Wade, A.J. (2009) A review of the potential impacts of climate change on surface water quality. *Hydrological Sciences*, 54(101-123), 101–123.
- Widmann, M. & Schär, C. (1997) A principal component and long-term trend analysis of daily precipitation in Switzerland. *International Journal of Climatology*, 17(12), 1333–1356.
- Wilby, R.L. (1994) Stochastic weather type simulation for regional climate change impact assessment. *Water Resources Research*, 30(12), 3395–3403.
- Wilby, R.L. & Wigley, T.M.L. (1997) Downscaling general circulation model output: a review of methods and limitations. *Progress in physical Geography*, 21(4), 530–548.
- Wilby, R.L., Wigley, T.M.L., Conway, D., Jones, P.D., Hewitson, B.C., Main, J. & Wilks D.S. (1998) Statistical downscaling of general circulation model output: a comparison of methods. *Water Resources Research*, 34(11), 2995–3008.
- Wilby, R.L., Hay, L.E. & Leavesley, G.H. (1999) A comparison of downscaled and raw GCM output: implications for climate change scenarios in the San Juan River basin, Colorado. *Journal of Hydrology*, 225(1-2), 67-91.
- Wilby, R.L. & Wigley, T.M.L. (2000) Precipitation predictors for downscaling: observed and general circulation model relationships. *International Journal of Climatology*, 20(1), 641–661.
- Wilby, R.L., Hay, L.E., Gutowski, W.J., Arritt, R.W., Takle, E.S., Pan, Z.T., Leavesley, G.H., Clark, M.P (2000) Hydrological responses to dynamically and statistically downscaled climate model output. *Geophysical Research Letters*, 27(8), 1199–1202.
- Wilby, R.L., Conway, D., Jones, P.D. (2002) Prospects for downscaling seasonal precipitation variability using conditioned weather generator parameters. *Hydrological Processes*, 16(6), 1215–1234.
- Wilby, R. L., (2002). sdsms — a decision support tool for the assessment of regional climate change impacts. *Environmental Modelling & Software*, 17(2), 147-159.
- Wilby, R.L. & Dawson, C.W. (2004) Statistical Downscaling Model: SDSM version 3.1 (software and user guide). [online]. Available at <http://www-staff.lboro.ac.uk/~cocwd/SDSM/> (accessed 1st March 2010).
- Wilby, R.L., Charles, S.P., Zorita, E., Timbal, B., Whetton, P., Mearns, L.O. (2004) *Guidelines for use of climate scenarios developed from statistical downscaling methods*. Data Distribution Centre of the Intergovernmental Panel on Climate Change.
- Wilby, R.L. (2005). Uncertainty in water resources model parameters used for climate change impact assessment. *Hydrological Processes*, 19(16), 3201–3219.

- Wilby, R.L. & Harris, I. (2006) A framework for assessing uncertainties in climate change impacts: Low-flow scenarios for the River Thames, UK. *Water Resources Research*, 42(2), 1-10.
- Wilby, R.L., Whitehead, P., Wade, A., Butterfield, D., Davis, R. & Watts, G. (2006) Integrated modelling of climate change impacts on water resources and quality in a lowland catchment: River Kennet, UK. *Journal of Hydrology*, 330(1-2), 204-220.
- Wilks, D.S. (1992) Adapting stochastic weather generation algorithms for climate change studies. *Climatic Change*, 22(1), 67-84.
- Wilks, D.S. & Wilby, R.L. (1999) The weather generation game: a review of stochastic weather models. *Progress in Physical Geography*, 23(3), 329-357.
- Willett, K.M., Jones, P.D., Gillett, N.P. & Thorne, P.W. (2008) Recent Changes in Surface Humidity: Development of the HadCRUH Dataset. *Journal of Climate*, 21(20), 5364-5383.
- Winder, M. & Schindler, D.E. (2004) Climate change uncouples trophic interactions in an aquatic ecosystem. *Ecology*, 85(8), 2100-2106.
- Winkler, J.A., Palutikof, J.P., Andresen, J.A. & Goodess, C.M. (1997) The simulation of daily temperature time series from GCM output. Part II: sensitivity analysis of an empirical transfer function methodology. *Journal of Climate*, 10(10), 2514-2532.
- Wood, A.W., Maurer, E.P., Kumar, A. & Lettenmaier, D.P. (2002) Long Range Experimental Hydrologic Forecasting for the Eastern U.S. *Journal of Geophysical Research*, 107(D20), 1-15.
- Wood, A.W., Leung, L.R., Sridhar, V., Lettenmaier, D.P. (2004) Hydrologic implications of dynamical and statistical approaches to downscaling climate model outputs. *Climatic Change*, 62(1), 189-216.
- Woodward, G., Perkins, D.M. & Brown, L.E. (2010) Climate change and freshwater ecosystems: impacts across multiple levels of organization. *Philosophical transactions of the Royal Society of London. Series B, Biological sciences*, 365(1549), 2093-2106.
- Worrall, F., Burt, T. & Adamson, A. (2006) Long-term changes in hydrological pathways in an upland peat catchment—recovery from severe drought? *Journal of Hydrology*, 321(1-4), 5-20.
- Wright, J.F., Clarke, R.T., Gunn, R.J. M., Kneebone, N.T. & Davy-Bowker, J. (2004) Impact of major changes in flow regime on the macroinvertebrate assemblages of four chalk stream sites, 1997-2001. *River Research and Applications*, 20(7), 775-794.
- Wrona, F.J., Prowse, T.D., Reist, J.D., Hobbie, J.E., Lucie, M.J., Vincent, W.F., Wrona, F.J. *et al.* (2010) Climate Change Impacts on Arctico Freshwater Ecosystems and Fisheries Effects Change Climate and Structure Ecosystem on Aquatic Function Biota. *Fisheries Bethesda*, 35(7), 359-369.

- Wuethrich, B. (2000) How climate change alters rhythms of the wild. *Science*, 287(5454), 793-795.
- Xenopoulos, M., Lodge, D. & Alcamo, J. (2005) Scenarios of freshwater fish extinctions from climate change and water withdrawal. *Global Change*, 11(10) 1557-1564.
- Xu, C. & Vandewiele, G., (1994). Sensitivity of monthly rainfall-runoff models to input errors and data length. *Hydrological sciences journal*, 39(2), 157–176.
- Xu, C. & Halldin, S. (1997) The effect of climate change on river flow and snow cover in the NOPEX area simulated by a simple water balance model. *Nordic hydrology*, 28(4), 273–282.
- Xu, C. & Singh, V.P. (1998) A review on monthly water balance models for water resources investigations. *Water Resources Management*, 12(1), 31–50.
- Xu, C. (1999) From GCMs to river flow: a review of downscaling methods and hydrologic modelling approaches. *Progress in Physical Geography*, 2(23), 229-249.
- Xu, C. (2000) Climate Change and Hydrologic Models: A Review of Existing Gaps and Recent Research Developments. *Water Resources Management*, 13(5), 369-382.
- Xu, C., Letcher, B.H. & Nislow, K.H. (2010) Context-specific influence of water temperature on brook trout growth rates in the field. *Freshwater Biology*, 55(11), 2253-2264.
- Xu, C., Tunemar, L., Chen, Y. & Singh, V. (2006) Evaluation of seasonal and spatial variations of lumped water balance model sensitivity to precipitation data errors. *Journal of Hydrology*, 324(1-4), 80-93.
- Xu, Y., Gao, X. & Giorgi, F. (2010) Upgrades to the reliability ensemble averaging method for producing probabilistic climate-change projections. *Climate Research*, 41(1), 61-81.
- Yamamoto, R. & Sakurai, Y. (1999) Long-term intensification of extremely heavy rainfall intensity in recent 100 years. *World Resource Review*, 11(2), 271–81.
- Yan, Z., Bate, S., Chandler, R.E., Isham, V.S. & Wheeler, H.S. (2002) An analysis of daily maximum windspeed in northwestern Europe using Generalized Linear Models. *Journal of Climate*, 15(15), 2073–2088.
- Yang, C., Chandler, R.E., Isham, V.S. & Wheeler, H.S. (2005) Spatial-temporal rainfall simulation using generalized linear models. *Water Resources Research*, 41(11), 1-13.
- Yang, J., Reichert, P., Abbaspour, K., Xia, J., & Yang, H. (2008) Comparing uncertainty analysis techniques for a SWAT application to the Chaohe Basin in China. *Journal of Hydrology*, 358(1-2), 1-23.

- Yarnal, B., Comrie, A.C., Frakes, B. & Brown, D.P. (2001) Developments and prospects in synoptic climatology. *International Journal of Climatology*, 21(15), 1923-1950.
- Ye, M., Meyer, P. D., & Neuman, S.P. (2008) On model selection criteria in multimodel analysis. *Water Resources Research*, 44(3), 1-12.
- Yokohata, T., Emori, S., Nozawa, T., Ogura, T., Kawamiya, M., Tsushima, Y., Suzuki, T., *et al.* (2008) Comparison of equilibrium and transient responses to CO₂ increase in eight state-of-the-art climate models. *Tellus A*, 60(5), 946-961.
- Young, P. (1998) Data-based mechanistic modelling of environmental, ecological, economic and engineering systems. *Environmental Modelling & Software*, 13(2), 105-122.
- Young, P.C., Parkinson, S. & Lees, M.J. (1996) Simplicity out of complexity in environmental modelling: Occam's razor revisited. *Journal of Applied Statistics*, 23(2-3), 165-210.
- Yu, P. S., Yang, T.C. & Kuo, C.C. (2006) Evaluating long-term trends in annual and seasonal precipitation in Taiwan. *Water Resources Management*, 20(6), 1007-1023.
- Zeebe, R.E., Zachos, J.C. & Dickens, G.R. (2009) Carbon dioxide forcing alone insufficient to explain Palaeocene-Eocene Thermal Maximum warming. *Nature Geoscience*, 2(8), 576-580.
- Zhai, P., Zhang, X., Wan, H. & Pan, X. (2005) Trends in total precipitation and frequency of daily precipitation extremes over China. *Journal of Climate*, 18(7), 1096-1108.
- Zhang, X., Harvey, K.D., Hogg, W.D. & Yuzyk, T.R. (2001) Trends in Canadian stream flow. *Water Resources Research*, 37(4), 987-998.
- Zhang, X., Zwiers, F.W., Hegerl, G.C., Lambert, F.H., Gillett, N.P., Solomon, S., Stott, P.A., *et al.* (2007) Detection of human influence on twentieth-century precipitation trends. *Nature*, 448(7152), 461-465.
- Zhang, K., Kimball, J.S., Mu, Q., Jones, L.A., Goetz, S.J. & Running, S.W. (2009a) Satellite based analysis of northern ET trends and associated changes in the regional water balance from 1983 to 2005. *Journal of Hydrology*, 379(1-2), 92-110.
- Zhang, X., Srinivasan, R. & Bosch, D. (2009b) Calibration and uncertainty analysis of the SWAT model using Genetic Algorithms and Bayesian Model Averaging. *Journal of Hydrology*, 374(3-4), 307-317.
- Zorita, E. Hughes J, Lettenmaier, D. & von Storch, H. (1995) Stochastic characterisation of regional circulation patterns for climate model diagnosis and estimation of local precipitation. *Journal of Climate*, 8(5), 1023-1042.

- Zorita, E. & von Storch, H. (1999) The analog method as a simple statistical downscaling technique: comparison with more complicated methods. *Journal of Climate*, 12(8), 2474–2489.
- Zydlewski, G.B., Haro, A. & McCormick, S.D. (2005) Evidence for cumulative temperature as an initiating and terminating factor in downstream migratory behavior of Atlantic salmon (*Salmo salar*) smolts. *Canadian Journal of Fisheries and Aquatic Sciences*, 62(1), 68–7.

Appendix I

**Projected changes in mean temperature (minimum and maximum) for the
Burrishoole catchment estimated on a seasonal and monthly basis.**

2020s Maximum Temperature	<i>Jan</i>	<i>Feb</i>	<i>Mar</i>	<i>Apr</i>	<i>May</i>	<i>Jun</i>	<i>Jul</i>	<i>Aug</i>	<i>Sept</i>	<i>Oct</i>	<i>Nov</i>	<i>Dec</i>	<i>Winter</i>	<i>Spring</i>	<i>Summer</i>	<i>Autumn</i>
<i>C4IRCA3 HadCM3Q16 A1B</i>	0.60	1.05	1.14	1.17	1.16	1.31	2.19	2.06	1.63	1.72	1.56	1.32	0.99	1.15	1.86	1.64
<i>C4IRCA3 ECHAM5 A2</i>	0.84	0.00	-0.06	0.13	0.88	0.52	1.12	0.91	0.35	0.76	0.41	-0.01	0.28	0.32	0.85	0.51
<i>CNRM-RM4.5 ARPEGE A1B</i>	0.90	0.09	0.28	0.45	0.55	0.31	0.91	0.62	0.68	0.67	0.60	0.47	0.50	0.42	0.62	0.65
<i>CNRM-RM5.1 ARPEGE A1B</i>	1.09	0.29	0.30	0.42	0.44	0.15	0.68	0.62	0.60	0.66	0.59	0.49	0.64	0.38	0.49	0.62
<i>DMI-HIRHAM5 ARPEGE A1B</i>	1.05	0.21	0.30	0.42	0.35	-0.03	0.77	0.71	0.36	0.31	0.66	0.73	0.68	0.36	0.49	0.44
<i>DMI-HIRHAM5 ECHAM5-r3 A1B</i>	0.47	-0.21	0.43	0.46	-0.21	0.06	0.41	0.47	-0.03	0.43	0.64	-0.29	0.00	0.23	0.32	0.35
<i>ETHZ-CLM HadCM3Q0 A1B</i>	1.07	0.70	0.87	0.80	0.66	0.76	1.13	1.45	1.13	0.98	1.00	1.10	0.97	0.78	1.12	1.04
<i>ICTP-REGCM3 ECHAM5-r3 A1B</i>	0.50	-0.12	0.41	0.92	0.46	-0.01	0.70	0.69	0.03	0.46	0.72	-0.27	0.04	0.59	0.47	0.40
<i>KNMI-RACMO2 ECHAM5-r3 A1B</i>	0.40	-0.16	0.45	0.66	0.45	0.04	0.69	0.62	0.00	0.42	0.81	-0.24	0.00	0.52	0.45	0.41
<i>METNOHIRHAM BCM A1B</i>	-0.25	0.60	-0.11	0.20	0.85	0.30	-0.35	-0.07	0.24	0.15	0.41	0.78	0.37	0.31	-0.04	0.27
<i>METNOHIRHAM HadCM3Q0 A1B</i>	0.99	0.75	0.91	0.80	0.98	0.65	1.14	1.51	1.22	0.77	0.98	1.09	0.95	0.90	1.10	0.99
<i>METO-HadRM3Q0 HadCM3Q0 A1B</i>	1.29	0.97	1.29	1.23	1.31	0.88	1.92	1.87	1.50	1.06	1.01	1.08	1.12	1.27	1.56	1.19
<i>METO-HadRM3Q3 HadCM3Q3 A1B</i>	1.31	0.95	0.87	0.26	0.35	0.87	1.48	0.68	0.57	0.86	1.02	1.14	1.14	0.50	1.01	0.82
<i>METO-HadRM3Q16 HadCM3Q16 A1B</i>	0.80	1.14	1.18	1.37	1.00	1.35	1.65	1.78	1.36	1.69	1.62	1.48	1.14	1.18	1.60	1.56
<i>MPI-M-REMO ECHAM5-r3 A1B</i>	0.45	-0.11	0.42	0.40	0.16	-0.13	0.55	0.64	0.12	0.48	0.80	-0.28	0.02	0.32	0.36	0.47
<i>OURANOSMRCC4.2.1 CGCM3 A1B</i>	-0.02	0.07	-0.06	-0.57	-0.21	0.40	1.48	1.44	1.54	1.23	1.37	1.15	0.41	-0.28	1.11	1.38
<i>SMHIRCA BCM A1B</i>	-0.11	0.73	0.00	0.17	0.44	-0.04	-0.12	-0.51	0.11	0.32	0.37	0.65	0.41	0.20	-0.23	0.27
<i>SMHIRCA ECHAM5-r3 A1B</i>	0.37	-0.09	0.46	0.57	0.32	-0.08	0.76	0.88	0.13	0.56	0.67	-0.41	-0.04	0.45	0.53	0.45
<i>SMHIRCA HadCM3Q3 A1B</i>	1.37	1.05	0.93	0.36	0.90	1.34	1.13	1.46	1.10	1.04	1.01	1.27	1.24	0.74	1.31	1.05
<i>SDSM HadCM3 A2</i>	0.25	0.35	0.29	0.40	0.55	0.38	0.13	0.93	0.40	0.29	0.12	-0.55	0.01	0.41	0.48	0.27
<i>SDSM HadCM3 B2</i>	0.28	0.56	0.24	0.74	0.42	0.23	0.51	0.81	0.74	0.71	0.45	-0.30	0.17	0.46	0.52	0.64
<i>SDSM CSIROmk2 A2</i>	0.72	0.74	0.83	1.84	0.92	1.01	1.23	1.00	1.24	1.30	1.37	1.32	0.93	1.19	1.08	1.31
<i>SDSM CSIROmk2 B2</i>	1.44	1.47	1.03	1.65	1.54	1.88	1.28	1.63	2.15	1.23	1.41	1.24	1.38	1.40	1.59	1.59
<i>SDSM CGCM2 A2</i>	1.03	0.79	0.83	1.42	1.70	1.77	1.61	1.59	0.90	0.62	0.55	1.32	1.05	1.32	1.66	0.69
<i>SDSM CGCM2 B2</i>	1.88	1.21	0.92	1.39	1.19	1.46	1.73	1.43	1.04	0.79	0.84	1.38	1.50	1.16	1.54	0.89

Table I-1 Projected changes in mean monthly and seasonal maximum temperature for the Burrishoole catchment calculated over the 2020s horizon (2010-2039) relative to the 30 year control period. (1961-1990). The table is colour coded to highlight increases/decreases.

2050s Maximum Temperature	Jan	Feb	Mar	Apr	May	Jun	Jul	Aug	Sept	Oct	Nov	Dec	Winter	Spring	Summer	Autumn
<i>C4IRCA3 HadCM3Q16 A1B</i>	1.02	1.58	1.77	2.31	2.17	2.37	3.61	3.92	2.85	2.68	2.10	1.76	1.45	2.08	3.31	2.55
<i>CNRM-RM5.1 ARGEGE A1B</i>	0.76	1.24	1.08	1.24	1.33	0.59	0.87	1.55	1.19	0.94	0.94	0.68	0.88	1.22	1.01	1.02
<i>DMI-HIRHAM5 ARPEGE A1B</i>	0.69	1.12	1.03	1.33	1.16	0.40	1.08	0.98	0.88	0.76	1.01	0.81	0.87	1.17	0.82	0.88
<i>DMI-HIRHAM5 ECHAM5-r3 A1B</i>	0.97	0.54	0.85	0.81	0.63	1.20	1.74	2.10	1.59	1.51	1.76	0.41	0.64	0.76	1.68	1.62
<i>ETHZ-CLM HadCM3Q0 A1B</i>	1.62	1.72	1.62	1.74	0.82	1.23	2.12	2.40	1.78	1.78	1.79	2.01	1.78	1.39	1.92	1.78
<i>ICTP-REGCM3 ECHAM5-r3 A1B</i>	0.66	0.43	0.55	0.81	1.18	1.20	1.22	1.92	1.30	1.37	1.52	0.29	0.46	0.85	1.45	1.40
<i>KNMI-RACMO2 ECHAM5-r3 A1B</i>	0.66	0.49	0.63	0.78	1.40	1.36	1.32	1.93	1.28	1.41	1.57	0.43	0.53	0.94	1.54	1.42
<i>METO-HadRM3Q0 HadCM3Q0 A1B</i>	1.99	2.28	2.28	2.40	1.72	1.69	2.90	2.75	2.13	2.09	2.10	2.10	2.12	2.13	2.46	2.11
<i>METO-HadRM3Q3 HadCM3Q3 A1B</i>	2.19	1.64	1.40	0.82	0.39	0.86	2.47	0.80	0.77	1.32	1.05	1.39	1.74	0.87	1.38	1.05
<i>METO-HadRM3Q16 HadCM3Q16 A1B</i>	1.26	2.05	1.82	2.46	2.00	2.29	2.93	3.52	2.56	2.71	2.14	1.73	1.67	2.09	2.92	2.48
<i>MPI-M-REMO ECHAM5-r3 A1B</i>	0.83	0.64	0.69	0.46	0.99	1.01	1.27	2.01	1.59	1.69	1.75	0.55	0.67	0.72	1.43	1.68
<i>SMHIRCA BCM A1B</i>	0.89	1.24	0.58	1.22	1.27	1.15	0.53	0.67	0.77	0.74	0.83	1.13	1.08	1.02	0.78	0.78
<i>SMHIRCA ECHAM5-r3 A1B</i>	0.65	0.58	0.65	0.87	1.25	1.38	1.80	2.56	1.77	1.64	1.62	0.33	0.52	0.93	1.92	1.68
<i>SMHIRCA HadCM3Q3 A1B</i>	1.91	1.37	1.11	1.08	1.02	1.65	1.88	1.71	1.42	1.17	0.88	1.13	1.47	1.07	1.75	1.16
<i>SDSM HadCM3 A2</i>	0.93	0.91	0.62	0.92	0.98	0.54	1.82	1.38	1.69	0.85	0.67	0.07	0.63	0.84	1.25	1.07
<i>SDSM HadCM3 B2</i>	0.76	0.22	0.35	0.73	1.19	0.86	1.18	1.62	0.88	0.77	0.91	0.20	0.40	0.75	1.22	0.85
<i>SDSM CSIROmk2 A2</i>	1.55	1.77	1.33	2.35	2.35	1.65	2.47	2.37	2.36	2.11	2.07	2.24	1.86	2.01	2.17	2.18
<i>SDSM CSIROmk2 B2</i>	2.04	1.96	1.51	2.37	2.86	2.48	2.22	2.34	2.91	1.84	2.45	2.06	2.02	2.25	2.34	2.39
<i>SDSM CGCM2 A2</i>	2.29	1.97	1.65	2.35	2.79	2.87	3.33	3.07	2.14	1.80	1.87	2.34	2.21	2.26	3.09	1.93
<i>SDSM CGCM2 B2</i>	1.89	1.39	1.22	2.23	2.41	2.34	2.56	2.36	1.62	1.28	1.28	1.80	1.70	1.95	2.42	1.39

Table I-2 Projected changes in mean monthly and seasonal maximum temperature for the Burrishoole catchment calculated over the 2050s horizon (2040-2069) relative to the 30 year control period. (1961-1990). The table is colour coded to highlight increases/decreases.

2080s Maximum Temperature	<i>Jan</i>	<i>Feb</i>	<i>Mar</i>	<i>Apr</i>	<i>May</i>	<i>Jun</i>	<i>Jul</i>	<i>Aug</i>	<i>Sept</i>	<i>Oct</i>	<i>Nov</i>	<i>Dec</i>	<i>Winter</i>	<i>Spring</i>	<i>Summer</i>	<i>Autumn</i>
<i>C4IRCA3 HadCM3Q16 A1B</i>	2.55	3.08	3.00	3.65	3.29	4.15	6.65	6.98	4.94	3.88	3.67	3.03	2.87	3.31	5.94	4.16
<i>CNRM-RM5.1 ARGEGE A1B</i>	1.27	1.47	1.37	1.70	1.69	1.21	1.68	1.98	1.65	1.23	1.28	1.32	1.35	1.58	1.63	1.38
<i>DMI-HIRHAM5 ARPEGE A1B</i>	1.15	1.02	1.07	1.74	1.57	0.89	1.26	1.75	1.19	0.97	1.21	1.28	1.16	1.46	1.30	1.12
<i>DMI-HIRHAM5 ECHAM5-r3 A1B</i>	1.59	1.13	1.26	1.47	1.02	1.23	1.57	2.23	2.00	2.09	1.90	1.34	1.36	1.25	1.68	2.00
<i>ETHZ-CLM HadCM3Q0 A1B</i>	2.01	1.56	2.02	2.05	1.56	1.49	2.48	2.70	2.61	2.54	2.13	2.09	1.89	1.87	2.23	2.43
<i>ICTP-REGCM3 ECHAM5-r3 A1B</i>	1.35	1.00	0.91	1.66	1.41	1.41	1.14	1.88	1.83	1.82	1.99	1.38	1.25	1.32	1.48	1.88
<i>KNMI-RACMO2 ECHAM5-r3 A1B</i>	1.29	1.16	1.04	1.45	1.54	1.48	1.15	1.88	1.85	1.82	2.10	1.48	1.32	1.34	1.50	1.92
<i>METO-HadRM3Q0 HadCM3Q0 A1B</i>	2.33	2.39	2.76	2.75	2.32	1.97	3.60	3.82	3.09	2.84	2.38	2.19	2.30	2.61	3.15	2.77
<i>METO-HadRM3Q3 HadCM3Q3 A1B</i>	2.25	1.97	1.69	0.84	1.20	1.76	4.06	2.04	1.07	1.33	1.70	1.95	2.05	1.25	2.63	1.37
<i>METO-HadRM3Q16 HadCM3Q16 A1B</i>	2.92	3.44	3.08	3.69	2.91	3.47	5.72	5.74	4.06	4.01	3.70	2.92	3.08	3.22	4.99	3.93
<i>MPI-M-REMO ECHAM5-r3 A1B</i>	1.44	1.34	1.11	1.19	1.20	1.22	1.23	1.79	2.35	2.15	2.28	1.60	1.46	1.17	1.42	2.26
<i>SMHIRCA BCM A1B</i>	1.36	2.20	1.04	1.37	1.92	1.64	0.99	1.94	1.14	1.27	1.61	1.75	1.76	1.44	1.52	1.34
<i>SMHIRCA ECHAM5-r3 A1B</i>	1.36	1.20	1.10	1.68	1.55	1.69	1.85	2.59	2.44	2.14	2.15	1.41	1.33	1.44	2.05	2.24
<i>SMHIRCA HadCM3Q3 A1B</i>	1.92	1.62	1.54	1.18	1.50	2.25	3.00	3.06	1.97	1.45	1.41	1.77	1.77	1.41	2.78	1.61
<i>SDSM HadCM3 A2</i>	1.38	1.30	1.66	2.02	2.26	1.90	3.51	3.32	2.71	2.04	1.33	0.86	1.18	1.98	2.92	2.03
<i>SDSM HadCM3 B2</i>	0.76	0.78	0.83	1.54	1.63	1.75	1.90	1.97	1.56	1.42	1.05	0.30	0.61	1.33	1.87	1.34
<i>SDSM CSIROmk2 A2</i>	3.03	2.76	2.29	3.98	3.31	2.83	4.38	3.88	3.55	3.24	3.22	3.70	3.17	3.19	3.71	3.33
<i>SDSM CSIROmk2 B2</i>	2.36	2.40	1.82	2.84	3.11	2.50	2.80	3.14	3.62	2.55	2.86	2.65	2.47	2.59	2.82	3.01
<i>SDSM CGCM2 A2</i>	2.57	2.32	1.85	3.24	3.71	4.20	4.39	3.96	3.04	2.43	2.40	3.06	2.66	2.93	4.18	2.62
<i>SDSM CGCM2 B2</i>	1.84	1.97	1.58	2.93	3.05	3.17	3.11	3.03	2.51	2.04	1.74	2.15	1.98	2.52	3.10	2.10

Table I-3 Projected changes in mean monthly and seasonal maximum temperature for the Burrishoole catchment calculated over the 2080s horizon (2070-2099) relative to the 30 year control period. (1961-1990). The table is colour coded to highlight increases/decreases.

2020s Minimum Temperature	Jan	Feb	Mar	Apr	May	Jun	Jul	Aug	Sept	Oct	Nov	Dec	Winter	Spring	Summer	Autumn
<i>C4IRCA3 HadCM3Q16 A1B</i>	0.73	1.32	1.60	1.30	1.43	1.34	1.68	2.05	1.82	2.25	1.92	1.59	1.21	1.45	1.70	2.00
<i>C4IRCA3 ECHAM5 A2</i>	0.92	0.04	0.08	0.23	0.68	0.65	0.68	0.93	0.43	0.83	0.59	-0.09	0.30	0.33	0.75	0.62
<i>CNRM-RM4.5 ARPEGE A1B</i>	0.80	0.01	0.14	0.21	0.43	0.46	0.42	0.58	0.31	0.45	0.65	0.44	0.43	0.26	0.49	0.47
<i>CNRM-RM5.1 ARGEGE A1B</i>	0.84	0.08	0.18	0.29	0.36	0.33	0.41	0.53	0.29	0.39	0.50	0.34	0.43	0.27	0.43	0.39
<i>DMI-HIRHAM5 ARPEGE A1B</i>	1.12	0.18	0.35	0.48	0.49	0.14	0.71	0.81	0.52	0.41	0.63	0.75	0.70	0.44	0.56	0.52
<i>DMI-HIRHAM5 ECHAM5-r3 A1B</i>	0.62	-0.11	0.75	0.78	0.09	0.24	0.46	0.64	0.19	0.57	0.74	-0.31	0.08	0.54	0.45	0.50
<i>ETHZ-CLM HadCM3Q0 A1B</i>	1.47	0.75	1.09	0.97	1.05	0.92	1.25	1.36	1.52	1.07	1.09	1.33	1.20	1.04	1.18	1.23
<i>ICTP-REGCM3 ECHAM5-r3 A1B</i>	0.57	0.09	0.75	0.87	0.55	0.24	0.67	0.90	0.16	0.57	0.70	-0.35	0.10	0.72	0.61	0.48
<i>KNMI-RACMO2 ECHAM5-r3 A1B</i>	0.56	0.05	0.72	0.61	0.59	0.28	0.70	0.91	0.19	0.62	0.85	-0.31	0.10	0.64	0.64	0.55
<i>METNOHIRHAM BCM A1B</i>	-0.20	0.63	-0.02	0.31	0.50	0.27	-0.09	0.15	0.36	0.29	0.60	0.85	0.42	0.26	0.11	0.42
<i>METNOHIRHAM HadCM3Q0 A1B</i>	1.23	0.84	1.21	0.95	1.26	0.80	1.12	1.45	1.51	0.70	1.18	1.35	1.15	1.14	1.13	1.13
<i>METO-HadRM3Q0 HadCM3Q0 A1B</i>	1.51	0.73	0.96	1.04	1.26	0.83	1.31	1.51	1.50	0.95	0.91	1.12	1.13	1.09	1.22	1.12
<i>METO-HadRM3Q3 HadCM3Q3 A1B</i>	1.17	0.80	0.85	0.37	0.46	0.96	0.87	0.92	1.02	0.80	1.13	1.27	1.09	0.56	0.92	0.98
<i>METO-HadRM3Q16 HadCM3Q16 A1B</i>	0.64	0.92	1.05	1.13	1.16	1.17	1.34	1.76	1.44	1.90	1.58	1.40	0.99	1.11	1.43	1.64
<i>MPI-M-REMO ECHAM5-r3 A1B</i>	0.44	0.15	0.76	0.46	0.42	0.20	0.68	0.96	0.39	0.64	0.86	-0.30	0.10	0.55	0.62	0.63
<i>OURANOSMRCC4.2.1 CGCM3 A1B</i>	0.24	0.36	0.32	0.03	0.24	0.21	1.11	1.02	1.40	0.90	1.22	1.00	0.54	0.20	0.79	1.17
<i>SMHIRCA BCM A1B</i>	-0.14	0.80	0.10	0.34	0.41	0.18	0.04	-0.29	0.15	0.28	0.34	0.63	0.42	0.28	-0.02	0.26
<i>SMHIRCA ECHAM5-r3 A1B</i>	0.37	0.09	0.80	0.41	0.40	0.30	0.76	0.99	0.20	0.68	0.81	-0.43	0.01	0.54	0.69	0.56
<i>SMHIRCA HadCM3Q3 A1B</i>	1.59	1.15	1.14	0.70	0.67	1.21	0.75	1.18	1.17	1.20	1.13	1.47	1.41	0.84	1.05	1.17
<i>SDSM HadCM3 A2</i>	0.37	0.35	0.15	0.39	0.75	0.59	0.07	0.56	0.49	0.35	0.09	-0.61	0.03	0.43	0.40	0.31
<i>SDSM HadCM3 B2</i>	0.39	0.66	0.13	0.73	0.70	0.52	0.36	0.63	0.90	0.84	0.53	-0.27	0.25	0.52	0.50	0.76
<i>SDSM CSIROmk2 A2</i>	0.82	0.61	1.02	1.48	0.80	0.69	0.75	0.75	1.21	1.45	1.48	1.51	0.99	1.09	0.73	1.38
<i>SDSM CSIROmk2 B2</i>	1.71	1.70	1.29	1.26	1.14	1.59	0.89	1.54	2.09	1.37	1.53	1.38	1.59	1.23	1.34	1.66
<i>SDSM CGCM2 A2</i>	1.30	0.84	0.86	1.42	1.09	1.40	0.87	1.53	0.90	0.75	0.61	1.35	1.17	1.12	1.26	0.75
<i>SDSM CGCM2 B2</i>	2.06	1.61	0.98	1.36	0.82	1.37	0.97	1.40	1.07	0.97	0.94	1.62	1.77	1.05	1.25	0.99

Table I-4 Projected changes in mean monthly and seasonal minimum temperature for the Burrishoole catchment calculated over the 2020s horizon (2010-2039) relative to the 30 year control period. (1961-1990). The table is colour coded to highlight increases/decreases.

2050s Minimum Temperature	Jan	Feb	Mar	Apr	May	Jun	Jul	Aug	Sept	Oct	Nov	Dec	Winter	Spring	Summer	Autumn
<i>C4IRCA3 HadCM3Q16 A1B</i>	1.37	2.01	2.30	2.06	2.29	2.16	2.49	3.56	2.96	3.25	2.49	2.13	1.83	2.22	2.74	2.90
<i>CNRM-RM5.1 ARGEGE A1B</i>	0.40	1.01	0.81	0.76	0.73	0.57	0.53	0.90	0.59	0.55	0.76	0.51	0.63	0.77	0.67	0.63
<i>DMI-HIRHAM5 ARPEGE A1B</i>	0.70	1.12	1.19	1.26	1.21	0.45	0.76	1.03	1.06	0.93	1.03	0.79	0.86	1.22	0.75	1.00
<i>DMI-HIRHAM5 ECHAM5-r3 A1B</i>	1.38	0.75	1.20	1.20	0.94	1.50	1.83	2.40	2.19	2.11	2.06	0.57	0.91	1.11	1.91	2.12
<i>ETHZ-CLM HadCM3Q0 A1B</i>	2.18	1.63	1.90	2.00	1.48	1.77	2.21	2.45	2.35	2.32	1.99	2.33	2.06	1.79	2.15	2.22
<i>ICTP-REGCM3 ECHAM5-r3 A1B</i>	0.88	0.70	0.82	1.13	1.17	1.50	1.48	2.15	1.60	1.71	1.77	0.38	0.65	1.04	1.71	1.69
<i>KNMI-RACMO2 ECHAM5-r3 A1B</i>	0.81	0.59	0.89	1.17	1.32	1.62	1.54	2.19	1.69	1.85	1.76	0.49	0.63	1.13	1.79	1.77
<i>METO-HadRM3Q0 HadCM3Q0 A1B</i>	2.21	1.61	1.88	2.07	2.00	1.87	2.02	2.25	2.20	2.08	2.04	2.17	2.01	1.98	2.05	2.11
<i>METO-HadRM3Q3 HadCM3Q3 A1B</i>	2.32	1.60	1.25	1.13	0.82	1.06	1.58	1.23	1.35	1.47	1.09	1.57	1.84	1.07	1.29	1.30
<i>METO-HadRM3Q16 HadCM3Q16 A1B</i>	0.98	1.62	1.68	1.59	1.84	1.95	2.06	2.91	2.45	2.64	1.95	1.77	1.45	1.71	2.31	2.35
<i>MPI-M-REMO ECHAM5-r3 A1B</i>	0.91	0.80	1.06	1.01	1.44	1.49	1.79	2.56	2.10	2.10	1.97	0.80	0.84	1.17	1.95	2.06
<i>SMHIRCA BCM A1B</i>	0.96	1.34	0.72	1.35	0.99	1.25	0.66	0.75	0.87	0.68	0.91	1.34	1.21	1.02	0.88	0.82
<i>SMHIRCA ECHAM5-r3 A1B</i>	0.92	0.78	1.14	1.14	1.25	1.62	1.79	2.43	1.95	2.01	2.03	0.66	0.79	1.18	1.95	1.99
<i>SMHIRCA HadCM3Q3 A1B</i>	2.32	1.57	1.33	1.33	1.21	1.59	1.35	1.71	1.53	1.41	1.04	1.28	1.73	1.29	1.55	1.33
<i>SDSM HadCM3 A2</i>	1.25	1.06	0.39	0.66	0.98	1.00	1.26	1.50	1.88	0.97	0.74	0.12	0.80	0.68	1.26	1.19
<i>SDSM HadCM3 B2</i>	0.95	0.26	0.26	0.93	1.35	1.08	0.93	1.31	0.96	0.89	1.04	0.30	0.51	0.85	1.11	0.96
<i>SDSM CSIROmk2 A2</i>	1.81	1.85	1.52	1.90	1.90	1.18	1.60	1.80	2.41	2.32	2.18	2.46	2.05	1.77	1.53	2.30
<i>SDSM CSIROmk2 B2</i>	2.12	2.06	1.81	1.97	2.06	2.01	1.41	2.21	2.82	2.04	2.65	2.19	2.12	1.95	1.88	2.50
<i>SDSM CGCM2 A2</i>	2.88	2.29	2.02	2.00	2.05	2.62	2.18	3.10	2.26	2.22	2.12	2.60	2.60	2.03	2.63	2.20
<i>SDSM CGCM2 B2</i>	2.19	1.39	1.45	1.99	1.82	1.92	1.60	2.36	1.64	1.57	1.44	1.93	1.85	1.75	1.96	1.55

Table I-5 Projected changes in mean monthly and seasonal minimum temperature for the Burrishoole catchment calculated over the 2050s horizon (2040-2069) relative to the 30 year control period. (1961-1990). The table is colour coded to highlight increases/decreases.

2080s Minimum Temperature	<i>Jan</i>	<i>Feb</i>	<i>Mar</i>	<i>Apr</i>	<i>May</i>	<i>Jun</i>	<i>Jul</i>	<i>Aug</i>	<i>Sept</i>	<i>Oct</i>	<i>Nov</i>	<i>Dec</i>	<i>Winter</i>	<i>Spring</i>	<i>Summer</i>	<i>Autumn</i>
<i>C4IRCA3 HadCM3Q16 A1B</i>	3.23	3.57	3.91	3.53	3.70	3.74	4.54	5.98	5.28	4.60	4.57	3.86	3.54	3.71	4.76	4.82
<i>CNRM-RM5.1 ARGEGE A1B</i>	0.89	0.86	1.11	1.04	1.28	0.96	0.87	1.14	1.04	0.92	1.14	1.01	0.92	1.15	0.99	1.03
<i>DMI-HIRHAM5 ARPEGE A1B</i>	1.32	1.16	1.46	1.60	1.79	0.96	1.09	1.64	1.51	1.26	1.44	1.29	1.26	1.62	1.23	1.40
<i>DMI-HIRHAM5 ECHAM5-r3 A1B</i>	2.15	1.46	1.85	1.95	1.66	1.87	2.13	2.83	2.59	2.68	2.23	1.71	1.78	1.82	2.28	2.50
<i>ETHZ-CLM HadCM3Q0 A1B</i>	2.62	1.51	2.46	2.27	2.42	2.11	2.59	2.96	3.38	2.93	2.43	2.46	2.21	2.38	2.56	2.91
<i>ICTP-REGCM3 ECHAM5-r3 A1B</i>	1.66	1.28	1.41	1.75	1.64	1.87	1.80	2.57	1.93	2.28	2.22	1.69	1.55	1.60	2.08	2.15
<i>KNMI-RACMO2 ECHAM5-r3 A1B</i>	1.52	1.26	1.39	1.67	1.78	2.00	1.83	2.54	2.10	2.33	2.28	1.76	1.52	1.61	2.13	2.24
<i>METO-HadRM3Q0 HadCM3Q0 A1B</i>	2.55	1.61	2.30	2.31	2.69	2.10	2.59	2.93	3.03	2.56	2.30	2.23	2.15	2.44	2.54	2.63
<i>METO-HadRM3Q3 HadCM3Q3 A1B</i>	2.33	1.93	1.71	1.33	1.40	1.78	2.32	2.21	1.85	1.43	1.62	2.06	2.10	1.48	2.10	1.63
<i>METO-HadRM3Q16 HadCM3Q16 A1B</i>	2.69	2.78	2.92	2.87	3.16	2.79	3.62	4.61	4.28	3.79	3.63	2.86	2.78	2.99	3.68	3.90
<i>MPI-M-REMO ECHAM5-r3 A1B</i>	1.70	1.52	1.63	1.81	1.90	1.97	2.09	2.85	2.59	2.71	2.48	1.87	1.70	1.78	2.31	2.59
<i>SMHIRCA BCM A1B</i>	1.47	2.57	1.31	1.53	1.47	1.72	1.10	1.91	1.29	1.41	1.80	1.98	1.99	1.43	1.57	1.50
<i>SMHIRCA ECHAM5-r3 A1B</i>	1.69	1.46	1.69	1.84	1.74	2.09	2.13	2.83	2.43	2.78	2.58	1.77	1.65	1.75	2.35	2.60
<i>SMHIRCA HadCM3Q3 A1B</i>	2.38	1.76	1.94	1.55	1.61	2.02	2.06	2.63	2.22	1.71	1.67	2.17	2.10	1.70	2.24	1.86
<i>SDSM HadCM3 A2</i>	1.76	1.57	1.74	2.09	2.52	2.15	2.68	3.31	3.06	2.44	1.57	1.10	1.47	2.11	2.72	2.36
<i>SDSM HadCM3 B2</i>	1.08	0.92	0.76	1.53	1.87	1.93	1.52	1.95	1.81	1.70	1.19	0.45	0.81	1.39	1.80	1.57
<i>SDSM CSIROmk2 A2</i>	3.58	2.88	2.57	3.23	2.65	1.97	2.71	3.17	3.54	3.53	3.39	4.05	3.52	2.81	2.62	3.49
<i>SDSM CSIROmk2 B2</i>	2.80	2.60	2.22	2.33	2.24	2.07	1.83	2.76	3.53	2.80	3.05	3.07	2.83	2.26	2.22	3.12
<i>SDSM CGCM2 A2</i>	3.16	2.74	2.18	2.81	2.56	3.46	2.89	4.17	3.22	2.92	2.70	3.66	3.20	2.51	3.51	2.95
<i>SDSM CGCM2 B2</i>	2.15	2.21	1.81	2.61	2.26	2.77	2.12	3.15	2.67	2.52	1.95	2.61	2.33	2.22	2.68	2.38

Table I-6 Projected changes in mean monthly and seasonal minimum temperature for the Burrishoole catchment calculated over the 2080s horizon (2070-2099) relative to the 30 year control period. (1961-1990). The table is colour coded to highlight increases/decreases.

Appendix II

Projected changes (%) in mean precipitation receipts for the Burrishoole catchment estimated on a seasonal and monthly basis.

2020s Precipitation Change (%)	Jan	Feb	Mar	Apr	May	Jun	Jul	Aug	Sept	Oct	Nov	Dec	Winter	Spring	Summer	Autumn
<i>C4IRCA3 HadCM3Q16 A1B</i>	3.1	0.6	-0.9	-7.6	23.9	-23.5	-7.9	-8.6	-3.2	6.1	6.5	5.6	3.4	4.0	-12.9	3.4
<i>C4IRCA3 ECHAM5 A2</i>	17.0	-1.5	6.0	3.5	1.7	-9.2	-20.1	-0.8	0.7	7.3	8.1	-2.3	5.1	4.1	-9.0	5.6
<i>CNRM-RM4.5 ARPEGE A1B</i>	10.9	3.3	0.5	-5.8	-7.9	-2.3	-4.6	-4.0	-9.4	7.6	20.9	3.2	6.1	-3.7	-3.7	7.1
<i>CNRM-RM5.1 ARGEGE A1B</i>	8.7	5.7	0.2	-8.8	2.7	-12.7	-2.6	0.9	-0.2	12.8	17.4	1.3	5.1	-1.6	-4.3	10.4
<i>DMI-HIRHAM5 ARPEGE A1B</i>	8.5	2.8	2.7	-12.5	-2.5	-17.0	12.5	-12.2	6.3	18.3	6.9	12.0	8.4	-3.0	-6.5	10.7
<i>DMI-HIRHAM5 ECHAM5-r3 A1B</i>	11.1	-6.8	26.4	8.4	17.1	19.7	-8.3	13.4	6.2	-0.8	10.2	-4.6	0.8	18.7	9.0	5.1
<i>ETHZ-CLM HadCM3Q0 A1B</i>	10.2	11.6	-0.3	1.3	-3.5	4.2	-0.5	-8.7	-3.9	-9.2	-3.6	16.5	12.9	-0.7	-2.4	-5.6
<i>ICTP-REGCM3 ECHAM5-r3 A1B</i>	14.4	4.7	13.4	1.1	6.2	-8.7	-7.3	8.7	6.9	-8.0	6.0	-11.4	2.2	7.9	-1.2	1.3
<i>KNMI-RACMO2 ECHAM5-r3 A1B</i>	10.1	2.3	11.7	-0.6	-1.9	-3.1	-11.3	4.9	11.5	0.9	11.0	-12.3	-0.4	4.4	-2.3	7.6
<i>METNOHIRHAM BCM A1B</i>	0.1	26.2	26.0	-5.5	-31.0	-8.6	-2.7	-6.5	0.4	12.1	1.7	24.0	15.6	1.2	-6.0	5.0
<i>METNOHIRHAM HadCM3Q0 A1B</i>	13.8	-0.1	8.6	-15.0	0.2	-2.8	4.1	-14.3	-1.3	-21.1	8.4	9.5	8.5	-0.6	-5.6	-4.8
<i>METO-HadRM3Q0 HadCM3Q0 A1B</i>	12.7	-2.1	-4.2	-12.8	-4.0	-10.9	0.9	1.3	9.2	-10.8	-4.9	9.2	7.5	-6.7	-2.6	-2.7
<i>METO-HadRM3Q3 HadCM3Q3 A1B</i>	27.2	-11.0	-7.7	16.0	11.4	7.5	2.6	-7.6	8.6	-0.4	6.1	9.5	10.6	4.4	0.0	4.6
<i>METO-HadRM3Q16 HadCM3Q16 A1B</i>	-2.1	-2.0	-4.2	-0.7	4.9	-16.9	-0.5	-9.7	-1.2	25.9	12.4	4.7	0.4	-0.7	-9.3	12.9
<i>MPI-M-REMO ECHAM5-r3 A1B</i>	8.9	0.6	8.4	11.7	-3.9	-10.7	-15.8	3.2	15.4	-3.2	-2.3	-13.3	-1.7	5.9	-6.6	2.7
<i>OURANOSMRCC4.2.1 CGCM3 A1B</i>	-18.8	-19.6	1.3	9.7	3.1	4.8	1.4	-1.5	0.2	-2.4	21.4	5.1	-9.9	4.1	1.2	6.6
<i>SMHIRCA BCM A1B</i>	3.4	23.5	28.5	3.9	-22.1	-0.8	-16.4	-2.6	-12.5	5.7	5.7	22.3	15.5	7.2	-6.0	0.2
<i>SMHIRCA ECHAM5-r3 A1B</i>	7.8	4.0	11.5	1.1	-8.3	-9.2	-9.2	-1.2	9.1	-0.2	10.3	-10.0	0.1	3.0	-5.9	6.2
<i>SMHIRCA HadCM3Q3 A1B</i>	29.4	-2.8	-7.8	27.8	13.2	-1.8	-6.8	-1.3	19.5	2.6	8.9	30.0	21.1	8.3	-3.0	9.9
<i>SDSM HadCM3 A2</i>	-6.7	-5.8	-3.4	-6.7	-9.4	18.9	6.8	-22.6	-0.2	-1.1	-3.1	5.0	-2.1	-6.0	-1.6	-1.5
<i>SDSM HadCM3 B2</i>	-0.3	4.1	8.8	-13.5	-6.1	17.6	-6.0	1.7	0.0	4.2	-1.7	-8.0	-2.0	-1.7	4.2	0.9
<i>SDSM CSIROmk2 A2</i>	10.1	12.8	4.0	-9.6	3.7	4.5	-5.2	-5.0	-0.4	8.5	2.3	12.0	11.5	0.1	-2.2	3.7
<i>SDSM CSIROmk2 B2</i>	4.5	1.8	-6.0	-0.8	8.7	8.2	-11.6	-4.2	4.5	-18.1	-10.4	7.0	4.8	-0.4	-2.7	-8.7
<i>SDSM CGCM2 A2</i>	7.7	-5.7	4.0	-0.8	-14.8	-19.3	-22.0	-1.4	4.8	5.0	11.2	6.1	3.8	-2.7	-12.9	7.1
<i>SDSM CGCM2 B2</i>	13.1	-14.4	13.2	9.0	-4.1	4.4	-3.4	0.0	-2.0	-18.9	5.3	5.3	3.4	7.1	0.4	-5.5

Table II-2 Projected changes (%) in mean monthly and seasonal precipitation receipts for the Burrishoole catchment calculated over the 2020s horizon (2010-2039) relative to the 30 year control period. (1961-1990). The table is colour coded to highlight increases/decreases.

2050s Precipitation Change (%)	Jan	Feb	Mar	Apr	May	Jun	Jul	Aug	Sept	Oct	Nov	Dec	Winter	Spring	Summer	Autumn
<i>C4IRCA3 HadCM3Q16 A1B</i>	-2.3	0.1	7.8	-12.9	10.1	-18.0	-8.0	-13.8	-18.6	10.7	12.9	17.8	5.8	2.4	-13.4	2.6
<i>CNRM-RM5.1 ARGEGE A1B</i>	-0.5	18.3	16.0	-0.3	-24.4	-29.3	-14.7	-16.9	-0.4	2.6	11.1	7.0	6.9	-0.2	-20.1	4.6
<i>DMI-HIRHAM5 ARPEGE A1B</i>	3.6	17.4	10.8	-7.9	-21.3	-21.5	0.9	-23.1	-1.3	6.3	-3.9	13.2	10.6	-3.3	-15.7	0.5
<i>DMI-HIRHAM5 ECHAM5-r3 A1B</i>	4.7	8.8	18.7	15.8	-5.4	-7.3	-7.8	13.6	6.0	6.3	16.5	-3.7	2.4	11.1	1.0	9.7
<i>ETHZ-CLM HadCM3Q0 A1B</i>	14.2	0.3	-0.8	-2.7	8.4	11.2	-8.6	-27.8	-7.5	-5.2	4.4	21.9	13.4	1.2	-10.4	-2.6
<i>ICTP-REGCM3 ECHAM5-r3 A1B</i>	-2.6	-4.2	19.8	1.1	1.7	-12.2	-2.8	-1.3	6.3	10.8	-4.9	-22.8	-10.7	9.4	-5.0	4.1
<i>KNMI-RACMO2 ECHAM5-r3 A1B</i>	-3.6	-0.2	9.2	-5.6	-6.7	-14.9	-14.7	-2.8	12.0	18.2	-4.6	-15.2	-7.2	0.5	-9.9	8.4
<i>METO-HadRM3Q0 HadCM3Q0 A1B</i>	12.4	-1.6	0.6	-3.8	8.1	-12.2	-3.9	-13.6	-0.6	5.4	3.7	17.1	10.5	1.4	-10.3	3.0
<i>METO-HadRM3Q3 HadCM3Q3 A1B</i>	32.0	-2.9	-8.7	26.1	9.2	1.1	-25.0	-14.6	7.7	15.0	6.2	3.8	12.3	6.3	-12.9	9.7
<i>METO-HadRM3Q16 HadCM3Q16 A1B</i>	-5.8	3.6	3.4	-4.5	0.4	-22.0	-8.5	-18.6	-13.0	6.0	16.6	8.8	2.1	0.3	-16.7	3.8
<i>MPI-M-REMO ECHAM5-r3 A1B</i>	-3.1	-7.5	15.5	12.0	-11.0	-20.5	-16.9	-14.2	5.3	17.0	-13.0	-25.6	-12.8	7.0	-16.9	3.1
<i>SMHIRCA BCM A1B</i>	12.3	36.1	28.8	15.5	-26.8	-3.7	-7.5	-15.3	-7.9	3.6	8.3	22.3	22.0	9.3	-9.6	1.7
<i>SMHIRCA ECHAM5-r3 A1B</i>	-4.8	-2.2	15.7	1.1	-12.2	-20.3	-14.4	-2.1	1.3	16.0	-2.6	-16.4	-8.6	3.7	-11.2	5.2
<i>SMHIRCA HadCM3Q3 A1B</i>	27.3	7.2	-5.6	18.5	16.9	-1.9	-19.0	-8.9	19.1	6.4	9.3	18.9	18.8	7.6	-9.6	11.3
<i>SDSM HadCM3 A2</i>	-1.2	8.8	-11.3	-21.8	-8.4	6.6	3.3	-20.3	-5.0	-15.2	1.2	2.8	2.9	-13.6	-5.4	-6.4
<i>SDSM HadCM3 B2</i>	3.3	0.3	-2.2	-0.8	-12.4	-1.3	-6.6	-20.2	-8.5	0.0	-0.2	12.5	5.9	-4.6	-10.6	-2.6
<i>SDSM CSIROmk2 A2</i>	17.4	12.7	5.0	-7.4	7.9	-19.7	-12.2	-16.7	-19.1	1.5	11.1	15.6	15.5	2.3	-16.3	-1.4
<i>SDSM CSIROmk2 B2</i>	33.5	9.7	-9.0	2.7	-6.6	6.5	-20.8	9.2	-2.8	-8.1	-1.5	21.5	23.1	-5.0	-0.6	-4.2
<i>SDSM CGCM2 A2</i>	20.7	0.8	-9.5	-10.5	-31.4	-14.0	-11.0	-1.7	4.8	-10.5	2.8	28.2	18.7	-16.0	-8.2	-1.3
<i>SDSM CGCM2 B2</i>	5.2	5.1	0.5	-15.7	-18.3	-1.0	-10.8	-12.4	-2.0	-5.6	8.9	24.1	12.4	-9.4	-8.5	0.5

Table II-1 Projected changes (%) in mean monthly and seasonal precipitation receipts for the Burrishoole catchment calculated over the 2050s horizon (2040-2069) relative to the 30 year control period. (1961-1990). The table is colour coded to highlight increases/decreases.

2080s Precipitation Change (%)	Jan	Feb	Mar	Apr	May	Jun	Jul	Aug	Sept	Oct	Nov	Dec	Winter	Spring	Summer	Autumn
<i>C4IRCA3 HadCM3Q16 A1B</i>	17.3	7.9	4.4	5.4	13.0	-23.3	3.5	-7.9	3.6	13.6	34.5	15.2	14.0	7.1	-9.3	17.9
<i>CNRM-RM5.1 ARGEGE A1B</i>	13.4	8.9	9.3	10.8	-20.2	-27.8	-13.4	-35.0	10.3	3.3	14.7	13.1	12.2	1.3	-26.4	9.3
<i>DMI-HIRHAM5 ARPEGE A1B</i>	14.3	4.8	6.4	-1.0	-25.6	-26.2	-0.2	-33.5	-0.7	-0.3	2.1	15.8	12.5	-4.5	-21.7	0.4
<i>DMI-HIRHAM5 ECHAM5-r3 A1B</i>	23.8	5.0	19.6	24.4	3.1	0.6	-3.5	15.3	-3.2	7.2	20.4	13.2	15.2	16.3	5.3	8.6
<i>ETHZ-CLM HadCM3Q0 A1B</i>	5.7	11.9	7.8	-6.5	-0.1	-4.8	-10.7	-11.9	0.8	10.5	7.4	2.0	6.0	1.5	-9.4	6.5
<i>ICTP-REGCM3 ECHAM5-r3 A1B</i>	16.6	1.8	12.2	6.7	3.0	-9.3	8.5	1.1	-5.2	-1.9	16.9	9.3	10.2	8.1	0.1	3.5
<i>KNMI-RACMO2 ECHAM5-r3 A1B</i>	18.2	11.4	18.1	3.9	-12.2	-12.1	-1.6	-5.0	2.2	4.9	21.3	10.0	13.4	5.5	-6.1	9.7
<i>METO-HadRM3Q0 HadCM3Q0 A1B</i>	10.5	4.9	4.7	2.5	10.7	-21.0	-12.4	-11.3	-4.5	18.6	12.9	6.2	7.4	5.7	-14.6	9.6
<i>METO-HadRM3Q3 HadCM3Q3 A1B</i>	14.1	12.9	8.3	41.9	-9.1	-20.7	-31.7	-27.5	11.4	8.5	14.8	24.1	17.5	13.1	-26.6	11.6
<i>METO-HadRM3Q16 HadCM3Q16 A1B</i>	15.4	6.4	3.9	12.9	10.5	-34.6	-9.0	-16.6	8.6	20.8	39.1	10.6	11.3	8.4	-19.9	23.4
<i>MPI-M-REMO ECHAM5-r3 A1B</i>	16.9	-8.6	7.1	18.2	-16.7	-23.5	-7.2	-13.1	2.6	-1.9	8.6	0.7	4.4	3.5	-14.4	3.1
<i>SMHIRCA BCM A1B</i>	23.0	39.7	39.6	27.6	-30.2	-1.2	-12.5	-9.3	-5.8	1.6	22.0	33.8	31.2	16.5	-7.8	6.3
<i>SMHIRCA ECHAM5-r3 A1B</i>	14.1	3.1	9.2	4.3	-13.8	-21.4	-6.1	-7.5	-1.7	6.7	20.6	10.9	10.1	1.3	-11.3	8.9
<i>SMHIRCA HadCM3Q3 A1B</i>	18.3	25.9	19.0	35.9	13.7	-7.6	-19.0	-11.0	29.1	7.2	21.0	23.3	22.2	22.4	-12.2	18.7
<i>SDSM HadCM3 A2</i>	16.6	5.3	1.1	-4.6	-6.0	-4.5	-19.2	-30.0	-14.7	-19.7	4.5	18.3	14.2	-2.5	-19.3	-9.7
<i>SDSM HadCM3 B2</i>	4.6	12.7	2.3	13.0	0.7	-5.3	-7.2	-10.5	-2.2	-9.5	-5.6	9.8	8.7	4.9	-8.0	-5.9
<i>SDSM CSIROmk2 A2</i>	9.6	33.2	-12.8	-2.3	13.5	-16.0	-1.1	2.4	-11.0	-0.1	-4.4	23.7	20.8	-2.4	-4.3	-4.9
<i>SDSM CSIROmk2 B2</i>	18.2	10.5	5.2	4.3	-7.9	3.5	-5.2	-8.4	2.7	-4.4	0.2	8.8	12.7	1.3	-3.9	-0.7
<i>SDSM CGCM2 A2</i>	22.0	5.7	-21.4	-32.2	-36.1	-25.4	-15.9	13.1	-5.1	-12.6	-8.2	11.2	13.9	-28.7	-7.2	-8.8
<i>SDSM CGCM2 B2</i>	22.0	3.9	-10.8	-20.5	-23.0	-10.5	-5.9	-13.3	-2.3	-12.4	9.5	12.6	14.0	-17.0	-10.3	-1.8

Table II-3 Projected changes (%) in mean monthly and seasonal precipitation receipts for the Burrishoole catchment calculated over the 2080s horizon (2070-2099) relative to the 30 year control period. (1961-1990). The table is colour coded to highlight increases/decreases.

Appendix III

Dotty plots from the Monte Carlo simulation conducted for each of the three rainfall-runoff models used in this study (TOPMODEL, HYSIM and HBV).

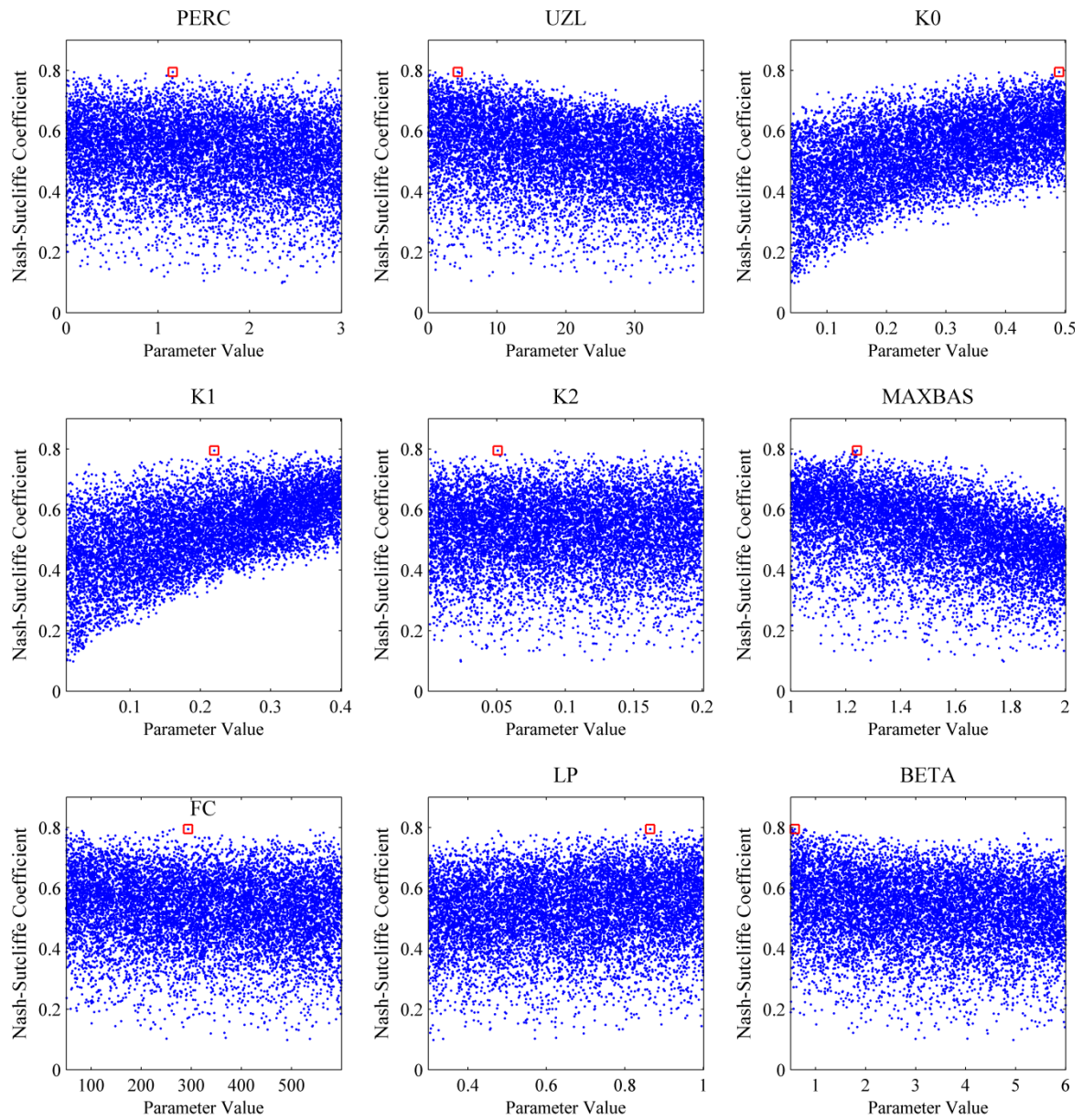


Figure III-1 Dot plots for the HBV-light model constructed using 10,000 sampled parameters sets. The Nash Sutcliffe (NS) efficiency criterion is used (y-axis). The red square denotes the parameter value with the highest NS score.

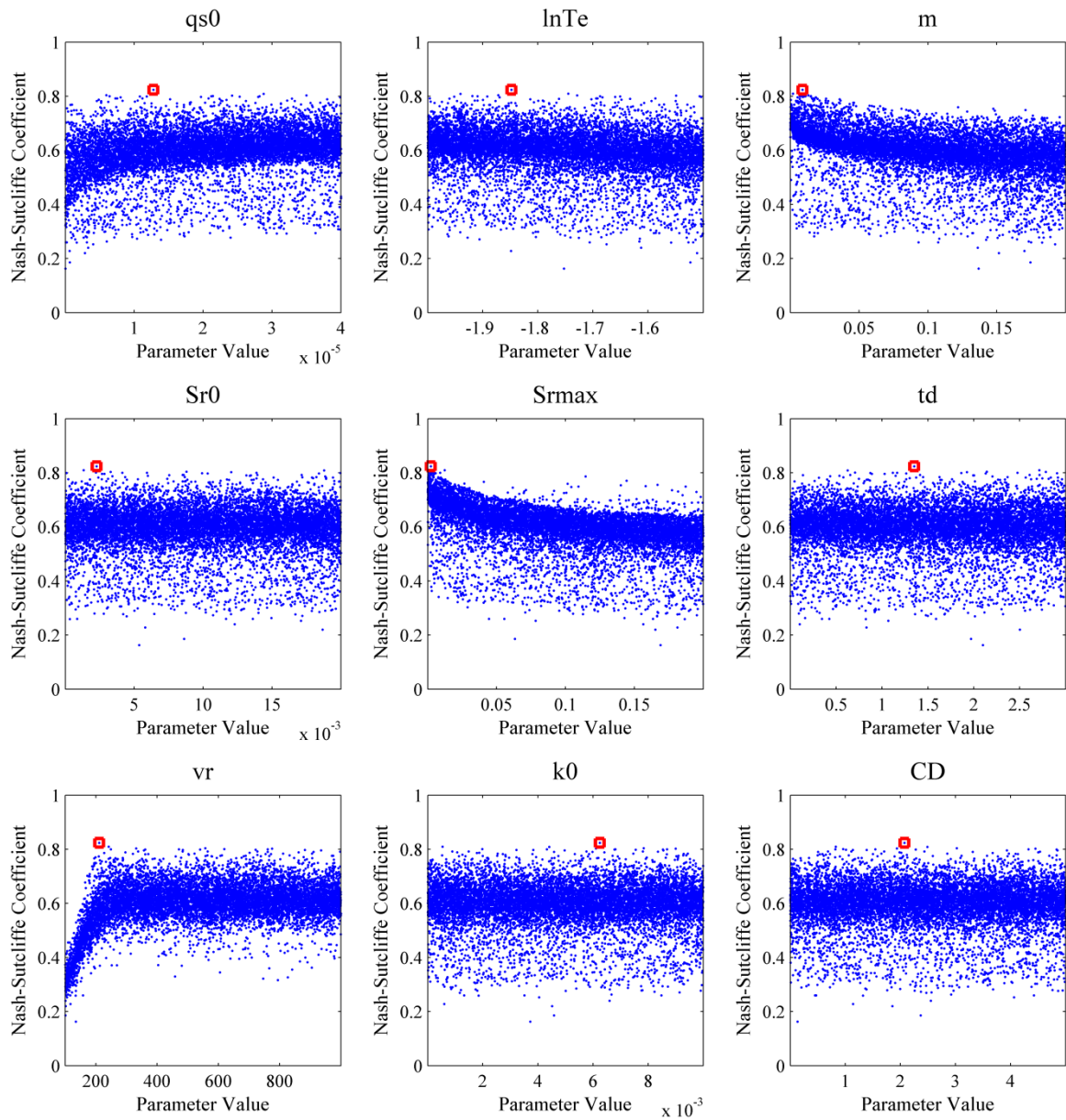


Figure III-2 Dotty plots for the TOPMODEL model constructed using 10,000 sampled parameters sets. The Nash Sutcliffe (NS) efficiency criterion is used (y-axis). The red square denotes the parameter value with the highest NS score.

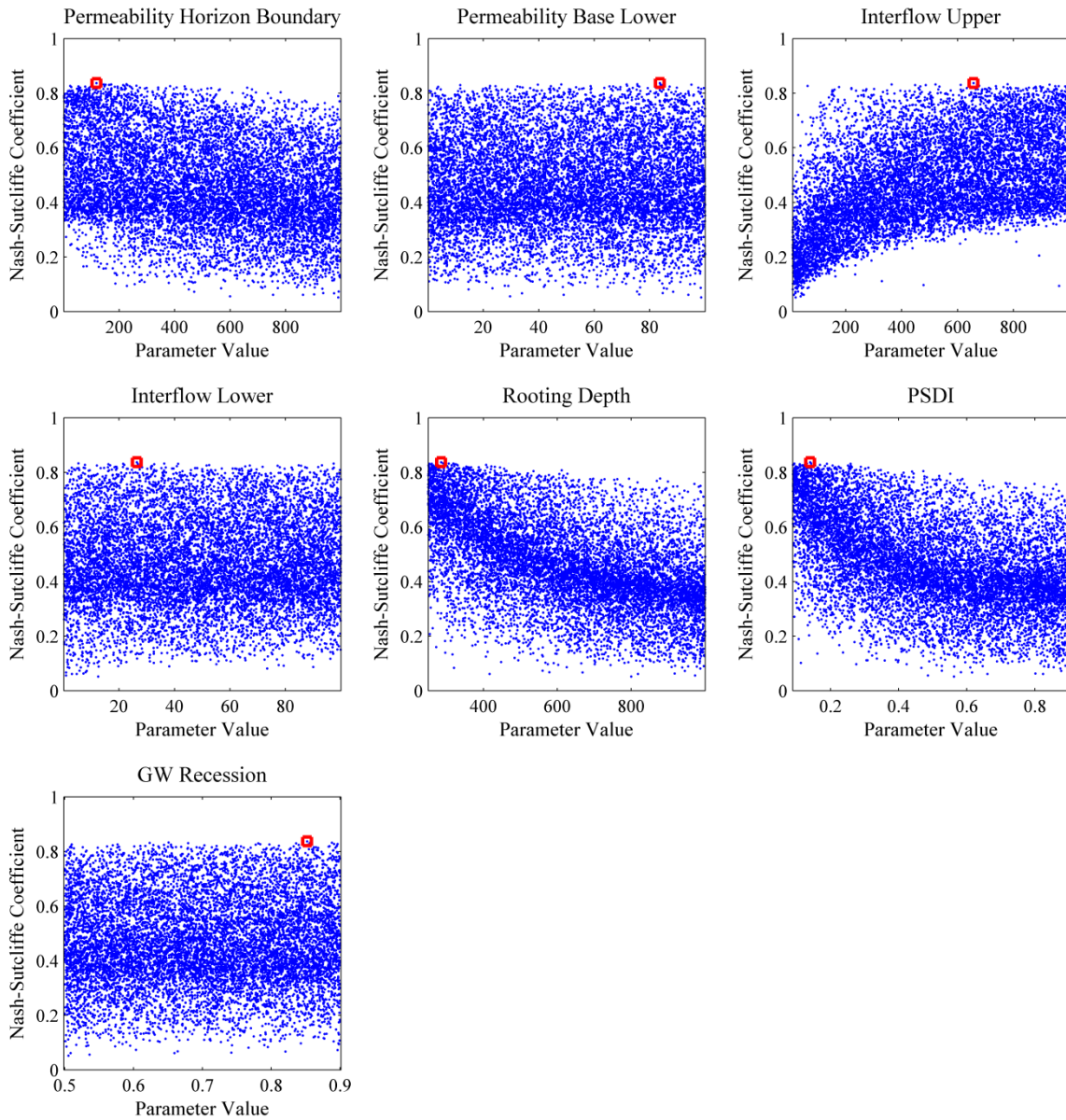


Figure III-3 Dotty plots for the HYSIM model constructed using 10,000 sampled parameters sets. The Nash Sutcliffe (NS) efficiency criterion is used (y-axis). The red square denotes the parameter value with the highest NS score.

Appendix IV

Projected changes in median (Q50), high (Q05) and low (Q95) flows for the Glenamong and Srahrevagh catchments respectively; estimated on a seasonal and monthly basis.

2020s Q50 Change (%)	Jan	Feb	Mar	Apr	May	Jun	Jul	Aug	Sept	Oct	Nov	Dec	Winter	Spring	Summer	Autumn
C4IRCA3 HadCM3Q16 A1B	-2.5	-5.8	-1.1	-16.5	5.2	-16.6	-13.4	-25.8	-3.2	3.6	9.1	0.7	-2.8	-1.6	-17.2	3.3
C4IRCA3 ECHAM5 A2	23.0	2.4	14.1	-14.4	-2.6	-10.2	-15.5	-6.3	-19.9	8.5	6.0	-3.6	8.1	-9.4	-13.8	0.6
CNRM-RM4.5 ARPEGE A1B	8.0	-3.5	-1.2	-13.7	-12.1	-11.3	-15.7	-25.3	-16.1	14.5	10.1	-3.1	1.1	-12.2	-16.1	6.8
CNRM-RM5.1 ARGEGE A1B	4.2	-6.5	-0.7	-14.5	-1.2	-13.2	-10.6	-9.5	-19.4	9.9	9.3	-8.7	-2.2	-8.7	-13.6	3.9
DMI-HIRHAM5 ARPEGE A1B	1.4	-4.1	3.7	-12.3	-5.1	-12.7	-10.6	-23.4	-11.0	12.2	5.2	-2.9	0.7	-9.5	-12.3	5.2
DMI-HIRHAM5 ECHAM5-r3 A1B	13.8	-1.8	41.0	-3.0	7.7	5.0	-3.8	-2.6	4.4	-1.6	5.9	-7.3	2.1	11.8	-2.1	3.4
ETHZ-CLM HadCM3Q0 A1B	-3.5	6.6	-2.2	-8.3	-12.5	-2.5	-6.5	-28.2	-28.9	-27.3	-17.3	6.9	5.1	-12.8	-11.7	-20.3
ICTP-REGCM3 ECHAM5-r3 A1B	18.0	-6.0	21.2	-13.2	-3.4	-14.5	-12.5	6.7	9.1	-10.1	-2.5	-20.1	-2.1	2.5	-10.2	-4.4
KNMI-RACMO2 ECHAM5-r3 A1B	11.2	5.4	6.8	-15.9	-9.1	-13.6	-13.1	-12.3	11.0	-3.2	0.2	-17.2	0.8	-7.9	-13.2	2.6
METNOHIRHAM BCM A1B	-6.9	27.3	34.1	-10.5	-18.8	-12.4	-6.3	-17.4	-6.0	11.1	5.8	37.9	19.4	-7.5	-12.6	5.7
METNOHIRHAM HadCM3Q0 A1B	5.1	6.5	9.4	-18.4	-15.2	-6.5	-7.7	-30.5	-22.1	-28.6	-1.0	2.9	2.8	-19.0	-12.8	-15.5
METO-HadRM3Q0 HadCM3Q0 A1B	-4.3	-9.5	-9.4	-25.4	-20.3	-12.8	-10.2	-25.9	-8.0	-19.6	-9.1	-1.2	-4.2	-25.4	-14.9	-13.1
METO-HadRM3Q3 HadCM3Q3 A1B	24.9	-14.2	-23.8	13.0	8.0	-2.5	-11.0	-14.0	6.2	-3.0	-5.8	14.5	7.3	-1.9	-7.6	-0.2
METO-HadRM3Q16 HadCM3Q16 A1B	-6.4	-3.7	0.2	-12.5	2.1	-14.8	-8.2	-28.5	-18.6	16.2	16.6	11.4	-0.9	-9.3	-14.9	9.0
MPI-M-REMO ECHAM5-r3 A1B	19.0	-2.9	5.7	-10.9	-10.8	-17.4	-13.2	2.3	23.2	-10.7	-4.0	-28.0	-4.0	-8.2	-14.0	-3.2
OURANOSMRCC4.2.1 CGCM3 A1B	-30.0	-35.2	-23.3	-5.6	-1.9	-7.4	-10.2	-24.2	-4.0	-16.8	22.6	-0.7	-24.4	-10.0	-12.9	0.9
SMHIRCA BCM A1B	10.2	38.9	57.5	-8.9	-18.0	-2.8	-10.1	-16.1	-10.5	5.2	15.5	37.3	29.7	1.6	-10.9	1.7
SMHIRCA ECHAM5-r3 A1B	13.3	0.9	15.1	-18.0	-11.9	-17.0	-10.4	-7.3	8.0	-7.6	-0.7	-15.1	-2.6	-9.4	-14.7	0.5
SMHIRCA HadCM3Q3 A1B	24.0	-3.1	-17.9	19.5	9.0	-6.4	-9.1	-13.5	9.9	-1.4	10.4	42.3	23.3	-1.4	-10.1	6.9
SDSM HadCM3 A2	-12.1	-5.5	-12.2	-15.3	-12.1	-2.1	-4.5	-29.3	-2.6	-14.9	-9.0	-9.0	-9.3	-17.6	-11.2	-9.7
SDSM HadCM3 B2	-3.9	8.6	5.2	-12.4	-14.9	-2.4	-9.9	-12.2	-3.5	-7.1	7.7	-17.2	-5.9	-14.5	-8.8	-3.0
SDSM CSIROmk2 A2	15.3	4.4	5.2	-9.9	-4.9	-6.4	-8.3	-17.3	-11.0	0.3	-7.2	10.1	9.0	-9.7	-10.6	-5.6
SDSM CSIROmk2 B2	1.6	7.6	-10.9	-16.3	-8.8	-4.6	-12.5	-16.2	-8.6	-21.4	-22.5	11.7	4.8	-15.8	-10.7	-16.7
SDSM CGCM2 A2	3.9	-5.0	-2.2	-9.1	-9.8	-16.8	-16.7	-22.1	-15.7	-1.4	5.5	5.6	-0.1	-12.4	-17.1	-4.5
SDSM CGCM2 B2	20.9	-9.9	4.1	-8.9	-1.3	-10.0	-9.8	-16.8	2.2	-19.1	7.7	8.1	-0.2	-8.3	-12.3	-5.0

Table IV-1 Projected changes (%) in the Q50 low flow statistics calculated on a monthly and seasonal basis for the Glenamong catchment. Changes are estimated for the 2020s horizon (2010-2039) relative to the 30 year control period. (1961-1990). Projected changes in Q50 are estimated using the median series from the multimodel simulation. The table is colour coded to highlight increases/decreases.

2050s Q50 Change (%)	Jan	Feb	Mar	Apr	May	Jun	Jul	Aug	Sept	Oct	Nov	Dec	Winter	Spring	Summer	Autumn
C4IRCA3 HadCM3Q16 A1B	-13.6	-10.1	-2.9	-25.2	-10.2	-16.6	-15.6	-33.9	-35.5	2.6	7.4	10.4	-6.8	-16.4	-19.7	-7.9
CNRM-RM5.1 ARGEGE A1B	-4.8	14.9	7.3	-7.3	-16.8	-21.9	-19.1	-27.4	-36.9	3.5	6.2	-3.1	-1.0	-19.5	-23.8	-3.1
DMI-HIRHAM5 ARPEGE A1B	-0.2	20.0	1.5	-12.4	-14.9	-21.2	-16.5	-34.1	-22.8	-4.0	-12.6	-8.1	2.7	-18.1	-19.8	-11.7
DMI-HIRHAM5 ECHAM5-r3 A1B	4.5	5.8	23.0	-3.2	-6.1	-9.9	-7.4	-11.1	1.1	5.8	1.6	-13.5	1.7	-0.4	-11.4	4.2
ETHZ-CLM HadCM3Q0 A1B	8.5	-2.0	-11.0	-12.8	-9.9	-0.9	-8.9	-32.0	-28.9	-22.4	-10.2	27.3	11.9	-13.7	-13.4	-21.1
ICTP-REGCM3 ECHAM5-r3 A1B	-12.7	-24.6	19.9	-8.1	-7.7	-15.6	-9.4	-19.8	-3.3	16.5	-14.6	-37.0	-24.1	0.2	-13.4	-2.2
KNMI-RACMO2 ECHAM5-r3 A1B	-7.8	-11.0	7.5	-15.0	-15.5	-18.9	-14.2	-28.6	7.0	19.3	-16.3	-30.1	-16.9	-11.8	-19.6	0.1
METO-HadRM3Q0 HadCM3Q0 A1B	-0.8	-10.3	-14.8	-17.4	-12.7	-12.1	-11.5	-27.9	-22.7	-9.4	0.8	5.1	-4.4	-19.8	-15.9	-10.2
METO-HadRM3Q3 HadCM3Q3 A1B	33.6	-10.5	-19.7	10.7	8.4	-7.6	-23.0	-21.7	14.1	8.3	3.1	0.4	10.1	2.7	-16.1	3.0
METO-HadRM3Q16 HadCM3Q16 A1B	-12.5	-7.5	1.5	-26.1	-13.7	-20.3	-15.4	-34.2	-41.8	-3.5	7.0	4.5	-5.4	-23.1	-20.7	-7.7
MPI-M-REMO ECHAM5-r3 A1B	-2.7	-16.8	18.6	-10.9	-12.9	-20.4	-16.8	-25.2	-7.4	16.5	-22.4	-42.6	-25.4	-9.4	-21.1	-6.1
SMHIRCA BCM A1B	29.1	51.7	61.0	3.1	-15.5	-8.4	-7.1	-26.8	-14.4	0.2	16.7	27.2	36.7	3.1	-12.0	-0.6
SMHIRCA ECHAM5-r3 A1B	-8.4	-14.4	17.0	-11.6	-13.7	-22.6	-14.1	-18.7	-9.9	13.1	-16.1	-27.1	-18.0	-7.2	-19.8	-3.8
SMHIRCA HadCM3Q3 A1B	37.2	5.9	-11.1	4.2	16.5	-8.0	-15.2	-22.3	9.2	0.1	6.4	26.3	25.9	4.4	-15.4	6.8
SDSM HadCM3 A2	0.8	17.1	-17.4	-24.5	-13.7	-3.9	-10.2	-29.0	-19.1	-29.8	-1.1	-1.2	5.1	-21.7	-13.6	-17.1
SDSM HadCM3 B2	2.1	-2.0	-2.8	-12.5	-16.7	-12.2	-11.1	-29.7	-24.6	-14.3	-0.9	14.6	4.4	-16.7	-15.5	-13.1
SDSM CSIROmk2 A2	21.9	20.0	10.2	-13.7	-6.5	-15.3	-12.7	-25.6	-39.4	-3.6	-0.5	12.6	14.8	-14.0	-17.0	-11.8
SDSM CSIROmk2 B2	29.7	20.6	-14.0	-9.7	-10.2	-7.5	-12.1	2.8	-1.8	-12.4	-10.2	21.6	25.1	-15.2	-8.4	-8.8
SDSM CGCM2 A2	22.8	-5.9	-13.2	-13.5	-17.5	-16.5	-14.1	-21.6	-15.8	-7.9	0.4	32.8	16.4	-21.9	-17.6	-4.1
SDSM CGCM2 B2	12.2	7.8	1.8	-20.7	-13.3	-13.9	-12.2	-26.2	5.5	-11.8	10.1	26.2	11.0	-20.9	-17.2	0.3

Table IV-2 Projected changes (%) in the Q50 low flow statistics calculated on a monthly and seasonal basis for the Glenamong catchment. Changes are estimated for the 2050s horizon (2040-2069) relative to the 30 year control period. (1961-1990). Projected changes in Q50 are estimated using the median series from the multimodel simulation. The table is colour coded to highlight increases/decreases.

2080s Q50 Change (%)	Jan	Feb	Mar	Apr	May	Jun	Jul	Aug	Sept	Oct	Nov	Dec	Winter	Spring	Summer	Autumn
C4IRCA3 HadCM3Q16 A1B	1.3	-4.1	-3.6	-13.1	-3.6	-18.4	-11.3	-28.9	-19.8	2.2	36.9	11.0	-1.1	-7.2	-17.5	7.8
CNRM-RM5.1 ARGEGE A1B	8.1	2.6	4.0	-2.6	-16.0	-24.4	-21.6	-38.8	-24.4	-8.1	5.1	6.2	4.3	-17.1	-29.3	-6.8
DMI-HIRHAM5 ARPEGE A1B	7.4	-0.2	-7.2	-10.4	-18.0	-23.8	-18.1	-37.4	-24.7	-15.5	-4.8	-3.8	2.6	-17.7	-22.5	-15.6
DMI-HIRHAM5 ECHAM5-r3 A1B	31.0	5.0	31.1	5.3	1.0	-0.1	-1.2	-0.6	-19.4	2.4	8.6	9.9	14.5	10.6	-3.3	4.0
ETHZ-CLM HadCM3Q0 A1B	2.7	-0.7	0.3	-14.9	-12.5	-11.5	-12.6	-30.0	-28.4	-8.6	-5.5	-0.8	2.9	-13.5	-17.1	-13.8
ICTP-REGCM3 ECHAM5-r3 A1B	14.5	-11.2	15.2	-2.9	-3.7	-14.2	-1.9	-12.8	-27.2	-7.8	7.6	3.9	4.9	0.9	-7.1	-7.3
KNMI-RACMO2 ECHAM5-r3 A1B	26.4	5.4	13.4	-1.6	-14.2	-18.1	-9.6	-26.4	-16.5	-5.5	15.1	4.7	12.2	-6.3	-16.2	-0.9
METO-HadRM3Q0 HadCM3Q0 A1B	1.8	-9.7	-7.1	-18.0	-14.5	-17.1	-14.8	-26.6	-33.2	-0.5	4.6	0.7	-3.2	-18.5	-17.6	-7.3
METO-HadRM3Q3 HadCM3Q3 A1B	7.5	9.2	9.2	60.9	-2.9	-15.5	-25.4	-32.2	3.9	5.8	8.5	26.7	13.3	22.9	-23.6	7.4
METO-HadRM3Q16 HadCM3Q16 A1B	5.2	2.7	7.4	-8.4	-0.2	-23.8	-15.9	-35.1	-29.9	7.0	40.8	8.3	3.9	-6.4	-22.6	6.6
MPI-M-REMO ECHAM5-r3 A1B	35.0	-10.5	3.6	7.2	-16.2	-23.4	-11.4	-20.3	-26.2	-12.7	10.6	-1.1	6.8	-9.2	-18.7	-7.6
SMHIRCA BCM A1B	45.1	50.4	72.0	11.5	-16.7	-3.9	-5.9	-25.4	-14.4	-4.1	45.1	60.6	54.6	0.7	-10.1	7.6
SMHIRCA ECHAM5-r3 A1B	26.4	-6.8	6.4	-7.7	-14.0	-22.8	-10.8	-22.4	-28.3	-3.4	6.6	10.5	6.9	-10.6	-18.4	-5.1
SMHIRCA HadCM3Q3 A1B	17.3	35.2	22.4	38.3	8.8	-11.1	-11.6	-31.1	14.0	4.9	28.5	34.0	27.4	20.0	-16.8	14.5
SDSM HadCM3 A2	13.0	5.3	-5.0	-14.9	-12.8	-9.3	-19.3	-35.9	-26.8	-28.9	-0.7	13.6	14.4	-15.9	-21.7	-19.1
SDSM HadCM3 B2	-0.2	21.9	-3.0	3.4	-9.9	-11.2	-13.4	-23.9	-5.9	-21.2	-5.1	2.8	8.0	-5.1	-14.8	-10.6
SDSM CSIROmk2 A2	9.4	31.6	-18.6	-10.7	-1.4	-14.0	-9.0	-15.5	-28.1	3.1	-10.5	25.5	20.4	-13.1	-14.0	-9.7
SDSM CSIROmk2 B2	12.6	16.6	2.3	-9.2	-10.7	-7.5	-7.5	-14.6	-10.3	-6.6	-11.4	8.1	12.4	-15.1	-9.3	-8.6
SDSM CGCM2 A2	28.4	4.2	-25.9	-30.0	-26.1	-26.2	-18.7	-14.3	-20.4	-17.0	-12.2	2.6	9.9	-30.8	-21.0	-15.2
SDSM CGCM2 B2	29.6	7.3	-23.0	-22.3	-15.6	-17.6	-12.8	-24.5	-8.2	-14.2	10.0	6.9	11.9	-24.2	-17.4	-3.2

Table IV-3 Projected changes (%) in the Q50 low flow statistics calculated on a monthly and seasonal basis for the Glenamong catchment. Changes are estimated for the 2080s horizon (2070-2099) relative to the 30 year control period. (1961-1990). Projected changes in Q50 are estimated using the median series from the multimodel simulation. The table is colour coded to highlight increases/decreases.

2020s Change Q05 (%)	Jan	Feb	Mar	Apr	May	Jun	Jul	Aug	Sept	Oct	Nov	Dec	Winter	Spring	Summer	Autumn
<i>C4IRCA3 HadCM3Q16 A1B</i>	5.1	-1.4	-6.6	-10.7	14.8	-34.3	-7.1	-16.7	-3.3	3.1	-1.8	1.0	1.4	-5.8	-19.0	1.5
<i>C4IRCA3 ECHAM5 A2</i>	9.2	-4.5	4.1	0.3	7.7	-1.1	-35.2	-19.5	12.0	3.2	-0.5	-0.8	1.0	5.8	-9.0	3.2
<i>CNRM-RM4.5 ARPEGE A1B</i>	4.7	3.2	-5.0	-13.0	0.6	-1.9	-14.4	8.5	-14.6	4.9	17.7	3.6	5.3	-5.6	3.9	3.9
<i>CNRM-RM5.1 ARPEGE A1B</i>	3.6	13.9	-0.9	-12.2	-2.5	-16.3	-1.7	5.2	-1.4	12.9	15.4	13.7	5.5	2.7	-8.9	7.3
<i>DMI-HIRHAM5 ARPEGE A1B</i>	15.3	1.4	4.0	-12.1	-0.8	-24.2	28.7	-18.3	11.7	18.7	8.9	24.8	15.9	-1.2	-15.3	13.2
<i>DMI-HIRHAM5 ECHAM5-r3 A1B</i>	3.5	-15.0	18.8	7.5	17.4	46.2	-3.8	20.0	7.2	0.3	6.2	1.7	2.0	19.1	16.2	3.9
<i>ETHZ-CLM HadCM3Q0 A1B</i>	12.5	6.0	-4.2	8.1	-6.0	3.5	-7.7	1.6	-0.3	-2.6	-4.2	21.9	17.8	0.5	-4.0	-3.1
<i>ICTP-REGCM3 ECHAM5-r3 A1B</i>	12.2	11.8	5.9	-6.5	3.2	-3.3	-0.2	7.0	10.6	-8.8	1.8	-6.3	0.5	5.1	-0.8	2.4
<i>KNMI-RACMO2 ECHAM5-r3 A1B</i>	4.0	2.9	4.7	-5.3	-4.3	2.5	-6.0	3.3	5.3	5.8	14.6	-12.3	-3.2	2.8	-0.2	7.5
<i>METNOHIRHAM BCM A1B</i>	5.7	18.3	15.8	-7.7	-40.1	-14.6	-5.4	-14.5	-0.5	6.1	-12.4	17.0	7.1	10.0	-8.3	2.8
<i>METNOHIRHAM HadCM3Q0 A1B</i>	18.3	-4.8	12.8	-20.5	3.8	-8.0	-3.5	-4.0	3.6	-21.3	12.8	3.6	9.0	-2.0	-11.3	-1.8
<i>METO-HadRM3Q0 HadCM3Q0 A1B</i>	20.3	-5.2	-11.1	-11.7	-2.7	-8.2	-14.3	11.0	15.4	-5.8	0.5	14.1	12.9	-9.8	-10.3	1.0
<i>METO-HadRM3Q3 HadCM3Q3 A1B</i>	21.0	-4.2	-9.5	0.7	7.8	21.7	14.2	-6.4	-4.2	8.5	10.0	6.0	5.1	-1.1	4.3	2.9
<i>METO-HadRM3Q16 HadCM3Q16 A1B</i>	-7.3	0.5	-10.2	-4.2	-7.6	-26.1	10.0	-6.6	3.3	27.3	9.6	-2.1	-0.5	-11.0	-16.0	11.7
<i>MPI-M-REMO ECHAM5-r3 A1B</i>	0.7	-0.7	6.3	24.7	1.2	-7.8	-21.8	1.7	9.5	-5.0	-0.9	-3.4	-1.5	11.7	-5.9	0.7
<i>OURANOSMRCC4.2.1 CGCM3 A1B</i>	-5.5	-3.8	6.0	13.0	0.2	11.1	16.9	-2.2	-3.2	4.6	11.6	3.0	0.4	5.5	5.9	4.7
<i>SMHIRCA BCM A1B</i>	-0.3	8.0	6.7	10.9	-21.3	-3.7	-27.3	8.5	-13.8	6.0	1.5	7.8	2.5	9.4	-3.1	-2.1
<i>SMHIRCA ECHAM5-r3 A1B</i>	0.7	1.8	7.7	5.9	-3.6	2.5	-12.8	-6.9	6.6	1.9	8.0	-10.4	-7.0	5.3	-8.9	4.0
<i>SMHIRCA HadCM3Q3 A1B</i>	26.8	0.9	4.5	9.2	22.5	0.8	-14.8	-5.2	19.5	5.0	9.0	22.3	22.5	6.3	-3.8	11.9
<i>SDSM HadCM3 A2</i>	1.5	-12.2	-3.0	-15.6	-21.2	36.0	11.9	-14.6	-6.3	2.6	-8.3	9.8	2.1	-6.3	-4.1	-2.4
<i>SDSM HadCM3 B2</i>	-3.1	-9.7	12.4	-28.9	3.2	19.7	-14.4	4.4	3.6	-3.3	-8.5	7.3	1.8	0.6	4.6	-3.4
<i>SDSM CSIROmk2 A2</i>	8.4	4.3	1.6	-12.9	-2.2	5.0	-24.5	-12.2	0.3	3.2	5.1	6.7	11.7	-4.6	-3.4	2.3
<i>SDSM CSIROmk2 B2</i>	3.5	-9.4	-13.0	2.4	-14.0	-3.9	-12.0	-12.6	4.9	-22.9	-11.7	1.9	0.5	-6.3	-8.9	-10.5
<i>SDSM CGCM2 A2</i>	4.7	-14.3	-1.6	10.6	-35.9	-29.6	-28.8	-7.0	-2.1	-0.4	4.3	5.4	3.0	-4.5	-19.4	0.3
<i>SDSM CGCM2 B2</i>	-3.1	-6.3	8.6	4.2	3.5	3.0	-25.9	-2.9	1.3	-24.9	6.7	2.2	3.5	-0.6	-4.2	-12.2

Table IV-4 Projected changes (%) in the Q05 low flow statistics calculated on a monthly and seasonal basis for the Glenamong catchment. Changes are estimated for the 2020s horizon (2010-2039) relative to the 30 year control period. (1961-1990). Projected changes in Q05 are estimated using the median series from the multimodel simulation. The table is colour coded to highlight increases/decreases.

2050s Change Q05 (%)	<i>Jan</i>	<i>Feb</i>	<i>Mar</i>	<i>Apr</i>	<i>May</i>	<i>Jun</i>	<i>Jul</i>	<i>Aug</i>	<i>Sept</i>	<i>Oct</i>	<i>Nov</i>	<i>Dec</i>	<i>Winter</i>	<i>Spring</i>	<i>Summer</i>	<i>Autumn</i>
<i>CAIRCA3 HadCM3Q16 A1B</i>	5.8	-3.3	4.2	-9.6	16.5	-17.2	-16.8	-9.5	-12.8	18.4	12.1	12.4	8.8	1.8	-13.8	9.9
<i>CNRM-RM5.1 ARGEGE A1B</i>	-0.5	10.1	20.0	-4.0	-34.6	-35.0	-21.0	-14.1	10.7	1.5	3.8	11.2	2.9	10.5	-25.7	1.8
<i>DMI-HIRHAM5 ARPEGE A1B</i>	14.9	2.6	11.4	-12.6	-32.3	-24.6	3.8	-29.6	5.5	6.7	3.7	38.4	18.8	-0.4	-23.4	3.5
<i>DMI-HIRHAM5 ECHAM5-r3 A1B</i>	5.0	1.2	20.4	17.7	6.3	5.1	-2.7	29.6	7.6	6.7	24.9	8.9	9.1	13.2	9.8	14.6
<i>ETHZ-CLM HadCM3Q0 A1B</i>	11.7	-0.8	4.4	-3.4	16.9	12.5	8.3	-19.9	-1.2	-1.3	12.7	12.7	11.1	2.4	-13.5	3.8
<i>ICTP-REGCM3 ECHAM5-r3 A1B</i>	-6.6	2.8	10.1	-11.8	4.5	-11.5	-9.2	3.1	9.4	6.9	-5.0	-10.9	-7.6	8.4	-5.0	6.4
<i>KNMI-RACMO2 ECHAM5-r3 A1B</i>	-5.9	2.8	2.8	-10.3	-9.4	-10.3	-20.3	13.0	3.1	19.3	3.8	-0.8	-0.8	-0.3	-8.0	9.9
<i>METO-HadRM3Q0 HadCM3Q0 A1B</i>	16.9	-3.3	2.3	-11.3	9.3	-12.6	-12.3	-6.9	3.6	10.0	4.0	19.3	16.6	-3.2	-17.1	6.4
<i>METO-HadRM3Q3 HadCM3Q3 A1B</i>	16.8	3.0	-10.8	21.2	0.7	10.9	-11.4	-9.5	-6.6	23.6	9.1	9.1	9.5	1.3	-10.9	12.4
<i>METO-HadRM3Q16 HadCM3Q16 A1B</i>	-8.9	-2.7	-3.4	-0.4	-8.0	-26.9	-5.7	-13.7	-9.3	7.8	17.2	3.6	0.1	-1.4	-27.0	7.7
<i>MPI-M-REMO ECHAM5-r3 A1B</i>	-6.8	-4.2	12.9	10.0	-7.2	-22.3	-13.3	-10.6	5.3	13.1	-7.2	-10.3	-8.2	7.2	-14.7	4.5
<i>SMHIRCA BCM A1B</i>	4.2	27.0	10.0	23.3	-19.7	-5.6	-15.8	-4.9	-0.2	5.9	-1.5	20.4	14.3	15.5	-10.5	2.1
<i>SMHIRCA ECHAM5-r3 A1B</i>	-6.6	9.1	16.7	-2.4	-5.6	-17.2	-18.6	-2.8	-3.2	16.9	8.7	-8.2	-5.7	7.0	-15.1	7.6
<i>SMHIRCA HadCM3Q3 A1B</i>	14.2	10.7	-5.6	5.7	8.4	-0.4	-22.3	-9.5	13.3	6.9	11.4	18.8	12.3	0.0	0.5	12.3
<i>SDSM HadCM3 A2</i>	-7.0	-3.1	-11.8	-32.6	-29.9	-2.4	27.0	-24.1	-6.5	-0.3	-8.1	-4.7	-2.6	-13.8	-11.7	-4.3
<i>SDSM HadCM3 B2</i>	7.4	-1.6	1.9	-6.0	-11.7	-13.8	-8.5	-23.8	-1.1	0.5	-7.7	22.5	8.7	1.6	-18.6	-5.5
<i>SDSM CSIROmk2 A2</i>	10.1	-8.1	-1.4	-6.1	4.7	-29.3	-36.9	-27.0	-22.1	-7.0	16.0	13.4	12.3	1.0	-29.8	-2.1
<i>SDSM CSIROmk2 B2</i>	31.1	-3.9	-13.3	-16.1	-20.4	-6.2	-45.7	-2.7	-15.7	-7.6	-2.6	14.5	18.5	-14.4	-1.3	-5.5
<i>SDSM CGCM2 A2</i>	8.8	1.5	-17.2	-11.0	-50.2	-29.4	-26.6	-1.0	0.7	-19.5	-5.5	21.6	13.6	-20.9	-16.4	-9.1
<i>SDSM CGCM2 B2</i>	-6.6	14.9	-7.1	-18.8	-31.9	-12.0	-43.4	-22.2	-10.8	-6.0	2.1	7.9	6.0	-12.4	-24.2	-8.0

Table IV-5 Percentage change in the Q05 low flow statistics calculated on a monthly and seasonal basis for the Glenamong catchment. Changes are estimated for the 2050s horizon (2040-2069) relative to the 30 year control period. (1961-1990). Projected changes in Q05 are estimated using the median series from the multimodel simulation. The table is colour coded to highlight increases/decreases.

2080s Change Q05 (%)	Jan	Feb	Mar	Apr	May	Jun	Jul	Aug	Sept	Oct	Nov	Dec	Winter	Spring	Summer	Autumn
C4IRCA3 HadCM3Q16 A1B	21.3	14.5	1.5	-5.1	11.1	-25.2	-9.3	-14.5	11.5	19.7	27.6	17.4	19.7	4.3	-16.4	24.3
CNRM-RM5.1 ARGEGE A1B	8.2	13.6	15.9	13.1	-16.7	-29.7	-9.7	-30.0	18.2	7.2	18.3	10.1	7.0	6.7	-28.3	11.2
DMI-HIRHAM5 ARPEGE A1B	22.7	1.5	9.6	-1.4	-23.9	-39.4	-9.5	-51.8	-4.4	3.1	16.6	35.9	23.8	4.6	-40.3	4.4
DMI-HIRHAM5 ECHAM5-r3 A1B	18.5	-1.6	14.7	30.3	11.4	10.9	-1.5	30.2	8.0	10.6	22.7	15.8	15.7	14.4	9.3	14.4
ETHZ-CLM HadCM3Q0 A1B	6.0	11.2	7.1	-0.4	8.9	8.8	-6.0	-1.7	15.2	22.1	9.8	9.1	8.5	6.1	-4.9	15.1
ICTP-REGCM3 ECHAM5-r3 A1B	13.3	9.8	11.0	6.5	2.6	4.8	-1.0	2.9	4.9	-2.1	13.3	11.6	12.7	6.0	-1.2	6.6
KNMI-RACMO2 ECHAM5-r3 A1B	6.9	13.5	10.7	1.8	-13.1	-0.4	0.9	10.1	0.0	14.3	27.6	13.5	11.7	8.0	-2.7	15.8
METO-HadRM3Q0 HadCM3Q0 A1B	20.8	4.8	-7.8	5.3	21.7	-21.7	-9.7	-6.9	0.8	28.4	11.5	16.0	19.7	5.3	-17.4	13.4
METO-HadRM3Q3 HadCM3Q3 A1B	13.3	5.9	-5.3	25.0	-0.9	-8.1	-10.2	-25.8	13.8	11.9	24.1	19.8	15.3	11.9	-22.6	15.6
METO-HadRM3Q16 HadCM3Q16 A1B	11.2	8.8	-9.6	10.2	18.3	-24.1	-10.0	-13.9	24.1	20.8	34.3	10.1	13.1	-4.5	-27.7	23.9
MPI-M-REMO ECHAM5-r3 A1B	2.3	-4.6	2.3	20.4	-14.5	-22.0	-11.6	-13.7	17.8	6.7	0.2	5.5	2.5	8.5	-17.9	8.6
SMHIRCA BCM A1B	7.2	26.7	24.3	42.8	-20.4	8.2	-26.3	2.3	-4.0	4.7	3.3	13.5	13.5	27.8	-6.4	2.2
SMHIRCA ECHAM5-r3 A1B	10.1	14.9	6.1	8.8	-6.0	-22.9	-17.8	-4.0	7.1	19.7	24.8	5.8	5.5	7.9	-13.9	15.2
SMHIRCA HadCM3Q3 A1B	15.8	20.2	16.8	12.1	24.5	2.3	-20.5	-1.8	34.8	13.9	12.7	25.8	21.0	17.4	-0.7	20.0
SDSM HadCM3 A2	19.6	-1.0	1.6	-11.3	-16.0	-0.2	-9.2	-20.9	-13.0	-8.6	-1.5	21.1	13.8	-1.7	-21.1	-5.4
SDSM HadCM3 B2	8.9	5.4	8.0	-0.6	2.9	-5.9	-7.6	-11.4	4.6	-8.1	-14.8	16.3	11.0	3.1	-8.1	-8.2
SDSM CSIROmk2 A2	11.7	8.6	-8.5	-15.6	-4.7	-32.1	-31.1	-16.9	-15.8	-1.1	1.4	14.9	17.3	-11.6	-14.5	-3.5
SDSM CSIROmk2 B2	18.1	6.2	-5.5	-5.9	-30.5	-12.9	-18.4	-28.9	0.1	0.7	12.5	-3.6	4.6	-7.0	-18.0	3.3
SDSM CGCM2 A2	13.8	10.7	-25.9	-29.6	-63.8	-40.0	-49.7	12.9	-8.4	-17.4	-18.5	7.9	11.2	-33.4	-10.0	-15.2
SDSM CGCM2 B2	4.1	12.1	-12.9	-24.0	-33.6	-17.6	-45.3	-28.1	-10.8	-12.7	1.9	4.3	11.0	-17.1	-27.0	-8.1

Table IV-6 Percentage change in the Q05 low flow statistics calculated on a monthly and seasonal basis for the Glenamong catchment. Changes are estimated for the 2080s horizon (2070-2099) relative to the 30 year control period. (1961-1990). Projected changes in Q05 are estimated using the median series from the multimodel simulation. The table is colour coded to highlight increases/decreases.

2020s Change Q95 (%)	Jan	Feb	Mar	Apr	May	Jun	Jul	Aug	Sept	Oct	Nov	Dec	Winter	Spring	Summer	Autumn
<i>C4IRCA3 HadCM3Q16 A1B</i>	-14.3	-1.0	9.2	-4.1	1.7	2.5	-8.9	-11.9	1.3	6.0	7.6	-0.2	-4.3	-0.6	-6.9	2.0
<i>C4IRCA3 ECHAM5 A2</i>	1.1	-1.6	-5.7	-1.6	-2.2	-2.7	-1.3	-1.5	-8.9	-11.6	-6.9	-5.8	-1.9	-2.3	-1.7	-8.0
<i>CNRM-RM4.5 ARPEGE A1B</i>	10.1	-5.6	0.2	-7.4	-7.6	-6.2	-5.7	-3.9	0.4	-8.8	-1.5	-16.2	-4.4	-3.9	-3.8	-8.9
<i>CNRM-RM5.1 ARPEGE A1B</i>	-0.9	-5.5	-6.3	-7.2	-4.9	0.4	5.0	-3.8	-18.7	-2.4	-3.6	-15.6	-9.5	-4.6	0.8	-17.6
<i>DMI-HIRHAM5 ARPEGE A1B</i>	-0.2	-6.0	0.1	-7.7	-5.4	0.9	-4.6	-6.8	-8.4	6.0	3.7	-13.3	-4.6	-5.0	-1.2	-8.2
<i>DMI-HIRHAM5 ECHAM5-r3 A1B</i>	22.2	-3.0	10.5	4.6	2.1	8.3	5.6	7.6	-1.5	7.6	7.6	-5.8	-2.9	3.8	6.6	5.3
<i>ETHZ-CLM HadCM3Q0 A1B</i>	-4.9	0.6	-3.9	-5.2	-4.6	-4.5	-3.6	-11.1	-3.6	-11.8	-16.1	-6.8	-2.9	-7.3	-7.4	-9.3
<i>ICTP-REGCM3 ECHAM5-r3 A1B</i>	0.2	-9.4	3.1	-1.2	-0.3	-6.3	-2.7	-5.3	-10.5	2.1	-3.4	-6.3	-4.6	-1.1	-4.7	-2.3
<i>KNMI-RACMO2 ECHAM5-r3 A1B</i>	0.6	-4.0	2.0	1.8	-2.3	-3.9	0.6	-4.5	-6.5	-1.4	1.5	-7.9	-3.4	0.1	-2.1	-3.3
<i>METNOHIRHAM BCM A1B</i>	3.1	2.8	23.6	-0.2	0.7	-1.2	3.8	-1.4	1.8	20.6	26.8	9.5	5.0	-0.3	1.9	9.8
<i>METNOHIRHAM HadCM3Q0 A1B</i>	-11.1	-3.7	-6.1	-8.6	-4.9	-7.4	-9.7	-14.2	-8.6	-25.1	-17.6	-1.5	-5.4	-9.5	-10.4	-17.2
<i>METO-HadRM3Q0 HadCM3Q0 A1B</i>	-21.7	-5.8	-13.2	-12.6	-13.6	-9.0	-3.4	-8.4	-9.9	-13.2	-23.2	-11.9	-13.4	-12.6	-7.5	-11.2
<i>METO-HadRM3Q3 HadCM3Q3 A1B</i>	1.7	-3.1	-9.4	0.3	3.9	3.4	2.2	9.8	15.9	-3.6	-6.0	26.4	1.4	1.7	4.7	0.9
<i>METO-HadRM3Q16 HadCM3Q16 A1B</i>	-14.5	-1.3	-0.3	-5.5	0.9	-4.3	-7.5	-6.7	5.3	-7.7	8.5	0.7	-5.6	-2.4	-6.7	-5.8
<i>MPI-M-REMO ECHAM5-r3 A1B</i>	-2.5	-11.3	1.7	-1.6	0.7	-1.4	-4.9	-6.9	-6.8	-8.7	1.9	-7.6	-7.4	-2.3	-4.2	-6.7
<i>OURANOSMRCC4.2.1 CGCM3 A1B</i>	-13.5	-2.1	1.7	-1.2	-3.5	-6.6	-8.9	-7.0	1.0	-0.2	0.9	-12.2	-10.6	-1.8	-7.4	-0.5
<i>SMHIRCA BCM A1B</i>	6.9	7.2	22.5	11.2	3.3	2.3	-0.1	0.0	-8.6	5.8	2.8	17.1	9.3	2.4	0.3	-4.1
<i>SMHIRCA ECHAM5-r3 A1B</i>	1.8	-11.2	7.9	-2.9	-2.6	-7.9	0.9	-8.6	-6.0	-5.7	4.1	-1.5	-2.8	-1.7	-5.3	-3.7
<i>SMHIRCA HadCM3Q3 A1B</i>	30.2	10.4	-0.7	5.1	8.8	9.7	6.9	15.8	20.3	4.4	-4.9	12.5	12.1	8.3	10.5	7.6
<i>SDSM HadCM3 A2</i>	-11.2	-14.0	-1.2	-6.2	-4.8	-4.6	-6.9	-14.1	-6.5	-17.6	-16.9	-5.3	-10.4	-5.0	-8.9	-9.9
<i>SDSM HadCM3 B2</i>	-9.0	4.1	10.5	-3.3	-1.0	-3.5	-1.9	-2.3	-1.0	1.3	-1.9	0.5	-2.2	-3.9	-1.6	-1.7
<i>SDSM CSIROmk2 A2</i>	3.6	1.8	9.3	-4.4	-0.9	-1.3	-3.4	-4.9	-9.1	-2.6	-8.0	-1.6	-1.4	-1.2	-3.5	-6.6
<i>SDSM CSIROmk2 B2</i>	-8.5	-4.7	-4.0	-5.5	-5.6	0.3	-2.8	2.8	-6.1	-11.7	-9.1	-5.4	-6.4	-4.6	-0.5	-6.3
<i>SDSM CGCM2 A2</i>	4.3	10.8	-2.0	-12.6	-1.5	1.1	-10.2	-5.1	-6.9	-3.2	-3.7	7.0	7.9	-4.1	-4.0	-3.8
<i>SDSM CGCM2 B2</i>	4.2	3.7	6.5	3.8	-5.5	-7.6	1.4	0.1	-0.3	-6.9	-2.9	8.2	2.5	-3.6	-2.2	-4.1

Table IV-7 Projected changes (%) in the Q95 low flow statistics calculated on a monthly and seasonal basis for the Glenamong catchment. Changes are estimated for the 2020s horizon (2010-2039) relative to the 30 year control period. (1961-1990). Projected changes in Q95 are estimated using the median series from the multimodel simulation. The table is colour coded to highlight increases/decreases.

2050s Change Q95 (%)	<i>Jan</i>	<i>Feb</i>	<i>Mar</i>	<i>Apr</i>	<i>May</i>	<i>Jun</i>	<i>Jul</i>	<i>Aug</i>	<i>Sept</i>	<i>Oct</i>	<i>Nov</i>	<i>Dec</i>	<i>Winter</i>	<i>Spring</i>	<i>Summer</i>	<i>Autumn</i>
C4IRCA3 HadCM3Q16 A1B	-4.5	-4.9	2.2	-3.6	-2.2	-1.1	-9.5	-14.2	-15.7	-14.3	-16.9	-3.6	-4.5	-2.5	-8.2	-15.8
CNRM-RM5.1 ARGEGE A1B	-10.8	-5.2	-1.4	-1.0	-4.9	-1.8	3.9	-7.5	-14.1	-23.3	-2.1	-15.4	-5.8	-4.4	-2.0	-20.3
DMI-HIRHAM5 ARPEGE A1B	-13.7	-3.3	-1.7	-6.4	-5.4	-3.2	1.9	-5.3	-9.7	-4.0	-9.5	-14.0	-5.1	-5.6	-1.4	-9.2
DMI-HIRHAM5 ECHAM5-r3 A1B	6.2	-6.5	-3.7	4.7	3.7	1.7	0.0	3.3	0.6	10.8	-11.0	-16.2	-9.1	3.2	2.1	2.5
ETHZ-CLM HadCM3Q0 A1B	6.6	2.0	-1.2	2.5	1.9	6.9	1.1	-9.2	-6.8	-6.3	-19.3	3.1	1.9	-0.5	-4.0	-8.1
ICTP-REGCM3 ECHAM5-r3 A1B	-9.0	-10.0	-3.7	-2.9	-0.4	-6.0	-6.9	-5.0	-9.3	4.4	-15.0	-22.5	-13.8	-1.4	-6.2	-4.2
KNMI-RACMO2 ECHAM5-r3 A1B	-15.1	-4.9	-0.5	-0.2	-2.2	-4.3	-5.6	-9.5	-8.7	3.9	-7.7	-18.4	-12.3	-1.7	-7.1	-3.4
METO-HadRM3Q0 HadCM3Q0 A1B	-17.2	-8.1	-7.6	-4.8	-6.0	-7.8	-10.1	-8.9	-10.1	-12.3	-2.9	3.1	-11.4	-5.6	-9.5	-9.0
METO-HadRM3Q3 HadCM3Q3 A1B	20.8	-5.7	-4.6	4.5	-1.5	-2.4	-7.6	4.4	13.3	-3.6	-15.2	12.1	-0.7	2.2	-2.3	1.1
METO-HadRM3Q16 HadCM3Q16 A1B	-10.2	-6.7	-6.6	-7.8	-3.1	-6.4	-12.4	-13.2	-12.1	-22.6	-4.8	-6.7	-7.3	-6.4	-10.6	-17.8
MPI-M-REMO ECHAM5-r3 A1B	-15.1	-10.3	-7.5	-4.0	-4.4	-5.8	-9.3	-13.0	-14.3	1.3	-14.4	-21.1	-15.6	-5.5	-9.4	-9.4
SMHIRCA BCM A1B	22.5	9.9	23.3	10.7	2.9	1.1	-0.9	-4.3	-7.3	-8.6	-10.9	15.3	14.0	3.0	-1.2	-10.3
SMHIRCA ECHAM5-r3 A1B	-14.0	-12.3	-1.4	-4.9	-2.8	-9.5	-4.7	-7.9	-10.5	-4.7	-5.1	-16.5	-14.2	-3.3	-7.3	-5.9
SMHIRCA HadCM3Q3 A1B	31.0	9.3	-2.9	7.9	7.1	3.5	0.5	5.4	12.1	-2.8	-11.6	13.4	11.9	7.7	2.6	3.2
SDSM HadCM3 A2	-1.4	-3.4	0.8	-7.5	-5.9	-5.1	-14.2	-17.0	-13.7	-20.2	-11.8	-0.2	-2.7	-6.1	-12.3	-18.7
SDSM HadCM3 B2	-9.7	0.7	-1.7	-3.9	-2.5	-2.8	-6.8	-12.3	-9.2	-17.2	-1.9	7.3	-3.0	-5.0	-6.7	-15.8
SDSM CSIROmk2 A2	7.4	4.3	5.4	-5.1	-3.3	-5.3	-6.6	-8.0	-21.9	-13.6	-13.6	6.0	3.1	-2.7	-6.8	-20.0
SDSM CSIROmk2 B2	14.4	-6.1	0.2	-0.6	1.3	2.3	-0.3	8.4	0.9	-7.2	-3.4	-5.3	-3.6	0.1	0.9	-0.9
SDSM CGCM2 A2	20.6	4.2	-1.9	-8.1	-3.8	3.0	0.6	0.6	-3.3	-16.1	0.6	13.4	6.6	-4.9	2.1	-7.5
SDSM CGCM2 B2	9.4	15.7	-2.6	-5.4	-9.7	-4.6	2.2	-4.8	-10.1	-7.8	-0.4	22.2	12.5	-7.9	-2.0	-6.7

Table IV-8 Percentage change in the Q95 low flow statistics calculated on a monthly and seasonal basis for the Glenamong catchment. Changes are estimated for the 2050s horizon (2040-2069) relative to the 30 year control period. (1961-1990). Projected changes in Q95 are estimated using the median series from the multimodel simulation. The table is colour coded to highlight increases/decreases.

2080s Change Q95 (%)	Jan	Feb	Mar	Apr	May	Jun	Jul	Aug	Sept	Oct	Nov	Dec	Winter	Spring	Summer	Autumn
C4IRCA3 HadCM3Q16 A1B	-7.0	2.3	9.2	5.1	5.7	5.5	-1.0	-7.3	5.0	-0.7	11.2	6.5	2.3	6.3	-1.3	-2.2
CNRM-RM5.1 ARGEGE A1B	-10.7	-0.8	-4.4	-1.2	-3.0	-2.9	2.4	-9.2	-18.9	-11.3	-4.8	-5.6	-4.2	-3.4	-3.3	-20.7
DMI-HIRHAM5 ARPEGE A1B	-7.3	-2.8	-1.2	-6.6	-8.0	-5.6	-1.5	-9.2	-12.4	-11.4	-10.2	-16.5	-7.3	-6.9	-4.9	-16.8
DMI-HIRHAM5 ECHAM5-r3 A1B	22.4	5.6	14.0	6.4	7.9	6.9	4.7	8.2	-5.7	8.3	-2.3	-4.6	3.2	8.1	6.6	-6.6
ETHZ-CLM HadCM3Q0 A1B	4.6	-8.0	6.4	-0.8	5.4	3.4	0.8	-4.3	-1.0	-4.8	0.4	-6.6	-3.2	-0.4	-1.7	-4.1
ICTP-REGCM3 ECHAM5-r3 A1B	12.1	-5.7	4.8	-1.5	-0.8	-4.2	0.7	1.3	-13.2	-5.6	0.4	-3.4	-0.9	-0.1	-1.0	-10.9
KNMI-RACMO2 ECHAM5-r3 A1B	6.2	0.6	11.0	4.4	-1.1	-3.1	4.7	2.5	-7.5	-4.2	7.3	-3.4	0.2	0.7	1.3	-6.6
METO-HadRM3Q0 HadCM3Q0 A1B	-9.9	-6.0	1.3	-7.2	-2.5	-6.5	-7.3	-6.1	-6.8	-7.7	2.9	-6.2	-7.4	-4.3	-7.4	-7.0
METO-HadRM3Q3 HadCM3Q3 A1B	0.0	-1.3	1.7	11.3	1.0	-2.8	-5.7	7.6	19.0	-4.1	-2.0	25.8	6.5	3.1	-1.3	0.3
METO-HadRM3Q16 HadCM3Q16 A1B	-14.1	3.0	1.8	2.9	4.8	-1.9	-5.5	-3.9	2.6	-12.4	18.2	5.5	-1.6	2.6	-3.6	-10.1
MPI-M-REMO ECHAM5-r3 A1B	8.3	-10.5	0.2	-5.5	-3.5	-6.2	-4.4	-6.5	-15.1	-10.6	-1.0	-2.7	-5.4	-5.1	-6.7	-12.8
SMHIRCA BCM A1B	43.3	20.0	10.7	25.9	7.0	10.3	4.4	-0.6	-11.8	-1.7	24.9	31.6	25.3	7.2	4.7	-5.4
SMHIRCA ECHAM5-r3 A1B	6.6	-9.7	4.2	-3.7	-5.2	-8.4	2.9	-5.5	-14.8	-5.3	9.9	5.0	-1.5	-2.5	-3.5	-13.4
SMHIRCA HadCM3Q3 A1B	22.8	11.8	11.2	13.5	12.3	3.2	2.3	3.1	17.3	4.2	7.9	33.9	19.7	12.5	1.9	8.0
SDSM HadCM3 A2	9.7	-9.0	7.4	-7.6	-7.5	-10.8	-13.7	-21.4	-15.1	-22.5	-12.9	17.2	3.5	-7.2	-15.7	-19.1
SDSM HadCM3 B2	-16.4	1.5	4.5	2.7	-0.2	-6.6	-7.2	-15.0	-4.6	-18.5	-10.3	-0.9	-5.3	-2.2	-8.8	-12.7
SDSM CSIROmk2 A2	13.6	17.4	5.9	-7.0	-4.9	-5.8	-2.5	0.0	-14.0	-3.9	-12.4	14.6	11.9	-3.7	-3.1	-12.6
SDSM CSIROmk2 B2	1.1	-2.0	-2.4	-1.1	-1.4	1.2	4.0	7.0	-8.3	3.1	-9.4	4.0	0.4	-2.2	3.7	-3.1
SDSM CGCM2 A2	13.4	0.1	1.2	-14.9	-13.2	-9.9	-8.6	-6.2	-3.3	-15.9	-9.1	3.2	3.4	-13.8	-8.9	-8.7
SDSM CGCM2 B2	12.1	14.9	-6.0	-4.4	-9.5	-8.1	0.8	0.2	-5.9	-5.3	-1.2	7.3	9.0	-7.3	-2.9	-6.2

Table IV-9 Projected changes (%) in the Q95 low flow statistics calculated on a monthly and seasonal basis for the Glenamong catchment. Changes are estimated for the 2080s horizon (2070-2099) relative to the 30 year control period. (1961-1990). Projected changes in Q95 are estimated using the median series from the multimodel simulation. The table is colour coded to highlight increases/decreases.

2020s Q50 Change (%)	Jan	Feb	Mar	Apr	May	Jun	Jul	Aug	Sept	Oct	Nov	Dec	Winter	Spring	Summer	Autumn
C4IRCA3 HadCM3Q16 A1B	-1.3	-6.9	-2.3	-10.3	24.0	-24.3	-12.7	-13.0	1.1	3.6	13.6	2.2	-3.7	3.8	-16.8	2.1
C4IRCA3 ECHAM5 A2	26.8	3.0	7.2	-9.1	2.6	-11.1	-17.1	1.0	-15.9	9.7	7.0	-2.6	5.5	-2.8	-9.9	1.2
CNRM-RM4.5 ARPEGE A1B	10.1	-2.9	-1.8	-11.3	-17.4	-13.0	-18.7	-10.1	-12.4	13.0	14.8	-5.8	1.0	-7.0	-13.8	5.8
CNRM-RM5.1 ARGEGE A1B	1.6	-6.7	-2.1	-14.4	0.4	-11.8	-9.8	-3.3	-12.6	10.2	11.0	-6.8	-1.6	-4.4	-8.9	3.6
DMI-HIRHAM5 ARPEGE A1B	2.9	-4.2	6.9	-13.6	-7.9	-17.5	-13.9	-12.9	-8.1	13.0	6.2	-3.4	0.4	-5.3	-14.0	5.9
DMI-HIRHAM5 ECHAM5-r3 A1B	15.2	-5.3	40.5	9.0	10.8	10.5	-11.5	1.4	2.5	0.0	11.3	-5.4	4.7	17.4	-0.4	2.0
ETHZ-CLM HadCM3Q0 A1B	-0.4	8.2	0.9	-3.7	-6.3	-0.1	-6.2	-20.9	-15.3	-20.0	-13.7	13.9	6.2	-5.3	-8.4	-18.0
ICTP-REGCM3 ECHAM5-r3 A1B	25.2	-3.0	18.5	-3.3	5.0	-10.2	-12.3	6.3	7.8	-7.6	3.2	-21.0	-0.9	8.6	-5.2	0.1
KNMI-RACMO2 ECHAM5-r3 A1B	15.1	4.7	12.3	-7.9	5.1	-10.7	-16.3	0.1	10.8	-5.4	2.3	-18.5	3.0	1.5	-10.0	3.8
METNOHIRHAM BCM A1B	-5.1	22.1	33.7	-5.4	-28.8	-16.3	-6.1	-13.7	-8.9	13.3	5.1	43.9	19.3	-2.4	-12.8	5.2
METNOHIRHAM HadCM3Q0 A1B	6.5	5.7	10.1	-10.4	-11.4	0.1	-6.6	-24.5	-12.1	-26.9	-1.1	11.2	2.5	-7.5	-10.5	-12.9
METO-HadRM3Q0 HadCM3Q0 A1B	-3.8	-6.3	-7.2	-19.1	-16.0	-11.2	-6.6	-18.8	-0.7	-15.3	-5.1	0.8	-3.6	-11.3	-12.2	-7.9
METO-HadRM3Q3 HadCM3Q3 A1B	23.2	-10.3	-20.3	12.6	19.3	2.4	0.8	-11.8	4.8	-6.3	-4.2	16.4	9.5	2.9	-1.4	-2.0
METO-HadRM3Q16 HadCM3Q16 A1B	-6.2	-4.1	0.5	-2.2	12.7	-21.4	-7.4	-17.0	-6.9	18.1	18.6	14.6	0.0	1.7	-14.1	9.3
MPI-M-REMO ECHAM5-r3 A1B	17.2	-4.4	7.8	-3.1	1.4	-19.5	-17.2	3.6	21.6	-9.7	-4.5	-25.5	-3.4	0.1	-11.0	1.0
OURANOSMRCC4.2.1 CGCM3 A1B	-28.3	-29.1	-18.2	7.1	0.0	-5.4	-8.1	-13.5	2.2	-13.2	24.9	0.0	-22.1	-3.2	-9.0	3.4
SMHIRCA BCM A1B	9.8	28.6	55.9	-1.1	-24.7	-2.8	-18.8	-8.7	-15.0	4.4	12.9	40.8	25.9	4.2	-13.7	-0.2
SMHIRCA ECHAM5-r3 A1B	15.6	-1.2	15.5	-8.6	-3.9	-19.5	-11.2	-3.8	3.9	-5.1	0.3	-11.9	0.0	0.0	-12.3	0.0
SMHIRCA HadCM3Q3 A1B	28.8	-6.5	-16.5	24.2	15.2	-5.6	-10.4	-7.3	10.7	0.4	13.7	50.7	22.2	3.9	-8.0	8.8
SDSM HadCM3 A2	-6.4	-3.6	-5.6	-13.0	-6.5	4.7	7.7	-22.6	-2.7	-11.1	-8.0	-7.7	-4.6	-8.2	-3.5	-7.1
SDSM HadCM3 B2	-2.9	6.8	10.0	-12.1	-14.0	8.3	-7.5	-1.8	-2.9	-2.0	3.4	-18.0	-3.7	-6.3	-0.7	-0.1
SDSM CSIROmk2 A2	15.7	6.1	3.8	-5.6	-4.2	2.9	-11.4	-6.3	-6.6	-1.0	-3.4	10.8	9.4	-2.9	-4.0	-6.1
SDSM CSIROmk2 B2	3.1	7.2	-6.3	-3.9	4.4	12.9	-16.5	-8.9	1.0	-16.7	-18.0	12.3	7.3	-2.4	-3.3	-12.5
SDSM CGCM2 A2	7.5	-1.5	0.9	1.5	-11.9	-20.8	-22.6	-8.5	-6.1	-1.3	9.5	8.5	2.4	-2.6	-17.0	-0.2
SDSM CGCM2 B2	22.2	-13.5	7.4	4.3	-2.0	-5.5	-6.1	-5.2	0.5	-17.3	6.6	9.1	3.6	3.9	-5.4	-3.8

Table IV-10 Projected changes (%) in the Q50 low flow statistics calculated on a monthly and seasonal basis for the Shrevagh catchment. Changes are estimated for the 2020s horizon (2010-2039) relative to the 30 year control period. (1961-1990). Projected changes in Q50 are estimated using the median series from the multimodel simulation. The table is colour coded to highlight increases/decreases.

2050s Q50 Change (%)	Jan	Feb	Mar	Apr	May	Jun	Jul	Aug	Sept	Oct	Nov	Dec	Winter	Spring	Summer	Autumn
C4IRCA3 HadCM3Q16 A1B	-11.0	-8.8	0.1	-19.0	-0.1	-20.5	-15.8	-22.8	-22.5	5.6	9.8	12.9	-6.2	-7.1	-17.8	-4.9
CNRM-RM5.1 ARGEGE A1B	-5.6	13.5	7.7	-3.5	-23.7	-29.7	-23.7	-23.1	-21.4	5.3	6.3	-0.9	-0.1	-10.9	-25.6	-0.9
DMI-HIRHAM5 ARPEGE A1B	3.4	17.6	7.8	-9.2	-23.4	-33.1	-21.3	-25.5	-15.5	-4.6	-9.1	-6.3	3.3	-10.7	-27.1	-9.8
DMI-HIRHAM5 ECHAM5-r3 A1B	4.6	1.3	24.0	7.8	-7.3	-11.7	-12.9	-6.2	2.8	9.4	6.2	-15.1	2.2	7.9	-11.1	4.7
ETHZ-CLM HadCM3Q0 A1B	10.2	-2.3	-7.5	-2.3	-3.6	2.0	-10.3	-29.0	-20.2	-17.3	-5.5	34.4	12.5	-4.8	-12.6	-15.7
ICTP-REGCM3 ECHAM5-r3 A1B	-7.9	-19.1	16.3	3.0	-2.8	-13.0	-9.4	-13.2	0.8	17.7	-12.4	-35.8	-20.9	6.9	-10.7	0.2
KNMI-RACMO2 ECHAM5-r3 A1B	-3.4	-8.0	8.5	-6.8	-3.8	-20.9	-17.1	-17.0	10.5	15.2	-13.0	-29.3	-13.3	-1.8	-18.1	2.6
METO-HadRM3Q0 HadCM3Q0 A1B	-0.2	-6.7	-11.6	-6.0	0.2	-10.2	-14.2	-21.9	-15.8	-8.3	4.8	7.9	-0.8	-5.8	-15.6	-6.3
METO-HadRM3Q3 HadCM3Q3 A1B	31.9	-7.0	-16.6	13.3	25.7	-4.7	-29.8	-23.9	6.2	6.8	4.3	2.8	12.6	7.5	-18.8	2.5
METO-HadRM3Q16 HadCM3Q16 A1B	-10.9	-5.1	6.5	-11.0	-9.5	-27.7	-15.7	-22.6	-26.3	-0.2	9.8	8.3	-4.1	-5.3	-21.3	-4.7
MPI-M-REMO ECHAM5-r3 A1B	-0.9	-15.3	19.9	-2.6	-2.6	-22.2	-22.0	-19.2	-1.1	13.7	-19.9	-38.7	-20.3	2.8	-21.0	-3.9
SMHIRCA BCM A1B	28.6	44.5	53.2	9.6	-23.2	-11.1	-13.8	-20.8	-13.7	-1.2	15.8	30.4	34.2	5.7	-15.1	-0.9
SMHIRCA ECHAM5-r3 A1B	-5.2	-11.8	16.9	-3.3	-6.7	-27.4	-16.8	-13.1	-7.7	13.2	-18.0	-24.6	-15.9	-0.6	-18.4	-5.6
SMHIRCA HadCM3Q3 A1B	42.8	5.3	-13.9	16.6	28.1	-9.5	-22.9	-16.7	5.6	-0.3	13.0	32.2	25.8	8.9	-16.5	8.2
SDSM HadCM3 A2	7.2	13.3	-12.1	-25.7	-9.2	0.8	-2.1	-19.8	-13.7	-24.1	-5.1	-2.2	7.6	-14.7	-6.8	-13.8
SDSM HadCM3 B2	5.1	1.9	0.5	-10.3	-16.7	-6.6	-6.2	-23.1	-18.0	-9.0	-2.1	17.6	7.8	-8.5	-11.2	-9.0
SDSM CSIROmk2 A2	21.9	19.4	5.1	-9.8	-2.5	-13.6	-14.9	-15.1	-25.2	-1.7	2.3	14.0	16.6	-2.6	-14.6	-9.4
SDSM CSIROmk2 B2	30.7	14.9	-12.2	-1.7	-5.0	2.6	-18.5	6.6	-0.5	-11.1	-11.6	27.8	26.7	-7.3	-2.9	-9.6
SDSM CGCM2 A2	25.1	0.0	-10.5	-6.9	-28.0	-16.8	-13.6	-6.1	-6.9	-6.2	5.2	38.5	18.3	-15.2	-12.7	-2.1
SDSM CGCM2 B2	11.7	6.4	3.8	-15.7	-22.4	-11.2	-6.9	-14.9	3.7	-11.2	8.7	31.0	14.6	-13.9	-11.3	0.6

Table IV-11 Projected changes (%) in the Q50 low flow statistics calculated on a monthly and seasonal basis for the Shrevagh catchment. Changes are estimated for the 2050s horizon (2040-2069) relative to the 30 year control period. (1961-1990). Projected changes in Q50 are estimated using the median series from the multimodel simulation. The table is colour coded to highlight increases/decreases.

2080s Q50 Change (%)	Jan	Feb	Mar	Apr	May	Jun	Jul	Aug	Sept	Oct	Nov	Dec	Winter	Spring	Summer	Autumn
C4IRCA3 HadCM3Q16 A1B	5.7	-1.4	-3.7	-6.3	6.3	-29.3	-7.0	-10.4	-8.0	3.2	40.4	10.2	-0.8	-1.4	-16.1	7.9
CNRM-RM5.1 ARGEGE A1B	9.3	-1.8	3.2	6.7	-22.8	-34.6	-28.9	-41.9	-17.7	-7.4	7.2	8.9	4.8	-4.3	-35.8	-4.0
DMI-HIRHAM5 ARPEGE A1B	9.2	0.1	-2.4	-3.3	-26.7	-37.6	-22.9	-31.2	-19.9	-15.4	-3.1	-2.1	1.9	-12.2	-30.5	-13.9
DMI-HIRHAM5 ECHAM5-r3 A1B	31.4	0.9	30.6	18.6	-1.1	-1.6	-8.0	-3.0	-12.8	5.5	16.4	12.0	14.1	15.6	-5.1	4.9
ETHZ-CLM HadCM3Q0 A1B	3.6	2.7	3.5	-7.4	-8.9	-17.1	-17.0	-24.2	-21.0	-4.6	-3.7	2.1	2.8	-4.0	-18.8	-11.2
ICTP-REGCM3 ECHAM5-r3 A1B	20.2	-8.6	11.6	8.8	1.6	-10.6	1.7	-6.7	-17.4	-3.9	12.2	2.8	7.7	8.9	-5.1	-1.2
KNMI-RACMO2 ECHAM5-r3 A1B	33.3	2.3	16.2	0.6	-8.6	-21.7	-12.0	-17.8	-11.6	-7.0	18.9	6.2	13.5	0.6	-17.1	0.0
METO-HadRM3Q0 HadCM3Q0 A1B	1.2	-5.9	-4.9	-6.2	-2.0	-24.4	-20.3	-20.3	-19.5	2.1	10.8	2.8	-1.4	-0.6	-21.3	-4.4
METO-HadRM3Q3 HadCM3Q3 A1B	6.0	9.8	14.7	43.8	-1.8	-28.3	-41.2	-41.4	-0.6	2.6	10.6	34.0	15.3	18.1	-35.6	6.9
METO-HadRM3Q16 HadCM3Q16 A1B	7.0	3.6	10.5	7.6	8.6	-42.2	-21.1	-25.9	-20.4	10.1	47.2	12.6	4.2	8.4	-28.4	11.2
MPI-M-REMO ECHAM5-r3 A1B	40.4	-10.8	4.6	9.1	-12.2	-29.5	-12.5	-15.8	-14.8	-10.2	7.5	1.5	8.1	-0.2	-18.9	-4.2
SMHIRCA BCM A1B	44.8	45.6	70.9	16.2	-30.4	-8.0	-14.7	-21.3	-13.4	-6.3	41.9	70.7	54.1	2.9	-15.4	6.5
SMHIRCA ECHAM5-r3 A1B	30.2	-5.7	5.3	-1.4	-13.5	-30.8	-10.6	-18.5	-20.9	-2.3	5.8	14.3	9.0	-4.4	-19.3	-3.7
SMHIRCA HadCM3Q3 A1B	18.9	32.1	16.9	38.3	12.3	-21.7	-20.5	-33.2	10.7	1.8	32.9	41.5	27.0	21.0	-24.8	15.7
SDSM HadCM3 A2	21.1	8.8	-3.1	-10.9	-8.6	-13.0	-25.4	-33.2	-15.6	-24.8	2.3	12.4	16.6	-5.5	-24.1	-15.7
SDSM HadCM3 B2	3.3	21.0	4.4	9.6	-3.7	-8.7	-11.5	-14.7	-2.0	-16.1	-4.1	0.3	9.0	3.2	-11.6	-6.7
SDSM CSIROmk2 A2	9.2	33.7	-18.6	-1.6	12.1	-10.5	-6.2	1.4	-17.0	3.5	-5.8	30.8	21.6	-3.3	-5.0	-7.3
SDSM CSIROmk2 B2	12.9	11.4	2.7	2.7	-4.1	3.8	-5.5	-6.2	-2.8	-8.7	-9.7	12.8	13.9	-1.8	-2.8	-7.0
SDSM CGCM2 A2	31.5	7.4	-20.3	-31.2	-40.2	-30.3	-16.7	5.8	-8.7	-14.3	-9.1	4.9	13.2	-27.8	-15.5	-10.2
SDSM CGCM2 B2	31.1	5.7	-15.1	-18.4	-24.2	-18.7	-5.9	-9.2	-2.9	-14.3	9.5	10.3	15.0	-18.4	-10.2	-3.9

Table IV-12 Projected changes (%) in the Q50 low flow statistics calculated on a monthly and seasonal basis for the Shrevagh catchment. Changes are estimated for the 2080s horizon (2070-2099) relative to the 30 year control period. (1961-1990). Projected changes in Q50 are estimated using the median series from the multimodel simulation. The table is colour coded to highlight increases/decreases.

2020s Q05 Change (%)	Jan	Feb	Mar	Apr	May	Jun	Jul	Aug	Sept	Oct	Nov	Dec	Winter	Spring	Summer	Autumn
C4IRCA3 HadCM3Q16 A1B	5.1	2.2	-2.8	-8.3	27.5	-28.5	-11.0	-11.5	-5.0	2.8	-0.2	2.5	4.1	-3.0	-19.5	3.4
C4IRCA3 ECHAM5 A2	14.0	-2.3	6.6	1.7	8.2	-1.0	-33.1	-19.0	13.9	3.7	0.4	-0.2	2.4	7.8	-10.4	5.7
CNRM-RM4.5 ARPEGE A1B	9.5	5.8	-2.4	-11.1	8.5	-5.9	-12.9	10.8	-20.2	0.3	23.0	7.6	7.6	-5.5	3.8	2.5
CNRM-RM5.1 ARGEGE A1B	6.9	13.9	3.0	-14.1	-3.6	-16.7	1.4	5.7	-4.6	16.0	19.1	17.3	8.0	3.7	-7.7	8.5
DMI-HIRHAM5 ARPEGE A1B	15.7	4.1	3.7	-14.7	4.3	-29.1	13.0	-25.0	13.1	20.9	10.4	27.5	14.1	-1.6	-17.4	14.3
DMI-HIRHAM5 ECHAM5-r3 A1B	4.2	-15.0	24.5	10.9	15.3	47.6	-3.0	23.3	6.3	1.1	8.6	0.4	4.0	24.6	18.7	2.9
ETHZ-CLM HadCM3Q0 A1B	16.9	7.5	-4.5	11.6	-8.5	7.5	0.3	0.2	2.7	-0.7	-6.4	26.8	20.3	2.6	1.5	0.1
ICTP-REGCM3 ECHAM5-r3 A1B	10.8	15.1	12.1	2.4	2.3	-1.6	9.0	7.6	9.3	-11.4	1.5	-8.4	0.5	5.6	-1.7	1.2
KNMI-RACMO2 ECHAM5-r3 A1B	4.4	4.8	8.6	-4.5	-5.2	5.4	-11.1	3.8	7.5	9.2	13.5	-13.2	-5.6	4.5	1.7	6.4
METNOHIRHAM BCM A1B	6.9	18.9	18.8	-10.3	-39.1	-19.6	-4.5	-12.1	2.5	6.8	-14.9	16.2	8.5	9.5	-10.8	4.4
METNOHIRHAM HadCM3Q0 A1B	25.5	-3.5	14.8	-22.4	3.5	-3.0	-7.2	-5.8	8.0	-22.6	15.0	9.9	15.9	-0.2	-10.4	-1.7
METO-HadRM3Q0 HadCM3Q0 A1B	25.4	-2.5	-11.8	-10.4	2.6	-9.1	-9.8	19.2	20.6	-8.7	1.9	16.6	16.1	-10.3	-5.7	1.0
METO-HadRM3Q3 HadCM3Q3 A1B	25.8	-2.2	-3.3	6.9	7.4	25.4	14.5	-5.7	-6.0	7.8	11.7	3.6	6.9	1.7	7.8	2.1
METO-HadRM3Q16 HadCM3Q16 A1B	-7.6	4.6	-12.6	0.3	-5.0	-25.2	3.4	-3.5	0.4	31.5	10.4	-1.4	-1.2	-10.2	-15.0	15.8
MPI-M-REMO ECHAM5-r3 A1B	0.7	1.8	10.4	26.6	-3.0	-11.0	-18.7	0.0	13.8	-6.4	-0.9	-5.0	-2.1	15.0	-7.4	1.0
OURANOSMRCC4.2.1 CGCM3 A1B	-4.6	-2.3	9.7	17.5	6.8	14.5	20.9	0.6	-4.0	8.2	16.7	5.7	2.2	5.0	7.0	4.2
SMHIRCA BCM A1B	0.6	11.0	9.4	13.3	-18.1	-3.4	-21.7	6.6	-15.6	6.2	1.3	11.0	2.4	11.1	-3.9	2.0
SMHIRCA ECHAM5-r3 A1B	1.3	4.5	9.3	9.4	-2.4	-3.0	-17.7	-3.2	9.2	0.9	8.5	-12.1	-5.1	6.5	-7.2	1.0
SMHIRCA HadCM3Q3 A1B	27.5	3.6	4.7	8.0	26.9	7.5	-16.6	-2.8	21.5	4.6	14.4	21.3	22.9	9.0	-3.6	13.1
SDSM HadCM3 A2	2.4	-14.8	-1.5	-15.5	-18.6	29.9	11.5	-17.4	-5.2	0.6	-8.0	12.6	4.2	-6.7	-1.7	-4.6
SDSM HadCM3 B2	-2.9	-9.9	18.5	-29.0	-3.4	20.8	-12.2	4.0	-0.1	0.5	-8.8	6.6	1.9	4.6	8.8	-2.4
SDSM CSIROmk2 A2	8.9	4.8	3.5	-10.4	-2.2	9.0	-22.0	-10.2	0.9	6.1	6.6	8.0	13.2	-6.3	-3.5	8.0
SDSM CSIROmk2 B2	6.5	-7.5	-12.6	7.2	-8.5	1.0	-5.8	-14.5	7.2	-25.2	-13.4	1.6	-0.1	-5.9	-6.9	-9.5
SDSM CGCM2 A2	10.6	-13.2	-1.1	14.3	-29.6	-26.9	-26.8	-6.0	-2.4	-0.1	10.0	9.5	0.9	-4.3	-14.0	4.1
SDSM CGCM2 B2	-4.2	-9.2	13.4	9.5	4.9	12.4	-16.8	-6.9	4.1	-25.9	11.6	1.6	5.6	0.0	-1.0	-9.9

Table IV-13 Projected changes (%) in the Q05 low flow statistics calculated on a monthly and seasonal basis for the Shrevagh catchment. Changes are estimated for the 2020s horizon (2010-2039) relative to the 30 year control period. (1961-1990). Projected changes in Q05 are estimated using the median series from the multimodel simulation. The table is colour coded to highlight increases/decreases.

2050s Q05 Change (%)	Jan	Feb	Mar	Apr	May	Jun	Jul	Aug	Sept	Oct	Nov	Dec	Winter	Spring	Summer	Autumn
C4IRCA3 HadCM3Q16 A1B	5.5	3.0	11.8	-6.1	26.2	-16.6	-14.7	-8.7	-14.7	23.0	15.9	14.9	13.8	5.3	-14.0	9.4
CNRM-RM5.1 ARGEGE A1B	1.0	12.8	24.5	-6.2	-29.7	-37.0	-21.2	-12.7	12.1	2.3	6.5	14.6	4.8	14.7	-26.7	4.3
DMI-HIRHAM5 ARPEGE A1B	15.4	5.9	12.5	-14.5	-31.2	-30.4	-1.3	-37.6	8.5	8.2	3.0	42.3	17.6	-1.0	-25.4	3.4
DMI-HIRHAM5 ECHAM5-r3 A1B	7.7	1.9	26.8	19.7	5.5	9.1	-2.0	37.4	8.2	8.3	28.4	8.6	12.7	18.4	10.3	15.1
ETHZ-CLM HadCM3Q0 A1B	13.4	2.4	4.5	0.1	15.6	17.0	14.6	-22.2	-3.6	-3.2	13.4	14.5	13.2	5.2	-9.1	5.4
ICTP-REGCM3 ECHAM5-r3 A1B	-9.0	7.3	17.5	-6.3	2.0	-12.5	0.8	4.0	8.8	7.1	-7.6	-12.0	-9.0	8.9	-5.4	7.5
KNMI-RACMO2 ECHAM5-r3 A1B	-5.9	4.0	7.5	-11.7	-10.8	-10.5	-21.0	15.6	7.9	24.7	2.7	-0.1	-1.7	1.3	-6.4	11.7
METO-HadRM3Q0 HadCM3Q0 A1B	22.3	0.4	3.9	-8.9	11.6	-11.6	-6.1	-4.1	8.5	10.6	5.6	23.1	19.4	-5.8	-14.6	7.3
METO-HadRM3Q3 HadCM3Q3 A1B	18.3	5.6	-10.6	30.6	1.3	5.6	-9.4	-7.1	-7.1	26.2	9.6	7.8	11.4	4.3	-9.9	13.0
METO-HadRM3Q16 HadCM3Q16 A1B	-8.3	0.8	-3.8	2.3	-4.0	-24.9	-4.4	-12.6	-11.1	8.9	22.2	2.5	0.2	1.2	-21.9	12.0
MPI-M-REMO ECHAM5-r3 A1B	-6.4	-2.3	18.5	13.6	-4.4	-23.8	-12.7	-11.4	9.1	14.2	-9.7	-11.0	-9.4	9.6	-17.1	8.0
SMHIRCA BCM A1B	6.1	32.3	12.6	23.7	-19.2	-6.2	-9.2	-5.6	-1.3	4.6	-2.0	24.9	16.0	19.3	-9.4	5.0
SMHIRCA ECHAM5-r3 A1B	-4.1	9.3	19.7	-2.6	-3.1	-20.9	-20.2	0.1	-1.4	19.8	8.9	-8.6	-4.1	9.1	-15.1	5.4
SMHIRCA HadCM3Q3 A1B	14.4	14.7	-4.4	9.6	11.8	-0.7	-27.3	-8.8	14.9	6.7	15.2	19.5	14.2	0.8	-2.8	11.2
SDSM HadCM3 A2	-4.5	-4.0	-10.7	-33.2	-31.4	-5.1	31.3	-26.9	-7.5	-2.4	-9.3	-4.1	-0.3	-15.7	-10.4	-7.4
SDSM HadCM3 B2	6.3	-0.2	6.3	-3.7	-16.0	-11.9	-7.8	-24.7	-4.8	4.4	-5.8	24.8	10.8	2.9	-15.3	-4.1
SDSM CSIROmk2 A2	11.0	-7.5	1.2	-3.5	11.5	-27.2	-32.9	-25.4	-24.1	-4.2	20.3	14.9	13.3	0.6	-26.9	2.3
SDSM CSIROmk2 B2	34.1	0.2	-12.4	-14.2	-15.9	3.4	-28.0	-3.0	-16.7	-7.6	-3.0	18.5	20.5	-13.8	0.2	-6.7
SDSM CGCM2 A2	14.8	4.7	-17.0	-8.4	-43.9	-30.5	-14.9	-3.0	6.8	-20.3	-2.9	26.8	13.6	-22.4	-15.8	-6.2
SDSM CGCM2 B2	-7.6	17.6	-3.7	-16.7	-27.3	0.9	-35.0	-22.9	-8.2	-4.9	7.4	10.8	11.5	-13.7	-21.7	-9.2

Table IV-14 Projected changes (%) in the Q05 low flow statistics calculated on a monthly and seasonal basis for the Shrevagh catchment. Changes are estimated for the 2050s horizon (2004-2069) relative to the 30 year control period. (1961-1990). Projected changes in Q05 are estimated using the median series from the multimodel simulation. The table is colour coded to highlight increases/decreases.

2080s Q05 Change (%)	Jan	Feb	Mar	Apr	May	Jun	Jul	Aug	Sept	Oct	Nov	Dec	Winter	Spring	Summer	Autumn
C4IRCA3 HadCM3Q16 A1B	22.9	23.6	3.8	0.6	25.1	-20.7	4.8	-9.0	14.0	19.1	34.5	21.0	21.0	7.5	-13.5	27.9
CNRM-RM5.1 ARGEGE A1B	12.3	15.9	23.7	13.6	-16.0	-29.9	-10.4	-27.6	22.6	7.6	24.5	16.7	10.3	8.5	-28.0	15.5
DMI-HIRHAM5 ARPEGE A1B	22.7	7.5	10.4	0.8	-23.4	-42.3	-14.7	-54.1	-4.1	5.9	20.4	40.3	23.7	6.9	-39.7	5.2
DMI-HIRHAM5 ECHAM5-r3 A1B	19.1	-3.5	18.4	28.9	11.8	13.3	0.8	34.1	7.2	10.8	25.2	16.1	19.9	17.5	7.7	13.3
ETHZ-CLM HadCM3Q0 A1B	7.5	15.1	9.2	1.6	8.0	11.4	-1.9	-2.7	18.5	25.0	7.6	12.4	7.0	8.0	-2.0	19.9
ICTP-REGCM3 ECHAM5-r3 A1B	13.4	13.4	16.9	13.2	-2.6	4.2	9.5	4.8	4.8	-1.1	14.2	11.8	13.7	6.2	-0.4	4.3
KNMI-RACMO2 ECHAM5-r3 A1B	7.1	16.4	16.0	2.1	-15.1	-0.9	-2.3	8.3	3.6	19.7	29.7	16.4	12.6	12.0	-2.8	15.8
METO-HadRM3Q0 HadCM3Q0 A1B	24.3	6.4	-8.3	12.4	29.5	-21.8	-6.2	-5.1	4.1	30.6	14.0	19.5	24.5	5.0	-12.3	16.4
METO-HadRM3Q3 HadCM3Q3 A1B	16.4	8.1	-3.5	35.8	-4.8	-12.7	-12.7	-29.3	16.3	13.8	26.1	21.1	21.0	14.8	-20.6	17.5
METO-HadRM3Q16 HadCM3Q16 A1B	10.9	11.7	-11.0	15.5	20.3	-21.7	-5.7	-6.4	27.2	23.5	38.3	9.5	13.6	-3.7	-19.0	32.3
MPI-M-REMO ECHAM5-r3 A1B	2.3	-3.4	4.8	24.8	-14.2	-21.8	-14.2	-14.7	21.8	6.7	-2.3	7.2	2.6	10.9	-18.6	8.3
SMHIRCA BCM A1B	9.4	34.5	28.4	45.1	-15.8	10.8	-17.2	-3.0	-6.0	5.2	2.5	15.9	15.6	31.9	-3.8	5.5
SMHIRCA ECHAM5-r3 A1B	11.7	15.5	10.3	10.3	-6.8	-26.8	-16.8	-3.4	10.0	19.8	26.5	8.0	9.8	6.2	-13.8	15.0
SMHIRCA HadCM3Q3 A1B	16.3	22.0	19.6	14.8	29.6	5.4	-24.5	-0.9	36.4	14.7	18.2	27.3	20.2	20.1	0.9	21.9
SDSM HadCM3 A2	23.3	-0.5	5.0	-13.4	-10.6	-1.8	-4.4	-27.7	-13.2	-8.3	-2.4	24.8	19.4	-0.3	-20.6	-9.7
SDSM HadCM3 B2	6.1	6.5	10.9	4.3	0.6	-7.5	-6.1	-9.3	-0.2	-7.4	-15.0	16.3	12.0	6.2	-5.7	-8.8
SDSM CSIROmk2 A2	12.2	10.7	-7.7	-11.6	5.0	-28.7	-20.4	-14.2	-15.8	1.0	2.8	18.7	20.4	-12.6	-12.6	-3.4
SDSM CSIROmk2 B2	21.1	9.6	-3.4	1.0	-29.6	-6.5	-11.1	-29.5	-2.8	1.3	16.5	-4.3	6.1	-5.4	-13.5	7.1
SDSM CGCM2 A2	20.5	14.5	-26.2	-31.2	-51.1	-29.3	-33.3	16.9	-5.9	-17.1	-19.3	12.9	11.2	-34.6	-4.5	-12.0
SDSM CGCM2 B2	2.5	11.2	-13.7	-21.5	-27.5	-8.0	-35.7	-29.2	-8.1	-11.6	6.7	6.4	15.2	-18.0	-23.3	-7.8

Table IV-15 Projected changes (%) in the Q05 low flow statistics calculated on a monthly and seasonal basis for the Shrevagh catchment. Changes are estimated for the 2080s horizon (2070-2099) relative to the 30 year control period. (1961-1990). Projected changes in Q05 are estimated using the median series from the multimodel simulation. The table is colour coded to highlight increases/decreases.

2020s Q95 Change (%)	Jan	Feb	Mar	Apr	May	Jun	Jul	Aug	Sept	Oct	Nov	Dec	Winter	Spring	Summer	Autumn
C4IRCA3 HadCM3Q16 A1B	-18.2	-3.6	16.3	-10.3	17.7	-0.1	4.9	-18.2	29.5	21.8	17.7	5.0	-5.7	4.5	-3.2	18.6
C4IRCA3 ECHAM5 A2	8.6	-3.1	-10.5	-1.6	0.7	-19.4	-7.4	2.8	-9.9	-16.5	-8.3	-6.3	-1.4	-3.2	-8.9	-9.9
CNRM-RM4.5 ARPEGE A1B	12.4	-10.4	11.6	-9.0	-27.6	-7.7	1.7	4.4	7.4	0.9	9.2	-7.5	-7.3	-15.4	-1.7	-4.2
CNRM-RM5.1 ARGEGE A1B	1.1	-19.6	-3.9	-3.0	-17.2	-3.6	6.4	0.9	-38.5	16.2	1.5	-27.8	-21.7	-7.3	1.7	-21.4
DMI-HIRHAM5 ARPEGE A1B	-3.7	-13.5	7.6	-16.1	-14.7	-0.3	-5.8	-14.5	-8.9	16.0	-0.8	-13.1	-9.9	-10.3	-7.3	-7.7
DMI-HIRHAM5 ECHAM5-r3 A1B	31.4	-8.4	23.3	11.2	0.6	19.5	-14.4	-7.5	-8.6	8.9	4.5	-5.1	0.1	6.3	-3.9	2.2
ETHZ-CLM HadCM3Q0 A1B	-9.8	13.5	-4.1	-6.2	-15.6	-2.9	6.5	-4.1	-0.5	-30.0	-19.7	3.6	5.0	-10.7	-0.6	-19.0
ICTP-REGCM3 ECHAM5-r3 A1B	19.4	-12.2	15.5	0.9	-3.9	-14.4	-16.5	-17.4	-16.3	24.7	-4.8	-12.6	-3.8	0.2	-16.3	3.0
KNMI-RACMO2 ECHAM5-r3 A1B	17.6	-12.3	-2.7	8.7	-4.7	-6.9	-2.0	-14.1	-19.8	10.9	-1.4	-15.2	-5.2	1.5	-8.0	-1.6
METNOHIRHAM BCM A1B	11.9	3.5	62.7	10.7	-27.6	-24.5	7.6	-22.1	4.8	60.3	31.4	13.7	8.8	-14.3	-9.7	22.8
METNOHIRHAM HadCM3Q0 A1B	-15.8	5.4	-8.0	-17.4	1.6	-0.2	1.0	-21.0	1.7	-43.6	-17.2	11.7	-3.0	-10.4	-5.1	-23.3
METO-HadRM3Q0 HadCM3Q0 A1B	-21.4	-6.6	-14.3	-25.8	-17.6	-10.9	7.3	-15.5	-0.3	-21.8	-27.1	-7.9	-12.0	-19.8	-7.5	-16.1
METO-HadRM3Q3 HadCM3Q3 A1B	4.4	-8.9	-18.9	6.5	21.9	4.7	-19.1	12.7	71.4	-2.0	-18.1	13.4	-1.7	8.6	1.4	1.4
METO-HadRM3Q16 HadCM3Q16 A1B	-24.1	-2.9	-0.8	-6.0	6.8	-8.4	12.3	-7.0	12.1	-5.3	32.6	10.6	-4.7	-0.5	-2.7	9.0
MPI-M-REMO ECHAM5-r3 A1B	4.7	-14.5	6.9	-2.4	-0.3	0.6	-17.4	-20.2	-5.2	15.2	4.0	-12.7	-9.8	-0.2	-12.8	2.1
OURANOSMRCC4.2.1 CGCM3 A1B	-16.5	-2.6	33.3	0.5	0.9	-8.5	-26.3	-13.4	22.8	-3.1	1.3	-15.3	-17.3	8.2	-15.0	6.3
SMHIRCA BCM A1B	17.6	12.6	63.5	31.0	-26.5	-14.9	-21.0	-11.1	-18.0	20.8	0.8	41.2	21.8	-4.8	-15.9	-0.5
SMHIRCA ECHAM5-r3 A1B	13.7	-22.3	13.3	-8.4	-8.1	-18.3	-10.0	-25.2	-6.2	4.4	16.4	-6.1	-6.5	-2.9	-19.0	4.3
SMHIRCA HadCM3Q3 A1B	51.9	13.9	-14.1	9.4	9.8	7.6	-4.0	-4.8	41.0	-1.3	-7.7	35.9	20.6	6.0	-2.3	11.6
SDSM HadCM3 A2	-10.9	-15.2	13.1	2.6	-5.1	13.6	-10.0	-24.5	-2.6	-25.0	-24.3	-4.1	-9.0	0.0	-11.4	-14.4
SDSM HadCM3 B2	-12.7	27.5	47.0	5.7	-9.8	7.5	-6.7	4.7	6.7	3.5	4.7	9.7	7.4	2.3	-3.7	4.6
SDSM CSIROmk2 A2	17.8	1.0	40.3	-21.9	-3.3	3.4	-9.6	-10.0	-11.9	-2.2	-10.7	-5.6	-0.3	-0.4	-7.8	-8.6
SDSM CSIROmk2 B2	-4.1	-1.5	-0.7	14.2	10.0	23.1	1.8	15.7	-5.6	-13.4	-19.8	-4.2	0.1	12.0	10.5	-10.7
SDSM CGCM2 A2	16.1	18.9	4.6	-21.7	-7.4	8.0	-9.3	-2.4	0.1	0.0	2.1	5.3	14.0	-11.2	-3.9	-0.7
SDSM CGCM2 B2	18.8	7.0	11.8	21.9	-18.3	-15.9	19.8	7.5	7.9	-8.1	6.3	19.3	6.8	-3.6	2.0	0.7

Table IV-16 Projected changes (%) in the Q95 low flow statistics calculated on a monthly and seasonal basis for the Shrevagh catchment. Changes are estimated for the 2020s horizon (2010-2039) relative to the 30 year control period. (1961-1990). Projected changes in Q95 are estimated using the median series from the multimodel simulation. The table is colour coded to highlight increases/decreases.

2050s Q95 Change (%)	Jan	Feb	Mar	Apr	May	Jun	Jul	Aug	Sept	Oct	Nov	Dec	Winter	Spring	Summer	Autumn
C4IRCA3 HadCM3Q16 A1B	10.8	-4.9	6.3	-12.2	-1.8	0.4	0.6	-20.0	-15.2	-23.0	-14.7	-2.6	-0.6	-4.7	-4.5	-22.6
CNRM-RM5.1 ARGEGE A1B	-19.7	-9.1	0.3	7.6	-16.6	-16.6	-6.4	-21.1	-32.8	-28.5	4.7	-18.0	-12.3	-3.0	-14.1	-27.6
DMI-HIRHAM5 ARPEGE A1B	-17.4	-1.8	5.1	-7.3	-12.8	-18.2	-6.1	-14.8	-3.9	-5.3	-12.1	-3.3	-3.3	-11.1	-15.0	-11.6
DMI-HIRHAM5 ECHAM5-r3 A1B	10.3	-20.1	-6.6	-1.5	-16.1	-22.4	-17.9	-9.6	1.5	22.6	-13.8	-35.0	-21.5	-12.3	-17.9	2.1
ETHZ-CLM HadCM3Q0 A1B	7.6	9.4	-3.0	5.0	-3.3	-12.0	0.4	-28.6	-13.8	-9.3	-29.9	35.2	12.1	-3.3	-16.0	-19.6
ICTP-REGCM3 ECHAM5-r3 A1B	-8.0	-12.3	-2.0	3.0	-7.6	-21.0	-29.8	-20.4	-5.8	36.1	-21.2	-43.7	-24.8	-2.5	-24.2	-1.7
KNMI-RACMO2 ECHAM5-r3 A1B	-23.0	-12.6	-10.8	-1.0	-14.3	-12.0	-33.4	-27.4	-6.1	26.8	-7.7	-41.6	-25.6	-8.0	-23.3	2.7
METO-HadRM3Q0 HadCM3Q0 A1B	-25.2	-20.3	-6.4	-10.1	-5.7	-10.7	-5.9	-30.8	-9.3	-9.9	-4.5	13.9	-9.1	-5.5	-17.1	-8.3
METO-HadRM3Q3 HadCM3Q3 A1B	27.7	-16.8	-8.8	14.3	3.9	4.8	-25.2	8.9	65.4	1.2	-24.8	9.5	-2.2	12.1	-2.1	1.1
METO-HadRM3Q16 HadCM3Q16 A1B	-3.6	-9.9	-8.3	-21.8	0.2	-15.2	7.0	-15.9	-13.9	-26.0	-7.6	-0.9	-3.9	-10.3	-9.3	-20.5
MPI-M-REMO ECHAM5-r3 A1B	-26.6	-8.2	-5.7	-6.7	-13.0	-10.0	-27.7	-30.8	-15.0	56.5	-19.3	-42.7	-27.6	-9.4	-22.0	-3.2
SMHIRCA BCM A1B	54.5	12.5	60.4	14.1	-38.4	-12.8	-19.0	-24.4	-14.9	-11.8	-14.4	20.6	24.7	-16.0	-17.2	-12.9
SMHIRCA ECHAM5-r3 A1B	-20.5	-20.2	-5.6	-13.3	-10.8	-26.9	-24.3	-27.4	-7.9	13.6	2.1	-37.8	-24.4	-10.6	-26.3	1.2
SMHIRCA HadCM3Q3 A1B	53.0	9.4	-8.0	25.1	13.1	6.1	-21.7	-5.9	34.5	-9.4	-19.7	31.8	21.3	13.4	-12.1	1.9
SDSM HadCM3 A2	11.1	6.5	20.2	0.0	3.8	23.3	-27.7	-34.5	-15.8	-29.3	-15.9	5.3	8.9	5.5	-16.8	-21.5
SDSM HadCM3 B2	-6.0	15.2	14.7	4.8	-9.6	0.1	-11.7	-27.8	-15.2	-22.4	8.0	16.9	6.4	-3.2	-15.0	-14.7
SDSM CSIROmk2 A2	19.4	4.7	25.5	-24.1	-2.7	-6.8	2.0	-15.7	-35.4	-13.9	-3.9	11.2	10.6	-7.6	-7.7	-23.5
SDSM CSIROmk2 B2	20.2	-10.4	-4.3	13.7	-3.8	-8.0	-4.8	28.7	5.4	-4.1	-12.2	-4.6	-2.4	4.7	1.7	-2.3
SDSM CGCM2 A2	37.4	4.6	-6.1	-18.5	-21.5	0.9	-3.8	6.4	-0.1	-28.7	-0.9	22.5	9.7	-19.8	-1.2	-11.7
SDSM CGCM2 B2	18.7	23.5	-0.6	3.6	-19.1	-12.8	29.2	3.6	-7.7	-11.3	6.3	33.0	24.6	-11.8	4.0	-3.6

Table IV-17 Projected changes (%) in the Q95 low flow statistics calculated on a monthly and seasonal basis for the Shrevagh catchment. Changes are estimated for the 2050s horizon (2040-2069) relative to the 30 year control period. (1961-1990). Projected changes in Q95 are estimated using the median series from the multimodel simulation. The table is colour coded to highlight increases/decreases.

2080s Q95 Change (%)	Jan	Feb	Mar	Apr	May	Jun	Jul	Aug	Sept	Oct	Nov	Dec	Winter	Spring	Summer	Autumn
C4IRCA3 HadCM3Q16 A1B	-5.6	5.9	10.7	5.6	22.8	-7.3	13.0	-20.9	15.0	13.6	31.5	13.5	5.7	14.1	-5.3	10.8
CNRM-RM5.1 ARGEGE A1B	-18.8	-1.3	-9.1	10.7	-11.1	-16.8	-8.5	-8.8	-37.9	3.0	4.1	-8.8	-7.8	-3.8	-10.6	-30.8
DMI-HIRHAM5 ARPEGE A1B	-8.5	-0.3	-7.0	-9.2	-24.6	-25.7	-11.6	-13.9	-14.0	-16.3	-17.0	-21.8	-11.2	-19.5	-18.4	-18.7
DMI-HIRHAM5 ECHAM5-r3 A1B	39.1	3.1	27.5	4.5	6.0	-6.8	-7.7	-0.7	-29.2	16.9	-11.4	-10.4	3.6	5.2	-6.5	-17.8
ETHZ-CLM HadCM3Q0 A1B	10.3	-6.1	28.5	-15.5	0.3	-3.3	3.6	-9.0	-0.3	-5.1	8.6	8.0	3.5	-8.2	-2.7	1.0
ICTP-REGCM3 ECHAM5-r3 A1B	44.7	-11.4	14.3	-1.7	-12.8	-22.6	-3.3	-0.4	-37.5	-0.5	1.4	0.3	2.4	-7.1	-9.5	-22.0
KNMI-RACMO2 ECHAM5-r3 A1B	22.9	-6.6	12.7	2.2	-9.9	-9.5	4.1	4.5	-29.4	-3.8	8.6	-16.7	-3.7	-4.4	-0.8	-16.9
METO-HadRM3Q0 HadCM3Q0 A1B	-14.0	-13.0	14.7	-21.4	8.4	-10.0	-15.8	-25.6	-1.5	-7.9	9.0	-5.3	-9.5	-4.0	-16.2	-2.5
METO-HadRM3Q3 HadCM3Q3 A1B	-4.7	-1.0	6.1	28.7	-11.4	-2.5	-36.1	-13.4	45.9	-1.2	-2.5	34.4	10.5	5.0	-18.3	-7.1
METO-HadRM3Q16 HadCM3Q16 A1B	-19.0	5.0	1.2	-7.8	9.7	-21.4	0.7	-9.7	-1.8	-13.2	34.7	1.8	-1.9	2.9	-12.7	-11.1
MPI-M-REMO ECHAM5-r3 A1B	26.6	-14.8	4.8	-3.3	-8.7	-10.1	-5.1	-6.1	-37.2	15.3	5.3	0.6	-3.3	-5.9	-9.1	-19.3
SMHIRCA BCM A1B	84.7	32.6	19.1	54.6	-33.8	-22.3	-22.3	-27.2	-32.7	4.0	28.5	50.3	49.6	-10.9	-21.3	-5.6
SMHIRCA ECHAM5-r3 A1B	20.7	-25.5	3.3	-10.0	-10.2	-26.8	-7.0	-13.0	-42.5	7.5	15.4	5.3	-4.1	-8.1	-16.7	-19.3
SMHIRCA HadCM3Q3 A1B	28.1	19.2	18.3	34.6	3.9	-3.8	-35.1	-19.3	29.2	-13.7	13.6	78.0	33.5	18.7	-21.0	2.3
SDSM HadCM3 A2	27.2	-2.3	35.5	2.6	-2.1	15.6	-34.6	-43.5	-22.7	-33.7	-9.1	52.2	23.0	2.0	-26.9	-25.0
SDSM HadCM3 B2	-20.4	13.7	28.9	15.5	10.0	-9.8	-21.2	-33.6	-2.2	-23.4	-17.1	4.5	-0.6	14.4	-23.8	-11.7
SDSM CSIROmk2 A2	28.8	23.4	33.4	-22.3	3.6	2.3	-5.8	9.2	-18.0	2.9	-8.8	23.6	25.1	3.9	-3.2	-13.6
SDSM CSIROmk2 B2	7.3	-2.2	-8.4	20.3	-0.1	10.7	7.9	16.8	-11.2	10.6	-11.8	9.6	7.3	6.0	12.4	-4.4
SDSM CGCM2 A2	33.9	10.8	5.3	-29.2	-40.4	-9.0	2.2	1.0	5.2	-23.2	-3.5	1.1	14.4	-34.5	-7.2	-8.2
SDSM CGCM2 B2	25.2	19.3	-8.9	-14.9	-39.5	-13.1	26.4	12.9	-4.3	0.1	10.5	13.4	17.1	-26.9	5.0	-0.4

Table IV-18 Projected changes (%) in the Q95 low flow statistics calculated on a monthly and seasonal basis for the Shrevegh catchment. Changes are estimated for the 2080s horizon (2070-2099) relative to the 30 year control period. (1961-1990). Projected changes in Q95 are estimated using the median series from the multimodel simulation. The table is colour coded to highlight increases/decreases.

Appendix V

Results of the Reliability, Resilience and Vulnerability analysis conducted for the Glenamong and Srahrevagh catchments.

Reliability	Q05						Q 50						Q95					
	Glenamong			Srahrevagh			Glenamong			Srahrevagh			Glenamong			Srahrevagh		
	2020s	2050s	2080s	2020s	2050s	2080s	2020s	2050s	2080s	2020s	2050s	2080s	2020s	2050s	2080s	2020s	2050s	2080s
C4IRCA3 HadCM3Q16 A1B	5.17	5.93	7.01	5.33	6.11	7.25	47.54	44.34	47.18	48.20	45.90	48.67	91.17	87.42	95.18	94.84	92.91	95.37
C4IRCA3 ECHAM5 A2	5.26	-	-	5.46	-	-	48.65	-	-	48.95	-	-	91.04	-	-	93.26	-	-
CNRM-RM4.5 ARPEGE A1B	5.60	-	-	5.72	-	-	47.92	-	-	48.77	-	-	93.39	-	-	93.09	-	-
CNRM-RM5.1 ARGEGE A1B	5.84	5.62	6.13	5.85	5.66	6.24	47.50	45.01	45.22	48.61	45.87	45.50	92.26	87.89	87.27	92.65	91.64	90.44
DMI-HIRHAM5 ARPEGE A1B	5.88	5.53	5.85	5.96	5.70	5.94	47.91	45.04	43.41	47.85	45.14	43.45	93.04	88.80	86.50	92.84	91.98	90.44
DMI-HIRHAM5 ECHAM5-r3 A1B	5.94	6.31	6.82	6.11	6.52	7.00	52.15	49.95	52.50	52.50	50.37	52.93	97.62	96.32	98.06	94.97	92.22	94.02
ETHZ-CLM HadCM3Q0 A1B	5.40	5.64	5.91	5.59	5.87	6.04	46.19	46.47	46.04	46.50	46.91	46.54	90.42	92.27	92.68	93.14	92.04	93.47
ICTP-REGCM3 ECHAM5-r3 A1B	5.20	5.07	5.89	5.37	5.27	6.14	49.98	47.23	50.03	49.85	47.41	50.07	91.40	89.86	92.63	93.55	91.81	92.96
KNMI-RACMO2 ECHAM5-r3 A1B	5.20	5.39	6.71	5.35	5.47	6.74	48.94	46.38	48.52	49.48	46.45	48.77	92.82	90.06	94.18	94.06	91.57	93.28
METNOHIRHAM BCM A1B	5.28	-	-	5.53	-	-	51.72	-	-	51.92	-	-	94.84	-	-	93.05	-	-
METNOHIRHAM HadCM3Q0 A1B	5.30	-	-	5.28	-	-	45.59	-	-	46.49	-	-	89.20	-	-	92.74	-	-
METO-HadRM3Q0 HadCM3Q0 A1B	5.63	5.74	5.89	5.81	6.12	6.13	44.98	45.62	44.78	45.66	46.62	45.99	87.86	90.44	89.33	91.94	92.74	92.79
METO-HadRM3Q3 HadCM3Q3 A1B	5.58	5.78	6.18	5.63	5.98	6.29	49.91	49.03	50.15	50.29	49.32	50.51	96.23	94.13	93.86	95.72	94.45	91.74
METO-HadRM3Q16 HadCM3Q16 A1B	5.37	5.16	6.50	5.69	5.46	6.63	47.98	44.45	47.39	49.26	45.70	49.03	91.47	85.98	92.17	94.38	92.03	91.87
MPI-M-REMO ECHAM5-r3 A1B	5.13	4.68	5.29	5.33	4.77	5.38	47.91	45.35	47.45	48.12	45.50	47.37	90.21	85.98	88.45	93.66	91.55	92.93
OURANOSMRCC4.2.1 CGCM3 A1B	5.69	-	-	5.82	-	-	46.23	-	-	46.95	-	-	91.12	-	-	94.13	-	-
SMHIRCA BCM A1B	5.29	5.93	6.88	5.37	6.15	6.89	51.68	51.83	53.22	51.34	51.66	53.22	94.26	95.25	97.50	93.14	91.92	92.35
SMHIRCA ECHAM5-r3 A1B	5.29	5.24	6.46	5.39	5.41	6.55	48.67	46.09	46.80	49.11	46.10	47.32	90.76	88.36	90.54	92.63	91.22	91.80
SMHIRCA HadCM3Q3 A1B	6.84	6.25	7.16	6.99	6.23	7.35	50.84	50.63	52.85	50.95	51.07	52.95	98.56	96.67	97.05	95.90	94.82	93.36
SDSM HadCM3 A2	4.79	4.37	4.96	4.87	4.62	5.22	46.35	45.98	46.39	46.94	46.57	46.43	88.98	87.79	84.90	93.41	93.33	90.76
SDSM HadCM3 B2	4.99	4.89	4.90	5.10	4.97	4.98	49.57	46.89	49.29	49.48	47.13	50.00	92.65	88.52	89.93	94.85	93.27	93.28
SDSM CSIROmk2 A2	5.83	5.43	5.53	5.93	5.71	5.69	48.74	46.59	47.56	49.09	47.47	49.66	92.05	87.80	91.40	93.98	92.33	95.01
SDSM CSIROmk2 B2	4.34	5.22	4.95	4.48	5.41	5.18	46.98	48.49	48.27	48.43	49.92	50.06	91.87	94.30	94.08	95.66	94.62	95.92
SDSM CGCM2 A2	4.76	4.81	4.40	4.88	5.06	4.56	47.39	46.17	43.28	47.68	46.91	44.06	90.58	90.45	84.39	92.82	92.46	89.17
SDSM CGCM2 B2	4.88	4.76	4.75	5.07	4.85	4.93	49.11	47.62	46.25	49.81	48.38	47.03	92.10	90.45	89.30	94.47	93.59	92.01

Table V-1 The projected reliability of median (Q50), low (Q95) and high (Q05) flows estimated on an annual basis for the Glenamong and Srahrevagh catchments respectively. Each statistic is calculated for three future time horizons (2020s, 2050s and 2080s) relative to the 30 year control period (1961-1990). Projected changes in each statistic are estimated using the median series from the multimodel simulation. The table is colour coded to highlight differences in the results from individual climate scenarios.

Resilience	Q05								Q50								Q95							
	Glenamong				Srahrevagh				Glenamong				Srahrevagh				Glenamong				Srahrevagh			
	Ctrl	2020s	2050s	2080s	Ctrl	2020s	2050s	2080s	Ctrl	2020s	2050s	2080s	Ctrl	2020s	2050s	2080s	Ctrl	2020s	2050s	2080s	Ctrl	2020s	2050s	2080s
C4IRCA3 HadCM3Q16 A1B	4.4	4.4	5.0	5.8	4.4	4.5	5.3	6.1	19.4	18.6	16.5	18.2	18.9	19.0	17.3	19.4	18.6	17.0	15.9	19.4	16.2	21.9	18.4	20.9
C4IRCA3 ECHAM5 A2	4.3	4.4	-	-	4.3	4.5	-	-	20.8	19.3	-	-	20.7	20.0	-	-	19.5	17.2	-	-	25.2	19.8	-	-
CNRM-RM4.5 ARPEGE A1B	4.4	4.9	-	-	4.4	5.0	-	-	18.2	16.8	-	-	17.2	16.8	-	-	12.7	12.3	-	-	17.2	16.6	-	-
CNRM-RM5.1 ARPEGE A1B	4.5	5.1	4.9	5.3	4.5	5.1	4.9	5.4	18.4	17.4	15.4	15.6	17.6	17.4	15.2	15.0	10.9	12.3	12.8	12.1	18.4	15.2	15.2	14.9
DMI-HIRHAM5 ARPEGE A1B	4.4	4.8	4.8	5.0	4.5	4.9	5.0	5.1	17.7	16.3	15.0	14.3	16.6	15.5	14.3	13.2	13.1	12.3	11.8	12.0	20.1	16.4	17.7	14.7
DMI-HIRHAM5 ECHAM5-r3 A1B	4.5	5.0	5.3	5.6	4.5	5.1	5.3	5.8	20.3	22.8	19.9	21.1	20.6	23.4	20.2	22.0	23.2	21.5	19.4	23.9	28.5	25.6	19.8	22.9
ETHZ-CLM HadCM3Q0 A1B	4.1	4.5	4.6	5.2	4.2	4.6	4.8	5.2	18.8	18.1	17.4	17.7	18.5	17.8	17.7	18.5	13.5	13.4	13.0	15.1	18.8	17.0	15.1	17.5
ICTP-REGCM3 ECHAM5-r3 A1B	4.1	4.3	4.3	5.0	4.0	4.4	4.5	5.1	20.7	20.3	19.2	19.6	20.7	20.4	19.2	19.9	20.8	16.6	17.9	17.0	25.9	20.9	19.7	21.1
KNMI-RACMO2 ECHAM5-r3 A1B	4.1	4.6	4.6	5.6	4.0	4.8	4.7	5.6	20.0	19.4	18.1	18.4	20.3	19.5	18.3	18.6	18.6	17.7	15.4	17.7	21.4	20.3	17.6	22.0
METNOHIRHAM BCM A1B	4.4	4.6	-	-	4.4	4.8	-	-	19.9	19.3	-	-	19.5	19.2	-	-	17.0	16.8	-	-	20.1	18.6	-	-
METNOHIRHAM HadCM3Q0 A1B	4.3	4.4	-	-	4.3	4.4	-	-	19.2	17.0	-	-	18.9	16.9	-	-	15.6	13.3	-	-	18.2	18.6	-	-
METO-HadRM3Q0 HadCM3Q0 A1B	4.3	4.7	4.9	5.1	4.3	4.8	5.2	5.3	19.8	16.9	18.3	18.0	19.5	17.6	18.9	18.8	17.2	15.4	14.6	14.4	21.0	17.0	16.2	17.5
METO-HadRM3Q3 HadCM3Q3 A1B	4.2	4.5	4.9	5.2	4.2	4.5	5.0	5.3	17.5	17.7	16.8	16.4	17.3	17.5	16.3	15.7	12.1	15.0	11.8	11.5	13.0	16.2	15.1	10.9
METO-HadRM3Q16 HadCM3Q16 A1B	4.3	4.6	4.6	5.4	4.3	4.7	4.8	5.6	20.4	19.5	17.4	17.9	19.9	20.4	17.9	18.7	16.6	14.9	14.6	15.9	19.0	19.8	19.2	15.9
MPI-M-REMO ECHAM5-r3 A1B	3.7	3.9	3.5	4.0	3.5	3.9	3.4	4.0	17.9	17.5	16.2	16.6	18.3	17.4	16.0	16.8	19.7	15.6	14.6	17.0	23.5	19.9	17.2	21.0
OURANOSMRCC4.2.1 CGCM3 A1B	4.3	4.8	-	-	4.4	4.9	-	-	20.4	19.4	-	-	21.3	20.3	-	-	17.2	17.3	-	-	20.4	22.7	-	-
SMHIRCA BCM A1B	4.1	4.3	4.9	5.6	4.1	4.4	5.1	5.6	21.5	20.7	19.2	20.1	21.4	20.8	19.7	20.1	18.4	18.0	17.9	16.1	22.8	20.2	17.2	16.2
SMHIRCA ECHAM5-r3 A1B	4.2	4.5	4.5	5.4	4.2	4.6	4.6	5.4	20.2	19.6	18.3	18.1	20.7	19.6	18.7	18.5	18.1	15.5	15.9	16.1	24.3	20.8	17.7	19.2
SMHIRCA HadCM3Q3 A1B	4.1	5.4	5.2	6.1	4.1	5.5	5.1	6.2	18.4	18.7	18.7	18.7	18.4	19.0	18.8	18.8	16.5	15.2	15.9	13.7	17.2	20.7	18.3	13.0
SDSM HadCM3 A2	4.2	3.9	3.6	4.0	4.3	4.0	3.8	4.2	19.5	18.4	17.8	17.7	19.2	18.7	18.1	18.1	19.2	17.4	17.1	13.7	20.6	23.0	21.8	17.7
SDSM HadCM3 B2	4.2	4.2	4.0	3.9	4.2	4.3	4.1	3.9	20.4	20.0	18.3	18.3	19.8	19.8	18.1	18.4	15.9	18.4	19.0	16.7	22.6	23.8	20.2	18.6
SDSM CSIROmk2 A2	4.0	4.6	4.2	4.4	4.0	4.6	4.4	4.4	21.6	20.4	18.2	20.7	21.6	20.2	19.0	22.3	22.1	19.9	18.1	20.3	26.1	25.5	22.8	23.9
SDSM CSIROmk2 B2	4.0	3.5	4.0	3.8	4.0	3.5	4.0	3.9	21.3	19.7	19.8	19.5	20.9	20.1	19.9	20.9	17.7	22.2	19.0	23.0	25.2	31.8	23.7	28.2
SDSM CGCM2 A2	4.1	3.8	4.1	3.6	4.1	3.8	4.2	3.7	22.6	20.3	18.8	18.0	22.3	20.7	19.6	18.5	15.7	15.2	17.8	13.2	23.7	22.9	24.7	20.6
SDSM CGCM2 B2	4.1	4.1	3.8	3.8	4.0	4.3	3.9	3.9	22.6	21.2	19.1	18.9	21.5	21.9	19.9	19.4	16.9	16.5	19.8	17.7	22.4	23.6	26.5	20.6

Table V-2 The projected resilience of median (Q50), low (Q95) and high (Q05) flows estimated on an annual basis for the Glenamong and Srahrevagh catchments respectively. Each statistic is calculated for three future time horizons (2020s, 2050s and 2080s) relative to the 30 year control period (1961-1990). Projected changes in each statistic are estimated using the median series from the multimodel simulation. The table is colour coded to highlight differences in the results from individual climate scenarios.

Vulnerability	Q05								Q50								Q95							
	Glenamong				Srahrevagh				Glenamong				Srahrevagh				Glenamong				Srahrevagh			
	192	205	207	197	208	205	230	187	73	55	79	54	73	55	62	49	35	25	26	37	34	19	23	33
C4IRCA3 HadCM3Q16 A1B	192	205	207	197	208	205	230	187	73	55	79	54	73	55	62	49	35	25	26	37	34	19	23	33
C4IRCA3 ECHAM5 A2	250	218	-	-	250	218	-	-	53	73	-	-	43	49	-	-	20	34	-	-	17	24	-	-
CNRM-RM4.5 ARPEGE A1B	228	276	-	-	226	276	-	-	58	60	-	-	58	75	-	-	32	35	-	-	31	31	-	-
CNRM-RM5.1 ARGEGE A1B	207	215	208	224	218	215	215	224	83	88	84	78	83	87	84	78	41	39	64	42	36	40	63	42
DMI-HIRHAM5 ARPEGE A1B	211	217	269	236	211	217	269	236	75	62	87	108	74	61	73	104	30	39	37	69	34	49	35	60
DMI-HIRHAM5 ECHAM5-r3 A1B	217	199	208	181	217	212	209	181	48	53	62	45	42	53	54	46	17	19	26	18	14	27	35	30
ETHZ-CLM HadCM3Q0 A1B	217	198	227	213	224	248	227	213	73	61	60	72	75	72	65	51	55	39	52	31	22	28	44	27
ICTP-REGCM3 ECHAM5-r3 A1B	224	244	234	193	233	244	234	193	43	72	50	47	40	68	49	46	21	40	39	29	24	26	29	25
KNMI-RACMO2 ECHAM5-r3 A1B	226	219	210	196	224	209	210	200	53	85	57	70	51	78	61	47	21	25	53	21	19	20	50	19
METNOHIRHAM BCM A1B	245	270	-	-	245	270	-	-	53	82	-	-	53	82	-	-	32	27	-	-	34	29	-	-
METNOHIRHAM HadCM3Q0 A1B	240	232	-	-	240	232	-	-	72	82	-	-	72	82	-	-	33	45	-	-	32	29	-	-
METO-HadRM3Q0 HadCM3Q0 A1B	292	229	262	222	281	196	247	209	72	58	55	83	72	58	62	75	45	32	47	58	22	34	42	30
METO-HadRM3Q3 HadCM3Q3 A1B	227	259	247	199	228	252	224	202	69	110	62	104	69	89	61	105	63	30	32	44	59	57	31	35
METO-HadRM3Q16 HadCM3Q16 A1B	230	219	229	194	230	228	229	194	66	69	83	77	53	69	78	77	27	38	39	35	27	36	26	33
MPI-M-REMO ECHAM5-r3 A1B	317	308	274	256	317	308	305	256	52	86	56	66	52	78	56	61	24	38	40	41	17	18	35	28
OURANOSMRCC4.2.1 CGCM3 A1B	249	224	-	-	220	219	-	-	63	63	-	-	48	63	0	0	21	57	-	-	22	35	-	-
SMHIRCA BCM A1B	295	240	201	218	267	238	251	218	50	84	90	71	50	84	79	67	31	27	28	26	31	33	31	49
SMHIRCA ECHAM5-r3 A1B	205	226	191	192	211	201	191	196	55	76	57	59	54	76	57	55	43	29	39	31	19	27	35	25
SMHIRCA HadCM3Q3 A1B	338	171	257	181	272	188	257	181	61	92	59	71	81	83	59	74	28	20	24	46	27	23	17	50
SDSM HadCM3 A2	243	202	275	208	243	202	222	208	68	96	67	83	70	100	55	60	29	30	46	41	33	27	33	36
SDSM HadCM3 B2	234	285	221	252	234	285	223	263	87	85	62	96	87	57	62	96	36	35	51	37	28	24	40	37
SDSM CSIROmk2 A2	211	235	268	209	211	235	268	224	58	53	87	101	59	49	78	81	18	25	31	43	31	28	45	39
SDSM CSIROmk2 B2	249	216	229	232	249	254	229	232	64	53	60	67	57	46	60	72	29	27	33	20	25	23	21	16
SDSM CGCM2 A2	222	279	251	258	255	264	251	258	80	68	97	121	77	68	68	85	46	37	36	53	41	30	25	46
SDSM CGCM2 B2	246	281	259	229	266	281	240	247	129	98	77	119	67	68	65	119	48	33	32	87	41	28	26	76

Table V-3 The projected vulnerability of median (Q50), low (Q95) and high (Q05) flows estimated on an annual basis for the Glenamong and Srahrevagh catchments respectively. Each statistic is calculated for three future time horizons (2020s, 2050s and 2080s) relative to the 30 year control period (1961-1990). Projected changes in each statistic are estimated using the median series from the multimodel simulation. The table is colour coded to highlight differences in the results from individual climate scenarios.